UNIVERSITY OF
LIVERPOOL

Assessing the viability of using foraminifera from Mersey Estuary saltmarsh sediments to reconstruct former sea level

Thesis submitted in accordance with the requirements of the University of Liverpool for the degree of Doctor in Philosophy

Hayley Mills

July 2011

Abstract

The viability of using a foraminifera-based transfer function method to reconstruct the local relative sea-level for the Mersey Estuary was assessed in this study, which has not been previously investigated in the UK in the context of application in a strongly macrotidal setting. A total of 105 surface samples were collected across two saltmarshes. Foraminiferal analysis was carried out, along with several environmental variables (organic matter content, salinity, pH, and grain size) to establish the species distribution of foraminifera and their relationship with elevation. Two main zonations were found: a high-to-middle marsh zone occupied by *Haplophragmoides* spp*., J. macrescens* and *M. fusca;* and a low marsh zone composed of increasing numbers of calcareous species including *Elphidium* spp*.;* and *Haynesina* spp*.* Foraminiferal distributions along each transect were found to be controlled predominantly by elevation and distance from tidal influence, whilst combined datasets reflected intra- and inter-site variability in the assemblages. Elevation was still found to have an important control over the distributions, with a strong relationship between the species zonations and elevation (r^2 = 0.8). Therefore, the dataset (82 samples) formed a local training set in which a transfer function for the relationship between foraminifera species and elevation was developed. WAPLS was used as it produced the highest predictive ability (r^2_{jack} = 0.85) and lowest prediction errors ($RMSEP_{jack}$ = 0.11 m). Regional and combined (local plus regional) transfer functions were also developed but the local transfer function produced the most accurate and reliable reconstruction. Reconstructions were carried out for both saltmarshes with reference to a sediment chronology which was established using radionuclides and pollution indicators. The reconstructions demonstrated the vast difference in the saltmarsh development and record of sea level between the sites. Oglet Bay developed as a result of increased accommodation space arising from changing estuary morphology, resulting in rapid accretion (2.34 cm $year^{-1}$) and was found to be strongly influenced by tidal channel migration. Decoy Marsh accreted at a slower pace (0.32 cm $year^{-1}$) and was less affected by tidal or morphological changes. Both reconstructions were affected by decalcification resulting in the reconstructions dating back to 1978 at the most. The reconstructed rates of sea-level change were 1.8 cm $year^{-1}$ for Oglet Bay and 1.1 cm $year^{-1}$ for Decoy Marsh, both of which over-estimate the trend from the monthly instrumental record (1.04 cm $year^{-1}$) over the same period. The study highlights the problems which may arise when conducting research in an inner estuary which is strongly macrotidal, including tidal range changes, tidal asymmetry, and decalcification, but also demonstrates that a relatively precise and reliable reconstruction is achievable.

Acknowledgments

Firstly I would like to thank my supervisors Prof. Andrew Plater, Dr. Jason Kirby and Dr. Simon Holgate for their encouragement, support, expertise and guidance throughout, as well as help with the many fieldwork trips. I am particularly grateful to Andy for his time and patience especially during the last stages of the thesis, and always seeing the positive in everything! Thanks also go to Jason Kirby for introducing me to the subject and encouragement to continue in academia, and also to Simon Holgate for his advice and help throughout.

I am grateful to all the technical staff in the geography department who have helped me over the past 5 years including Hilda Hull, Irene Cooper, Alan Henderson, Bob Jude, Sandra Mather, Suzanne Yee, with extra thanks to Irene for her help using the laboratory equipment.

I would also like to thank the other members of staff in the department who were always available for advice if needed, including John Boyle for help in using the XRF, and particularly Richard Chiverrell who has given his time, help and encouragement when needed.

I am also grateful to Peter Appleby and Gayane Piliposyan, for carrying out the radionuclide analysis, Ben Horton and Robin Edwards for allowing me to use their dataset and for assistance when needed, and to Alan Bowden for his interest, expertise, and help in foraminifera identification.

I would like to thank all the post-graduates in the department for their support and friendship over the years as well as for being willing and enthusiastic field helpers. Thanks to my office mates Claire, Rubina and John, and to Lee, Katherine, Ian, Claire, Tim, Jen, Bev, Dan, Becky, and Andy. I wouldn't have lasted till the end without all the coffee and lunch breaks, as well as nights out together.

I would also like to thank my friends and family. I am especially grateful to my mum, dad and Katie for their constant support and encouragement throughout all my studies. As well as to Stephen who listened to every problem I encountered along the way, and provided encouragement and help throughout.

I acknowledge the department of Geography, University of Liverpool and Proudman Oceanographic Laboratory, who funded this research, with thanks to Quaternary Research Association for an additional grant. Lastly I would like to thank both my internal and external examiners John Boyle and Jerry Lloyd for their constructive critique and advice.

Contents

List of abbreviations

C2 Component 2

C2 software (Juggins, 2007)

CA Correspondence Analysis

CCA Canonical Correspondence Analysis

DBD Dry Bulk Density

DCA Detrended Correspondence Analysis

DCCA Detrended Correspondence Analysis

DM Decoy Marsh

DMSS1-2 Decoy Marsh surface samples, transects 1-2

GIA Glacio-isostatic Adjustment

HAT Highest Astronomical Tide

HOF Huisman-Olff-Fresco

LOI Loss on Ignition

MAT Modern Analogue Technique

MHWST Mean High Water Spring Tide

MHW Mean High Water

ML Maximum Likelihood

MLWST Mean Low Water Spring Tide

MSL Mean Sea Level

MTL Mean Tidal Level

OB Oglet Bay

OBDM Oglet Bay and Decoy Marsh

OBSS1-3 Oglet Bay Surface samples, transects 1-3

PCA Principle Components Analysis

pCCA partial Canonical Correspondence Analysis

PME Palaeo-Marsh Elevation

RMSE(p) Root Mean Squared Error (prediction)

pRDA partial Redundancy Analysis

PLS Partial Least Squares

RA Reciprocal Averaging

RDA Redundancy Analysis

SLIP Sea Level Index Point

SWLI Standardised Water Level Index

WA Weighted Averaged

WA-Tol Weighted Tolerances

WAPLS Weighted Averaged Partial Least Squares

List of figures

List of tables

1. Introduction and Aims

With growing concerns over sea levels rising due to anthropogenically induced global warming, understanding past changes in sea level is becoming more important in order to put the current changes into context, and to improve sea-level predictions for the future. The development of more precise and accurate methods of sea-level reconstruction allow resolutions to be achieved which are more comparable to the scale of current changes and are important in improving understanding. Sea-level reconstructions using saltmarsh sediments have the potential to link to, and extend back, instrumental records (e.g. Donnelly et al., 2004; Gehrels et al., 2005) which can give additional context to current sea-level changes (Woodworth, 1999b).

Foraminifera within saltmarsh sediments have been utilised successfully in many studies in the UK and elsewhere due to their strong and quantifiable relationship with elevation (e.g. Horton et al., 1999a; Gehrels, 2000; Hayward et al., 2010; Rossi et al., 2011). It is a widely utilised method with many sites across the UK investigated for their modern surface distributions (e.g. Horton and Edwards, 2006). There have been several sea-level reconstructions utilising foraminifera within the UK (e.g. Edwards and Horton, 2000; Edwards, 2001, Massey et al., 2008), however been fewer foraminifera based transfer function reconstructions in macrotidal environments with only Hill et al. (2007) reconstructing sea-level in a strongly macrotidal environment in the UK using diatoms. The current study will test the feasibility of carrying out such methods on the sediments within the River Mersey (North West England) which is a strongly macrotidal estuary.

The sediments within the Mersey Estuary have not been utilised to produce a sea-level record for the area. Wilson et al. (2005a, b) assessed δ^{13} C and C/N as an alternative to microfossils for sea-level reconstructions in the Mersey Estuary, and although the sea level was not reconstructed. Shennan et al. 2006 reconstructed sea level for the Mersey using sea-level index points, glacial isostatic modelling and ice-sheet reconstructions for the past 15000, although the points were not from the Estuary itself. This study will attempt to reconstruct sea level at a higher resolution than previous long term regional studies in the area using a sediment-based method. The reconstruction will try and link with the existing sea-level record from the Liverpool tide gauge in attempt to both reproduce and extend the record.

The Mersey Estuary has one of the longest records of sea level obtained from tidal gauges and historical records (Woodworth, 1999b). The long record offers a unique opportunity and is valuable in this study as it will assist in verifying and assessing the reliability of the reconstruction on a longer timescale than other studies where tide gauges only date back a hundred years or so (e.g. Gehrels et al., 2005). Agreement between the reconstructed records and the tide gauge record will determine the robustness and validity of the sea-level reconstruction (Gehrels et al., 2005).

The Mersey Estuary also offers other advantages, as firstly, it will be less affected by isostatic adjustment than other parts of the UK and therefore, should reflect more of a eustatic sea-level component of change. Secondly, it has the potential to produce a good chronology for the industrial period utilising pollution indicators, due to its extensive and well documented industrial history.

The main aim of the study is to test the viability of using a foraminifera-based transfer function method for sea-level reconstruction using saltmarsh sediments from within the Mersey Estuary.

The objectives of the study are to:

- Assess whether the modern saltmarsh environment and foraminifera assemblages have the potential to form a training set in which a local transfer function can be developed.
- Carry out a stratigraphic and geochemical study of the saltmarsh to understand the sedimentation processes which have occurred and to select a core from which a fossil record will be established.
- Produce a chronology based upon radionuclides and pollution indicators.
- Develop additional transfer functions based upon regional and combined regional and local datasets which will be compared with the locally trained transfer function.
- Produce a local sea-level curve based upon the most appropriate foraminifera-based transfer function and the established chronology which will be compared with the instrumental record.

These objectives will allow the exploration of potential problems associated with carrying out such a study in a macrotidal environment, testing the methodology and applicability of the established methods, particularly within an estuary setting.

It will allow: insights into the sea-level changes which are occurring at the sites located within the estuary where sea level has not been reconstructed; establish whether a local modern foraminifera study is necessary before a reconstruction is carried out, or whether a regional transfer function based upon previous studies can be utilised, thus reducing time and costs; ascertain whether the metal profiles within the sediments are good enough to be used as chrono-markers in order to produce a constrained chronology; and determine how well a foraminifera-based transfer function reconstruction based within a macrotidal setting performs.

1.1. Background and literature review

1.2. Sea level

Sea levels change on a range of temporal and spatial scales. Short term sources of variability include: air pressure, winds, storm magnitude and frequency, ocean temperatures and salinity, currents and tides. Inter-annual and annual variations are caused by seasonality, ocean circulation and nodal changes (Pugh, 2004). Longer time scale relative sea-level changes result from the independent movements of the sea surface and the movements of the land surface (Pirazzoli, 1996). The sea surface can be modified by changes in oceanic water volume, water density, water masses and the deformation of the shape of the ocean basin (Fairbridge, 1961; Pirazzoli, 1996). The land surface can be modified by changes in a range of geological factors including, tectonic activity, consolidation of coastal sediments, and isostatic adjustment of the Earth's surface to land ice and loading from the ocean itself (Pugh, 2004).

Present sea-level changes are predominantly related to changes in ocean volume and glacio-isostatic adjustment (GIA). Ocean volume changes are related to thermal expansion caused by warming, as well as decreases in salinity, whereby, the density of the water decreases causing a rise in sea level as the volume of the ocean increases (Church et al., 2001). In addition, warming can also cause ocean ice melting resulting in gravitational changes in sea-level near ice margins (Plater, and Kirby, in press). The large heat capacity of the oceans means that there will be a delay before oceans reach thermal equilibrium with

new temperatures, therefore, changes in sea level occurring today may be the result of past changes (Pugh, 2004).

The changing mass of grounded ice may also change the volume of the ocean. As water is stored as ice on the Earth's surface, increasing temperatures will increase inputs of water to the oceans increasing volume. When cooler, water is removed from the volume as it is held in storage as ice. Glaciers and ice caps are sensitive to changes in temperature, and in addition to present day forcings, ice sheets may still be adjusting to past conditions (Church et al., 2001).

The land surface may be altered due to transfers of mass from grounded ice sheets to the ocean and the adjustment of the mantle to these (Church et al., 2001). When ice sheets are present they press the crust of the Earth down into the mantle, which then rebounds when the ice melts and the weight lifts i.e. glacio-isostatic movements (Plater and Kirby in press). In addition 'continental levering' occurs when the increased postglacial load depresses the adjacent continental shelf and ocean basin causing the adjacent land mass to rise (Clarke et al., 1978). The depression of the ocean basin from the transfer of load from the land to ocean is known as hydro-isostasy (e.g. Stochi and Spada, 2009). When the ice melts it also creates an area of uplift at its margins which is known as a fore bulge. When a fore bulge is located on the ocean floor and collapses due to ice melt, space is created which allows water to flow into and increases the size of the ocean basin, which is known as 'ocean siphoning' (Plater and Kirby, in press). Major melting of ice ended approximately 6000 years ago, however, resulting isostatic movements are still occurring today as a result of the slow viscous response of the Earth (Church et al., 2001; Shennan and Horton, 2002) as well as rapid deformations of the Earth's surface due to the response to modern melting. Other smaller contributions to present day sea-level change may be caused by variations in the amount of water retention in lakes and reservoirs, groundwater and permafrost (Pugh, 2004).

1.2.1. Tidal levels

Sea levels change on a daily basis due to tidal oscillations controlled by the gravitational forces of the moon and sun. The major tidal constituents contributing to the astronomical tide are the M_2 and S_2 which are the principle lunar and solar semidiurnal constituents respectively. In most locations, the largest constituent is the M_2 tidal constituent and therefore most locations have a semidiurnal tide, having two high and two low tides a day with each tidal cycle taking an average of 12.24 hours (Pugh, 2004). In shallow water, a

short-period harmonic term is introduced into the formula of tidal constituents to take account of the change in the form of a tide wave resulting from shallow water conditions (M_4). M_4, M_6, and M_8 are the harmonics of the principle lunar constituents and S_4, S_6 etc. are the harmonics of the principle solar semidiurnal constituents.

There are two main features of a tidal cycle: the 'range' which is measured as the height between successive high and low tidal levels; and the 'period' which is the time between one high water and the next (Pugh, 2004) (figure 1.1). Semidiurnal tides have a range which usually increases and decreases cyclically over a 14 day period. This cycle, related to the phases of the moon is repeated every 29.5 days. There are three main classifications of tidal range based upon size. Micro-tidal, which has a tidal range of <2 m, meso-tidal which has a range between 2-4 m and macro-tidal which has a tidal range >4 m (Hayes, 1976). The mean spring tidal range is calculated from the difference between the Mean High Water Spring (MHWS) and Mean Low Water Spring (MLWS) tides. Mean Tidal Level (MTL) is a reference level often referred to and is calculated as half the mean spring tidal range. The Mean Sea Level (MSL) is the mean level of the tide measured over a set period of time (Pugh, 2004).

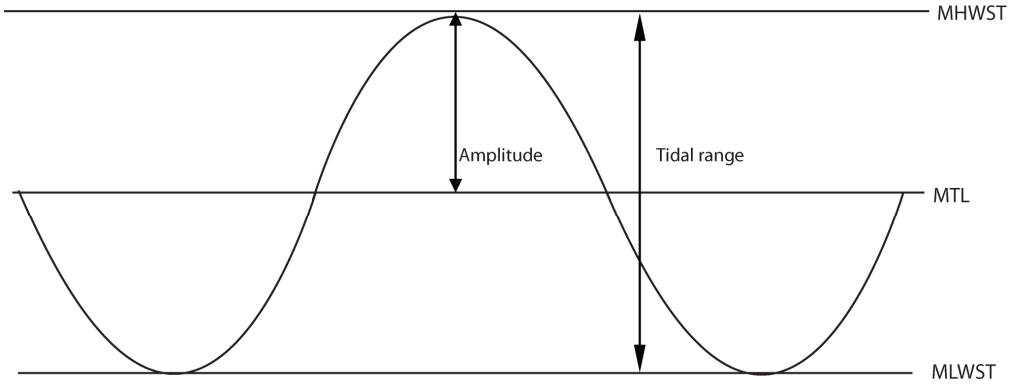

Fig. 1.1 Reference tidal levels.

Estuaries and other inlets are affected by tides, however, as they are smaller in area they undergo changes which are more related to the laws of hydraulics and wave motion rather than related to gravitational forces directly (Clark, 2007). Throughout the open ocean, the tide is usually symmetrical with the crest of the undulation causing high water and the trough causing low water. However, on entering an estuary, the tide undergoes some distortion as waves do in shallower water near the shore (Clark, 2007). The velocity at

which the tide moves up an estuary is governed by the equation for the propagation of waves in shallow water and is therefore a direct function of depth (Perillo, 1996). Because of this depth dependence, tides in estuaries are deformed during upstream propogation (Perillo, 1996). Distortion occurs in terms of amplitude, symmetry and duration of the flood and ebb tides (Woodroffe, 2003). In estuaries, tidal flows become modified as a result of changes in depth, friction, landward constriction of the channel, and reflection from channel banks, shoals, and the channel head (Woodroffe, 2003).

The topography as well as bottom friction affect the propagation of the tide, with a narrowing of the estuary causing the range of the tide to increase landward (Steele, 2009). The rate at which the estuary narrows determines the tidal amplitude of the tide along the estuary (Nichols and Briggs, 1985). If the rate of narrowing is in equilibrium with the tidal flow the tidal range remains relatively constant along the channel. If the channel narrows rapidly the energy is concentrated and, therefore, the tidal amplitude and range increases upstream, whereas if the channel widens rapidly the tidal range will decrease (Woodroffe, 2003). Figure 1.2, taken from Woodroffe (2003) shows the changes in the tide which can occur along an estuary in relation to the constrictions of the channel. In high tidal range estuaries, the currents and the range of the tide generally increase towards the head, until in the riverine section the river flow becomes important (Steele, 2009).

In many estuaries the degree of tidal asymmetry increases upstream also, thereby magnifying the differences between ebb and flood velocities and slack-water durations (Perillo, 1996). As the speed of the tidal wave varies with depth, the wave travels more rapidly when the water is deeper at high tide than when it is shallower at low tide. As a result, the duration of the flood limb gets progressively shorter and the ebb duration gets longer upstream (Woodroffe, 2003). Therefore, flows become increasingly asymmetric in duration and velocity which can also be seen in figure 1.2.

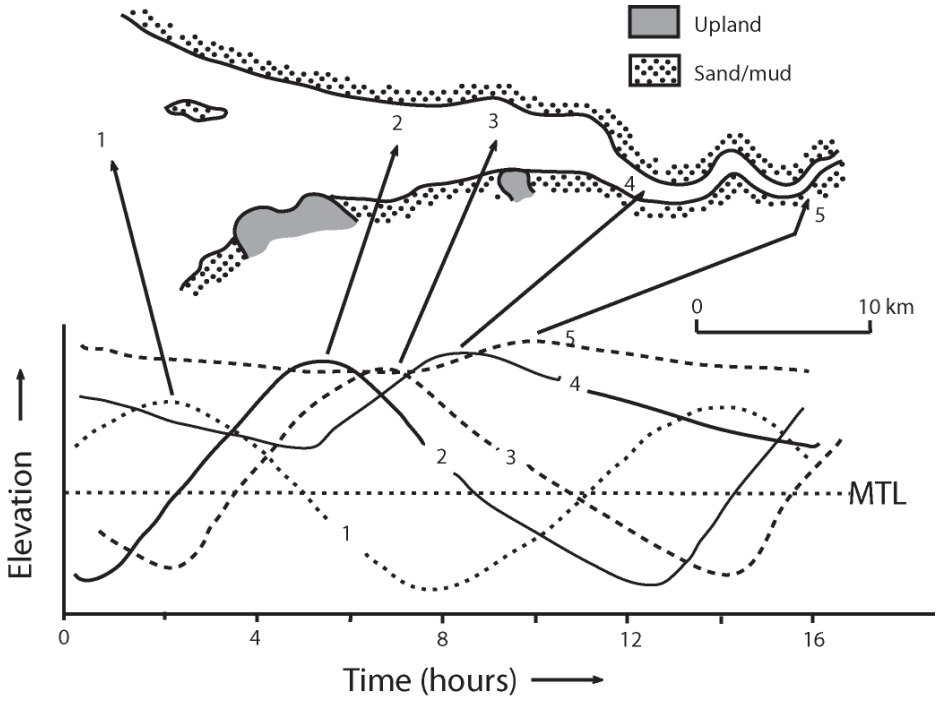

Figure 1.2 Distortion of tidal wave propagating up a schematic estuary. The tidal amplitude varies as a result of changes in width (taken from Woodroffe (2003)).

In some cases the effect of friction combined with the slope of the bed reaches a critical state where the wave crest catches up with the trough and forms a bore. In a tidal bore the crest of the tide takes the form of a breaking wave which advances up the estuary. There is a very rapid reversal of the tidal flow which takes place as the wave passes and a rapid rise in the water level (Ghosh, 1998).

1.2.2. Present day sea-level observations

Knowledge of present-day sea-level change is derived from tide-gauge observations and satellite altimetry measurements. Investigations of these have led to varying conclusions, with both the rate and causes of the 20th century global sea-level rise being contentious (Miller and Douglas, 2006). Estimates range from 1.4 mm to 2.4 mm year^{-1} (Church et al., 2001) with the IPCC third assessment report concluding that the rate is within the range of 1-2 mm year^{-1} during the 20th century (Church et al., 2001) and this was also supported by Woodworth et al. (1999). The IPCC fourth assessment report concluded that sea-level had risen an average of 1.7 mm year^{-1} during the last century (Solomon et al., 2007). Some studies have concluded that the tide gauge data have shown no significant acceleration in the rate of rise during the latter half of the 20th century (e.g. Douglas, 1992). However, other studies suggest that the rate is higher than for the previous century (Woodworth et al., 1999). Gehrels et al. (2005) and Donnelly et al. (2004) examined both recent geological

and instrumental data and suggest that the sea-level rise observed during the 20th century was significantly larger than that measured over timescales of several centuries.

The cause of the current rise in sea level is also uncertain. Anthropogenic sources of global warming and resultant sea-level rise are considered to be the dominant cause of present data sea-level changes (Solomon et al., 2007). However, there is uncertainty as to; how much of the increasing sea levels is anthropogenically related, how much, if any, is natural; if there are accelerations in the sea-level rise; and the timings of these. For example, geological data indicates that ocean volumes have increased since the main phase of deglaciation about 7000 years ago (Church et al., 2001) and, therefore, the rise may be a continuation of this. Other studies have found increases in sea levels as a response to the little ice age (LIA) recovery. For example, increased flooding, correlated with climatic warming at the end of the LIA was found on several marshes in New England and England (Thomas et al., 1993) and in Chesapeake Bay (Kearney and Stevenson, 1991). Many other studies have also reported that the sea-level rise occurring presently is natural in origin. An example is that of Gehrels (1999) were it was concluded that rapid sea-level rise was occurring before the 18th century and, therefore, must contain a natural component related to the recovery from the LIA. This supported previous studies in North America including van de Plassche et al. (1998).

It is important that information about former sea-level changes over the last few centuries or millennia is obtained to place the more recent changes in a longer historical context (Woodworth, 2006). Instrumental records, however, only date back to the later part of the 19th century, when the rate of sea-level rise may have already been influenced by human activity (Donnelly et al., 2004). Therefore, the need for accurate high resolution sea-level reconstructions have become even more important.

1.3. Past records of sea level

Changes in sea level and its relationship with climate have, and are being investigated in numerous ways, on varying temporal and spatial scales. Over the recent time period (past 100 years or so), instrumental measurements have been made using tide gauges and over the last 17 years satellite altimetry has been used. Both of these allow investigations of changes over short timescales which are important in the context of anthropogenic influences on climate and sea-level. Woodworth et al. (1999) and Ekman (2003) in the UK and Europe have examined tidal gauges to determine whether there has been accelerated sea- level rise in recent decades. Woodworth (1999b) used the few long tide gauge records from North West Europe and suggested that the acceleration first became apparent in the latter part of the 19th century. Whilst Jevrejeva et al. (2008) suggested that it may have been earlier. Tide gauges provide accurate relative sea-level records for coastal areas, however, the data they provide are limited both spatially and temporally, and satellite altimetry whilst providing world-wide data for sea level, it is only available since 1992.

Over millennial timescales, geophysical models of GIA can be used to estimate large scale changes in land movements and sea levels using ice thickness and rheology. Ice thickness and extent is determined by geomorphological evidence including, trim lines and moraine deposits, and is used along with rheology information about the Earth's surface to model the growth and decay of the last major ice sheets and determine the effect upon relative sea-levels (Lambeck, 1995). Many GIA models cover the UK including, Lambeck (1995), Peltier et al. (2002), Shennan and Horton (2002) and Shennan et al. (2006). In these studies there are, however, major differences in the models used, the input parameters, and the results (Shennan et al., 2006). Advances in the method allow a good degree of fit between results and observations, however, not all sites can be accurately represented (Milne et al., 2006) and further development is needed, including the incorporation of an ice-sheet model that is based on quantitative, glaciological model simulations (Shennan et al., 2006). Geophysical models also do not capture submillenial-scale variability and have variable height accuracy estimates ranging from 1-2 m for the mid-to-late Holocene and 3-5 m changes in sea level for the late glacial (Lambeck, 1995) in absolute terms, although rates of change may be more accurate.

Both the models and instrumental methods of establishing sea-level records are supported and validated by reconstructed sea levels from coasts. These are derived from a number of different geomorphological, geological and biological indicators (Lambeck, 1995) and can

also provide a chronology on which they can be based. Submerged and raised coastal features, including beaches (e.g. Sissons, 1983), peats (e.g. Tooley, 1978), forests, tidal flats, saltmarshes, beachrock, marine carbonates, marine notches, wave-cut terraces, and coastal barrier sands can be used. These data sources are coupled with macrofossils, including ooids, corals, algae, gastropods, macrophytes, ostracods, shell middens and marine molluscs, and microfossils including, foraminifera, diatoms, and testate amoebae in order to reconstruct former sea levels. The timescales, resolution and spatial applicability of these techniques vary along with their accuracy, but many are capable of reconstructing metre-scale changes on millennial to century timescales.

1.4. Saltmarsh sediments

Tidal saltmarshes are areas bordering saline water bodies vegetated by herbs, grasses and shrubs, which are subjected to periodic inundations of sea water by tidal flooding. The frequency and duration of submergence that occur will decrease with increasing elevation on the marsh (Adam, 1990). Saltmarsh sedimentation can be linked to the magnitude, frequency, duration of tidal inundation and can keep pace with moderate rates of sea-level rise and their sediments alone have been used to reconstruct former sea-level (e.g. Shennan, 1982; Allen, 1991). However, these reconstructions were based on the assumption that accretion is in quasi-equilibrium with sea-level rise, causing the over- or under-estimation of sea-level reconstructions if accretion is higher or lower than sea-level rise (Haslett et al., 2001).

The biological indicators (pollen, foraminifera, diatoms and testate amoebae) contained within the sediments them can preserve a more reliable record of sea-level change (Haslett et al., 2001), and during the past 60 years have been investigated and used extensively to provide reconstructions of Holocene sea level. Saltmarsh biota can be used to reconstruct palaeo-sea levels due to their ecological zonations which can be linked with tidal heights (Murray, 1971). Due to competition for space, different species develop different tolerance levels to exposure and submergence, creating zones of unique species assemblages, which if they can be linked with specific elevation ranges can provide a tool for sea-level reconstructions (Gehrels, 2000). If the elevation of the biota in the modern environment is known in relation to chosen tidal level (also known as a reference water level e.g. MTL), this is known as the indicative meaning, and can be used in a sea-level reconstruction.

Vegetation zones were the first to be examined and their development was attributed to many factors, including salinity, substrate, temperature, tidal inundation and flooding

duration (Chapman, 1938; Adams, 1963). Following these, some studies examined the relationships between saltmarsh vegetation and altitude specifically (e.g. Beeftink, 1966). Using pollen assemblages as a proxy for sea level was common in early sea-level reconstructions, with Godwin (1940) producing the first sea-level curve using this method. However, using pollen to reconstruct sea level based upon vegetation zonations has several problems. Firstly, the identification key for pollen types may be too coarse and, secondly, the dispersal of pollen may give a misleading impression of the vegetation cover (Freund et al., 2004). Therefore, other techniques using micro-biota were developed and utilised, including foraminifera, diatoms and testate amoebae, which do not suffer the disadvantages of using pollen and have the advantage of having more narrowly constrained vertical zones (Gehrels, 2000). High quality sea-level records were then able to be reconstructed which could show changes of a sub-metre magnitude on shorter temporal scales (Church et al., 2001). This resulted in fewer pollen-based sea-level reconstructions being carried out. Although, more recently, in areas where foraminifera and diatom assemblages cannot be utilised due to poor preservation, pollen assemblages have utilised again for reconstructions (e.g. Engelhart et al., 2007).

The distribution and zonation of micro-biota was first described for inter tidal diatoms over 70 years ago (Carter, 1933). Since then there have been numerous studies describing their distributions relating to a number of environmental variables, e.g. substrate (Whiting and McIntire, 1985) but particularly in relation to salinity (e.g. Palmer and Abbott, 1986) resulting in a classification based upon this. More recently, studies relating microfossil distributions to tidal inundation have been investigated, and strong relationships have been found (e.g. Nelson and Kashima, 1993; Zong and Horton, 1998, 1999).

Foraminiferal studies dating back to 1950 (Phleger and Walton, 1950) have recognised altitudinal relationships to their distribution and have established distinct assemblage zones across saltmarshes. As with diatoms, however, several studies have found other variables to be important in constraining their distributions, including substrate (e.g. Matera and Lee, 1972) and salinity (e.g. de Rijk and Troelstra, 1997) as well as pH, vegetation cover etc. Since the first study by Phleger and Walton (1950), who described four ecological zones for the Great Marshes of Massachusetts, many studies have established similar ecological zones, including that of Scott and Medioli (1978, 1980b). Many studies have since concluded that elevation is the dominant factor influencing saltmarsh foraminiferal distributions (e.g. Horton et al., 1999b), therefore, many palaeo-sea level and coastal

studies that have utilised foraminifera (e.g. Edwards and Horton, 2000; Edwards, 2001, Donnelly et al., 2004; Massey et al., 2008; Gehrels et al., 2006; Kemp et al., 2009b).

The first application of intertidal foraminifera in sedimentary records for sea-level studies, was to locate the occurrence of marine influence and marine conditions within a sequence using the switch from sediments devoid of foraminifera to those containing the microfauna (Scott and Medioli, 1980b). It then followed that sea-level reconstructions were based upon the mono-specific assemblage of *Trochammina macrescens* (*T. macrescens*) found near the landward edge of the saltmarsh (Scott and Medioli, 1978). More detailed relative sea-level records were then able to be produced using the zones described, including studies in Connecticut saltmarshes (e.g. Varekamp et al., 1992) where the zonation scheme was used in a qualitative way based upon visual comparison with modern zones.

For over 20 years, a quantitative approach using sea-level index points (SLIPs) has been used and developed based upon microfossils which have precise and consistent relationship to sea level (e.g. Shennan and Woodworth, 1992). In order for a SLIP to be used to reconstruct sea level it must have information regarding its location, altitude, age and its vertical relationship to a reference water level, i.e. the indicative meaning. SLIPs are based upon the principle of switches between terrestrial and marine sedimentation which reflect changes in the balance between land and ocean levels (Horton and Edwards, 2005), i.e. transgressions and regressions.

There are many limitations to this method, for example, SLIPs can only be used at contacts between marine and terrestrial sediments and can only provide information about the tidal level at that specific point, with no information on variations between points (Edwards, 2001). Organic-minerogenic contacts are also limited spatially and temporally in late Holocene sediment sequences, therefore, sequences may only contain a few or even no SLIP data, meaning sea-level reconstructions using these sediments would be impossible (Edwards, 2001). There may also be large margins of error associated with the precise determination of SLIPs and, therefore, it is required that the former sea-level curve is plotted as a generalised band of sea-level change (Shennan, 1986). When examining changes during the late Holocene these error bands become of comparable magnitude to the sea-level variations and, therefore, are inappropriate for reconstructing high-resolution sea-level changes (Horton and Edwards, 2005).

1.4.1. Ecological-based transfer functions

The transfer function approach is an extension of the SLIP approach and it allows quantification of the indicative meaning as well as the quantification of errors associated with sea-level reconstructions (Gehrels, 2007). It offers a number of advantages including; an increased range of sedimentary environments which are able to be utilised, defined error terms as well as consistent, objective and replicable treatment of data (Edwards et al., 2004b). The approach also permits stratigraphically constrained sea-level data to be treated as sequences, rather than a collection of isolated points, and therefore improves the resolution of relative sea-level records which could not be achieved by the use of standard SLIPs (Edwards and Horton, 2006). In contrast to the traditional SLIP approach, whereby comparing reconstructed altitudes is done in isolation, transfer functions allow sequences of change to be used to match a collection of data together (Edwards and Horton, 2006). The application of a regional transfer function (see page 18) allows more replicability and therefore the direct comparison of records from different sites (Edwards and Horton, 2006).

The first application of microfossils to the reconstruction of relative sea level applied in a quantitative way was applied by Guilbault et al. (1995). Previously transfer functions had been used in many other applications for example sea-surface temperatures and lake water quality. Since then the method has been applied worldwide due to its advantages over the previous method of SLIPs, improving the precision and accuracy of the reconstructions.

The precision which can be achieved using a microfossil-based transfer function varies with the conditions of the site chosen, along with the type and number of microfossils used. Precision is not constant due to the non-linear relationship between height of the marsh surface and tidal flooding duration (Gehrels, 2000). The most accurate precision which has been achieved to date has been as high as +/- 0.05m (Gehrels et al., 2001). This level may be accomplished by using a local transfer function and a multi-proxy approach of three micro fossil indicators (foraminifera, diatoms and testate amoebae). A similar study which was carried out examining foraminifera, diatoms and macrophytes, also came to the same conclusion that a combination of proxies provides the most accurate results (Patterson et al., 2005). The most accurate results using a foraminifera-based transfer function are 0.09 m from Edwards et al. (2004a), 0.07 m from Horton et al. (2003) and 0.06 m from Gehrels et al. (2005). The SLIP method can also produce accurate results also with Scott and

Medioli (1980b) finding an error of +/-0.05 m although this was only based upon the monospecific high marsh zone of *J. macrescens.*

Foraminifera are single celled marine protozoa and are found throughout the intertidal to marine environment. As described above, foraminifera may exhibit a zonation in relation to elevation across the saltmarsh; a schematic diagram of this can be seen in figure 1.3. There are two main distinguishable species varieties, agglutinated species which form from detrital material cemented to a cell membrane, and calcareous species which form from secreted calcium carbonate. Agglutinated species are usually located higher within the tidal frame than calcareous species which are less common in intertidal marsh settings. Agglutinated species offer greater potential for sea-level reconstructions as their distributions are more constrained than calcareous species which are often subjected to inwashing and tidal mixing in the low marsh/mudflat environment (Horton and Edwards, 2003). Foraminifera may be benthic, and live in the top surface of sediment, planktonic and inhabit the water column or infaunal and live within the sediment.

This study will be primarily utilising intertidal benthic foraminifera which were chosen as the micro-fossil for this study as they are thought to be the most accurate sea-level indictors (Scott and Medioli, 1978), they are usually well preserved, easily detectable and occur in high numbers in modern environments as well as within sedimentary records (Horton et al., 1999).

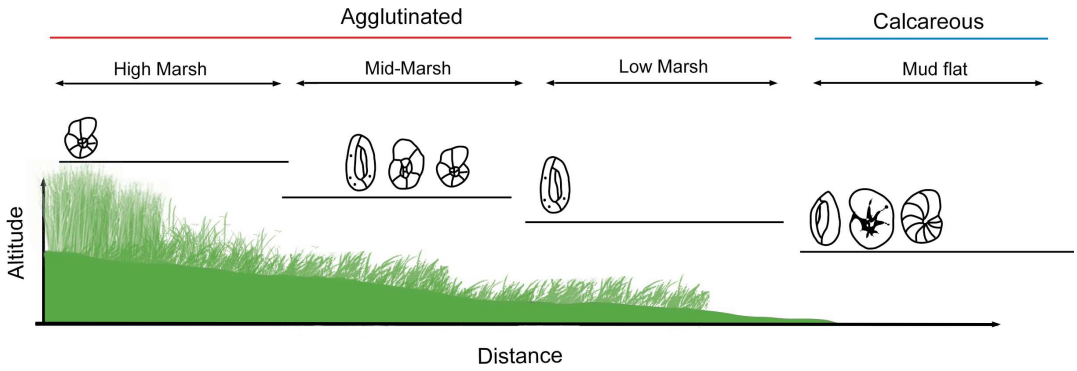

Figure 1.3 Simple illustration of the distribution of foraminifera species across a saltmarsh.

Transfer function development

Contemporary studies

The transfer function method was first developed by Imbrie and Kipp in 1971, and was used to determine ocean surface temperatures and salinity using marine foraminifera. It was the first time a procedure was used for the quantitative reconstruction of past environmental variables from fossil assemblages (Birks, 1995). The aim of a transfer function is to express the value of an environmental variable as a function of an environmental proxy. The method is based upon a uniformitarian approach. The relationship between the modern proxy (i.e. foraminifera) and the ecological parameter (i.e. height above sea level) to be reconstructed must be investigated first in a field setting which is presumed to be similar to the palaeo-environment (Gehrels, 2002).

The first step in creating and applying a transfer function, therefore, begins with an investigation of the modern relationship between the modern proxy and the tidal. There have been many studies investigating the contemporary distributions of foraminifera (e.g. Horton et al., 1999b), testate amoebae (e.g. Charman et al., 2002) and diatoms (e.g. Zong and Horton, 1998) in relation to elevation.

It is important to establish what the main controlling factor affecting the contemporary distribution of the particular microfossil is, as several environmental variables can affect the distribution of the micro-biota. Most studies measure several environmental variables along with elevation including salinity, pH, organic matter content and grain size. In the majority of studies the distribution of foraminifera across the saltmarsh surface was found to be attributed mostly to elevation (i.e. tidal inundation) therefore, allowing them to be utilised for sea-level reconstruction purposes (e.g. Gehrels et al., 2002, 2005, 2006; Edwards, 2001; Edwards and Horton, 2000, 2006; Edwards et al., 2004a ; Donnelly et al., 2004; Horton and Edwards, 2005, 2006; Horton et al., 1999b, 2005; Patterson et al., 2005). However it is not true in all cases with some studies suggesting that other factors have a greater influence. de Rijk (1995) and de Rijk and Troelstra (1997) suggested that in Massachusetts marshes, salinity was more important than elevation in controlling distributions. They found a positive correlation between the abundance of *Jadammina macrescens* (*J. macrescens*) and *T. comprimata* with mean salinity, and a negative correlation between the abundance of *Haplophragmoides manilaensis* with salinity. Murray (1973) suggested that salinity is the first ecological control for estuarine foraminifera and

Patterson (1990) also invoked a combination of both elevation and salinity to explain the patterns observed on high marshes in British Columbia.

Other factors may also complicate the foraminifera distribution, including substrate, vegetation cover and pH. Gonzalez-Regalado et al. (2001), Matera and Lee (1972) and Steineck and Bergstein (1979) found relationships between foraminifera species and grain size. Gonzalez-Regalado et al. (2001) found in Spanish estuaries that *Trochammina inflata* (*T. inflata)* and *J. macrescens* prefer organic-rich muds. In contrast, Matera and Lee (1972) in Long Island and Steineck and Bergstein (1979) in New York found there were strong correlations between coarse substrates and *T. inflata*, showing that there may be inter-site variability. Sediment particles between 2 to 20 μm are used as building material by agglutinated foraminifera, therefore, if there are few particles within this range, this may limit agglutinated foraminifera populations (Horton, 1999). Vegetation cover can have an effect on foraminifera populations as it interacts chemically and physically with environmental variables, with the composition and density of vegetation influencing foraminifera populations (Horton, 1999). Duchemin et al. (2005) found higher faunal densities in areas with a vegetation cover compared with those in areas without vegetation, confirming observations of Steineck and Bergstein (1979). Plants may also provide shelter from the negative impacts of low tide, such as desiccation or tidal currents that may transport foraminifera away to other areas (Duchemin et al., 2005). Lastly, a low or high pH may create stress and restrict growth of calcareous foraminifera and, therefore, may limit their distribution (Horton, 1999) as well as causing preservation problems.

Despite the great variability in the local environmental conditions of different saltmarshes, foraminiferal distributions are found to be similar in most temperate areas (Leorri et al., 2011). For example UK saltmarshes show similar species assemblages and zonations across the marsh surface with high and middle marsh zones being dominated by *J. macrescens, T. inflata* and *M. fusca*, and low marsh and tidal flat zones dominated by *E. williamsoni, H. germanica* and *Quinqueloculina* spp. Examples of foraminifera zonations can be seen in figure 1.4 and 1.5.

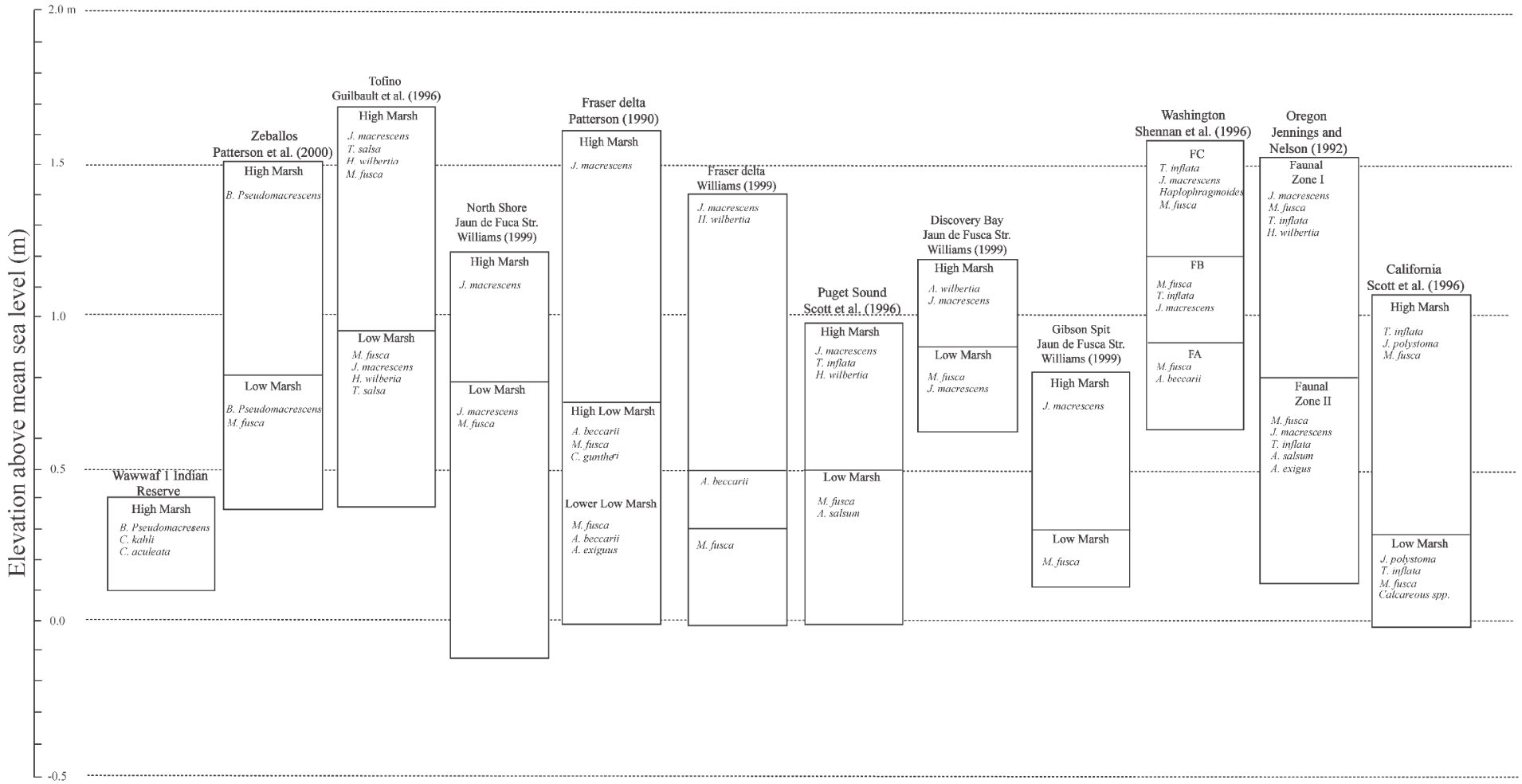

Figure 1.4 Summary of foraminifera assemblages relative to elevation of north coast America (taken from Williams, 1999).

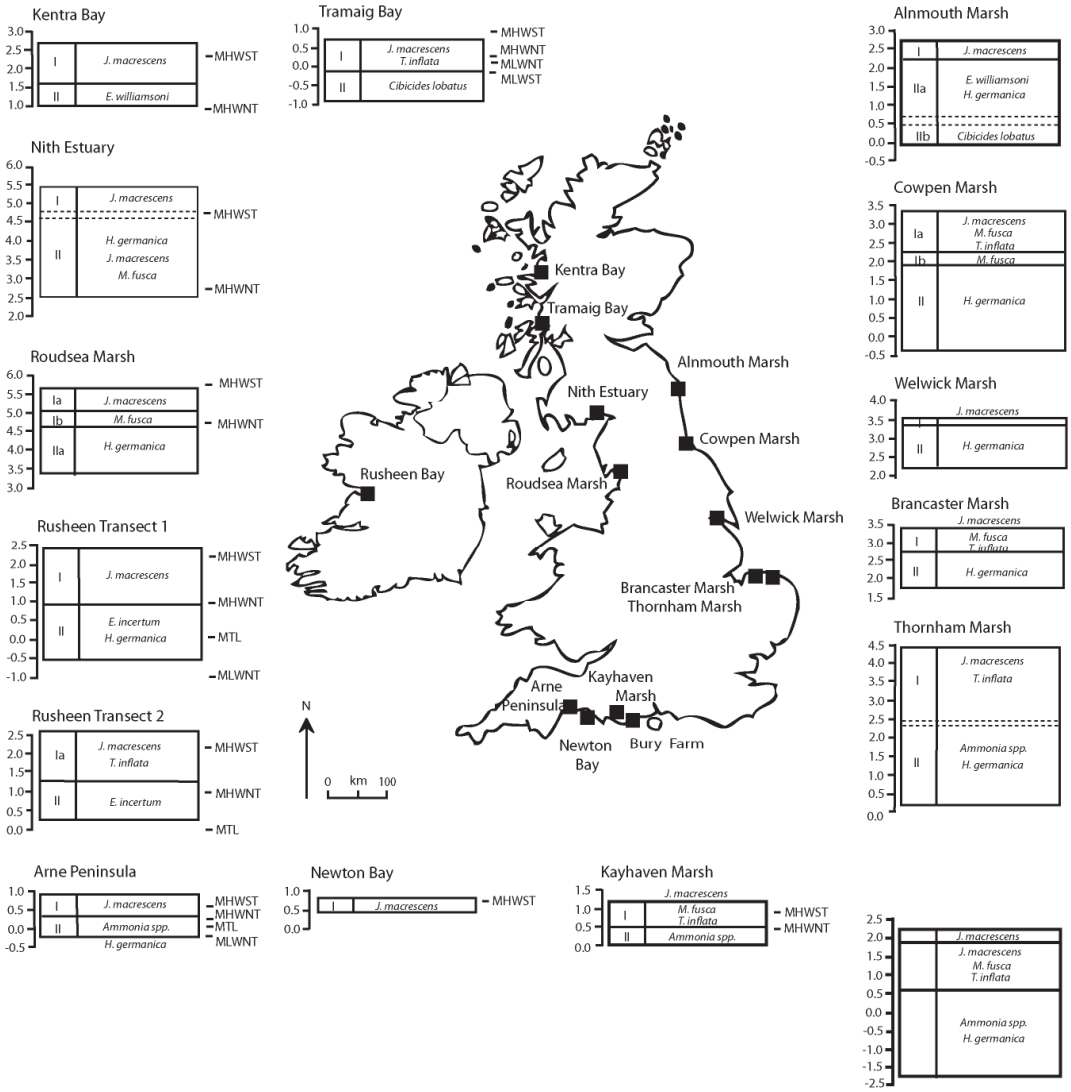

Figure 1.5 Summary of foraminifera assemblages relative to altitude of from British Isle and Ireland (taken from Horton and Edwards, 2006).

Due to the many variables which may have an effect on the distributions of the foraminifera, the salinity, grain size, pH, organic matter content and vegetation cover along with altitudinal data must be collected (e.g. Horton, 1999; Horton et al., 1999b; Edwards et al., 2004b; Gehrels and Newman, 2004). If altitude is found to be the most dominant factor affecting the distribution of foraminifera across the saltmarsh surface the data will then be used to form a training set (e.g. Horton et al., 1999b, 2007; Gehrels et al., 2002, 2005, 2006, 2008; Edwards et al., 2004a; Leorri and Cearreta, 2009; Leorri et al., 2011; Rossi et al., 2011).

Local versus regional

The reconstruction can be based upon a training set which contains data collected from an area local to that of the fossil record, producing a local transfer function, or may be compiled from a wider area containing a number of data from various differing saltmarshes, producing a regional transfer function. There has been debate as to which dataset provides the best analogue for reconstructions (Allen and Haslett, 2002; Horton and Edwards, 2005). The assumption of using a local data set is that the conditions the modern saltmarsh is experiencing will provide the most appropriate analogue to those found in the fossil record (Horton and Edwards, 2005). An advantage of using this approach is that other environmental variables which may affect and complicate the distribution, for example salinity and hydrographic regime, will be reduced (Horton and Edwards, 2005). Gehrels (1994) supports the use of a local transfer function based upon a local training set as the errors associated with inter-site and intra-site variability may be kept to a minimum. A local transfer function has also been advocated by Allen and Haslett (2002) as they recognise that there may be associated errors when incorporating data from areas which differ in their faunal characteristics, species ranges and oceanographic conditions.

In contrast, many studies (e.g. Horton and Edwards, 2005; Edwards et al., 2004a) have argued that the most appropriate approach is a regional transfer function which includes a compilation of many modern training sets from a range of sites which differ in their, physical, biological and hydrographic characteristics (Edwards et al., 2004a). This approach has been developed in order to consider the assemblages of similar areas as a whole, whilst discerning subtle variations, and quantifying the variability within them (Edwards et al., 2004a). A regional transfer function is capable of capturing the spatial variability (Edwards et al., 2004a) and allows reliable results if the past environmental conditions differ significantly from that of the present (Horton and Edwards, 2005). It has also been argued that the most appropriate analogue to use may not necessarily be located at the study site, but may be found some distance away. Zong et al. (2003) found that the best analogues for a study in Alaska were found 150 km away, rather than from a local site.

Horton and Edwards (2005) compared the results of a regional transfer function and a local transfer function. It was concluded that the transfer functions developed from regional training sets are better suited to the analysis and reconstruction of sedimentary sequences as they include a variety of modern analogues compared with those based upon local data (Horton and Edwards, 2005). Gehrels (2000) also concluded that data from a wide range of

sites varying in their environmental controls have greater predictive power compared with local. Local transfer functions, however, do have the advantage of increased precision, but reconstructions using local data only may be deemed unreliable due to the abundance of 'no analogue' situations (Horton and Edwards, 2005), which can be avoided if regional training sets are used.

The most appropriate solution which will be undertaken in this study is to carry out a local study first, as well as using data from other regions if the problem of no modern analogue arises. The modern data collected will also provide supplementary data to the regional transfer function creating a combined dataset.

Developing a transfer function

If it is determined that the modern distribution of foraminifera is primarily dependent upon elevation, foraminifera can then be used as a proxy for elevation which can then be converted into sea-level data. In order to convert the foraminifera data into the elevation data, the relationship between the two is usually quantified through the use of a transfer function (Horton and Edwards, 2006).

There are several different statistical methods which can be used for palaeoenvironmental reconstructions, each appropriate for different research problems. Most palaeosea-level reconstructions are based on methods which use response models and their inverse, the transfer function. These methods assume that each species lives in a given range of environmental conditions (Guiot and de Vernal, 2007). Distinction can be made between techniques using this approach based upon the type of response model that is used.

There are two response models, the first are linear-based methods which assume a linear response model of the environmental proxy to the environment, whereby the abundance of taxa increases or decreases with the environmental variable of interest (Birks, 1995). The second are unimodal-based methods, which assumes that individual taxa have a Gaussian distribution along the environmental gradient, and peaks in abundance at the most favourable condition (Birks, 1995). Unimodal response models are considered the most robust reconstruction method (Telford et al., 2004; Telford and Birks, 2005).

There are also two different statistical approaches which can be used, the first is the classical approach which expresses the foraminifera data as a function of elevation. ter Braak (1995) suggested that this approach may perform better at the extremes of data and

with slight extrapolation. The second is the inverse approach which expresses elevation as a function of the foraminifera data. This approach performs slightly better when the fossil samples are from the central part of the distribution of the modern training set (ter Braak, 1995). The inverse approach may also be more suitable when other environmental variables are important in influencing the proxy assemblages as it considers each environmental variable individually (ter Braak, 1995).

In a simple inverse regression, the functions are estimated from the training set by regressing the environmental variables on the environmental proxy and the unknown environmental variable is then estimated directly from the modern regression equation (Birks, 1995). The inverse approach is more widely used than the classical approach and if the environmental variable being reconstructed equals its distribution in the modern training set, inverse regression is a statistically efficient procedure (Birks, 1995). However, there are many problems inherent in using the simple inverse regression method (see Birks, 1995, p178), therefore various other techniques were developed in order to overcome these, including restricted inverse regression, principle components analysis (PCA), partial least squares regression (PLS) canonical correlation analysis (CCA), and redundancy analysis (RDA), all of which assume a linear or at least monotonic data distribution (Birks, 1995).

In palaeoclimate reconstructions the most common technique used is a restricted inverse linear regression often when using pollen data over large geographical areas to reconstruct past climatic variables (Birks, 1995). PCA is an ordination technique and was the basis of the Imbrie and Kipp (1971) study. PCA maximises the variance in the predictor variables, however, it does not take into account the predictive value for the environmental 'response' variable of interest (Birks, 1995). An alternative is PLS whereby the components are chosen to maximise the covariance with the response variable (Birks, 1995). In both of these analyses, data are discarded so these are known as biased methods (Birks, 1995).

Non-linear, unimodal response methods include maximum likelihood (ML) and weighted averaging (WA). ML regression and calibration is regarded as the most 'statistically rigorous approach to environmental reconstruction' (Birks, 1995), however ML methods are not commonly used in palaeoecological reconstructions. Weighted averaging (WA) regression and calibration has the same aims as ML but is mathematically simpler, performs as well or better than ML and has, therefore, been applied more widely (Birks, 1995). WA offers many advantages over other techniques including; ecological plausibility, simplicity, rigorous underlying theory, good predictive power, relatively insensitive to outliers, performance in

'no analogue' situations, and performs best with noisy, species-rich data (Birks, 1995). It is fairly robust when samples are not entirely evenly distributed along the environmental gradient (ter Braak and Looman, 1986). However, WA alone does have some disadvantages, including considering each environmental variable separately and disregarding the correlations which may be caused by other influential environmental variables that remain in the biological data after fitting the environmental variable (Birks, 1995).

The incorporation of PLS into WA overcomes some of the weaknesses associated with WA. The method was developed by ter Braak and Juggins (1993) and ter Braak et al. (1993) and takes into account any residual correlations which would be disregarded in WA. WAPLS improves predictions by using any structure present in the WA residuals which would otherwise been discarded. It therefore, in effect, considers the influence of additional environmental variables (ter Braak and Juggins, 1993). WAPLS shows little improvement over WA if there is a lot of unstructured noise in the data, however, it shows a large improvement if the noise is structured in the form of a secondary environmental gradient (Birks, 1995). ter Braak et al. (1993) recommended WAPLS as a simple and robust method to be used until a more sophisticated method is developed. Another modification to WA is WA with tolerance down weighting (WA-Tol). This method attempts to improve WA by giving more weight to species with narrow ranges, because these have a better indicator value (Gehrels, 2000).

Another method which may be used is correspondence analysis regression (CA), it is the unimodal-based equivalent of PCA and is therefore often more suitable with species. CA has many of the same problems associated with PCA, with WAPLS providing a technique to overcome these. Canonical correspondence analysis (CCA) is the constrained version of CA and is an intermediate between CA and WA (Birks, 1995).

An alternative to these approaches are analogue-based methods which are used in paleo-reconstructions and are not based upon response models and calibration as the above methods. Analogue-based methods are based upon the principle that a given assemblage of taxa in the fossil record is most likely to have occurred under a combination of environmental conditions characterising similar modern assemblages of taxa (Birks, 1995). This approach makes comparisons between assemblages, in contrast to the response model approach which uses the direct relationship between taxa and the environmental variable in question (Guiot and de Vernal, 2007). Examples of this method include the modern analogue technique (MAT) and the response surface method.

MAT numerically compares the biological assemblage in a fossil sample with the assemblages in modern samples that have associated environmental data. The modern sample that is most similar to the fossil sample is found, and the past environment for that sample is inferred to be the modern environmental variable for the analogous modern sample. This is repeated for all samples and a simultaneous reconstruction for several environmental variables is made for the fossil record (Birks, 1995). MAT is often the easiest way to compare the fossils to their modern counterparts, however, the accuracy and reliability of this type of reconstruction is dependent on the range of environmental conditions represented in the modern training set and, therefore, a large training set is usually needed to model the faunal assemblages found in all environmental conditions (Southall et al., 2006). MAT has also been criticised as being over-optimistic when assessing errors (Telford and Birks, 2005).

Response surface methods are another 'similarity approach' which can be used for paleo-reconstructions. They are two or three dimensional graphic representations of occurrence and/or abundance of taxa considered individually in modern environmental space (Birks, 1995). The main aim of response surfaces are to find the combination of modern environmental variables that support an assemblage of similar composition and abundance to the fossil assemblage (Birks, 1995). This method suffers from the same disadvantage as MAT with a large amount of training set data needed from a wide environmental range (Birks, 1995).

In most palaeosea-level reconstructions based upon micro-biota several statistical techniques are tested and the most appropriate of these is chosen. The performance of the transfer functions are usually tested with other statistical methods which can be applied to the data. As all quantitative palaeoenvironmental reconstruction methods will produce a result no matter what data are used, the transfer functions reliability should be tested whatever method or methods are used (Birks, 1995). Imbrie and Webb (1981) stated that there is no simple means of evaluating how reliable the result is, however, there are statistical methods available which can be used to provide some information about the performance and may be useful in making comparisons between the different methods. To test the performance of the transfer function 'apparent' measures, coefficient of determination (r^2) and root mean squared error (RMSE) are used in most studies (Edwards and Horton, 2000).

RMSEP is calculated to measure the prediction errors, and the r^2 is calculated to measure the strength of the relationship between observed *versus* predicted values. Both of these are 'apparent' measures and are useful when comparing the performance of different transfer functions (Edwards and Horton, 2000). However, Birks (1995) stated that RMSE is consistently under-estimated and r^2 over-estimated when solely based upon the training set, and for an independently calculated RMSEP, independent data must be used (Guiot and de Vernal, 2007).

Split-sampling or cross-validation is needed to derive more reliable and realistic estimates of prediction error and to evaluate the predictive abilities. Split-sampling involves randomly splitting the modern data set into a training set and a test set, and then using the training set to predict the environmental variable for all samples in the test set. This provides a realistic assessment of the RMSEP and r^2. As large test sets are not often available, the test set can be simulated by statistical cross-validation. Jack-knifing is the simplest and most common cross-validation technique (Birks, 1995). It is a leave-one–out method whereby the reconstruction procedure is applied *n* times using a training set in which one sample is left out in turn (*n*-1). The calibration function based on the *n*-1 sites in the training set is applied to the one sample in the test set which has been omitted (Birks, 1995). This produces a predicted value for the sample. By subtracting the predicted value from the observed value, this generates a prediction error for the sample ($RMSEP_{jack}$) (Birks, 1995). Its measures are reliable indicators of the true predictive ability of the transfer function as they are less biased by sample re-substitution (Dixon, 2003). There may be a disadvantage of using this technique as the test set and the training set are the same and hence will be located geographically close and therefore the full independency of the data might not be achieved due to autocorrelation (Guiot and de Vernal, 2007).

When applying the transfer function to a fossil core the $RMSEP_{jack}$ is used (Edwards and Horton, 2000). $RMSEP_{jack}$ is a measure of the overall errors of the training set. It does not provide sample-specific errors for each fossil sample as the observed value is not known for the fossil samples (Birks, 1995). r^2_{jack} can be calculated for each observed value when the sample is included in the test set but excluded from the training set. For a sample-specific RMSEP for individual fossil and modern samples, standard error (SE) of prediction (SE_{pred}) can be derived by using bootstrapping (Birks et al., 1990) as bootstrapping determines a confidence interval (Dixon, 2003).

These measures determine the predictive ability of the transfer function. However, other methods should be used to determine if the estimates which they produce are reliable. A useful evaluation procedure is to reconstruct the same environmental variable using several numerical methods to look for differences in the reconstructions and to attempt to produce a consensus reconstruction based on several methods (Birks, 1995). If possible an independent measure should be carried out by comparing the results with a transfer function based upon a different environmental proxy, therefore testing for validity. Another approach would be to compare the estimates to known historical records if they are available. For example, if a reconstructed sea-level record has good chronological control then the record can be compared with observational tide gauge data for the area (Gehrels, 2000).

However, in many cases another environmental proxy may not be available to use or may be too costly and time-consuming. Observed historical records may not be available for the area, therefore, there are assessments of 'reliability' which are often used. MAT is considered a standard method which is used to assess the reliability of reconstructions based on other methods (Guiot and de Vernal, 2007). As stated earlier MAT can be used to predict values of elevation, however in this case it is used to identify fossil assemblages without modern equivalents to provide an independent assessment of the reliability of WA predictions (Edwards and Horton, 2000).

Another test of reliability would be to use another transfer function approach. The similarity of the results of each transfer function tests whether or not the statistical technique used is significantly determining the outcome (Edwards and Horton, 2000). The most common transfer function used is ML when using WAPLS as the principal transfer function method, since ML is a classic approach which compliments WAPLS which is an inverse approach (Edwards and Horton, 2000).

More recently, Telford and Birks (2011) developed a statistical technique to test the significance of the transfer functions and reconstructions. Statistically significant transfer functions can be determined by comparing the results of the transfer function created from real modern data with a transfer function created from random data. This is determined by comparing the amount of variance the transfer functions explains in the fossil data. A transfer function based upon real modern data which explain less variance in the fossil record than a transfer function based upon random data then the transfer function is

deemed to be insignificant, therefore caution should taken when interpreting the results (Telford and Birks, 2011).

Different studies use different statistical methods to develop and assess which transfer function is the most suitable to achieve the aims of that study. For palaeosea-level reconstructions carried out in US saltmarshes, foraminifera distributions often display linear variation with elevation and therefore, methods reflecting this provide better results. For example, Gehrels (1999) tested several models and found PLS produced the highest statistical predictive power (r^2) and RMSEP. Gehrels (2000) tested four different methods, WA, WA-Tol, PLS and WAPLS and also found the method PLS to be the better method. In contrast to US saltmarshes, the UK-wide training set was found to have a unimodal distribution with respect to a standard water level index (SWLI) (Horton, 1999). This form of response is therefore, effectively modelled by unimodal techniques. WA regression and calibration has been the most commonly used technique (e.g. Edwards and Horton, 2000; Horton et al., 2000; Edwards, 2001). More recently WAPLS has been chosen as the most favourable method (e.g. Edwards et al., 2004a; Horton and Edwards, 2005; Massey et al., 2006a, 2008). MAT was also applied in most of these studies in order to test the reliability of the estimates.

The accuracy of the reconstructed values depends on the selection of regression model and the composition of the training set (Gehrels, 2000). The reliability of the values depends upon how well the data fits the assumptions which are made in the calibration process. There are many assumptions in quantitative palaeoenvironmental reconstructions. The five main assumptions taken from Birks (1995) are as follows:

1. Taxa in the training set are related to the environment in which they live;

2. The environmental variable to be reconstructed is related to an ecologically important determinant in the ecological system of interest;

3. Taxa in the training set are the same as in the fossil record and their ecological responses to the environmental variable of interest has not changed over the time of the record;

4. Mathematical methods adequately model the biological responses to the environmental variable and yield calibration functions with sufficient predictive powers to allow useful, accurate and unbiased reconstructions;

5. Other environmental variables have negligible effect on the taxa or if not are the same in the training set as they are in the fossil record.

The foremost assumption for sea-level reconstructions is (5), which is to say that elevation is the dominant environmental variable which affects the distribution of the proxy, and other environmental variables do not exert a strong or changeable influence on the distribution through time (Horton and Edwards, 2006). It is however, more realistic to expect other environmental variables to influence the foraminifera distribution to some degree and introduce scatter to the data. This reduces the precision of the reconstruction which can be made. Therefore, it must also be assumed that the joint distribution of these variables with elevation is the same in the training set data and the fossil data (Birks, 1995). Le and Shackleton (1994) assessed this assumption and showed that transfer functions do have potential pitfalls regarding their sensitivity to joint distribution, however they are a reliable method when applied within the calibration range and used with caution (Horton and Edwards, 2006). Methods like WAPLS as described above, use the structure present in the WA residuals and therefore consider the influence of additional environmental variables (ter Braak and Juggins, 1993).

Another assumption which is important to recognise in saltmarsh foraminifera studies in particular, is that the composition of modern foraminifera assemblages are representative of those in the fossil record. In reality many process may introduce error, including post-depositional destruction, transport or reworking, as well as infaunal foraminifera activity. By comparing the assemblage composition of fossil data with the training set data this may reveal whether the fossil record has experienced post-depositional change. An assessment of modern analogues may also be used using MAT (Juggins, 1992).

A further important assumption made by transfer functions, in addition to those discussed above which is not often considered, is that the test sites are independent of the modelling sites. However, in ecological data there is often strong spatial autocorrelation between samples (Belyea, 2007). Positive spatial autocorrelation is the tendency of sites close to each other to resemble one another more than randomly selected sites (Belyea, 2007). The value of an autocorrelated variable at one site can be partially predicted from its value at neighbouring sites, with the strength of correlation decreasing with increasing distances (Telford and Birks, 2005). Species-environment relationships derived from training sets that do not account for spatial autocorrelation have misleadingly inflated explanatory powers and will be biased in their ranking of environmental variables (Belyea, 2007). Statistical

analysis may place emphasis on environmental factors that have no bearing on species' distribution and abundance, and may fail to place sufficient emphasis on true abundance-environment relationships leading to omission of important variables (Keitt et al., 2002).

As transfer functions assume the test sites are independent, autocorrelation may also cause unrealistic estimates of the reconstructions errors and an inappropriate model choice (Telford and Birks, 2005). This is because for most standard statistical procedures used for performance testing independence is assumed and autocorrelated data violate that assumption (Legendre, 1993). Different statistical methods used to develop a transfer function will be affected by spatial autocorrelation to a different extent (Belyea, 2007). Telford and Birks (2005), using planktonic foraminifera data, examined the consequence of spatial autocorrelation on the performance evaluation of WA, WAPLS, and MAT. They showed that r^2 between observed and estimated values from a transfer function model based on an autocorrelated environment can be high even in the absence of relationships between the species and the environmental parameter reconstructed. They concluded that MAT and ANN could be misleading because of their incapacity to maintain a spatial autocorrelation structure. Guiot and de Vernal (2007) used independent data sets to take into account potential effects of spatial autocorrelation problems. They found that the estimates based on the independent data sets were not fundamentally different from the conclusions based on the validation data set obtained from random selection and concluded that the results found by Telford and Birks (2005) were not definite. Segurado et al. (2006) suggested that semi- or non-parametric models, e.g. general additive models and classification trees are more robust to spatial autocorrelation than parametric models (e.g. general linear models). Telford and Birks (2005) argued global response models (e.g. likelihood logit regression and WA) are more favourable over those which find local structure in assemblage data (e.g. MAT and artificial neural networks).

Recently, the 'neutral theory' (Bell, 2000; Hubbell, 2001; Chave et al., 2002) has also questioned the reliability of the use of transfer functions. The theory is based upon the view that community dynamics are driven entirely by chance, ecological drift and dispersal rather than relating to functional differences among species and responding to the environment which is the niche theory (Belyea, 2007). As it is accepted that some cosmopolitan species may have different optima in different regions it is likely that this is due to neutrality and if so it may be unreliable to assume that it will be transferable into the past as the optima may also have changed since then (Belyea, 2007).

The validation of transfer functions using jack-knifing or bootstrapping methods may also result in problems if neutrality exists as they will not detect the context-sensitive nature of the relationships and may overestimate the explanatory power of niche-based models (Belyea, 2007). Therefore, as with overcoming autocorrelation, independent validation methods should be used if possible. One method to assess whether the species-environment relationship could be explained by neutral processes is using a null model approach which will detect whether the relationship is valid or not (Belyea, 2007).

The final assumption that is made by transfer functions is that the spatial patterns of distribution are accurate analogues for temporal changes, and that local dynamics are easily translated to regional dynamics (Belyea, 2007). However, Peters et al. (2006) stated that local spatial structures of communities interact with regional dynamics in hierarchical and non-linear ways, and that community dynamics at a local point are dependent on historical effects and ecological context. Therefore, the transfer function may reconstruct the effects of local processes rather than regional ones (Camill and Clark, 2000).

2. Study site

The Mersey Estuary has been chosen for the present study for several reasons, firstly Liverpool has a one of the longest instrumental records of sea-level change in the World, extending back to 1768 (Woodworth, 1999), which makes it particularly valuable in verifying and assessing the accuracy of a sea-level reconstruction over a longer timescale. Secondly, it has the potential to produce a good chronology for the industrial period utilising pollution indicators, due to its well documented industrial history. Thirdly, it will be less affected by isostatic adjustment than other parts of the UK. Lastly, the estuary is strongly macrotidal and offers the opportunity to assess the applicability of the foraminifera-based transfer function within this environment.

The Mersey Estuary is situated in North West England and is one of the largest estuaries in Britain. It is divided into four separate regions; Upper Estuary, Inner Estuary, the Narrows and Outer Estuary (figure 2.1). The Upper Estuary is a narrow meandering channel, 17 km in length, which widens into the Inner Estuary which is a large and shallow basin 20 km in length and up to 5 km wide. The estuary constricts into the Narrows which is up to 30 m deep and experiences strong tides. The channel then widens into the Outer Estuary which is the convergence of Liverpool Bay and the Irish Sea (NRA, 1995). The estuary is made up of many different environments including coastal dunes, intertidal sands and muds, rocky shores and saltmarsh (Blott et al., 2006). Saltmarshes and mudflats border the Inner Estuary including at Ince Banks, Oglet Bay, and Frodsham marsh (figure 2.1).

The estuary experiences a macrotidal regime with a spring tidal range of 8.4 m and a mean tidal range of 4.5 m at Liverpool. The tidal range decreases further upstream in the Inner Estuary due to effects of the estuary's topographic features upon the propagation of the tidal curve upstream (Admiralty, 2010) (figure 2.2). Mean high water spring tides at Hale Head are 4.9 m and mean high water neap tides are 2.9 m. Due to the constriction of the Narrows there is very limited penetration of waves from the Irish Sea and wave energy is also relatively low in the Inner Estuary (Blott et al., 2006).

The River Mersey has one of the largest catchments in Britain (5000 km^2) containing the conurbations of Liverpool and Manchester and many industrial areas including Birkenhead, Ellesmere Port, Runcorn, Widnes, Warrington, and St. Helens, all contributing to the pollution of the estuary, resulting in it being identified as one of the most polluted in Europe (NRA,1995).

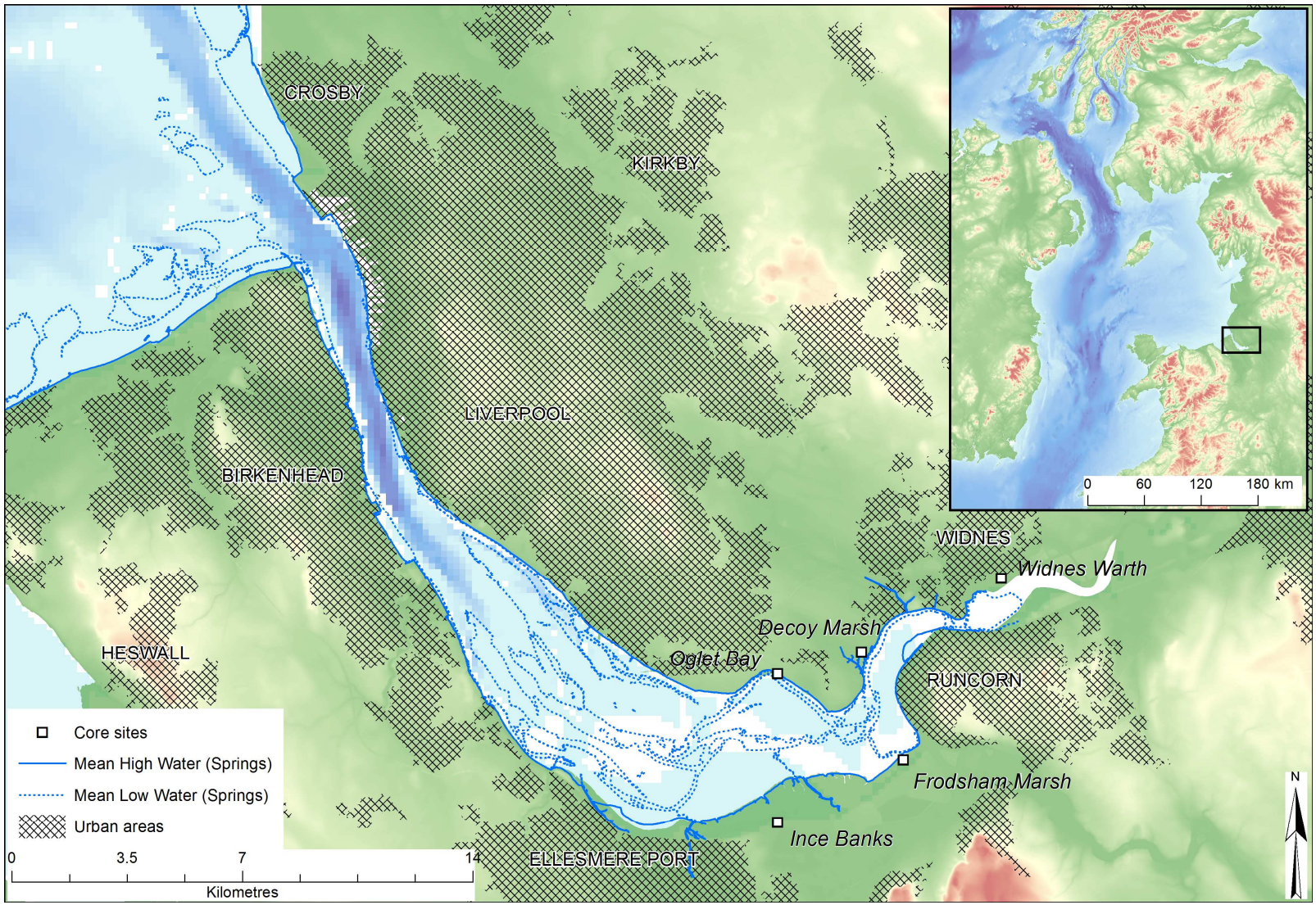

Figure 2.1 Location of the Mersey Estuary, NW England.

2.1. Sea level in the Mersey Estuary

There have been no previous investigations reconstructing former sea-levels in the Merseyside region using a quantitative microfossil-based approach. Previous studies include Tooley (1974) who produced a sea-level curve for the north west of England which was based upon a sequence of stratigraphic intercalations in the Lancashire mosslands and dated back to approximately 9000 BP. The curve was drawn through the use of SLIPs from tidal flat and lagoonal zones of the Mersey and Ribble estuaries and shows several transgressions and regressions. The amplitude and period of each oscillation is considered to have resulted from increased ocean volume from de-glaciation as well as glacio-isostatic rebound which was occurring. The oscillating curve shows periods of very rapid rise followed by apparent standstill and falls. There was a rapid increase from about 9000 to 7000 years BP followed by a more gradual trend of increasing sea level.

More recently, sea-level curves for the area have been established from GIA models reconstructing glacial rebound and sea-level changes for the whole of the British Isles. In Lambeck (1993), three sea-level curves were produced for the region from Morecambe, the Ribble Estuary, and Formby, establishing sea-level changes dating back to approximately 9000 years. There are, however, many limitations in the curve including height errors which range from 1 to 2 m (Lambeck, 1993). In general, the North West area also suffers from insufficient knowledge relating to the Irish Sea, including the thickness of the ice, the limits of the ice and the rates of ice retreat (Lambeck, 1996), and have led to discrepancies between model output and observations around Liverpool Bay (Shennan and Horton, 2002). Further information is required relating to the pre-Holocene relative sea level and the response of the coast during the mid-to-late Holocene when local factors will be more important in determining change (Plater, 2004).

Other studies carried out within the estuary include those by Wilson et al. (2005a, b) where δ^{13} C and C/N were assessed as an alternative to microfossils in sea-level reconstructions. It was concluded that δ^{13}C and C/N are good indicators of palaeoenvironmental change and the relationship between δ^{13}C and C/N and elevation is preserved in the sediment. The sea level was not reconstructed but the studies showed the potential of using δ^{13}C and C/N for reconstructions in the Mersey Estuary.

Present sea-level data from the area can be gathered from the tide gauge record which is available. Liverpool has one of the longest tide gauge records in the UK dating back to 1858 (Woodworth et al., 1999). Datasets of high water, however, date back to as early as 1768

and have been used as a proxy for mean sea level (Woodworth, 1999b). Together with the Georges Pier, Princes Pier, and Gladstone Dock gauges, the information is the second longest near-continuous record in the world, after Amsterdam (1682) (Woodworth, 1999b). The MSL record indicates that the average rate of rise from 1768 to the present was 0.83 +/- 0.06mm per year with an acceleration of 0.33 +/- 0.10 mm per year per century and shows comparable results with other records from Europe (Woodworth, 1999b).

2.2. Tidal propagation

The Mersey Estuary is affected by a semidiurnal tide with a progressive flow. It is generally flood dominant with the ebb having a slightly longer phase compared to the flood. At Liverpool (Gladstone) the ebb is 6.75 hours, whilst the flood is 5.5 hours (Thomas, 2000). As with other estuaries, the tide undergoes distortion on entering the estuary due to changes in the depth and width compared to the open ocean.

Analysis of 7 tide gauges in the Mersey Estuary by Gifford and Partners (2004) illustrated that from the Narrows to Eastham in the Inner Estuary, there is a tidal amplification effect, which increases the tidal range. The mean spring tidal range for Gladstone dock is 8.4 m which increases to 9 m at Eastham (Rossiter et al., 1956). Further upstream from the mouth the tidal range decreases and the distortion increases. Rossiter et al. (1956) carried out simultaneous tidal height observations at several points within the Mersey Estuary for 6 months starting in 1954 and showed the dramatic change in the tidal cycle along the estuary. By the time the tide reaches Widnes, the spring tidal range has decreased to 4.5 m and has a more prolonged ebb. Further upstream again at Fiddlers Ferry in the Upper Estuary (approximately 36 km upstream from the mouth) the mean spring tidal range decreases to 3 m and it has a very distorted tidal curve, with a flood of about 1 hour and an ebb of 11 hours (figure 2.2). The maximum tidal amplification is somewhere between Eastham and Hale Head further upstream from this the tidal range begins to decrease. It is not possible to locate the exact location of the maximum as the Inner Estuary dries out at low water (Gifford and Partners, 2004).

Due to the large tidal range in the Mersey Estuary a tidal bore occurs, were the onset of the flood can be seen as a wave travelling upstream. Gifford and Partners (2004) found that the tidal bore is most prominent when there are very high tides (>10 m) at Liverpool which occurs a few days a year or when other favourable conditions occur for example a period of dry weather reducing the fresh water in the rivers (Gifford and Partners, 2004). Davies (1988) studied the tidal bore between 1985 and 1988, and made over 50 observations of

the bore. It was found that the average speed of the bore was 10 km hour^{-1} and it increases in speed as it travels upstream. When the high tide was predicted to be lower (<9.9 m) the bore's speed is reduced and it arrives at Warrington later (35.5 km upstream of Liverpool) (Davies, 1988).

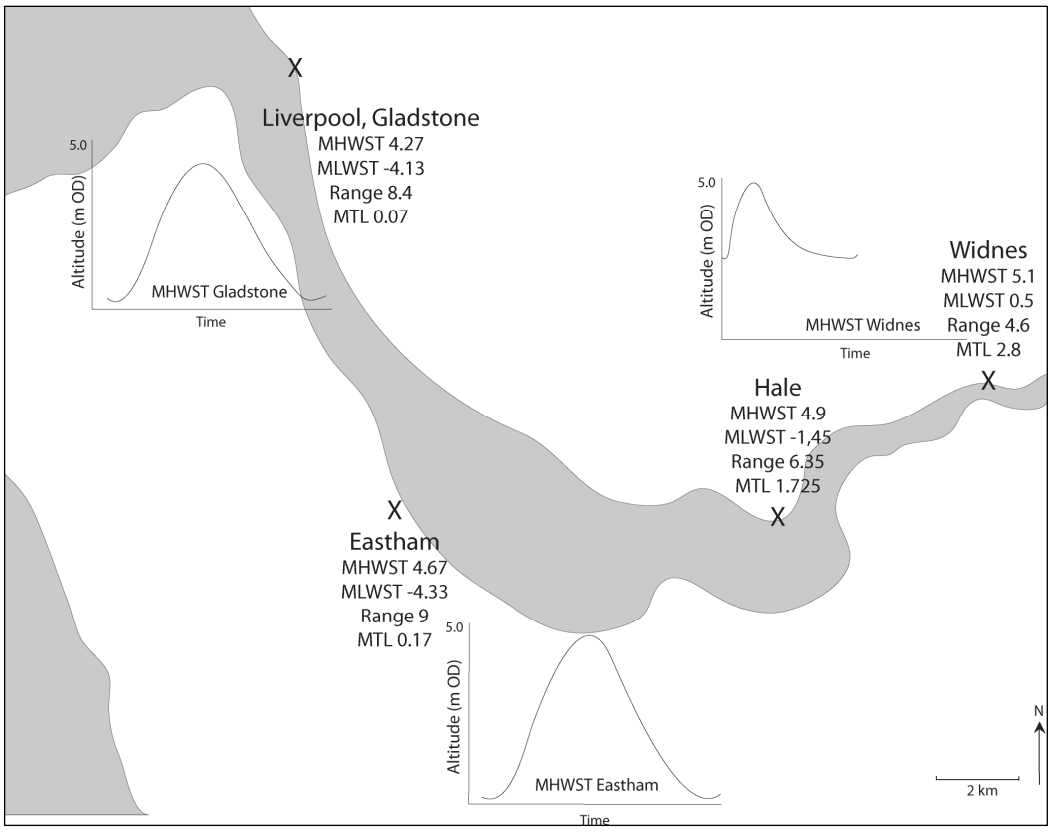

Figure 2.2 Tidal propagation in the Mersey Estuary (tidal values taken from Rossiter et al., 1956).

2.3. History of the Mersey Estuary

2.3.1. Capacity changes of the Mersey Estuary

The Mersey Estuary has undergone major changes in morphology and sediment volume over the last 150 years. The Outer Estuary has experienced most of the change as the area is largely unconfined and is more sensitive (Blott et al., 2006). Most of the change which has taken place in the Inner Estuary has been through re-distribution of sediments between and within the intertidal and subtidal zones as the area is largely confined by cliffs and embankments (Blott et al., 2006).

Due to the importance of the River Mersey for navigation more data are available than for other estuaries. The Mersey Docks and Harbour Company, for example, produced a succession of bathymetric charts, with surveys being carried out in the years 1906, 1936, 1956, 1977 and 1997. These data have been used in several studies investigating the estuary's changes over this time period including O'connor (1987), Thomas et al. (2002), Lane (2004) and Blott et al. (2006).

Many studies have established that from 1906 to 1977 the estuary was slowly infilling, with the largest rate of accretion occurring between 1936 and 1956. O'Connor (1987) estimated, using the bathymetric charts along with capacity figures produced by the Water Pollution Research Laboratory in 1938, that 80 Mm^3 of estuary volume was lost. Thomas et al. (2002) and Lane (2004) both made similar estimates of the loss in volume. Lane (2004) found there was a decrease by 60 Mm^3 or 8% in overall estuary volume. Thomas et al. (2002) estimated a 10% in volume over 70 years. Lane (2004) also found that the largest changes in volume occurred in the Inner Estuary with some exceeding 10% between years, compared with in the Narrows were the volume only changed a few percent between years. Gifford and Partners (2004) made similar estimates for the estuary capacity.

Lane (2004), Gifford and Partners (2004) and Blott et al. (2006) also calculated the sedimentation over this time period. At the beginning of the 20^{th} century (1906-1936) accretion rates were modest (Blott et al., 2006) estimated at 5 mm $year^{-1}$ (Gifford and Partners, 2004). Between 1936 and 1956 there was a significant increase in accretion, estimated as 26 mm $year^{-1}$ by Blott et al. (2003) and similarly 24 mm $year^{-1}$ by Gifford and Partners (2004), which coincided with a reduction in dredging of the channels during World War II (Blott et al., 2006). In the second half of the century (1956-1977) the rate of infilling was found to slow down, reducing to 3 mm $year^{-1}$ (Gifford and Partners, 2004). After 1977

erosion began to take place, increasing the estuary volume by 10 Mm^3 between the years 1977 and 1997 (Lane, 2004). Gifford and Partners (2004) estimated that after 1977 the Inner Estuary began to erode at a rate of 19 mm $year^{-1}$. Blott et al. (2006) also made an estimate of the erosion of the intertidal zone in the Inner Estuary to be 3.7 mm $year^{-1}$.

Several factors could have contributed to the observed morphological and sediment volume changes. An estuary's capacity is controlled by a number of inter-related factors, some of which encourage accretion, reducing the capacity (negative factors) while other factors can increase the capacity (positive factors) (O'Connor, 1987). The negative factors taken from O'Connor (1987) include: sediment dynamics, plant and animal life, wave/current interactions and surges, tidal curve distortion, gravitational circulations (density currents), flood and ebb channels, and engineering works. Positive factors include; construction of tidal docks and marinas, large river discharges, meandering of low water channels, introduction of pollutants lethal to plants/animal life, and capital/maintenance dredging (O'Connor, 1987).

Blott et al. (2006) discussed some of the important factors which may have contributed to the observed changes in the estuary, these include the geomorphology, sediment availability, freshwater discharge, relative sea level, tidal regime, wind climate, land reclamation and dredging and building. Blott et al. (2006) concluded that the main factors contributing to the changes which have taken place over this time period were dredging and training wall construction. Gifford and Partners (2004) related the decrease in estuary volume in the Inner Estuary between 1906-1977 to increased supply of sediment to the estuary due to training wall construction in the Outer Estuary and changes in the mobility of the low water channels. Thomas et al. (2002) attributed the reduction in sediment volumes in the Inner Estuary since 1977 and increase in water volumes to dredging, a reduced rate of sediment supply from the Outer Estuary and rising sea level.

2.3.2. Tidal constituents in the Mersey Estuary

Lane (2004) investigated the hydrodynamic and sediment transport using a 3D fine-resolution model utilising the bathymetry, tide gauge and acoustic doppler current profiler data. Lane (2004) modelled tidal constituents for the period 1906 to 1997. It was found that most change in the tidal characteristics occurred in the Inner Estuary due to the decrease in volume. Figure 2.3 shows the modelled results of the tidal amplitude for the time period taken from Lane (2004). The results show a decrease in M_2 amplitude at Widnes between 1906 and 1956 from 2.2 m to 1.5 m, the tidal constituents in the lower estuary were not affected by the changing bathymetries and at Stanlow on the southern banks on the Inner Estuary show only small changes. In contrast, at Hale, the results show an increase of 1 m in the M_2 amplitude and 1 m decrease in Z_0 in 1977 due partly to the migrating low water channels, (Lane, 2004). The migrating low water channels were mapped for the areas of Oglet Bay and Decoy Marsh from aerial photographs between 1971 and 2000 (figure 2.5 and 2.7). Figure 2.4 and 2.6 also show the extent of the saltmarshes for the same time period.

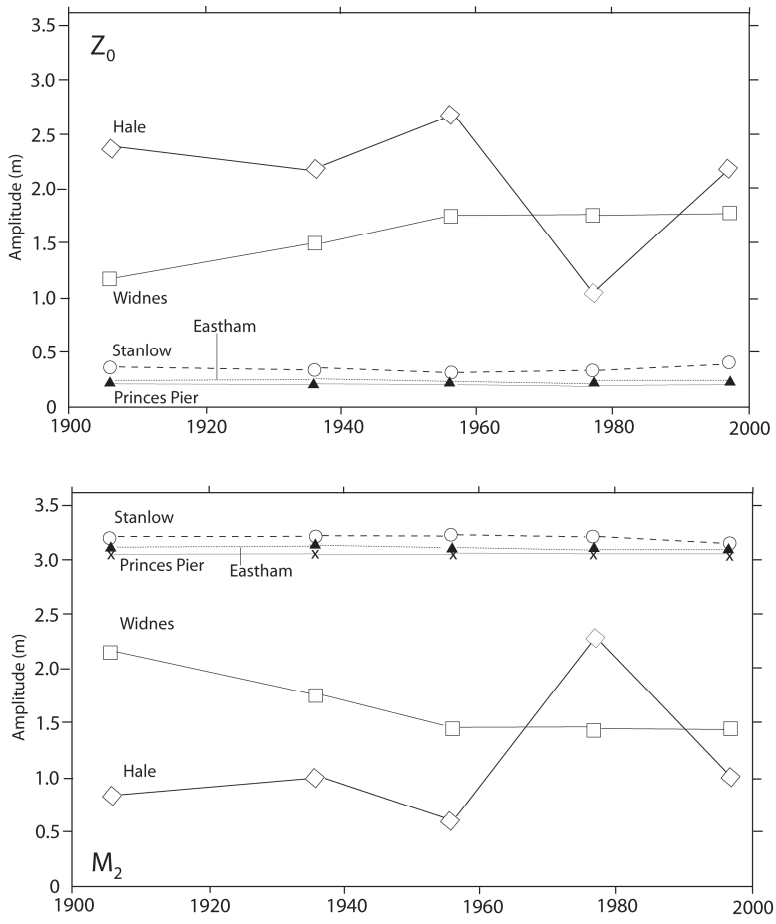

Figure 2.3 Tidal elevation amplitudes from the Mersey Estuary for M_2 and Z_0 constituent and different bathymetries (1906-1997) (Lane, 2004).

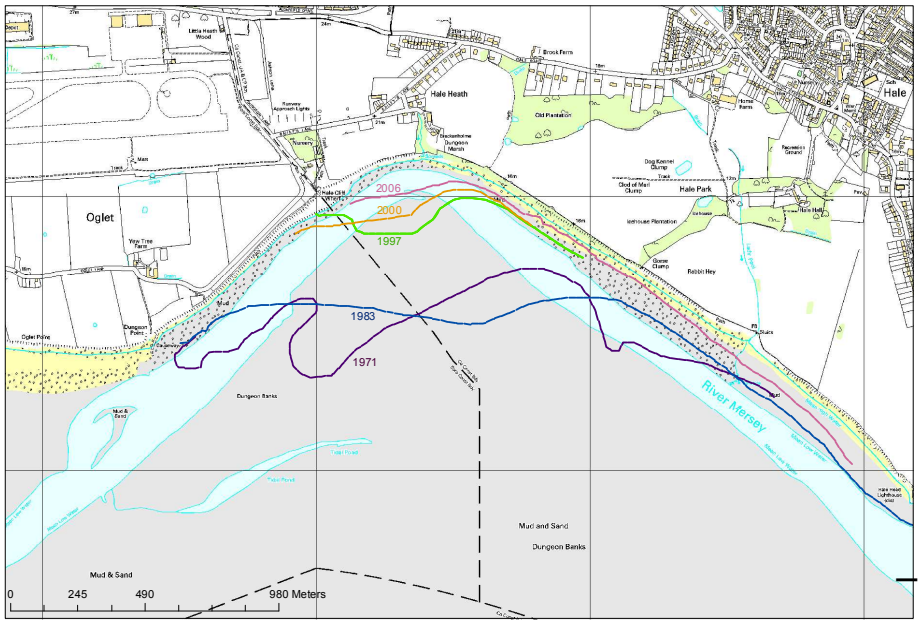

Figure 2.4 Oglet Bay saltmarsh extent from 1971 from aerial photographs over the 2008 OS map.

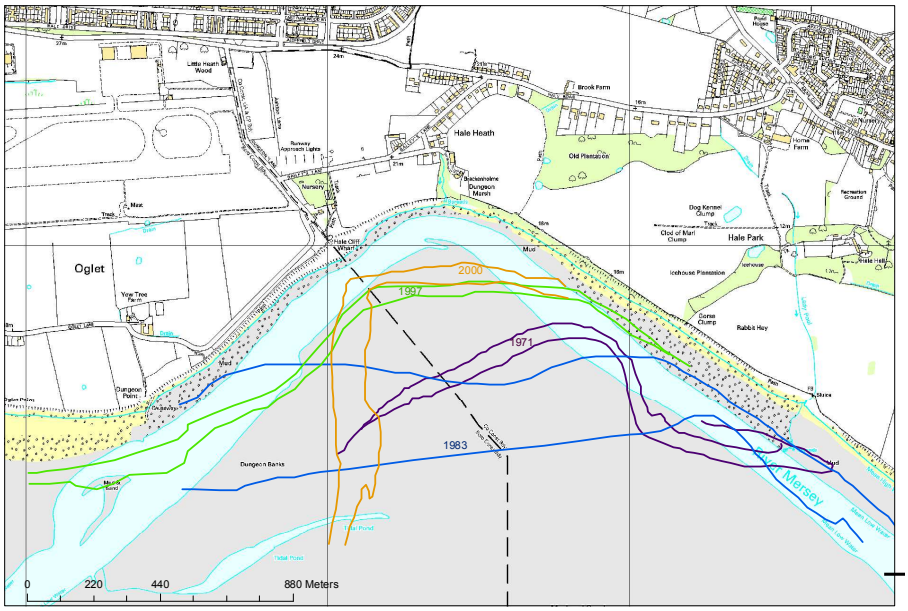

Figure 2.5 Location of low water channels from aerial photographs over the 2008 OS map.

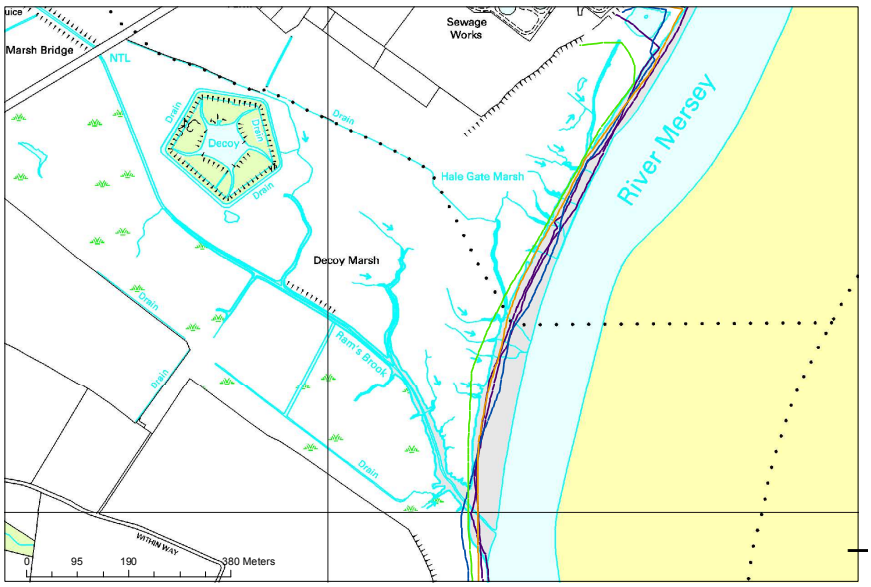

Figure 2.6 Decoy saltmarsh extent from 1971 from aerial photographs over the newest OS map.

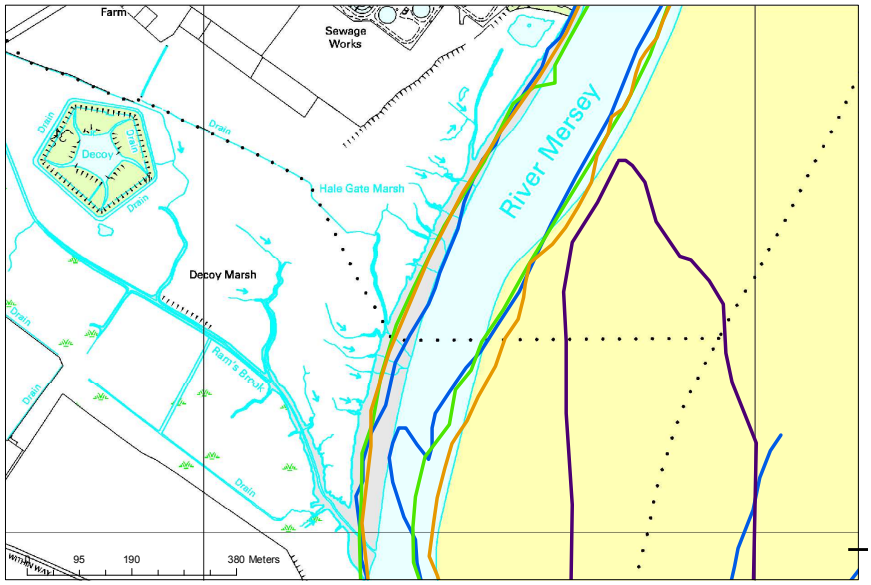

Figure 2.7 Location of low water channels from aerial photographs over the newest OS map.

2.3.3. Anthropogenic Activity within the Mersey Estuary

Anthropogenic activities have directly affected the estuary and may have had an influence on some of the changes which have occurred in the estuary. These are summarised in table 2.1.

Table 2.1 Anthropogenic activity within the Mersey Estuary (from Thomas et al., 2002 and Gifford and Partners, 2004).

	Activity	**Year completed**
	Transporter Bridge demolished	1961
	Runcorn Bridge construction	1954-1961
WWII	Crosby Training walls extended	1945-1957
	Training walls at Queens North and South Training Bank extended	1946-1957
	South Training Bank construction	1935-1938
Recession WWI	Queens North Training Bank construction	1933-1938
	Askew Spit Training Bank construction	1933-1935
	Crosby bend training walls constructed	1914 -1935
	Taylor's bank revetment constructed	1909-1910
	Sea approach channels dredged	1908
	Transporter Bridge construction	1901-1905
	River Weaver diverted Slag tipping to form embankment between Hale head and Runcorn	1896
	Manchester ship canal construction	1894
	Queens channel Liverpool Bay dredged Eastham channel dredged	1890 1890-1950
	Runcorn Railway Bridge construction	1868
Start of Industrial Revolution	Piers for Runcorn Railway Bridge construction	1865

2.4. Industrial history of Merseyside

The industrial history of Merseyside will be discussed in the following section in order to provide some background information of possible pollution inputs to the sediments which may be used to provide a chronology.

The Mersey Estuary has been identified as one of the most polluted in Europe (NRA, 1995). The area on and surrounding its banks have been heavily industrialised since the 18th century (Fox et al., 1999) and have been dominated by numerous industries including chemical, manufacturing, mining, quarrying, ship building, and smelting. Table 2.2 provides a summary of the main industrial activities which have taken place within Merseyside from 1600s to 1975.

Due to the former perspective that estuaries had the capability to 'dilute' and 'disperse' pollutants, industries became concentrated around these, resulting in industrial and domestic waste being discharged into the water as well as pollution being released into the atmosphere (Williams et al., 1994). The city of Liverpool was no exception, with a large port and trade with America enhancing the rapid development of industry within the region, leading the rest of the world in the industrial revolution (Handley and Wood, 1999).

The first significant pollution input in the area was between 1840 and 1980 (Fox et al., 1999), with crude sewage being first discharged into the estuary in 1848 (NRA, 1995). During the beginning of the Industrial Revolution (1850), coal combustion and smelting developed in the area as well as the chemical industry which grew rapidly between 1850 and 1900 (Fox et al., 1999). The chemical industry was predominantly located on the northern shore, then later on the south bank near Ellesmere Port. Chemical industry processes included copper smelting and the production of ammonia, chlorine, sodium carbonate and caustic soda (Hardie, 1950).

Copper works were first established in St. Helens in the 1850s (Rees, 1991) and the first copper smelting industries using arsenopyrite as part of the processing was established from 1885 (Fox et al., 1999). The copper industry then declined around 1925, with some increases later, at the time of World War II (WWII) (1939-1945) and in the late 1950s (Harland et al., 2000). The copper industry was then significantly reduced between 1959 and 1961.

The chlorine production industry developed in Runcorn from 1897 using Hg in the production process (Fox et al., 1999). There was increased demand during WWI, increasing

Hg pollution as a result. This was followed by a recession in the industry during the 1920s and 1930s (Fox et al., 1999), which was followed by further expansion of the chlor-alkali industry during WWII (Fox et al., 1999).

Mining and quarrying was also carried out during the Industrial Revolution. Since the 17th century, coal mining took place in Knowsely (Rees, 1991). However, the majority of mining took place in St. Helens between 1866 and 1988. Pb sulphide, Zn sulphide and coal were mined, with most of the mining occurring between 1870s and 1960s (Rees, 1991).

Manufacturing industries were also present in the area including the manufacture of Pb components, and petrochemicals. Many manufacturing industries established in St. Helens including glass works which operated between 1773 and 1903 (Rees, 1991). The 'le blank' process used in the glass production produced residue waste products of calcium sulphide and As and was established in 1822 in St. Helens. Other industries included locomotive and ship building industries which were established around the 1850s in St. Helens and the Wirral (Rees, 1991), as well as iron foundries which began in the early 19th century in the Wirral and began in St. Helens in 1896 (Rees, 1991). More recently, major oil refining, car assembly and support industries have operated within the Mersey catchment (Hardie, 1950).

The first increase in Pb pollution occurred during the Industrial Revolution between 1850 and 1890, followed by a further increase with the introduction of tetraethyl Pb petrol around 1945 (Valette-Silver et al., 1993). The introduction of unleaded petrol has reduced this potentially toxic hazard in developed industrialised countries (De Vos et al., 2006).

More recently the development and expansion of industries on Merseyside has declined due to the changing patterns of consumer demand, international competition, and political climate (NRA, 1995). The Mersey Estuary has undergone schemes to reduce the levels of pollution (NRA, 1995) and introduced new technologies developed to clean-up contaminants such as Hg which led to a decline in Hg pollution in the estuary since the end of the 1970s (Fox et al., 1999). Several acts and regulations were also introduced including the 1974 Control of Pollution Act, as well as the formation of organisations such as the Mersey Basin Campaign which was established in 1981 (NRA, 1995). All of which have contributed to the decline in pollution in the region.

Table 2.2 Summary timeline of industries and pollutants in Merseyside.

Event	Pollutant	Year
	Mercury effluent clean up	1975
	End of mining and quarrying	1988
	Reduction in lead- introduction of unleaded petrol.	1986
	Decline of lead industry	1960s
	Decline of copper industry	1959-1961
	Increase in copper industry	1957
	Increase in lead- introduction of lead petrol.	1945
WWII	Increase in copper industry. Increase in chlorine production industry. Increase in lead Increase in zinc	1939-1945
Recession	Decline in copper industry	1925
	Decline in chlorine production industry	1920-1930
WWI	Increase of chlorine and mercury	1914-1918
	Metal production using zinc	1910-1950
	Increase in lead industry	1905
	Chlorine production industry using mercury	1897
	Iron foundries	1896
	Increase in arsenic-copper smelting using arsenopyrite	1885
	Copper smelting Mercury production	1870
	Mining and quarrying	1866
Start of Industrial Revolution	Lead industry – lead smelting	1858-1900
	Coal combustion Ship building Copper works Chemical industry	1850-1900 1850-1890 1850 1890
	'Le Blanc process' calcium sulphide and arsenic production.	1822
	Crude sewage discharged	1848
	Iron foundries	Early 1800s
	Glass works	1773-1903
	Mining and quarrying	1600s

2.5. Selection of saltmarshes within the Mersey Estuary

To locate study sites which were suitable to carry out a foraminifera-based sea-level reconstruction, several sites within the Mersey Estuary were investigated. The first step in the investigation was to examine map evidence which provides information about how long the saltmarsh has been present and therefore provide an approximate age of the saltmarsh sediments. The historical maps also provide information about the dynamics of the saltmarsh environment. The study site was also investigated initially to determine the topography and altitudinal range of saltmarsh and different environments which are found on the marsh, as the contemporary training set should have as many sub-environments as possible over a large enough altitudinal range. In addition, the presence of foraminifera on the study site and preserved in the sediment was also important to determine.

Historic maps of Oglet Bay were examined and date back to approximately 1886 (figure 2.8) and the saltmarsh itself consisted of good vegetation zones and altitudinal range. A pilot study was carried out to determine if foraminifera were present on the saltmarsh, and if it would be possible to utilise them in a sea-level reconstructions. Surface samples were collected and the foraminifera assemblages produced a species zonation across the saltmarsh which was agreeable with previous studies and was likely to be related to altitude. This indicated that the current saltmarsh environment was potentially suitable to provide a contemporary training set data. Following on from this pilot study, a 95 cm core was collected (OB1) and analysed to ensure foraminifera were present in the sediment. It was concluded that Oglet Bay would provide an appropriate location for the study.

Cores were collected and examined for foraminifera from Frodsham Marsh, located on the southern banks of the Mersey Estuary. Foraminifera were found within the sediment, but only the top 10 cm proved to have sufficient foraminifera of which most were calcareous species and below 20 cm no foraminifera were found. This site was, therefore, discarded.

Following this, Ince Banks, located adjacent to Frodsham saltmarsh was explored. It is a large, grazed, flat saltmarsh, with the Manchester Ship Canal running along the back of the marsh along with a man-made embankment. Several cores and surface samples were collected and two were examined for foraminifera. It was determined that Ince Banks was not a suitable saltmarsh as the foraminifera record in the upper saltmarsh core was not complete enough, as both calcareous and agglutinated species had not been preserved well and, the lower saltmarsh core did not contain many agglutinated species to provide the

best results for sea-level reconstructions. Most of the foraminifera species found were inwashed marine species. It is likely that the saltmarsh development is being squeezed backwards due to rising sea-level (and tidal channel movement) and the constriction from the Manchester Ship Canal which had been constructed behind the saltmarsh. This may have resulted in the loss of the high marsh, which was reflected in the core which showed a change from a high marsh environment to a lower marsh up-core.

Widnes Warth was then explored as a potential study site. Fox et al. (1999) studied this site for historical pollution and found a very successful record from the site. Therefore this pollution record could be used to provide a chronology for the core. A short core was collected from the high marsh. Foraminifera were found throughout the core, although agglutinated species were found only in the 2-4 cm with the majority of foraminifera species being calcareous species. It was, therefore, considered as having low potential for a sea-level study.

Finally, Decoy Marsh was investigated. Figure 2.9 shows that the marsh was present at 1849 and therefore had the potential for a record of at least 150 years. Surface samples and cores were collected from the site, and although foraminifera were only found in the top 10 cm, all foraminifera were agglutinated species, with no calcareous species present. Several surface samples were analysed for foraminifera with most having abundant and common agglutinated species. This site was therefore considered to have the most potential out of those sites studied previously.

As the preservation of foraminifera was poor at several locations within the Mersey Estuary, diatoms were also examined to determine if they may have greater potential to reconstructed former sea-level. Both surface sediments and core material were examined for diatoms at Oglet Bay, Ince banks and Widnes Warth. It was found that the sediments contained mostly marine species with few saltmarsh species, with no species zonation across the marshes. It was therefore concluded that diatoms were not suitable as an alternative or additional sea-level proxy.

Coring sites located beyond the present saltmarsh environment which may contain older saltmarsh sediments were considered but was found not to be viable. Oglet Bay saltmarsh has a small cliff behind the saltmarsh and therefore there are no saltmarsh sediments which are older than those on the current marsh. The other saltmashes within the estuary, e.g. Widnes Warth, Ince Banks and Frodsham Marsh, all have canals bordering the back of

the marsh and therefore could not be utilised either. Other areas which border the estuary which may have had potential for older sediments were found to have been disturbed.

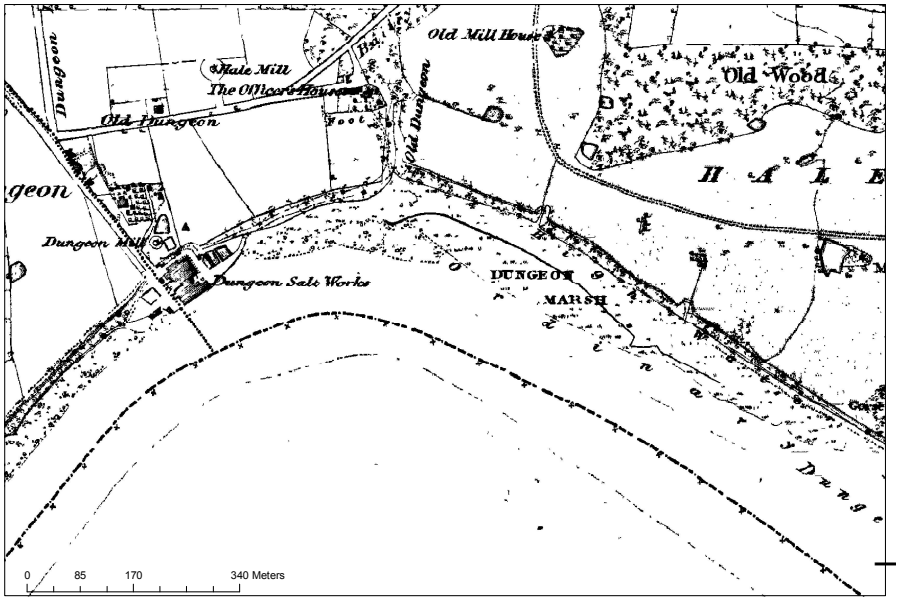

Figure 2.8 Oglet Bay (Dungeon Banks) from 1849 map.

Figure 2.9 Decoy Marsh from 1849 map.

The two sites chosen for this study were therefore Oglet Bay and Decoy Marsh. Oglet Bay is a saltmarsh located on the northern banks of the Inner Estuary (figure 2.1). The saltmarsh is thought to have been present for the last 150 years or more and is still active today (figure 2.8). The area was previously used as a quay up until 1690 when it was no longer navigable, and relicts of the harbour wall still remain (Forshaw, 1990).

Decoy Marsh is also located on the northern banks of the Inner Estuary (figure 2.1) it is also thought to have been present for at least 150 years (figure 2.9). The marsh is named after a Duck Decoy which is located on the marsh is a scheduled ancient monument constructed in the 17th century. Today both sites are also recognised by the RSPB and are Special Protection Areas (SPA) (English Nature, 2001).

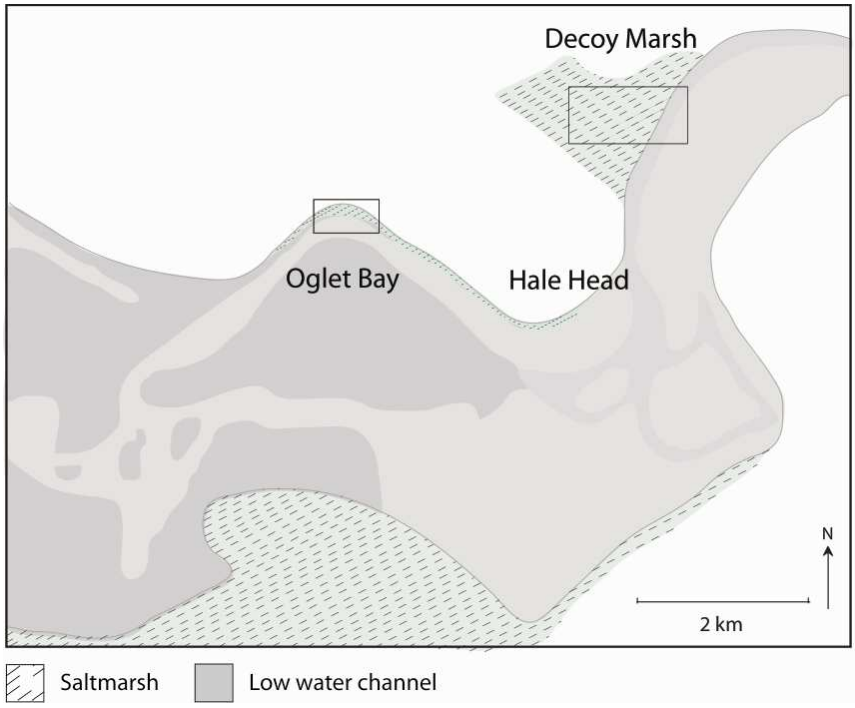

Figure 2.10 Location of study sites Oglet Bay and Decoy Marsh within the Inner Mersey Estuary (see figure 3.1 for the inserts of Oglat Bay and Decoy Marsh).

3. Material and Methods

3.1. Methodological considerations

Before the methodology of the study is set out below, there are several methodological issues which need to considered in order for the correct methodology to be established and for the correct interpretation of the results. Considerations relating to the foraminifera-based transfer function, and the establishment of a chronology will be discussed in the chapter, followed by the methods which have been applied in this study.

3.1.1. Foraminifera-based transfer function considerations

There are several issues which need to be considered in order to determine what the most appropriate transfer function methodology is, as the methodology chosen may affect the results of the modern distribution data and as a consequence the sea-level reconstruction. Factors which will be discussed in the following section include: the depth at which the foraminifera inhabit which will determine the depth which should be sampled; whether live, dead or total (live plus dead) assemblages are the most representative; whether the foraminifera assemblages change with each season and therefore which time of year the saltmarsh should be sampled; and whether one sample alone is representative of the marsh. There are also considerations which need to be made in relation to the setting of the saltmarsh including the current and past changes in tidal range. In addition, taphonomic processes can affect the modern surface data as well as the fossil record. The fossil record also has the potential to be altered through sediment compaction. Each of these factors will be considered in turn below including i) infaunal species, ii) Live versus dead versus total assemblages, iii) Seasonality, iv) Patchiness, v) Tidal range change, vi) Altitudinal uncertainty, vii) Tidal range and transport, viii) Taphonomic problems, iix) Compaction.

i) Infaunal species

The depth at which foraminifera occur in the saltmarsh is important as a sample must be collected which is representative of the foraminifera living on the marsh at that point in time in respect to the local environmental conditions (Scott et al., 2001). If a 1 cm slice is taken and a significant proportion of foraminifera are infaunal then this sample will not be representative. Infaunal occurrences may also change the composition of dead assemblages that accumulate in sub-surface sediments and therefore effect the palaeosea-level reconstruction. If there is a significant infaunal population at the study site it is important that they are recognised, as it would have several implications on the palaeo-

reconstructions: 1. the surface samples would not give an accurate representation of the living population at the sample site; 2. living foraminifera will be counted as fossil specimens; 3. mixing of living foraminifera with fossil assemblages might obscure to some degree a change in autochthonous foraminifera assemblages (Gehrels, 2000).

Reconstructions using foraminifera assume that infaunal populations do not constitute a significant proportion of the total assemblages recovered and, therefore, only the top few centimetres of the surface are used in acquiring modern training set data. However, there has been disagreement about what depth below the marsh surface will provide the best modern analogue for palaeoecological interpretations with a number of studies questioning the reliability of this approach.

Many studies carried out on North American saltmarshes have found infaunal foraminifera populations to be significant in most cases (e.g. Hippensteel et al., 2002; Martin et al., 2003; Ozarko et al., 1997; Duchemin et al., 2005). Tobin et al. (2005) however, argued and concluded that even with the existence of infaunal populations they did not have any significant effect on the formation of death assemblages. Duchemin et al. (2005) concluded that the use of distribution models exclusively based on surface assemblages must be corrected by considering infaunal taxa.

In contrast to the studies in North America, whereby infaunal foraminifera activity is common, most studies carried out in Europe have found that foraminifera are mainly found in the top few centimetres of sediment (Horton, 1997; Alve and Murray, 2001; Horton and Edwards, 2006). Horton (1997) and Horton et al. (1999a) found living and dead assemblages from surface samples did not vary significantly with depth for Cowpen Marsh, UK. Horton and Edwards (2006) also examined infaunal populations at Rusheen Bay, west coast of Ireland, and found that foraminifera lived primarily in epifaunal habitats in the uppermost cm, even though the thin oxygenated layer extended to a depth of 3 cm. Therefore, Horton and Edwards suggested in contrast to Duchemin et al. (2005) that foraminifera of the 0-1 cm interval can function as the model upon which British and Irish fossil marsh deposits can be related to former sea levels.

There are many suggestions as to the reason for infaunally occurring foraminifera and the differences between saltmarshes. It was thought the distribution of foraminifera with depth was related to the oxygen levels in the sediment as it was previously thought that foraminifera could only occupy the top oxygenated layers. However, foraminifera have

been found to occur below the oxic boundary and therefore, may not be limited by oxygen concentrations (Moodley and Hess, 1992). Alve and Murray (2001) also found that the majority of living foraminifera found in the Hamble estuary were restricted to the top 0.25 cm of sediment whilst the redox boundary was located at around 1 cm depth. They therefore concluded that the redox boundary was not the main limiting factor in down-core abundance, and this inference has since been supported by the results from Horton and Edwards (2006) for Rusheen Bay west Ireland. Horton (1997) and Horton et al. (1999a) suggested that the silt substrate in the marsh at Cowpen, NE England prevents any significant penetration of the subsurface by foraminifera and is not favourable in supporting infaunal fauna.

Most substrates in saltmarshes in the UK are minerogenic in origin compared with North American saltmarsh which are usually more organic in nature, therefore, this might explain some of the difference in infaunal activity in the two different environments. The differences concerning the infaunal character of foraminifera species between study sites was suggested by Horton and Edwards (2006) to be due, in part, to spatial and temporally variability, reflecting seasonal and local environmental conditions and chance bioturbation.

Overall, it seems that where and how deep infaunal foraminifera are present in sediments is site specific. North American saltmarshes appear to have higher abundances of infaunal foraminifera present with several of these having significant numbers to affect the overall proportions of the populations. Most studies have found that infaunal populations may be present but in low numbers including the few studies of saltmarshes in the UK and Ireland in which no significant infaunal populations were found to affect the sample size collected for modern training set data. Therefore collecting only the top 1 cm is still the conventional practice (e.g. Horton, 1999; Horton et al., 1999a, b, 2003, 2005; Gehrels et al., 2001 Gehrels and Newman, 2004; Edwards et al., 2004a; Duchemin et al., 2005; Tobin et al., 2005; Southall et al., 2006) and this method will therefore be carried out in this study.

ii) Live versus dead versus total assemblages

Determining which foraminifera are dead and which were alive is necessary when counting surface samples for contemporary population distribution studies as either live, dead or total assemblage constitutes can be counted in order to represent the modern environment (Horton et al., 1999b). There has been debate as to which is the most reliable dataset to use.

Murray (1973) suggested that the living assemblage may represent the fossil record more accurately because seasonality, transport, and taphonomy could bias the total assemblages. The living population also reflects the impact of factors such as, predation, reproduction mode, sources and distribution pattern of food particles and species interactions (Schafer, 1968; Buzas, 1968). These, however, may cause small-scale spatial and temporal variability between the live and dead assemblages because of patchiness and seasonal changes in the live assemblage composition as well as post-mortem changes such as transport and carbonate dissolution in the dead assemblage. Therefore, Murray and Alve (1999) suggested that caution should be taken in using the distribution of living foraminifera as a basis for paleoecological interpretation.

As the living population varies greatly from season to season, the total population of the upper cm (representing the integrated population of several years) may remain relatively constant (Scott and Medioli, 1980a) and, therefore, tends to represent a more homogenous spatial and temporal distribution compared to the live. The total integrates all the living seasonal and spatial variation combined into an average signal and tends to reduce between-sample variance and is more indicative of steady state conditions (Scott and Medioli, 1980b). Gehrels (1994) suggested that because fossilised deposits contain the former total population, the relative abundances of total foraminifera populations on the present day marsh surface are suitable for application in stratigraphic studies. Scott and Medioli (1980b) also concluded that total assemblages were the best to use in Chezzetcook Inlet, Nova Scotia as the total assemblage did not change significantly over a three year period and integrated most small scale seasonal and spatial variations and reliably reflected the prevailing conditions (Tobin et al., 2005). Many studies, including Buzas (1968), Scott and Leckie (1990), Jennings et al. (1995) and Scott et al. (2001), are based upon total assemblages as it is believed that they more closely resemble the assemblage that will be fossilised rather than the live or dead assemblage (Murray, 2000).

In British marshes, Horton (1999) and Horton and Edwards (2003) found that dead rather than total assemblages were the most appropriate for palaeoenvironmental studies because they closely resemble sub-surface samples. They concluded that if the live assemblages are variable then their combination with the dead assemblage to produce total will degrade the usefulness of the dead assemblage (Horton and Murray, 2006). The dead assemblage represents the time-averaged input from the death of living individuals and, therefore, it is common that the species diversity of a dead foraminifera assemblage is

greater than that of living assemblage from the same sample unless post-mortem losses have altered the former or the sedimentation rate is high, as the dead assemblage represents the accumulation of the empty test from successive living assemblages (Murray, 2003).

Using the total assemblage is also misleading as it does not recognise any test loss which will occur after the live component dies (Murray, 2000). Total assemblages disregard taphonomic changes that will affect live assemblages after death (Murray, 1982, 1991, 2000). Whereas the effects of post-mortem modifying processes, including, transport (loss or gain) and destruction of tests are included in the dead assemblage (Murray and Alve, 1999). Death assemblages importantly do not show as much spatial and temporal fluctuations as live assemblages (Horton et al., 2005) which is important when needing a representative modern sample on which to base a palaeo-reconstruction and may also further complicate reconstructions (Horton et al., 1999c).

Murray (2000) demonstrated that the better record produced by total assemblages rather than live or dead in studies is simply an artefact of the statistical method used. As the total assemblage (live plus dead) is compared with the live and dead, the total will appear highly similar, as it is being compared with itself and, therefore, the similarity will be greater than that of the live and dead assemblages (Murray, 2000). Murray (2000) concluded ecological studies should not be use total assemblages as it can hinder the interpretation of fossil assemblages.

Considering the above, this study will follow the conventional methodology used for most UK studies (e.g. Horton et al., 1999a, b; Gehrels et al., 2001; Horton and Edwards, 2005; Horton and Edwards, 2006; Massey et al., 2006a) and the dead component will be used, as this should be more representative of the overall foraminiferal distribution as it will be 'time-averaged' and it will also be more similar to the fossil record.

iii) Seasonality

The time of year in which sampling of surface sediment is carried out is important and can affect the accuracy of the results produced by the transfer function as studies have reported seasonal cycles in living foraminifera. Reiter (1959), in California, found that the largest living populations were in autumn; Parker and Athearn (1959), in Massachusetts also found spring and autumn to have the highest populations. In New York, Buzas (1968) with similar studies by Jones and Ross (1979), Scott and Medioli (1980a), Alve and Murray

(1995) and Murray and Alve (1999), observed that the total number of living individuals was at its largest during the summer months. Horton and Murray (2006) observed that populations of dead calcareous species were also at its highest in the late spring and early summer months.

Buzas (1968) observed an explanation for this seasonality in foraminifera distribution, where it was discovered that the greatest total number of living individuals in the summer months correlated with maximum temperature and abundance of zooplankton and phytoplankton. Therefore, Horton and Edwards (2006) suggested that the increase in productivity of the saltmarsh during summer months is reflected in the summer rise in foraminifera. Another explanation is that it reflects seasonal reproduction which occurs in the spring and early autumn which has been documented for foraminifera in marsh environments (Hippensteel et al., 2000).

Dead foraminiferal assemblages are found to be the most appropriate for palaeosea-level reconstructions as these are found to be less influenced by seasonal fluctuations than live populations as discussed above (Horton and Edwards, 2006). However, they may influence reconstructions derived from their modern distributions, as Horton and Edwards (2003) illustrated. Over the course of a year, surface samples were collected at stations across Cowpen Marsh, NE England. It was observed that seasonal variations of modern dead foraminiferal assemblages did occur and that they modified the elevation and range of the vertical assemblage zones established (Horton and Edwards, 2006). Horton and Edwards (2006) also collected foraminifera samples at three-monthly intervals for a year for saltmarsh sites at Welwick, Thornham and Brancaster, UK, and it was also found that the vertical zonation at each study area varied during the year in response to the seasonality of dead foraminifera distributions, and that the boundary between, the vegetated zone, occupied by agglutinated species, and the tidal flat zone, occupied by calcareous species moved throughout the year. The results from this study demonstrated that a modern sample taken in one three-month periods can significantly under-estimate or over-estimate the boundary between the zones by as much as 0.94 m (Horton and Edwards, 2006).

Horton and Edwards (2003), found that difficulties may arise when populations of calcareous species are at its highest which Horton and Murray (2006) found to be in the late spring and early summer months, and therefore, samples should be taken in late summer, autumn, winter and early spring when the influence of agglutinated species is greater (Horton and Murray, 2006). Buzas (1968) concluded that a modern assemblage

sampled at any one time may or may not be in equilibrium with the environment or be typical of assemblages over a longer time period. Horton and Edwards (2003) recommend that samples should be taken in every season in order to provide the best quality data. However, if only one set of measurements can be carried out Horton and Edwards (2003) suggest that the winter months may represent the most reliable alternative since the greatest precision achieved by the monthly transfer functions was during the winter months when calcareous species declined in numbers and agglutinated species reaching their peak (Horton and Edwards, 2003). Therefore following Horton and Edwards (2003), sampling will be carried out during or as close as possible to the winter months.

iv) Patchiness

In addition to seasonality affecting the distribution of modern dead foraminifera, Murray (2000) considered that differences in monthly records could be attributed to patchiness in distribution patterns. Buzas et al. (2002) found that in a lagoon in Florida, the dominant species showed patch-scale variability in abundance both spatially and temporally. They suggested that distributions formed heterogeneous continua with differences in standing crop over short distances. They consider that asynchronous reproduction within a single species would lead to differences in abundance and through time, to differences in the spatial position of patches on a scale of a few metres; they introduce the concept of asynchronous or aperiodic pulsating patches (Murray, 2003). Therefore, a single sampling event or even a group of replicates at one station will only record some of the species present (Buzas et al., 1977). In view of this small-scale spatial and temporal variability, caution should be taken in using the distribution of living foraminifera as a basis for paleoecological interpretation (Murray, 2000). The present study will try and take this into account by sampling several different areas across the same marsh.

v) Tidal range change

Another problem which may arise in sea-level reconstructions are changes in the tidal ranges. The indicative meanings of any SLIP derived from the upper marsh will only reflect a true MTL position if the tidal range has remained unchanged (Gehrels, 1999) therefore, these should be taken into account in areas where change has occurred. If changes have occurred and an incorrect tidal frame is applied to each unit boundary, the potential exists to over or underestimate the position of MSL. However, few studies have included tidal range changes in calculations as this often requires the use of specialist models (Edwards and Horton, 2006). One example is Gehrels et al. (1995) were the tidal amplification

contribution in Maine was modelled. This was then used as part of the reconstruction of the sea-level in Gehrels (1999) to correct for the palaeo-tidal changes which had occurred. In studies were large changes in tidal range have taken place, care should be taken to correct for this or incorporate these into the error margins. In studies which cover a short time period the tidal range is unlikely to have undergone a major change in range unless anthropogenic engineering has taken place in the estuary.

Another issue arises when using sites located within estuaries, as tidal amplification causes changes in tidal range up estuary (section 2.2). This is important when the nearest tide gauge to the study site is not located in vicinity but in the outer estuary, therefore incorrect tidal levels may be used. Where possible, tide gauges should be installed at the site of the fossil record and the modern surface samples in order to gather accurate tidal information. However, in most studies this is not possible, therefore the nearest first or secondary port information is used. If inaccurate levels are used this may result in over or under-estimate the position of MSL. The above problems related to tidal range change temporary and spatially will be considered during the study and the effects this may have on the resulting reconstruction.

vi) Altitudinal uncertainty

When using a regional transfer function complied of different sites with tidal ranges from microtidal to macrotidal, the elevation is standardised and presented in the form of a standard water level index (SWLI) (Edwards and Horton, 2006). The transfer function then estimates sea-level as a SWLI, because this value is expressed as a proportion of the tidal range, those sites which are macrotidal will have greater vertical errors associated with values than from a microtidal site (Edwards and Horton, 2006). Microtidal marshes also lie closer to equilibrium with sea level and, therefore, could provide higher precision results (Leorri et al., 2009).

Although errors may be greater due to the large tidal range, studies from macrotidal sites have been successful. Edwards and Horton (2006) reconstructed the sea level along the North Norfolk coast which has a tidal range of 6.5 m and therefore had uncertainties of +/- 0.6 m. Horton et al. (2006) investigated surface foraminifera in 15 different study sites around the UK, 11 of which were macrotidal, ranging from 4.0 to 8.4 m. These were complied to form part of a regional training set to develop a transfer function. Hill et al. (2007) also investigated the use of diatoms to reconstruct sea level for the macrotidal Severn Estuary and found it to be successful despite the large tidal range.

vii) Tidal range and transport

Large tidal ranges can also lead to problems relating to mixing of sediments caused by the physical processes. In macrotidal areas, transport due to tidal action may be a significant process and can introduce exotic species which are likely to be in the dead assemblages and not represented by the living individuals (Murray and Alve, 1999). The transport of foraminifera tests in estuaries from more marine environments has been reported from macrotidal or semidiurnal mesotidal estuaries with strong tidal flows, including the Severn, UK (Murray and Hawkins, 1976), the Humber rivers, UK (Brasier, 1981), the Elbe river, Germany (Wang and Murray, 1983) and the Qiangtam and Yangtze Rivers, China (Wang et al., 1985).

If the site is strongly affected by sediment mixing on the surface and with depth, the distribution of foraminifera across the saltmarsh surface will be affected and therefore the training set data for the transfer function. It may also affect the distribution of the fossil foraminifera and therefore the interpretation and reconstruction of the sea level. In addition, Andersen et al. (2000) found that the mixing layer in sediments is deeper in macrotidal sites than microtidal.

Microtidal environments are, however, not immune to local transport and mixing with the transport of tests due to waves and wave induced currents occurring. Micro- and mesotidal marshes are also more likely to be influenced by storm events (French, 2006). These episodic or periodic (e.g. seasonal) variations in the burial rate can potentially accentuate or destroy the geological signal (Bentley et al., 2006).

The Mersey estuary is a macrotidal estuary, therefore issues relating to these must be considered, including identifying if any remobilisation and mixing has occurred in the surface samples and whether they are suitable to use, as well as trying to identify if the sediment record has been affected also.

viii) Taphonomic problems

The dead foraminifera, both modern and fossil, may be subjected to many processes which may disturb the record, in addition to those associated with tidal range. These include the destructing of the tests themselves along with the mixing and transportation of the tests.

Preservation

Preservation problems are a common problem in foraminifera studies, as dissolution may occur particularly in calcareous species resulting in foraminifera being removed from the record (Edwards and Horton, 2000). It has been observed that calcareous foraminifera are poorly preserved in marsh sediments (e.g. Jonasson and Patterson, 1992; de Rijk and Troelstra, 1999). Parker and Athearn (1959) and Bradshaw (1968) found that calcareous species may be present in the living assemblages but not found in the fossil assemblage.

The destruction of the calcareous tests is caused by carbonate dissolution and is attributed to the reducing conditions below the oxidized the sediment layer (Murray, 1973). The process is complex and may be caused by several processes including corrosive bottom or sediment pore waters which may be brought about by metabolisation of organic matter and bacterial destruction (Murray and Alve, 1999). The potential for dissolution varies with foraminifera characteristics and the depositional environment, particularly its chemical properties. The dissolution of calcareous foraminifera is predominantly affected by pH, which varies with the depositional environment change with burial, therefore foraminifera occurrence in surface sediments does not imply subsequent preservation, e.g. *Elphidium* spp. were found in surface samples in South Aligator Australia but their tests dissolved after death. A similar post-mortem dissolution was seen in the Severn Estuary England by Murray (1973). Calcareous dissolution in mollusc shells occurs in highly bioturbated areas (often of slow sediment accumulation) where the build-up of alkalinity is inhibited by water-flushing in burrows and oxidation of solid phase sulphides during particle reworking, with the best mollusc shell preservation occurring in regions least affected by biological physical disturbance (Aller, 1982; Murray and Alve, 1999).

Complete dissolution does not always occur and the effects of the process can be seen on the test. Tests may be etched and weakened (Murray, 1967; Murray and Wright, 1970) or show partial decalcification and organic linings may be exposed, the dissolution of foraminifera carbonate by bacteria may also lead to pitting (Freiwald and Schonfeld, 1996). Tests may become fragile and easily broken including some agglutinated tests which are

poorly held together with cement (e.g. Schroder, 1988; Murray, 1991; de Rijk and Troelstra, 1999).

Fragile agglutinated and calcareous foraminifera are often lost via oxidation of organic test cements and dissolution respectively (Hippensteel et al., 2000). Dissolution and preservation varies with species (Wang and Chappell, 2001), thus, fossil assemblages may be numerically dominated by more preservable species. Goldstein et al. (1995) found taxa that are most likely to be preserved in Georgia US included *Arenoparella Mexicana, Haplophragmoides wilberti, Reophax nana, Textularia palustris, Siphotrochammina lobata, T. inflata* and *T. macrescens*. Taxa which are less likely to be preserved included *Pseudothurammina limnetis, Ammotium salsum, Ammobaculites dilatatus, M. fusca* (Goldstein et al., 1995) *Ammonia beccarii* and *Elphidium* spp. (Hippensteel et al., 2000). Culver and Horton (2005) and Hippensteel et al. (2000) found *M. fusca* foraminifera were also the most likely to be lost to post-mortem degradation. However, Scott et al. (1995) did not see any taphonomic effects on this species in Chezzetcook Inlet where the cores spanned up to 4000 years.

Differential preservation of foraminifera is also related to changes in sediment porewater chemistry with season and depth. A shallow (0-20 cm) mixed layer exists in which test destruction is most intense (Martin, 1999) and below which test abundances tend to become less variable (Hippensteel et al., 2000). The interval from the surface to 20-30 cm is a zone of extensive geochemical activity that can potentially alter assemblages and is subject to relatively deep bioturbation by invertebrates, especially in the low marsh (Hippensteel et al., 2000). One major problem with differential preservation of foraminifera in the upper 60 cm and especially the upper 20 cm of sediment as it may produce an apparent palaeoenvironmental change that could potentially be misinterpreted as a rapid fall in sea level over the last 100-200 years which was found by Hippensteel et al. (2000) in Delaware Bay.

Identifying if, and how much, dissolution has occurred is therefore important. Murray and Alve (1999) stressed that comparative studies over a period of more than a year of the living and dead assemblages should be made, or alternatively the amount of dissolution can also be gauged by comparing the living and dead assemblages from the same samples, accepting that there may be some differences caused by seasonal variability in living assemblages (Murray and Alve, 1999).

Although dissolution is common in most studies it has been found not to hamper subsurface interpretations (Tobin et al., 2005). The problem of calcareous foraminifera present in surface samples and not present in fossil assemblage may however, cause problems with transfer function development based upon these modern surface samples. This was overcome by a new transfer function developed by Edwards and Horton (2000), which was based upon agglutinated foraminifera and test linings. This transfer function can then be applied to sedimentary sequences were calcareous foraminifera have undergone dissolution, see for example Edwards (2001).

Mixing

Experimental studies indicate that considerable reworking and transport of sediment can occur before its final burial in the marsh. This conclusion is based on the fact that the quantity of sediment deposited during two consecutives tides can often introduce several times the amount of sediment corresponding to the annual accretion rate (Boorman et al., 2002). Sediment mixing results from both physical (e.g. tidal flushing) and biological processes (e.g. bioturbation) (Smoak and Patchineelam, 1999). Bioturbation is especially important in saltmarshes and can be caused by burrowing organisms including Fiddler crabs which rework the saltmarsh surface between successive high tides. Other common burrowing organisms in saltmarshes are snails, mussels, shrimp and blue crabs. Vegetation also affects the amount of reworking which occurs. The presence of macrophyte roots can affect the distribution of burrows. Where root densities are greatest in the high marsh, bioturbation is expected to be minimal (Hippensteel et al., 2000). Plant densities decrease in the low marsh and, therefore, burrow depths may increase to 30 cm or more (Sharma et al., 1987). The amount of sediment mixing will also depend upon local ecological and taphonomic factors such as the depth of infaunal distributions and seasonal changes of porewater chemistry (Hippensteel et al., 2000). The possible influence of climatic factors on bioturbation rates must be also considered. These factors are also strongly related to the tidal range.

Sediment mixing results in a reduction of temporal precision, potentially affecting the resolution of the rates and magnitudes of sea-level change recorded in sedimentary sequences (Leorri et al., 2009). Sediments may also be reworked and redeposited in younger sediments resulting in erroneous tidal levels calculated.

Some of the problems associated with sediment mixing can be overcome by choosing a study site which suffers little mixing. As sediment mixing intensity and accumulation rates vary with marsh elevation, suitability for high-resolution sea-level studies also vary with elevation (Leorri et al., 2009). Leorri et al. (2009) suggest that the high or mid-marsh is most suitable for high-resolution sea-level studies, because it is farthest removed from physical reworking and has the thinnest mixed layer. The low marsh is more likely to be subjected to physical reworking due to storms. Furthermore, long-term (>50 year) changes of marsh elevation are determined by mean high water level in which low marsh accumulates relatively quickly, while the high marsh remains in 'equilibrium' with mean high water (Temmerman et al., 2004; Goodman et al., 2007). Leorri et al. (2009) in Delaware Bay found rapid burial rates and thick mixed layer in low marsh areas therefore preventing low marsh from use in high-resolution sea-level studies with very good temporal resolution for the high marsh which have lower rates.

Lithological, chronological and geochemical data will be used in this study to help identify discrepancies in sediment profiles which will assist in determining if, and how, much sediment mixing has occurred.

iix) Compaction

Compaction can cause large errors in sea-level reconstructions and occurs due to the overlying weight of the sediment above or as a result of its own weight (autocompaction). Factors such as unit thickness, depth of overburden, time since deposition, water content and the composition of the sediments, all contribute to the amount of autocompaction which may occur (Tooley, 1978; Pizzuto and Schwendt, 1997; Paul and Barras, 1998).

It is important that autocompaction is recognised in all sea-level studies as it can affect all sediments, but it is particularly significant in high precision sea-level reconstructions from the late Holocene as the magnitude of the sea-level change can be similar to the magnitude of the errors (Paul and Barras, 1998).

Where compaction has occurred in sediments, sea-level reconstructions using biostratigraphic data would underestimate the position of mean sea level (Haslett et al., 1998; Allen, 2000) due to the lowering of their position relative to the current sea level and thus over-estimate the long-term rate of relative sea-level rise (Edwards and Horton, 2006). Allen (2000) showed from field and experimental data that index points can be lowered by as much as 3-4 m from their true position. As the compaction of sediments is not equal

through the sedimentary sequence, those which are older will experience more compaction and displacement than the younger, thus, reconstructed sea-level curves from these sequences may show erroneous changes in levels due to compaction differences rather than actual environmental changes (Edwards and Horton, 2006).

The effects of compaction have been widely studied and acknowledged (e.g. Jelgersma, 1961; Tooley, 1978; Shennan, 1986; Haslett et al., 1998; Shennan et al., 2000) but as of yet there is no current standard method of decompacting sediment sequences (Edwards, 2006).

Many attempts have been made to try and 'decompact' the sediments for example; Kaye and Barghoorn (1964) used tree trunk and branch distortion to estimate the amount of compaction. Several studies including Bloom (1964), Belknap and Kraft (1977), and Haslett et al. (1998) also used geometrical approaches, using the changing altitude of the top of isochronous peat bed tops (Allen, 2000). A model described by Paul and Barras (1998) and followed by Massey et al. (2006b) used geotechnical procedures to estimate autocompaction and used this to decompact sediments. The parameters which the model was based upon included; the compression index, the bulk density and the groundwater level which in turn were used to derive effective stress and thus volume reduction (Massey et al., 2006b). Brain (2006) created an empirically-based model to correct for autocompaction more accurately in intertidal sediments. This also uses geotechnical parameters including the effective stress and the in situ compacted voids ratio based upon lithology and compression testing of the sediments. Using these modelling techniques (Paul and Barras, 1998; Shaw and Ceman, 1999; Massey et al., 2006b; Brain, 2006) is difficult in most sea-level reconstructions due to the absence of geotechnical data, and the inability to quantify past factors including sediment and water level (Edwards, 2006).

Most studies which try and account for compaction use SLIPs from basal peats only, as these are assumed to be free of compaction as the underlying consolidated Pleistocene deposits are thought to be unaffected by compaction (Jelgersma, 1961) (e.g. van de Plassche, 1979; Gehrels et al., 2002,, 2005, , 2006; Donnelly et al., 2004). However, basal peats themselves may have undergone some compaction, where the deposits are thick and/or the dated materials have not come from the very base (Allen, 2000). There may also be problems relating to the interpretation and indicative meaning of these samples as van de Plassche (1979) observed that initial peat growth may be influenced by groundwater gradients (Horton and Edwards, 2006). Using only basal peats to reconstruct sea level also

limits the amount of sediments which can be used, reducing the amount of sea-level information available.

Most sea-level reconstruction studies which have included autocompaction estimates, have been located in organic-rich marshes of America, in comparison to mineral-rich UK marshes were there have been few studies, as it is assumed that these sediments are less susceptible to compaction (Edwards, 2001) and is therefore negligible (e.g. Edwards and Horton, 2000). Other studies have acknowledged autocompaction may have occurred but have not attempted to account for it (e.g. Boomer and Horton, 2006; Nikitina et al., 2000).

Although compaction is an important problem in sea-level reconstructions which should be considered and corrected for where possible, it is not viable in this present study to 'decompact' the sediments. As UK minerogenic sediments are less susceptible to compaction (Edwards, 2001) and the cores which will be collected for the fossil record in the present study will be short in length and located in the high marsh it is likely that the compaction will be negligible (e.g. Edwards and Horton, 2000). Dry bulk density will however be carried out for both the fossil records in order to determine if there are any major changes in density which may be caused by autocompaction.

3.1.2. Chronology considerations

There are several different methods which can be applied to assign a chronology. The chosen method depends upon the time frame which the record is within and the dateable material available. Methods include radioisotopes, luminescence and chronostratigraphic markers including tephra and pollution. Each of the available methods have their own problems and errors associated with them and interpolation of dates may also increase errors further (Gehrels, 1999).

The principle limitation of reconstructed records is the coarsely constrained chronology which produces large uncertainties in the timing of changes (Edwards and Horton, 2006). The principal problems with dating include uneven temporal and spatial data distribution and the differing magnitude of associated errors, which results in variable age control (Edwards and Horton, 2006).

Radiocarbon

Past studies reconstructing sea levels using traditional radiocarbon methods were relatively imprecise, primarily due to uncertainties involved with conventional dating of large peat samples using radiocarbon dating (Belknap and Kraft, 1977). As accurate sea-level records are based upon precise ages, more detailed chronologies had to be utilised (Edwards and Horton, 2006). Accelerator Mass Spectrometry (AMS) radiocarbon ages on plant macrofossil fragments embedded within the sediment have provided more precise ages for SLIPs (Gehrels et al., 1992) and provide the chronology for most sediment sequences. In studies where the sediments are several thousands of years old, AMS radiocarbon may provide a suitable chronology alone, if enough accurate dates can be ascertained (e.g. Zong and Horton, 1999).

AMS radiocarbon dating has several disadvantages, including the limited availability of suitable organic deposits resulting in poorly constrained chronologies (Edwards and Horton, 2006). Where plant macrofossils are not available, AMS radiocarbon dating of calcareous foraminifera may be used and offers the potential for increasing the temporal precision of the resulting relative sea-level records (Horton et al., 2000). AMS radiocarbon dating also has the disadvantage of having large errors associated with them. The method in general may also produce erroneous dates. It may also be difficult to date the last few centuries due to the levelling of the calibration curve (Stuiver et al., 1998) which results in the production of a wide range of ages (Gehrels et al., 2006).

More recently, ^{14}C bomb spike calibration has been used to provide high resolution chronologies spanning the last few centuries, overcoming the problem associated with the levelling of the calibration curve. The approach has been successfully applied to peat sequences (e.g. Shotyk et al., 2003; Garnett and Stevenson, 2004) and saltmarsh sediments (e.g. Marshall et al., 2007). However, as with other dating techniques, independent age markers may be needed.

Luminescence

For sediments older than 300 years, AMS radiocarbon and luminescence are the most appropriate techniques which can be employed, for example, Horton and Edwards (2005) based their chronology on radiocarbon ages as well as infrared stimulated luminescence ages (IRSL) for sediments aged between 2000 and 7000 BP. However the use of IRSL dates may have large age uncertainties (Edwards and Horton, 2006). Luminescence has not been

used on younger sediments as it was thought that there would be incomplete resetting of the signal before or during deposition and weak luminescence signals (Madsen et al., 2005). However, recent studies have investigated the use of optically stimulated luminescence (OSL) on younger sediments and determined that it may now be possible to obtain OSL dates on a scale of decades to a few hundred years (Madsen et al., 2005).

Metal Pollution

Estuaries are predominantly areas of deposition and act as an important sink for sediments and the metals associated with them, natural or otherwise (Ridgway and Shimmield, 2002; Spencer et al., 2003). Estuaries are often areas of port, industrial and urban development which results in large amounts of contaminants entering the surrounding environment (Ridgway and Shimmield, 2002).

Anthropogenically derived contaminants can enter the sediments directly through effluent discharge as well as through deposition from atmospheric pollution. They are transferred from solution to sediments by adsorption onto suspended particulate matter and deposited with relatively short lag times (Spencer et al., 2003). The supply of industrial pollution in association with incremental sedimentation can provide saltmarshes and mudflats with a stratigraphic record of metal pollution (Berry and Plater, 1998). Concentrations may then reflect the pollution deposited in the environment at the time of deposition (Cundy et al., 2003). Increases in the production of the contaminant will lead to increased input to the saltmarsh surface. It is, therefore, possible to relate peaks in concentrations to past changes in the industrial history of the area which may allow a chronology to be produced for the profile in the form of 'event dating' (Spencer et al., 2003). In order to use pollution to provide a chronology; knowledge of the distribution of contaminated material, an understanding of the processes which influence its accumulation and knowledge of the industrial activities in the area are all required.

Radionuclides

^{210}Pb

Younger sediments are often dated using the radioisotope ^{210}Pb. This method can be used to date sediments which are up to 120 years old, and is a common technique used in saltmarsh sediments.

^{210}Pb is a natural radioactive isotope formed from the ^{238}U decay series (Anderson et al., 2006). ^{238}U which is present in the Earth's crust decays to ^{226}Ra and further to ^{222}Rn which escapes into the atmosphere and then decays to ^{210}Pb (Anderson et al., 2006). Precipitation brings ^{210}Pb to the Earth's surface where it adheres to fine-grained material and organic matter (Anderson et al., 2006). ^{210}Pb covers all surfaces which are exposed to the atmosphere including sediments, this forms the 'unsupported 'part of the ^{210}Pb. ^{238}U also decays from the mineral grains within the sediment also producing ^{210}Pb, known as 'supported' activity. The supported activity is then subtracted from the total content to give the 'unsupported' only or 'excess' content which is used in the analysis (Anderson et al., 2006). As ^{210}Pb has a half-life 22.3 years, it is possible by analysing the exponential decay of the content of the isotope with depth to date the sediment for last 120 years (approximately five half-lives) (Anderson et al., 2006).

When using ^{210}Pb it is important that an independent age control to validate the chronology is also used (e.g. Koide et al., 1973). However, according to Smith (2001) it is common to find that independent tracers are not used and it is assumed that no post-depositional mixing or single-particle sedimentation has taken place. Appleby and Oldfield (1992) and Smith (2001) stress that independent validation of ^{210}Pb chronologies must be an integral part of the overall methodology. ^{137}Cs and ^{241}Am, pollution markers, varves and tephra could all be used for this purpose. A disadvantage of ^{210}Pb is that it may be subject to the same diagenetic remobilisation processes as Pb, such as Fe and Mn cycling (Cundy and Croudace, 1996) and this may produce inaccurate estimates of sediment ages (Gubala et al., 1990).

$^{137}Cs\ and\ ^{241}Am$

The use of radionuclides can also be used in event dating to provide a chronology, and has been successfully applied in estuarine sediments around the country including the Mersey Estuary (e.g. Fox et al., 1999). The radionuclide ^{137}Cs (half-life 30 years) and ^{241}Pu (half life 14.4 years) which decays by beta-emission to ^{241}Am (half-life 432 years) are artificially-

generated radioactive nuclides that were released primarily by fallout from weapons testing and the Chernobyl reactor accident (Faure et al., 2005).^{137}Cs and ^{241}Am can therefore be used to assign the dates 1963 from the peak in weapons testing and 1986 from Chernobyl (Michel et al., 2001). The ^{241}Am from fresh nuclear weapons test debris is essentially zero (Krey et al., 1976) and its presence in older deposits is through in-growth from ^{241}Pu.

These radionuclides are particularly useful chronostratigraphic markers as they have very specific time frame in which it has been released into the environment. Weapons testing began in 1952 and peaked in 1963 when a ban was then introduced and resulted in a rapid decline in deposition of the radionuclide (Carpenter et al., 1987). Identification of peaks in ^{137}Cs in sediment records potentially enables the determination of these dates (e.g. Aston and Stanners, 1979; Delaune et al., 1978; Andersen et al., 2000). However, another input of radionuclides to the North West of the England, is the discharge from the nuclear fuel reprocessing facility at Sellafield, Cumbria. This provides the main delivery of increased concentrations of radionuclides to the Irish Sea and therefore to sediments on the west coast of the UK and the east coast of Ireland. Discharge of radionuclides from Sellafield were at its peak in the mid-1970s which can provide a chronological marker for these sediments (Fox et al., 1999).

The use of Sellafield-derived radionuclides has an advantage over fallout sources as the radionuclides from nuclear reactors are disposed of directly into the coastal waters and are therefore rapidly transported into nearby estuaries, compared with the accumulation from fallout which may be longer (Aston and Stanners, 1979). It is important to note, however, that Irish Sea saltmarsh sediments preserve a record of the time-integrated discharge of Sellafield-derived radionuclides and not an annual record, due to intense mixing of contaminated offshore sediment before deposition in saltmarshes (Harvey et al., 2007).

Considerations of using pollution and radionuclide event dating

The input of pollution to sediments is not the only factor determining the concentrations of heavy metals and radionuclides within the profile. It is important to understand the other processes effecting the metals and radioisotopes in the sediment as it can affect the interpretation of the profile. Other factors which can complicate the interpretation include: bioturbation and mixing of the sediments, grain size, composition, diagenesis, post-depositional mobility, organic matter content, varying sedimentation rate and erosion of

the sediment record (Valette-Silver, 1993). Therefore, a false impression of contamination may be recorded in the profile.

In order for pollution to be used to provide accurate chronologies there are several requirements that must be fulfilled: 1) since deposition of the marker horizon, sediment accumulation must be at a uniform rate; 2) little post-depositional mixing should have taken place or should be included in the model; 3) and little variation in the sediment characteristics which may affect the distributions (Morris et al., 2000).

Sediment characteristics which may affect the concentrations include the particle size which has a marked effect on the concentrations of pollutants per unit sediment mass (Aston et al., 1985). The finest sediments have a greater potential for trace metal binding than coarser grained particles due to their large surface area to volume ratios and the high density of metal binding sites potentially available (Kersten and Forstner, 1986; Schoer, 1985; Horowitz et al., 1989; Loring and Prosi, 1986) Therefore, significant changes in grain size in the profile could lead to features in the concentration of metals and ^{137}Cs and ^{241}Am (Sharma et al., 1987) which do not represent real changes in contamination levels but a change in grain size (Fox et al., 1999).

The same is true for organic matter content which has strong affinities with some metals as well as ^{137}Cs and ^{241}Am, therefore, increases in organic matter may result in increases in concentrations. Heavy metals may become associated with organic matter during initial deposition (Salomons and Forstner, 1984), then later may be redistributed by early aerobic degradation of organic matter. This may result in a gradual decrease in metal concentration with depth (Allen, 1990; Valette-Silver, 1993).

Organic matter plays an important role in forming complexes with heavy metals, as well as retaining heavy metals in an exchangeable form. The complexes are different for each metal and they also affect each metal differently. For example, Cu is bound and rendered unavailable mainly through the formation of organic complexes (Kirkham, 1977), while Cd is retained in an exchangeable form and is more readily available (Haghiri, 1974).

Post-depositional changes from diagenesis and remobilisation of metals and radionuclides, as well as the reworking of sediments themselves also cause problems. Mn and Fe are the most affected by diagenesis. Surface enrichment of Mn is common and related to redox cycling in the sediment (Spencer et al., 2003) with early-diagenetic remobilisation and reprecipitation in the oxic zone (Spencer et al., 2003). The reduction of Fe and Mn ions

results in the mobilisation of these metals and diffusion to oxic surface sediments where they are reprecipitated as oxides or occasionally carbonates (Farmer and Lovell, 1984). Other metals which may be affected by mobilisation include Cu, Pb and Zn which commonly co-precipitate with sulphides below the redox-cline and therefore may show enrichment at depth (Croudace and Cundy, 1995; Zwolsman et al., 1993). Fuller (1977) found that in acidic soils (pH 4.2-6.6) the elements Cd, Ni, and Zn are highly mobile and Pb practically immobile, in neutral to alkaline (pH 6.7-7.8), Cr is highly mobile, Cd and Zn are moderately mobile and Ni is immobile.

^{137}Cs has also been found to be mobile and in many cases the value of it as a chronological marker has been significantly reduced (Appleby et al., 1991). However, many sequential observations of ^{137}Cs over 20 years have found the persistence of the ^{137}Cs peak corresponding to the mid-1970s regardless of the remobilisation (Pulford et al., 1998). ^{241}Am which has been found to exhibit less post-depositional re-dissolution (Appleby et al., 1991).

Post-depositional mixing may occur and may also alter the vertical profiles of the radionuclides. This includes the bioturbation of sediments by benthic fauna and the mixing of sediment by physical reworking (Aston and Stanners, 1979). In addition other processes which may cause problems include delays between delivery and sedimentation, as this may lead to an under-estimate of sediment accumulation rates (Milan et al., 1995).

Although there are many potential problems which could affect the sediment record, Cundy et al. (2003) found that saltmarsh cores from even the most heavily disturbed estuarine sites can provide useful information on variations in historical contaminant input. Saltmarshes are generally less susceptible to post-depositional disturbance and reworking of sediments as they are stabilised, and have a dense root system (Cundy et al., 1997) as well as anoxic conditions at depth which inhibit bioturbation (McCaffrey and Thomas, 1980). However, for sediments which have been vigorously mixed or reworked, large-scale compositional variations are present or where significant early-diagenic remobilisation has taken place, only general information on the scale of contamination can be observed (Cundy et al., 2003). Care should be taken in understanding the processes which may have occurred and affected the sediment profile whilst making interpretations.

3.2. Fieldwork

3.2.1. Sample collection for the contemporary foraminiferal study

A total of 105 samples were collected from five surface transects across two saltmarshes. The locations of these transects can be seen in figure 3.1. A description of each of the transects follows. Twenty seven sediment samples were collected in November 2007 along a transect (OBSS1) 69 m in length across the width of Oglet Bay saltmarsh from the back of the high marsh, at the upland edge, to the low marsh. The samples were taken every 1.5 m until the slope of the saltmarsh decreased, when samples were then taken every 3 m. The samples were not taken at equal vertical intervals (e.g. Horton and Edwards 2006; Edwards et al., 2004) as it proved difficult due to the small microtopography of the saltmarsh. Most of the samples taken for this transect were located within the *Phragmites* spp. (samples 1-13). A second Oglet Bay transect (OBSS2) was carried in November 2008 where a total of 19 surface samples were collected over a distance of 39 m, the majority of samples (1-12) being located within the *Phragmites* spp. Samples were collected every 1.5 m, again increasing to 3 m on the flatter part of the marsh. A third transect (OBSS3) was carried out in early March 2009 in an area further west along the saltmarsh, in a location which was not occupied by *Phragmites* spp. at the back of the marsh. A total of 30 surface samples were taken, firstly every 1 m across the saltmarsh starting from the highest trash-line until 17 m whereby the slope decreased and samples were collected every 2 m. Decoy Marsh was sampled in January 2010, where 10 surface samples (DMSS1) were collected from the back of the ridge of Decoy Marsh, 100 m in length. Additional samples were collected in March 2010, a total of 19 surface samples (DMSS2) were collected, starting 30 m from the location of the first sample from DMSS1 (figure 3.1).

All samples were levelled to a fixed temporary benchmark and later levelled to an Ordnance Datum benchmark (Flush bracket, Hale, Childe of Hale Hotel, benchmark number 10558, 16.208 m OD). Sediment samples for analysis of both foraminifera and environmental variables were collected. A standardised volume of 10 cm^3 was taken for foraminiferal analysis allowing comparisons with other studies including; Phleger and Walton (1950), Scott and Medioli (1980a), Horton et al. (1999a, 1999b, 2000, 2005), Gehrels et al. (2001, 2005, 2006). To ensure the correct volume of sample was collected at each sampling point a small cylindrical pot was used which had a surface area of 10 cm^2 and was 1 cm deep. At the same time a volume of 30 cm^3 was taken for analysis for other environmental variables, pH, salinity, grain size, organic matter.

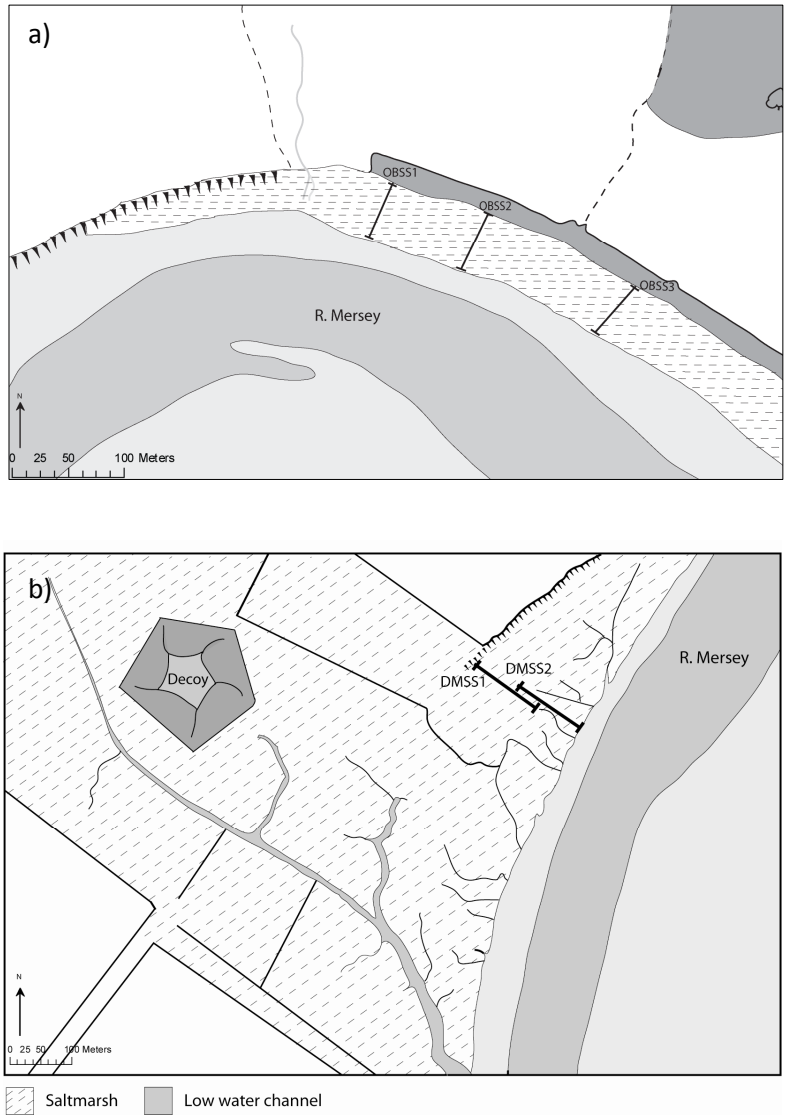

Figure 3.1 Location of modern surface transects from a) Oglet Bay b) Decoy Marsh (see figure 2).

3.2.2. Core collection for the stratigraphic study of Oglet Bay saltmarsh

Systematic transects of cores were examined across the Oglet Bay saltmarsh, in order to provide information about the past environment and environmental conditions of Oglet Bay, to establish an appropriate location in which to take a core. A total of 50 cores were taken and examined using the Troels-Smith (1955) method of classification. The location of the cores can be seen in figure 3.2 and table 3.1. Each transect was spaced 50 m apart and in each transect between 2 and 5 cores were examined which were spaced 10 m apart. The length of the core retrieved was dependent on: reaching the underlying bedrock; whether the sediment was retrievable and not being re-sampled; or when the sediment was no longer penetrable. The depth varied between 0.13 m and 5 m. The same methodology was not conducted on Decoy Marsh due to the practical limitations of sampling due to restrictions relating to permission and the protection of rare bird species.

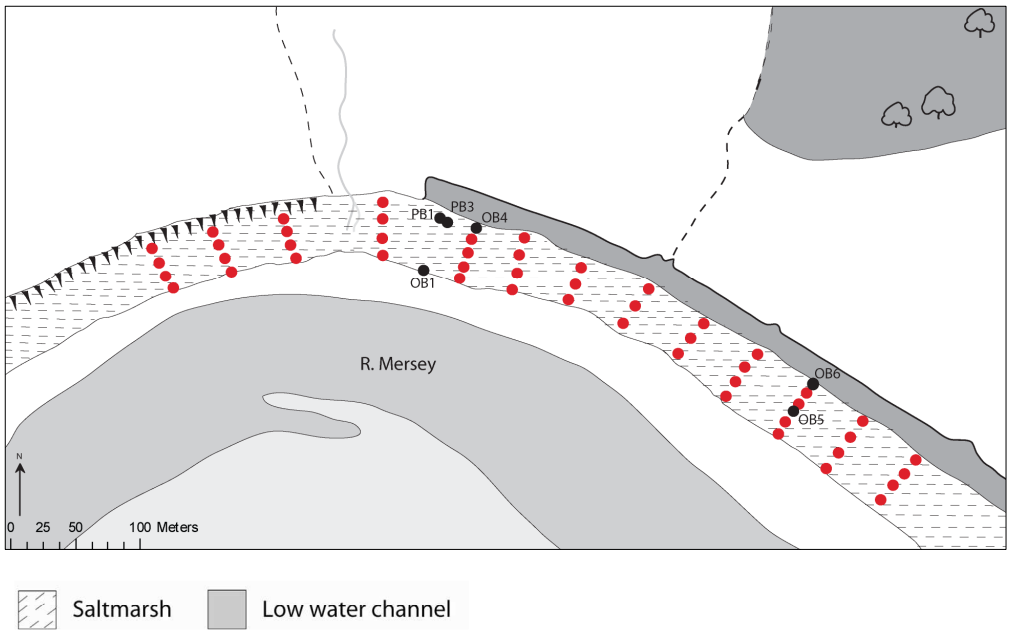

Figure 3.2 Location of a) red circles show sediment cores examined for lithology b) black circles show sediment cores collected for geochemical analysis from Oglet Bay.

Table 3.1 Location and altitude of cores analysed.

Core Name	Grid Reference	Location	Altitude (m OD)
OB1	345250, 381980	Low Marsh	4.482
OB4	345473, 382130	Mid-Marsh	4.822
OB5	345678,382019	Mid-Marsh	5.012
OB6	345689,382030	High Marsh	5.252
PB1	345786, 382125	Mid-Marsh	4.822
PB3	345498, 382122	Mid-Marsh	4.682
DMC1	348234, 382686	High Marsh	5.595

3.2.3. Core collection for the geochemistry analysis of saltmarsh sediments

Several cores were collected from various locations across the saltmarsh (figure 3.2 and table 3.1) in order to determine if there is a distinct pattern in pollution across the saltmarsh as a whole. Each core was levelled to a temporary benchmark then later to Ordnance Datum. Core OB1 was located on the edge of the low marsh using 2 monolith tins 50 cm in length, a total of 95 cm with an overlap of 5 cm. Core OB4 was collected in the *Phragmites* spp. vegetation zone close to the boundary of *Phragmites* spp. and *Scirpus maritimus* 26 m from the back of the saltmarsh in the same location as surface sample transect OBSS1. It was collected using a wide gouge corer (5.5 cm diameter) and was 74 cm in length. Core PB1 was collected at a similar location to the previous core OB4 and was 70 cm in length. Core PB3 was taken 20 m east along the saltmarsh from OB4, also taken within the *Phragmites* spp. reeds and was 90 cm in length. Cores OB6 and OB5 were collected from an area further east along the saltmarsh, in a location absent of *Phragmites* spp. OB6 was collected from an upper marsh location and was 26.5 cm in length. OB5 was collected from a mid-marsh environment and was 83 cm in length. Cores were taken from different locations in order to find a core which maximised sediment depth, had the best potential for sea-level reconstruction based upon foraminifera preservation and species type as well as being representative of the marsh. The core analysed from Decoy Marsh (DMC1) taken from a high marsh location was 42 cm in length below which was only sand.

The cores were returned whole to the laboratory where they were sliced every 1 cm. The cores PB1 and PB3 were very wet and unconsolidated therefore both were frozen in order to slice the core without compressing it, and thereby removing water and air, changing the dry bulk density of the sediment.

3.2.4. Core collection for foraminiferal fossil analysis from Oglet Bay and Decoy Marsh

Two cores were collected for fossil foraminifera analysis, one from each of the saltmarsh sites. OB5 was taken from Oglet Bay, and was collected from the eastern side of the saltmarsh, in a location absent of *Phragmites* spp. (figure 3.3a). It was sampled from a mid-to-high marsh environment and was 84 cm in length. DMC1 was collected from a high marsh location from Decoy Marsh (figure 3.3b) and was 42 cm in length.

Figure 3.3 Location of cores a) OB5 from Oglet Bay b) DMC1 from Decoy Marsh.

3.3. Laboratory work

3.3.1. Foraminifera analysis

Foraminiferal analysis was carried out for both the contemporary samples and fossil samples from cores OB5 and DMC1. On return to the laboratory, the contemporary samples were stained using a rose bengal solution (Walton, 1952; Murray and Bowser, 2000). The solution was made with a 30% ethanol solution (300 ml Ethanol and 700 ml distilled water) to which rose bengal (1.5 g) and sodium bicarbonate (1.5 g) were added. The rose bengal solution was added to the samples within 24 hours of collection and shaken to ensure all foraminifera took up the stain and soaked for at least 24 hours following Gehrels (2002).

Both sets of samples (contemporary and fossil) then followed the same methodological procedure. The samples were sieved through a 500 µm sieve and collected in 63 µm sieve following the methods of Scott and Medioli (1980a). They were then washed into beakers and the decanted material of random samples were examined to check for any foraminifera before being discarded (Gehrels, 2002; Horton and Edwards 2006). A wet-splitter was used in order to divide the sample into equal amounts allowing the volume of the amount counted to be known. A wet-splitter maximises the number of samples that may be processed whilst minimising loss or damage to foraminiferal tests and maintains a representative sub-sample (Gehrels, 1994). It is the most accurate and time efficient preparation method (Edwards et al., 2004). To test whether the $1/8^{th}$ was representative of the whole sample, $1/8^{th}$ (one section of the splitter) of a randomly selected sample was counted, as well as the whole sample. Similar assemblages (<5% difference) were found for the two counts. Therefore it was deemed suitable to use only $1/8^{th}$ of the samples if enough total and dead tests were counted.

The samples were counted wet to assist in the detection of rose bengal-stained foraminifera for the contemporary samples following Scott and Hermelin (1993) Gehrels (1994, 2002), Edwards et al. (2004) and Horton and Edwards (2006). In addition, wet counting is also favoured over drying the sample as drying can cause many problems including: consolidation or 'pancaking' as a result of drying out of organic residue which is often irreversible (Scott and Medioli, 1980a; Scott, et al., 2001); identification problems due to organic matter adhering to the tests making them difficult to identify (Patterson et al., 2005); the clumping of sediment together, making specimen picking difficult; and finally the

organic linings of foraminifera that mark the dissolution of calcareous foraminifera or the breakdown of agglutinated tests may be lost (Scott et al., 2001).

A manageable amount of sediment was then transferred to a counting tray and counted wet under a binocular microscope at typical magnifications of x50, using Haynes (1973) and Murray (1971b, 1979) for identification. Species of *Ammonia beccarii*, *Elphidium* and *Quinqueloculina* were combined into generic groups (Hayward et al., 2004a; Horton and Edwards, 2006). A known sample volume was counted fully and repeated until at least 150 individuals were identified as well as at least 100 dead foraminifera (Fatela and Taborda, 2002).

3.3.2. Salinity and pH analysis

Salinity and pH were analysed for the surface samples as part of the environmental variables analysed for the contemporary study. The variables were measured at the same time using a 1:2 soil to water mix, made using 20 ml of sample which was made up to 70 ml with double distilled water. The sample was stirred and left for one hour. Both variables were measured using a K&M 7002 conductivity and pH probe and was calibrated for both pH and salinity. Salinity was converted into ‰ salinity using a standard equation (Salinity ‰ = 0.6679 (conductivity in mS cm^{-1}) – 0.1513) following Gehrels and Newman (2004).

3.3.3. Organic matter content analysis

Organic matter content was analysed for both the surface samples and the collected cores. The organic matter was calculated using the loss on ignition method (LOI). Sub-samples of the collected sediment were weighed and freeze-dried at 35° C until all moisture was removed. The samples were then re-weighed to determine soil moisture content excluding hydroscopic moisture. To remove all the moisture, the samples were further sub-sampled (0.5 g) into 10 ml porcelain crucibles, weighed, oven-dried at 105° C overnight, and then re-weighed to determine the amount of hydroscopic water present. The samples were then placed into the furnace at 450° C for 4 hours to remove all the organic matter present. The samples were then re-weighed and the percentage of organic matter was calculated using the soil moisture lost and the loss on ignition results.

3.3.4. Dry bulk density analysis

Dry bulk density (DBD) was calculated for cores OB5 and DMC1 to be used for radionuclide determination as well as to establish whether compaction has occurred. To calculate DBD, a 1 ml volume of sediment was cut out of each slice, measuring the volume of the cube as accurately as possible. The sub-sample was then weighed, frozen, freeze-dried and then re-weighed. The DBD was calculated by;

DBD = Volume / Dry weight

3.3.5. Grain size analysis

Grain size analysis was carried out for the surface samples as well as the cores for fossil foraminifera analysis OB5 and DMC1. The grain size distributions of the samples were measured using a Coulter Laser Granulometer (LS200). As the samples were very rich in organic matter, this was removed by digestion before grain size analysis was carried out. Approximately 5 g of wet or dry sample was sieved through a 2 mm sieve into a beaker then 20% hydrogen peroxide was added. The samples were heated gently on a hot plate and any floating organic material removed with tweezers to quicken the process. The samples remained on the hot plate alternating between adding more 20% hydrogen peroxide and double distilled water until all the organic matter was removed. A small amount of sediment (<1 cm^2) from each of the digested sample was then mixed on a watch glass with calgon to disaggregate the sediment. Once smooth, the mixture was added to the granulometer and the grain size measured when satisfactory obscuration was reached. The data were then processed using the computer program *GRADISTAT* (Blott, 2000).

3.3.6. XRF analysis

XRF analysis was carried out for 6 cores from Oglet Bay and one core from Decoy Marsh. The metal concentrations were determined using a BRUKER S2 Ranger energy dispersive X-ray fluorescence (XRF) and Atomic Adsorption Analysis (AAS). This analysis was carried out on several cores for Oglet Bay as well as for OB5 and DMC1. A sub-sample of core material was freeze-dried at 35°C until all moisture was removed. The sediment was then disaggregated into powder form using a pestle and mortar. A thin layer of the resulting sample was placed and lightly pressed with a plunger into a 25 mm-deep polythene tube which had a polypropylene film stretched across the base. The samples were then analysed along with certified standard reference materials of Buffalo River Sediment (srm2704) and Stream Sediment (GBW07305) which were used for calibration at the beginning of the

analysis. In addition, a standard silica disc (Baxs-S2) was measured along with each set of samples measured. These were measured in addition to the samples to ensure consistency between measurement runs. As the samples were organic-rich, each sample was adjusted for the organic matter content using the LOI data in order to calculate the mass attenuation correction which is applied using the theoretical coefficients of Theisen and Vollath (1969).

3.3.7. Hg analysis

Hg concentrations were carried out for cores OB1, OB4, OB5 and DMC1 on a sub-sample of the sliced cores. This was carried out for sediment from every other centimetre in the core. The wet sub-sample was firstly dried in a drying oven at 60 °C. The samples were then put into tinfoil-made pots and covered with blue roll and left in the oven overnight along with three standards; River Sediment (2704), San Joaquin (2709) and Light Sandy Soil (7002). Once the samples were dry, they were sub-sampled further by weighing 0.25 g (to 4 decimal places) of each into acid-washed polythene tubes. 1 ml of concentrated AnalaR nitric acid was added and then placed in a shallow water bath at 90 °C for one hour. Once removed and cooled, 7 ml of double distilled water was added to each sample and shaken thoroughly. The samples were then left to settle for 30 minutes, flicked twice to bring clean liquid to the top of the tube, and this was repeated three times. The samples were then centrifuged at 1200 rpm for 15 minutes and the supernatant decanted. Along with the samples and sediment standards, three acid standards were also made which contained only 1ml of concentrated AnalaR nitric acid and 7 ml of double distilled water. Once each sample had been prepared, a standard of $SnCl_2.2H_2O$ solution was made by placing 5 g of $SnCl_2.2H_2O$ in a conical flask with 20 ml of concentrated HCl and stirred. 80 ml of double distilled water was added and the sample was stirred. The solution was placed on a magnetic stirrer for the rest of the laboratory analysis. A Hg standard reagent was made at a dilution of 1:1000. 5 ml of concentrated HCl was added to 100 µl of Hg stock in a 100 ml flask and made up to 100 ml with double distilled water.

The samples were measured using an AAS. The instrument was first calibrated by measuring several standards including a blank sample. To make a blank sample 40-50 ml of double distilled water was put in a conical flask and 2 ml of the stannous chloride solution was added and a stopper put in the flask until it was ready to be measured. The program was then run and after 10 seconds of measuring the Drechsel head was fitted to the flask. After 80 seconds of measuring the Drechsel head was removed and rinsed with double distilled water. The standard samples measured were 10, 20, 40, 100 and 200 ng. A 10 ng

standard was made by adding 10 µl of Hg reagent to 40-50 ml of double distilled water and 2 ml of stannous chloride solution. The samples were prepared by adding 1-5 ml of the sample to 45-49 ml of double distilled water and 2 ml of stannous chloride solution added.

If the sample concentration was below that of the blank, the sample was re-measured using more sample. If the concentration of Hg in the sample was higher than that of the standard, less sample was used or a new standard was made using a higher concentration of Hg reagent. All samples were measured, including the sediment standards and acid standards. Every 5 samples a QBlank and QCheck of a standard (20 ng) were measured. Once all were measured, further Hg standards and blanks were measured.

The peak absorption for each sample was read from the signal graph produced by the AAS. The height of the increase was measured from each graph, measuring from the baseline readings to the top of the peak where it levelled off. The data was then entered into EXCEL and a calibration curve made. The results were then adjusted for standard drift in the values between blank and standard checks.

The samples were then corrected for the dilution and weight and the results produced in mg/g as follows; the unknown concentrations were converted to ng per measurement vessel using the calibration curve then converted into ng per sample.

The used mass (g) = (original sample weight (gm) x used extractant volume)/ dissolution volume (ml).

The sample concentration in (ng/g) was then calculated by dividing the AAS measurement by the used mass (g). To convert to mg/g, the sample concentration was further divided by 1000.

3.3.8. Radionuclide analysis

^{210}Pb dating was commissioned from the Quaternary Research Association and the Department of Geography, and was carried out on the cores OB5 and DMC1. Radiometric analyses were carried out in the Environmental Radioactivity Research Centre (ERRRC), University of Liverpool. ^{210}Pb, ^{226}Ra, ^{137}Cs and ^{241}Am were analysed by direct gamma assay using Ortec HPGe GWL (well-type) and GMX series coaxial low background intrinsic germanium detectors (Appleby et al., 1986). ^{210}Pb was determined via its gamma emissions at 46.5 keV, and ^{226}Ra by the 295 keV and 352 keV γ-rays emitted by its daughter radionuclide ^{214}Pb following 3 weeks storage in sealed containers to allow radioactive

equilibration. ^{137}Cs and ^{241} Amwere measured by their emissions at 662 keV and 59.5 keV respectively. To determine the absolute efficiencies of the detectors, calibrated sources and sediment samples of known activity were used and corrections were made for the effect of self absorption of low energy γ-rays within the sample (Appleby et al., 1992). (See appendix 4 for full dating report).

3.3.9. Statistical analysis

Statistical analysis was carried out for the different datasets individually. For clarity and ease of understanding, the statistical analysis methodology will not be included in this chapter but will precede the results in each of the chapters 4, 5 and 6.

4. Contemporary distributions of foraminifera

4.1. Introduction

Before a sea-level reconstruction is carried out at a study site, the relationship between foraminiferal assemblages with elevation within the tidal frame must be tested. The distribution of the foraminifera must be documented and defined in order to determine whether the modern dataset is appropriate to use for a sea-level reconstruction.

Contemporary foraminifera distribution data were collected with the aim of establishing whether they could be used to provide a modern training set. A total of 9 environmental variables were measured and used in the analysis including; elevation, salinity, pH, organic matter, grain size which is divided into clay%, silt% and sand%, percentage of *Phragmites* spp. vegetation cover and lastly distance from tidal influence. When the transects were combined the additional variable transect number was added in order to try and account for the different locations of the samples.

4.2. Statistical analysis

4.2.1. Data handling

Samples which had less than 150 individual foraminifera were removed from the analysis along with samples which had less than 100 dead foraminifera, with the exception of 5 samples which contained between 50-100 dead individuals. These were included in the dataset as the dominant species in these samples made up at least 50% of the sample, with no co-dominant species. Species which contributed less than 5% to the sample were also removed following Fatela and Taborda (2002), who concluded that species must represent at least 5% of the data in order for species to be significant in statistical analysis where a total of 100 foraminifera counts are made. The species data were converted into percentages before representing the data in species diagrams and carrying out statistical analysis.

Abundance was presented in the diagrams along with the percentage of agglutinated and calcareous species. As different amounts of sediment volume were counted for each sample (from 1.25 cm^2 to 10 cm^2), abundance was calculated as the number of individual tests per 5 cm^2. As this also ranged significantly from 50 to 3500 tests per sample, in order to present this on the diagram, the values were converted into percentages out of the maximum abundance value. Therefore, direct comparisons of abundances between

transects cannot be read from the diagrams, but this can only be used to identify trends in foraminifera numbers along the transect.

4.2.2. Foraminiferal zonations

The *Tilia* program (Grimm, 1991) was used to present the data and to perform cluster analysis using the *CONISS* program. Both stratigraphically constrained (e.g. Charman et al., 1998; Massey et al., 2006; Charman et al., 2002; Szkornik et al., 2006; Gehrels et al., 2001). and unconstrained (e.g. Horton, 1999; Horton et al., 1999b; Edwards et al., 2004b; Horton and Edwards, 2005; Engelhart et al., 2007; Horton and Edwards, 2006; Roe et al., 2009; Horton and Culver, 2008; Kemp et al., 2009a) cluster analyses were carried out on non-transformed data, based upon unweighted Euclidean distance. Stratigraphically constrained cluster analysis (i.e. in the order collected along the saltmarsh) was carried out in order to establish the distribution of the foraminifera across the marshes. Unconstrained cluster analysis was also carried to determine if there were any ecological zonations in the data related to elevation. In order to determine if elevation is related to the zonations established, it is important that cluster analysis is stratigraphically unconstrained as constrained cluster analysis will usually be constrained by elevation and, therefore, the zonations will be automatically related to the variable. Unconstrained cluster analysis re-orders the samples moving those which are similar close together and separating those which are dissimilar. The CONISS total sum of squares can then be used to delineate any zonations in the species data. These groups may be related to elevation, with each zone occupying a different height on the modern saltmarsh. Alternatively elevation may not be controlling factor, and groups may overlap in elevation reflecting changes due to other environmental variables. Following Horton et al. (1999b), scatterplots of cluster order vs. environmental variable can be used to determine what the zonations are most related to. Pearson product-moment correlation coefficient using the software package *Past* (Hammer and Harper, 2004) was used to determine the correlation coefficients (r^2) between the order of the samples from the cluster analysis and other environmental variables, along with the significance (p-value).

4.2.3. Ordination

The results were plotted in 2-dimensional space to determine if there were any patterns in the data and which samples and species were similar or associated with each other. Constrained ordination was additionally used to determine which environmental variables the species data were related to (Birks, 1995).

To determine which constrained ordination methods should be used, whether unimodal e.g. Canonical Correspondence Analysis (CCA), or linear e.g. Redundancy Analysis (RDA), the ordination methods e.g. Detrended Correspondence Analysis (DCA) (details of the different methods can be found in chapter 1.4.1) can be used to see how unimodal the data are. DCA (the unimodal equivalent of Principle Component Analysis, PCA) is an ordination technique which constructs a theoretical variable that best explains the species data by choosing the best values for the site that maximises the dispersion of the species scores. This is termed the first ordination axis. A second axis can also be constructed which also maximises the dispersion of the species scores, however it must not be correlated with the previous axis. The data are 'detrended' in order to overcome problems in CA due to the 'arch effect' where the second axis often shows a systematic quadratic relation to the first axis (Birks, 1995).

DCA was performed using the *Decorana* function in *Vegan* package (Oksanen et al., 2011) in *R* to determine whether linear or unimodal statistical methods are the most appropriate to use for that dataset (Birks, 1995). The unconstrained ordination gives a measure of the total heterogeneity in the species data with the total variability shown by the length of the axis (Leps and Smilauer, 2003). Birks (1995) stated that if the ordination axis length is <2 standard deviations (SD) the species are linear, whereas if it is >2 SD then several species must be unimodal. ter Braak (1995) also stated that response curves will be linear if the lengths of the ordination axes are <2 SD and states that for the species to be strongly unimodal the ordination axes length is >4 SD. Leps and Smilauer (2003) stated that if the gradient length is >4 SD, a unimodal method is most appropriate and if <3 SD a linear method may be more appropriate, with the area between 3 and 4 SD being ambiguous, with both working reasonably well. ter Braak and Prentice (1988) found the range of 1.5 – 3 SD both PCA and CA/DCA, or both RDA and CCA, can be used.

Oksanen (2011) stated that the origin of this method of using the length of the ordination axis is obscure, with the method often used in micropalaeontology reconstructions yet not

being based upon any research which shows that DCA is as good as, or better than PCA with short gradients (Oksanen, 2011). However, there was a study were DCA was found to perform better than PCA when the data are, compositional percentages, contain many zeros, and there are many variables (Anderson and Willis, 2003; Legendre and Legendre, 1998; ter Braak, 1995b). The method of DCA was created by Hill and Gauch (1980) as an improvement of the reciprocal averaging (RA) method. One of the main problems with RA was the arch effect (described above) which was corrected by DCA. The other problem was that the distances in the ordination space did not have a consistent meaning relating to compositional changes. Hill and Gauch (1980) corrected this and scaled the axes to SD units with a definite meaning of ordination length. Hill and Gauch (1980) found that if a species is unimodal, the full Gaussian curve was completed within 4 SD.

DCA can also be used to determine whether any of the measured environmental variables can be related to the theoretical axes and whether they are significant or not. The function *Envfit* was used in *Vegan* (Oksanen et al., 2011) which finds vectors of environmental variables and relates them to the DCA axis, determining the significance using a permutation test.

To further examine the relationship of the environmental variables and species, constrained ordination analyses were carried out. CCA and RDA are the constrained versions of DCA and PCA, respectively. These select combinations of the included variables that maximises the dispersion of the species scores as opposed to a theoretical variable like DCA and PCA. The CCA chooses the best weights for the variables and gives the results on the first axis. The second and further axes (as many axes as variables can be extracted) also select linear combinations of the variables that maximise dispersion of the species scores but uncorrelated to the previous axis (as CA) (ter Braak, 1995).

To test the significance of the environmental variables included in the analysis, an automatic forward and backward stepwise model using permutation tests was adopted using *Step* in *Vegan* (Oksanen et al., 2011). The analysis adds and removes the environmental variables depending on whether they improve the model or not. It builds the model so that it maximizes the adjusted r^2 at every step, and stops when the adjusted r^2 starts to decrease (Blanchet et al., 2008). CCA and/or RDA were then re-run with the significant variables only.

As stated above, the length of the gradient of the axis from the DCA can be used to establish whether unimodal (CCA) or linear (RDA) methods should be used to analyse the data. There is no definite value to determine which method is the most appropriate to use. Therefore, when ordination axis lengths are low (>4 SD), when either method may be appropriate, both analyses were carried out and the method which provided the results explaining the largest proportion of variance was considered the most appropriate (e.g. Puntí et al., 2009).

A further extension of the constrained ordination is partial canonical/constrained ordination which can be used to determine the effects of a single variable after removing the effects of the other variables. In partial canonical ordination the variables are replaced by the residuals obtained by regressing each of the variables on the covariables. Examples of studies where this has been carried out include; Horton et al. (1999b), Zong and Horton (1999), Sawai et al. (2004), Horton and Edwards (2006), Szkornik et al. (2006), Hill et al. (2007), Riveiros et al. (2007) and Horton and Culver (2008).

Peres-Neto et al. (2006) showed, however, that partitioning of CCA or RDA as it is currently applied is a biased method, and that adjustments are necessary to provide more accurate estimations and in order for comparisons between variables explaining community structure to be valid. Discrepancies between non-adjusted and adjusted fractions in variation partitioning were found to depend upon the difference between the numbers of variables in each set of predictors and the sample size. Therefore, comparisons between different studies are not appropriate. In order to compare the study sites accurately, the same method of adjusting must be used for all studies, or only studies with equal sample size and equal numbers of measured variables can be compared.

Varpart in the *Vegan* package (Oksanen et al., 2011) conducts variation partitioning based upon Peres-Neto et al. (2006). In order for the method to be unbiased, the adjusted r^2 is used to assess the partitions explained by the explanatory variables and combinations. Two to four explanatory variables can be calculated along with their combined effects. *Varpart* provides more information than partial CCA (pCCA) or partial RDA (pRDA) as it shows how the intercorrelation between the variables are divided, and so which variables are contributing the most to the intercorrelation proportion.

This function currently only allows RDA to be used in the multivariate partitioning as it is much more complicated to estimate the adjusted R^2 for CCA, and therefore unbiased analysis of CCA is not currently implemented (Legendre, 2007). The other disadvantage of using *Varpart* is that it is limited by the number of variables which can be used. As eight variables have been measured in this study, if more than four of these variables are found to be significant it is difficult to use *Varpart* for partitioning, therefore pCCA and pRDA are applied.

To test the difference between using pCCA, pRDA and adjusted variation partitioning all the data from the 5 transects was used along with four selected variables to determine how similar or different the results are for these data. The first two axes from DCA for the data are 2-3 SD so either method could be used. Table 4.1 shows the results of the three different methods for the same data. This illustrates that the main difference is the amount of explained variance in the data. The CCA method accounts for less variance than RDA or *Varpart,* this may be because the data is more linear than unimodal and therefore linear methods are more appropriate. As each method has a different amount of explained inertia, particularly the difference between RDA and CCA, the percentages of each variable from the total inertia is different between the methods. However, the proportions each variable contributes to the explained amount is similar between all methods, particularly the variation partitioning and the pRDA percentages when they are rounded to the nearest whole number. The main difference between these two methods is the proportion of intercorrelation which is less for *Varpart.* This may be because the correlation is split between the variables, whereas the intercorrelation from pRDA is calculated from the residual inertia which is not explained by the individual variables combined. Although not perfect, the use of pRDA is reasonable to use when more than 4 variables need to be included in the analysis. Where 2 to 4 variables are found to be significantly affecting the species data *Varpart* is used to identify the contributions made by the environmental variables individually and with other variables.

Correlations were also carried out for the environmental variables to see which variables were related or associated with each other using *Past* (Hammer and Harper, 2004). Distance from tidal influence was included as a variable, because, unlike most other studies the elevation in the transects did not always increase with increasing distance from the seaward edge and is therefore considered as a separate variable to elevation. As the transects differ in the vegetation present, particularly *Phragmites* spp*.,* the presence and

absence of *Phragmites* spp. was also included as a variable in the analysis in order to determine if this affects the species distribution data.

Table 4.1 Example of the different methods used to 'partial-out' the variance for all data (live DM) with only four variables included.

Method	VARPART			pCCA			pRDA		
	Variance	% of total variance	% of explained variance	Variance	% of total variance	% of explained variance	Variance	% of total variance	% of explained variance
Total	0.5243			0.39409			0.5475		
Organic matter	0.04561	5%	9	0.03082	3%	8	0.0497	5%	9
Phragmites spp.	0.11598	12%	22	0.07417	7%	19	0.1175	12%	22
Elevation	0.19574	20%	37	0.1335	13%	34	0.1944	19%	36
pH	0.06633	7%	13	0.08274	8%	21	0.0697	7%	13
Intercorrelation	0.10064	10	19	0.07286	7	19	0.1162	12	21

4.2.4. Response models

In addition to the analyses described above, response models were used to mathematically describe the observed relationship between species and elevation. Response models are simple mathematical representations of the species distribution along the elevation gradient. They were used in order for the response patterns to be described clearly. The response of different species to the elevation gradients have been produced for each transect, as well as for the combined data, to identify the elevations at which each species can be found as well as the optimum elevation. The response of individual species can be modelled in different ways e.g. generalised linear models (GLMs) (Nelder and Wedderburn, 1972), generalised additive models (GAMs) (Hastie and Tibshirani, 1986) or Huisman-Olff-Fresco models (HOF) (Huisman et al., 1993). HOF models were used in this study as they allow more flexible expression of different response curve shapes and are more appropriate to use for ecological data (Huisman et al., 1993). The HOF model method fits a model from a series of five pre-determined models (figure 4.1) and was carried out using the *Gravy* (gradient analysis in vegetation) package in *R* (Oksanen et al., 2011). The HOF method fits a hierarchical set of five increasingly complex response models. This allows the simplest possible model to be chosen which describes the observed pattern the most (Huisman et al., 1993). The different models can be seen in figure 4.1 and are described as follows: Model 1 has no trend; Model 2 shows an increasing or decreasing trend to the maximum; Model 3 shows an increasing or decreasing trend below the maximum attainable response; Model 4 is a unimodal response curve; and Model 5 has a skewed response curve in which the most parsimonious model is selected using a least likelihood

criteria. WA using *C2* (Juggins, 2007) was also used to determine the elevation optima and maxima for each of the species.

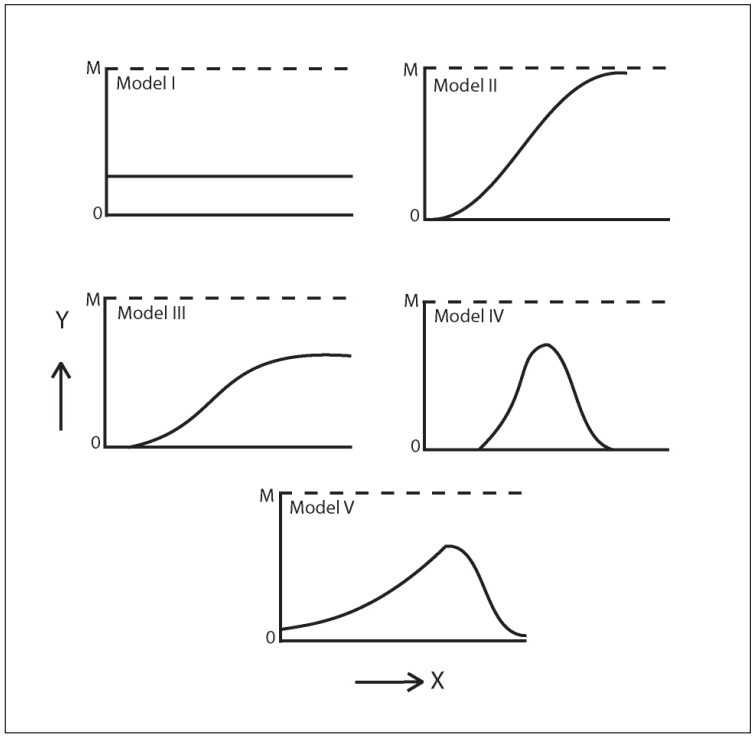

Figure 4.1 HOF models (Huisman et al., 1993).

4.3. Results of contemporary data

4.3.1. Environmental variables

Figures 4.2 and 4.3 show the measured environmental variables along the transects. The three transects from Oglet Bay show similar altitudes ranging from 4.362 to 5.872 m OD, with a range of 1.51 m. The upper elevation of the saltmarsh was restricted due to the 12 m cliff at the back of the marsh and lower marsh was restricted to the 1 m drop in elevation to the mudflat which is currently eroding. Oglet Bay has an obvious vegetation succession across the saltmarsh with *Phragmites* spp. in areas at the back of the marsh, followed by *Scirpus maritimus*, *Spartina* spp*.* A*ster tripolum* and *Agrostis stolonifera* (table 4.2). Decoy Marsh has a much higher altitude, ranging from 5.285 to 5.882 m OD with a much smaller altitudinal range of 0.597 m. It is vegetated by low grasses, i.e. *Festuca rubra* and is currently grazed by horses.

Table 4.2 Example of vascular plant zonation at Oglet Bay.

Altitude (m OD)	Vascular plants
5.672	*Phragmites australis*
4.822	*Scirpus maritimus*
4.792	*Scirpus maritimus* *Limonium vulgare* *Agrostis stolanifera* *Aster trioplum*
4.722	*Agrostis stolonifera* *Lumonium vulgare* *Aster tripolum*
4.652	
4.532	Spartina spp. *Agrostis stolonifera*
	Mud flat

All transects and sites have low salinities ranging from 0 to 4.46‰, which is freshwater. Transects OBSS1 and DMSS2 have the highest salinities, whilst transect OBSS3 has the lowest. All transects increase in salinity with increasing distance from the high marsh.

The organic matter content is similar for all transects and ranges from 66 to 6%; the lowest organic matter content can be seen in Decoy Marsh compared with higher organic matter content in Oglet Bay. The organic matter content was found to decrease along all the transects towards the water. pH ranges from 8.4 to 7 and is similar for all transects, decreasing along the transects away from the high marsh.

The grain size of most of the transects is predominantly silt, making up approximately 80% of the composition, followed by clay which makes up roughly 10%, with sand contributing the least (<10%). Transects OBSS2 and DMSS1 show no significant changes in grain size along the marsh. In contrast, OBSS1 and OBSS3 show an increase in grain size in the high marsh area at the back of the marsh, with higher sand content up to 70%. DMSS2 has an increase in grain size in the lower marsh, with sand increasing to 40% of the composition and reduced silt content.

Correlation coefficients were determined for the variables for each transect and combined datasets. These show (tables 4.3 to 4.8) that many of the variables from OBSS1 (table 4.3) are correlated strongly and significantly with each other. For example salinity has a significant and strong relationship with pH, silt, clay, *Phragmites* spp. presence, elevation and distance. Elevation is also related to many variables, i.e. distance, sand, clay, silt, organic matter content, pH and salinity.

Less highly inter-correlated variables were found for OBSS2 (table 4.4) with elevation relating to distance, salinity, organic matter content and *Phragmites* presence. For OBSS3 (table 4.5) elevation is related to distance, salinity, pH, sand, silt and clay; and salinity is related to many variables: elevation, distance, silt and sand. When variables were combined for Oglet Bay there were less significant correlations, with elevation and distance having a positive relationship, and distance being related to clay, silt and organic matter. It was found for the combined Decoy Marsh variables (table 4.7) that organic matter was related to many variables, i.e. transect, elevation, distance, sand, clay and silt. Transect is related to distance, clay and organic matter. Elevation is related to distance, sand and organic matter. When all data from both sites are combined (table 4.8) organic matter is related to most variables, distance, transect, clay and silt; transect is related to clay, silt, and organic matter; and elevation is only strongly related to distance.

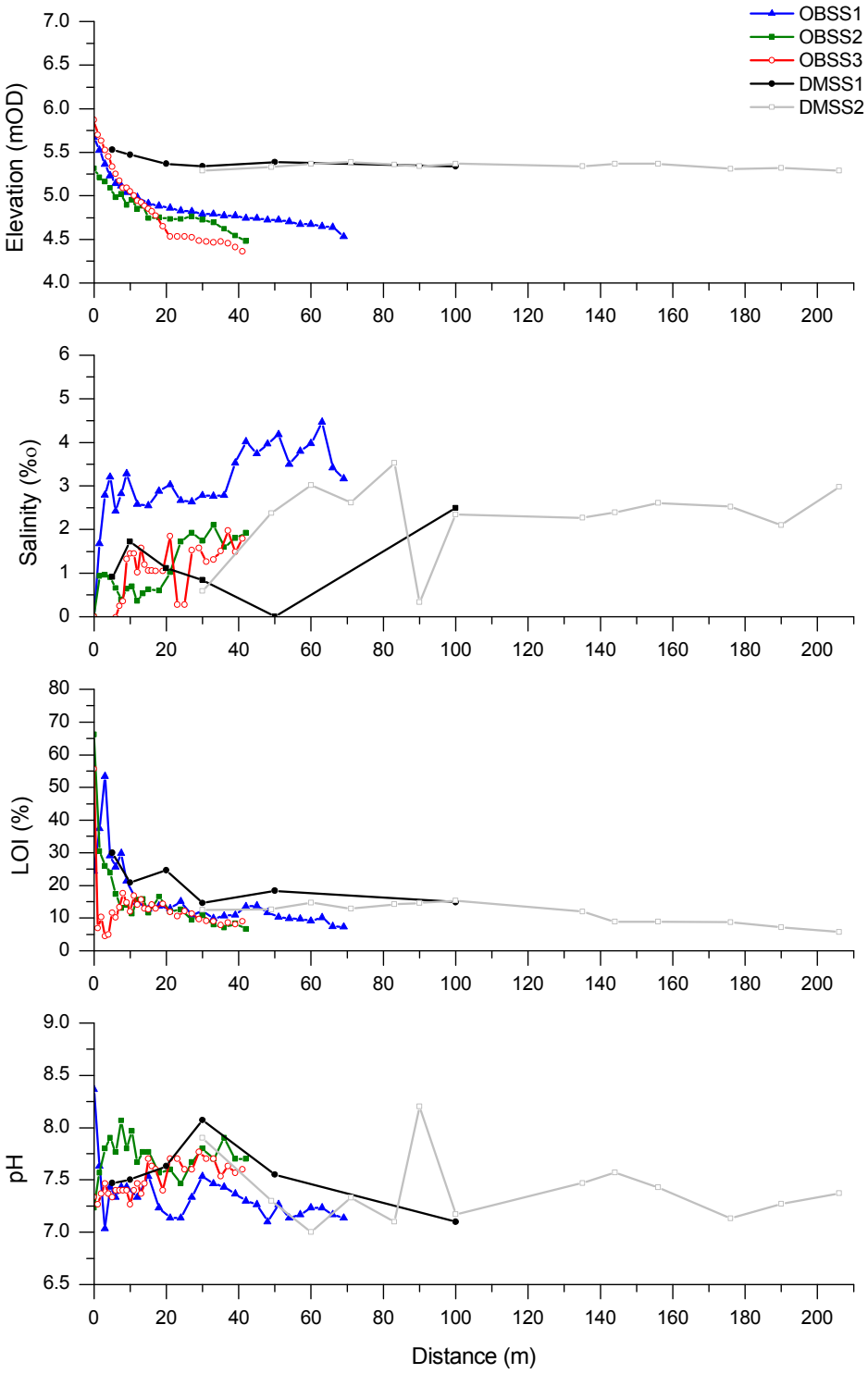

Figure 4.2 Environmental variables (elevation, salinity, organic matter, pH) from all 5 transects.

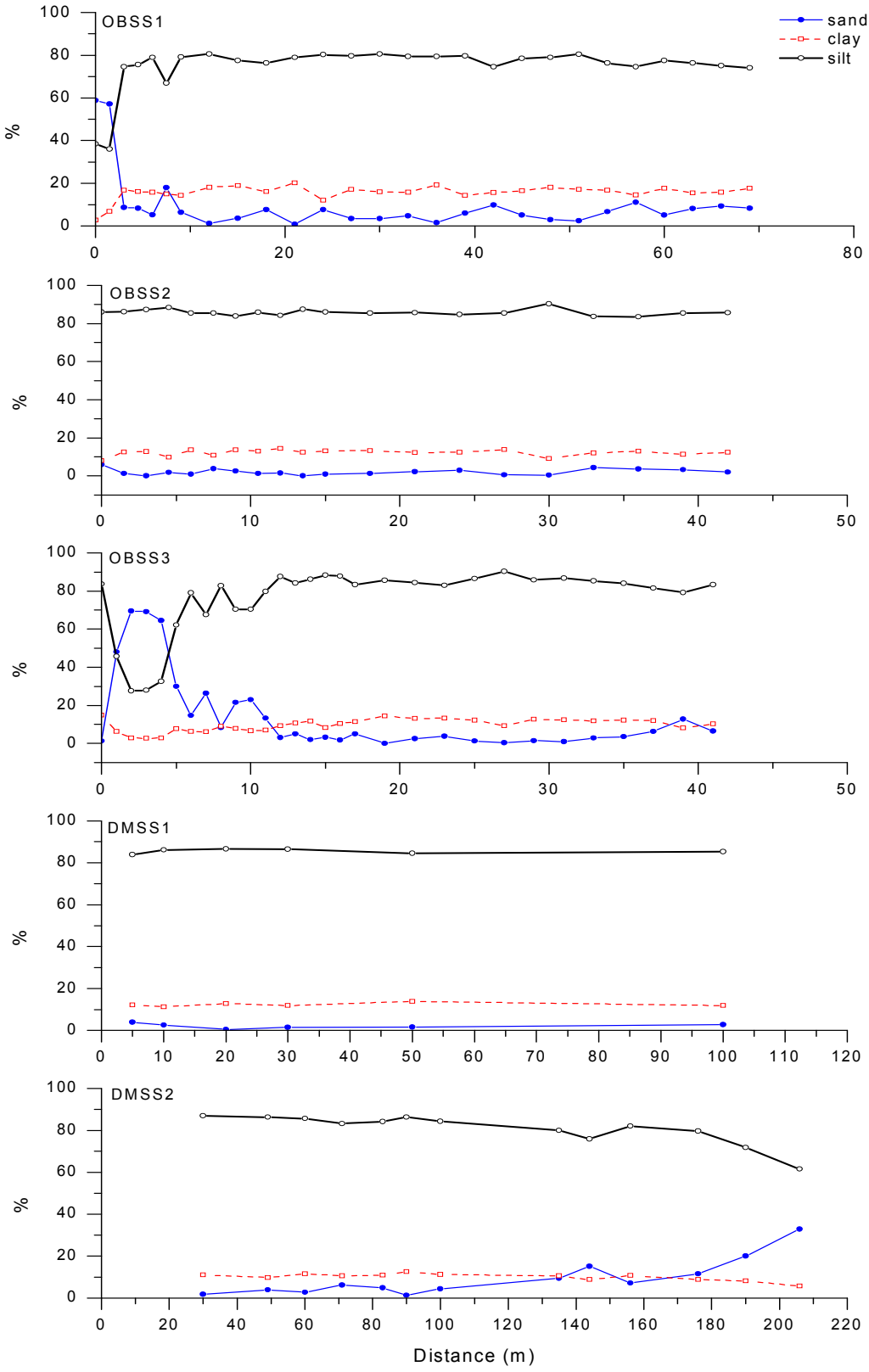

Figure 4.3 Grain size fractions for each transect.

Table 4.3 Correlation coefficient matrix of environmental variables from OBSS1, p-values in grey and r^2 >0.6 in bold.

	Sand %	Clay %	Silt %	Organic matter	pH	Salinity	*Phragmites spp.*	Elevation	Distance
Sand %	0	0	0	0.019	0	0	0.102	0	0.050
Clay %	**-0.913**	0	0	0.064	0	0	0.157	0	0.068
Silt %	**-0.991**	**0.851**	0	0.015	0	0	0.100	0	0.054
Organic matter	0.450	-0.361	-0.462	0	0.346	0.027	0	0	0.000
pH	**0.713**	**-0.714**	**-0.687**	0.189	0	0	0.144	0	0.009
Salinity	**-0.685**	**0.643**	**0.674**	-0.425	**-0.763**	0	0.001	0	0
Phragmites spp.	0.322	-0.280	-0.323	**0.643**	0.289	**-0.612**	0.000	0	0
Elevation	**0.726**	**-0.657**	**-0.721**	**0.829**	**0.646**	**-0.775**	**0.750**	0	0
Distance	0.381	-0.356	-0.375	**0.728**	0.492	**-0.701**	**0.886**	**0.864**	0

Table 4.4 Correlation coefficient matrix of environmental variables from OBSS2, p-values in grey and r^2 >0.6 in bold.

	Sand %	Clay %	Silt %	Organic matter	pH	Salinity	Phragmites pp.	Elevation	Distance
Sand %	0	0.035	0.032	0.115	0.171	0.998	0.293	0.866	0.636
Clay %	-0.473	0	0.013	0.013	0.416	0.796	0.990	0.200	0.730
Silt %	-0.481	-0.545	0	0.402	0.639	0.796	0.312	0.269	0.424
Organic matter	0.363	**-0.546**	0.198	0	0.007	0.009	0.184	0.000	0.002
pH	-0.319	0.193	0.112	**-0.581**	0	0.863	0.646	0.619	0.891
Salinity	-0.001	0.062	-0.062	**-0.565**	0.041	0	0.027	0.001	0
Phragmites spp.	-0.247	-0.003	0.238	0.310	-0.110	-0.495	0	0.005	0.001
Elevation	0.040	-0.299	0.260	**0.789**	-0.118	-0.680	**0.598**	0	0
Distance	-0.113	-0.082	0.190	**0.644**	-0.033	**-0.836**	**0.700**	**0.929**	0

Table 4.5 Correlation coefficient matrix of environmental variables from OBSS3, p-values in grey and r^2 >0.6 in bold.

	Sand %	Clay %	Silt %	Organic matter	pH	Salinity	Elevation	Distance
Sand %	0	0	0	0.118	0.003	0	0	0.001
Clay %	**-0.856**	0	0	0.041	0.004	0.009	0.001	0.002
Silt %	**-0.995**	0.803	0	0.154	0.004	0	0	0.001
Organic matter	-0.291	0.375	0.267	0	0.169	0.408	0.044	0.086
pH	-0.522	0.509	0.508	-0.258	0	0.006	0	0
Salinity	**-0.605**	0.467	**0.612**	-0.157	0.491	0	0	0
Elevation	**0.693**	**-0.588**	**-0.691**	0.371	**-0.778**	**-0.763**	0	0
Distance	**0.571**	-0.537	**-0.559**	0.318	**-0.740**	**-0.719**	**0.924**	0

Table 4.6 Correlation coefficient matrix of environmental variables from Oglet Bay, p-values in grey and r^2 >0.6 in bold.

	Sand %	Clay %	Silt %	Organic matter	pH	Salinity	Elevation	Distance	*Phragmites spp.*	Transect
Sand %	0	0	0	0	0.138	0.107	0.001	0.346	0.039	0
Clay %	0.473	0	0	0	0.642	0.694	0	0	0.001	0
Silt %	0.552	**0.992**	0	0	0.506	0.522	0	0	0.001	0
Organic matter	0.357	**0.95**	**0.927**	0	0.708	0.957	0	0	0.003	0
pH	-0.153	-0.048	-0.069	-0.039	0	0	0.318	0.866	0.018	0.612
Salinity	0.166	0.041	0.066	-0.006	-0.55	0	0.005	0.429	0.403	0.002
Elevation	0.097	0.527	0.532	0.515	-0.103	-0.286	0	0	0.805	0
Distance	0.55	**0.813**	**0.779**	**0.875**	0.017	-0.082	**0.632**	0	0.461	0
Phragmites spp.	0.328	-0.325	-0.331	-0.297	0.241	-0.086	0.026	-0.076	0	0
Transect	-0.211	**0.762**	**0.79**	**0.676**	0.052	-0.306	0.426	0.472	-0.5	0

Table 4.7 Correlation coefficient matrix of environmental variables from Decoy Marsh, p-values in grey and r^2 >0.6 in bold.

	Sand %	Clay %	Silt %	Organic matter	pH	Salinity	Transect	Elevation	Distance
Sand %	0	0	0	0.003	0.319	0.055	0.069	0.118	0
Clay %	**-0.917**	0	0	0	0.194	0.007	0.008	0.050	0
Silt %	**-0.993**	**0.863**	0	0.008	0.381	0.101	0.125	0.163	0
Organic matter	**-0.637**	**0.729**	**0.589**	0	0.528	0.032	0	0	0
pH	-0.242	0.311	0.213	0.154	0	0	0.365	0.855	0.184
Salinity	0.447	**-0.598**	-0.388	-0.493	**-0.782**	0	0.021	0.410	0.022
Transect	0.425	**-0.586**	-0.364	**-0.733**	-0.220	0.525	0	0.018	0.007
Elevation	-0.371	0.455	0.334	**0.783**	-0.045	-0.201	-0.534	0	0.015
Distance	**-0.811**	**0.760**	**0.800**	**0.817**	0.319	-0.523	**-0.600**	**0.549**	0

Table 4.8 Correlation coefficient matrix of environmental variables from Oglet Bay and Decoy Marsh, p-values in grey and r^2 >0.6 in bold.

	Sand %	Clay %	Silt %	Organic matter	pH	Salinity	Elevation	Distance	*Phragmites spp.*	Transect
Sand %	0	0	0	0	0.138	0.107	0.001	0	0.039	0
Clay %	0.473	0	0	0	0.642	0.694	0	0	0.001	0
Silt %	0.552	**0.992**	0	0	0.506	0.522	0	0	0.001	0
Organic matter	0.357	**0.950**	**0.927**	0	0.708	0.957	0	0	0.003	0
pH	-0.153	-0.048	-0.069	-0.039	0	0	0.318	0.013	0.018	0.612
Salinity	0.166	0.041	0.066	-0.006	-0.550	0	0.005	0	0.403	0.002
Elevation	0.328	0.527	0.532	0.515	-0.103	-0.286	0	0.409	0.805	0
Distance	**0.817**	0.546	**0.605**	0.366	-0.252	0.422	0.085	0	0	0
Phragmites spp.	-0.211	-0.325	-0.331	-0.297	0.241	-0.086	0.026	-0.373	0	0
Transect	0.550	**0.762**	**0.790**	**0.676**	0.052	-0.306	0.426	0.506	-0.500	0

4.3.2. Foraminiferal assemblages

Ninety-six out of the 105 samples collected were analysed for foraminifera. Eighty-two samples remained after samples which did not contain more than 150 individuals and 100 dead individuals were removed (with the exception of five samples). This removed one uppermost sample from OBSS1, one sample from OBSS2, eight samples from OBSS3, and four samples from DMSS1. Most of the samples were removed because they did not contain any foraminifera due to their high altitude (above HAT). More than 23,500 individuals of 34 species were identified but once minor species were removed (>5%) the dataset was reduced to 13 species.

Oglet Bay

Transects OBSS1 and OBSS2 were dominated by two agglutinated species *Haplophragmoides* spp*.* and *Miliammina fusca* (figures 4.4 and 4.5). OBSS1 was also dominated by the calcareous species *Ammonia beccarii* spp*.* In contrast, OBSS3 is dominated by more agglutinated species, *Haplophragmoides* spp*. Jadammina macrescens, M. fusca* and *Trochammina inflata* (figure 4.6).

Figures 4.4 to 4.18 show the results of the foraminifera data in relation to elevation, along with the constrained cluster analysis results. Figure 4.4 shows three main foraminifera zones for OBSS1. The first, high marsh zone (1a) characterised by *Haplophragmoides* spp*., M. fusca and J. macrescens* with few *Ammonia beccarii* spp*.* The middle marsh zone (1b), dominated by less *Haplophragmoides* spp*., M. fusca* and greater dominance of *Ammonia beccarii* spp. The next lower zone (1c) is distinguished by its lower number of *Haplophragmoides* spp. and *Ammonia beccarii* spp*.,* as well increased amounts of calcareous species (*Ammonia beccarii* spp., Elphidium spp*.*)

OBSS2 (figure 4.5) is divided into three main zones. The first higher marsh zone (2a) is dominated by *Haplophragmoides* spp*., M. fusca* and a small amount of *Balticammina pseudomacrescens.* The middle zone (2b) is distinguished by having no *B. pseudomacrescens* present, then a low marsh zone (2c) by low numbers of *Haplophragmoides* spp*.,* increased amounts of *J. macrescens* and increases in all calcareous species (*Ammonia beccarii* spp., *Elphidium* spp*. Haynesina* spp*. Brizalina* spp*.*)

The cluster analysis carried out for OBSS3 (figure 4.6) shows the foraminifera assemblage divided into three distinct groups. The main high marsh group (3a) identified is dominated by *Haplophragmoides* spp*., J. macrescens,* and *M. fusca.* The middle marsh group (3b) is

distinguishable by its higher abundance of calcareous species. Sample 11 is singled out on its own as it is distinguished from the above and below due to its higher *T. inflata*. The low marsh group (3c) is dominated by more *Haynesina* spp. with the absence of *Haplophragmoides* spp.

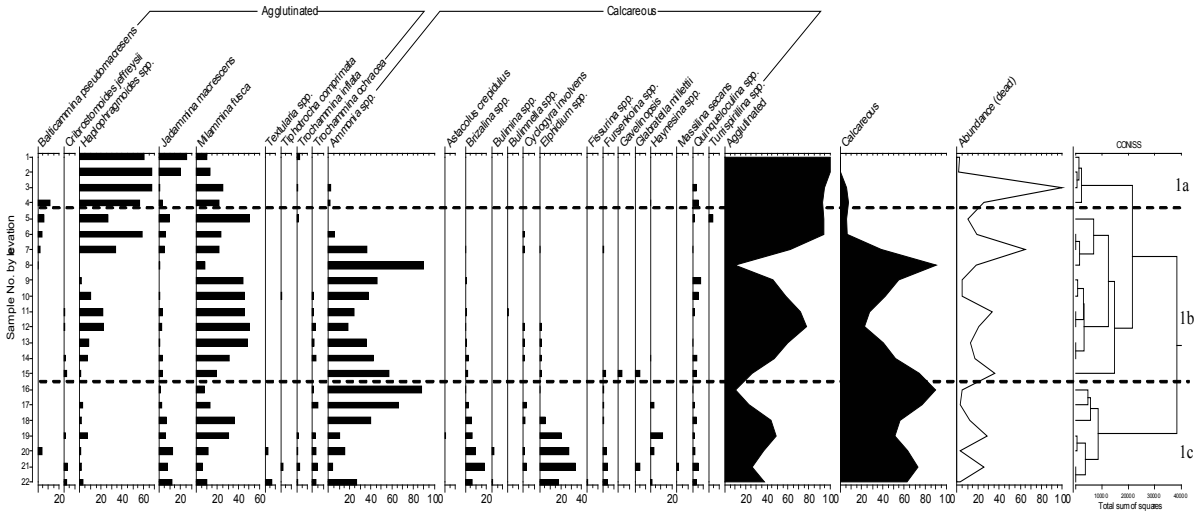

Figure 4.4 Relative percentages of dead foraminifera abundance for OBSS1. Ordered by elevation from high (1) to low (22), with constrained cluster analysis based upon unweighted Euclidean distance.

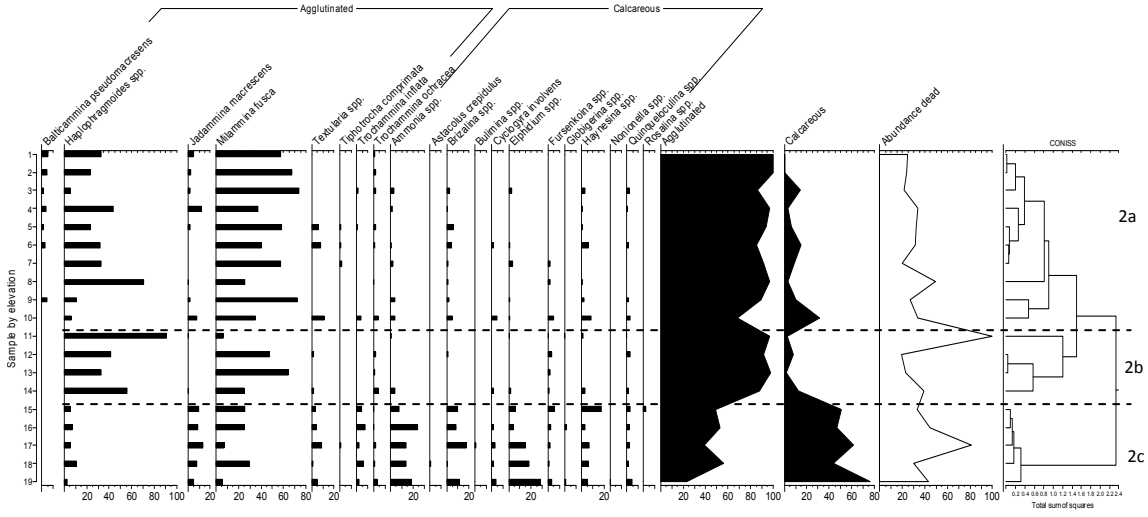

Figure 4.5 Relative percentages of dead foraminifera abundance for OBSS2. Ordered by elevation from high (1) to low (18), with constrained cluster analysis based upon unweighted Euclidean distance.

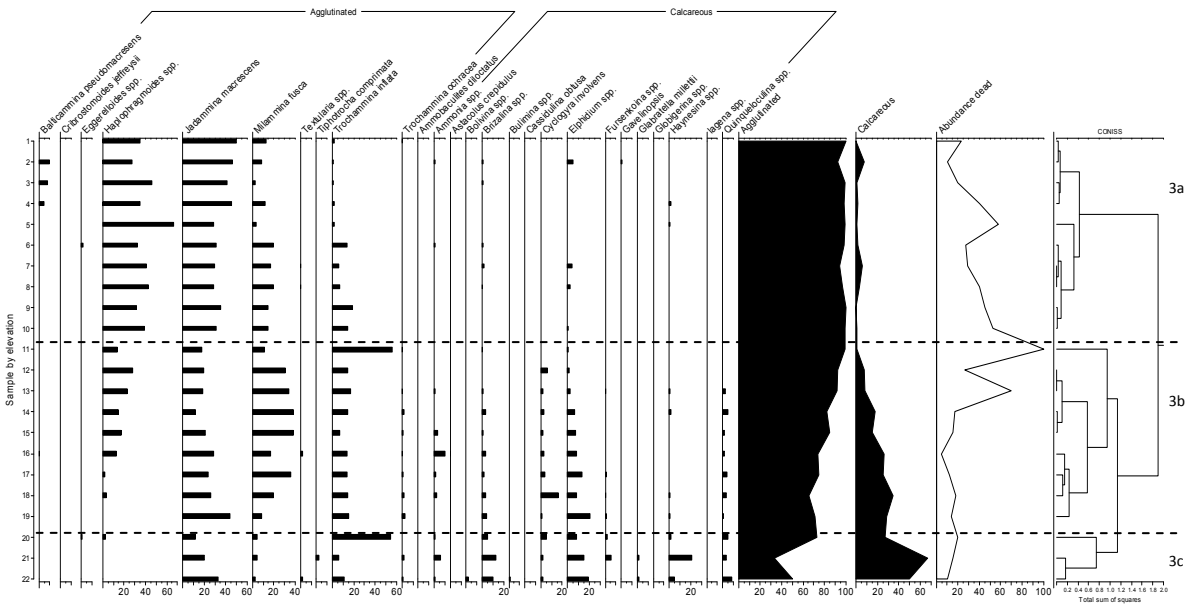

Figure 4.6 Relative percentages of dead foraminifera abundance for OBSS3. Ordered by elevation from high (1) to low (22), with constrained cluster analysis based upon unweighted Euclidean distance.

The data from the Oglet Bay transects were combined and can be seen in figure 4.7. The samples collected from the highest elevations (OBa) contain high percentages of *Haplophragmoides* spp*., J. macrescens,* and *M. Fusca, B. pseudomacrescens* with some *Ammonia beccarii* spp*.* increasing lower down. The middle elevation samples (OBb) have less *Haplophragmoides* spp*.* and *J. macrescens,* with increasing amounts of calcareous species including *Ammonia beccarii* spp*.* Finally, the lower elevation samples (OBc) contain less *Ammonia beccarii* spp. and *Haplophragmoides* spp*.* with increasing numbers of *J. macrescens* and increasing calcareous species, in particular *Elphidium* spp*.*

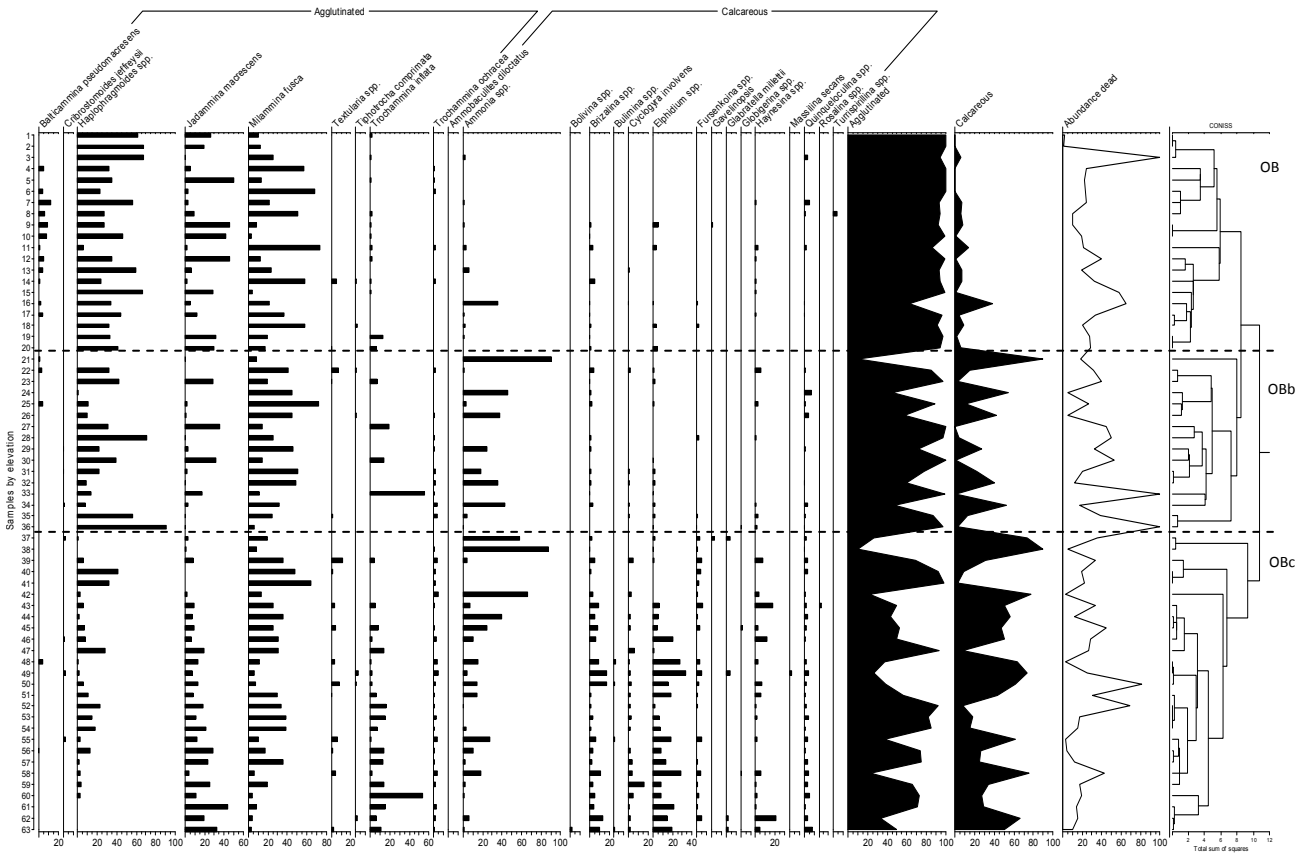

4.7 Relative percentages of dead foraminifera abundance for combined Oglet Bay transects. Ordered by elevation from high (1) to low (63), with constrained cluster analysis based upon unweighted Euclidean distance.

Figures 4.8 to 4.10 show the results of the live data for all three Oglet Bay transects. OBSS1 (figure 4.8) live data can be seen to be very similar to the dead assemblages (figure 4.4) particularly for the agglutinated species. However, there are several calcareous species (*Elphidium* spp*. and Brizalina* spp.) which are absent in the live data. The constrained cluster analysis was found to be very similar to the dead data with the only noticeable difference being an increase in the number of samples of the zone 1a L (figure 4.8) compared to 1a (figure 4.4).

Figure 4.9 shows the live assemblage for OBSS2. When compared with the dead data (figure 4.5), the live data have similar abundance and distribution of agglutinated species. The diversity of the calcareous species in the live data is much less than in the dead assemblage and the abundance of these is also reduced. The zonations defined by the constrained cluster analysis for the live data were found to be the same as those in the dead data.

The results of the live data for OBSS3 can be seen in figure 4.10. Similarly to the OBSS1 and OBSS2 assemblages, the number of calcareous species is reduced in the live data as well as the abundance of these. The agglutinated species for both the live and dead for OBSS3 are similar, although there is a greater number of *T. inflata* present in the live data. The constrained cluster zonations for live assemblage also changes as a result of the increase of *T. inflata* at the lower part of the marsh, as well as a decrease in numbers of *M. fusca*, resulting in only two main zones (figure 4.10).

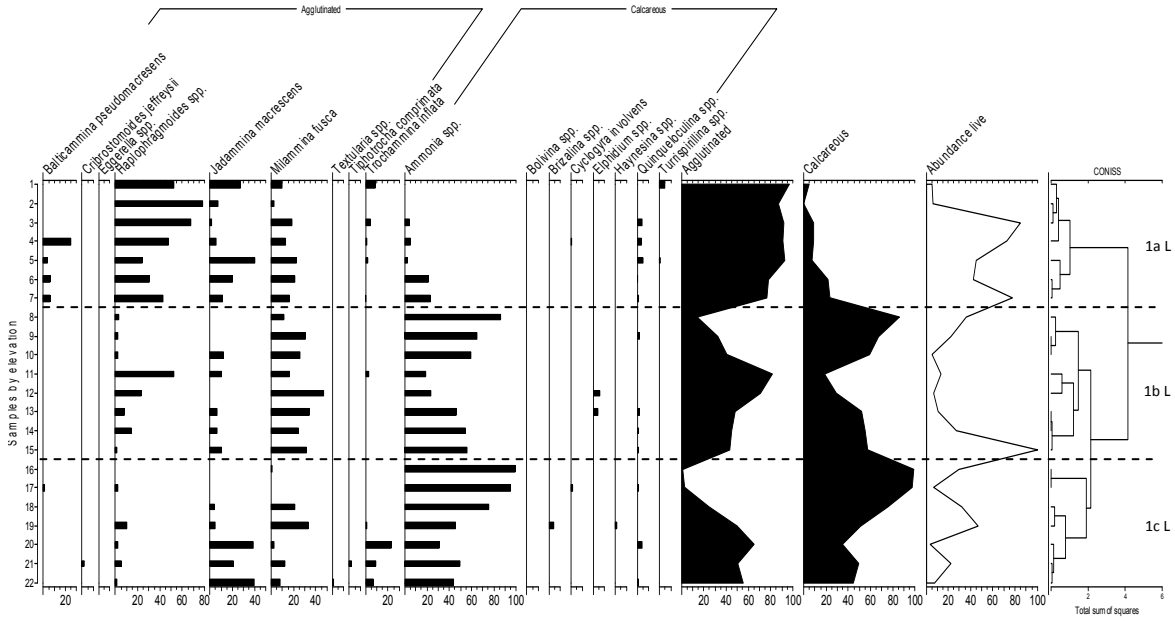

Figure 4.8 Relative percentages of live foraminifera abundance for OBSS1. Ordered by elevation from high (1) to low (22), with constrained cluster analysis based upon unweighted Euclidean distance.

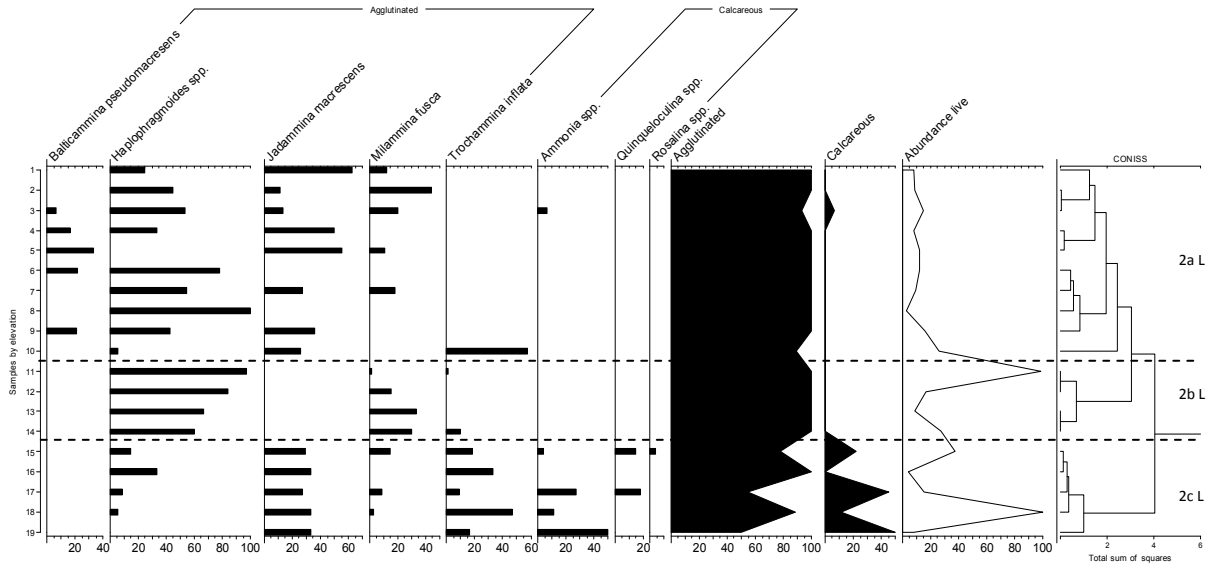

Figure 4.9 Relative percentages of live foraminifera abundance for OBSS2. Ordered by elevation from high (1) to low (19), with constrained cluster analysis based upon unweighted Euclidean distance.

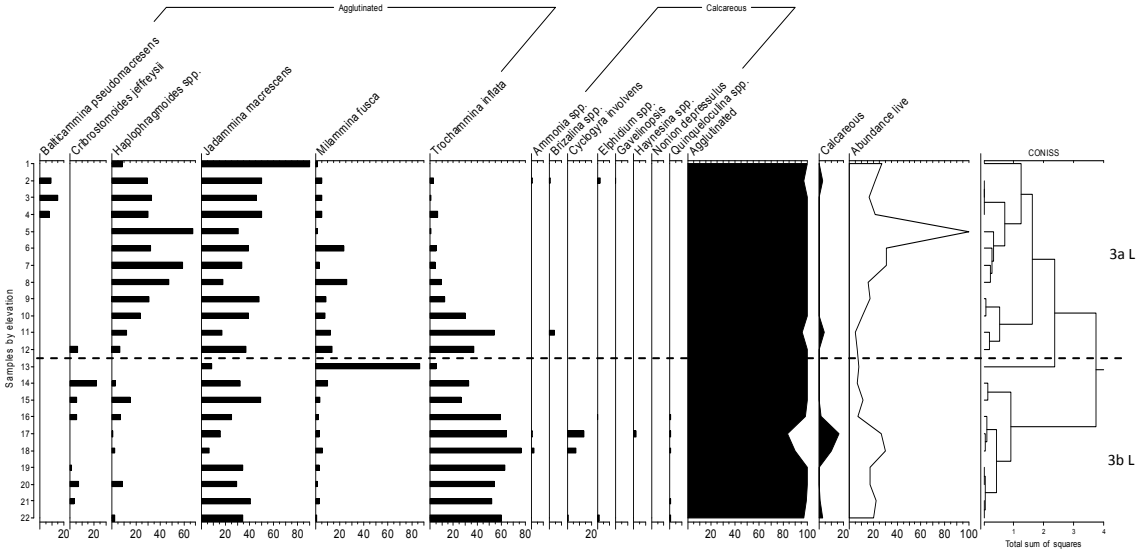

Figure 4.10 Relative percentages of dead foraminifera abundance for OBSS3. Ordered by elevation from high (1) to low (22), with constrained cluster analysis based upon unweighted Euclidean distance.

Decoy Marsh

DMSS1 (figure 4.11) contains only six samples, as four were removed due to too few foraminifera present. The cluster analysis reveals two zones. The higher altitude zone (4a) has *B. pseudomacrescens, Haplophragmoides* spp*., J. macrescens,* and *M. fusca* present whilst the lower of the group (4b) is contains little *B. pseudomacrescens* and *M. fusca.* The cluster analysis applied to DMSS2 (figure 4.12) identifies two species zones. The majority of the samples are very similar, most probably due to the samples having similar elevations. The only difference is the absence of some agglutinated species in the lower part of the marsh.

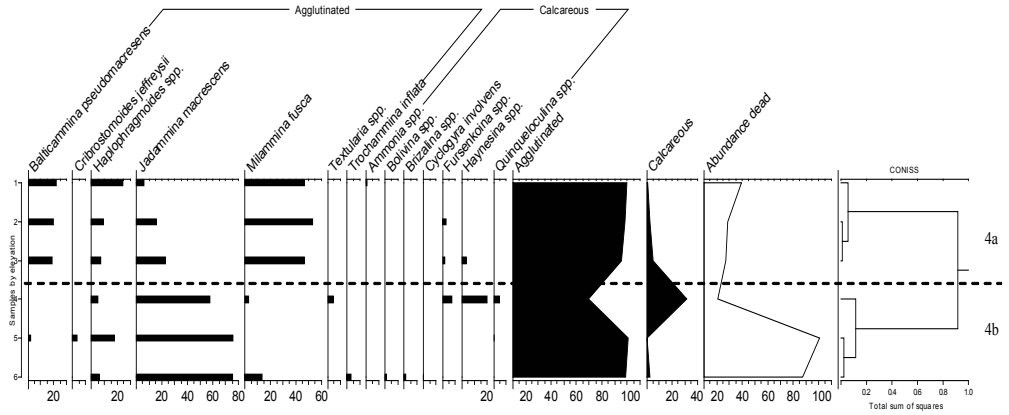

Figure 4.11 Relative percentages of dead foraminifera abundance for DMSS1. Ordered by elevation from high (1) to low (6), with constrained cluster analysis based upon unweighted Euclidean distance.

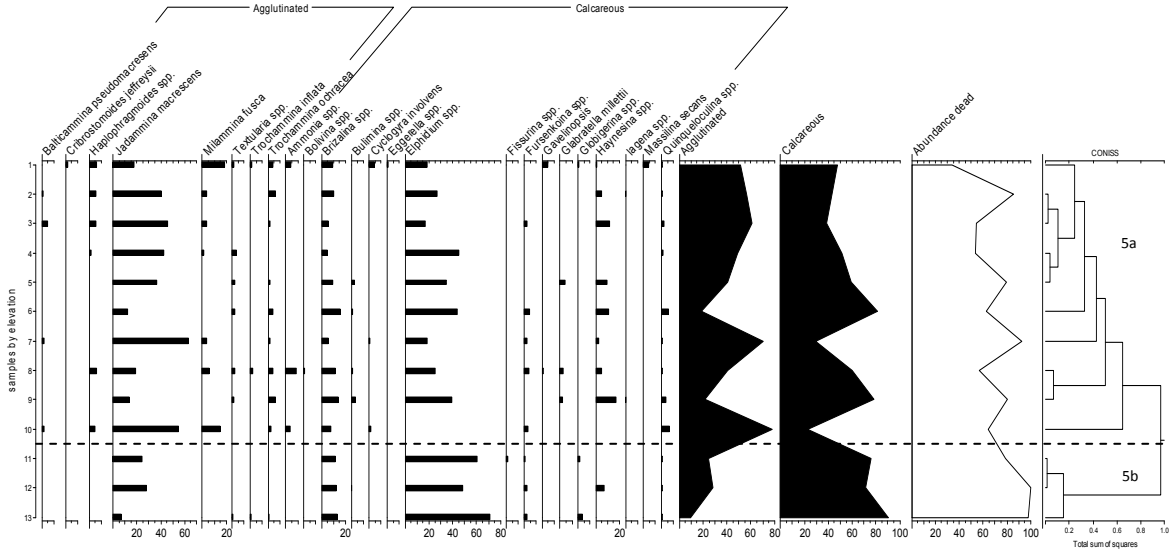

Figure 4.12 Relative percentages of dead foraminifera abundance for DMSS2. Ordered by elevation from high (1) to low (12), with constrained cluster analysis based upon unweighted Euclidean distance.

The two transects from Decoy Marsh show different assemblages, the main difference being the presence of calcareous species, particularly *Elphidium* spp., throughout the DMSS2 transect, compared with DMSS1 where few calcareous species were found. This is problematic when adding the two transect data together as the samples overlap in elevation but the percentage of calcareous to agglutinated varies up and down in relation to which transect the sample was taken (figure 4.13). There are three clear zones identified, 6a, which contains two samples whish have high *B. pseudomacrescens, Haplophragmoides* spp*.* and *M. Fusca.* The second (6b), contains high *J. Macrescens, low M. Fusca,* and greater *Elphidium* spp*.* Zone 6c is very similar to zone 6b.

The live data for the two transects can be seen in figures 4.14 and 4.15. The live data in DMSS1 shows a similar assemblage to the dead data. This is reflected in the constrained cluster analysis were similar zones can be defined. The live data in DMSS2, however, only contain the agglutinated species with no calcareous species present. The constrained cluster analysis also reveals different zonations. Figure 4.10 shows the DMSS1 and DMSS2 live data combined and reveals that these assemblages are much more consistent than the dead data. The combined assemblage can be divided into two main zones, a higher zone, 6a L, which is distinguished from the lower zone 6b L by the higher numbers of *B. pseudomacrescens.*

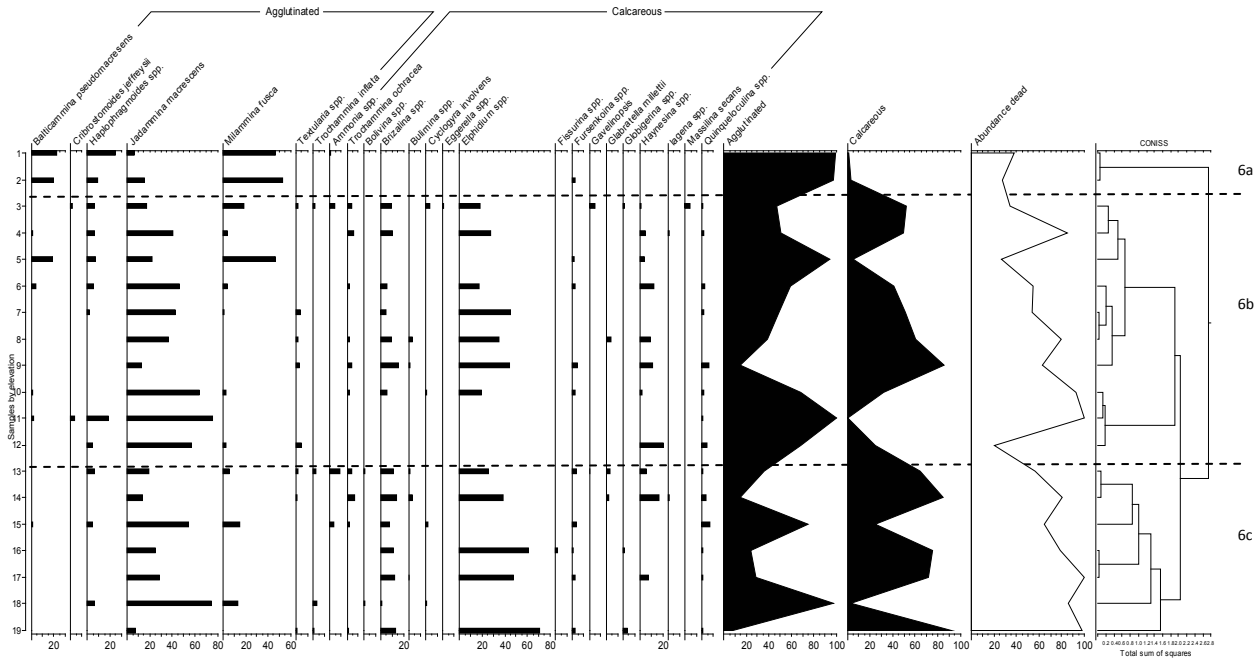

Figure 4.13 Relative percentages of dead foraminifera abundance for combined Decoy Marsh transects. Ordered by elevation from high (1) to low (18), with constrained cluster analysis based upon unweighted Euclidean distance.

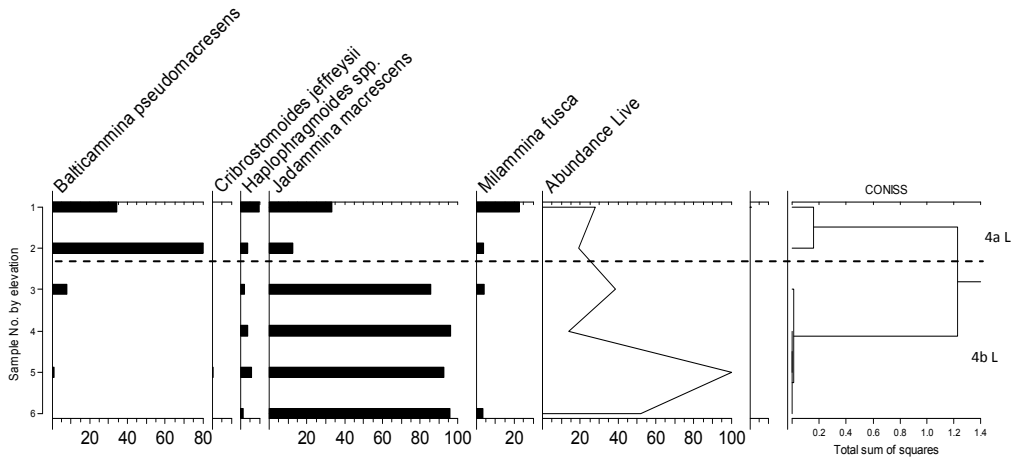

Figure 4.14 Relative percentages of live foraminifera abundance for DMSS1. Ordered by elevation from high (1) to low (6), with constrained cluster analysis based upon unweighted Euclidean distance.

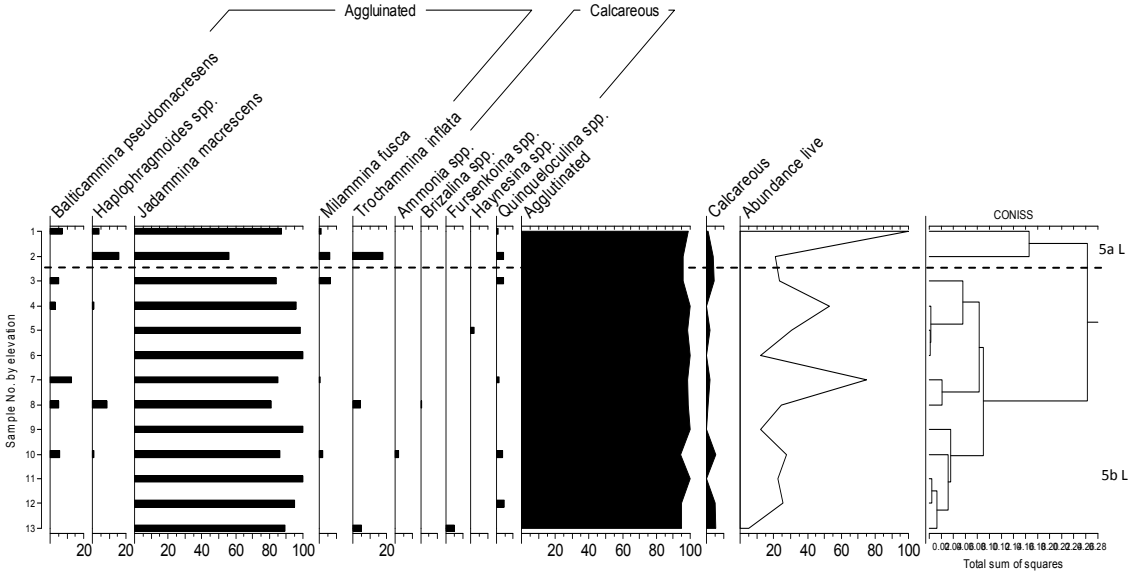

Figure 4.15 Relative percentages of live foraminifera abundance for DMSS2. Ordered by elevation from high (1) to low (13), with constrained cluster analysis based upon unweighted Euclidean distance.

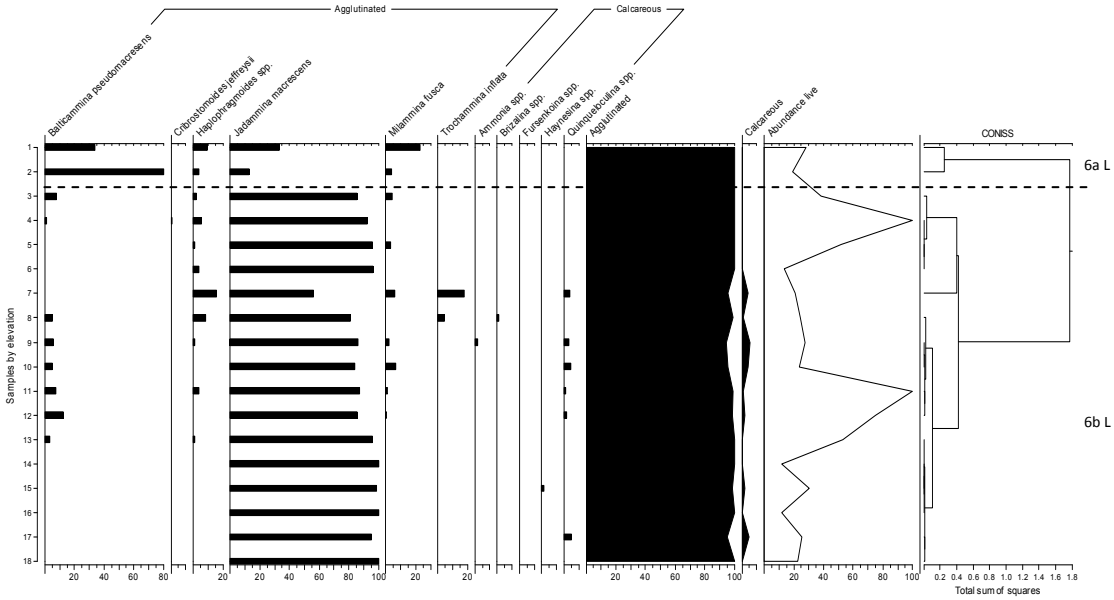

Figure 4.16 Relative percentages of live foraminifera abundance for combined Decoy Marsh. Ordered by elevation from high (1) to low (18), with constrained cluster analysis based upon unweighted Euclidean distance.

Combined Oglet Bay and Decoy Marsh

Figure 4.17 shows the combined (ODBDM) dead data for both sites. It shows that there is a complicated distribution in relation to elevation, and there seems to be no clear zonation. It shows there to be calcareous species present in the very highest elevations as well as the lowest. *Haplophragmoides* spp., *J. macrescens* and *M. fusca* are found to be the most dominant species, and these are present at all altitudes in all transects. *T. inflata* and *Ammonia beccarii* spp. appear to be present in the lower altitudes and *B. pseudomacrescens* present in the higher samples. The assemblage has been divided into three zones, zone 7a comprising of high abundances of *J. Macrescens* and *Elphidium* spp. Zone 7b which comprises of greater abundances of *Haplophragmoides* spp. and *M. Fusca* and less *Elphidium* spp. Zone 7c contains a similar assemblage but with greater abundance of *Elphidium* spp. and *Ammonia app.*

As discussed above, the live and dead data from Decoy Marsh are different in their species composition and abundance due to the presence and high abundance of calcareous species in the dead DMSS2 data which is not present in the DMSS1 data. There is evidence to suggest that the dead species data from Decoy Marsh are unreliable. The live data in DMSS2 contain only agglutinated species with no calcareous species present. This is unusual as it would be expected that it would be the dead data that contain less calcareous due to dissolution processes. It is possible that the dead calcareous component was

inwashed onto the marsh by an extreme high tide and is anomalous for several reasons. As two transects were taken from the same location which overlap in elevation and distance, it would be expected that they show similar results and similar species. However, the fact that there is a difference between the two suggests that this is related to the time the sampling was carried out. Seasonality may be a factor as the second transect was sampled in the beginning of spring, however, the change in populations occurs in the dead data whereas we would expect a change more in the live if caused by a bloom or increased population. The only other difference between the time of sampling is the spring equinox which took place after the collection of DMSS1 but before collection of transect DMSS2. The foraminiferal composition of DMSS2 contains both high marsh and low marsh species, with several shelf species indicating that there has been a mixing of the species across the marsh. It is unlikely that the calcareous species are inhabiting the marsh due to the high elevation within the tidal frame and also the live data show a much lower abundance of calcareous species. The most likely explanation, therefore, is that the dead calcareous species have been inwashed due to an extraordinary high tide which took place before the sampling, i.e. the spring equinox which occurred in March 2010.

Therefore, the live DMSS data were added to the dead Oglet Bay data to test whether this improved the results by giving a clearer zonation. Figure 4.18 shows the combined assemblage and a clearer zonation can be seen. The constrained cluster analysis reveals two distinct zones. The higher elevational samples (7a L) contain predominantly *J. macrescens*. It is distinct from the zone below (7b L) due to its low numbers of *Haplophragmoides* spp. and *M. fusca*. The higher zone (7a L) contains predominantly Decoy Marsh samples which are at a higher elevation than Oglet Bay, with the Oglet Bay transects in the lower zone (7b L).

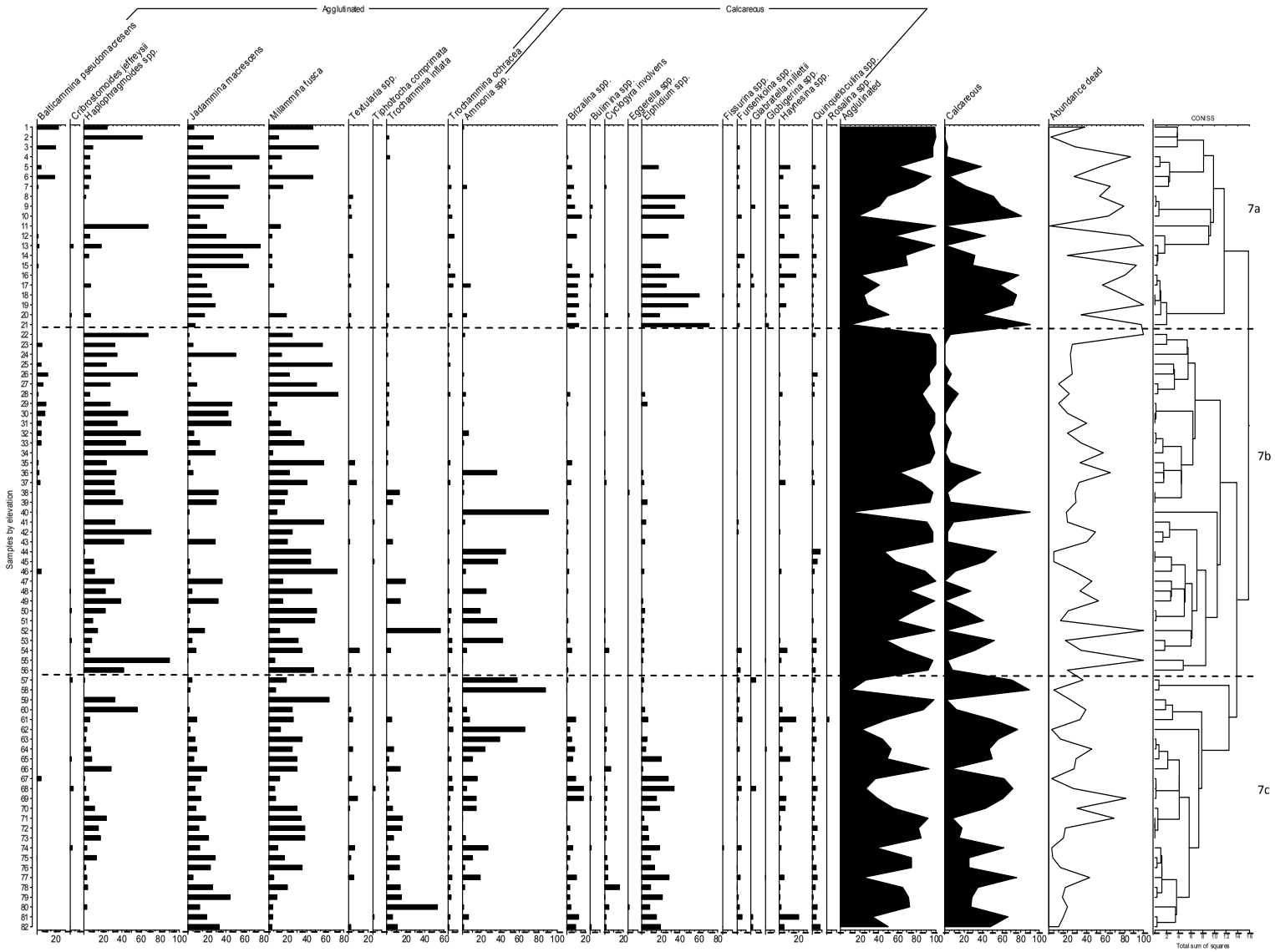

Figure 4.17 Relative percentages of dead foraminifera abundance for combined Oglet Bay and Decoy Marsh transects. Ordered by elevation from high (1) to low (82), with constrained cluster analysis based upon unweighted Euclidean distance.

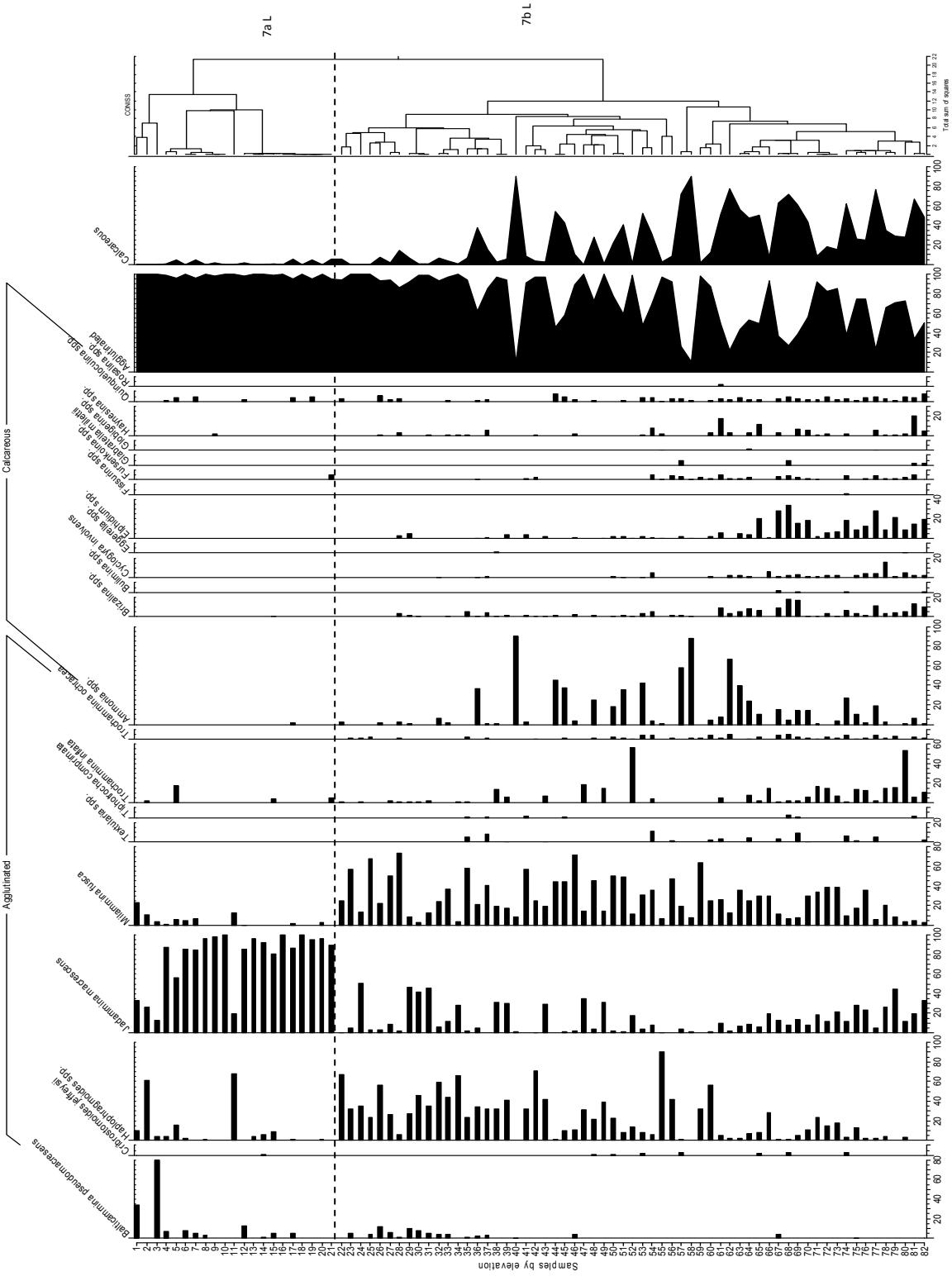

Figure 4.18 Relative percentages of live foraminifera abundance for combined Oglet Bay and Decoy Marsh transects. Ordered by elevation from high (1) to low (82), with constrained cluster analysis based upon unweighted Euclidean distance.

4.3.3. The relationship between foraminiferal assemblages and environmental variables

Oglet Bay

OBSS1

Table 4.9 and figure 4.19 show the DCA results for OBSS1. The species *Haplophragmoides* spp. and *B. pseudomacrescens* seem to be related to the higher marsh samples and *Quinqueloculina* spp. the lower elevation samples.

The measured environmental variables which were most related to each DCA axis were determined and can be seen in table 4.9 and figure 4.19**.** It shows that axis 1 is positively related to clay and salinity and negatively with organic matter, *Phragmites* spp., elevation and distance from the marsh edge, i.e. tidal influence. This indicates that the samples and species which are located in the left, negative, part of the diagram are related to high organic matter, *Phragmites* spp*.,* high elevation and high distance from the marsh edge, whilst those in the right, positive, part are more closely related to salinity.

This can be further examined using a constrained analysis where measured environmental variables as opposed to theoretical variables are used. This can be seen in figure 4.19. The lengths of the first two DCA axes shown in table 4.9 are low (<3 SD) and therefore ambiguous, i.e. both unimodal and linear methods of statistical analysis could be used. Both unimodal (CCA) and linear methods were carried out and it was determined that RDA was most appropriate as it explained more of the variance in the data. The results of the RDA can be seen in table 4.10 and show that the nine variables included explain 70% of the total variance. *Step* in *Vegan* (Oksanen et al., 2011) was used to determine which environmental variables contributed significantly to explaining the total inertia. The results show that elevation and distance were significant in explaining the species data (50%) (figure 4.11). *Varpart* in *Vegan* (Oksanen et al., 2011) was used to determine how this explained proportion was divided between elevation and distance, and the results of which can be seen in table 4.12 and figure 4.20. It shows that elevation (22%) makes up most of the explained variance followed by the intercorrelation (13%) then distance (11%).

Table 4.9 DCA results for OBSS1

	DCA1	DCA2	DCA3	DCA4
Eigenvalues	0.4956	0.365	0.04958	0.08084
Decorana values	0.4974	0.2609	0.03034	0.02025
Axis lengths	2.3562	2.3188	0.7449	0.95689

	DCA1	DCA2	r2	Pr(>r)	Significance (p value)
Sand %	-0.6642	0.747557	0.1989	0.097	0.1
Clay %	0.645549	-0.76372	0.2507	0.055	0.1
Silt %	0.671098	-0.74137	0.1638	0.142	1
Organic matter	-0.99968	0.025348	0.6591	0.001	0.001
Salinity	0.909165	0.416436	0.3794	0.016	0.05
PH	-0.73013	-0.68331	0.1527	0.2	1
Phragmites spp.	-0.91709	-0.39867	0.5885	0.001	0.001
Elevation	-0.98528	-0.17093	0.7929	0.001	0.001
Distance	-0.84939	-0.52777	0.8599	0.001	0.001

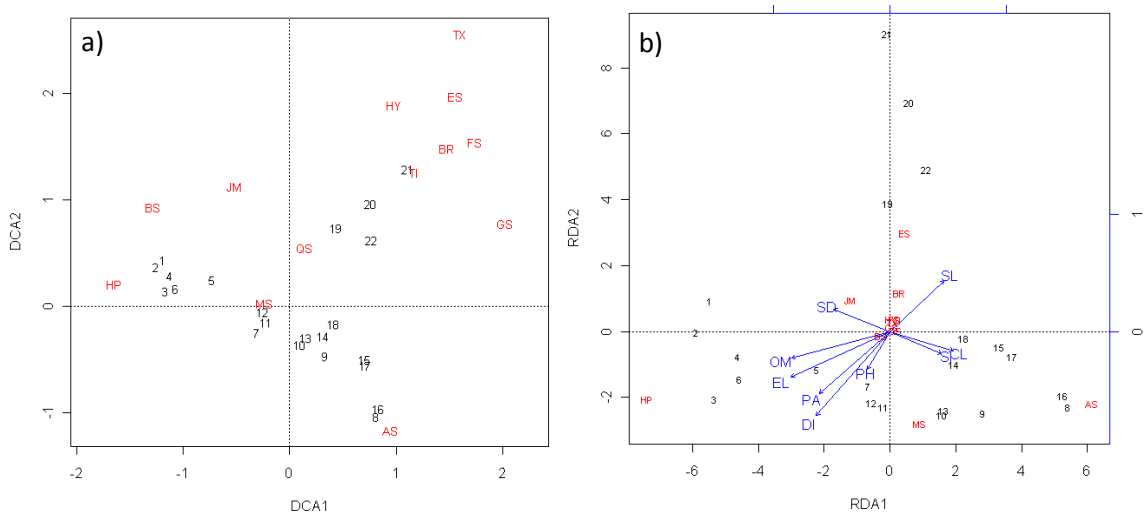

Figure 4.19 a) DCA b) RDA plots for OBSS1. AS=*Ammonia beccarii spp., BS= B. pseudomacrescens,* BR=*Brizalina spp.,* ES= *Elphidium spp.,* FS= *Fursenkoina spp.*, GS=*Glabratella milletti,* HP= *Haplophragmoides spp.,* HY= *Haynesina spp.*, JM= *J. macrescens,* MS= *M. fusca,* QS= *Quinqueloculina spp.*, TX=*Textularia spp.,* TI= *T. inflata*. SD=sand, SL=salinity, OM=organic matter, EL=elevation, PA=*Phragmites* spp. presence, DI=distance, PH=Ph, CL=clay, SI=silt.

Table 4.10 RDA for OBSS1 with all environmental variables.

	Inertia	Proportion	Rank
Total	1811.6859	1	
Constrained	1262.6022	0.6969	8
Unconstrained	549.0837	0.3031	13

Table 4.11 RDA for OBSS1 with only significant variables included (elevation and distance).

	Inertia	Proportion	Rank
Total	1811.686	1	
Constrained	909.540	0.502	2
Unconstrained	902.146	0.498	13

Table 4.12 Variance partitioning with significant variables only for OBSS1.

Variable	Variance	Significance	% of total inertia	% of constrained inertia
All	0.44962			
Elevation	0.21608	0.002	22	48
Distance	0.10642	0.013	11	24
Intercorrelations	0.12713		13	28

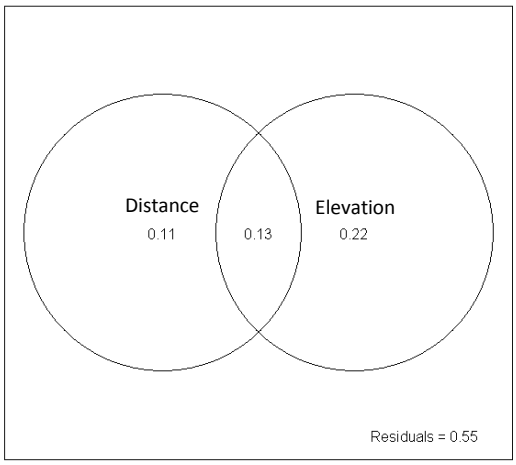

Figure 4.20 Diagram of variance partitioning with significant variables only for OBSS1.

Figure 4.21 shows the species response curves to elevation for the different species with the best fit models. The species coefficients from WA also show the optimum elevations for each species. It shows *M. fusca, Ammonia beccarii* spp. and *Haplophragmoides* spp. having unimodal distributions, *B. pseudomacrescens* and *J. macrescens* occupying a high marsh position, and *Brizalina* spp., *Elphidium, Gavelinopsis* spp., *Haynesina* spp., *Textularia* spp. and *T. inflata* having optima in the low marsh. WA using *C2* (Juggins, 2007) provides the optima and tolerances for each of the species (table 4.13). These have been plotted in figure 4.22 and show that the calcareous species seem to have a narrow vertical distribution and the agglutinated higher marsh species have a wider distribution, particularly *J. macrescens*.

Unconstrained cluster analysis for OBSS1 divides the assemblage into three zones (figure 4.23). The first is dominated by *Haplophragmoides* spp., *J. macrescens* and *M. fusca*. The second is dominated predominantly by *M. fusca, Ammonia beccarii* spp. and calcareous species. The third is similar to the second but with less calcareous species. The second and third zones overlap in elevation, therefore the transect is divided by the first CONISS division only, giving two groups, a high and low marsh (figure 4.24). Figure 4.25 and table 4.14 shows the results of the correlations (r^2) of the sample cluster order and the environmental variables, and shows organic matter content (0.65), salinity (-0.6), *Phragmites* spp. (0.73), elevation (0.77) and distance (0.76) to be significant.

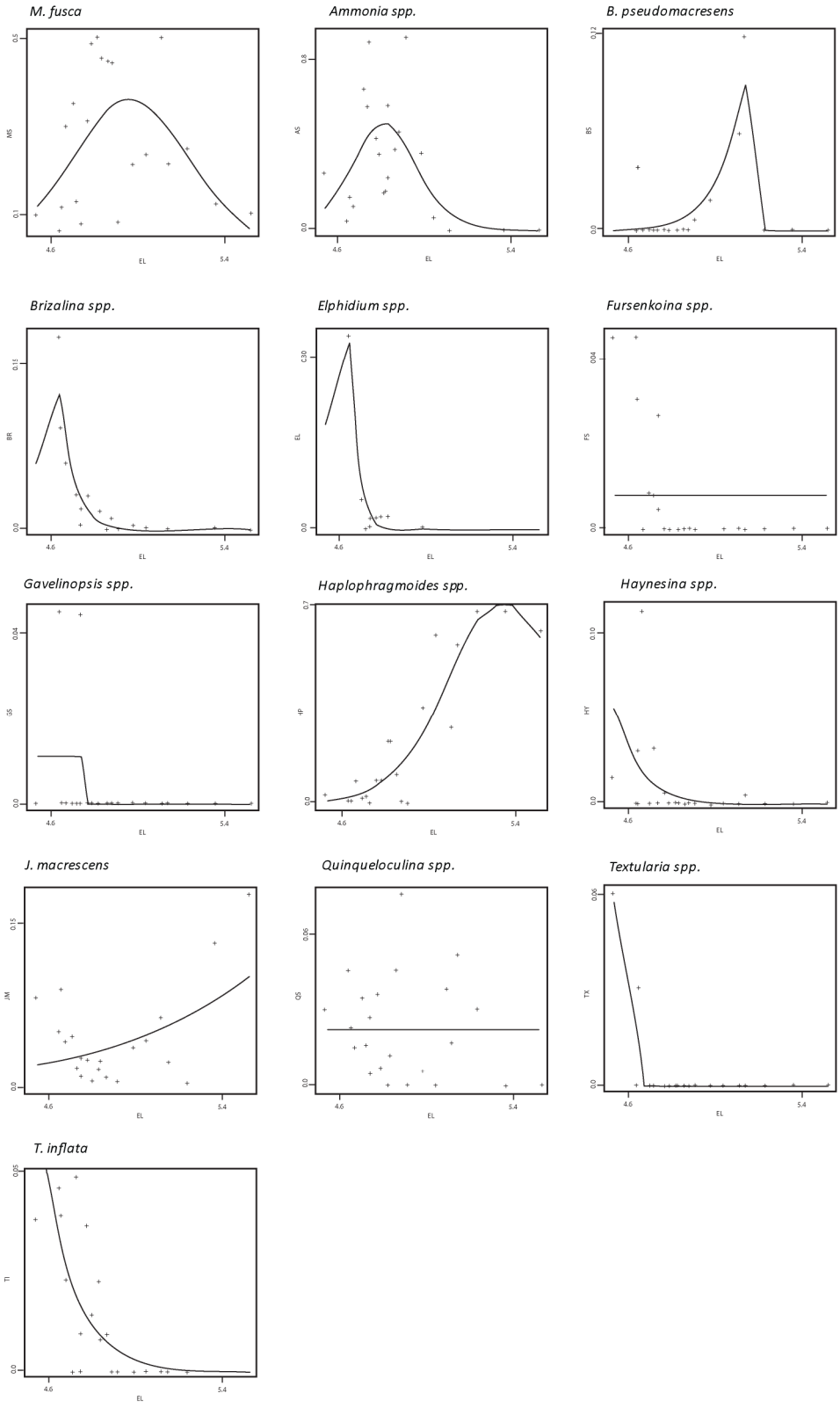

Figure 4.21 Species response curves to elevation for OBSS1.

Table 4.13 Species coefficients from WA for OBSS1.

Species	Count	Max	N2	Optimum	Tolerance
Ammonia beccarii spp.	19	90.26	12.0428	4.79254	0.113636
B. pseudomacrescens	6	11.79	3.75841	5.03635	0.191055
Brizalina spp.	14	17.61	6.3304	4.67071	0.0837709
Elphidium spp.	11	33.52	4.82113	4.64422	0.0718213
Fursenkoina spp.	8	4.55	5.00906	4.64379	0.0967557
Glabratella milletti	2	4.55	1.99994	4.68972	0.0707107
Haplophragmoides spp.	20	67.86	9.37802	5.14155	0.249273
Haynesina spp.	6	11.36	2.70293	4.67829	0.107507
J. macrescens	21	26.44	10.3907	5.01026	0.377013
M. fusca	22	50.42	16.3635	4.88806	0.200988
Quinqueloculina spp.	17	7.62	11.8649	4.83649	0.203714
Textularia spp.	2	6.06	1.80783	4.57044	0.0848528
T. inflata	11	4.84	8.45199	4.69491	0.096214

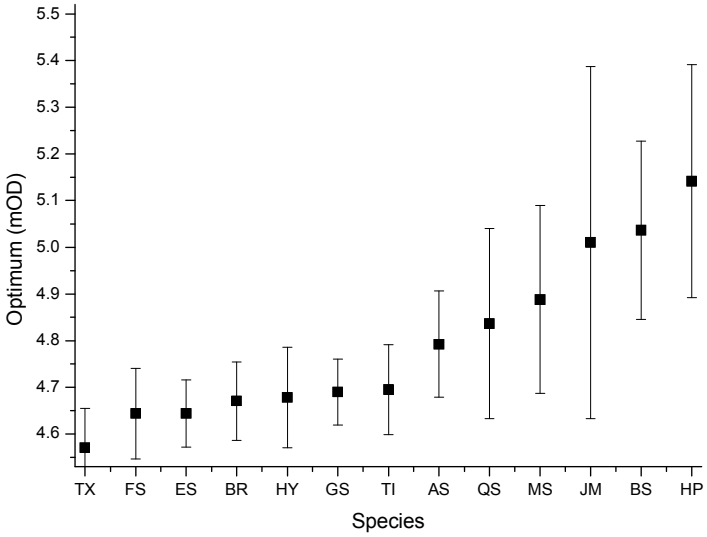

Figure 4.22 Optimum altitude of species from OBSS1 with tolerance levels (results from WA, c2) (Y axis altitude gradient). BS=*B. pseudomacrescens,* BR=*Brizalina spp.,* ES=*Elphidium spp.,* FS=*Fursenkoina spp.*, GS=*Glabratella milletti,* HP=*Haplophragmoides spp.,* HY=*Haynesina spp.,* JM=*J. macrescens,* MS=*M. fusca,* QS=*Quinqueloculina spp.*, TX=*Textularia spp.,* TI=*T. inflata*.

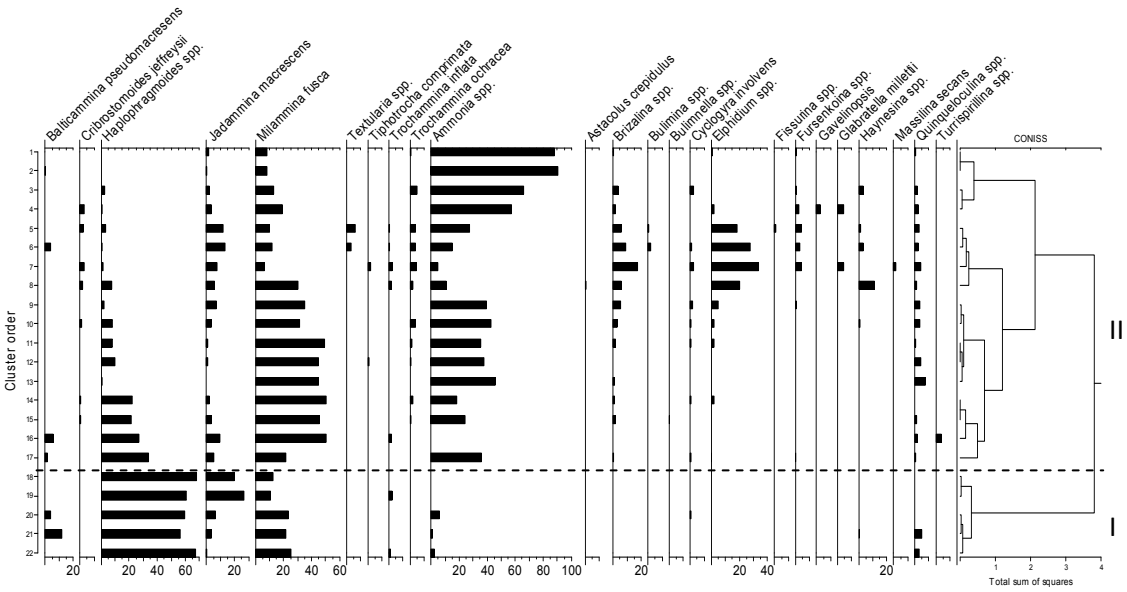

Figure 4.23 OBSS1 unconstrained cluster analysis based on unweighted Euclidean distance for relative percentages of dead foraminifera abundance.

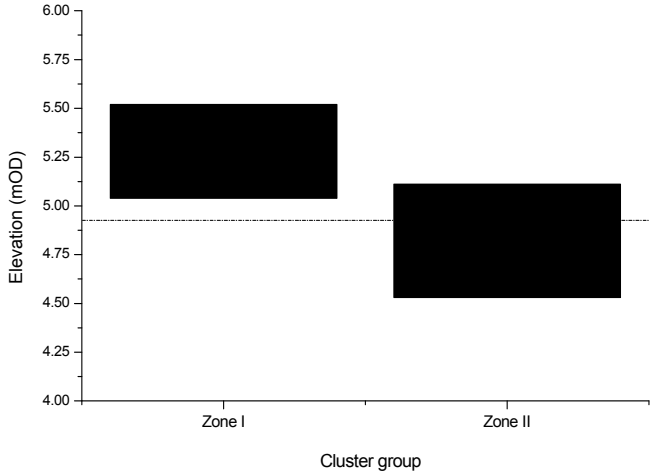

Figure 4.24 OBSS1 cluster zones related to elevation.

Table 4.14 Correlations for cluster order and variables for OBSS1.

Variable	r^2	p-value
Sand %	0.262822	0.237323
Clay %	-0.35176	0.108408
Silt %	-0.22214	0.320424
Organic matter	**0.646805**	**0.001142**
Salinity	**-0.60126**	**0.003079**
pH	0.265775	0.2319
Phragmites spp.	**0.730449**	**0.000113**
Elevation	**0.769644**	**2.82E-05**
Distance	**0.763202**	**3.61E-05**

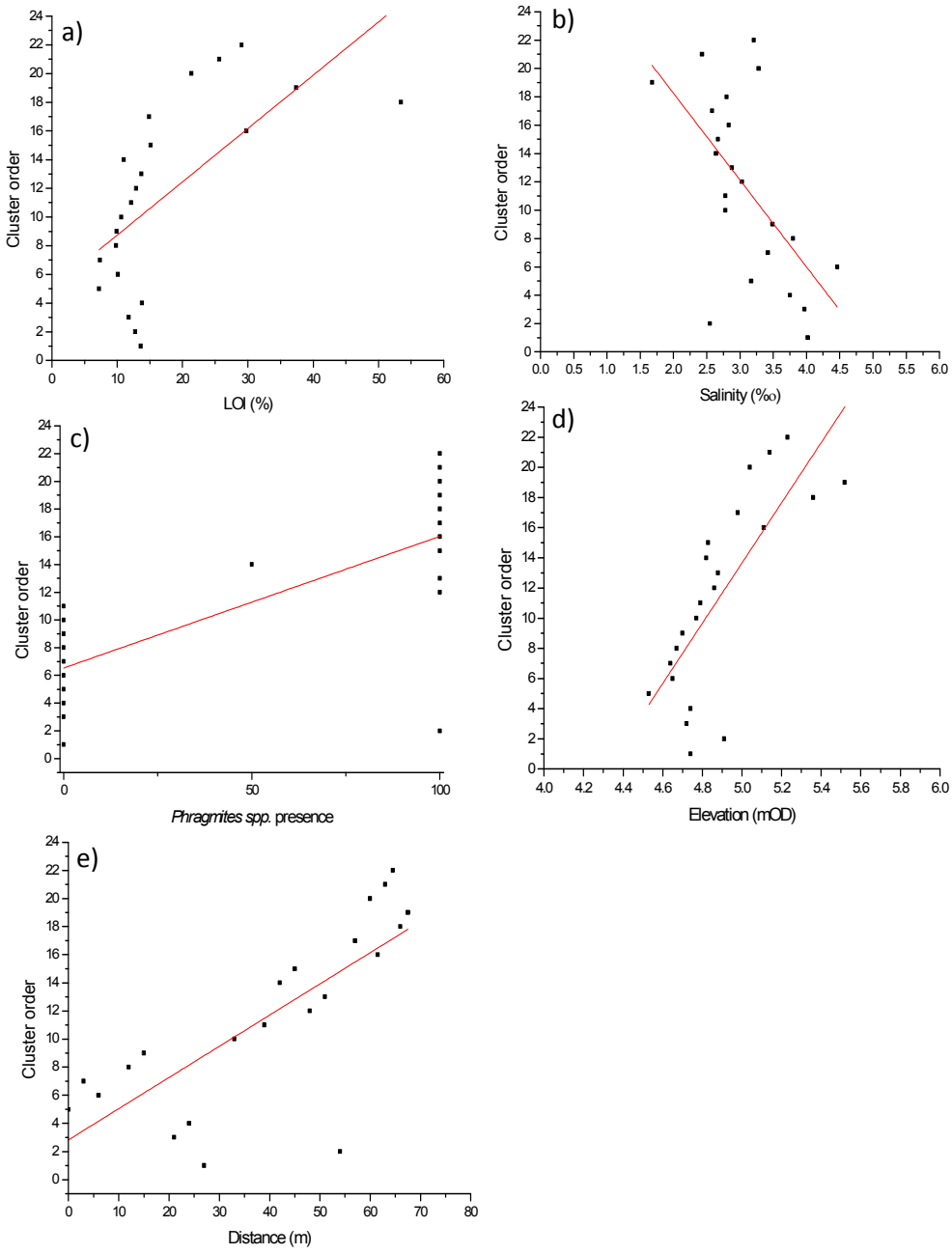

Figure 4.25 Correlations between cluster order and significant variables for OBSS1. a) organic matter, b) salinity, c) *Phragmites spp*. presence, d) elevation, e) distance.

OBSS2

Table 4.15 and figure 4.26 show the results of the DCA analysis for OBSS2. The environmental variables which were most related to each DCA axes were determined and can be seen in table 4.15 and figure 4.26 also. It shows that axis 1 is positively and significantly related to salinity and negatively and significantly related to organic matter, *Phragmites* spp*.,* elevation and distance. This indicates that the samples and species which are located in the left, negative, part of the diagram are related to organic matter, *Phragmites* spp*.,* elevation and distance, whilst those in the right positive part are more related to higher salinity. Species *B. pseudomacrescens*, *Haplophragmoides* spp*.* and *M. fusca* were found to be related to the higher elevation samples and *T. inflata* and *J. Macrescens,* along with calcareous species associated with the lower samples.

The relationships can be further examined using a constrained analysis where measured environmental variables as opposed to theoretical variables are used and can be seen in figure 4.26. The lengths of the first DCA axis is between 1 and 3 SD. The results of the CCA were found to explain more variance than that of the RDA results, therefore CCA was used and the results can be seen in table 4.16. The CCA shows that the nine variables included explain 73% of the total variance. The most significant variables were found to be *Phragmites* spp., elevation and distance. These were included in the CCA alone and explain 55% of the variance (table 4.17). Permutation tests were carried out to determine how significant each individual variable was to the species distribution. It was established that *Phragmites* spp. individually (without the elevation and distance) had a p-value >0.05, therefore this was removed before the variation partitioning was carried out. This reduced the amount of variance explained by the significant variables (elevation and distance) to 36% (table 4.18). The results of the variation partitioning show that elevation contributes 7% to the total inertia whilst distance contributes 17%, leaving 13% attributed to the correlation of the two variables (figure 4.27). The percentages of total variance/inertia, converted into percentage out of the explained proportion, gives 19% elevation, 46% distance and 36% intercorrelation.

Table 4.15 DCA results for OBSS2.

	DCA1	DCA2	DCA3	DCA4
Eigenvalues	0.4527	0.1595	0.08734	0.14075
Decorana values	0.4588	0.059	0.02785	0.01588
Axis lengths	2.5207	1.3198	0.92234	1.26007

	DCA1	DCA2	r2	Pr(>r)	Significance (p value)
Sand %	0.999839	-0.01793	0.1281	0.364	1
Clay %	-0.86572	-0.50053	0.0601	0.606	1
Silt %	-0.63178	0.775148	0.0101	0.922	1
Organic matter	-0.52658	0.850125	0.5486	0.003	0.01
pH	0.32226	0.946651	0.0469	0.694	1
Salinity	0.881357	-0.47245	0.6598	0.001	0.001
Phragmites spp.	-0.91197	0.410268	0.5363	0.003	0.01
Elevation	-0.51871	0.854952	0.6038	0.002	0.01
Distance	-0.65706	0.753843	0.8021	0.001	0.001

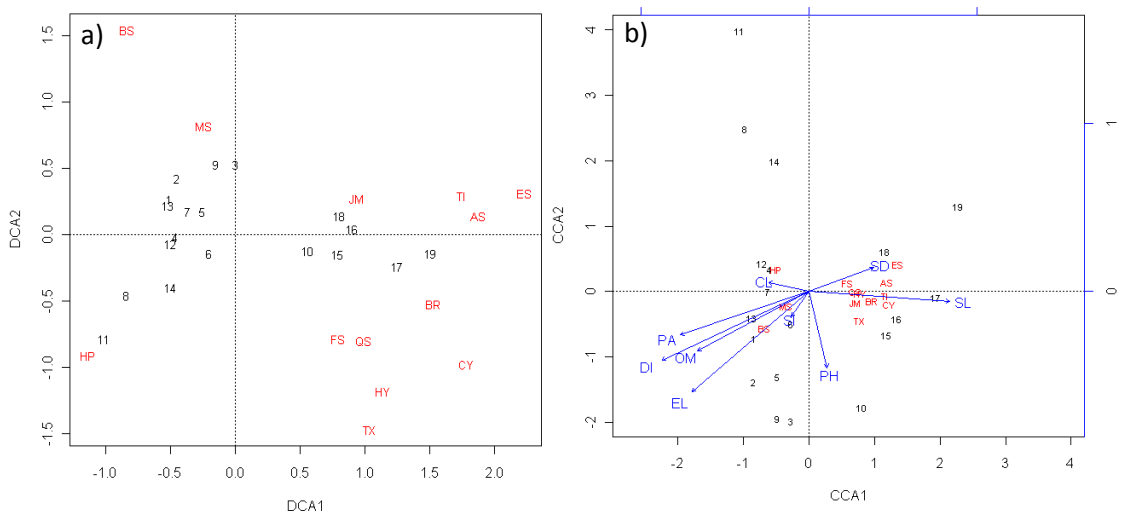

Figure 4.26 a) DCA b) CCA plot for OBSS2. *AS=Ammonia beccarii spp.,* BS= *B. pseudomacrescens,* BR=*Brizalina spp.,* ES= *Elphidium spp.,* FS= *Fursenkoina spp.*, GS=*Glabratella milletti,* HP= *Haplophragmoides spp.,* HY= *Haynesina spp.*, JM= *J. macrescens,* MS= *M. fusca,* QS= *Quinqueloculina spp.*, TX=*Textularia spp.,* TI= *T. inflata*. SD=sand, SL=salinity, OM=organic matter, EL=elevation, PA=Phragmites presence, DI=distance, PH=Ph, CL=clay, SI=silt.

Table 4.16 CCA for OBSS2 with all environmental variables.

	Inertia	Proportion	Rank
Total	0.8744	1	
Constrained	0.6362	0.7276	9
Unconstrained	0.2382	0.2724	9

Table 4.17 CCA for OBSS2 with only significant variables (elevation, *Phragmites spp.,* and distance).

	Inertia	Proportion	Rank
Total	0.8744	1	
Constrained	0.4771	0.5457	3
Unconstrained	0.3973	0.4543	12

Table 4.18 Variance partitioning with significant variables only for OBSS2.

Variable	Variance	Significance	% of total inertia	% of constrained inertia
All	0.36426			
Elevation	0.06869	0.06	7	19
Distance	0.16643	0.004	17	46
Intercorrelations	0.12914		13	36

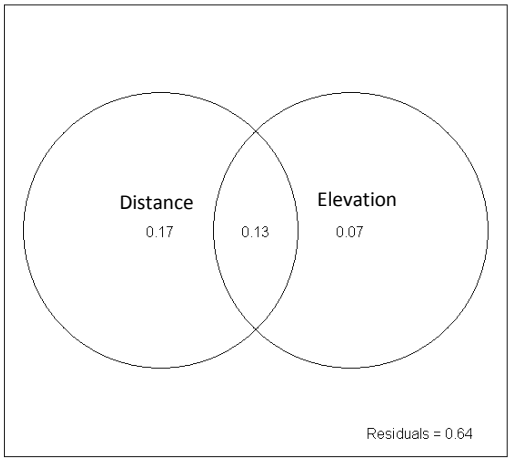

Figure 4.27 Diagram of variance partitioning with significant variables only for OBSS2.

Figure 4.28 shows the species response curves to elevation for the different species with the best fit models. The species coefficients from WA also show the optimum elevations for each species. It shows *B. pseudomacrescens* and *M. fusca* occupy high marsh, and *Ammonia beccarii* spp*., Cyclogyra involvens, Quinqueloculina* spp*., Fursenkoina* spp*., Elphidium* spp*. and inflata* have an optimum in the low marsh. WA using *C2* (Juggins, 2007) provides the optima and tolerances for each of the species (table 4.19). These have been plotted in figure 4.29 and show that all species have similar vertical distributions, with *J. macrescens* having a wider distribution.

Unconstrained cluster analysis for OBSS2 divides the assemblage into two main zones, high and low (figures 4.30 and 4.31). The high marsh zone is dominated by *Haplophragmoides* spp. and *M. fusca,* and a low zone dominated by *M. fusca* and calcareous spp. The unconstrained and constrained analyses have similar divisions. The correlation with the

order of the unconstrained cluster analysis and the variables can be seen in figure 4.32 and table 4.20, and show that organic matter (r^2=-0.63), salinity (r^2=0.63), elevation (r^2=-0.63) and distance (r^2=-0.75) are all significant.

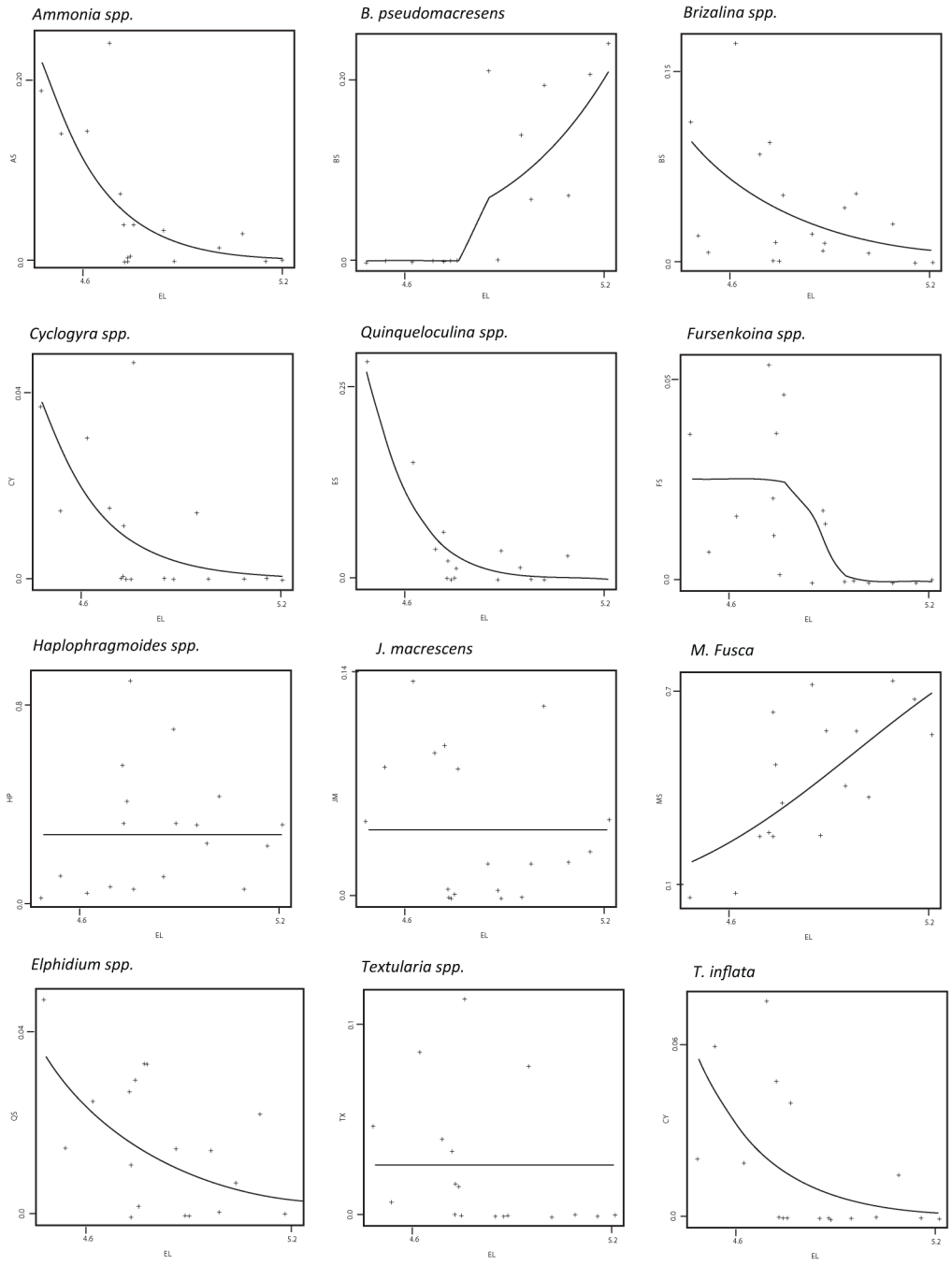

Figure 4.28 Species response curves to elevation for OBSS2.

Table 4.19 Species coefficients from WA for OBSS2.

Species	Count	Max	N2	Optimum	Tolerance
Ammonia beccarii spp.	13	24	6.60305	4.65348	0.153823
B. pseudomacrescens	7	4.93	6.03835	5.04808	0.142186
Brizalina spp.	14	17.36	7.56505	4.718	0.179728
Cyclogyra involvens	7	4.67	5.48164	4.66276	0.151596
Elphidium spp.	12	28.27	4.98962	4.60918	0.168987
Fursenkoina spp.	12	5.41	8.53355	4.70561	0.116038
Haplophragmoides spp.	19	90.58	11.0453	4.85962	0.167122
Haynesina spp.	14	17.57	7.31923	4.72697	0.162127
J. macrescens	15	13.5	9.25802	4.78309	0.226446
M. fusca	19	73.33	14.7127	4.90268	0.191127
Quinqueloculina spp.	13	4.71	9.88244	4.72141	0.184103
Textularia spp.	10	11.33	6.9632	4.7503	0.164724
T. inflata	8	7.5	5.71852	4.6812	0.153551

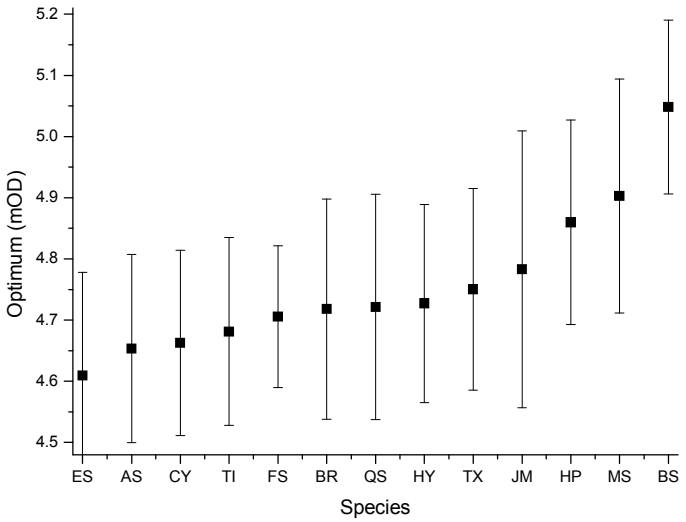

Figure 4.29 Optimum altitude of species from OBSS2 with tolerance levels (results from WA, c2) (y axis altitude gradient). *AS=Ammonia beccarii spp.,* BS= *B. pseudomacrescens,* BR=*Brizalina spp.,* CY= *Cyclogyra involvens,* ES= *Elphidium spp.,* FS= *Fursenkoina spp.*, GS=*Glabratella milletti,* HP= *Haplophragmoides spp.,* HY= *Haynesina spp.,* JM= *J. macrescens,* MS= *M. fusca,* QS= *Quinqueloculina spp.*, TX=*Textularia spp.,* TI= *T. inflata*.

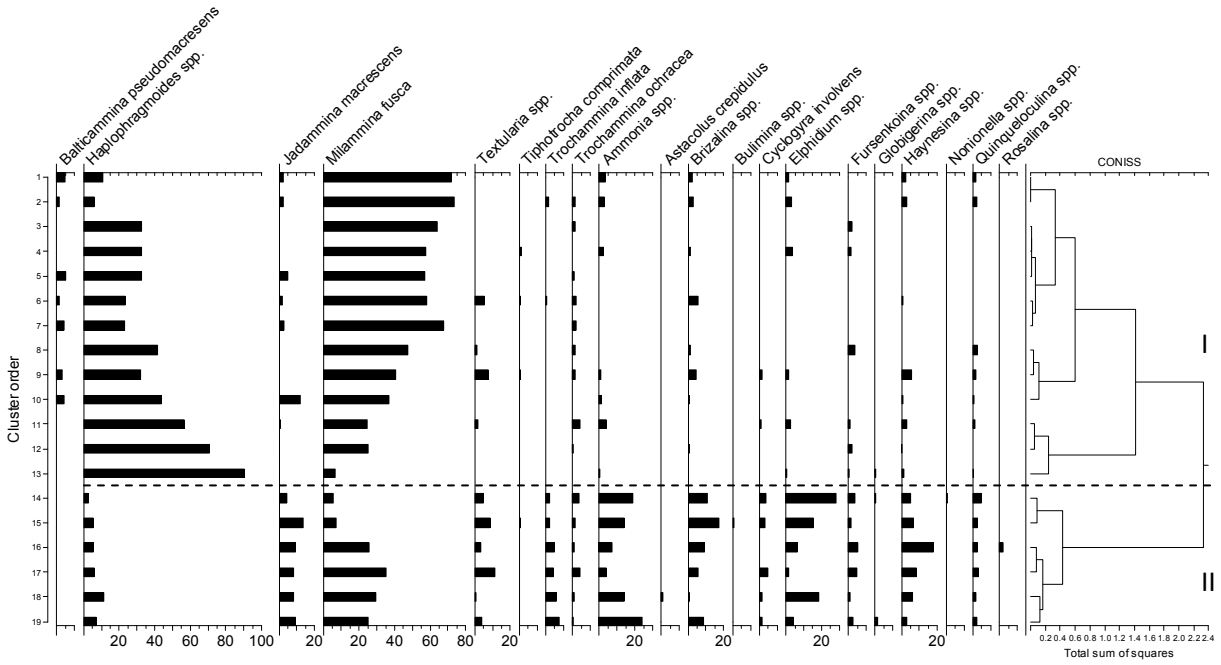

Figure 4.30 OBSS2 unconstrained cluster analysis based on unweighted Euclidean distance for relative percentages of dead foraminifera abundance.

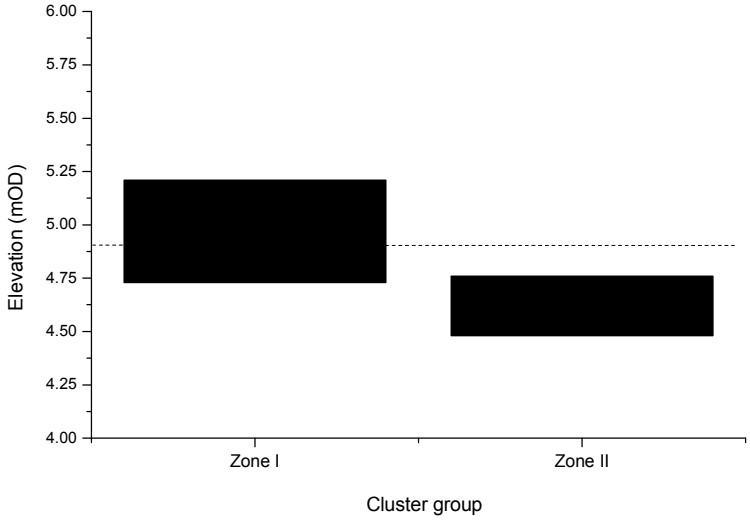

Figure 4.31 OBSS2 cluster zones related to elevation.

Table 4.20 Correlations for cluster order and variables for OBSS2.

Variable	r^2	p-value
Sand %	0.195325	0.422921
Clay %	-0.2056	0.398444
Silt %	0.012494	0.959515
Organic matter	**-0.63171**	**0.003716**
pH	0.025475	0.917551
Salinity	**0.633089**	**0.00362**
Phragmites spp.	-0.44799	0.054413
Elevation	**-0.62941**	**0.003883**
Distance	**-0.7546**	**0.000189**

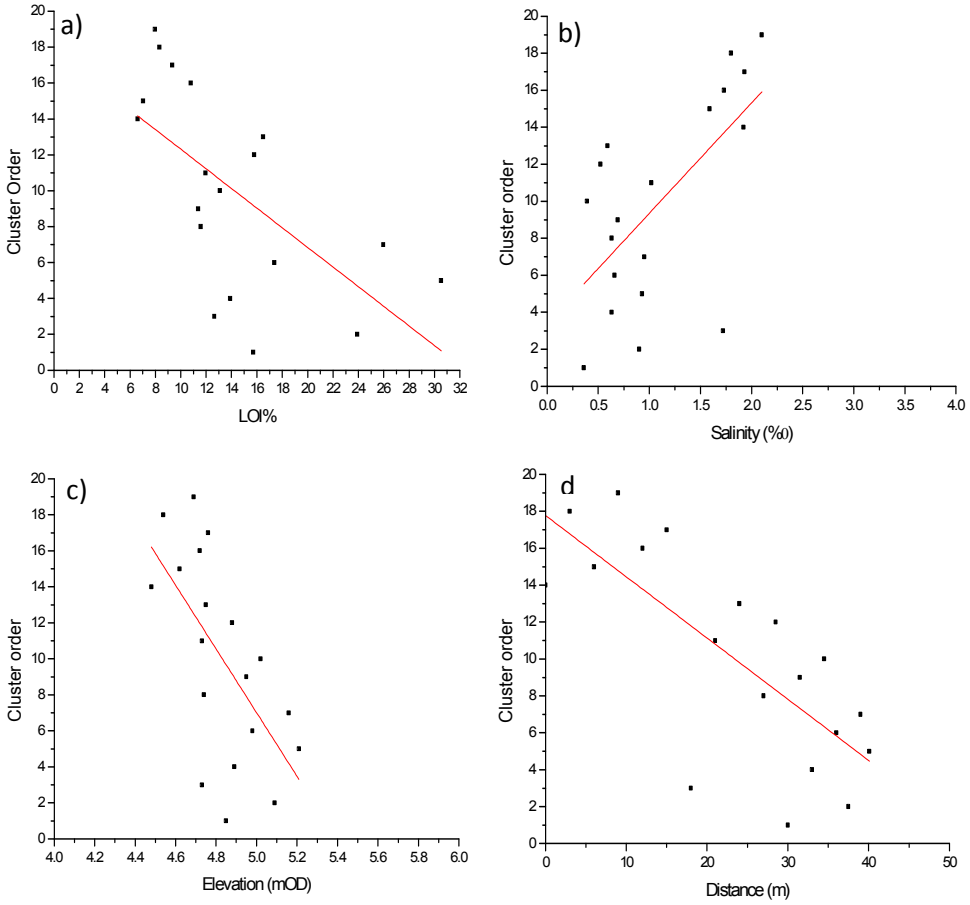

Figure 4.32 Correlations between cluster order and significant variables for OBSS2. a) organic matter b) salinity, c) elevation d) distance.

OBSS3

Table 4.21 and figure 4.33 show the results of the DCA analysis for OBSS3. The lengths of the first two DCA axes are between 1-3 SD, therefore either method could be applied. The environmental variables which were most related to each DCA axis can be seen from table 4.21. It shows that axis 1 is positively and significantly related to pH and clay, and negatively and significantly related to organic matter, elevation and distance. This indicates that the samples and species which are located in the left, negative part of the diagram are related to high organic matter, elevation and greater distance from the marsh edge, whilst those in the right positive part are more related to higher pH and higher clay content. The DCA biplot shows that those species which are at the edge of the diagram have low abundances and include *B. pseudomacrescens, Textularia* spp*., Fursenkoina* spp*., Cyclogyra involvens* and *T. inflata.*

The linear method of RDA proved the most appropriate method (as the variables explained more of the variance in the data using RDA compared to CCA) and the results of this constrained ordination can be seen in table 4.22. Using this method, the variables explain 67% of the variance. The RDA with the most significant variables was re-run and the results show that elevation and distance to be significant and explain 57% of the variance, similar to OBSS2 (table 4.23). Variance partitioning was carried out along with significance testing and can be seen in table 4.24 and figure 4.34. Distance (16%) and elevation (18%) show to explain similar amounts of the variance, not surprisingly as the distance along the saltmarsh is very similar to the elevation in this transect, with the correlation between the two being 0.93 (table 4.5).

Table 4.21 DCA results for OBSS3.

	DCA1	DCA2	DCA3	DCA4
Eigenvalues	0.3436	0.1534	0.08686	0.06608
Decorana values	0.3547	0.1128	0.03869	0.02418
Axis lengths	2.3447	1.4654	0.90913	0.78053

	DCA1	DCA2	r2	Pr(>r)	Significance (p value)
Sand %	-0.66801	0.744153	0.2564	0.054	0.1
Clay %	0.763958	-0.645266	0.3234	0.021	0.05
Silt %	0.620006	-0.784597	0.1818	0.151	1
Organic matter	-0.98622	-0.165444	0.7462	0.001	0.001
pH	0.825897	-0.563821	0.4974	0.001	0.001
Salinity	0.926269	0.376863	0.1175	0.276	1
Elevation	-0.99933	0.036484	0.7685	0.001	0.001
Distance	-0.97279	-0.231701	0.891	0.001	0.001

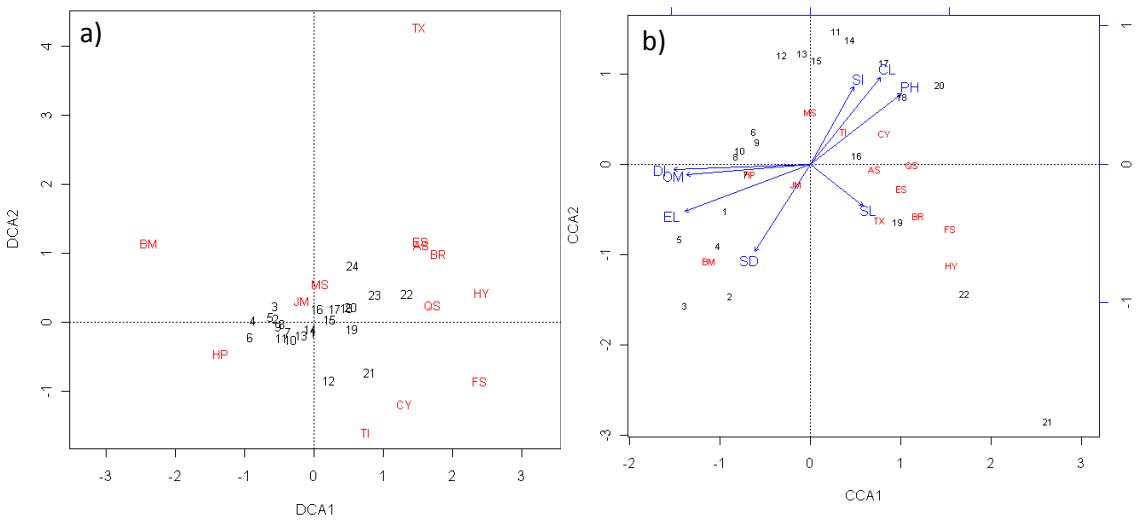

Figure 4.33 a) DCA b) RDA for OBSS3. AS=*Ammonia beccarii spp.*, BS= *B. pseudomacrescens,* BR=*Brizalina spp.,* CY= *Cyclogyra involvens***,** ES= *Elphidium spp.,* FS= *Fursenkoina spp.*, GS=*Glabratella milletti,* HP= *Haplophragmoides spp.,* HY= *Haynesina spp.,* JM= *J. macrescens,* MS= *M. fusca,* QS= *Quinqueloculina spp.*, TX=*Textularia spp.,* TI= *T. inflata*. SD=sand, CL=clay, SI=silt, SL=salinity, PH=pH, EL=elevation, DI=distance, OM=organic matter.

Table 4.22 RDA results for OBSS3 with all variables.

	Inertia	Proportion	Rank
Total	906.5486	1	
Constrained	610.2802	0.6732	8
Unconstrained	296.2684	0.3268	13

Table 4.23 RDA results for OBSS3 with only significant variables (elevation and distance).

	Inertia	Proportion	Rank
Total	906.5486	1	
Constrained	517.5856	0.5709	2
Unconstrained	388.9629	0.4291	13

Table 4.24 Variance partitioning with significant variables only for OBSS3.

Variable	Variance	Significance	% of total inertia	% of constrained inertia
All	0.52578			
Elevation	0.17625	0.001	18	34
Distance	0.16048	0.001	16	31
Intercorrelations	0.18905		19	36

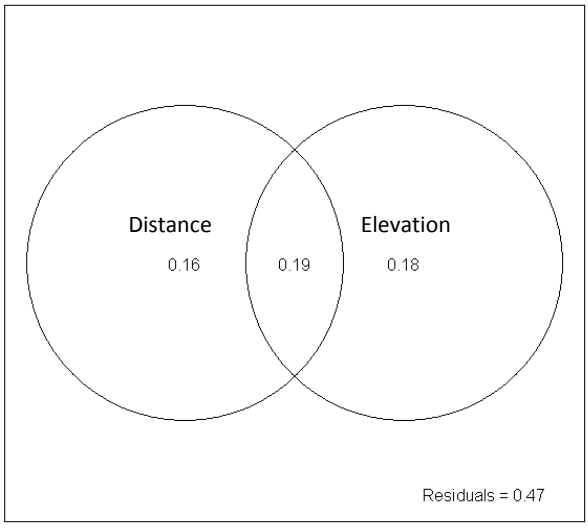

Figure 4.34 Diagram of variance partitioning with significant variables only for OBSS3.

Figure 4.35 shows the species response curves to elevation for the different species with the best fit models. The species coefficients from WA also show the optimum elevations for each species. It shows that *B. pseudomacrescens* and *J. macrescens* occupy the high marsh, and *Ammonia beccarii* spp*., Brizalina* spp*., Cyclogyra involvens,* Elphidium spp*., Haynesina* spp*., M. fusca,* and *Quinqueloculina* spp*.* have optima in the low marsh. WA using *C2* (Juggins, 2007) provides the optima and tolerances for each of the species (table 4.25). These have been plotted as ranges in figure 4.36, which shows that *B. pseudomacrescens* has a very narrow tolerance. It also shows that *Textularia* spp*.* has a high elevational optimum. However, in figure 4.35, which shows all the species occurrences, it can be seen that *Textularia* spp*.* occupies all areas across the marsh in low numbers and the optimum is not in the high marsh but has one sample which has higher numbers at this high elevation.

Unconstrained cluster analysis reveals two main zones (figure 4.37); a high marsh zone dominated by *Haplophragmoides* spp*., J. macrescens* and *M. fusca,* and low zone dominated by J*. macrescens, M. fusca and T. Inflata,* with calcareous species including *Elphidium* spp*.* The correlation with the order of the unconstrained cluster analysis and the variables can be seen in figure 4.39 and table 4.26 and show that clay (r^2=0.50), organic matter (r^2=-0.54), elevation (r^2=-0.74) and distance (r^2=-0.65) are well correlated with cluster order.

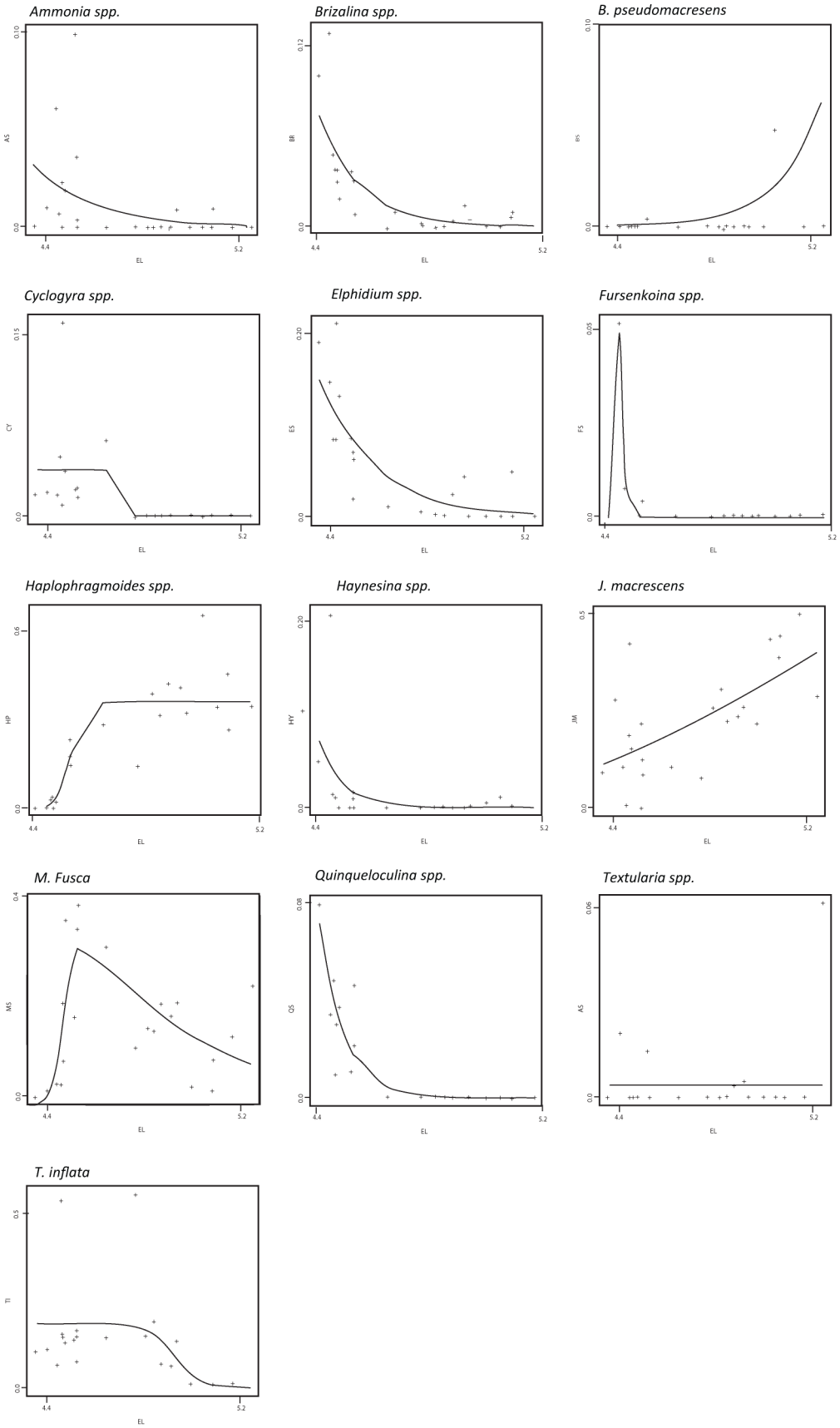

Figure 4.35 Species response curves to elevation for OBSS3.

Table 4.25 Species coefficients from WA for OBSS3.

Species	Count	Max	N2	Optimum	Tolerance
Ammonia beccarii spp.	10	9.96	4.78751	4.53013	0.15702
B. pseudomacrescens	4	9.62	2.88865	5.07456	0.089404
Brizalina spp.	16	12.93	6.97255	4.50555	0.163664
Cyclogyra involvens	11	16.03	5.2692	4.5041	0.073788
Elphidium spp.	16	21.15	9.53581	4.52269	0.16776
Fursenkoina spp.	6	5.17	3.15176	4.4621	0.021351
Haplophragmoides spp.	19	66.04	13.9686	4.88966	0.204575
Haynesina spp.	9	20.69	2.31064	4.47837	0.166807
J. macrescens	22	50.3	19.3271	4.79283	0.271049
M. fusca	22	38.76	15.0653	4.68051	0.223801
Quinqueloculina spp.	10	8	7.37568	4.47161	0.047915
Textularia spp.	4	2	2.81973	4.54214	0.22696
T. inflata	22	55.95	10.5878	4.63317	0.189621

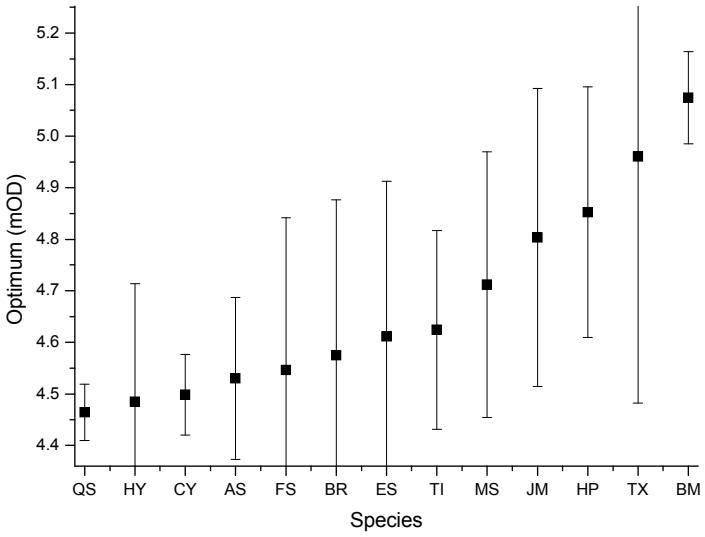

Figure 4.36 Optimum altitude of species from OBSS3 with tolerance levels (results from c2) (y axis altitude gradient). *AS=Ammonia beccarii spp.,* BS= *B. pseudomacrescens,* BR=*Brizalina spp.,* CY= *Cyclogyra involvens***,** ES= *Elphidium spp.,* FS= *Fursenkoina spp.*, GS=*Glabratella milletti,* HP= *Haplophragmoides spp.,* HY= *Haynesina spp.,* JM= *J. macrescens,* MS= *M. fusca,* QS= *Quinqueloculina spp.*, TX=*Textularia spp.,* TI= *T. inflata*.

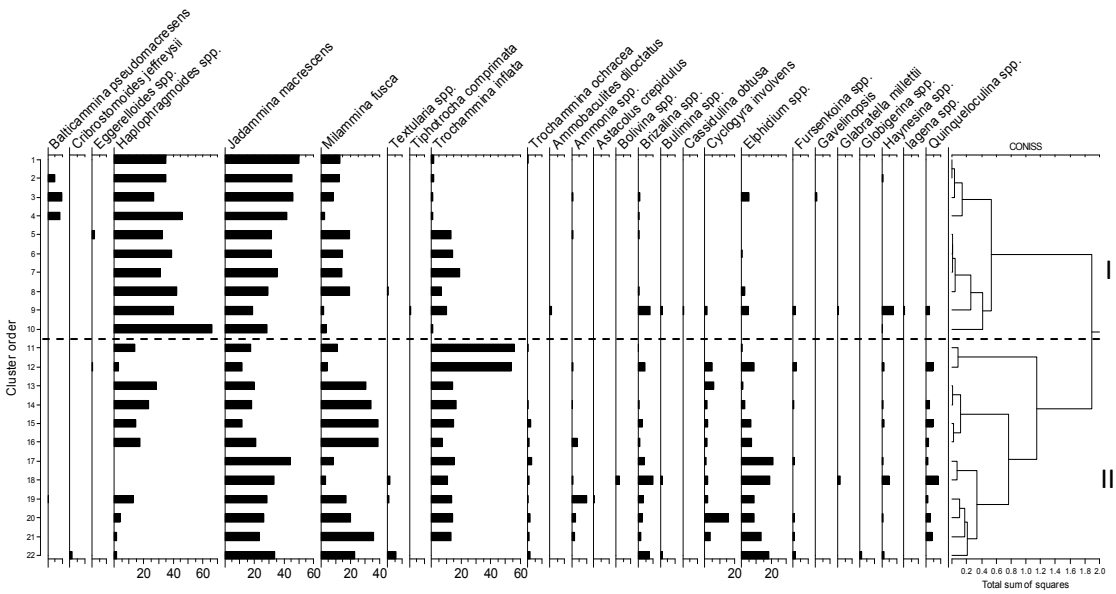

Figure 4.37 OBSS3 unconstrained cluster analysis based on unweighted Euclidean distance for relative percentages of dead foraminifera abundance.

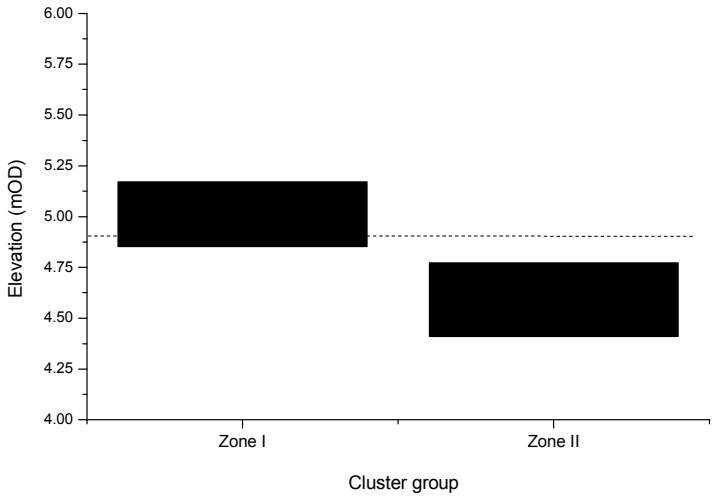

Figure 4.38 OBSS3 cluster zones related to elevation.

Table 4.26 Correlations for cluster order and variables for OBSS3.

Variables	r^2	p-value
Sand %	-0.32898	0.13492
Clay %	**0.508932**	**0.015567**
Silt %	0.218945	0.327607
Organic matter	**-0.53874**	**0.009683**
pH	0.498367	**0.018243**
Salinity	0.155007	0.490955
Elevation	**-0.73655**	**9.27E-05**
Distance	**-0.6477**	**0.001118**

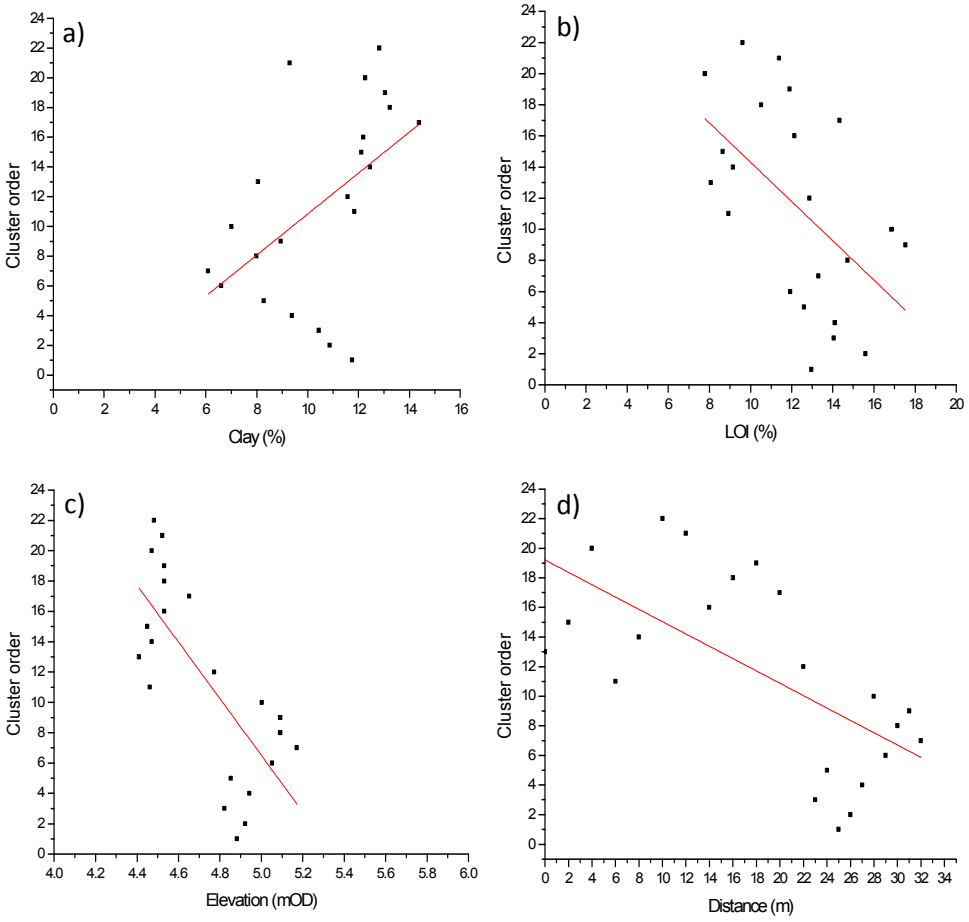

Figure 4.39 Correlations between cluster order and significant variables for OBSS3. a) clay %, b) organic matter content c) Elevation d) distance.

Combined Oglet Bay

Table 4.27 and figure 4.40 show the DCA results for all the data from the combined Oglet Bay data. An additional variable was added to the data when all three transects were combined. The transect number was included in order to represent the location of the transect on the marsh as well as the sampling time (e.g. Charman et al., 2002).

The lengths of the first two DCA axes are between 2 and 3 SD, indicating both RDA and CCA could be used. The biplot diagram for the DCA (figure 4.40 and table 4.27) show which variables are most related to each DCA axis. Axis 1 can be seen to be related positively and significantly with clay and pH, and negatively significantly with many variables, such as organic matter, salinity, elevation, distance and transect. Axis 2 is only negatively and significantly related to clay and pH. The RDA method of constrained ordination was found to have slightly better results than CCA, therefore this method was used. The biplot of this can be seen in figure 4.40. The DCA biplot shows *Brizalina* spp*., Elphidium* spp. and *Ammonia beccarii* spp. to be related to the lower marsh samples and *Haplophragmoides* spp. related to the higher marsh samples. The RDA biplot shows that the lower samples are related to high silt content, high clay content and high pH. The higher samples are more related to higher distance, higher elevation, higher organic matter and higher sand content.

The results of the RDA shows that the 10 variables included explain 55% of the total variance. The RDA with only the significant variables included can be seen in table 4.29, which shows that distance, transect, pH, organic matter, and elevation explain 52% of the total inertia. In order to determine how much each of these variables contributes to this variance, pRDA was used as there were more than four significant variables contributing. The results of the pRDA can be seen in table 4.30 and shows that most of the variance can be explained by transect number (14%), pH (13%) and intercorrelations (13%). The amount of variance explained by the other environmental variables was very low.

Table 4.27 DCA results for all Oglet Bay data.

	DCA1	DCA2	DCA3	DCA4
Eigenvalues	0.436	0.3148	0.17815	0.1884
Decorana values	0.4651	0.301	0.09779	0.05092
Axis lengths	2.891	2.3077	1.55946	1.61027

	DCA1	DCA2	r2	Pr(>r)	Significance (p value)
Sand %	-0.87637	0.48164	0.0854	0.044	0.5
Clay %	0.75574	-0.65487	0.4648	0.001	0.001
Silt %	0.82582	0.56394	0.0045	0.884	1
Organic matter	-0.69588	-0.71816	0.373	0.001	0.001
Salinity	-0.62402	0.7814	0.2082	0.002	0.01
pH	0.80056	-0.59925	0.257	0.001	0.001
Phragmites spp.	-0.1892	-0.98194	0.5201	0.001	0.001
Distance	-0.36138	-0.93242	0.5128	0.001	0.001
Transect	-0.52272	0.85251	0.5021	0.001	0.001
Elevation	-0.61252	-0.79046	0.5211	0.001	0.001

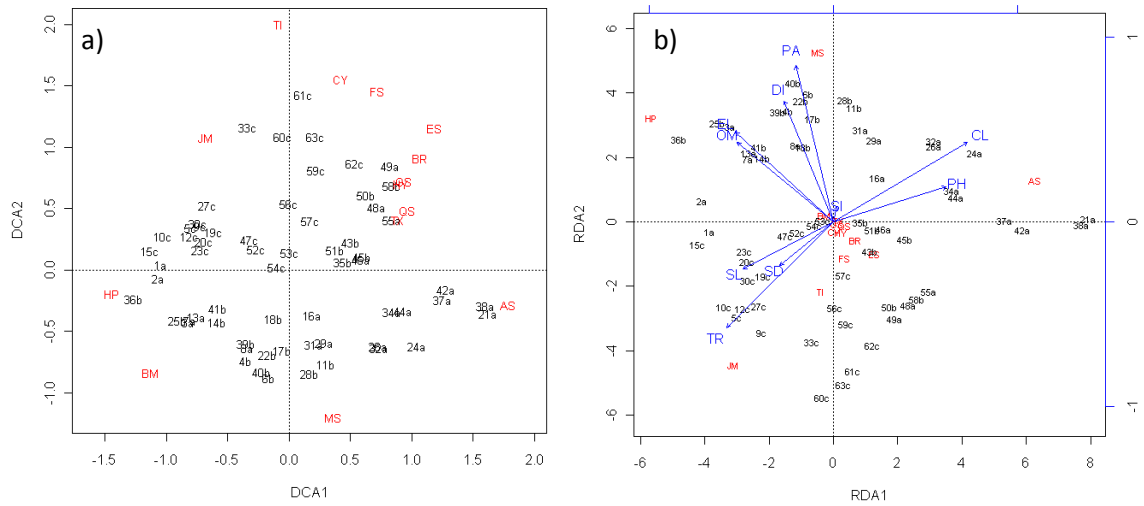

Figure 4.40 a) DCA b) RDA for all data. AS=*Ammonia beccarii spp., BS= B. pseudomacrescens,* BR=*Brizalina spp.,* CY= *Cyclogyra involvens***,** ES= *Elphidium spp.,* FS= *Fursenkoina spp.*, GS=*Glabratella milletti,* HP= *Haplophragmoides spp.,* HY= *Haynesina spp.,* JM= *J. macrescens,* MS= *M. fusca,* QS= *Quinqueloculina spp.*, TX=*Textularia spp.,* TI= *T. inflata*. SD=sand, CL=clay, SI=silt, SL=salinity, PA=Phragmites spp., PH=pH, EL=elevation, DI=distance, TR=transect, OM=organic matter. a=OBSS1, b=OBSS2, c=OBSS3, d=DMSS1, e=DMSS2.

Table 4.28 RDA for all Oglet Bay data and all variables.

	Inertia	Proportion	Rank
Total	1741.5214	1	
Constrained	956.7136	0.5494	10
Unconstrained	784.8105	0.4506	14

Table 4.29 RDA for all Oglet Bay data with significant variables (distance, transect, pH, elevation, organic matter).

	Inertia	Proportion	Rank
Total	1741.5241	1	
Constrained	904.7066	0.5195	5
Unconstrained	836.8175	0.4805	14

Table 4.30 pRDA with significant variables only for all Oglet Bay.

Variable	Variance	Significance	% of total inertia	% of constrained inertia
All	0.5195			
pH	0.12910	0.001	13	25
Distance	0.05496	0.001	6	11
Transect	0.1377	0.001	14	27
Organic matter	0.02433	0.036	2	5
Elevation	0.03899	0.002	4	8
Intercorrelations	0.13442		13	26

Figure 4.41 shows the species response curves to elevation for the different species with the best fit models. The species coefficients from WA also show the optimum elevations for each species. It shows that *Ammonia beccarii* spp*., B. pseudomacrescens* and *Elphidium* spp*.* are unimodal in their distribution; *Haplophragmoides* spp*.* occupies the high marsh; and *Brizalina* spp*., Cyclogyra involvens*, Elphidium spp*., Fursenkoina* spp*., Haynesina* spp., *Quinqueloculina* spp*.* and *T. inflata* all have optima in the low marsh. WA using *C2* (Juggins, 2007) provides the optima and tolerances for each of the species (table 4.31). These have been plotted in figure 4.42 and show that most of the species have similar altitudinal ranges with some of the calcareous species having the narrowest ranges.

Unconstrained cluster analysis was carried out on the combined OB data and four main zones identified (figure 4.43). Three of the zones (I, II, IV) cover the same altitudinal range and species composition, including *Haplophragmoides* spp*., M. fusca*, with varying amounts of *J. macrescens* and *Ammonia beccarii* spp. The other zone (III) has similar dominant species but with higher proportions of *T. Inflata* and calcareous species. Figure 4.44 shows the two main cluster groups and the altitudinal range they cover.

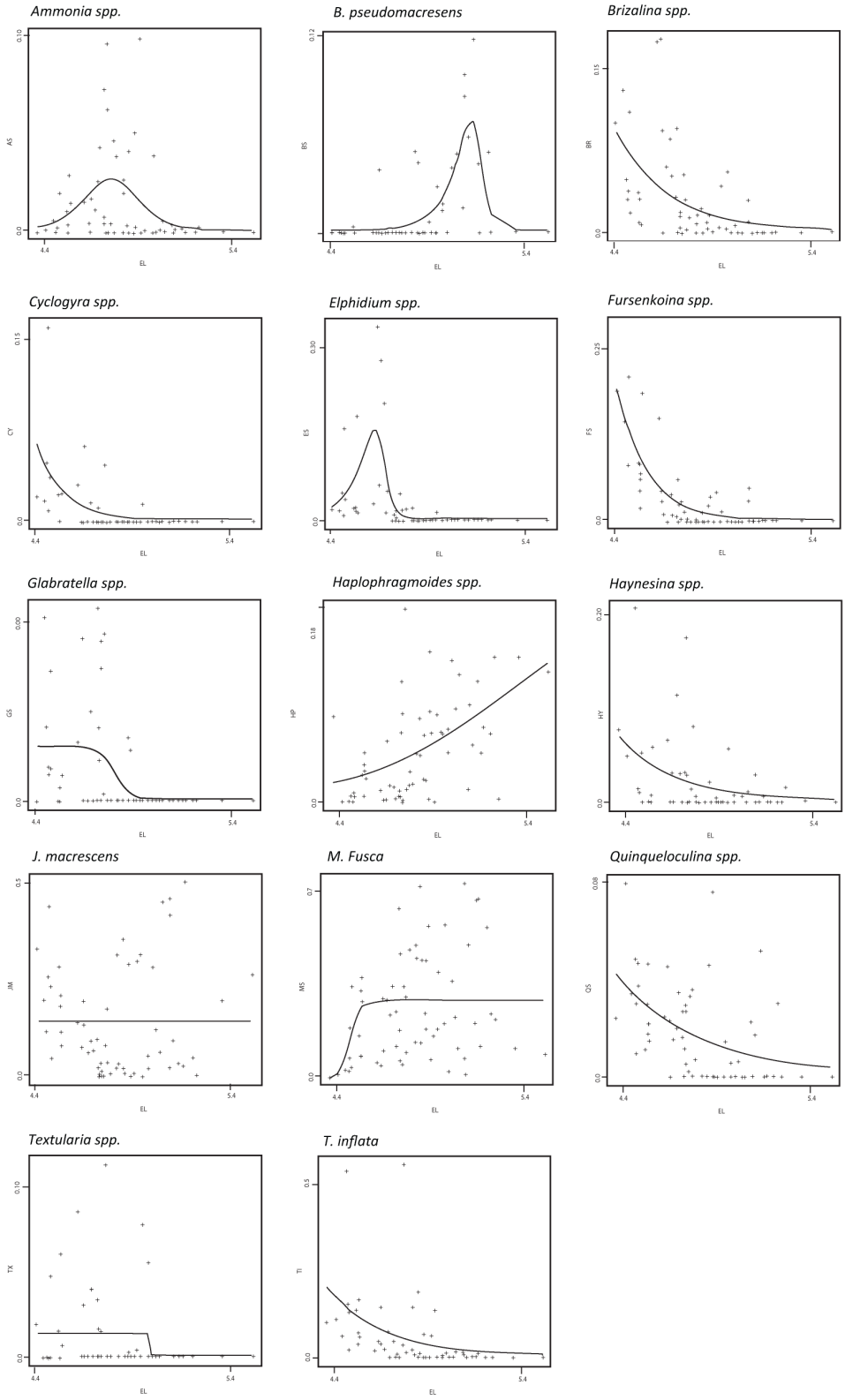

Figure 4.41 Species response curves to elevation for all Oglet Bay.

Table 4.31 Species coefficients from WA for all Oglet Bay.

Species	Count	Max	N2	Optimum	Tolerance
Ammonia beccarii spp.	41	90.26	16.2823	4.76408	0.133213
B. pseudomacrescens	6	11.79	3.75841	5.03635	0.191055
Brizalina spp.	45	17.61	21.5298	4.66933	0.2066
Cyclogyra involvens	18	16.03	8.88384	4.54864	0.123476
Elphidium spp.	40	33.52	19.0543	4.62497	0.209277
Fursenkoina spp.	27	5.41	17.3932	4.65863	0.164595
Glabratella millettii	2	4.55	1.99994	4.68972	0.070711
Haplophragmoides spp.	58	90.58	33.1407	4.94365	0.234743
Haynesina spp.	30	20.69	11.9192	4.65646	0.192713
J. macrescens	58	50.3	31.8147	4.8421	0.298779
M. fusca	63	73.33	42.379	4.8492	0.217575
Quinqueloculina spp.	39	8	27.0178	4.67908	0.209854
Textularia spp.	17	11.33	10.7952	4.75828	0.231338
T. inflata	41	55.95	14.6085	4.64199	0.179318

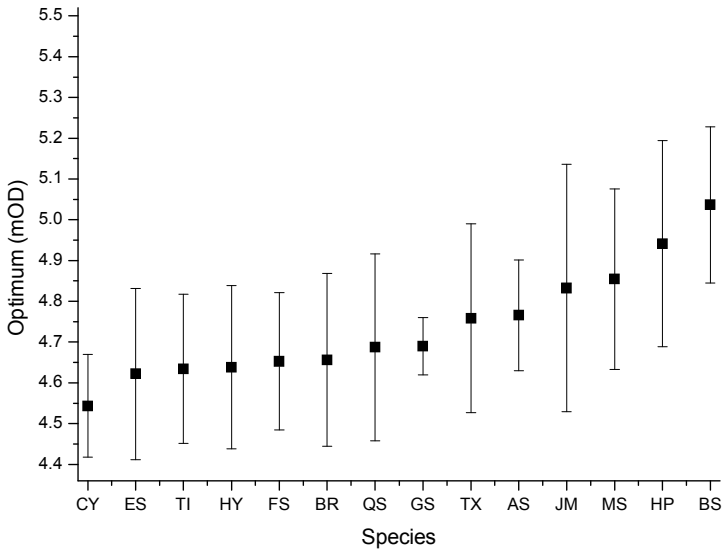

Figure 4.42 Optimum altitude of species from OB with tolerance levels (results from c2) (y axis altitude gradient). *AS=Ammonia beccarii* spp., BS= *B. pseudomacrescens,* BR=*Brizalina spp.,* CY= *Cyclogyra involvens,* ES= *Elphidium spp.,* FS= *Fursenkoina spp.*, GS=*Glabratella milletti,* HP= *Haplophragmoides spp.,* HY= *Haynesina spp.,* JM= *J. macrescens,* MS= *M. fusca,* QS= *Quinqueloculina spp.*, TX=*Textularia spp.,* TI= *T. inflata*.

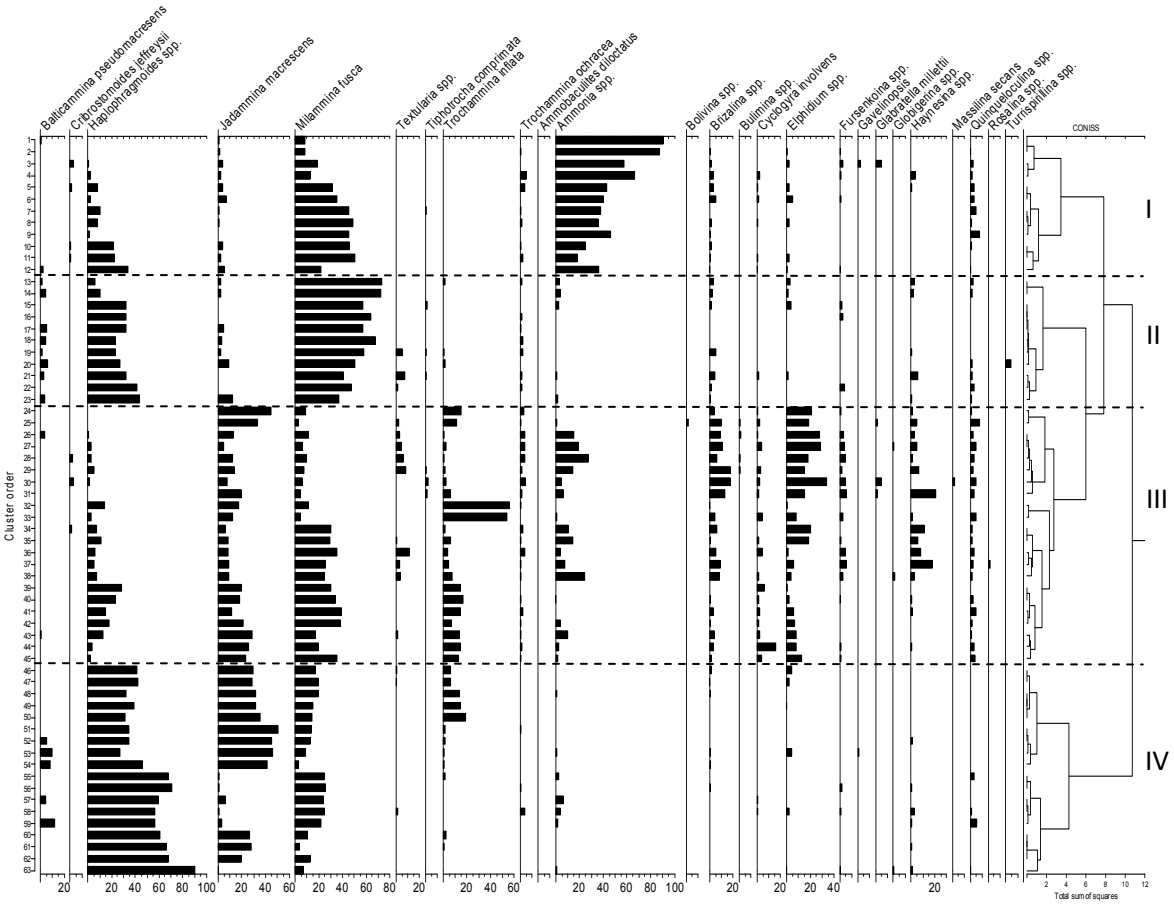

Figure 4.43 Oglet Bay unconstrained cluster analysis based on unweighted Euclidean distance for relative percentages of dead foraminifera abundance.

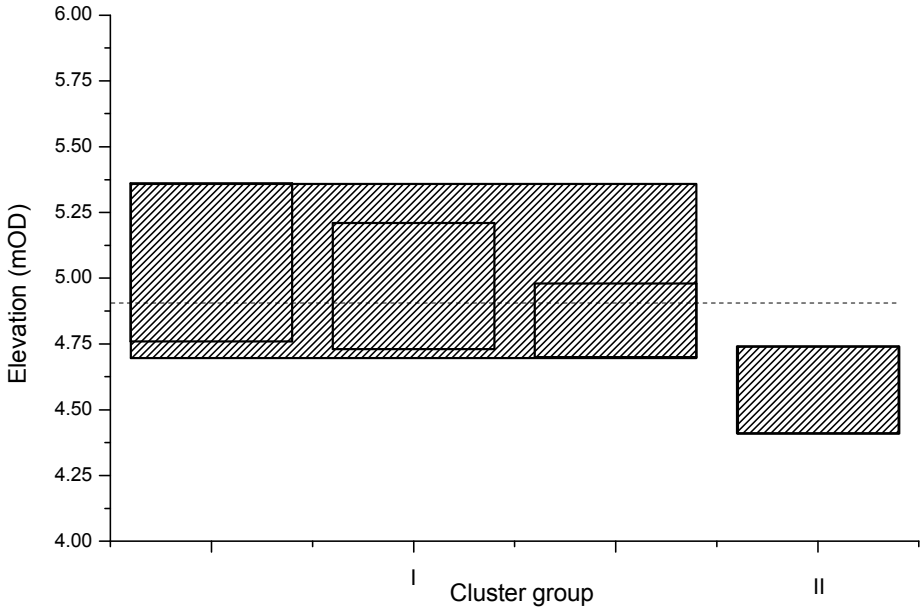

Figure 4.44 OB cluster zones related to elevation.

Table 4.32 Correlations for cluster order and variables for OB.

Variables	r^2	p-value
Sand %	-0.29037	**0.020967**
Clay %	0.083914	0.513201
Silt %	0.280582	**0.02592**
Organic matter	-0.35712	**0.004064**
Salinity	0.253341	**0.045137**
pH	-0.18406	0.148717
Phragmites spp.	-0.11622	0.364349
Distance	**-0.52832**	**8.57E-06**
Transect	0.131607	0.303875
Elevation	**-0.65074**	**7.77E-09**

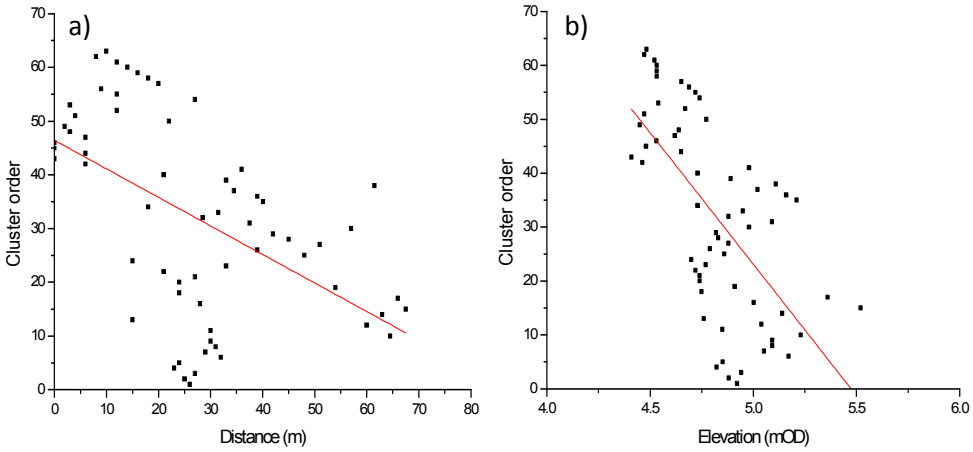

Figure 4.45 Correlations between cluster order and significant variables for OB. a) distance b) elevation.

Decoy Marsh

Combined Decoy Marsh dead data

The two transects taken from Decoy Marsh were combined together as the numbers are very low using the individual transects. Table 4.33 and figure 4.46 show the DCA results for Decoy Marsh. It has the highest ordination axis length of 3 SD but the RDA was still found to perform the 'best', and can be seen in table 4.34. The correlations between the DCA axis and the variables, which can be seen in table 4.33, show that the first ordination axis is highly positively related to high organic matter, elevation and distance from the marsh edge, and negatively with salinity, i.e. the axis shows a gradient from low to high marsh. The second axis was found to be positively and significantly with sand content and transect number and negatively with clay and silt content.

The results of the RDA show that the nine environmental variables account for 77% of the inertia in the species data. With only the significant variables included (distance, clay, organic matter, transect) this reduces to 73% (table 4.35). As only four variables were proven to be significant, variation partitioning was used. The permutation tests used to test the significance of the variables individually found that only organic matter and clay were significant. The results of variation partitioning with the two variables can be seen in table 4.36 and figure 4.47. It shows that both clay (24%) and organic matter (25%) contribute equal amounts to the observed inertia, with 11% due to their intercorrelations.

Table 4.33 DCA for all Decoy Marsh data.

	DCA1	DCA2	DCA3	DCA4
Eigenvalues	0.5511	0.1853	0.16338	0.11723
Decorana values	0.5706	0.1188	0.04287	0.02173
Axis lengths	3.0043	1.5696	1.33346	1.23952

	DCA1	DCA2	r2	Pr(>r)	Significance (p value)
Sand %	-0.62553	0.780202	0.5297	0.004	0.01
Clay %	0.571584	-0.820544	0.6564	0.001	0.001
Silt %	0.645312	-0.76392	0.4638	0.007	0.01
Organic matter	0.999508	0.031373	0.8487	0.001	0.001
pH	0.970107	-0.242677	0.0547	0.605	1
Salinity	-0.97975	0.20025	0.2608	0.086	0.1
Transect	-0.79535	0.606148	0.6976	0.001	0.001
Elevation	0.985162	0.171625	0.5391	0.003	0.01
Distance	0.99384	-0.110824	0.7803	0.001	0.001

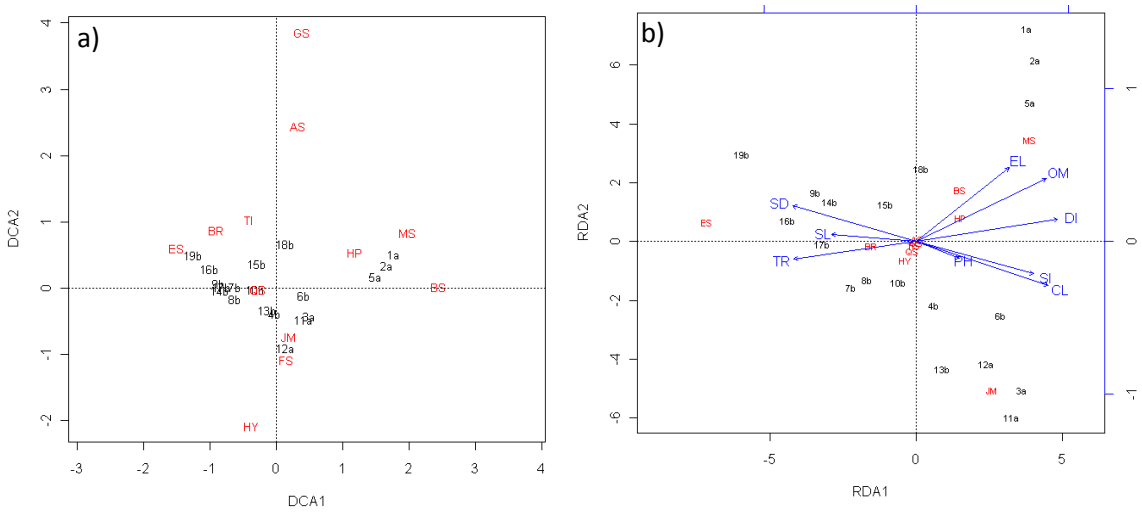

Figure 4.46 a) DCA b) RDA for all DM. AS=*Ammonia beccarii spp.,* BS= *B. pseudomacrescens,* BR=*Brizalina spp.,* CY= *Cyclogyra involvens,* ES= *Elphidium spp.,* FS= *Fursenkoina spp.*, GS=*Glabratella milletti,* HP= *Haplophragmoides spp.,* HY= *Haynesina spp.,* JM= *J. macrescens,* MS= *M. fusca,* QS= *Quinqueloculina spp.*, TX=*Textularia spp.,* TI= *T. inflata*. SD=sand, CL=clay, SI=silt, SL=salinity, PA=Phragmites spp., PH=pH, EL=elevation, DI=distance, TR=transect, OM=organic matter.

Table 4.34 RDA with all variables from all Decoy Marsh.

	Inertia	Proportion	Rank
Total	1520.368	1	
Constrained	1170.5412	0.7699	9
Unconstrained	349.8356	0.2301	9

Table 4.35 RDA with significant variables from all Decoy Marsh (distance, clay, organic matter. transect number).

	Inertia	Proportion	Rank
Total	1520.377	1	
Constrained	1105.967	0.7274	4
Unconstrained	414.4093	0.2726	12

Table 4.36 Variance partitioning with significant variables only for all Decoy Marsh.

Variable	Variance	Significance	% of total inertia	% of constrained inertia
All	0.59788			
Clay %	0.23790	0.001	24	40
Organic matter	0.25301	0.003	25	42
Intercorrelations	0.10697		11	18

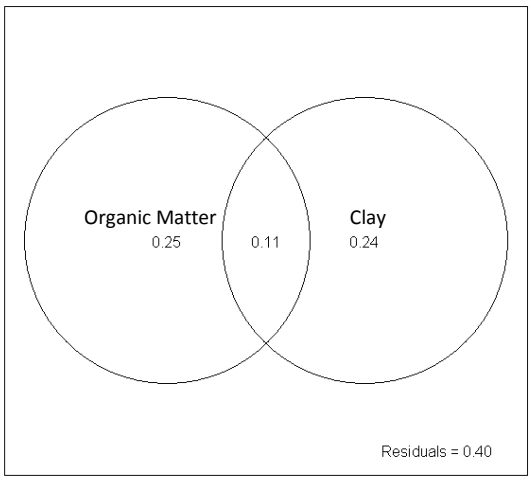

Figure 4.47 Diagram of variance partitioning with significant variables only for all Decoy Marsh.

Figure 4.48 shows the species response curves to elevation for the different species with the best fit models. It shows that *Glabratella millettii*, *Haynesina* spp., *Quinqueloculina* spp., and *T. inflata* are unimodal in their distribution. *B. pseudomacrescens, Haplophragmoides* spp. and *M. fusca* have optima in the high marsh, with many species having no optimum. WA using *C2* provides the optima and tolerances for each of the species (table 4.37); these have been plotted in figure 4.49 and show that the dominant agglutinated species have the largest vertical ranges.

The unconstrained cluster analysis for DMSS can be seen in figure 4.50. As discussed earlier, as the altitudinal range for this site is very small and there is little change in species composition. The assemblage can be seen to be divided into two zones. Zone I contains high abundance of *B. pseudomacrescens*, *J. macrescens* and the presence of *Haplophragmoides* spp. Zone II also has a high abundance of *J. macrescens* but a greater abundance of *Elphidium* spp. and fewer *B. pseudomacrescens* and *Haplophragmoides* spp.

The correlation of the cluster order has been carried out, however, and can be seen in figure 4.51 and table 4.38. It shows that sand (0.53), silt (-0.54), organic matter (-0.41), and distance (-0.60) are all significant variables relating to the order of the samples.

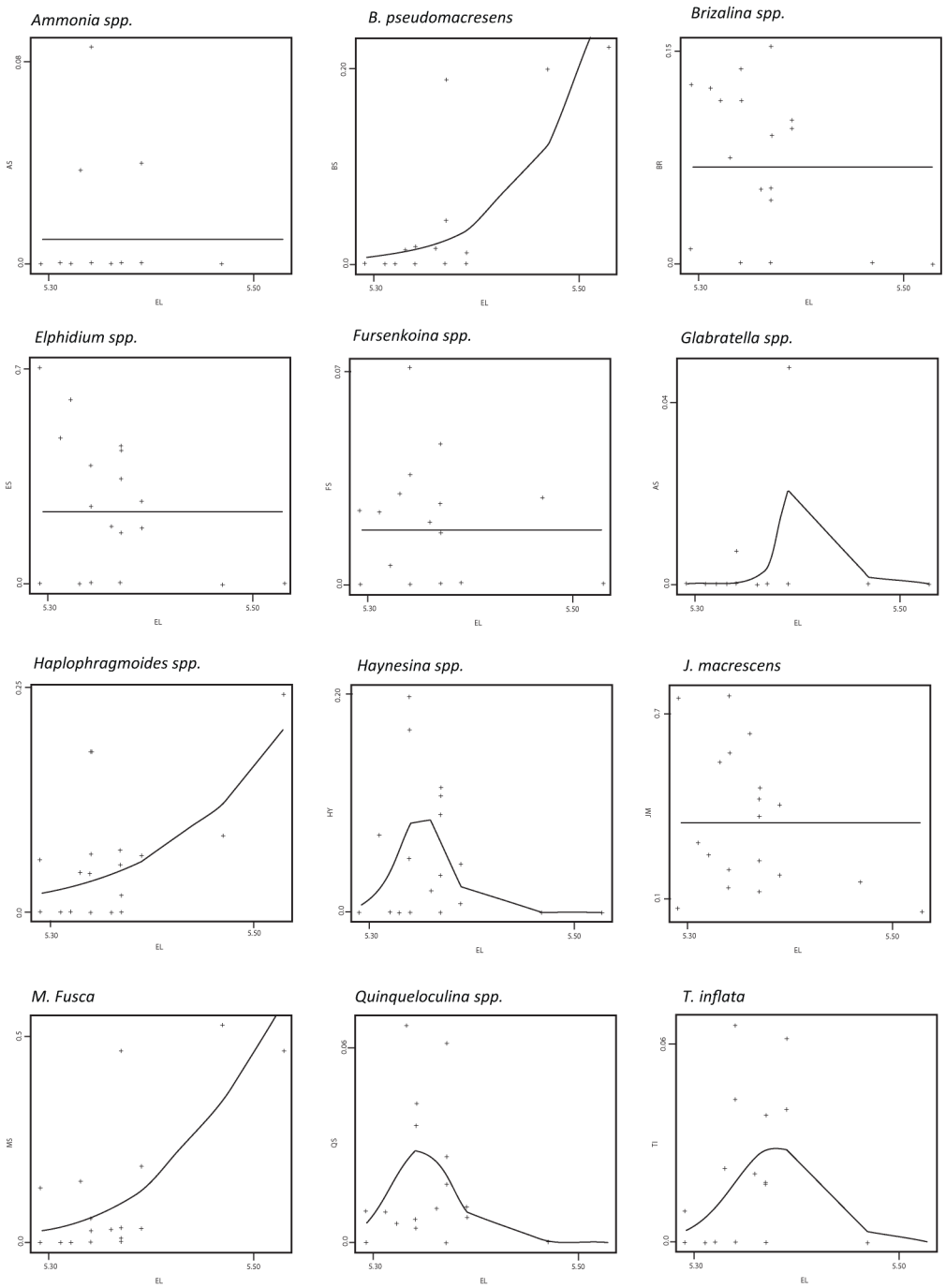

Figure 4.48 Species response curves to elevation for all Decoy Marsh.

Table 4.37 Species coefficients from WA for all Decoy Marsh.

Species	Count	Max	N2	Optimum	Tolerance
Ammonia beccarii spp.	4	8.63	2.8513	5.36002	0.05845
B. pseudomacrescens	8	22.33	3.99583	5.4462	0.081805
Brizalina spp.	14	15.38	11.861	5.34574	0.032952
Elphidium spp.	12	71.08	10.0317	5.34143	0.034904
Fursenkoina spp.	11	7.14	8.51356	5.35348	0.045332
Fursenkoina spp.	2	4.8	1.2934	5.38348	0.035355
Haplophragmoides spp.	12	24.27	7.66781	5.4055	0.087997
Haynesina spp.	11	20	7.38116	5.35243	0.021889
J. macrescens	19	76.15	13.6165	5.34933	0.040045
M. fusca	12	52.86	5.66625	5.4229	0.084692
Quinqueloculina spp.	14	6.72	7.79315	5.3487	0.024415
T. inflata	10	6.59	7.7378	5.36076	0.026747

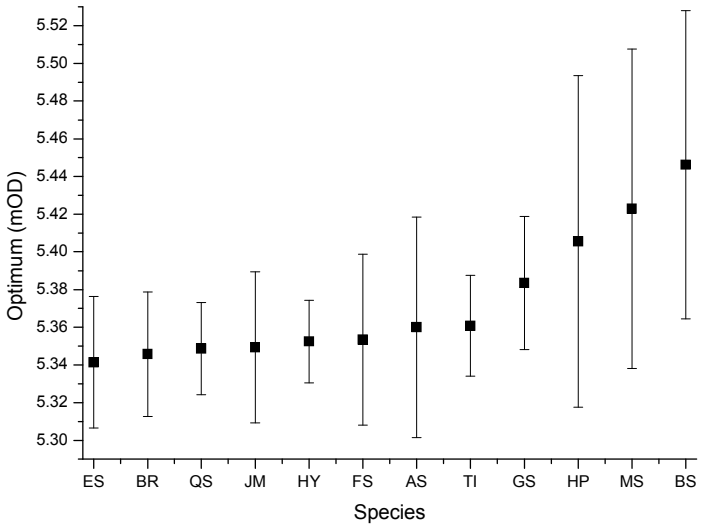

Figure 4.49 Optimum altitude of species from Decoy Marsh with tolerance levels (results from WA, c2) (y axis altitude gradient). AS=*Ammonia beccarii spp.,* BS= *B. pseudomacrescens,* BR=*Brizalina spp.,* CY= *Cyclogyra involvens***,** ES= *Elphidium spp.,* FS= *Fursenkoina spp.*, GS=*Glabratella milletti,* HP= *Haplophragmoides spp.,* HY= *Haynesina spp.,* JM= *J. macrescens,* MS= *M. fusca,* QS= *Quinqueloculina spp.*, TX=*Textularia spp.,* TI= *T. inflata*.

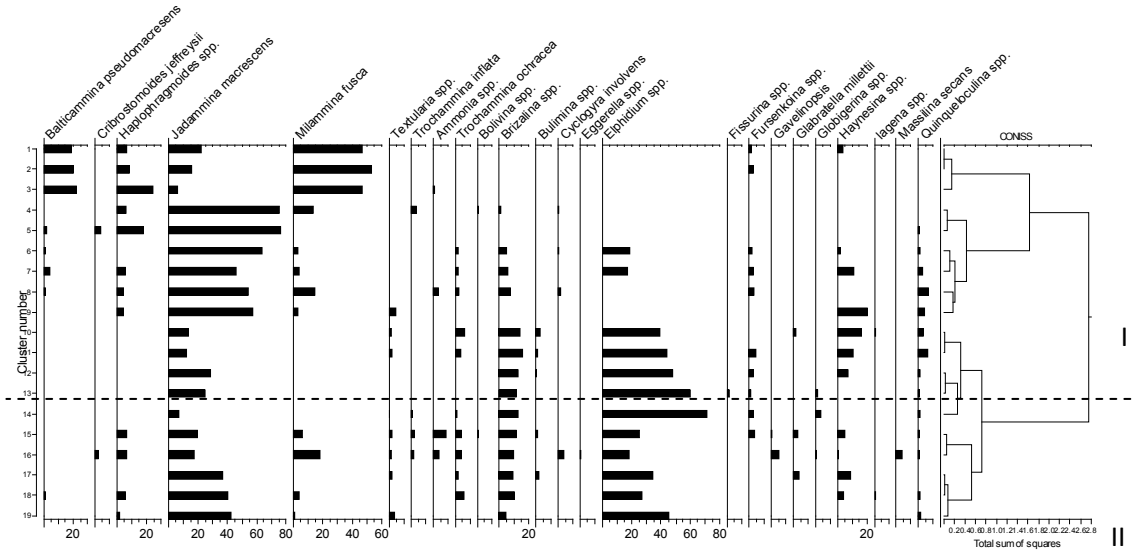

Figure 4.50 Decoy Marsh unconstrained cluster analysis based on unweighted Euclidean distance for relative percentages of dead foraminifera abundance.

Table 4.38 Correlations for cluster order and variables for Decoy Marsh.

Variables	r^2	p-value
Sand %	**0.53307**	**0.02273**
Clay %	-0.41217	0.089195
Silt %	**-0.53916**	**0.020945**
Organic matter	**-0.40793**	**0.092866**
pH	0.002796	0.991214
Salinity	0.068495	0.787118
Transect	0.363449	0.138198
Elevation	-0.1564	0.535417
Distance	**-0.59755**	**0.008824**

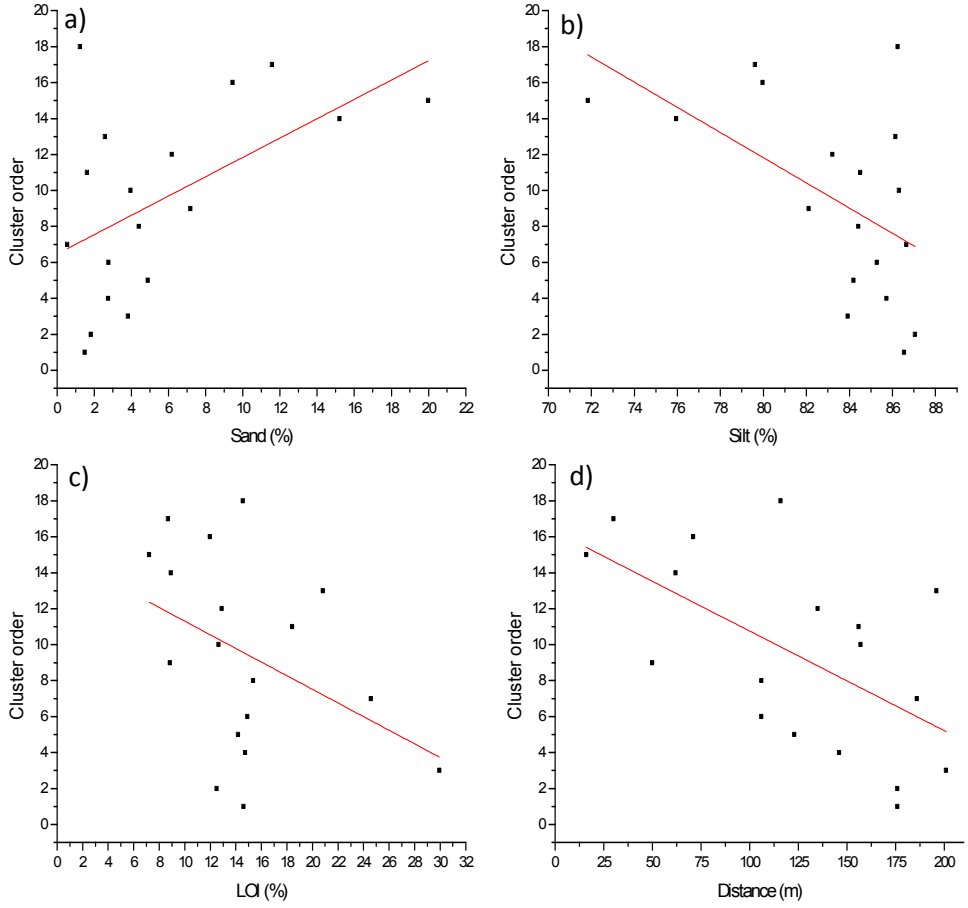

Figure 4.51 Correlations between cluster order and significant variables for Decoy Marsh. a) sand %, b) silt %, c) organic matter content, d) distance.

Combined Decoy Marsh live data

The results of the DCA for the live DM data can be seen in table 4.39. The first two axes have a length between 1 and 2 SD. The first ordination axis was found to be correlated positively with organic matter, elevation and distance, and negatively with transect number. The second axis is also positively related to distance. The biplots (figure 4.52) show that many of the species and samples clustered together, with only three samples being distinguished from each other (1, 2 and 18).

The RDA results show that the nine variables explain 76% of the variance (table 4.40). It was found that distance, elevation and clay were significant and explained 67% of the variance (table 4.41). *Varpart* and permutation tests revealed that only distance and elevation are significant independently. With these significant variables alone the variance explained reduces to 51% (table 4.42). Most of this variation is due to intercorrelation (23%) followed by elevation (20%), with distance only explaining 9%.

Table 4.39 DCA for live Decoy Marsh data.

	DCA1	DCA2	DCA3	DCA4
Eigenvalues	0.4792	0.2068	0.06039	0.35128
Decorana values	0.483	0.1674	0.02399	0.01016
Axis lengths	1.6416	1.2156	0.50068	1.72493

	DCA1	DCA2	r2	Pr(>r)	Significance (p value)
Sand %	-0.61023	-0.79222	0.1512	0.23	1
Clay %	0.87709	0.48032	0.0548	0.654	1
Silt %	0.56422	0.82563	0.1804	0.183	1
Organic matter	0.95734	0.28898	0.4332	0.043	0.05
pH	0.35669	0.93422	0.0706	0.578	1
Salinity	-0.44553	-0.89527	0.1515	0.309	1
Transect	-0.93864	0.3449	0.2228	0.093	0.1
Elevation	0.8982	-0.43959	0.625	0.014	0.05
Distance	0.68744	0.72624	0.4825	0.003	0.01

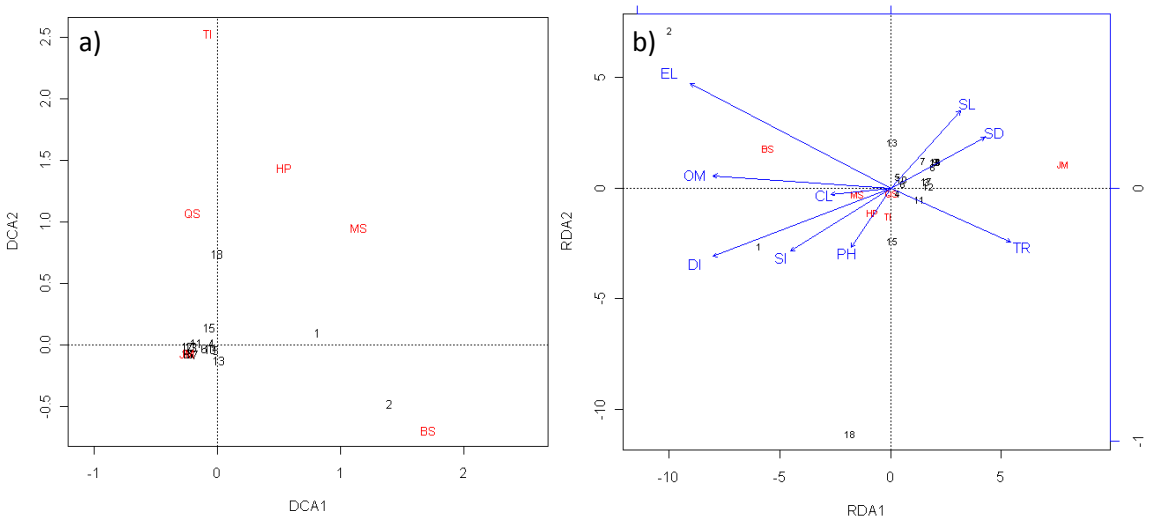

Figure 4.52 a) DCA b) RDA for live Decoy Marsh data. BS= *B. pseudomacrescens,* HP= *Haplophragmoides spp.,* JM= *J. macrescens,* MS= *M. fusca,* QS= *Quinqueloculina spp.*, TI= *T. inflata*. SD=sand, CL=clay, SI=silt, PH=pH, EL=elevation, OM=organic matter content, SL=salinity, TR=transect, DI=distance.

Table 4.40 RDA results for Decoy Marsh live data.

	Inertia	Proportion	Rank
Total	1042.2693	1	
Constrained	808.7163	0.7759	6
Unconstrained	233.5530	0.2241	6

Table 4.41 RDA for live Decoy Marsh data with significant variables only (distance, elevation, clay).

	Inertia	Proportion	Rank
Total	1042.2693	1	
Constrained	688.2642	0.6604	3
Unconstrained	354.0051	0.3396	6

Table 4.42 Variation partitioning of significant variables for live Decoy Marsh.

Variable	Variance	Significance	% of total inertia	% of constrained inertia
All	0.50743			
Distance	0.08657	0.001	9	17
Elevation	0.19539	0.002	20	39
Intercorrelations	0.22547		23	44

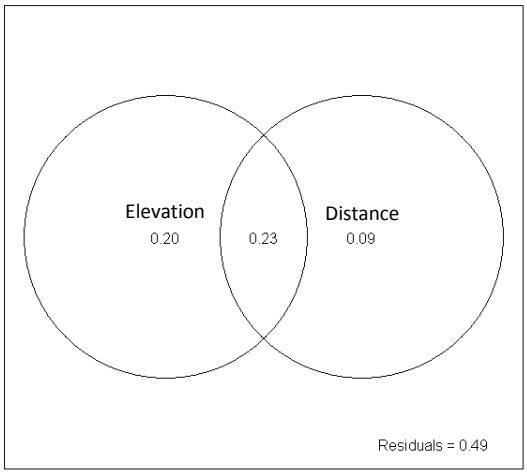

Figure 4.53 Variation partitioning of live Decoy Marsh.

Figure 4.54 shows the species response curves to elevation for the different species using the best fit models. It shows that *B. pseudomacrescens* and *M. fusca* have optima in the high marsh whereas *J. macrescens* and *T. inflata* occupy the low marsh. WA provides the optima and tolerances for each of the species (table 4.43). These have been plotted in figure 4.55 and show that several of the species (*Haplophragmoides* spp*., T. inflata* and *M. fusca*) have tolerances that are outside the sampled altitudinal range as the mudflat was not sampled and the upper marsh samples did not have any foraminifera and therefore were not included. *J. macrescens* was found to have the narrowest vertical range.

The unconstrained cluster analysis for DMSS live data can be seen in figure 4.56. As discussed earlier, as the altitudinal range for this site is very small and there is little change in species composition. The assemblage so two clear zonations (figure 4.56). Zone I which predominately contains *J. macrescens* and zone II which is distinguishable by its increased presence of B. *Pseudomacrescens.* The correlation of the cluster order has been carried out however, and can be seen in table 4.44 and figure 4.57. It shows that organic matter (r^2=0.61), and elevation (r^2=0.67) are significant variables relating to the order of the samples.

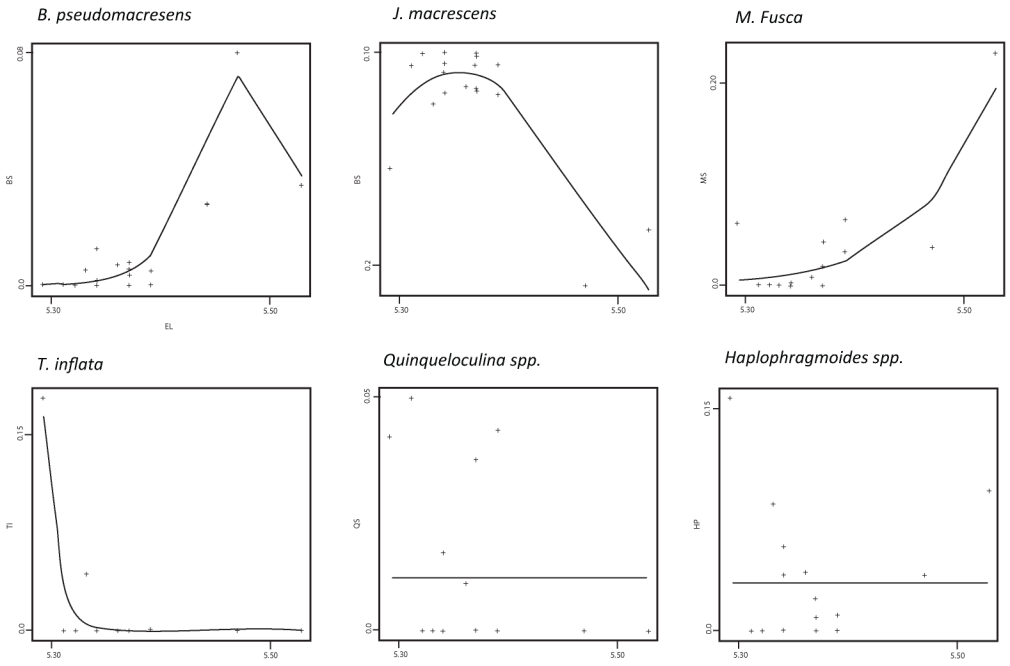

Figure 4.54 Species coefficients of live Decoy Marsh data.

Table 4.43 Species coefficients for live Decoy Marsh data.

Species	Count	Max	N2	Optimum	Tolerance
B. pseudomacrescens	10	80	3.31281	5.44943	0.077181
Haplophragmoides spp.	11	15.75	6.34261	5.36982	0.092539
J. macrescens	18	100	16.6372	5.3563	0.039678
M. fusca	9	23.02	3.76618	5.44528	0.103257
T. inflata	2	17.81	1.45722	5.29779	0.028284
Quinqueloculina spp.	6	4.95	5.02884	5.3394	0.042989

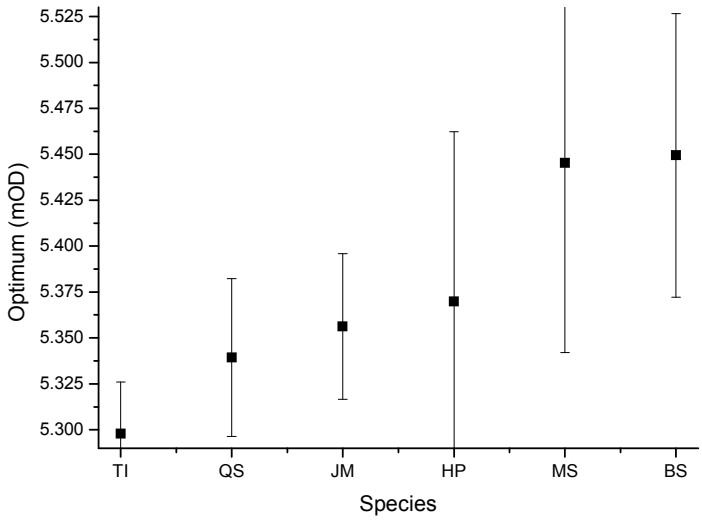

Figure 4.55 Optimum altitude of species from all Decoy Marsh live data with tolerance levels (results from WA, c2) (y axis altitude gradient). BS= *B. pseudomacrescens,* HP= *Haplophragmoides spp.,* JM= *J. macrescens,* MS= *M. fusca,* QS= *Quinqueloculina spp.*, TI= *T. inflata*.

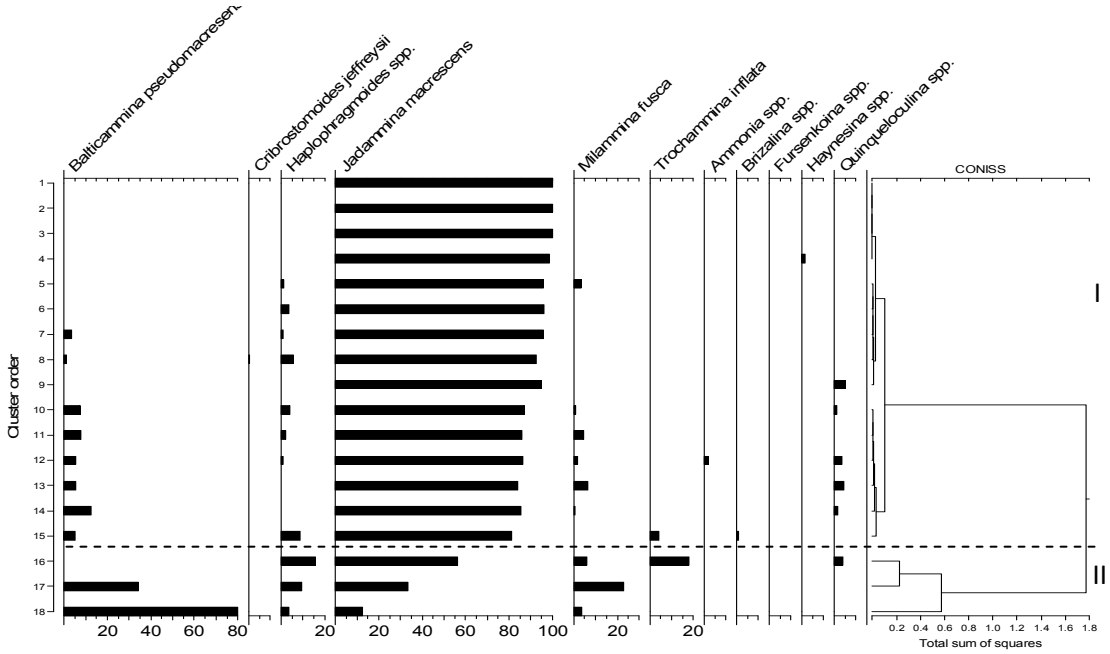

Figure 4.56 Decoy Marsh live unconstrained cluster analysis based on unweighted Euclidean distance for relative percentages of dead foraminifera abundance.

Table 4.44 Correlations for cluster order and variables for DM live

Variables	r^2	p-value
Sand %	-0.34343	0.162921
Clay %	0.372814	0.127581
Silt %	0.308809	0.21245
Organic matter	**0.611784**	**0.006972**
pH	-0.21104	0.400559
Salinity	0.089732	0.723276
Transect	-0.18172	0.470489
Elevation	**0.672535**	**0.002228**
Distance	0.333161	0.176701

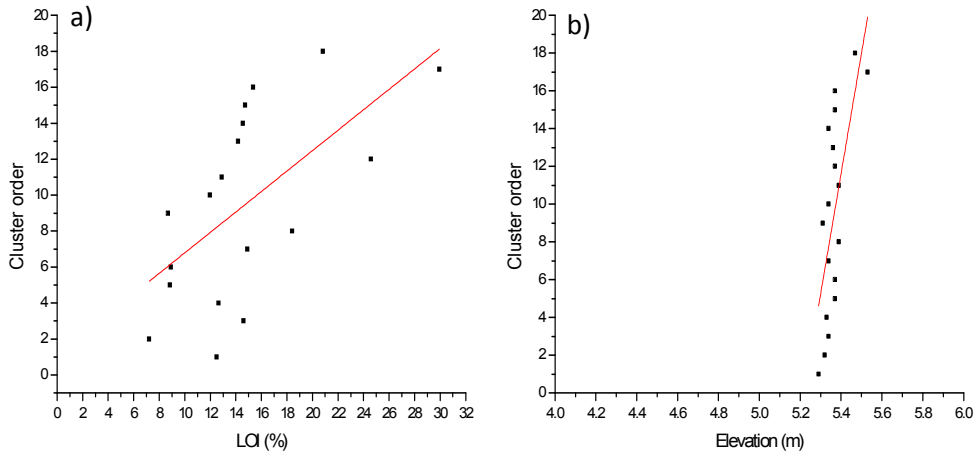

Figure 4.57 Correlations between cluster order and significant variables for Decoy Marsh live data. a) organic matter content, b) elevation.

Combined Oglet Bay and Decoy Marsh data

All dead data

All the species and environmental data were combined from both sites, and the data analysis was repeated. The DCA can be seen in table 4.45 and shows the first two axes have lengths of 3 SD. Table 4.45 also shows that the first ordination axis was found to be correlated positively with transect and distance, and negatively with *Phragmites* spp. and clay. Axis 2 was found to relate positively to clay and negatively with sand, clay, organic matter and transect. There does not seem to be any gradient or clear relationships identifiable from the biplot of the DCA, which is seen in figure 4.58. Similarly, the biplots of the RDA analysis (figure 4.59) show no obvious elevational gradient. Elevation, distance and sand can be seen to have a positive relationship and these are negatively related to clay. The RDA results (table 4.46) show that the all 10 variables explain 52% of the total inertia. The significance test shows that transect, salinity, organic matter, *Phragmites* spp., clay, elevation and sand are significant in explaining the variance. With these variables alone, these account for 50% (table 4.47). pRDA was used to determine which variables account for the most of the explained inertia (table 4.48), and it was found that the variables individually account for very little, with most of the variance being explained by the correlation of these variables (32%).

Table 4.45 DCA for all data.

	DCA1	DCA2	DCA3	DCA4
Eigenvalues	0.4865	0.4122	0.1768	0.18864
Decorana values	0.4903	0.3931	0.1597	0.06605
Axis lengths	3.0301	3.0411	1.8438	1.68938

	DCA1	DCA2	r2	Pr(>r)	Significance (p value)
Sand %	0.69281	-0.72112	0.0758	0.042	0.05
Clay %	-0.66051	0.750818	0.4967	0.001	0.001
Silt %	-1	0.002826	0.0005	0.983	1
Organic matter	-0.58837	-0.80859	0.3711	0.001	0.001
Salinity	-0.03872	0.99925	0.2807	0.001	0.001
pH	-0.11666	-0.99317	0.0349	0.242	1
Phragmites spp.	-0.99453	-0.10445	0.3643	0.001	0.001
Distance	0.702077	-0.7121	0.0535	0.123	1
Transect	0.889001	-0.45791	0.6013	0.001	0.001
Elevation	0.435779	-0.90005	0.1548	0.002	0.01

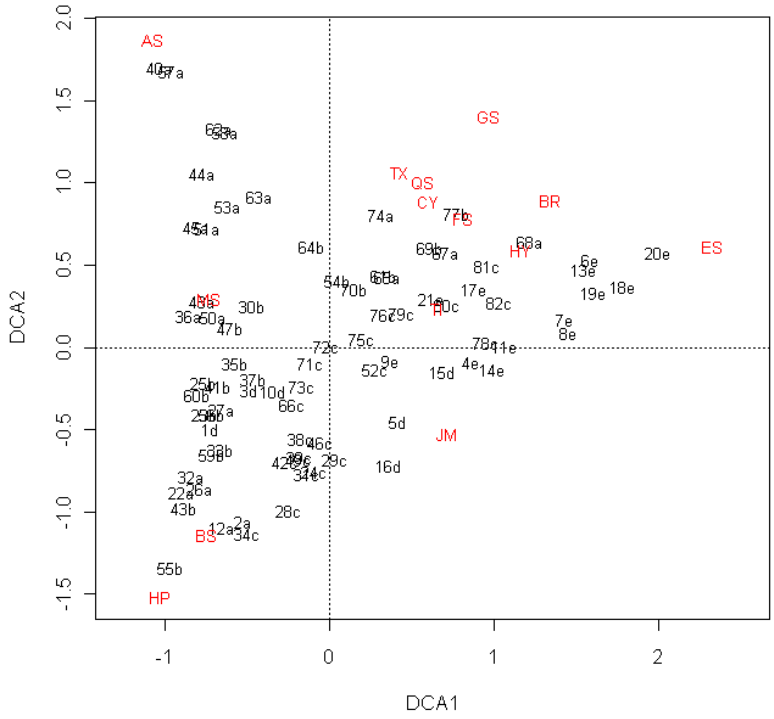

Figure 4.58 DCA for all data. AS=*Ammonia beccarii* spp., BS= *B. pseudomacrescens,* BR=*Brizalina spp.,* CY= *Cyclogyra involvens,* ES= *Elphidium spp.,* FS= *Fursenkoina spp.*, GS=*Glabratella milletti,* HP= *Haplophragmoides spp.,* HY= *Haynesina spp.*, JM= *J. macrescens,* MS= *M. fusca,* QS= *Quinqueloculina spp.*, TX=*Textularia spp.,* TI= *T. inflata*. a=OBSS1, b=OBSS2, c=OBSS3, d=DMSS1, e=DMSS2.

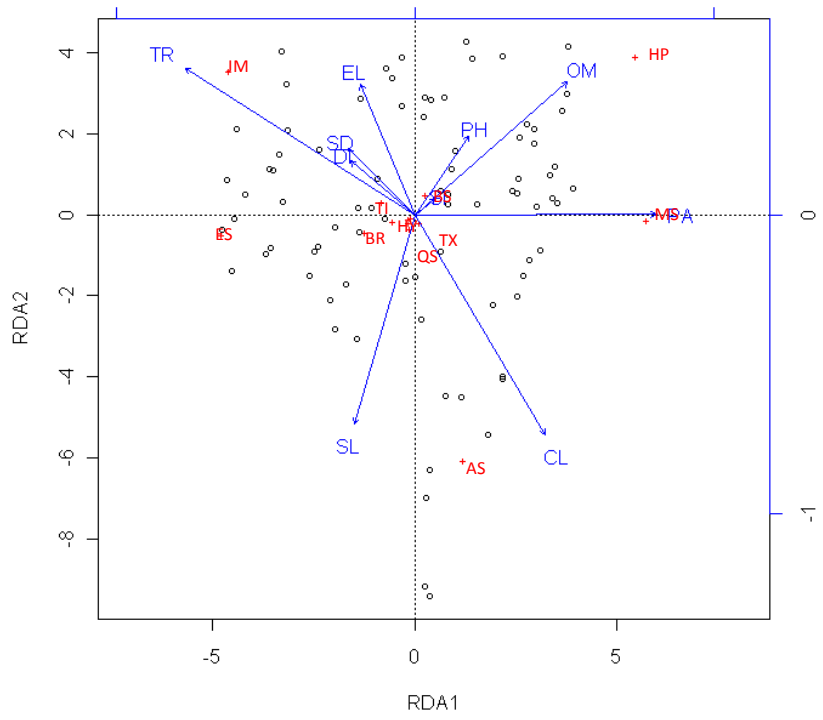

Figure 4.59 RDA for all data. SD=sand, CL=clay, SI=silt, SL=salinity, PA=Phragmites spp., PH=pH, EL=elevation, DI=distance, TR=transect, OM=organic matter.

Table 4.46 RDA for all data.

	Inertia	Proportion	Rank
Total	1944.3127	1	
Constrained	1014.0926	0.5216	10
Unconstrained	930.2201	0.4784	14

Table 4.47 RDA for all data with only significant variables (transect, salinity, organic matter content, *Phragmites spp.,* clay, elevation, and sand).

	Inertia	Proportion	Rank
Total	1944.3127	1	
Constrained	970.3477	0.4991	7
Unconstrained	973.9650	0.5009	14

Table 4.48 pRDA for all data.

Variable	Variance	Significance	% of total inertia	% of constrained inertia
All	0.4991			
Sand	0.01558	0.042	2	3
Phragmites spp.	0.0305	0.003	3	6
Clay %	0.01628	0.031	2	3
Organic matter	0.03237	0.002	3	7
Elevation	0.01755	0.03	2	4
Transect	0.04068	0.001	4	8
Salinity	0.02727	0.006	3	6
Intercorrelations	0.31887		32	64

Figure 4.60 shows the species response curves to elevation for the different species using the best fit models. It shows that *Ammonia beccarii* spp., *Haplophragmoides* spp. and *M. fusca* have a unimodal distribution in relation to elevation; *B. pseudomacrescens, Elphidium* spp. and *J. macrescens* occupy the high marsh; and *Cyclogyra involvens, G. millettii, Textularia* spp., *Quinqueloculina* spp. and *T. inflata* have low marsh optima. WA using *C2* (Juggins, 2007) provides the optima and tolerances for each of the species (table 4.49). These have been plotted in figure 4.61 and show that *B. pseudomacrescens* has a narrow vertical range and *J. macrescens* has a large altitudinal tolerance.

The unconstrained cluster analysis (figure 4.62) reveals six different assemblage zones, several of which are related to transect number, with zone I relating to OBSS1, zone III related to OBSS3, and zone V related mostly with DMSS2. As the zonations overlap in altitude they have not been plotted showing the altitudinal range they cover. The correlations between cluster order and variables have been carried out and can be seen in table 50. It shows that *Phragmites* spp. presence and elevation are the only significant variables.

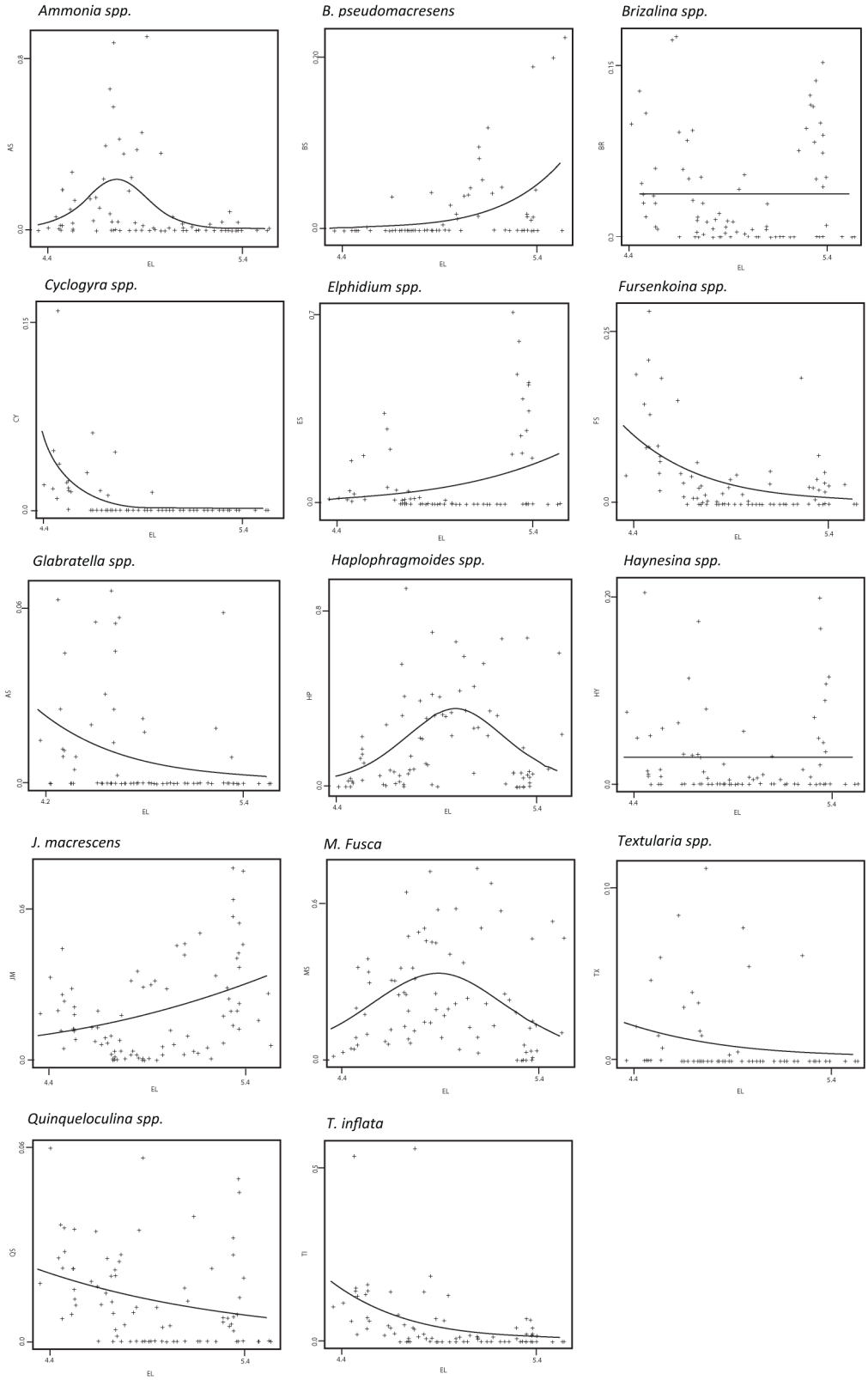

Figure 4.60 Species coefficients for species with elevation all data.

Table 4.49 Species coefficients for all data.

Species	Count	Max	N2	Optimum	Tolerance
Ammonia beccarii spp.	42	90.26	16.389	4.76564	0.135833
B. pseudomacrescens	17	11.79	11.4315	5.05191	0.137431
Brizalina spp.	44	17.61	20.5426	4.64423	0.16909
Cyclogyra involvens	18	16.03	8.88384	4.54864	0.123476
Elphidium spp.	29	33.52	9.79112	4.61112	0.102462
Fursenkoina spp.	36	28.27	16.3813	4.56498	0.16356
Glabratella millettii	20	5.41	13.4995	4.65086	0.136792
Haplophragmoides spp.	58	90.58	33.7881	4.95616	0.237033
Haynesina spp.	29	20.69	11.6328	4.64856	0.180272
J. macrescens	58	50.3	30.8904	4.82614	0.292921
M. fusca	63	73.33	42.4194	4.84935	0.2173
Quinqueloculina spp.	40	8	27.9694	4.69449	0.226517
Textularia spp.	16	11.33	9.79657	4.70981	0.173562
T. inflata	41	55.95	14.6085	4.64199	0.179318

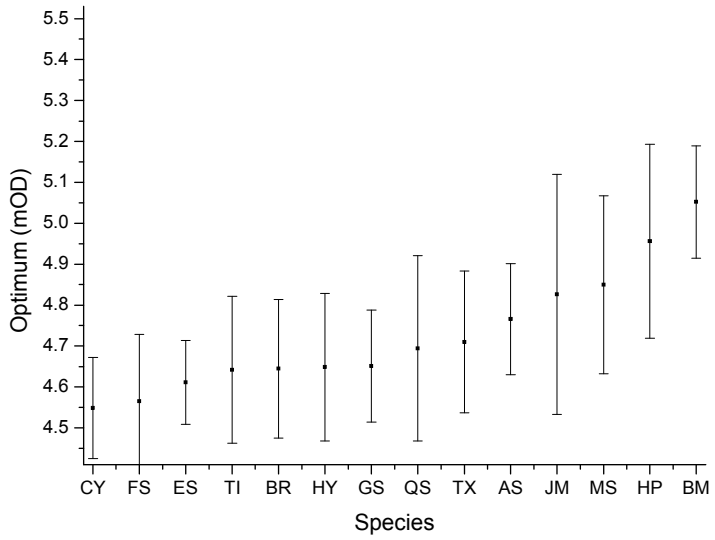

Figure 4.61 Optimum altitude of species for all data with tolerance levels (results from WA, c2) (y axis altitude gradient). AS=*Ammonia beccarii spp.*, BS= *B. pseudomacrescens,* BR=*Brizalina spp.,* CY= *Cyclogyra involvens,* ES= *Elphidium spp.,* FS= *Fursenkoina spp.*, GS=*Glabratella milletti,* HP= *Haplophragmoides spp.,* HY= *Haynesina spp.,* JM= *J. macrescens,* MS= *M. fusca,* QS= *Quinqueloculina spp.*, TX=*Textularia spp.,* TI= *T. inflata*.

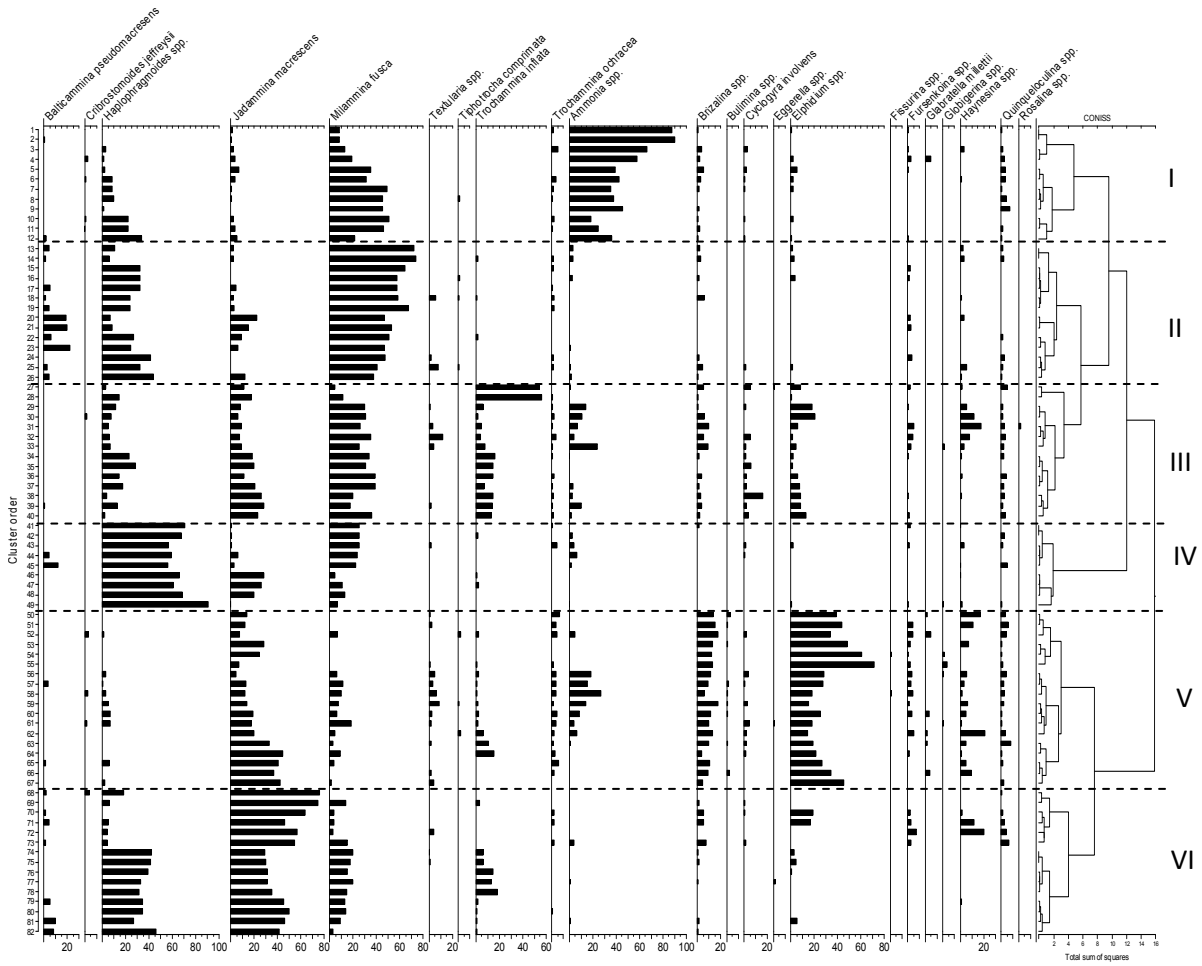

Figure 4.62 Oglet Bay and Decoy Marsh unconstrained cluster analysis based on unweighted Euclidean distance for relative percentages of dead foraminifera abundance.

Table 50 Correlations between cluster order and variables for all data.

Variables	r^2	p-value
Sand %	-0.04092	0.71679
Clay %	0.158621	0.157254
Silt %	-0.02006	0.858951
Organic matter	-0.21705	0.051609
Salinity	0.082157	0.465906
pH	-0.15815	0.1585
Phragmites spp.	-0.34863	**0.001425**
Distance	-0.10796	0.337404
Transect	0.012128	0.914426
Elevation	-0.22294	**0.045443**

Combined Oglet Bay dead data and Decoy Marsh live data

As the live data from Decoy Marsh appears to be related to elevation and distance from tidal influence. These data were added to the dead Oglet Bay data. The results can be seen in tables 4.51 to 4.58 and figures 4.63 to 4.70. The results of the DCA (table 4.51) show the gradient length to be between 2-4 SD. Axis 1 is significantly and positively related to clay and *Phragmites* spp., and negatively related with sand, distance and elevation. Axis 2 is significantly and positively related to salinity and negatively related to organic matter, *Phragmites* spp., distance and elevation. The biplot of the DCA (figure 4.63) shows that the species *Brizalina* spp*., G. milletti, Haynesina* spp*., C. involvens, Textularia* spp*.* and *Fursenkoina* spp*.* are all associated with each other as well as the species *B. pseudomacrescens* and *Haplophragmoides* spp*.* The biplot for the RDA shows that *J. macrescens* is most associated with transect number, and *Ammonia beccarii* spp. which appears to be associated with clay content. Other species are not seen to be directly associated with any variables.

The results of the RDA show that 52% can be explained by the 10 variables included (table 4.52). Transect, elevation, salinity, sand, *Phragmites* spp*.* and organic matter, were found to be significant and these explain 49% (table 4.53). Permutation tests from the pRDA shows that organic matter was not significant on its own, so was removed before pRDA was carried out. Table 4.54 shows that most of the variance is from intercorrelations between the variables (33%), followed by the transect number (7%). Other variables have only low proportions.

Table 4.51 DCA with all data (DM live).

	DCA1	DCA2	DCA3	DCA4
Eigenvalues	0.5722	0.3731	0.2007	0.24725
Decorana values	0.5788	0.304	0.1132	0.08347
Axis lengths	3.3772	2.7288	2.2988	2.50209

	DCA1	DCA2	r2	Pr(>r)	Significance (p value)
Sand %	-0.89415	-0.44776	0.0862	0.032	0.05
Clay %	0.940594	0.339534	0.3022	0.001	0.001
Silt %	0.769656	0.638459	0.0117	0.655	1
Organic matter	-0.05208	-0.99864	0.2379	0.001	0.001
Salinity	0.141567	0.989929	0.0761	0.057	0.1
pH	0.996478	-0.08385	0.0219	0.439	1
Phragmites spp.	0.793015	-0.6092	0.3965	0.001	0.001
Distance	-0.75003	-0.6614	0.3737	0.001	0.001
Transect	-1	-0.00195	0.6455	0.001	0.001
Elevation	-0.64754	-0.76203	0.5202	0.001	0.001

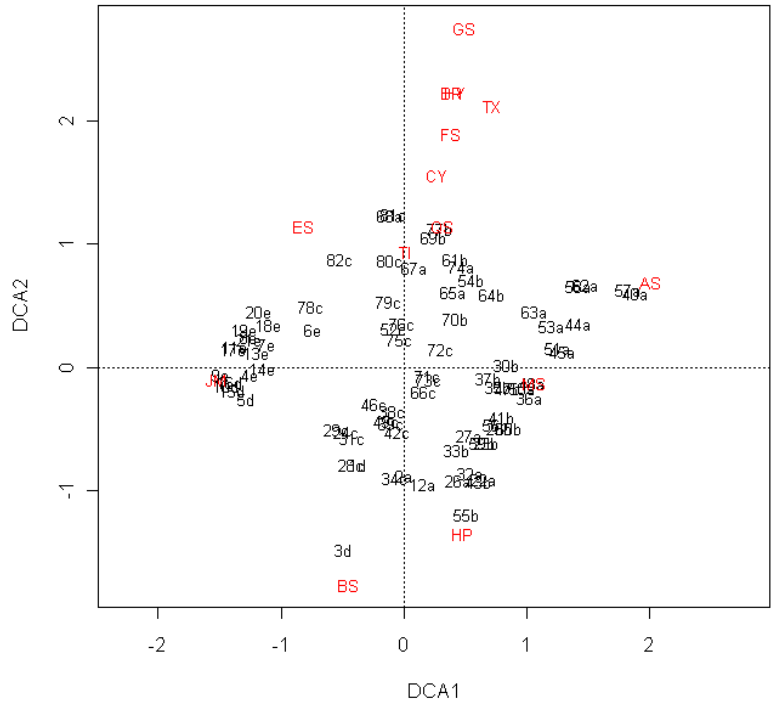

Figure 4.63 DCA for all data (DM live). AS=*Ammonia beccarii spp., BS= B. pseudomacrescens,* BR=*Brizalina spp.,* CY= *Cyclogyra involvens,* ES= *Elphidium spp.,* FS= *Fursenkoina spp.*, GS=*Glabratella milletti,* HP= *Haplophragmoides spp.,* HY= *Haynesina spp.,* JM= *J. macrescens,* MS= *M. fusca,* QS= *Quinqueloculina spp.*, TX=*Textularia spp.,* TI= *T. inflata.* a=OBSS1, b=OBSS2, c=OBSS3, d=DMSS1, e=DMSS2.

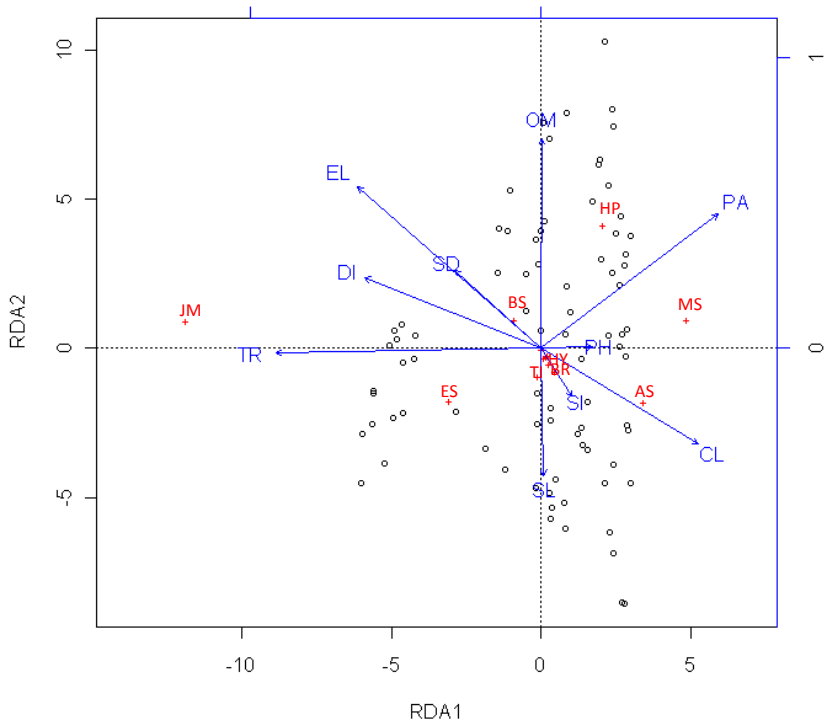

Figure 4.64 RDA for all data (DM live). SD=sand, CL=clay, SI=silt, SL=salinity, PA=*Phragmites spp*., PH=pH, EL=elevation, DI=distance, TR=transect, OM=organic matter. AS=*Ammonia beccarii spp*., BS= *B. pseudomacrescens,* BR=*Brizalina spp.,* CY= *Cyclogyra involvens,* ES= *Elphidium spp.,* FS= *Fursenkoina spp.*, GS=*Glabratella milletti,* HP= *Haplophragmoides spp.,* HY= *Haynesina spp.,* JM= *J. macrescens,* MS= *M. fusca,* QS= *Quinqueloculina spp.*, TX=*Textularia spp.,* TI= *T. inflata*.

Table 4.52 RDA for all data (DM live).

	Inertia	Proportion	Rank
Total	2793.4505	1	
Constrained	1449.1704	0.5188	10
Unconstrained	1344.2801	0.4812	14

Table 4.53 RDA with all data (DM live) with significant variables only (transect, elevation, salinity, sand, *Phragmites spp.* and organic matter).

	Inertia	Proportion	Rank
Total	2793.4505	1	
Constrained	1449.1704	0.4868	6
Unconstrained	1344.2801	0.5132	14

Table 4.54 pRDA of all data (DM live).

Variable	Variance	Significance	% of total inertia	% of constrained inertia
All	0.4882			
Sand %	0.01973	0.047	2	4
Elevation	0.03737	0.001	4	8
Transect	0.07021	0.001	7	14
Phragmites spp.	0.01694	0.048	2	4
Salinity	0.02622	0.008	3	5
Intercorrelations	0.32654		33	67

Figure 4.65 shows the species response curves to elevation for the different species with the best fit models. It shows that *Ammonia beccarii* spp*.*, *Haplophragmoides* spp*.* and *M. fusca* have unimodal distributions in relation to elevation; *B. pseudomacrescens* and *J. macrescens* occupy the high marsh, similar to OBDM; and *Brizalina* spp*., Elphidium* spp*., Fursenkoina* spp*., G. millettii, Quinqueloculina* spp. and *T. inflata* can be seen to have low marsh optima. WA using *C2* provides the optima and tolerances for each of the species (table 4.55), which have been plotted in figure 4.63 to show that most of the species have similar tolerances, with *B. pseudomacrescens* having a narrow vertical range and *J. macrescens* a larger altitudinal tolerance.

The unconstrained cluster analysis (figure 4.67) reveals five different assemblage zones: zone (a) is most related to Decoy Marsh due to the dominance of *J. macrescens*; zone (c) is more related to OBSS1 due to the high abundance of *Ammonia beccarii* spp.; a lower marsh zone (e) contains all Oglet Bay transects but predominantly OBSS3 containing more calcareous species; and finally, the other two zones (b and d) have similar assemblages of *Haplophragmoides* spp*.* and *M. fusca.* Figure 4.68 shows two main distinguishable cluster groups zone I which contains the zones a, b, c, and e (figure 4.67), and zone II which contains the lower marsh zone (figure 4.67).

The correlation coefficients for cluster order and variables (table 4.56 and figure 4.69) show that distance (0.6), transect (0.53) and elevation (0.8) are significant and have strong correlations.

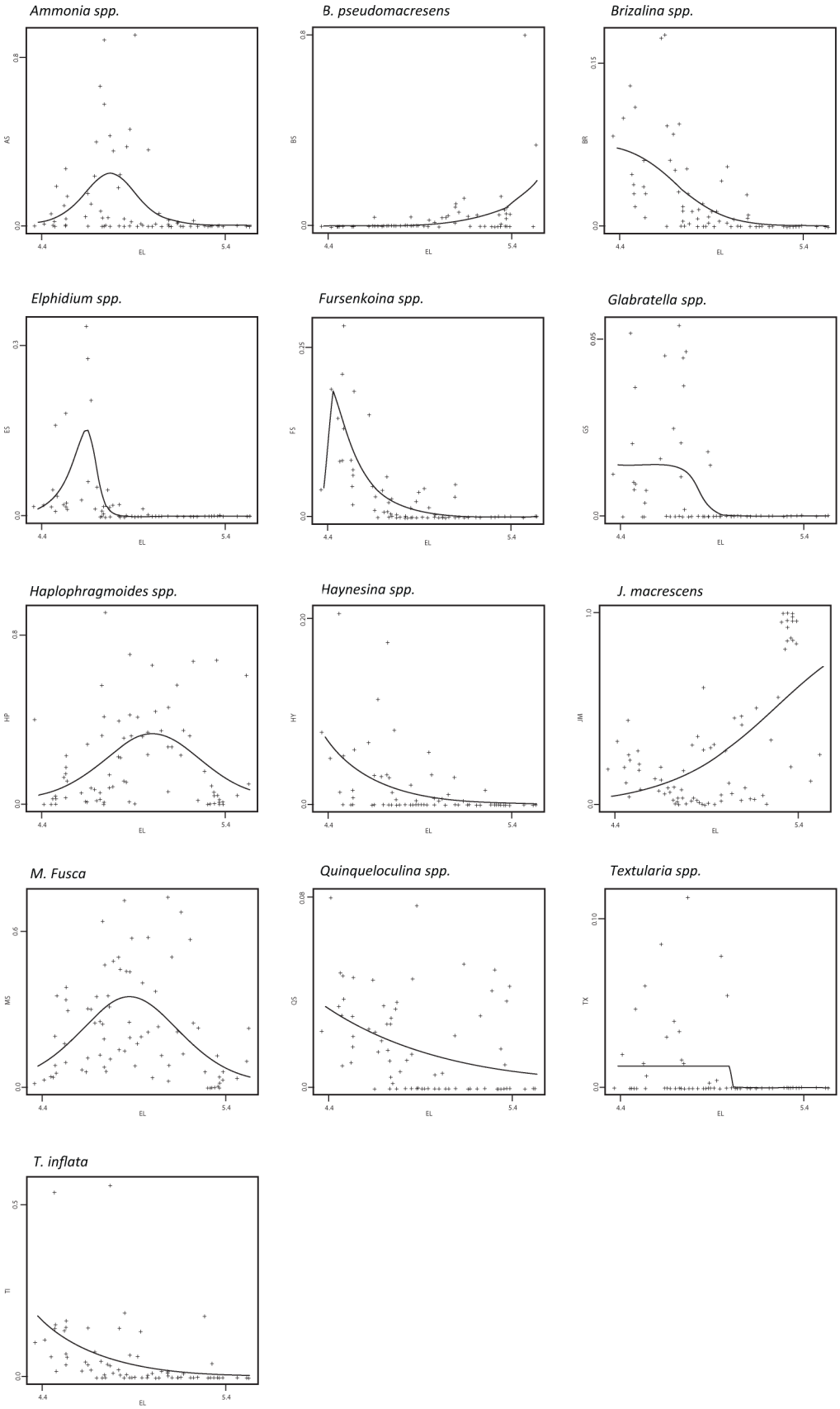

Figure 4.65 Species coefficients of all data (DM live).

Table 4.55 Species coefficients for all data (DM live).

Species	Count	Max	N2	Optimum	Tolerance
Ammonia beccarii spp.	42	90.26	16.389	4.76564	0.135833
B. pseudomacrescens	27	80	6.63727	5.3246	0.223185
Brizalina spp.	45	17.61	21.5298	4.66933	0.2066
Elphidium spp.	29	33.52	9.79112	4.61112	0.102462
Fursenkoina spp.	37	28.27	17.271	4.61729	0.244691
Glabratella millettii	21	5.41	14.179	4.66942	0.172324
Haplophragmoides spp.	70	90.58	36.156	4.9713	0.245845
Haynesina spp.	30	20.69	11.9192	4.65646	0.192713
J. macrescens	77	100	35.8707	5.16337	0.313155
M. fusca	73	73.33	45.3326	4.87125	0.239283
Quinqueloculina spp.	46	8	32.998	4.7934	0.314835
Textularia spp.	17	11.33	10.7952	4.75828	0.231338
T. inflata	43	55.95	15.8612	4.68009	0.235042

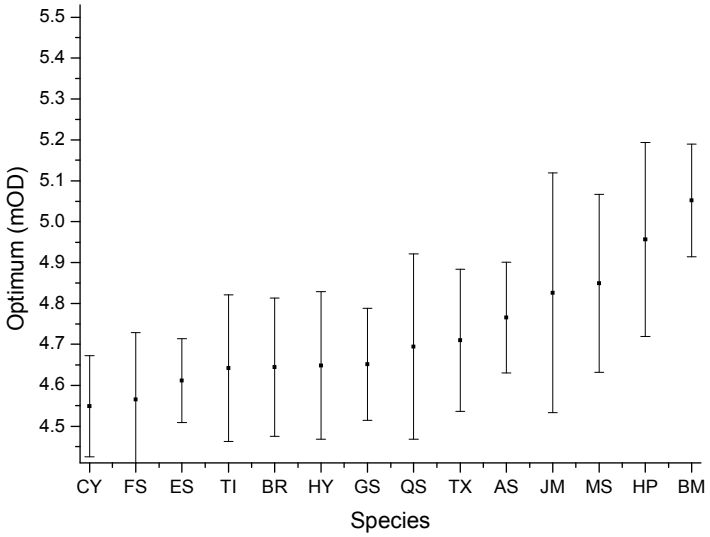

Figure 4.66 Optimum altitude of species from OBDM live with tolerance levels (results from WA, c2) (y axis altitude gradient). AS=*Ammonia beccarii spp*., BS= *B. pseudomacrescens,* BR=*Brizalina spp.,* CY= *Cyclogyra involvens,* ES= *Elphidium spp.,* FS= *Fursenkoina spp.*, GS=*Glabratella milletti,* HP= *Haplophragmoides spp.,* HY= *Haynesina spp.,* JM= *J. macrescens,* MS= *M. fusca,* QS= *Quinqueloculina spp.*, TX=*Textularia spp.,* TI= *T. inflata.*

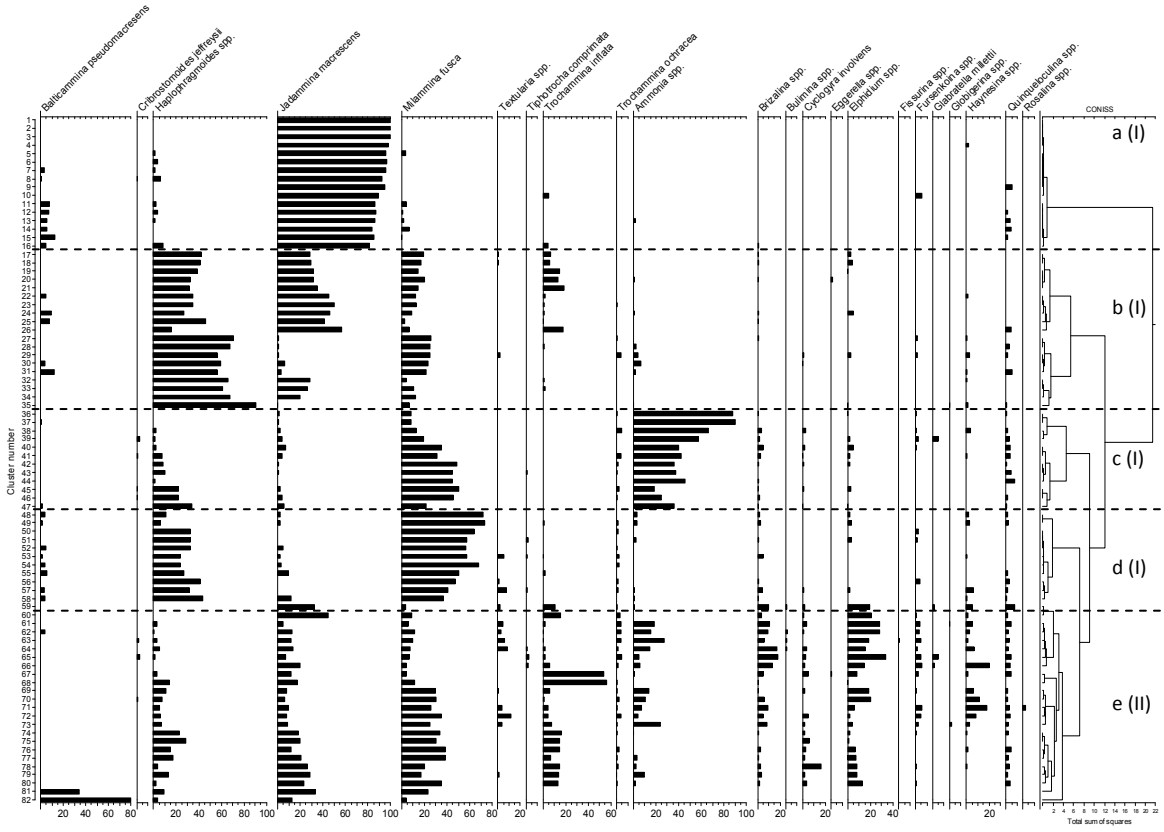

Figure 4.67 Oglet Bay and Decoy Marsh live unconstrained cluster analysis based on unweighted Euclidean distance for relative percentages of dead foraminifera abundance.

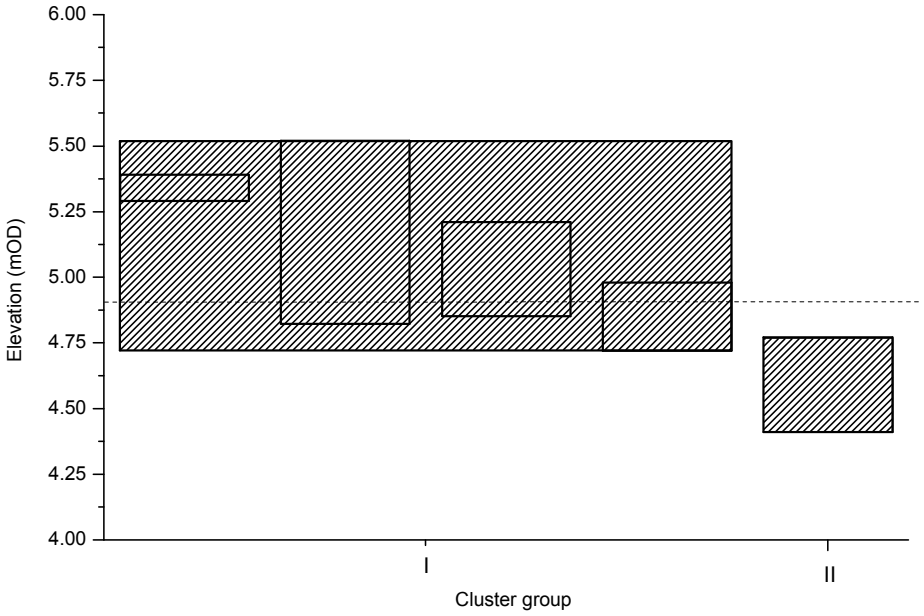

Figure 4.68 OBDM (DM live) cluster zones related to elevation.

Table 4.56 Correlations between cluster order and variables for all OBDM (DM live).

Variables	r^2	p-value
Sand %	0.164621	0.147121
Clay %	-0.3304	**0.002941**
Silt %	-0.04802	0.674291
Organic matter	0.356434	**0.001263**
Salinity	-0.13326	0.241683
pH	-0.05518	0.629069
Phragmites spp.	0.022296	0.845363
Distance	**0.603531**	**3.93E-09**
Transect	**0.531883**	**4.55E-07**
Elevation	**0.800637**	**8.34E-19**

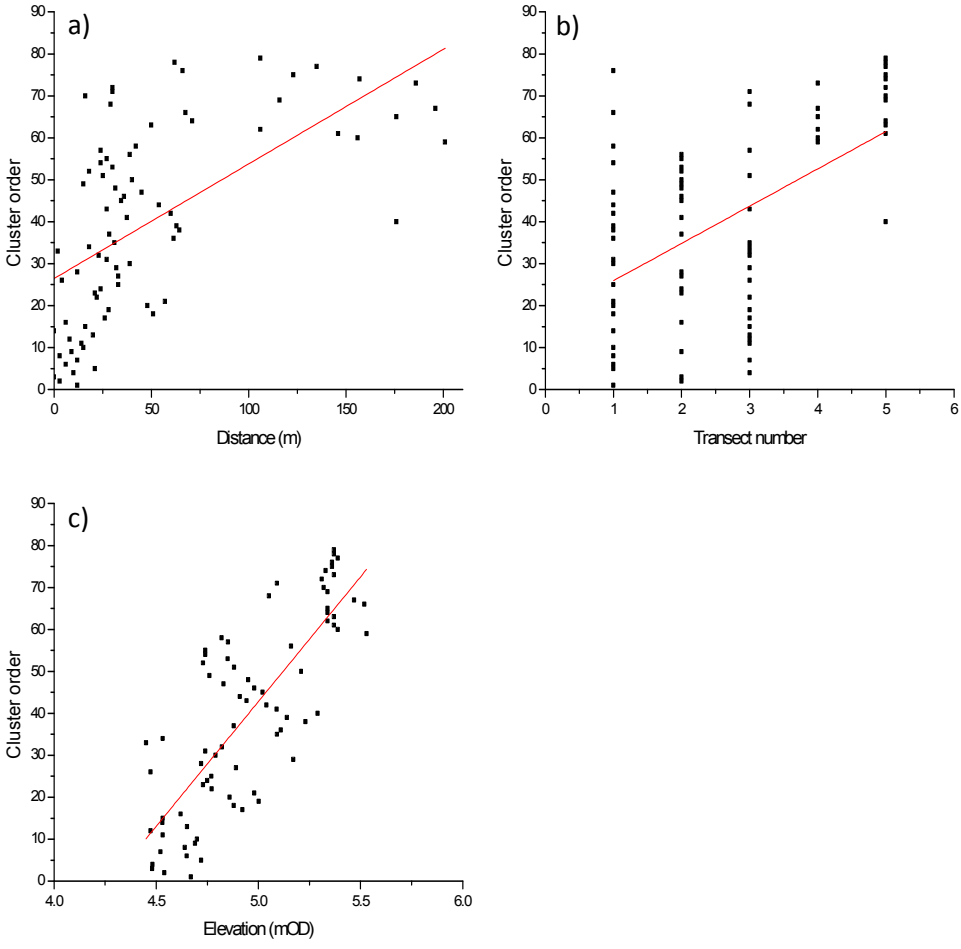

Figure 4.69 Correlations between cluster order and significant variables for all data (DM live). a) distance, b) transect number c) elevation.

4.4. Interpretation of contemporary data

4.4.1. Environmental variables

Figure 4.2 clearly illustrates the contrast in altitude and width between the saltmarshes at Oglet Bay and Decoy Marsh. Oglet Bay has a maximum length of ≈70 m compared with the ≈200 m of Decoy Marsh. The difference in altitude is also large, with Decoy Marsh having an altitude which is on average 0.54 m above Oglet Bay. Although the two sites have very different altitudes and lengths, the other environmental variables appear to be similar across the two saltmarshes.

The salinity of the marshes varied between 0 and 4.5 ‰, which is low salinity and largely freshwater. All transects increase in salinity with increasing distance from the high marsh, which would be expected due to the increase of tidal influence. It is important to consider, however, that salinity data may not be very reliable as the conductivity measurements have only been taken once for each transect and, therefore, may not representative of the prevailing salinity conditions. The salinity of the marsh depends on several parameters which can change seasonally to hourly, depending upon the balance between precipitation, evapotranspiration and tidal inundation. Therefore, higher salinities will be recorded after a high tide or high evapotranspiration, and low salinities during lower tides and higher precipitation. For reliable salinity data, measurements should be taken more than once, in order to cover all of the circumstances in which salinity may change and a mean may be taken.

Organic matter was found to be higher in Oglet Bay than Decoy Marsh, which is likely to be related to the greater and denser vegetation at the former, and grazing which occurs at the latter. The organic matter content decreases along all the transects, which is also attributable to vegetation cover which decreases away from the high marsh.

pH in this study ranges from 8.36 to 7, which corresponds to the average seawater pH of 7.5 to 8.4, and is similar for all transects. The pH was found to decrease in most of the transects down the marsh, however it would be expected that the pH would increase towards the sea as seawater usually has higher pH than freshwater. In addition, organic matter which contains humic acids decreases the pH, therefore the pH would increase along the transect due to a decrease in organic matter content and vegetation.

Although the majority of the samples contain mostly silt followed by clay, in some samples sand makes up most of the grain size composition. For example increases in grain size can

be seen in the high marsh of OBSS1 and OBSS3 in the area at the back of the marsh, with sand content up to 70%. This is likely to be due to runoff from the small cliff at the back of the marsh, and therefore unrelated to marine input. DMSS2 follows a more expected grain size distribution across the marsh with increases in mean grain size and sand increasing in the lower part of the marsh due to the higher tidal flow velocities across the lower marsh.

4.4.2. Foraminiferal assemblages

Both the unconstrained and constrained cluster analysis reveal that, in general all transects at Oglet Bay can be divided into two main zones, a high-to-mid marsh zone and a low marsh zone (figures 4.24, 4.31, 4.38 and 4.44). In contrast, the transects at Decoy Marsh consist of one zone, i.e. high marsh only, as the altitudinal range is very small. The most dominant species occupying the high-to-mid marsh from both sites are *Haplophragmoides* spp*., J. macrescens* and *M. fusca.* The low marsh environment comprises less agglutinated species, including *Haplophragmoides* spp*.* and *J. macrescens* with more calcareous species, mostly *Ammonia beccarii* spp*., Brizalina* spp*.,* and *Elphidium* spp*.* Although the transects can be combined to produce high and low marsh zones (figure 4.68), there are clear differences between the two sites as well as intra-site variability.

Most ecological data have normal distributions relating to a variable, with an optimum within this. For some of the species this can be seen clearly, however, other species appear to have more linear relationship with elevation, exhibiting an increasing or decreasing trend. This occurs at the edges of the marsh where the sampling ends, and may be because the full extent of the environment has not been captured. For example, at the lower end of the saltmarsh, the existence of eroding cliff edge means the full extent of marsh is not sampled. In the high marsh *J. macrescens* (figures 4.21 and 4.35) has a linear distribution in relation to elevation, due to species data above the optimum not being included because of the very low numbers of foraminifera. *J. macrescens* has a distribution towards the lower end of the marsh in Decoy Marsh (figure 4.48 and figure 4.54), but, in reality, *J. macrescens* in Decoy marsh occupies a higher elevation than *J. macrescens* in Oglet Bay (figure 4.70) as these locations are significantly higher than lower transect counterparts at Oglet Bay.

T. inflata occupies the lower marsh environment in both sites, occupying an altitude between 4.43 and 4.79 m OD with an optimum between 4.63 and 4.69 m OD (figure 4.70). The distribution of *M. fusca* from these sites is not so clear, with the abundance of the species extending across the marshes. In OBSS1 *M. fusca* has a unimodal distribution across the marsh, with the optimum in the middle of the marsh. In OBSS2 this species was most

commonly found in the high marsh and in OBSS3 it was found to have its optimum at lower altitudes, although the optima are similar in altitude between 4.71 and 4.90 m OD (figure 4.70). *B. pseudomacrescens* was found to occupy the high marsh environment for all sites and transects (figure 4.70). The range in altitude that this species occupies is between 4.85 and 5.16 m OD, with an optimum range between 5.04 and 5.07 m OD which is a very narrow optimum.

The calcareous species at Oglet Bay were found to have linear distributions occupying the lower marsh environment, with some species having tolerances below that of the sampling elevation. This suggests that their distribution extends to the tidal flat environment, which was not sampled, or extends further out into the estuary or beyond. Species which dominate the low marsh environment include *Ammonia beccarii* spp*., Brizalina* spp., and *Elphidium* spp*. Ammonia beccarii* spp*.* has a wide distribution due to occurrence in the high marsh environment of OBSS1, otherwise it is more commonly found at a lower marsh altitude (figure 4.70). Transect OBSS3 has samples at lower elevations than the other transects and, therefore, low marsh species occur at lower elevations. It is more difficult to determine the altitudinal range each species occupies as the lower end of the distribution is not known (figure 4.70).

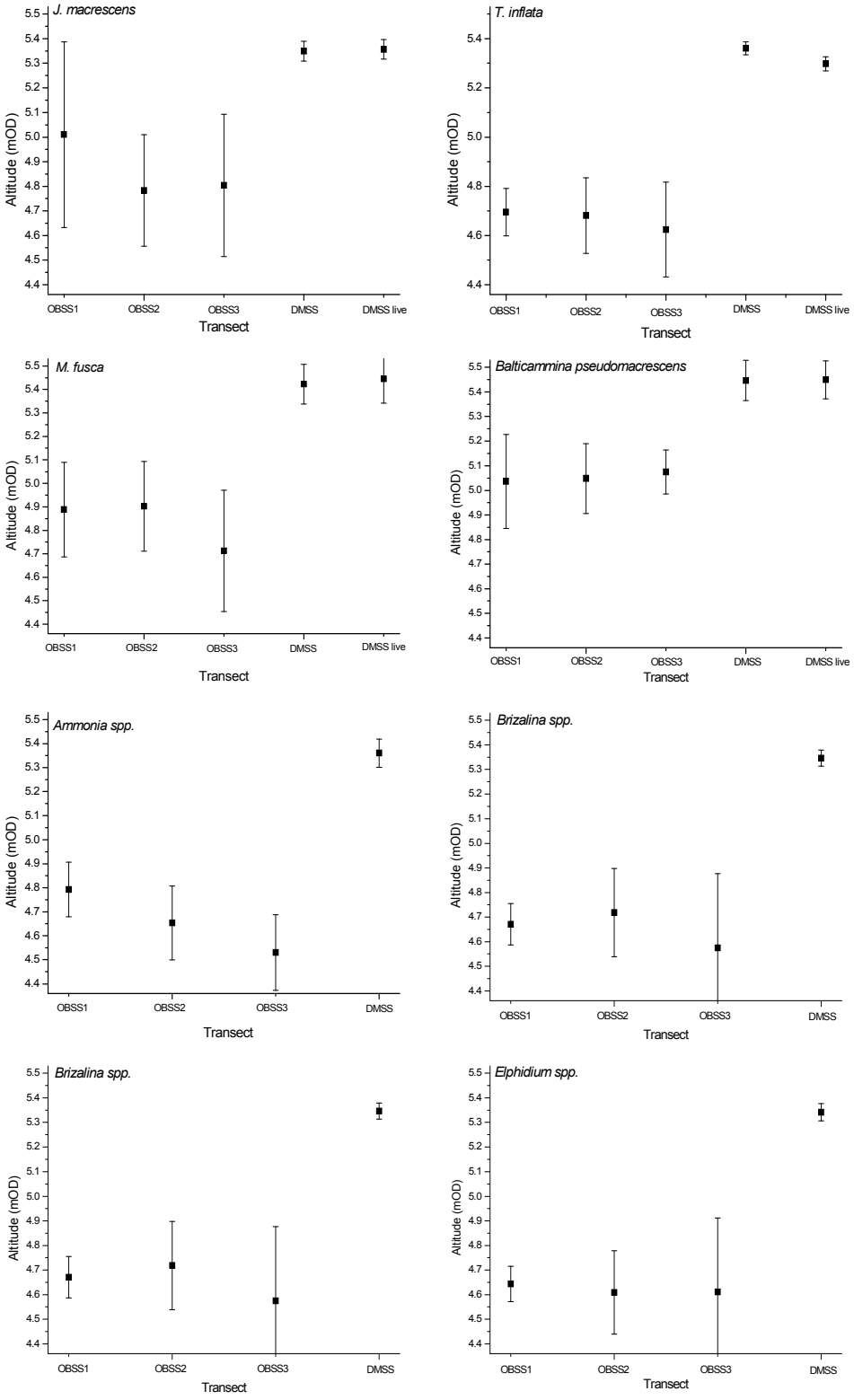

Figure 4.70 Altitudinal ranges for the most dominant species in each of the transects.

4.4.3. The relationship between foraminiferal assemblages and environmental variables

Oglet Bay

The DCA and RDA biplots for OBSS1 (figure 4.19) show a clear elevational gradient in species distribution from high to low marsh, with high organic matter, elevation, distance from tidal influence, and the presence of *Phragmites* spp*.,* associated with samples located in the high marsh and the lower samples associated with higher salinities. Therefore, it is likely that the distribution is related to elevation. This was further explored using RDA (table 4.12 and figure 4.20) and confirmed that elevation and distance were the only significant variables ($p > 0.05$, 999 permutations) and these alone accounted for 45% of the variance found in the species data, of which 48% was from elevation alone. Further statistical analysis used to evaluate the relationships between species distributions and environmental variables included unconstrained cluster analysis. This identified two main zonations, a high marsh zone occupying an altitude range of 5.52-5.04 m OD and a low marsh zone occupying an altitude of 5.11-4.53 m OD with an overlap of 0.07m, indicating that the zones are related to altitude (figure 4.24). To explore this further, the relationship between the cluster order and elevation were examined by scatterplots and correlation coefficients (figure 4.25 and table 4.14). For OBSS1, this indicated that distance (0.76) and elevation (0.77) have the highest correlations with cluster order, although *Phragmites* spp. (0.73) and salinity (-0.6) also have high correlations with cluster order. This is to be expected as *Phragmites* spp*.* is strongly correlated with elevation (0.75) and distance (0.89) and salinity is strongly negatively correlated with elevation (-0.77) and distance (-0.7) (table 4.3).

Similar results were found for OBSS2 whereby only elevation and distance were significant and accounted for 36% of the variance in the species data, although distance made up 46% of this, as opposed to elevation in the OBSS1 data (table 4.17). Unlike OBSS1, whereby elevation decreases down-marsh and distance from tidal influence increases up-marsh, in OBSS2 as well as the other transects in Oglet Bay and Decoy Marsh, elevation does not necessarily decrease with increasing distance down-marsh, with greater variability in elevation across the marsh (figure 4.4). Therefore, distance from tidal influence may be more representative of tidal flooding rather than altitude. In OBSS2 the intercorrelation between distance and elevation makes up 13% of the total variance, and 36% of the explained proportion of the variance. This is reflected in the correlations of distance and elevation that have a strong positive correlation of 0.93 (table 4.4). Distance also has the

highest correlation with cluster order (-0.75), although other variables also have strong correlations, including elevation (-0.63), organic matter (-0.63) and salinity (0.63) (table 4.20), all of which are correlated which other each. The unconstrained cluster analysis reveals two main zones related to altitude, with a high marsh zone occurring between 5.21-4.73 m OD and a low marsh zone occurring between 4.76-4.48 m OD with a small overlap of 0.03 m (figure 4.31). The OBSS2 CCA and DCA biplots (figure 4.26) show a similar gradient of high to low marsh as OBSS1, with samples located in the high marsh, having the presence of *Phragmites* spp., high distance from tidal influence, high organic matter and high elevation, and low marsh samples having high sand content and salinity.

Again, in OBSS3 only, distance and elevation are significant in explaining the species distribution in the data, accounting for 57%, made up equally between elevation (34%), distance (31%) and intercorrelation (36%) (table 4.23). As with the previous two transects from Oglet Bay, elevation and distance have a positive correlation (0.63) although not as strong. In addition to the variation partitioning, results from the biplots of RDA and DCA (figure 4.33) show a gradient from high marsh to low marsh comparable with the other transects, although in this transect sand is more associated with high elevations and clay and silt are more associated with the low marsh environment. This is due to the high sand content in samples from the high marsh (figure 4.2). The cluster analysis also supports the suggestion that elevation is predominant in controlling the species distribution with cluster zonations related to altitude, with a high marsh zone occurring between 5.172 – 4.852 m OD and a low marsh zone between 4.772 – 4.41 m OD (figure 4.38). The cluster order, as with the previous transects, was correlated with the variables and elevation was found to be related the most with the order (-0.74), although distance was also significant and had a strong correlation of -0.65 with cluster order. Clay and organic matter, which were found to have strong positive correlations with distance (0.81 and 0.88, respectively) and also had some correlation with the cluster order (clay 0.51, and organic matter -0.54) (table 4.26).

All three transects show that foraminiferal zonation appears to be related to elevation, particularly transects OBSS1 and OBSS3, along with distance from tidal influence. The data from Oglet Bay were then combined into one dataset to determine if elevation and distance were still the predominant factors controlling the species distributions. In contrast with the three individual transects, the DCA and RDA biplots show a more complicated picture of the relationships with species, samples and variables, with no clear gradient (table 4.21 and 4.22). There are associations with elevation, organic matter, distance and

the presence of *Phragmites* spp., as well as an association between sand, salinity and transect number. Most of the distribution in the data seems to be related more to transect number or location on the marsh, with OBSS2 associated with higher elevation, higher organic matter, higher distance and the presence of *Phragmites* spp., whereas OBSS3 samples are more associated with higher sand content, higher salinity and transect number. This reflects the spatial differences in the environmental variables between the transects, and can also be seen in the correlations between variables (table 4.6) where transect number is related strongly to clay (0.76), silt content (0.79), organic matter content (0.68) and correlated, though not as strongly, with distance (0.47) and elevation (0.43).

Unconstrained cluster analysis revealed four zones (figure 4.43). These can also be seen to be related to transect number, with zone I relating more to OBSS1, zone II more related to OBSS2 and zones III and IV more related to OBSS3. All of these zones overlap in their elevation. Three of these zones have similar compositions of species, with the main difference being the presence of *Ammonia beccarii* spp. which is present in OBSS1. Therefore these zones were combined, leaving two zones a higher marsh zone occupying an altitude between 5.52-4.73 m OD, which contains samples from all three transects; and a low marsh zone between 4.77-4.46 m OD, with an overlap of 0.04 m OD (figure 4.44). The lower zone predominantly contains samples from OBSS3, which is to be expected as OBSS3 contains the lowest samples (figure 4.2). The zones were reordered slightly, moving the lowest zone to the bottom, and this order was correlated with the different environmental variables (table 4.32). This revealed that the strongest correlations were with elevation (-0.65) and distance (-0.53).

pRDAs were used to determine how much each of the variables contributes to the overall explained proportion of the variance in the data which was 55% with all variables, but then reduced to 52% with only the significant variables included ($p>0.05$, 999 permutations, distance, transect number, pH, elevation and organic matter). This confirmed that most of the variance in the species data is related to the location on the saltmarsh, with transect number accounting for 14% of the variance and 27% of the explained proportion. However, pH was also found to contribute a large amount to the distribution in the data, making up 13% of the total variance and 25% of the explained proportion. This may also reflect the differences in the transects, as each has a different average pH. Distance and elevation contribute much less to the distributions, distance contributing 6% to the total variance (11% of the explained proportion) and elevation contributing to only 4% of the total

variance (8% of the proportion explained) (table 4.30). It is important to consider that transect number incorporates all the differences between the sampling sites, therefore any difference in pH, sand content and elevation, which all differ between transects, will be incorporated in this one variable. Although in pRDA this will be removed, it will be included in the intercorrelation proportion. In addition, the variables themselves correlate with each other. This results in a large proportion of the variance being a combination of the variables (intercorrelation), contributing 13% of the total variance, (26% of the proportion explained).

Decoy Marsh

For Decoy Marsh both the live and dead data were analysed separately, with each dataset giving different results. The biplots of RDA and DCA for the dead DMSS data (figure 4.46) were similar to transects from Oglet Bay reflecting a gradient across the marsh from low marsh, with high sand content, high salinity and higher transect number, to samples from the high marsh being associated with higher elevation, organic matter, distance from tidal influence, silt and clay. Although it appears from this that there is an elevational gradient across the marsh, the RDA revealed that only clay and organic matter content were significant in explaining the variance in the species data (explaining 60%). Out of this, organic matter contributes 25% of the variance (40% out of the explained variance), and clay contributes 24% of the total (42% of the explained proportion), leaving the remaining 11% (or 18% of the explained variance) due to intercorrelation (table 4.36).

In contrast live foraminifera DMSS data have significant variables of distance and elevation, which explain 51% of the variance in species data, similar to the transects from Oglet Bay (table 4.41). To determine the proportions of these variables, variance partitioning was carried out. This revealed that most of the variance was explained by the intercorrelation between distance and elevation, contributing 23% to the total variance (44% of the explained proportion) (table 4.42). The live data were also found to show a gradient of elevation across the marsh shown on the RDA and DCA biplots (figure 4.52) with high marsh samples associated with high elevation, organic matter content, clay, distance, silt and pH, and low marsh samples associated more with a higher transect number, sand content, and salinity.

In terms of cluster analysis the elevational range of Decoy Marsh samples is small, just 0.24 m OD, therefore using cluster analysis to divide the assemblage further may be inappropriate as all zones are considered high marsh. The cluster order was correlated with the environmental variables to determine whether elevation was a factor in the cluster results (table 4.38 and 4.44). It was found that the dead foraminifera sample order was most related to distance (-0.60), whilst elevation was found to be not significant at all. Other significant variables were found to be sand (0.53), silt (-0.54) and organic matter content (-0.41). The correlation coefficients for Decoy Marsh between the environmental variables can be seen in table 4.7**,** and show that distance is very strongly related to grain size, i.e. sand (-0.81), clay (0.76) and silt (0.8), as well as organic matter content (0.82), which may explain the significant correlations of cluster order with sand, silt and organic matter.

For the live species data the cluster order was found to be related mostly to elevation (0.67) not distance. The only other significant variable which cluster order is related to organic matter content (0.61). Elevation and organic matter also have a very strong positive correlation (0.78).

Combined Oglet Bay and Decoy Marsh

The data were combined in two ways, firstly with all dead species combined and secondly the dead Oglet Bay data with live Decoy Marsh data. The first dataset (OBDM) was first explored by RDA and DCA biplots (figures 4.58 and 4.59). From these plots it was difficult to determine any gradient in the data particularly related to elevation, with no clear patterns, although samples from OBSS1 seem to be associated more with high clay content as well as the species *Ammonia beccarii* spp*.,* which is not surprising since high proportions of *Ammonia beccarii* spp*.* were found in OBSS1. It also appears that samples from DMSS2 are more associated with high elevation, sand content, distance and transect number. This is not unexpected as the Decoy Marsh samples have the highest elevations in the dataset (they also have the highest distance value as the marsh is longer in length, and the samples have the highest value in the transect number of 5).

Unconstrained cluster analysis was carried out and 6 zones were delineated. It appears that there is no clear environmental variable controlling the cluster zonations (table 50). The results of RDA show similar results to the cluster results, with no variable accounting for a large proportion of variance in the species data (table 4.48), but a large proportion made up

from the intercorrelation of the variables (32% of the total variance, 64% of the explained variance 50%).

The results for the combined data using the live Decoy Marsh data were found to be completely different from that of the dead combined data. The biplots from DCA and RDA show no clear gradient and it is also difficult to find any associations and relationships, although elevation and transect number have the greatest influence on the data (longest arrow lengths). Unconstrained cluster analysis revealed five zones. The correlation coefficients for cluster order and variables (table 4.44) show that the elevation is the most dominant factor effecting the cluster zonations, with a correlation coefficient of 0.8. The other significant variables include distance, which is also correlated strongly (0.60), and transect number (0.53). Although the zonations from the unconstrained cluster suggest that the species data are related to elevation, the results of the variance partitioning and permutation tests are similar to those of the dead OBDM with most of the variance explained by intercorrelation of the variables (transect number, elevation, salinity, sand and *Phragmites* spp. presence), i.e. 33% of the total variance and 67% of the explained variance (49%). The highest proportion of the explained variance from a variable was for transect number (14%) followed by elevation (8%). As with the combined OB data, it is important to keep in mind that elevation and transect number do correlate (0.43) as Decoy Marsh transects contain the highest samples and OBSS3 contains the lowest samples. Variation partitioning also revealed that transect number and elevation share 34% of the variance they explain (not shown).

As discussed in the results section, the live and dead data from Decoy Marsh are different in their species composition and there is evidence to suggest that the dead species data from Decoy Marsh are unreliable. For this reason statistical analysis was carried out on both datasets. The live data from Decoy Marsh proved to be more dependent upon elevation than the dead data, and this was also reflected in the combined Oglet Bay and Decoy Marsh data as discussed above.

Removing inwashed foraminifera is important in the screening of modern data as the use of foraminifera as a proxy for sea level relies upon on the assumption that the dead assemblages are formed in-situ from living populations. Allochthonous inputs of foraminifera to assemblages are not usually an issue in most studies for two reasons; firstly they contribute small amounts (<5%) to the assemblage and therefore are usually removed by data screening, and secondly, they can be used as a characteristic of the elevation which

they occur (Horton and Edwards, 2006). In several studies the lower altitudinal samples are removed as they are subjected to greater transport and bioturbation but also contain more inwashed foraminifera species (e.g. Edwards and Horton 2000, 2006; Kemp et al., 2009b; Leorri et al., 2011). Horton and Edwards (2006) overcome the issue of allochthonous species by combining all inwashed (shelf) species into an 'exotic' species component.

It may, therefore, be justifiable to use the live data from Decoy Marsh as these are more representative of the autochthonous species from Decoy Marsh as opposed to the dead data which are likely to be allochthonous. Most of the live data from Decoy Marsh have totals above 100 individuals, however six samples do have numbers between 50 and 100 individuals. These samples have dominant species which account for 80-100% of the assemblage, therefore the statistical analysis should be as reliable as for the dead data.

4.5. Discussion of contemporary data

4.5.1. Foraminiferal assemblages

When considered as a whole, the foraminifera assemblages recorded in the transects and study sites show many similarities to those in previously studied saltmarshes. The unconstrained cluster analysis revealed two main zonations, a high marsh zone and a low marsh zone. The high marsh zone is principally dominated by *Haplophragmoides* spp., *J. macrescens, B. pseudomacrescens* and *M. Fusca.* Similar zonations have been found in many studies with the high to middle marsh area usually occupied by the dominant and cosmopolitan intertidal foraminifera of *J. macrescens*, *T. inflata* and *M. fusca* e.g. Cowpen Marsh, NE England, and Roudsea Marsh, NW England (Horton and Edwards, 2006); Bury Farm Marsh, S England and central Broadlands saltmarshes, SE England (Coles and Funnel, 1981); North Norfolk marshes, E England (Boomer, 1998); the Severn Estuary, SE England (Haslett et al., 1997); and Welwick, Thornham and Brancaster marshes, E England (Horton et al., 1999b). Outside the UK, *J. macrescens* has also been found to dominate the high-to-middle area of saltmarshes, including European marshes (Leorri et al., 2008; Rossi et al., 2011). *J. macrescens* and *M. fusca* were found in a high marsh setting in Portugal (Leorri et al., 2011) and Patterson (1990) also found similar distributions in British Columbia in Western Canada, with *J. macrescens* and *T. inflata* co-dominant with decreased freshwater input. Similar to these studies, *J. macrescens* and *M. fusca* were found to occupy the high-to-middle marsh environment in the Mersey Estuary, however, unlike these previous works, this study has a higher proportion of *Haplophragmoides* spp. with less *T. inflata,* which was found to occupy a lower area of the marsh.

In general, *Haplophragmoides* spp. has been found to be an indicator of low salinity. De Rijk (1995) found that *Haplophragmoides manilaensis* was present at the most elevated areas of the marsh in Massachusetts, near the upland, in the upper marsh, and was associated with brackish water. *Haplophragmoides* spp. is also found to occupy the same environment as *J. macrescens*. Coles and Funnell (1981) in the central Broadlands identified a high marsh dominated by *J. macrescens* and *T. inflata* with minor influences of *Haplophragmoides* spp. Horton et al. (1999) found *Haplophragmoides* spp. in most studies in the UK in minor abundances in the high-to-middle marsh environment, including Bury Farm which was dominated by *J. macrescens* with lesser abundances of *Haplophragmoides* spp., *T. inflata* and *M. fusca*; the Arne Peninsula dominated by *J. macrescens, M. fusca* and *Haplophragmoides* spp.; and Roudsea Marsh dominated by *J. macrescens* with low frequencies of *Haplophragmoides* spp. and *M. fusca*. Oregon marshes were found by Jennings et al. (1995) to be dominated by *J. macrescens* with low frequencies of *M. fusca* and *Haplophragmoides* spp. in the high-to-middle marsh. Leorri et al. (2011) found a significant presence of *Haplophragmoides* spp. predominantly in the high marsh area in Northern Portugal marshes. Kemp et al. (2009a) found *J. macrescens* and *H. wilberti* to be dominant in the high marsh environment in North Carolina, and Gehrels et al. (2001) found *T. inflata, J. macrescens* and *M. fusca*, with significant occurrences of *Haplophragmoides* spp. from the Taf and Brancaster marshes. It is generally accepted that *Haplophragmoides* spp. is usually associated with lower salinities (Leorri et al., 2011), therefore, *Haplophragmoides* spp., *M. fusca*, *T. inflata* and *J. macrescens* all tend to occupy the highest marsh environments, but which species dominates depends upon the salinity. *Haplophragmoides* spp. and *M. fusca* increase with decreasing salinity (e.g., Hayward et al., 2004) and *J. macrescens* and *T. inflata* increase with decreasing freshwater input (Patterson, 1990).

Although *Haplophragmoides* spp. is common in most saltmarshes (as described above) it is unusual for the frequencies to be as high as they are in Oglet Bay. Horton and Edwards (2006) found that they may be locally abundant, with relative frequencies of greater than 20% in Bury Farm and Roudsea Marsh, but these abundances are still relatively low in comparison to the two transects on Oglet Bay where >80% of *Haplophragmoides* spp. was found in samples in OBSS2 and up to 60% in OBSS1.

The three Oglet Bay transects broadly have the same species present, however there are differences in the abundance of *Haplophragmoides* spp. Transects OBSS1 and OBSS2 have

greater abundance of *Haplophragmoides* spp. with less *J. macrescens,* whereas transect OBSS3 is dominated less by *Haplophragmoides* spp. and more *J. macrescens* is present. All three transects have significant amounts of *M. fusca* present throughout the transects.

Differences in transect location is likely to be the cause of this variation between transects, with transects OBSS1 and OBSS2 located in an area of lower salinity than OBSS3. The salinity data from the transects does not reflect this however (figure 4.2), and instead shows that OBSS1 has the highest salinity out of the three transects.

The P*hragmites* spp. vegetation does, however, provide evidence of the salinity conditions of the saltmarsh, as *Phragmites* spp. usually occupies areas with a freshwater input. OBSS1 and OBSS2 are located in an area where *Phragmites* spp. is present, which reflects a greater freshwater input likely to be coming from runoff and input from the back of the marsh as there is a small stream located near transects OBSS1 and OBSS2 which enters the back of the marsh. OBSS3 may reflect an 'unaffected' foraminifera zonation on Oglet Bay as it is located in an area away from the freshwater input where *Phragmites* spp. is absent most probably due to higher prevailing salinities. This is likely to be the reason why *Haplophragmoides* spp. is more highly abundant in OBSS1 and OBSS2 whereas *J. macrescens* is more abundant in OBSS3. In addition, the *Phragmites* spp. itself may be inhibiting the complete colonisation of cosmopolitan species *J. macrescens* and *T. inflata* as these species may not tolerate the dense vegetation compared with *Haplophragmoides* spp. and *M. fusca,* which may be more tolerant of this environment. de Rijk (1995) found that *Haplophragmoides* spp. was more vegetation tolerant. In transects OBSS1 and OBSS2 it can be seen that where the *Phragmites* spp. vegetation ends, *Haplophragmoides* spp. decrease in abundance and *J. macrescens* increases. Also, there is very high abundance of *J. macrescens* in the live data from Decoy Marsh. This may be due to the absence of *Phragmites* spp. vegetation but this marsh also has a much higher altitude.

Decoy Marsh live data are predominantly characterised by *J. macrescens* with some *B. pseudomacrescens* in the highest high marsh area. There are also some samples which only contain *J. macrescens.* Many other studies have also noted a monospecific assemblage of *J. macrescens* which occurs in the highest elevations on the saltmarsh. These include; Alnmouth marsh, NE England; Arne Peninsula, South England; Nith Estuary, SW Scotland; Thornham marsh, East England (Horton and Edwards, 2006); Maine, New England (Gehrels, 1994); Connecticut (Edwards et al., 2004); Outer Banks, North Carolina (Horton and Culver, 2008); and Nova Scotia (Scott and Medioli, 1978, 1980a). Although the samples from Decoy

Marsh which contain a monospecific assemblage of *J. macrescens* do not occur in the highest samples from the transect, the elevations at which they occur are still very high within the tidal frame.

Of those studies which distinguish between *J. macrescens* and *B. pseudomacrescens,* most do not contain great abundances of *B. pseudomacrescens* and the distribution is not found to be consistent. *B. pseudomacrescens* was first described from, and thought to be endemic to, the Baltic Sea (Bronnimann et al., 1989) but has now been recorded in several marshes from around the world, e.g. Maine (Gehrels and van de Plassche, 1999), Massachusetts (de Rijk, 1995a, b) British Columbia (Riveiros et al., 2007) and in very small numbers (0.5-2.2%) in Arne Peninsula, Bury Farm, and Newton Bay in Britain (Horton and Edwards, 2006).

Gehrels and van de Plassche (1999) found that *J. macrescens* and *B. pseudomacrescens* had different distributions on the saltmarsh in Maine, with *J. macrescens* occurring in the high marsh, while *B. pseudomacrescens* was found to be spatially variable across the saltmarsh. Therefore *J. macrescens* was found to be the better sea-level indicator on this marsh. de Rijk (1995) and de Rijk and Troelstra (1997) found that *B. pseudomacrescens (T. macrescens A)* dominated areas of the marsh in Massachusetts which had salinities lower than 20%. In contrast to most saltmarsh studies, de Rijk (1995) found *J. macrescens* (*T. macrescens B*) dominated areas which had higher salinities as opposed to those in the high marsh environment. The study of Riveiros et al. (2007) from British Columbia found a dominance of *B. pseudomacrescens* in the high marsh environment along with *J. macrescens*. Alve and Murray (1999) studied the Skagerrak–Kattegat coast and found *B. pseudomacrescens* was associated with the most elevated areas of the marsh. Alve and Murray (1999) also found the species in the highest part of a *Phragmites* spp. marsh in the River Cur, S England, suggesting that this species is found in the most landward terrestrial parts of the marsh and could define the uppermost limit of the marine influence, tolerating lower salinities than *J. macrescens* (Alve and Murray, 1999). Although the abundance of *B. pseudomacrescens* from British saltmarshes has been found to be low, it was found that when they do occur it is in the highest marsh samples along with *J. macrescens* (Horton and Edwards, 2006).

B. pseudomacrescens occurs in much higher numbers in Decoy Marsh and to a lesser extent the highest high marsh areas of Oglet Bay; it provides a narrower vertical distribution in Oglet Bay were the tolerance range is 0.32 m OD, and the range in the optimum range is 0.04 m OD, compared to *J. macrescens* were the tolerance range is 0.83 m OD and the optimum is 0.23 m OD. In contrast, the tolerance range of live *B. pseudomacrescens* from

Decoy Marsh (0.15 m OD) is greater than for live *J. macrescens* (0.08 m OD). This is likely to be related to the optimum altitude at which the species occurs. For *J. macrescens* this is much clearer as it has a unimodal distribution along the marsh, whereas *B. pseudomacrescens*' distribution is based upon one sample of high abundance, resulting in larger errors and tolerance range.

Decoy Marsh is at a very altitude high in the tidal frame, which is probably the reason for the higher abundances of B*. pseudomacrescens* compared to Oglet Bay. Both study sites are also very low in salinity due the location of the saltmarshes within the middle to upper part of the estuary, and therefore this may also explain why there are higher abundances of this species compared with other UK saltmarshes.

Mid-marsh environments are less distinguishable on most marshes as they may not be present, or if they are, they may reflect local conditions, for example tidal creeks, fresh water inputs and distance to the mouth of the estuary (Leorri et al., 2011). Mid-marsh environments are usually distinguished from the high marsh due to the higher presence of *M. fusca* and perhaps some calcareous species (Horton and Edwards, 2006). Some studies have further subdivided this zone, including Leorri et al. (2011) and Gehrels et al. (2001). Other studies have distinguished between high marsh and high, high marsh environments, e.g. Scott and Medioli (1978). However, most studies find two zones a high-to-middle marsh and low/mudflat zone, although the low marsh and mudflat zones are also sometimes separated (e.g. Horton, 1999; Horton et al., 1999b; Horton and Edwards, 2006).

Similar to most of the saltmarsh studies in the UK (e.g. Horton and Edwards, 2006), two assemblage zones were found in the transects from Oglet Bay. A high-mid marsh zone, as described above, and a low marsh zone which is similar to many other studies, being dominated by calcareous species, i.e. *Elphidium* spp., *Brizalina* spp*.* and *Haynesina* spp*.,* along with the dominant agglutinated species*, J. macrescens, M. fusca* and *T. inflata* (e.g. Horton, 1999; Kemp et al., 2009a; Gehrels et al., 2001).

In addition to the differences described above between this study and other studies, another unusual component of the species assemblage is the presence of *Ammonia beccarii* spp. in the high marsh environment in OBSS1. *Ammonia beccarii* spp*.* are generally found to occupy the low marsh environment along with other calcareous species (e.g. Horton et al., 1999a, b), so it is unusual to find high proportions of *Ammonia beccarii* spp. throughout the transect. Gehrels et al. (2001), however, found that *A. beccarii* was present in the higher

marsh environment in Brancaster saltmarshes and had a negative correlation coefficient with increased flooding. In contrast to this, Horton and Edwards (2006) found that *Ammonia beccarii* spp. appeared only in very low numbers occurring throughout Brancaster marshes. For the present study it appears that the high abundance of *Ammonia beccarii* spp. is very local, only occurring in one of the transects from the Oglet Bay saltmarsh. A possible explanation may be the influence of tidal mixing and transport, redistributing *Ammonia beccarii* spp. up the marsh, although the presence of *Ammonia beccarii* spp. in the dead as well live data suggests that the species are inhabiting the area, or that this redistribution is a regular occurrence. The presence of *Ammonia beccarii* spp. in the high marsh in Brancaster, was not able to be explained (Gehrels et al. 2001) and cannot be explained in this study either as there seems to be no noticeable changes in the environmental variables that were measured. Conditions for OBSS1 are similar to those at OBSS2, however little *Ammonia beccarii* spp. was found on OBSS2. Tidal mixing, especially in a macrotidal setting, may cause this anomalous presence of *Ammonia beccarii* spp.

4.5.2. The relationship between foraminiferal assemblages and environmental variables

In order for foraminifera to be used successfully in sea-level reconstructions the indicators must show a known and ideally a strong, quantifiable relationship to tidal elevation in the modern environment (Roe et al., 2009). The majority of studies demonstrate that saltmarsh foraminifera are most related to elevation due to tidal flooding. For the studies which do show elevation as a major controlling factor, the data are then used to reconstruct relative sea levels (e.g. Gehrels, 2000; Gehrels et al., 2002, 2005, 2006; Edwards, 2001; Edwards and Horton, 2000, 2006; Edwards et al., 2004a; Donnelly et al., 2004; Horton and Edwards, 2005, 2006; Horton et al., 1999b, 2005; and Patterson et al., 2005). There are, however, no clear guidelines or rules as to what proportion elevation has to contribute to the overall species variance for the data to be used to reconstruct former sea level.

There are many ways in which studies and authors determine whether elevation is an important control on foraminifera distribution, including constrained (e.g. Charman et al., 1998) and unconstrained (e.g. Horton, 1999; Horton et al., 1999b) cluster analysis, pCCAs (e.g. Horton et al., 1999a; Zong and Horton, 1999; Charman et al., 2002; Sawai et al., 2004; Horton and Edwards, 2005; Horton and Edwards, 2006; Szkornik et al., 2006; Engelhart et al., 2007; Hill et al., 2007; Horton and Culver, 2008; Roe et al., 2009), using the performance of transfer functions (e.g. Massey et al., 2006a; Leorri et al., 2011; Rossi et al., 2011), CCA

(e.g. Sherrod, 1999; Ng and Sin, 2003; Woodroffe and Long, 2009; Woodroffe and Long, 2010) and correlation coefficients using scatterplots (e.g. Horton, 1999; Horton and Murray, 2007).

Several studies use pCCAs to determine how much elevation contributes to the explained proportion of the variance in species data. The variance explained by elevation can vary between 3% (Sawai et al, 2004) to 32% (Horton and Edwards, 2006). Studies most commonly determine the proportion of the explained variance which is made up from the variable (most commonly elevation), as opposed to the overall variance, which can vary from 8% (Roe et al. 2009) to 42% (Horton and Edwards, 2006). These figures are misleading as it can appear that a variable which explains a high proportion of the amount explained may not contribute much in comparison to the overall variance e.g. if 80% is explained by the variable, it may only be 80% of an explained proportion of 20%, which is only 16% of total variance. Alternatively, the variable may only explain 25%, but it may be out of an explained proportion of 70%, therefore it explains 18% of the total variance (greater than the amount explained by the variable which explains 80% of an explained total of 20%). It may therefore be more useful to use the percentages from the overall variance. For comparative purposes in this study, the results from other published studies have been recalculated to produce values for explained variance from the total variance (table 4.57) in order to compare the results more easily. It is, however, still very difficult to compare the results of the pCCAs or pRDAs between studies as the figures depend upon the number of variables included in the analysis; the fewer variables included, the higher the proportions the variables make up. Using variation partitioning, as discussed in section 5.2.3, attempts to reduce the problems associated with studies having different sample sizes and the number of variables. However, currently only RDA can be used and only 4 variables included.

The explained proportion of variance for the present study ranges from 36 to 57%. This improves greatly for some of the transects when all the other measured variables are included, for example OBSS1 with the two significant variables included explains 45%, increasing to 70% when all nine other variables are included. In contrast, OBSS2 varies only a little from 36% with two variables to 38% with all nine variables. The unexplained proportion of 62-23% (all variables) may be due to other factors which were not measured at the time (e.g. nutrients) or may be that the variables which were measured do not reflect the averaged conditions of the marsh which the foraminifera assemblages reflect. The dead

assemblages reflect time-averaged populations, whereas salinity and pH, for example, reflect the sampling day's environment only. Other studies suggest that stochastic variation or random variation could explain the reason for the unexplained proportion. The explained proportions in this study (using all variables and the significant variables only), are similar to or greater than other studies where the unexplained variance varies between 80-21% (table 4.57) and is considerably greater than in studies with biological datasets with large numbers of zero values (Gasse et al., 1995; Zong and Horton, 1999).

The amount of the variance that the variables explain in itself is not important, but the amount of this made up from elevation is. For example, the amount explained may be low, but the proportion of this from elevation may be high. e.g. if only 25% of the variance is explained but most of this is from elevation than elevation could still make up a larger proportion of the variance, 7% for example (Hill et al. 2007), compared with a study which has a higher proportion explained 46% but with less explained by elevation 4% (Roe et al., 2004).

The results of the proportion of the variance controlled by elevation/SWLI, distance or tidal flooding for the studies can also be seen in table 4.57. Individually, the transects for the two sites appear to be strongly related to elevation and distance from tidal influence. Elevation explains most of the foraminifera species variance for OBSS1 (22%), OBSS3 (18%) and DMSS live (20%), with distance being more of a control for OBSS2, explaining 17% of the total variance and elevation explaining 7%. These results are at the upper end of the results from other studies which range from 3 to 32%, with an average percentage of 9% (table 4.57).

In the present study only the significant variables are included for variation partition, pRDAs or pCCAs, to reduce the number of variables which need to be used. In most studies, however, all variables are included even those which are not significant and in some cases all variables may not be significant (e.g. Charman et al. 2002; Roe et al., 2009).

When the Mersey data are combined into one dataset, the percentage explained by elevation falls dramatically to 4%, which is quite low with respect to the other studies. Charman et al. (2002) and Roe et al. (2009) have included results from individual sites along with the combined data and they also show that the combined dataset reduces the amount of variance explained, and also the amount of variance explained by elevation. This is similar to the results found in this study, where the amount explained by elevation in the individual transects is reasonable (7-22%) compared to the combined dataset (4%).

The majority of the explained variance for the combined dataset is mostly made up of intercorrelations between the significant variables (sand, elevation, transect number, *Phragmites* presence and salinity), accounting for 33% of the total variance and making up the majority of the explained variance of 49%. Combining the data emphasises the differences between the transects and results in the transect number contributing the most to the explained variance (7%). It is important to note that the 'transect number' contains information about the elevation also, as DMSS live contains the highest elevation samples and OBSS3 contains the lowest elevation samples, and 34% of the variance in transect number and elevation is shared; this correlation will be included in the intercorrelation proportion. Also, the 'transect number' variable may be artificially high due to the product of no overlap in 'number' between the transects and sites.

An alternative method of determining whether elevation influences the foraminiferal assemblage is to use cluster analysis. The cluster correlations for the transects confirmed the results from the pCCA and pRDAs as elevation had the highest correlations with the cluster orders. For OBSS1 (0.77) OBSS3 (0.74), DMSS live (0.67), with distance being more correlated with the results for OBSS2 (0.75). For the four sites cited in Horton et al. (1999b) the correlation coefficients varied between 0.73-0.82 for elevation and cluster order. This shows the results from this study to be reasonably good. In addition to determining the correlation coefficients for cluster order and elevation and distance, Pearson's product moment was carried out on all variables to determine which also had strong correlations and were significant. For most of the transects there were other variables which were also significant with strong correlations with cluster order, including *Phragmites* spp. (0.73) and salinity (0.60) for OBSS1, and these are likely to be due to the correlations in the environmental variable data with elevation and distance.

It is promising that the highest correlations found between cluster order and elevation is for the combined data (OBDM live) (0.8). The correlations reveal that the order of samples is mostly related to elevation (0.8) and distance (0.6) along with transect number (0.53); demonstrating that elevation is an important contributing factor to the foraminifera assemblages, although the results from the pRDA may not convincingly show this.

Some studies use CCAs alone (e.g. Sherrod, 1999; Ng and Sin, 2003; Woodroffe and Long, 2009; Woodroffe and Long, 2010) to determine how much elevation contributes to the amount of variance. These figures cannot be compared with the other methods used as this method does not exclude the influence of the other environmental variables which

correlate. This method, therefore, gives higher percentages of the amount explained by that variable compared with partial CCAs which removes this correlation, resulting in a combined intercorrelation portion. Another disadvantage of this method is that only the proportion elevation is contributing to the variance is determined, and it may be possible that another variable has an overriding influence on the foraminiferal assemblage distribution.

In reality, however, the reason that elevation can be used as the variable of interest is the fact that it is a proxy for flooding duration, which, in turn, determines the vegetation cover on the marsh, the grain size, the salinity, the organic matter content etc. which foraminifera are effected by. Therefore, if there are strong correlations between elevation, distance from tidal influence and the other variables, it is more likely that the foraminifera species will reflect changes in elevation. Therefore, perhaps using CCA alone with elevation should be used, as taking out the influence of the other variables correlating with elevation (i.e. partial CCA/RDA) is unrealistic. If elevation correlates highly with other variables, which it should if the other variables are to be expected to be related to flooding, then this will lead to higher intercorrelation percentages and lower elevation percentages in the pCCA and pRDA results.

Several studies use the performance of regression analysis, including Leorri et al. (2011) Massey et al. (2006a) and Rossi et al. (2011), to determine how well the transfer function will perform the reconstruction of elevation. This may be the most pragmatic way of comparing the results between studies, although which statistical test and component is used in the study effects the results. This approach will be carried out in chapter 6 in the transfer function development section.

Table 4.57 Examples of contributions of variables to the total inertia in species data for previous studies.

Biota	Study	Explained	Unexplained	Elevation/ SWLI	Distance	Flood duration	No. of variables
Foraminifera	Horton et al. (1999)	49	51	9	-	-	6
	Horton and Edwards (2005)	52	48	12	-	-	6
	Horton and Edwards (2006)	76	24	32	-	-	**5**
	Riveiros et al. (2007)	23	77	-	-	-	6
	Horton and Culver (2008)	43	57	9	-	-	-
Diatoms	Sawai et al. (2004)	20	80	3	-	-	5
	Szkornik et al. (2006)	38	62	9	-	-	3
	Hill et al. (2007)	25	75	7	-	7	6
	Roe et al (2009) WAUMP	46	54	4	-	-	6
	Roe et al (2009) WAWAT'L	51	49	7	-	-	6
	Roe et al. (2009) combined	39	61	3	-	-	6
	Zong and Horton (1999)	22	78	5	-	-	5
Pollen	Engelhart et al. (2007)	26	74	4	2		8
	Charman et al. (2002) all	49	51	-	-	8	6
	Charman et al. (2002) Brancaster	62	38	-	-	11	5
	Charman et al. (2002) Erme	79	21	-	-	7	5
	Charman et al. (2002) Taf	72	28	-	-	14	5
Present	OBSS1	45	55	22	11	-	2
Study	OBSS2	36	64	7	17	-	2
	OBSS3	57	43	18	16	-	2
	OB	52	48	4	6	-	5
	DMSS live	51	49	20	9	-	2
	OBDM live	49	51	4	-	-	2

4.5.3. Suitability of the datasets for studies of relative sea-level change

Taking single transect datasets the foraminiferal assemblages show they have great potential for quantitative sea-level reconstructions as they explain between 36-57% of the total variance in the data, which is comparable to other studies, where elevation and distance from tidal influence account significantly for this distribution. The variance partitioning shows that these two variables account for a large proportion of the variance, as well as the unconstrained cluster analysis. The DCA and RDA biplots also reveal a gradient related to elevation. The data cannot be used independently, however, as the sample sizes are very small (19-22 samples)

The data were combined (OBDMlive) in order to increase the sample size, and also to enable the capture of all environments and conditions on the marsh, as any of these conditions could have occurred in the past and are, therefore, in the fossil record. The

sample size was increased to 82 samples, with sample sizes of other studies ranging from 22 (Sherrod, 1999) to 165 (which includes 10 different sites) (Horton et al., 1999b).

The results for the combined dataset showed that the amount explained by the variables remained similar (49%) and was still comparatively high, but the amount explained by elevation and/or distance diminished. One explanation may be that the individual transect data have inflated relationships with elevation and distance due to autocorrelation and the fact that the samples were taken along a transect, therefore this relationship decreases when the full data are added together.

Combining the datasets together also adds additional variance and variation in the species and environmental data; the differences in species data will be explained by any difference in the variables and therefore may automatically be explained by the 'transect number' variable. However, in reality this is not a real variable and is simply highlighting the differences between the sites. When transect number is removed from the pRDA analysis and re-run, the permutation tests revealed that organic matter was not significant and was therefore removed. Table 4.58 shows that elevation makes up the largest proportion of the variance, closely followed by the *Phragmites* spp*.,* although the explained variance has reduced to 39%. It also shows that there is no intercorrelation between these variables (elevation, salinity and *Phragmites* spp.). The intercorrelation proportion which made up the majority of the variance when transect number was included, was therefore found to be between transect number and other variables, predominantly elevation.

Table 4.58 pRDA for OBDMlive with significant variables only and transect number removed.

Variable	Variance	Significance	% of total inertia	% of constrained inertia
All	0.388			
Elevation	0.1967	0.001	20	51
Phragmites spp.	0.17887	0.001	18	46
Salinity	0.01273	0.039	1	3
Intercorrelations	0		0	0

Elevation, does therefore, have an important control over the distribution of the species data and this is also supported by the order of the samples in the unconstrained cluster analysis, which was found to be highly correlated with elevation. The amount of variance explained by elevation alone with the three significant variables only is 20%. This is quite high in comparison with other studies were this varies between 3-32%, the average being 9% from the studies included in table 4.57. When all the significant variables were included

(including transect number) the amount reduced to 4%. Although this seems low, other studies, including Sawai et al. (2004), Roe et al. (2009), Zong and Horton (1999) and Engelhart et al. (2007), found similar results and concluded that the data were suitable to be used. These studies are, however, from diatom assemblages and pollen (Engelhart et al., 2007) which usually have less well-constrained species assemblages than foraminifera (Gehrels et al., 2001), and the foraminifera studies do have higher proportions explained by elevation 9-32%. However, none of these studies included transect/study site in their analysis, and if they were to do so this may reduce the amount explained by elevation also. For example, Charman et al. (2002) in their combined dataset include the variable 'site' and found that this explained highest proportion the variance.

Another important consideration is the macrotidal environment in which these sites are located. The Mersey Estuary is a very dynamic, high energy environment and Oglet Bay is also currently eroding. Therefore, the likelihood of marine and inner-shelf species being washed in as well as the reworking and movement of foraminifera across the marshes is greater. Therefore, all things considered and compared with other studies, the dataset is satisfactory and has the potential to be used for a palaeosea-level reconstruction.

4.6. Summary of contemporary data

The aims of this study were to document the distribution of the foraminifera across two different saltmarshes within the Mersey Estuary, to determine the controls on the foraminifera distribution, and establish whether the dataset is appropriate to use for a local sea-level reconstruction. A total of 105 surface samples were collected from two saltmarshes, Oglet Bay and Decoy Marsh; 82 of the samples met the criteria and were utilised in the study. Along with foraminiferal analysis, several environmental variables, including organic matter content, salinity, pH, and grain size, were analysed.

In general, the species assemblages were found to be similar to other studies in the UK and elsewhere, with two main zonations across the marsh: high-to-middle marsh zone occupied by *Haplophragmoides* spp*., J. macrescens,* and *M. fusca;* and a low marsh zone composed of similar agglutinated species with increasing numbers of calcareous species including *Brizalina* spp*., Elphidium* spp*.* and *Haynesina* spp*.* The biggest dissimilarity between the assemblages from this study and others is the greater abundance of *Haplophragmoides* spp., which reflects the low salinity of the marsh and estuary and the dense *Phragmites* spp. vegetation.

A large input of allochthonous calcareous species was found to dominate the dead assemblage from one transect from Decoy Marsh, creating a different assemblage to that found in the previous transect from the same location. It was concluded that these species were inwashed during an extreme tide relating to the spring equinox, and the problem was overcome by using the live data from Decoy Marsh which were consistent on both transects investigated.

All transects individually were found to be controlled predominantly by elevation and distance from tidal influence, whilst the combined data's main control was related to the site at which the transect was carried out, reflecting the intra- and inter-site variability in the assemblages. When 'transect number' was removed as a variable, elevation and *Phragmites* spp. presence were found have the greatest control, and the assemblage zonations were also found to be related to elevation.

The modern distribution data from this study was found to have a reasonable relationship with elevation when comparing the results with other studies, as elevation contributes 20% to the total inertia (when transect number was removed as a variable) for the combined dataset. The large number of samples and the amount of variance explained by the variables allow the dataset to be used for a local relative sea-level reconstruction. However, caution should be taken as some foraminifera reflect changes in salinity and vegetation cover along with elevation and/or distance from tidal influence.

5. Chronology and accretion history of sediment cores

5.1. Introduction

The construction of a reliable, high resolution sea-level record requires precise age determination (e.g. Marshall et al., 2007). The first step in creating a chronology for a core is to decide which dating method is the most appropriate and suitable to use. To gain an indication of the age of the sediments, historic maps (figures 2.8 and 2.9) were examined to see if the saltmarshes were present in the near past. This indicated that the saltmarshes were at least 150 years old as they were present in the 1886 Ordnance Survey map; older maps were not available. The second step was to use a historic record of environmental pollution to determine an approximate age. From the map evidence and the high concentration of heavy metals, it was determined that the cores were not older than 150 years old and therefore (other than pollution indicators) the most appropriate dating method to use was radionuclides, i.e. ^{210}Pb, ^{241}Am and ^{137}Cs.

The following chapter gives details of the methods used and discussion of the rationale for the assigned chronology from both the pollution indicators and radionuclides. It also provides a discussion of the stratigraphic framework for sampling the fossil record.

5.2. Stratigraphy

The sedimentary record provides an essential stratigraphic and chronological framework for sampling the fossil record. It is important to examine the sedimentary record as it provides information about the past environment and environmental conditions of the site (Scott and Medioli, 1986). The record can be used to understand the dynamics of the saltmarsh as well as the process of saltmarsh development (Coe and Church, 2003). This is also necessary when determining the suitability of the saltmarsh and establishing an appropriate location in which to take cores to provide a representative fossil record. Understanding the sedimentary record can therefore help to select the location of a 'type' core from the site, put the core into the wider context of the study site and assist in correlating between cores (e.g. Gehrels et al., 2006). Determining the overall pattern of sediment sequence can be used to establish whether the sediments are consistent or highly variable across the saltmarsh, as a consistent record is preferred for sea-level reconstruction (Horton and Edwards, 2006). The sedimentary record of Oglet Bay was examined by considering the sedimentology and geochemistry of the saltmarsh sediments.

The geochemistry of the sediments, particularly metal concentrations which are related to anthropogenically-derived pollution, can assist in: establishing a chronology based upon 'event markers' in the record and industrial history of the area, choosing a representative core, and help in cross-correlating between cores. It can also be used to help determine the nature of the sedimentation and establish that the stratigraphic sequence is a pattern in time and not space, i.e. progradation.

Changes that occur in the stratigraphy reflect changes in sedimentation which may be related to changes of the height within the tidal frame. As the sediment builds up, the marsh surface's location within the tidal frame increases and therefore the amount of sediment deposition it receives decreases, while the amount of organic deposition increases as vegetation becomes established (Pethick, 1981). This should occur at the same limiting tidal height across the saltmarsh and therefore the stratigraphy should show roughly the same pattern across the marsh. Variations from the established pattern of stratigraphy may be related to other influences such as storm events, higher inputs of fresh water runoff or local erosion of the record as well as marsh surface variability (Cahoon et al., 2000).

Although the sediments and sequence may be the same throughout the saltmarsh, they may not have formed at the same time, and therefore the ages of apparently similar sediments will be different. Younger sediments in the outer marsh will only show the top or most recent part of the record, whilst the inner marsh sediments are assumed to contain a full record, but one that is highly 'compressed' at the top due to minimal sedimentation i.e. limited in terms of vertical range (e.g. Allen, 1990; Plater and Appleby, 2004) (figure 5.1). The geochemical and radionuclide data from cores located at different parts of the saltmarsh can be used to determine how the accretion has taken place and can be used to choose a location which has a consistent pattern of sedimentary and pollution data.

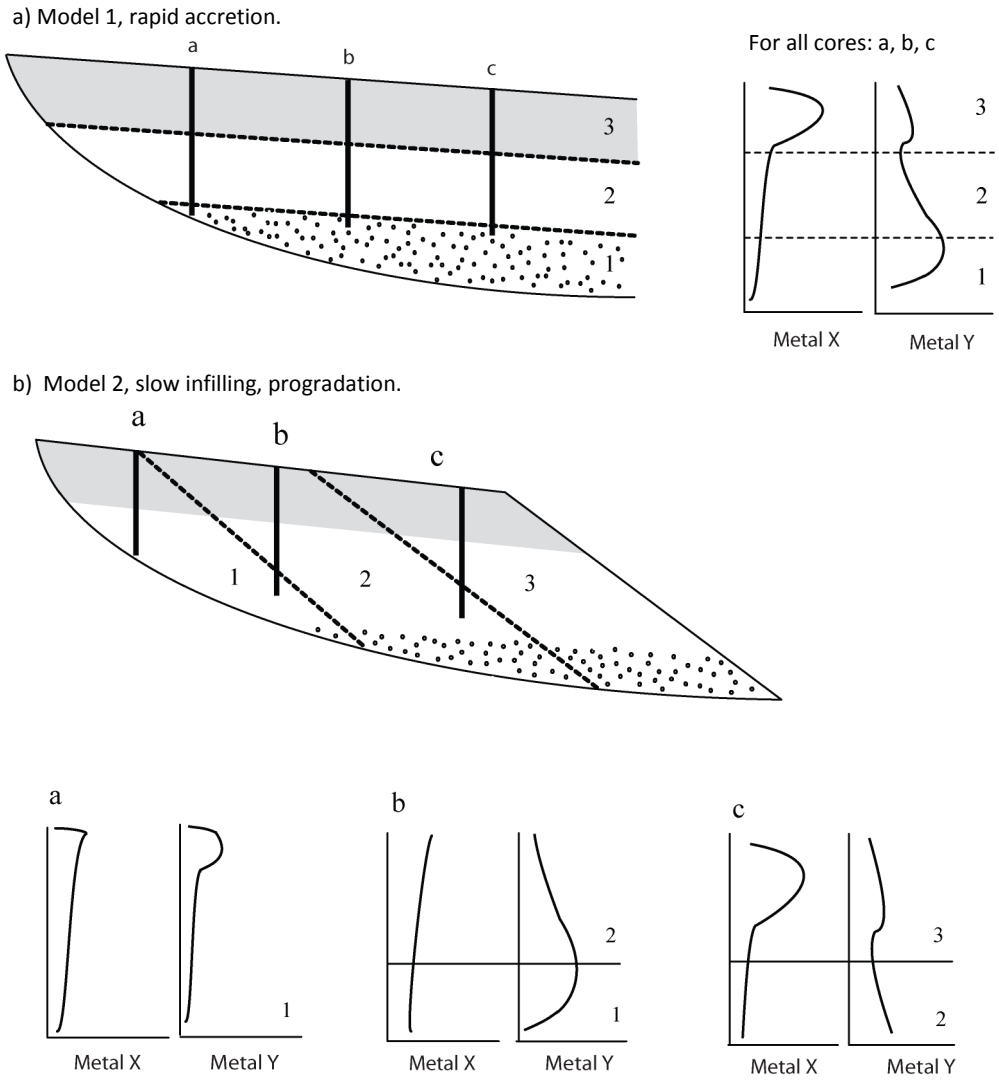

Figure 5.1 Simple schematic of two sediment accretion models for a saltmarsh. A) Rapid accretion which is related to sea-level rise. Sediments have built up synchronous and all three cores (a, b and c) show the same metal concentration trends. B) Slow infilling related to dynamics and sediment supply, were sediments have accreted building outwards. Although the sediment are the same, the cores a, b and c do not show the full metal concentration record but each captures a different time-period of pollution.

5.2.1. Results of stratigraphy

Figure 5.2 shows the general stratigraphic units from the transects of cores examined from Oglet Bay saltmarsh (figure 3.2). The cores generally increase in the length towards the lower saltmarsh with very shallow depths of sediment in the high saltmarsh due to the high elevation of the Devensian diamicton beneath. The thickness of the sediment was also found to be greatest on the western area of the saltmarsh where the underlying pre-Holocene surface developed on the diamicton drops in altitude. The general stratigraphy of the saltmarsh consists of pre-Holocene surface of red, poorly sorted coarse sand and gravel, found in cores which had a higher elevation of the Devensian diamiction. Above this were silts, interbedded with sand lenses, above which were several horizons of black-grey silts up to several metres thick. The top horizon consisted of brown, mottled, silty clay, with organic matter which varied in thickness from 0.02 to 0.47 m, both found in the highest marsh cores. Most of the sediments followed this pattern in sedimentary sequence with variations in the thickness and depth. The most obvious differences in sediments were the large horizons of dark sand near the bottom of the cores which can be seen in transects 4 and 5.

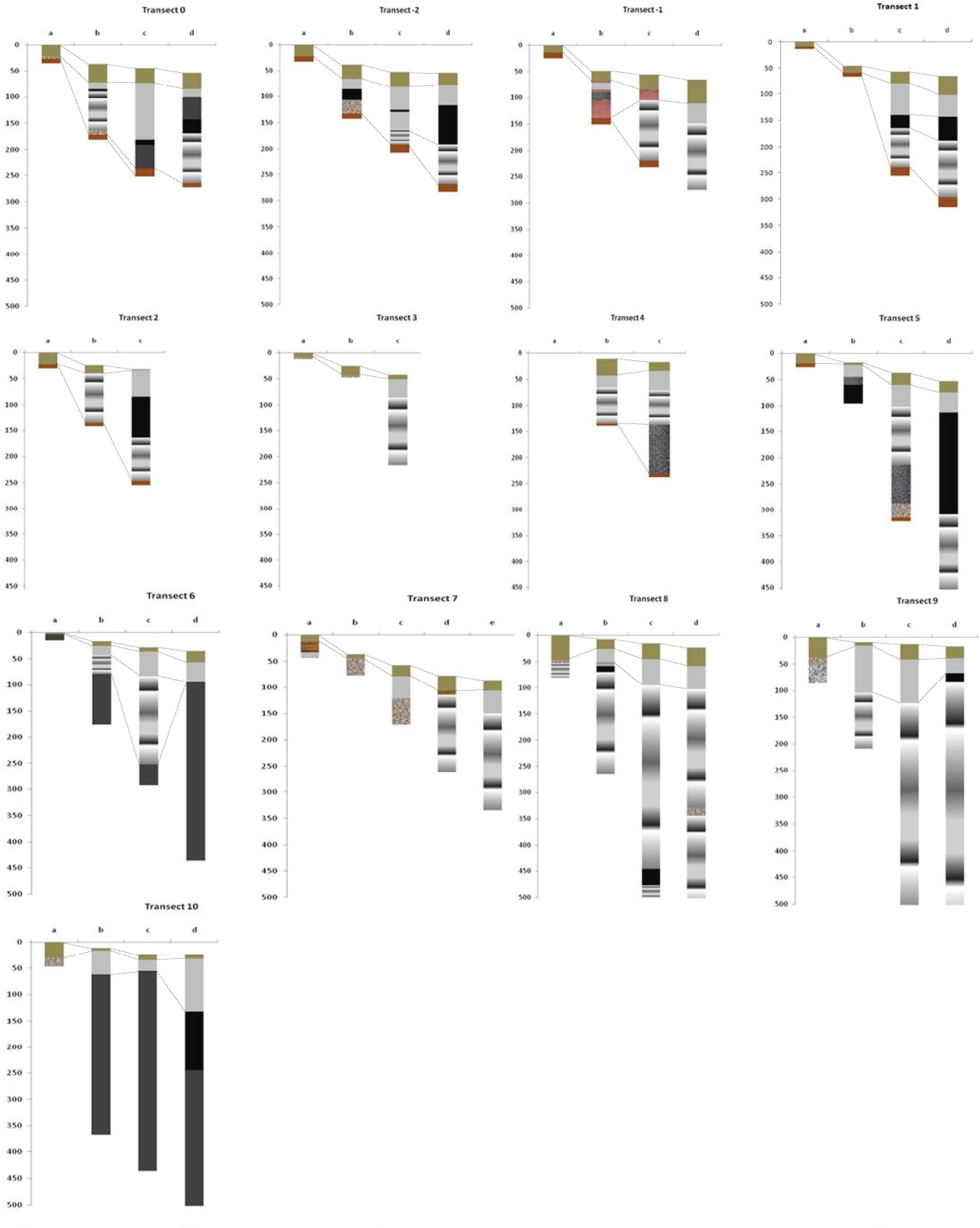

Figure 5.2 Basic stratigraphic units of cores taken from Oglet Bay Saltmarsh

5.2.2. Interpretation of stratigraphy

The underlying tidal sediments (figure 5.2) can be interpreted as three main environments following deposition of the poorly sorted Devensian till. Above the till, the sediments are interpreted as originating from a tidal channel, with alternating horizons of silts and sand, with some cores containing large sand units with the laminations changing from mainly sandy to mainly silty. The laminated deposits are interpreted as heterolithic tidal rhythmites recording changes in tidal cyclicity during a phase of rapid tidal sedimentation (e.g. Stupples and Plater, 2007). This initial phase of rapid tidal sedimentation may have been due to a change in estuary dynamics relating to the shifting of the low water channel in the estuary, therefore increasing accumulation space and resulting in rapid sedimentation which, in turn, reduces the accumulation space (Allison, 1949; Blott et al., 2006). Above the tidal channel deposits were grey-black silts which were likely to have been deposited on the upper part of a tidal flat environment; a mudflat-saltmarsh transition, developing as the location of the sedimentary surface within the tidal frame increase in elevation. The variation in colour from light grey to dark black is related to a condition of reductive diagenesis. Finally, above the tidal flat sediments were top horizons of brown silty clay, containing organic matter and herbaceous remains, which are interpreted as saltmarsh sediments. As the sediments have built up, the height within the tidal frame increases, therefore tidal inundation and sediment deposition decreases and vegetation becomes established (Pethick, 1981).

The sediments in the high marsh were much shallower than those in the low marsh as it was found that the underlying glacial till slopes towards the water giving the lower saltmarsh more accumulation space. The area at the top of the saltmarsh also receives less tidal inundation and less sediment than the lower marsh or tidal flat and therefore accumulation in this area will also be less. The bedrock was also found at a lower depth in the western area of the marsh as the sediments found here were greater than 5 m in length and the glacial till was not reached for many of the cores located here.

The presence of heterolithic tidal rhythmites suggests the tidal sediments have undergone rapid sedimentation and may therefore have a sediment accretion model similar to model 1 (figure 5.1a). However, it is not possible to determine this for certain, without the aid of the geochemistry data.

5.3. Geochemistry

To establish which accretion model is more suitable to describe the sedimentation which has taken place on the study site, a distinct pattern or trend in pollution must be identified and determined whether all cores exhibit the same pattern related to the industrial history of the area. The depth at which prominent features in the pattern occur in different cores can be used to establish if the sediments built up simultaneously related to rapid accretion or related to slower infilling whereby the sediments accumulated at different times (figure 5.1).

5.3.1. Normalisation of metal concentration data

Studies have found that heavy metals have an affinity with organic matter content and therefore increased organic matter can increase the heavy metal concentration as it can cause the retention of metals (Salomons and Forstner, 1984; Allen, 1990; Valette-Silver, 1993; Alloway, 1995). In addition, grain size can have a marked effect on the concentrations of pollutants per unit sediment mass (Aston et al., 1985). For sediments in the Mersey Estuary, Vane et al. (2009) found Hg to be highly related to organic matter content. Fox et al. (1999) found that the grain size distribution did not change throughout their Mersey Estuary cores and therefore had no influence on the trends seen in the metal profiles. However, Harland et al. (2000) found that the silt fraction of the sediments during the last 25 years was strongly correlated with Hg and other metals, and therefore the values were normalised to the silt % in the sediments.

In order to remove the effects of grain size and composition on heavy metals, and to determine if there are any anomalous metal concentrations, it is common to carry out a normalisation (Covelli and Fontolan, 1997). Normalisation is essential for establishing 'real' down-core trends in pollution in order to achieve a clearer pattern of metal pollution trends with time.

There is no one standard method for normalisation, with a variety of techniques being used (Jickells and Rae, 1997). A common technique is to normalise for grain size using a grain size proxy such as Al, Fe or Li (Wen et al., 1999). The grain size proxy which is used varies with the local conditions as the element must be an important constituent of one or more of the major trace metal carriers and reflect the variability in grain size (Loring, 1990) as well as not being a constituent of any anthropogenic activity (Covelli and Fontolan, 1997).

Al is often and successfully applied to normalise metals due to its high abundance in crustal rocks and low concentrations in anthropogenic sources (Alexander et al., 1993), and behaves conservatively in normal marine environments (Herut and Sandler, 2006). An advantage of using Al is that is it representative of mineralogical variation as well as grain size (Tam and Yao, 1998), it is also easy, precise and accurate to determine (Herut and Sandler, 2006).

Fe has also been successfully used for normalisation as it is a clay mineral element and has been used instead of Al in some cases. However, Fe can only be used to normalise if there is no anthropogenic source (Tam and Yao, 1998) and no diagenetic remobilisation, or precipitation has taken place (Herut and Sandler, 2006).

Li has also been found to be an alternative to Al, with Loring (1990) finding it to be superior for sediments derived from crystalline rocks which have been glacially eroded and equal to or superior to Al for non-crystaline rocks also (Covelli and Fontolan, 1997). It has been shown to be better for normalising marine sediments. However, it seems that its success depends on the study site (Herut and Sandler, 2006).

Rb is also an element which is used to normalise for grain size. Rb is most common in the clay and silt fraction of sediments and is usually not influenced by anthropogenic activity (Jickells and Rae, 1997). Rb has similar geochemical behaviour to Li and has been applied in many studies in the UK (Herut and Sandler, 2006).

Procedure

The following procedure was carried out in order to try to identify relationships between grain sizes fractions and organic matter content with metals. The procedure was carried out on surface data as these are not complicated by the temporally variable input of certain metals which might mask or complicate the relationships.

Grain size

To aid in the decision of which is the most appropriate and best grain size proxy to use in normalisation, an evaluation of the correlations between heavy metals (Pb, Cu, Ni, Zn, Cr, Fe, Hg), grain size indicators (Al, Ti, K, Rb), grain size percentages (sand, silt, clay), and grain size fractions (0-10 ϕ) was undertaken. Al, Ti, K, and Rb were chosen as the most appropriate grain size proxies as they are not input into the environment by anthropogenic activities and are not affected by remobilisation and precipitation.

Although grain size data are available to use instead of a proxy for the two principal cores, other cores which have been analysed for geochemistry do not have grain size data (from digested sediment) available. Therefore, a proxy must be used for normalisation. In addition, grain size data themselves are not necessarily the best data to be use for normalisation. In Covelli and Fontolan (1997), although grain size data were available, they chose to use a proxy for grain size by using an element which was the strongest correlation with grain size in order to carry out an enrichment factor analysis for geochemical baselines.

Correlation matrices were created for each of the datasets (see appendix 2) and from these it was firstly determined for each dataset whether the grain size proxies were correlated with each other and were, therefore, all reflecting the same environmental control. The same was done for the heavy metals. (For note, the relationships were classified as being correlated and having a relationship when the r^2 value was =>0.6 and the p value was <0.05). If high correlations between these were found, the correlations between the heavy metals and grain size fractions were then evaluated. High positive correlations show that the heavy metals are related to that fraction and, therefore, their concentrations may be effected by changes in the grain size and the grain size fraction could be used to normalise the metal data. Once a grain size fraction or proxy was chosen to represent the fine grained material with which heavy metals are associated, ratios of these were calculated and plotted. It was then determined which of the normalised results showed an improvement on the unmodified results, reducing the effect of grain size.

For the Oglet Bay surface samples, the grain size proxies mostly correlate well and these also correlate with some grain size fractions, predominantly the 8-9 ϕ size. The heavy metals all correlate with each other also, although not as strongly in some transects. In two of the transects (OBSS1 and OBSS2), the heavy metals do not correlate positively with grain size. This contrasts with OBSS3 were the heavy metals do correlate with grain size (tables A2.1 to A2.3).

DMSS2 correlations (table A2.5) show that the heavy metals are correlated with grain size and each other, and the grain size proxies are also highly correlated, suggesting that the fine grain size fractions as well as K, Al or Rb may be used to normalise the metals.

In DMSS1, Al, K, and Ti all correlate strongly, and the heavy metals Pb, Zn, Cu and Ni also correlate. Some of the heavy metals (Zn and Fe) and the grain size proxies (Si, Rb and Zr)

also correlate with some grain size fractions (Clay; 7-9 ϕ; 3-5 ϕ; 6-9 ϕ; and 3-5 ϕ, respectively). However, it can been seen in the correlation matrix that Al, K, and Ti also highly correlate with Ca, Mg and Sr as well as the clay %, and size fractions 4-5 ϕ, 5-6 ϕ and 8-9 ϕ. This suggests that the source of the fine sized material is not minerogenic but may be related to a biogenic shell component. Therefore, using a grain size fraction (8-9 ϕ) for normalisation will normalise for all fine grained sediment, irrespective of the source, compared with a grain size proxy, such as Al, which will normalise for grain size and mineral content.

A possible explanation for the differences in the two surface sample transects on the same study site may be related to the altitude of the samples. DMSS1 is located in the upper marsh area covering the top 100 m only, compared with DMSS2 which was taken along the saltmarsh concentrating on the lower marsh area. The lower marsh is more likely to have a higher minerogenic input of a fine grain sizes since it is inundated more compared with the higher marsh area which has a greater biogenic sediment accumulation. This has a consequence for the DMC1 core as it is likely that as the sediments have accumulated and the elevation of the marsh has increased accordingly, there may be a switch from a minerogenic accumulation of fine grained material to a more biogenic accumulation of fines higher up the core. This is problematic when choosing a 'normaliser', either a grain size fraction or a grain size proxy. If the grain size fraction which is correlated the most with the metals is used this will also adjust the data for the minerogenic input as well as the biogenic input of fine material which may be occurring towards the top of the core. In contrast, the proxies Rb and Al are more likely to represent the mineral fine grain size input only, and should provide a better normalisation.

It can be seen from the correlation matrix for DMC1 that Rb correlates with grain size fractions, metals and other proxies, and the heavy metals correlate, but not very highly, with the 8-9 ϕ grain size fraction. Due to the two different sources of fines this may be masking the correlations.

It was concluded that Al, Rb and the 8-9 ϕ grain size fraction correlate the best in Oglet Bay and Decoy Marsh, therefore these ratios were calculated and plotted for both cores to see if there were any differences, and to determine whether the data show any clearer temporal trend in heavy metal accumulation after normalisation for grain size.

The ratios for OB5 metals with Al and Rb (figures A3.1 and A3.2) did not show a significant difference with the non-normalised data. The grain size fraction-normalised data (figure A3.3) did show some difference, the most obvious an increased fall in the concentrations at a depth of 35 cm for all metals.

Comparing the plots for the unmodified metal data with the ratios of Rb and Al for DMC1 (figures A3.4 and A3.5) it can be seen that the normalisation does not change the trends of the metals significantly. The plot of the 8-9 ϕ grain size fraction-normalisation (figure A3.6) does however alter the trends considerably. The concentrations of metals at the top half of the core were increased and the peak in the lower half of the core was reduced. This supports the suggestion that there is a change in source of fines up-core and the increase in metals at the top of the core is related to the biogenic accumulation of fines and not minerogenic input.

It was, therefore, concluded that for DMC1 that the 8-9 ϕ fraction was not the most appropriate grain size normaliser. As Al and Rb ratios did not change the profiles significantly in either core these did not improve the results enough to justify the use of these instead of the non-normalised data.

Organic matter

Other than grain size, organic matter may also influence the metal concentrations in a core, therefore, the data may also need to be normalised for organic matter content (e.g. Kim et al., 1997). An evaluation of the correlations between heavy metals (Pb, Cu, Ni, Zn, Cr, Fe, Hg) and organic matter (LOI) were carried out similar to above, with correlation matrices created for each of the datasets (see appendix 2). If it was found from the correlations (appendix 2) that the metals were highly correlated with LOI then the heavy metals profiles may be disrupted by the effect of the organic matter content (Allen, 1990; Valette-Silver, 1993).

In the transects OBSS1 and OBSS2 from Oglet Bay, the heavy metals were found to be correlated with organic matter and did not correlate positively with grain size (tables A2.1 and A2.2). This may be due to the location of the transects, as OBSS1 and OBSS2 are located on a marsh area which is vegetated with *Phragmites* spp. providing more organic matter than at OBSS3 which does not have any *Phragmites* spp. present and where the metals were not strongly correlated with organic matter.

The correlations for the two transects from Decoy Marsh show different relationships. Metals from DMSS1 can be seen to correlate negatively with LOI %. Whilst in DMSS2, there are strong positive relationships with most of the metals as well as the clay and silt fractions. Again this is reflecting the different inputs of sediment across the marsh as described above.

The ratios for OB5 metals with the LOI data showed that the metals appear to be related to the organic matter content. For this reason the metals were normalised with organic matter content. Examining the DMC1 correlation matrix it can be seen that many of the metals are also highly correlated with LOI and, therefore, the concentrations may be more likely to be affected by the organic matter content than grain size. Similarly to OB5, these plots also show no significant difference with non-normalised plots. Most of the change in organic matter, however, occurs in the top 5 cm of the core and, therefore, it would be expected that the profiles would change most significantly in this part of the core. However, due to limitations in the amount of sediment in the top 5 cm of the core because of a large amount of vegetation present, organic matter content from the 4-5 cm slices only are available. Using this alone it appears that the metals increase rather than decrease at the very top of the core.

When the other cores from Oglet Bay are considered, it becomes apparent that cores PB1 and PB3 are both affected by organic matter content as it can be seen from figures 5.11 and 5.15 that the profiles of the heavy metals are similar to the organic matter content profile, although the correlation r^2 values do not confirm this. This appears to be because only the lower parts of the cores are affected by the LOI % whilst the upper parts appear not to be. This can be seen when metals are normalised with LOI %, that the lower part (>40 cm depth) of the cores seems to improve by reducing the observed falls in metal concentration which reflect declines in organic matter content, but the upper part of the 'normalised' data (<40 cm depth) does not reflect the true profile of metal flux in the environment as it removes some of the features which are unrelated to organic matter content. This seems counter-intuitive as it would be expected that the upper core would be more affected by organic matter due to increasing LOI %. In order to overcome this problem, a threshold LOI % and depth was determined to find where in the cores the metals stopped being correlated with each other and, therefore, affected by LOI so only this part of the core was normalised. This was done using scatterplots and correlations to determine the samples which were outliers and the depth and value of these. This was found to be a depth of 40

cm and 10% LOI for PB1 and 38 cm and 8% for PB3. The thresholds were determined when the maximum correlation was achieved whilst minimising the amount of samples being selected. The LOI % values were used below the threshold to normalise the metal concentrations and above the threshold depth the threshold value was used in order to ensure the upper part of the marsh was not normalised. The results of this can be seen figures 5.13 and 5.16. As the normalisation of the heavy metals with LOI seemed to improve the two cores PB1 and PB3, the same was done for OB5 to see if this improved the profiles. Scatterplots were also created for OB5 heavy metals and LOI % to see if this could also be the case for OB5. However, there was found to be no consistent outliers with similar LOI % occurring at similar depths. Therefore all OB5 samples were normalised with LOI. These profiles can be seen in figure 5.8.

Results of normalisation

Overall the non-normalised heavy metals Pb, Cu and Zn showed similar trends in all cores (figures 5.3, 5.5, 5.7, 5.9, 5.11 and 5.14) with general decreases in concentrations up-core, and therefore all have strong positive relationships. Some of the metal concentrations in the cores have perturbations from this trend which in most cases are related to changes in organic matter. Cores PB1 and PB3 (figures 5.11 and 5.14) have large falls in concentrations in these heavy metals as well as many other elements as described above, which in each case the same trends can be seen in LOI profiles, indicating that this is the likely cause for the fall in concentrations. Therefore, the heavy metals were normalised for the organic matter using LOI%. The profiles of the processed and un-processed heavy metals can be seen in figures 5.3 to 5.16.

Figure 5.3 shows the un-processed heavy metal results for OB1, the metals Hg, Pb, Cu, and Zn all show decreasing concentrations up-core and have strong positive correlations (table A2.6). When the heavy metals have been normalised for LOI (figure 5.4) there becomes a sharp increase in concentrations at a depth of 75 cm and moves the peak in Hg up to this depth from 80 cm.

Figure 5.7 shows the un-processed results from OB4. Hg, Pb, Cu and Zn show similar trends to OB1 with decreasing concentrations up-core. However, the profiles have a sharp decrease at approximately 47 cm. The heavy metal profiles normalised for LOI (figure 5.7) show that the sharp decrease in heavy metals at 47 cm becomes a sharp increase in Cu, Zn, Fe, Ni, and Cr although not in Pb or Hg. Below this is a sharp decrease due to the sharp increase in LOI %. Normalised Hg shows a more distinct peak in Hg at the bottom of the

core. Un-processed OB5 results (figure 5.7) show a trend of falling metal concentrations in Pb, Cu and Zn. The LOI profile, however, shows a slightly different trend, although the top 35 cm does show the highest LOI %. There are falls in LOI % at depths of approximately 70 cm and 40 cm which can also be seen in the Cu concentrations. At the same point, approximately 40 cm, Zr increases in concentration. Figure 5.8 shows the normalised heavy metals and creates sharp peaks in all the profiles at a depth of 68 cm.

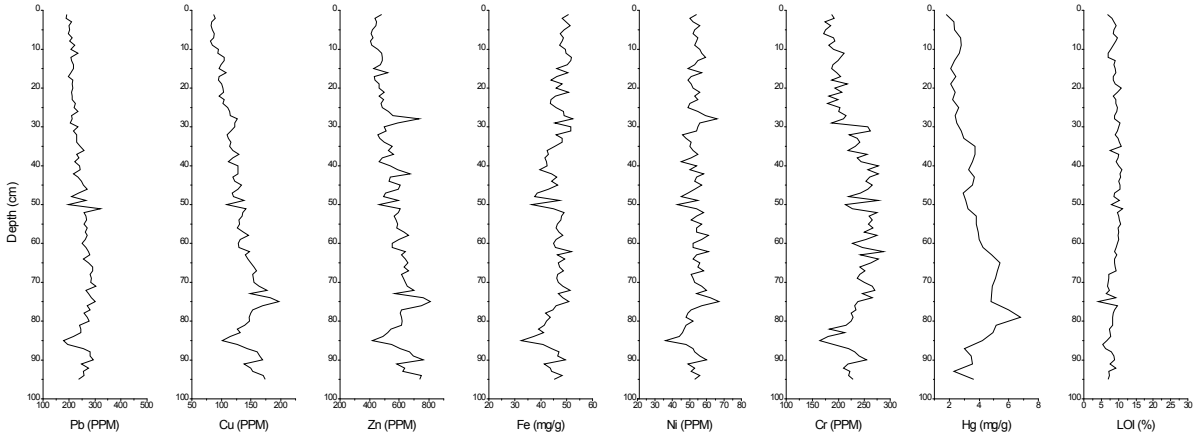

Figure 5.3 OB1 profiles of heavy metals.

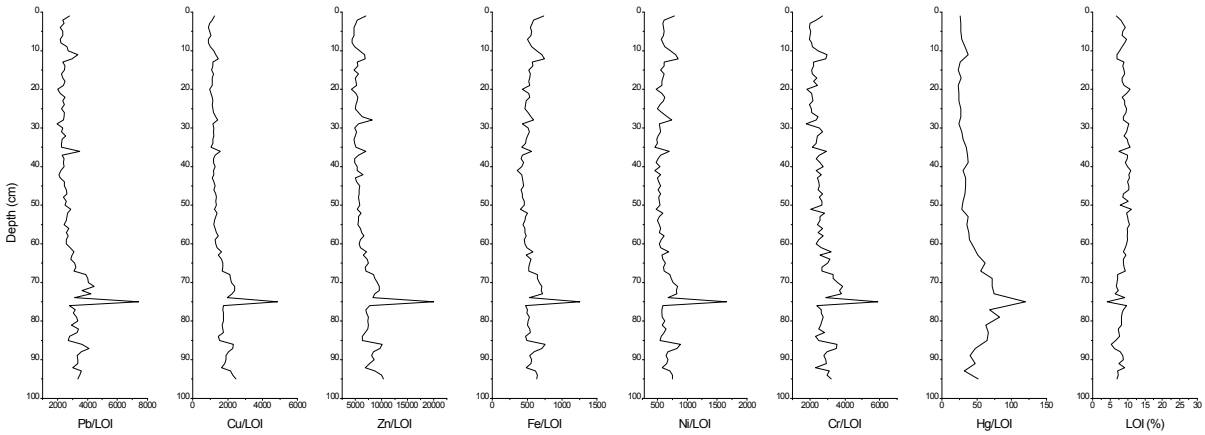

Figure 5.4 OB1 profiles of heavy metal ratios normalised for LOI.

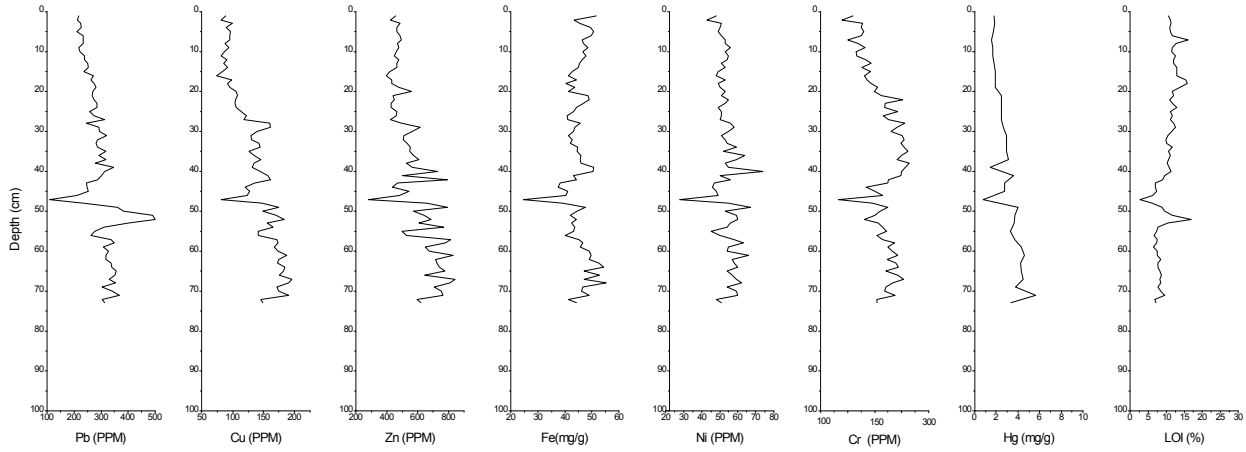

Figure 5.5 OB4 profiles of heavy metals.

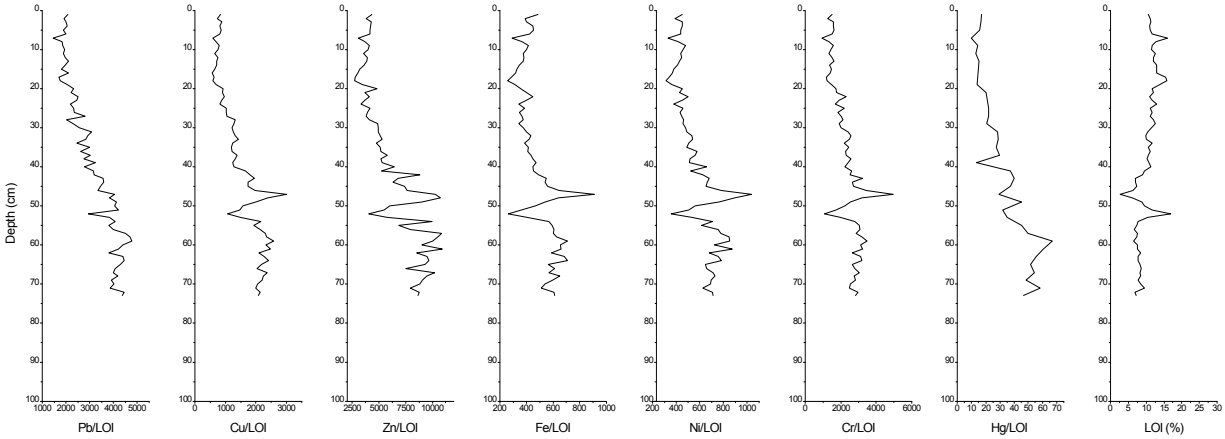

Figure 5.6 OB4 profiles of heavy metal ratios normalised for LOI.

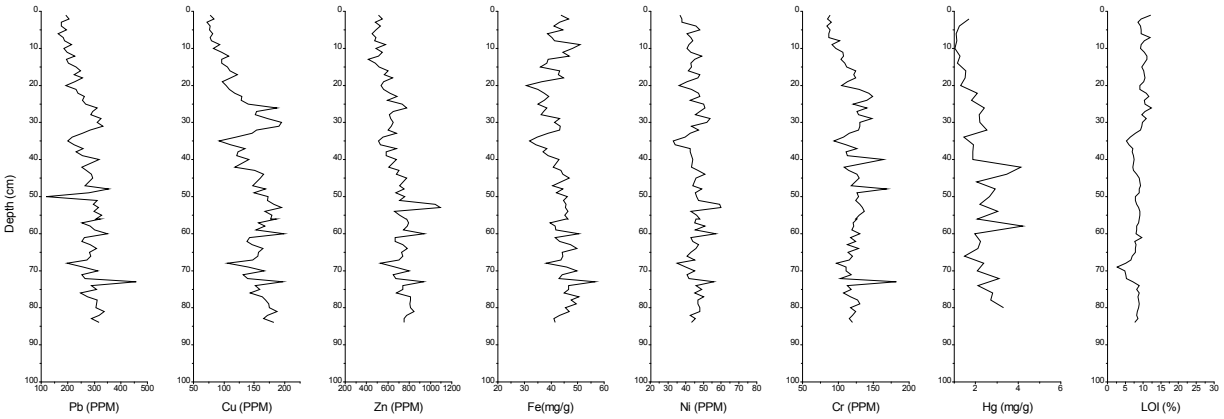

Figure 5.7 OB5 profiles of heavy metals.

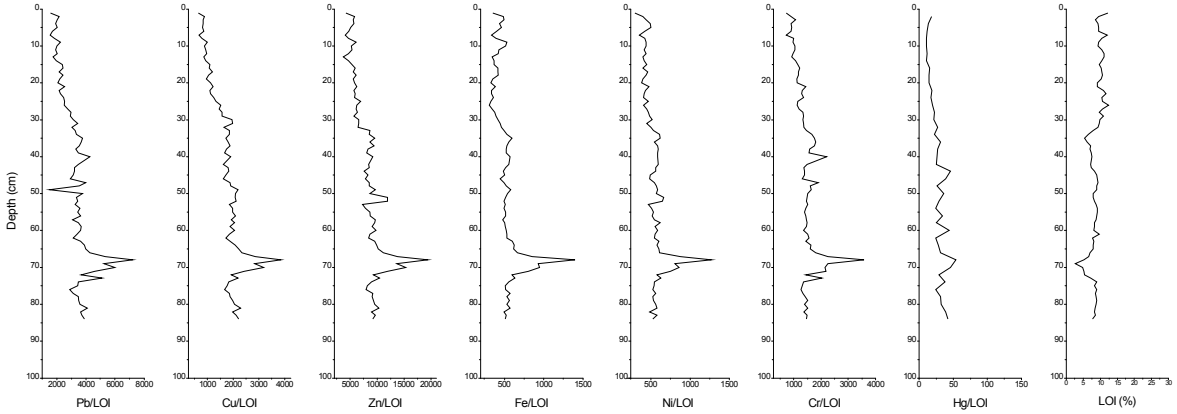

Figure 5.8 OB5 profiles of heavy metal ratios normalised for LOI.

Figure 5.9 shows the raw concentration profiles of metals from OB6. This core was very short in length (26 cm), therefore trends in the profiles are difficult to identify. However, as with the other cores, Pb and Cu show a fall in concentrations up-core, although Zn shows no trend of either an increase or decrease. After the heavy metals were normalised with LOI (figure 5.11), the variation in the profiles decreases and the profiles show a more gradual fall in concentrations. At the bottom of the core, the fall in LOI creates a sharp increase in all concentration profiles, except Zn.

The heavy metal profiles for core PB1 can be seen in figure 5.11. As with the other discussed cores, Pb, Cu and Zn show similar trends of decreasing concentrations up-core, however, the trend is interrupted by a decrease at approximately 50 cm depth which can also be seen in several other profiles including Ni, K, Al, Rb, Sr, Fe and LOI (figure 5.22). Figure 5.15 shows the heavy metal profiles from the PB3 core, again, Pb, Cu and Zn show a general trend of decreasing concentrations up-core, however, similar to PB1, the concentrations decrease at a depth of 50 cm and at approximately 75 cm. These decreases are present in many of the profiles including Ni, K, Zr, Al, Rb, Ca, Sr, Mn, Fe, Br and LOI (figure 5.24).

PB1 and PB3 are the cores in which the metal concentrations are most affected by the organic matter content, therefore, the metal profiles after normalisation with LOI show the most dramatic changes. Figures 5.12 and 5.15 show the heavy metal profiles normalised for LOI %. In figures 5.13 and 5.16, only the lower part of the cores were normalised with the LOI %, the upper part of the cores were all normalised by the threshold value which was determined previously. This removes the features which are related to variations in organic matter in the lower part of the core whilst keeping those which are unrelated to organic matter content in the upper part. LOI normalisation in PB1 (figure 5.13) removes the fall in

concentrations at a depth of 30 cm which is clearly an artefact of decreased organic matter content. In the Fe and Cr profiles, new peaks are created, in the other metal profiles it is more difficult to distinguish any peaks. In the Zn and Ni profiles there are peaks at a depth of 38 cm which have not been normalised, and are therefore present in the raw concentration profiles also.

Profiles of Pb, Fe, Ni and Cr concentration for PB3 (figure 5.16) all show similar profiles after normalisation, with peaks at 50 cm and 72 cm. In contrast, normalised profiles of Cu and Zn have emphasised the falls in concentration much more than the peaks and show similar trends. We can see that in the Zn profile there are increases in concentrations at the same points as in the other heavy metal profiles but the falls which are also present are much more noticeable. In the Cu profile, however, some of the peaks and falls occur at different depths, particularly at a depth of 48-50 cm where there is a sharp fall in organic matter causing an increase in the heavy metals, whereas in the Cu profile there is a decrease. This is due to a greater decrease in Cu concentrations then in the other metals at this point. It is important to note here that the Cu concentrations may not be as reliable given that Cu is not easily determined using the XRF.

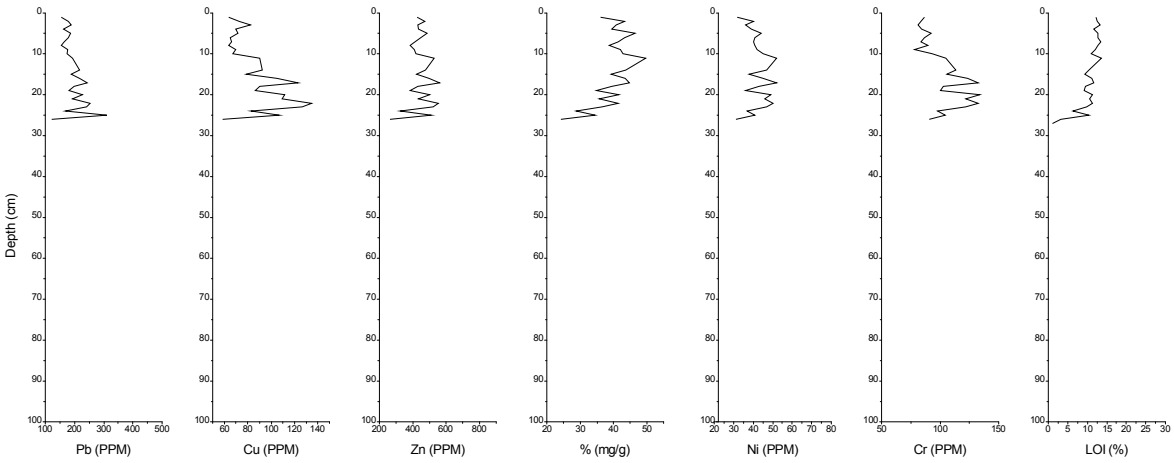

Figure 5.9 OB6 profiles for heavy metals.

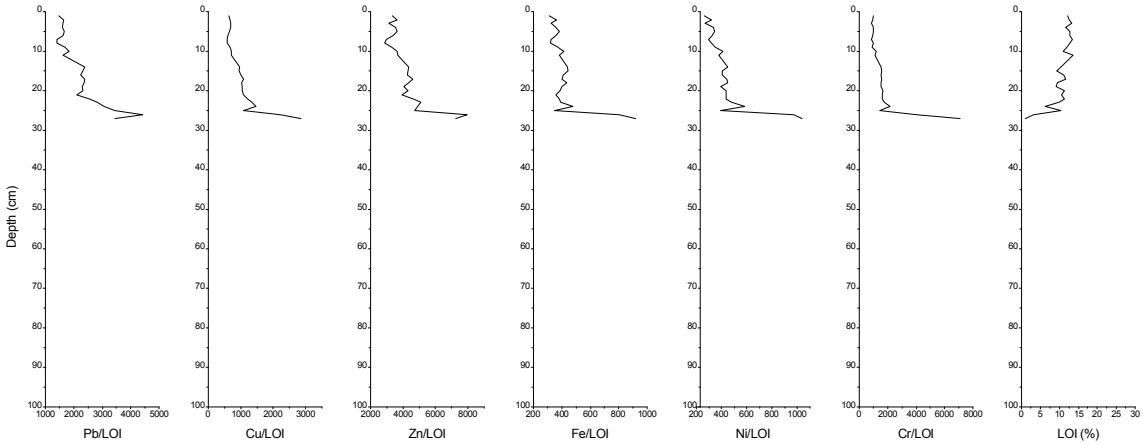

Figure 5.10 OB6 profiles for heavy metal ratios normalised for LOI.

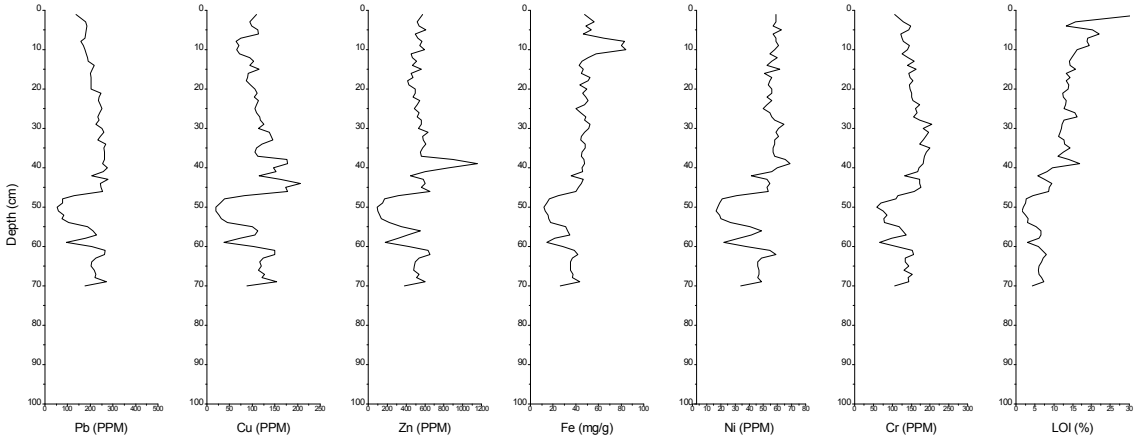

Figure 5.11 PB1 profiles of heavy metals.

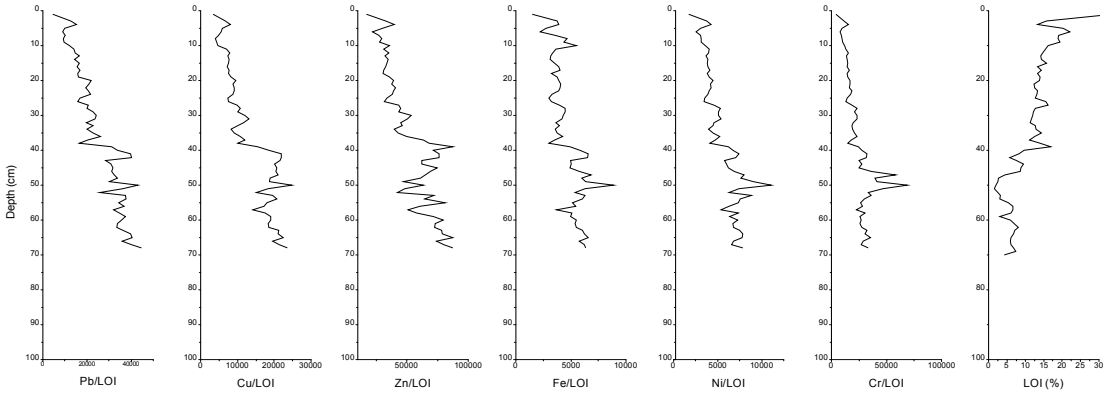

Figure 5.12 PB1 profiles of heavy metal ratios normalised for LOI.

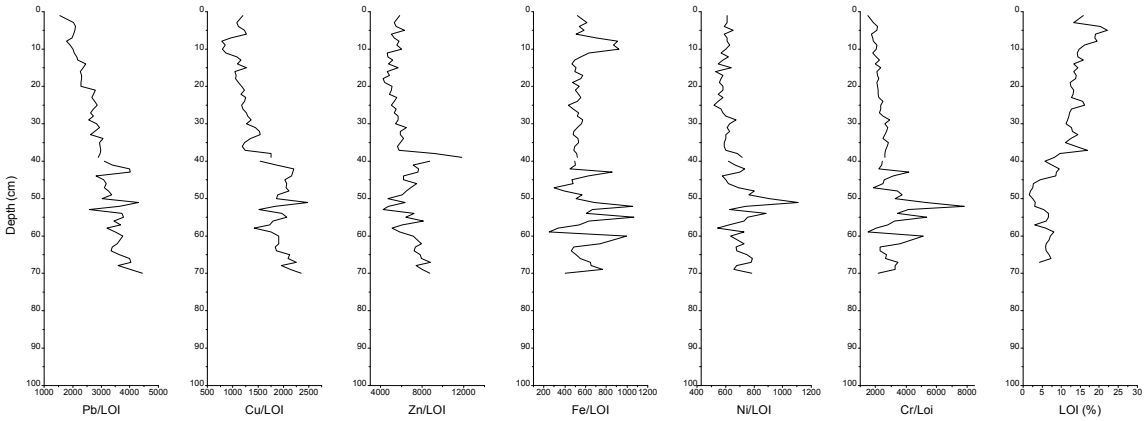

Figure 5.13 PB1 profiles with heavy metals. Samples 40 to 70 cm are normalised for LOI, whilst samples between 0 to 39 cm are not normalised. See text for further explanation.

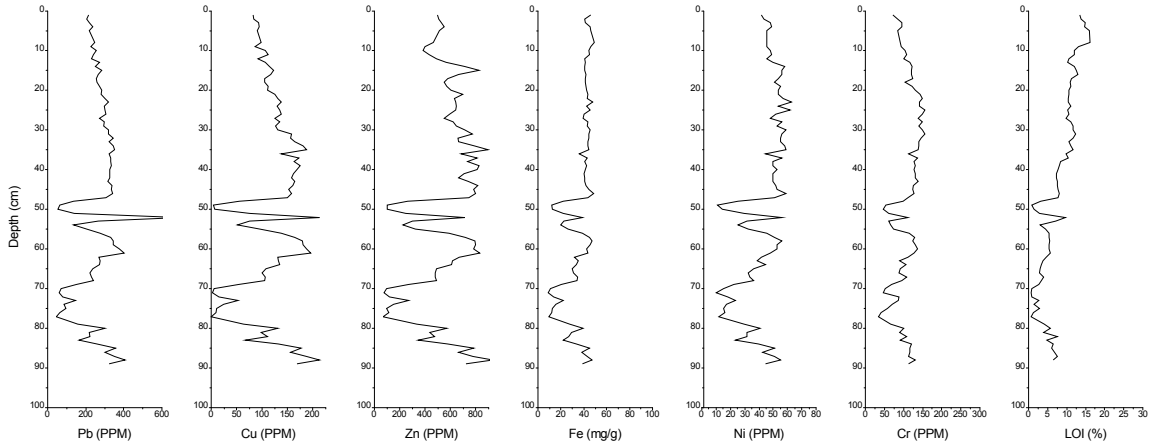

Figure 5.14 PB3 profiles of heavy metals

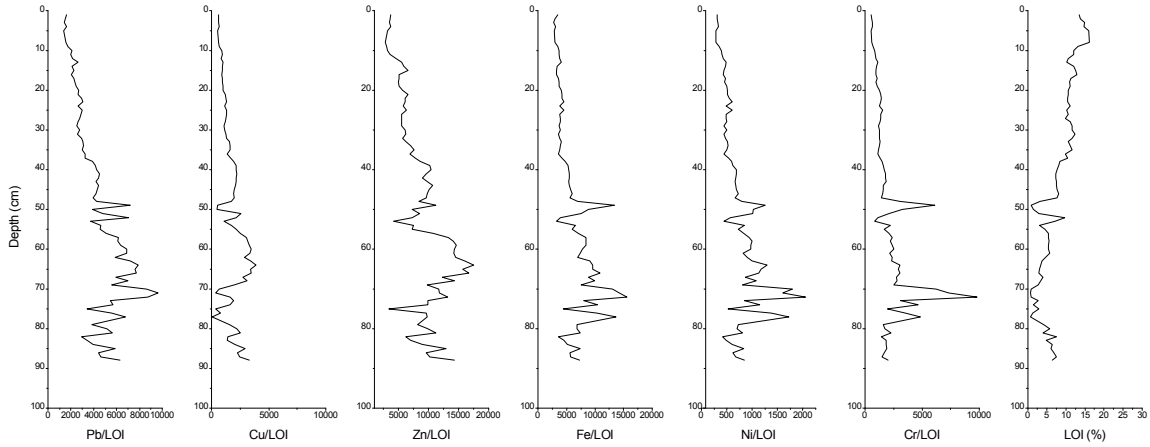

Figure 5.15 PB3 profiles of heavy metal ratios normalised for LOI.

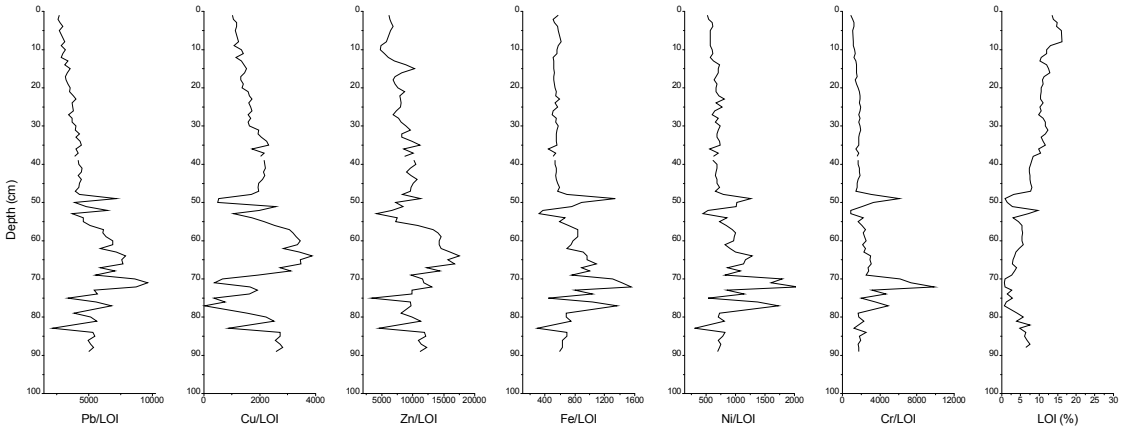

Figure 5.16 PB3 profiles with heavy metal Samples 38 to 50 cm are normalised for LOI, whilst samples between 0 to 37 cm are not normalised. See text for further explanation.

The LOI-normalised profiles for heavy metals for Decoy Marsh (figure 5.18) show a trend of increasing then decreasing of concentrations up-core for Pb, Cu, Cr and Zn, as do the un-processed results (figure 5.17). The small decrease in concentration which can most noticeably be seen in Pb in the non-normalised profile increases dramatically in the normalised profile, and can also been seen in the Cu and Zn profiles and less so in Fe and Ni profiles. The LOI-normalised profiles also emphasise the lower peak in concentrations in Pb, Cu and Zn. The Fe and Ni profiles show a dramatic rise in concentrations at the bottom of the core which cannot be seen in the un-normalised profiles. A similar trend in concentrations can be seen in the Cr normalised profile even though the un-normalised profile is similar to the other metals, Pb, Cu and Zn. The normalised Fe, Cr and Ni profiles do not seem to show a realistic trend in concentrations but seem only to be reflecting the organic matter content, therefore these will not be used in examining the pollution trends for dating.

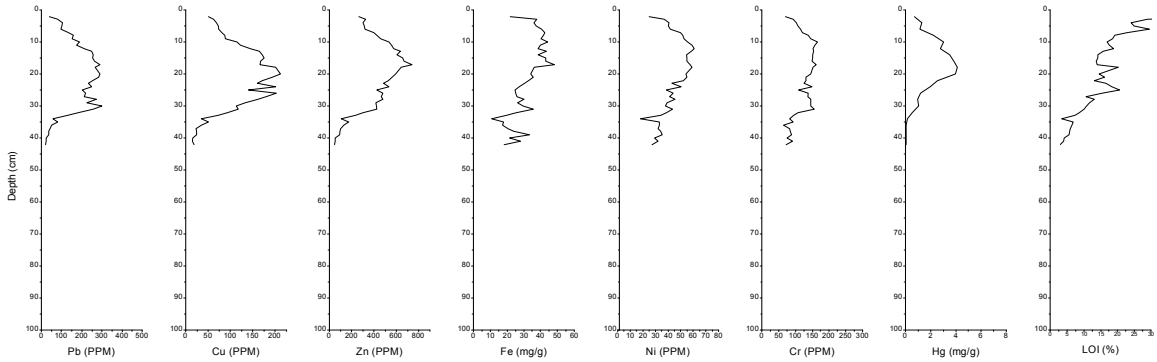

Figure 5.17 DMC1 profiles of heavy metals.

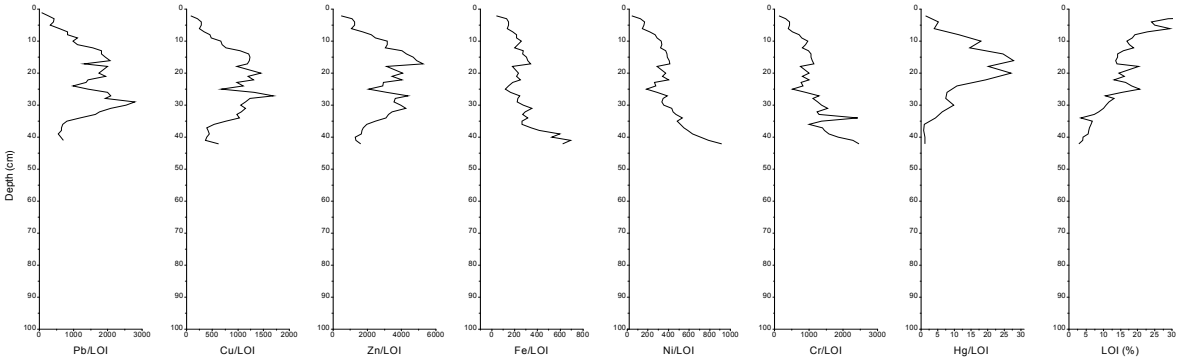

Figure 5.18 DMC1 profiles of heavy metal ratios normalised for LOI.

5.3.2. Results of Geochemistry

The following sections concentrate on the data which were established to be most appropriate to use from the above normalisation results and discussion. Organic matter content was found to be the most controlling factor influencing the metals concentration trends, therefore these were normalised for organic matter content by using the ratio with LOI %. The heavy metals (pollution indicators) were normalised for organic matter content for cores OB1, OB4, OB5, OB6 and DMC1 in order for clearer trends in metal history to be identified without the effects of changes in organic matter content. For cores PB1 and PB3 only the lower half of the cores below 40 cm for PB1 and 38 cm for PB3 were normalised for organic matter content as the upper half of the cores appear to be less affected by organic matter content. The other metals remain uncorrected in order to be used for the determination of the processes which the sediments have undergone and also establish the origins of the sediments if possible.

Figure 5.19 shows the results from OB1. Br, Cl and LOI show similar trends of increasing concentrations up to approximately 70 cm then an unchanging trend followed by decreasing concentrations up-core at approximately 15 cm. These metals also have some positive correlation (table A2.6). Other features in this core include an increase in Ca in the top 10 cm of the core and a very sharp peak in Mn at 30 cm with higher concentrations above this. The heavy metal profiles Pb, Cu, Zn, Fe, Ni, Cr and Hg show a general decrease in concentration up-core with sharp peaks at a depth of 75 cm. The peak at 75 cm is less sharp in Hg than in the other heavy metal profiles as it has a general increase and decrease between 90 and 70 cm.

The processed results from OB4 can be seen in figure 5.20 and show K, Al, Rb and LOI to have similar trends to the Br, Cl and LOI in OB1. They show increasing concentrations up-core between 70 and 50 cm followed by a decrease near the surface between 20 and 0 cm. These metals along with Sr, Ti and LOI show a sharp decrease at 48 cm. The Ca profile also shows a similar trend to OB1 with an increase at the top of the core in this case at approximately 15 cm which is also seen in the Sr profile. The heavy metal profiles show a decrease up-core similar to OB1. There is a perturbation in this trend at a depth between 55-45 cm where there is a sharp fall followed by a sharp peak in concentrations in Cu, Zn, Fe, Ni and Cr.

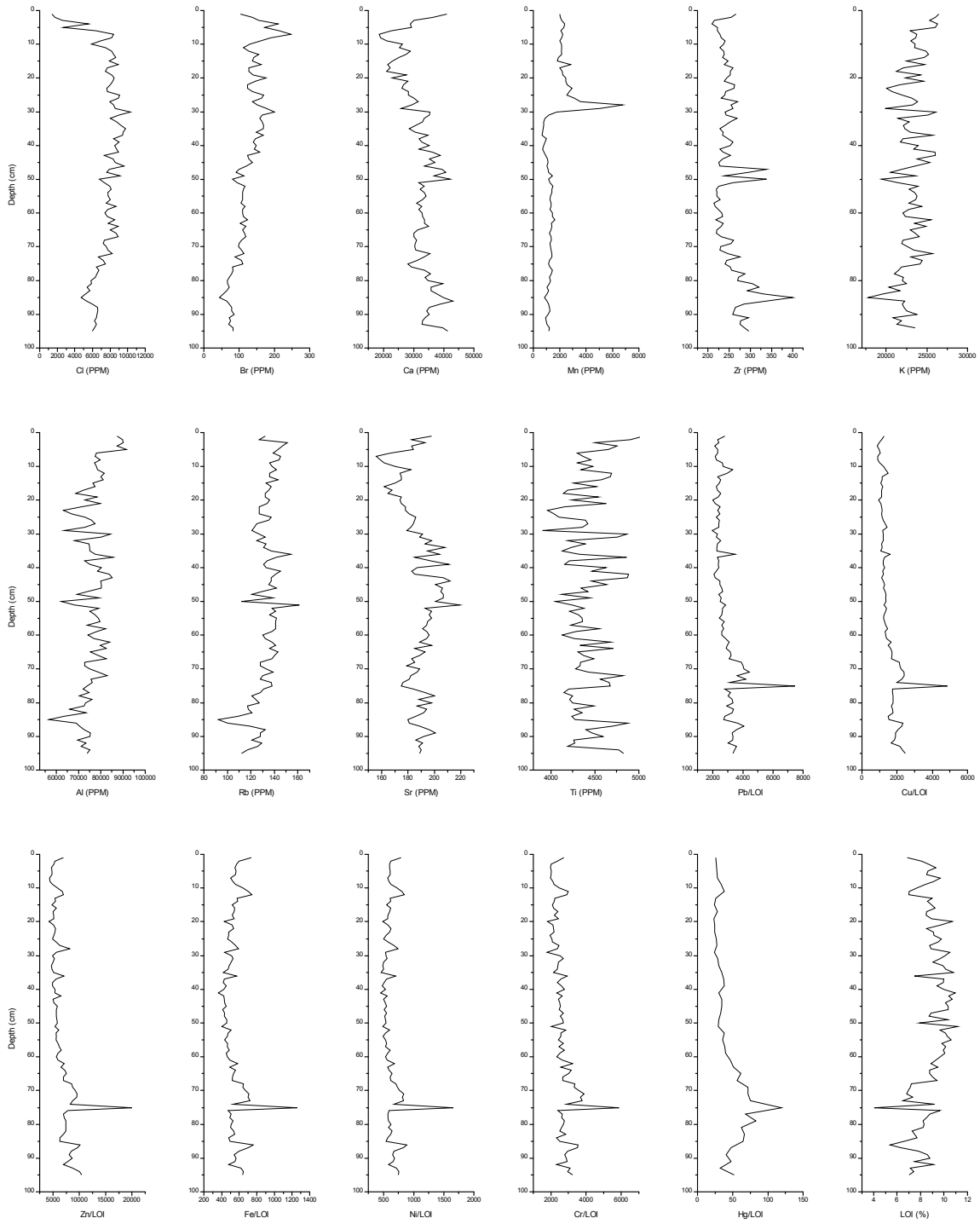

Figure 5.19 OB1 geochemical profiles.

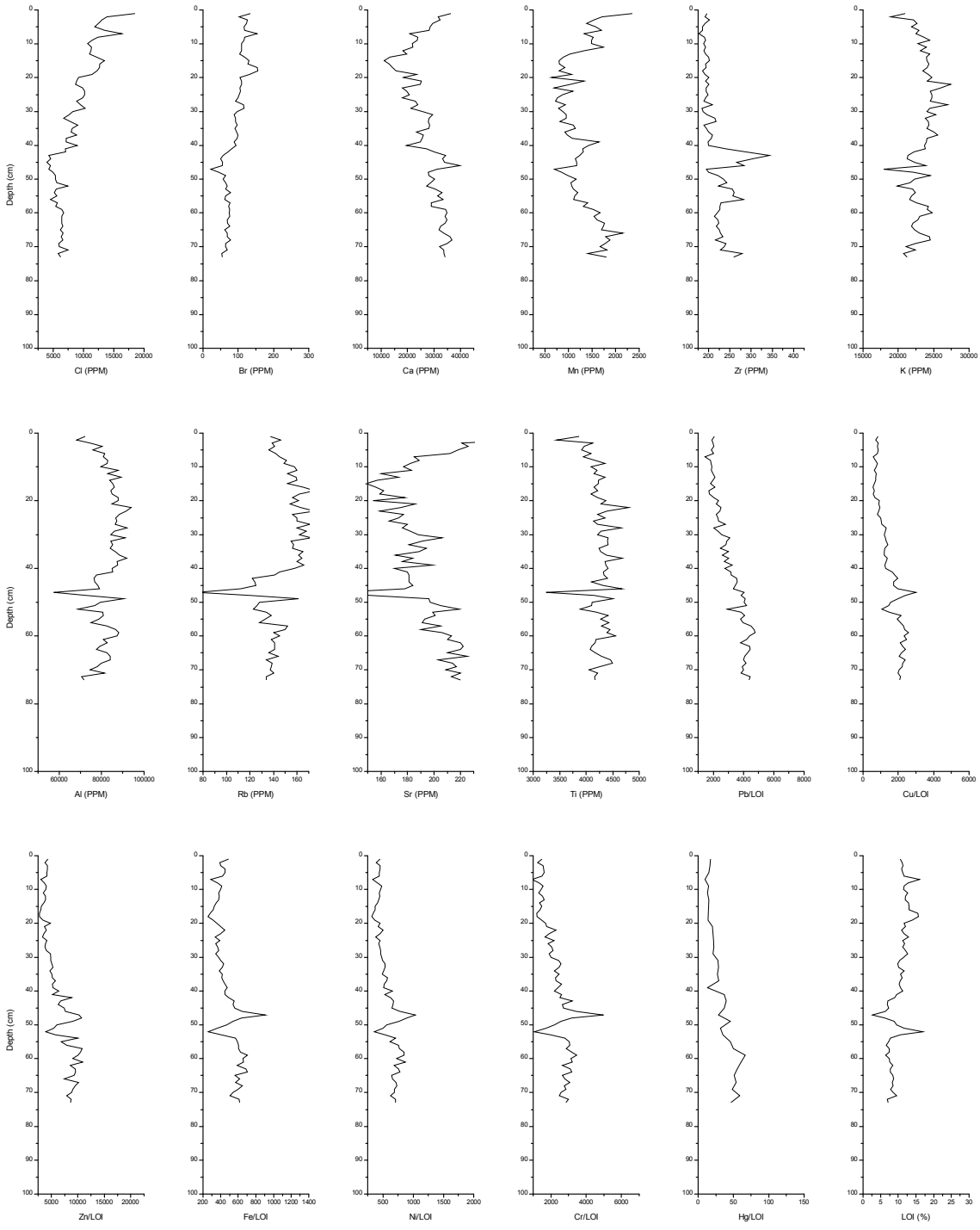

Figure 5.20 OB4 geochemical profiles.

Results from OB5 (figure 5.21) show a fall in concentrations of Ca and Sr up-core with an increase at approximately 5 cm depth which is also shown in Mn. Br and Cl have a strong positive correlation and have similar profiles with an increase and decrease which can be seen from 35 to 0 cm, with a fall before this between 50 and 35 cm. All heavy metal profiles show a slight decline in concentrations up-core, the most pronounced feature is the sharp peak in concentrations at a depth approximately 70 cm.

Ca and Sr in core OB6 (figure 5.22) show the same sharp increase, which can be seen in the other cores and occurs at a depth of 10 cm. Other metals (Cr, Br, Mn, Al, Rb and Ti) all show an increase between 25 and 10 cm followed by a decrease in concentrations up-core from 10 cm. The heavy metals all show decreasing trends up-core; at the bottom of the core the profiles show much higher concentrations which fall sharply, particularly for Fe, Ni, and Cr in the bottom 1 cm.

As with the other discussed cores, Pb, Cu and Zn show similar trends of decreasing concentrations in core PB1 (figure 5.24). Fe, Ni and Cr all shows increases in concentration at approximately 50 cm, at the same time Ni, K, Al, Rb, Sr, Fe and LOI have a decrease in concentrations. Br, Cl and LOI % all show very similar profiles up-core, increases in concentrations with a sharp increase in all three at a depth of 2 cm. Ca concentrations show a large variability up-core with an increase near the surface (4 cm) along with Mn, K, Ti and Al. Unlike the other cores there is no noticeable increase in Ca and Sr at the top of the profile, instead Sr and Mn show similar profiles of a sharp double peak at approximately 10 cm which can also be seen in the Fe profile.

Core PB3 (figure 5.24) shows Cl, Br and LOI % to have similar profiles of increasing concentrations up-core. Ca and Mn show increases near the surface of the core (5 cm). Ca, Mn, Zr, K, Al, Rb, Sr, Ti, Cu and LOI % all show large decreases in concentrations at 50 cm and 75 cm depths. This can also be seen in the LOI % to a lesser extent. The heavy metals Fe, Ni, and Cr all show sharp increases at these depths.

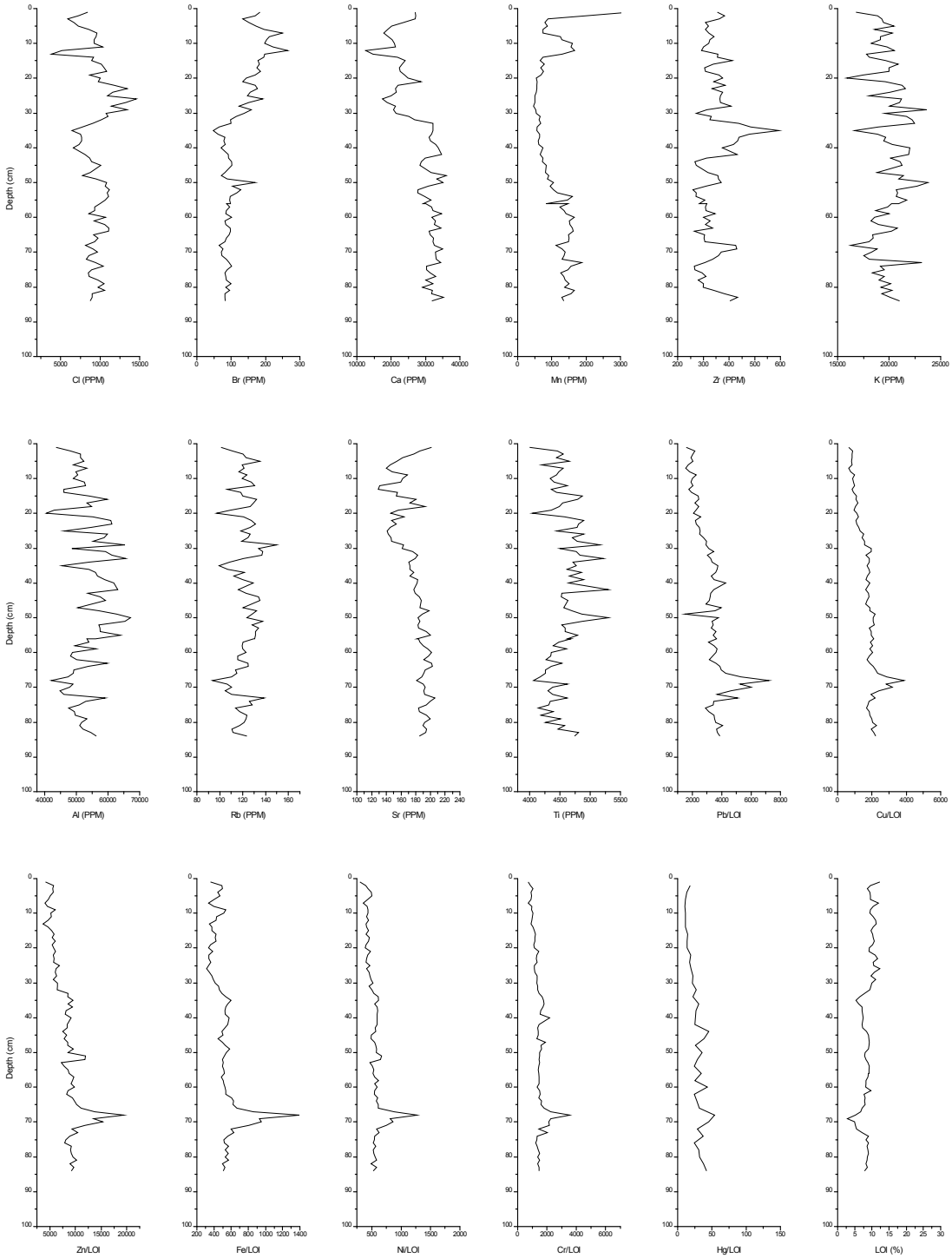

Figure 5.21 OB5 geochemical profiles.

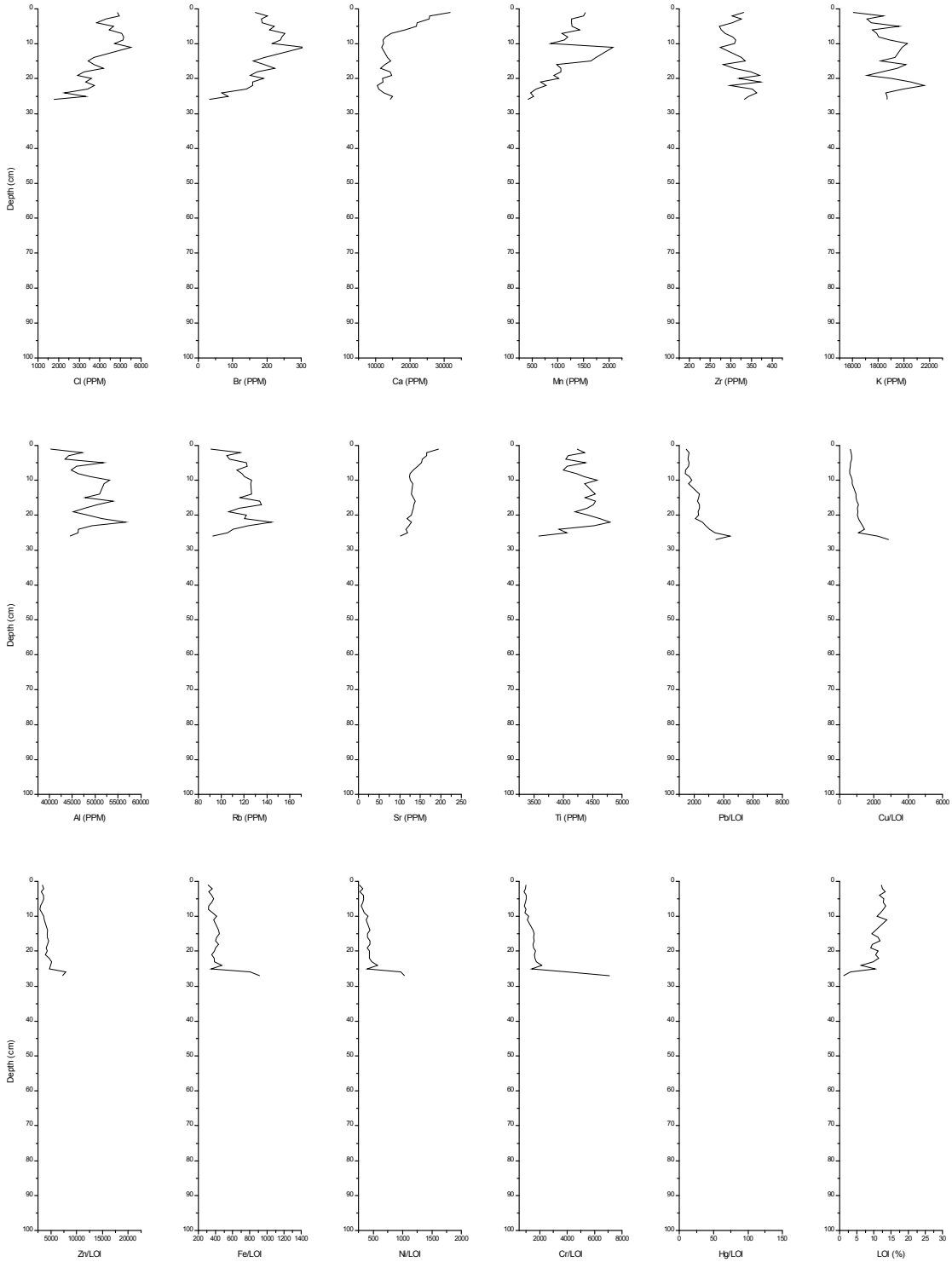

Figure 5.22 OB6 geochemical profiles.

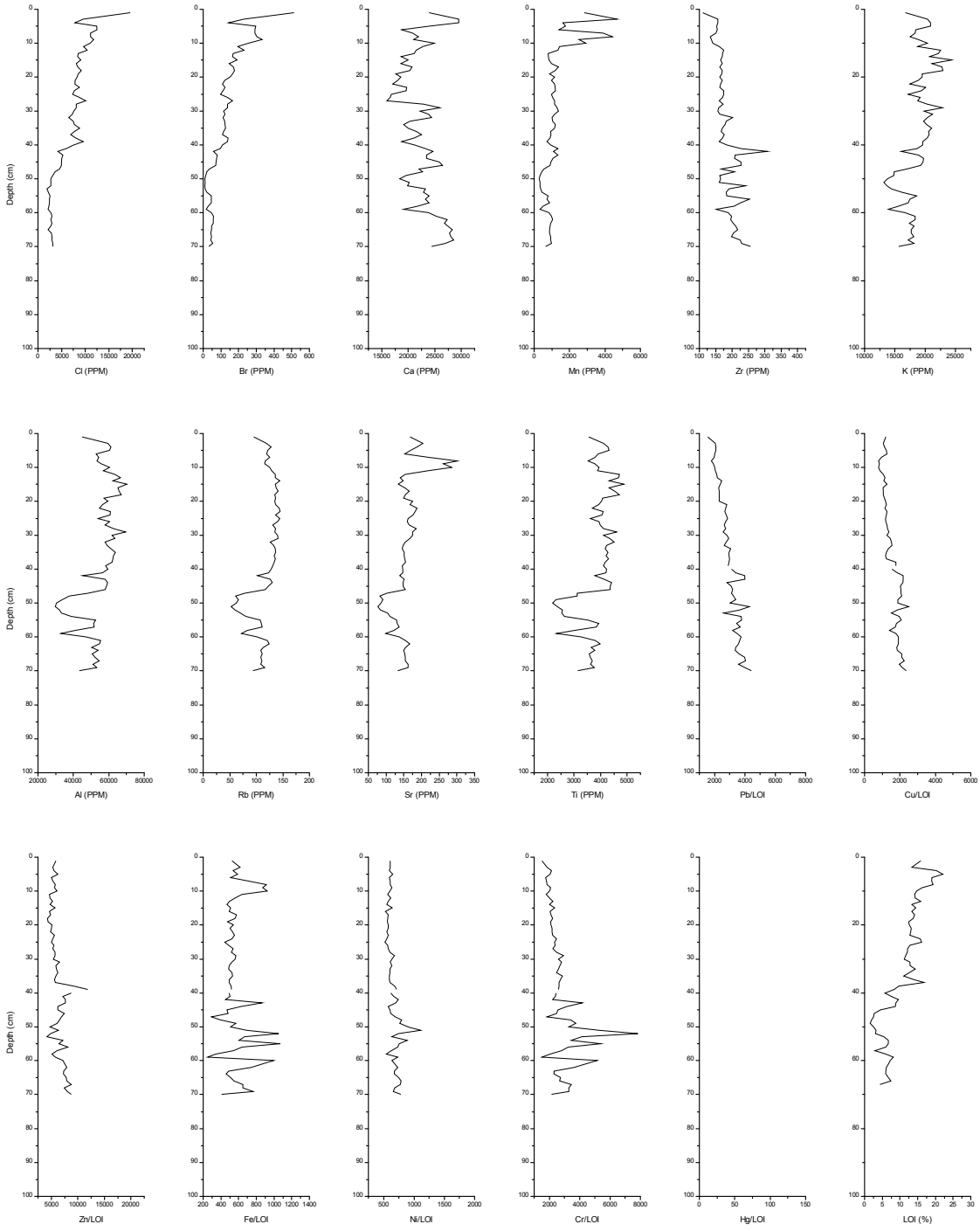

Figure 5.23 PB1 geochemical profiles.

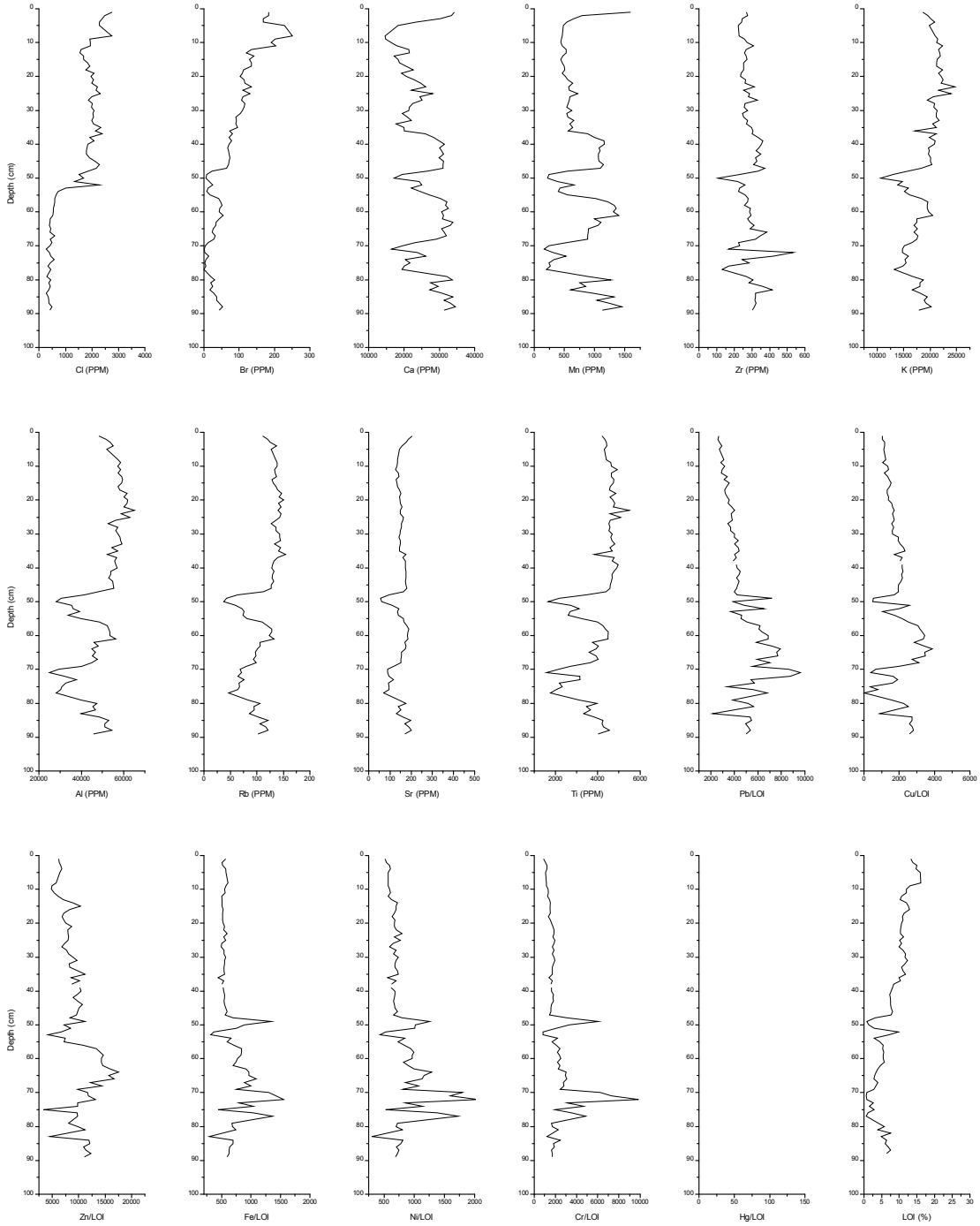

Figure 5.24 PB3 geochemical profiles.

DMC1 results can be seen in figure 5.25. Heavy metals Pb, Cu, Zr, Cr and Hg all show an increase in concentrations up-core up until approximately 20 cm followed by a decrease. Metals Pb, Cu, Zr, and Cr all show similar trends in concentrations with slight falls in concentrations at 25 cm depth, and this is reflected in the strong positive correlations between these (table A2.11). Although, Hg shows an increase up to 20 cm and decrease following this up-core, it only has one large peak at a depth of 20 cm, compared to the other heavy metal profiles which also have higher concentrations at a depth of 30 cm. Fe and Ni have different profiles to the other heavy metals with a less distinct increase and decrease up-core. Both profiles have a fall in concentrations at the top of the core similar to the other metals and also have a fall in concentrations at a depth of 34 cm similar to that which can be seen in Pb, Cu and Zn but is more noticeable. Al, K and Ti all have similar profiles and have strong positive correlations. The concentrations show little change up-core until the top 10 cm, where there is a decrease in concentrations. Metals Ca, Mn, S and Cl show similar profiles at the top of the core to other cores from Oglet Bay which have a sharp increase in concentration in the top 5 cm of the core, this can also be seen in the LOI profiles. However, the rest of the core below this peak is a decline in Ca with little variability which is seen in the Oglet Bay cores. Ca, Mn, S and Cl all have strong correlations with LOI % (appendix 2). LOI % are also highly correlated with other metals including Al, Ti, Ca, K, Fe, Cr, Ni, Rb and Sr.

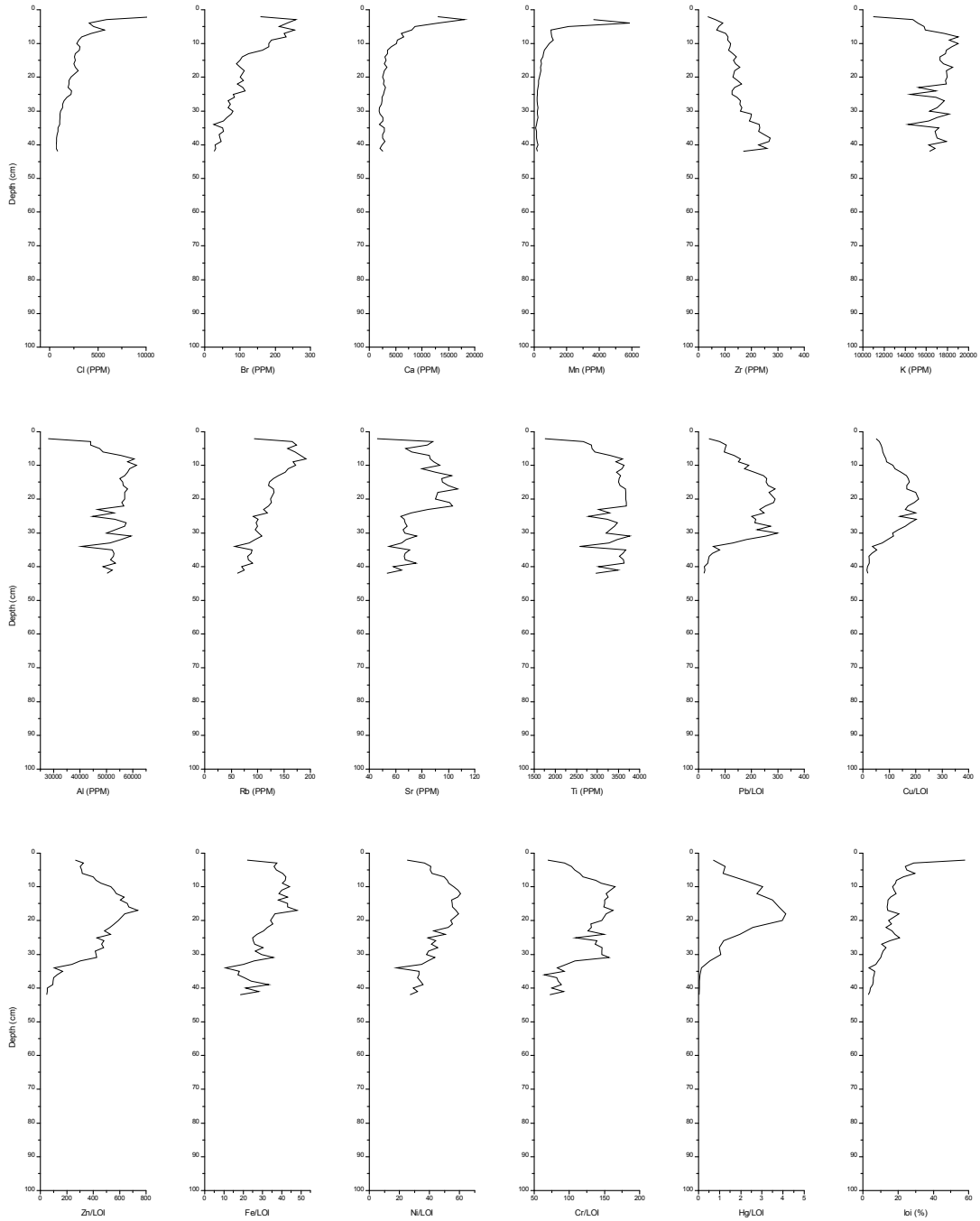

Figure 5.25 DMC1 geochemical profiles.

5.3.3. Interpretation of geochemistry

Figures 5.19 to 5.25 show the geochemical profiles of the cores that were collected for analysis. Ca and Sr have similar profiles at the top of the cores (OB1, OB4, OB5, OB6, PB3, DMC1) were they show a sharp increase between 10-5 cm and have a strong positive correlations of up to and 0.9 (OB6) (appendix 2). Several of the Mn profiles also show a sharp increase at the same points and also have strong positive correlations between Mn and Ca from 0.58 (OB4) to 0.95 (DMC1). Cl, S and LOI also have similar profiles to Ca, Sr and Mn in core DMC1 and these also correlate highly with each other. Below 10 cm there is great variability in the Ca concentrations in the Oglet Bay cores in particular, where there are several falls in Ca concentrations throughout the profiles and are most prominent in cores PB1, PB3, OB4 and OB5.

Several cores (OB1, OB5, OB6 and PB1) have different Mn profiles with peaks in Mn concentrations below the top of the core. The most obvious is in OB1 where there is a very sharp peak at a depth of 30 cm and above which higher Mn values occur. PB1 also has a sharp peak at approximately 10 cm above which is another sharp peak, this peak is also present in several other profiles in this core including Fe and P. OB5 and OB6 have similar profiles with a noticeable but less pronounced increase and decrease in Mn concentration at 5-15 cm and 15-20 cm, respectively, followed by a sharp increase in concentrations after this. In contrast, the DMC1 below 10 cm declines and remains low throughout the rest of core, with little change.

The presence of Ca in sediments can be related to lithological and biological processes. Ca minerals can occur as carbonate, sulphate, fluoride, silicate, and borate (Wenk and Bulakh, 2004). Ca sulphate minerals are present in sandstone (De Vos et al., 2006) and, therefore, may be a source for the Ca in the sediments. Seawater may also be a source for Ca and, is controlled by tidal effects (Ogichi et al., 2000), as well as the presence of skeletons and shell components formed from $CaCO_3$ which may increase the Ca in the sediment.

Sr is strongly associated with Ca and is indicative of calcareous rocks (De Vos et al., 2006). However, both Sr and Ca are highly mobile and Ca has been found to be the most important cation in governing the solubility of trace elements in soil (Kabata-Pendias, 2001). $CaCO_3$ will precipitate with saturation of seawater and this may be the likely reason for the increasing Ca and Sr concentrations at the top of most of the cores. Surface enrichment of Mn is also common and related to redox cycling in the sediment (Spencer et al., 2003); therefore, the increase in Mn in the cores may be caused by some early-

diagenetic remobilisation with reprecipitation in the oxic zone (Spencer et al., 2003). Therefore, it is possible that the increases present in the top of the cores in several elements including Ca, Sr and Mn are related to remobilisation or illustrate a marine biogenic influence. The loss of Ca in the lower part of the cores is also likely to be consequence of de-calcification, with the increases in Ca at some parts, related to reprecipitation.

Present in many of the cores are peaks in the Ca lower in the profiles than Mn and can also be seen in Zr. Zr content is generally inherited from the parent rocks and is a main component present in sandstone and mudstone (De Vos et al., 2006) which form the main geology of the area and, therefore, may represent a lithological input. As Zr can be interpreted to be related to coarse lithogenic control it is likely that these associations with Ca are related to a coarser lithogenic control. Seawater may also be a source for Ca, therefore, the increases may also be due to increased tidal influence during this time maybe due to storm activity increasing the input of coarser sand particles as well as shell material.

The most obvious and distinct features in the normalised heavy metal results for Oglet Bay cores are peaks in heavy metal concentrations towards the bottom of the cores (OB1, PB3, OB5) approximately 70-75 cm in depth. In OB1 and OB5, all of the metal profiles Pb, Cu, Zn, Fe, Ni, Cr and Hg show a peak in concentrations at depths of 70 and 75 cm, respectively. Metals Ni, Fe, Cr and Pb all show a peak at approximately 72 cm in PB3. There is also a possibility that a second peak may be identifiable at a shallower depth. This is most obvious in PB3 with a peak occurring at a depth of 50 cm as well as 72 cm. As PB1 only covers a depth to 70 cm, only one peak can be seen in the profiles these are most likely to correlate with the shallower peaks in PB3, as they occur at the same depth (50 cm). These second peaks in OB5 and OB1 are more difficult to identify.

Pollution indicators

To determine if the levels of concentrations in the sediments are natural or anthropogenic in source, it is necessary to compare the values with baseline data to evaluate the degree of heavy metal contamination (e.g. Covelli and Fontolan, 1997). Several reference baselines are available to do this. Average Shale Values (ASV) (e.g. Turekian and Wedepohl, 1961) or Average Crustal Abundance (ACA) data (Taylor, 1964) can provide the natural background values of elements found in different geology. When using average crustal abundance as a single baseline level it has the disadvantage of not taking into account natural geochemical variability which occurs. Therefore a baseline which is used must be appropriate for the geology rather than a generic average.

Another method is to compare the sediments to values attained from uncontaminated sediments from deep cores known to have been deposited before any large-scale industrialisation, or in a remote area which has not been affected by anthropogenic activities. This can provide an insight into the degree to which a particular system is polluted due to anthropogenic activity (e.g. French, 1993). When comparing values with uncontaminated sediments it is important to compare like with like and therefore both deposits must be mineralogically and texturally comparable to the baseline as higher concentrations may be related to finer-grained sediments (Covelli and Fontolan, 1997). In areas where sedimentation is rapid and pre-industrial metal concentrations are not reached in a core, this kind of baseline is not available to use (Alexander et al., 1993). It may also be very difficult to find present day sediments which have not been affected by anthropogenic activities.

Comparisons of the heavy metal concentrations from the cores will be made with the Earth's Crustal Value (ECV) (Alloway, 1995) as well as sandstone values (Alloway, 1995) which is the most common geology in the area. Values will also be compared with contaminated land guidelines to determine how polluted the sediments are, including the 'New Dutchlist' (Dutchlist, 1999), the 'Society of Chemical Industry Guidelines' (1980) and 'ICRCL' (1987).

Pb values for all cores range from 20 ppm up to 693 ppm all of which are above the ECV, the sandstone value (Alloway, 1995), and above the optimum value from the Dutchlist (1999). Only one sample from PB3 has a value which may be considered to be high enough for action if these were at the surface (Dutchlist, 1999). The majority of the Pb values in the cores can be classified as uncontaminated (SCIG, 1980).

The values for Cu are similar, most are above the ECV and sandstone value (Alloway, 1995), and above the optimum (Dutchlist, 1999), however, the cores are not classified as being contaminated.

Zn has high concentrations in all cores and above background levels of the EVC and sandstone value (Alloway, 1995), as well as the optimum, even at the top of most cores. Still only the bottom of the cores in Oglet Bay and the middle of DMC1 are high enough to be classified as being contaminated (SCIG, 1980) and for 'action' (Dutchlist, 1999).

Data are only available for Hg for 4 cores (OB1, OB4, OB5 and DMC1). Concentrations for Oglet Bay cores show the same general trend of decreasing up-core similar to the heavy metals above. OB1 and DMC1 show a rise in concentrations and a distinct peak which are not as clear in OB4 and OB5. The values are high for all cores with values above the EVC and sandstone value (Alloway, 1995), as well as being higher than the optimum (Dutchlist, 1999). The samples at the bottom of the cores and the middle of DMC1 are classified as contaminated (SCIG, 1980), however they are still lower than trigger concentrations from ICRCL (1987).

Ni has low concentrations in all cores below the background levels of the EVC. Although they are above the optimum classification from the Dutchlist (Dutchlist, 1999) the concentrations are still not considered as being contaminated (SCIG, 1980).

Cr concentrations vary between 34 ppm to 287 ppm, any values above the level of 200 ppm are considered to be contaminated (SCIG, 1980) so some samples in OB1 and OB4 are contaminated, however most are not considered as contaminated but are above the optimum (Dutchlist, 1999).

Table 5.2 Element concentration values from various sources (ppm).

Element	Earth's crustal value[1]	Sandstone Value[1]	Dutchlist[2]		Guidelines (Contaminated)[3]	Trigger concentrations[4]
			Optimum	Action		
Cr		35	100	380	200-500	1000
Cu	50	30	36	190	200-500	
Hg	0.05	0.29	0.3	10	3-10	20
Ni	80	2	35	210	0—200	
Pb	14	10	85	530	1000-2000	2000
Zn	75	30	140	720	500-1000	

[1]Mean heavy metal contents of Earth's crust and sandstone rock (Alloway, 1995).

[2]The new Dutchlist (Dutchlist, 1999).

[3]Values classified as contaminated from Society of Chemical Industry Guidelines (1980).

[4]Trigger concentrations from parks, playing fields and open spaces (ICRCL, 1987).

As all of the values for Pb, Zn, Cr and Hg, and most of Cu, are higher than the naturally occurring background levels, it is likely that the sources are therefore, not natural and the sediments have been enriched by anthropogenic activity. Pb, Zn, Cu, Cr and Hg can all be released through industrial activity (Galloway et al., 1982; Alloway, 1995)

As the heavy metals, Pb, Cu and Zn, show very similar profiles in most cores it is likely they may be related to industrial processes which release the elements simultaneously. Zn smelters release substantial amounts of Cu, Zn, Cd, Pb and Ni (Alloway, 1995), and Cu smelters and brass foundries' emissions are complex and may also release large quantities of As and Zn (Alloway, 1995).

Mining may also be a source for Zn and Pb as Pb sulphide, Zn sulphide and coal have all been mined in the Merseyside area since the 1600s, although the majority of the mining and smelting industries began to develop in the area in the late 1800s (Rees, 1991). Pb from vehicle exhausts, in the form of tetraethyl Pb was also, until recently, a significant source of Pb contamination, and in urban environments the road dusts containing very high levels of Pb (Archer and Barret, 1976). Other anthropogenic sources of Pb include, the production of metallic detritus, glass and pottery glazes, batteries, old lead-based paints, as well as, the corrosion of lead pipes and sewage sludge.

Sources for Hg into the environment are refuse incineration, non-ferrous metal production, iron and steel production, coal combustion and the chlor-alkali industry (Hutton and Symon, 1986). The main source of Hg to the Mersey Estuary is from Chlor-alkali production of Cl which began in 1897 and continues today. There are two chemical factories within the banks of the Estuary, 'INEOS Chlor' (formally known as 'ICI Chemicals and Polymers Ltd') located in Runcorn and 'Innospec Ltd' (formally known as 'Associated Octel Ltd') which is

located in Ellesmere Port, both of which used the Hg cathode process and discharged large amounts of Hg at some point. The factory at Ellesmere Port began using Hg later than in Runcorn, around 1958 (Harland et al., 2000). New technology to clean-up effluents along with new production methods for Hg were introduced in Runcorn in 1974, after which, levels of Hg discharge decreased and by the early 1980s. The discharge was reduced from 60 t of Hg, to 10 t, and by the year 2000 was 0.5 t per year (Harland et al., 2000). The new technology was not introduced to Ellesmere Port until 1993.

Fox et al. (1999) examined two sites in the Mersey Estuary, Widnes Warth saltmarsh on the northern banks and Ince Marsh on the southern banks of the River Mersey. The cores were analysed for heavy metals, DDT, and ^{137}Cs, ^{238}Pu and dated using event markers from Hg, DDT and radionuclides. Increasing amounts of Hg were found in the sediment core at Widnes Warth which was attributed to the increasing amounts of Hg discharged from these factories. Cl production increased during the two World Wars (1914-1918 and 1939-1945) and, therefore, Hg pollution during this time is also likely to have increased. The decline in Hg contamination can also be seen in the Widnes Warth core where there is a sharp decline in Hg sediment concentrations at a depth of about 15 cm.

Oglet Bay

As the heavy metal concentrations in the cores from Oglet Bay show a decline up-core it is likely that the sediment cores only provide a record after the initial increase in metal pollution by the developing industrial activity of the late 19th century but when the input into the environment began to decrease. Although high levels of metal concentrations have been found in the sediment cores which are well above the background levels of natural environments, the majority are not highly contaminated, also indicating that the peak in industrial activity cannot been seen in these cores. The industrial output has generally decreased since the late 1800s but peaks and falls in output have occurred in different industries since this time due to changes in circumstances, industries and regulations. In addition, the concentrations may also be low due to high sedimentation which has the potential to dilute the metal concentrations.

The cores from Fox et al., (1999) found Widnes Warth to provide a record from 1850s-1989 and Ince Marsh from 1944s-1991. Background geological levels were found at the bottom of the Widnes Warth core and showed a build-up of heavy metals due to significant involvement of heavy metals in the north-west industry. Comparisons between minimum and maximum concentration values for heavy metals from cores of a similar length (OB1,

OB4, OB5, PB1, PB3) to Widnes Warth can be seen in table 5.3. In general, the lowest values found for Widnes Warth were lower than that found in Oglet Bay and the highest values were higher than in Oglet Bay. Therefore, it is likely that the time-span the record covers for Oglet Bay is less than in Widnes Warth. The Oglet Bay cores are similar to the Ince Marsh core, which covers a period later than the era of maximum contamination for heavy metals. Fox et al. (1999) found that only As returned to pre-industrial levels whilst all other metals passed the peak concentrations returned to an intermediate level, this intermediate level may be reflected in the Oglet Bay cores were high values in heavy metals can be seen throughout the core although they do not show the peak contamination.

Table 5.3 Maximum and minimum heavy metal concentrations for Widnes Warth, Ince Banks (Fox et al., 1999) Oglet Bay and Decoy Marsh.

	Widnes Warth		Ince Banks		Oglet Bay		Decoy Marsh	
Metal	Min	Max	Min	Max	Min	Max	Min	Max
Pb (ppm)	50	550	150	300	50	500	20	300
Zn (ppm)	<100	2650	400	1150	300	1000	47	700
Hg (mg/g)	<0.2	7	3	7	0.8-1.77	4.5-6	0.03	4
Cu (ppm)	25	600	90	300	60	200	15	200
Cr (ppm)	40	300	120	200	84	182	65	165

As discussed earlier, after normalisation with LOI there are peaks in the metal concentrations at the bottom of the core. There are many possible explanations and causes of these peaks. The peaks present in Widnes Warth occur between 1920s and 1940s, therefore the sharp peaks may be related to this period. They may also be related to increases in pollution during World War II, thus giving a date of the mid 1940s. Peaks in the emissions of Hg occurred around the years 1905, 1927, 1938 and mid 1970s (Fox, et al., 1999) therefore the peaks could be related to any of these dates. It is difficult to establish which of these dates the peaks reflect as there are no other distinguishable trends or patterns in the profiles which can clarify this.

Sevilla (2009) as part of a BSc honours project collected two saltmarsh sediments cores from Oglet Bay which were of a longer length than those from the present study. One core (185 cm) which was taken in the low marsh and the second (195 cm) taken from the high marsh, mid-*Phragmites* spp. Measurements of metals using XRF were taken on amalgamated samples of 5 cm slices. Highest values found at the bottom of the cores and were higher than those from the above shorter cores. The following values are for the maximum concentrations Cu 284 ppm, Cr 287 ppm, Pb, 254 ppm, and Zn 1498 ppm, all of

these values are classified as being considered to be high enough for action if these were at the surface (Dutchlist, 1990). It is possible that these high values are from the higher values related to the onset of industrial activity around the 1800s when pollution output was at its highest. However the values were still not as high as those found in Widnes Warth which show the onset of industrial activity and background levels were still not reached at Oglet Bay. In the longer cores (Sevilla, 2009) increases can be seen in the lower half of the core approximately 155 cm with a decrease around 120 cm in Pb, Cu and Zn profiles. It may be that this rise and fall is more likely to be related to the increase in industrial activity during the World War II which is not present in the shorter cores. Therefore, the peaks in Hg in the Oglet Bay cores may be related to mid 1970s (Fox et al., 1999) and not reflecting the peaks in the emissions of Hg which occurred around the years 1905, 1927 and 1938 (Fox et al., 1999).

Although in pre-normalised profiles most of the trends found in the metals show no distinct patterns or features, other than those being related to changes in organic matter content and diagenesis, once the data have been normalised according to the LOI %, clearer trends can be established. It is not possible to attribute the peaks in metals in the Oglet Bay cores to a certain date, but it can at least be established that the peaks occur at a similar depth in each of the cores with a difference up to 5 cm depth only. If these peaks are the same time period in each of the cores this shows that the sedimentation model is likely to have been rapid accumulation due to infilling related to large accommodation space arising from earlier erosion of the site.

Decoy Marsh

The Decoy Marsh core differs from all the cores from Oglet Bay and has lowest Cu and Pb values, which were lower than the background found in Widnes Warth. Zn values were also much lower than the lowest value found in Widnes Warth and the lowest Hg value was 0.03 mg/g which is also lower (table 5.3). The highest values found in the Decoy Marsh core were ≈200 ppm for Cu, similar to Oglet Bay but less than half that of Widnes. Pb and Zn maximum values were found to be lower than Widnes, and Hg, which has a highest value of about 4 mg/g, is also less than Widnes and Oglet Bay.

In contrast to Oglet Bay there is an obvious increase in concentrations from background levels followed by a decrease at the top of the Decoy Marsh core, similar to that found in Widnes Warth (Fox et al., 1999). This reveals that DMC1 is likely to be much older than Oglet Bay, with the lower part of the core likely to be pre-industrial activity. The ‘take-off’

point for the industrial activity can be seen in Hg and other heavy metals Pb, Cu and Zn at approximately 34 cm (figure 5.25). A date of 1897 can be assigned to this point when Hg emissions began from the chemical factory at Runcorn. As the DMC1 seems to be older than that of the cores from Oglet Bay, more changes in industrial activity have occurred and, therefore, more dates may be assigned.

Other dates which may be considered is a peak in chlorine production, and therefore Hg pollution during the World War I (1914-1919). This may be present as a small peak in Hg at 30 cm depth and may also be the reason for the increase in Pb at this depth. A decline in industries including the copper industry and chlorine production occurred during the recession between 1920 and 1930 and this may be reflected in the decline in concentrations of Pb and Cu at a depth of 25 cm. This was followed by an increase in concentrations which may be related to an increased demand during the World War II (1939-1945). The peak in Hg is above this and may be related to continued diversification and expansion of the chemical industry between 1950 and 1970 (Fox et al., 1999). During the 1960s there was a decline in Pb and Cu industries and this may be reflected in the sharp fall in the normalised Pb and Cu profiles at a depth of approximately 18 cm. The final metal chrono-marker may the introduction of new technology to clean-up Hg effluents which occurred in the late 1970s. This may be seen in the Hg profile where there is a steep decline in concentrations at a depth of 10 cm. This is similar to what was found in the Widnes Warth core (Fox et al., 1999).

The core taken from Widnes Warth (Fox et al., 1999) was 1 m in length and contained a record spanning 139 years from the 1850s to 1989. In contrast, DMC1 is only 42 cm in length but it seems to contain the same record as Widnes Warth, covering a similar time span. This indicates that the accumulation rate for Decoy Marsh is much lower, in fact half the rate of Widnes, and thus has the potential to record sea-level change over the last 150 years or so.

The result of the radionuclides will not only to shed light on the uncertainty related to the ages assigned from the metal profiles in the cores, particularly in Oglet Bay, but will also provide a more substantial suite of dates to provide a more complete and confident chronology.

5.4. Radionuclides

Radionuclides have been used as event markers in the form of ^{137}Cs and ^{241}Am in this study following other studies in the Mersey Estuary (e.g. Jemmett, 1991; Oldfield et al., 1993; Fox at al., 1999). As the Mersey Estuary is located on the Irish Sea where the main source of ^{137}Cs and ^{241}Am is the Sellafield nuclear fuel processing plant located in Cumbria on the coast of the Irish Sea. The initial start of the discharge and subsequent changing of concentrations and ratios of the emissions can be used as markers for dating.

The radioisotope ^{210}Pb is an independent radiometric dating technique which can be used to date sediments which are up to 120 years old (Madsen et al., 2005) and is a technique which is frequently applied to saltmarsh sediments more recent in age (e.g. Smoak and Patchineelam, 1999; Appleby et al., 1986; Nikitina et al., 2000, Gehrels, 2000, Gehrels et al., 2002, 2005, 2008). Precipitation and dry disposition brings ^{210}Pb to the Earth's surface where it adheres to fine-grained material and organic matter (Anderson et al., 2006). The radioisotope ^{210}Pb has been utilised in this study in order not to rely solely upon event dating to provide a chronology. See chapter 3.1.2 (page 62) for more details.

The cores OB5 from Oglet Bay, and DMC1 from Decoy Marsh, were chosen to provide the sedimentary material for analysis of the past sea-level record in the Mersey Estuary. DMC1 was chosen as it was the least disturbed core taken from a high marsh environment from Decoy Marsh and had been analysed for geochemical analysis which revealed its approximate age. From the several cores were taken from Oglet Bay, OB5 was chosen firstly, based upon the stratigraphy of the marsh (figure 5.2) choosing a core which had as much saltmarsh sediment as possible, and secondly based on the geochemical analysis of the cores. Choosing a core which appeared to be the least disturbed, less affected by changes in grain size and organic matter changes and was representative of the marsh as a whole was a key prerequisite of the research design.

5.4.1. Results of radionuclides

Oglet Bay

The results of the radiometric analyses carried out by the Environmental Radioactivity Research Centre (ERRC) are given in table 5.4 and 5.5 and figure 5.26 and 5.27. Figure 5.26a shows the ^{137}Cs activity down-core, where the peak in ^{137}Cs can be seen at the bottom of the core at 72-73 cm. Concentrations of ^{137}Cs then decrease up-core but remain relatively high up until 30 cm, when they fall rapidly near the top of the core. ^{241}Am concentrations

can be seen in figure 5.26b and have a similar profile to ^{137}Cs with the maximum value occurring at the same depth, although the up-core decline in concentrations is less rapid then those of ^{137}Cs. The ^{241}Am/^{137}Cs activity ratio varies from around 0.25 near the base of the core to around 0.5 in sediments in the top 10 cm.

Inventories were calculated for both radionuclides, ^{137}Cs has an inventory of 813,880 Bq m^2 and ^{241}Am of 209,200 Bq m^2. These figures, however, under-estimate the true inventories contained in the sediment record at this location, since there is evidence that significant amounts of radionuclides are present below the base of the core. These can be compared with inventories of other cores taken in the area, for example the Dee Estuary, where values of ~189,000 Bq m^{-2} of ^{137}Cs and ~67,000 Bq m^{-2} of ^{241}Am (Rahman, 2010), it can be seen that both radionuclides have very high inventories in comparison, particular ^{241}Am.

Figure 5.26c shows the total and supported ^{210}Pb from OB5. The unsupported ^{210}Pb was calculated by subtracting ^{226}Ra concentrations from the total ^{210}Pb concentrations. Figure 5.26c shows that the ^{210}Pb activity exceeds that of the supporting ^{226}Ra in all samples. However, unsupported ^{210}Pb activities are very low and do not decline significantly with depth (table 5.4).

Table 5.4 Radionuclide concentrations in OB5.

Depth		^{137}Cs		^{241}Am		^{210}Pb					
						Total		Unsupported		Supported	
cm	g cm^{-2}	Bq kg^{-1}	±	Bq kg^{-1}	±	Bq kg^{-1}	±	Bq kg^{-1}	±	Bq kg^{-1}	±
0.5	0.3	329.6	3.2	173.6	1.7	62.2	7.5	33.9	7.7	28.3	1.6
2.5	1.6	341.9	3.3	171.4	1.8	62.8	7.8	30.0	8.0	32.8	1.8
4.5	3.1	348.8	3.4	177.5	1.8	45.1	7.7	17.2	7.9	27.8	1.5
6.5	4.6	385.4	2.9	180.2	1.5	60.8	7.1	33.5	7.2	27.3	1.3
8.5	6.0	387.8	2.7	201.7	1.5	49.2	6.2	17.4	6.3	31.8	1.4
10.5	7.4	400.5	3.0	193.2	1.5	42.1	5.8	13.1	6.0	29.0	1.2
16.5	11.5	685.0	3.6	276.9	1.6	50.8	5.9	25.3	6.1	25.6	1.2
20.5	14.4	710.3	3.8	258.5	1.7	35.0	6.2	8.8	6.3	26.2	1.3
24.5	17.2	1002.1	5.8	310.6	2.4	66.2	9.5	41.4	9.7	24.8	1.7
28.5	19.8	1309.7	6.0	412.1	2.4	46.2	8.7	17.7	8.9	28.5	1.6
32.5	22.7	1472.8	5.6	365.8	2.1	61.1	7.9	29.6	8.1	31.5	1.5
40.5	30.7	1370.5	5.9	316.2	2.0	49.8	8.2	23.0	8.4	26.8	1.5
48.5	37.3	1544.5	9.9	355.5	3.4	54.1	9.9	25.7	10.2	28.4	2.7
56.5	43.0	1532.1	8.3	334.8	2.9	62.7	11.5	35.0	11.7	27.7	2.1
64.5	49.1	1757.1	8.0	428.8	2.9	48.1	10.1	21.5	10.3	26.6	2.1
72.5	55.3	2602.8	8.9	530.9	2.9	66.2	9.9	37.2	10.1	29.0	2.0
80.5	61.3	1265.0	5.1	377.4	2.0	56.2	7.5	29.1	7.7	27.1	1.4

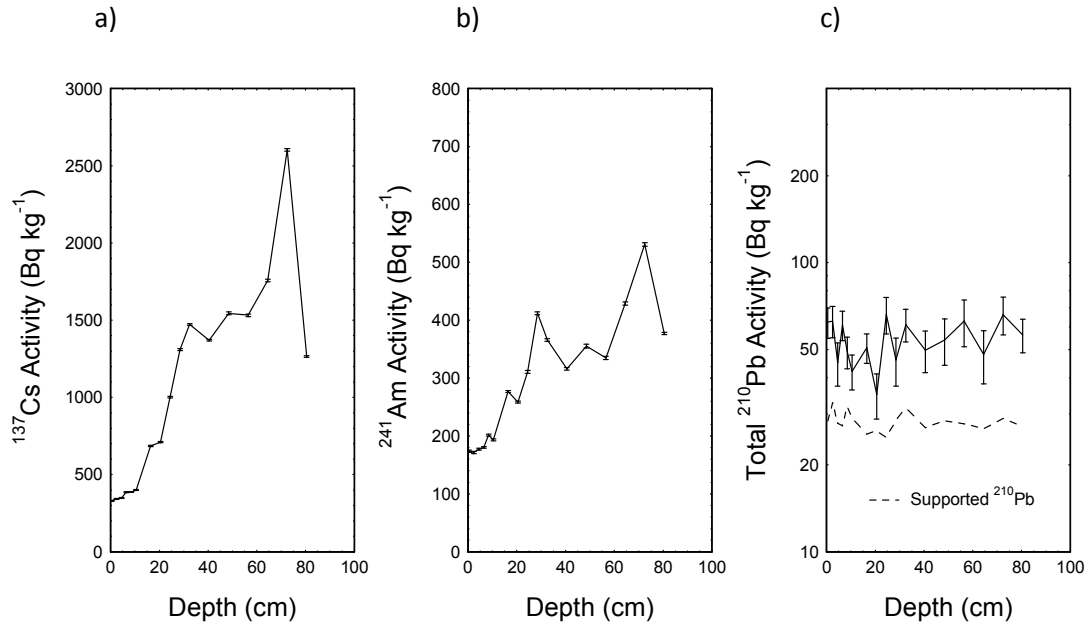

Figure 5.26 Fallout radionuclides in OB5 showing a) ^{137}Cs b) ^{241}Am c) total and supported ^{210}Pb concentrations versus depth.

Decoy Marsh

The radionuclide activities from DMC1 which can be seen in table 5.5 and figure 5.27 were found to be very different to those found in OB5. The onset of significant concentrations of ^{137}Cs up-core occurred at a depth of around 20 cm and increased rapidly until reaching a maximum between 11-13 cm (figure 5.27a). ^{241}Am concentrations (figure 5.27b) followed a similar pattern, though the onset occurred very slightly later and the peak was a little sharper and contained in the 11-12 cm section. The inventories were calculated to be 85710 Bq m^{-2} of ^{137}Cs and 24,938 Bq m^{-2} of ^{241}Am, which although are still high they are only 10% of the values recorded in the nearby Oglet Bay core (Appleby and Piliposyan, 2010).

The ^{210}Pb activity can be seen in table 5.5 and figure 5.27c. Although the unsupported ^{210}Pb activity (calculated as above) declined irregularly with depth, the overall trend was exponential, suggesting that sedimentation rates have been relatively constant at least in recent decades.

Table 5.5 Radionuclide concentrations in DMC1

						^{210}Pb					
Depth		^{137}Cs		^{241}Am		Total		Unsupported		Supported	
Cm	g cm^{-2}	Bq kg^{-1}	±	Bq kg^{-1}	±	Bq kg^{-1}	±	Bq kg^{-1}	±	Bq kg^{-1}	±
3.5	2.3	388.7	5.1	177.1	2.4	112.0	11.7	95.9	11.9	16.1	2.4
6.5	3.6	427.5	4.1	201.8	2.0	88.2	8.1	66.9	8.3	21.3	1.6
8.5	4.8	474.2	3.6	194.1	1.6	59.6	7.0	38.5	7.1	21.1	1.4
9.5	5.6	678.1	3.4	227.1	1.4	57.3	5.3	35.0	5.5	22.3	1.1
11.5	7.1	876.9	5.1	262.7	2.0	79.6	8.0	48.8	8.1	30.8	1.6
12.5	7.9	893.1	5.0	197.4	1.8	47.7	7.2	18.4	7.4	29.3	1.5
15.5	10.7	631.2	3.8	133.2	1.4	46.1	6.1	13.4	6.2	32.7	1.3
18.5	13.4	475.5	3.8	96.8	1.3	49.6	6.8	22.4	7.0	27.2	1.5
21.5	16.1	29.5	1.6	0.0	0.0	28.6	7.0	-1.0	7.2	29.5	1.6
24.5	19.2	7.3	0.8	1.6	0.5	35.3	4.6	9.3	4.7	26.0	1.0
27.5	22.7	1.9	0.8	0.0	0.0	28.4	4.2	2.3	4.3	26.0	1.2
30.5	26.2	1.5	0.7	0.0	0.0	27.4	5.2	0.9	5.3	26.5	1.1
35.5	33.2	0.0	0.0	0.0	0.0	24.4	5.3	-4.9	5.5	29.3	1.4

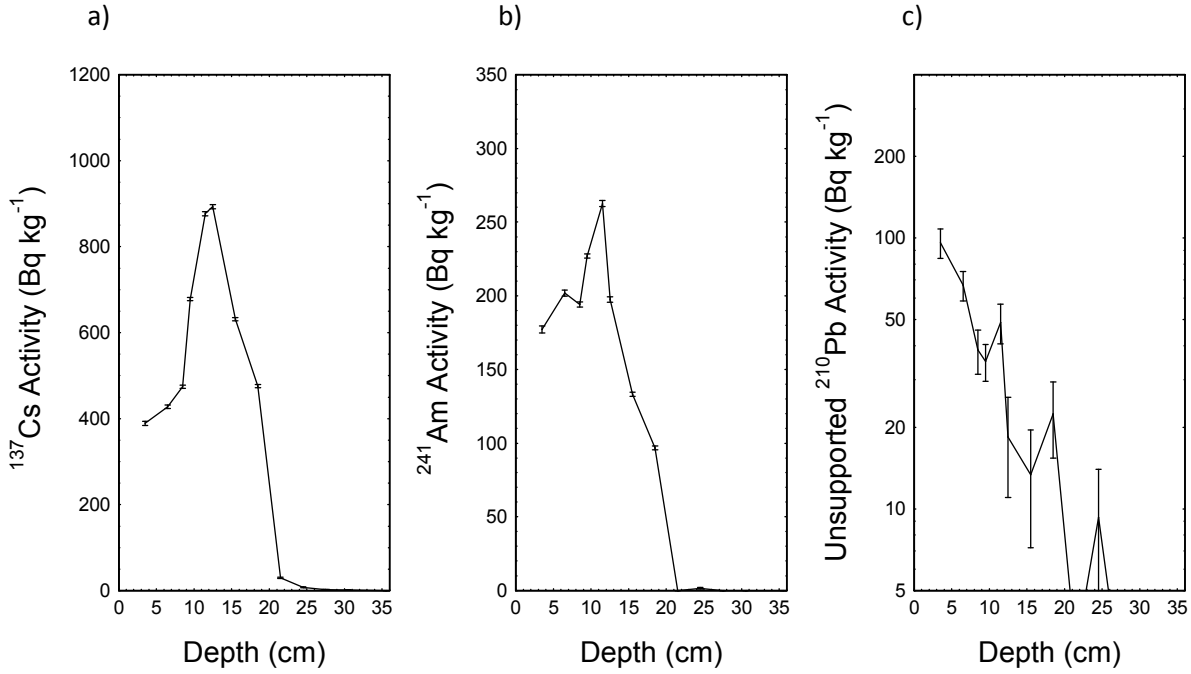

Figure 5.27 Fallout radionuclides in DMC1, showing a) 137Cs b) 241Am and c) unsupported 210Pb concentrations versus depth.

5.4.2. Interpretation of radionuclides

Oglet Bay

Discharges of ^{137}Cs from the Sellafield nuclear installation peaked during the years 1974-78, and discharges of ^{241}Am between during the years 1974-75 (Cook et al., 1997), therefore it is most likely that sediments in the 72-73 cm sample containing the highest ^{137}Cs and ^{241}Am date from the period 1974-78. The unsupported ^{210}Pb also supports the fact that the core spans no more than a few decades.

A chronology spanning the past 40 years was calculated using the ^{137}Cs and ^{241}Am data only, as it was not possible to calculate an independent ^{210}Pb chronology because of the incomplete nature of the ^{210}Pb record (Appleby and Piliposyan, 2010) (appendix 4). Figure 5.28 and table 5.6 show the calculated chronology of OB5 and imply a mean sedimentation rate since the mid-1970s of 2.3 cm $year^{-1}$. The results also suggest a significant acceleration in the sedimentation rate during past few decades, from around 1.2 cm $year^{-1}$ before 1980 to around 4 cm $year^{-1}$ during the past few years. However, as the sedimentation rate is calculated from the dry bulk density (g cm^2) it is likely that this just reflects the increase in organic matter up-core and not an increase in sedimentation rate.

Table 5.6 ^{210}Pb chronology of OB5

Depth		Chronology			Sedimentation Rate	
		Date	Age			
cm	g cm^{-2}	AD	Y	±	g cm^{-2} y^{-1}	cm y^{-1}
0.0	0.0	2007	0	0		
0.5	0.3	2007	0	1	2.4	3.5
2.5	1.6	2006	1	1	2.5	3.5
4.5	3.1	2006	1	1	2.5	3.6
6.5	4.6	2005	2	1	3.0	4.1
8.5	6.0	2005	2	2	3.1	4.5
10.5	7.4	2004	3	2	3.4	4.9
16.5	11.5	2003	4	2	3.4	4.8
20.5	14.4	2002	5	2	2.9	4.2
24.5	17.2	2001	6	2	2.6	3.7
28.5	19.8	2000	7	2	2.1	2.6
32.5	22.7	1999	8	2	1.9	2.3
40.5	30.7	1995	12	2	1.7	2.1
48.5	37.3	1991	16	2	1.5	1.8
56.5	43.0	1986	21	3	1.3	1.6
64.5	49.1	1981	26	3	1.0	1.3
72.5	55.3	1975	32	3	0.9	1.2
80.5	61.3	1966	41	5	0.8	1.0

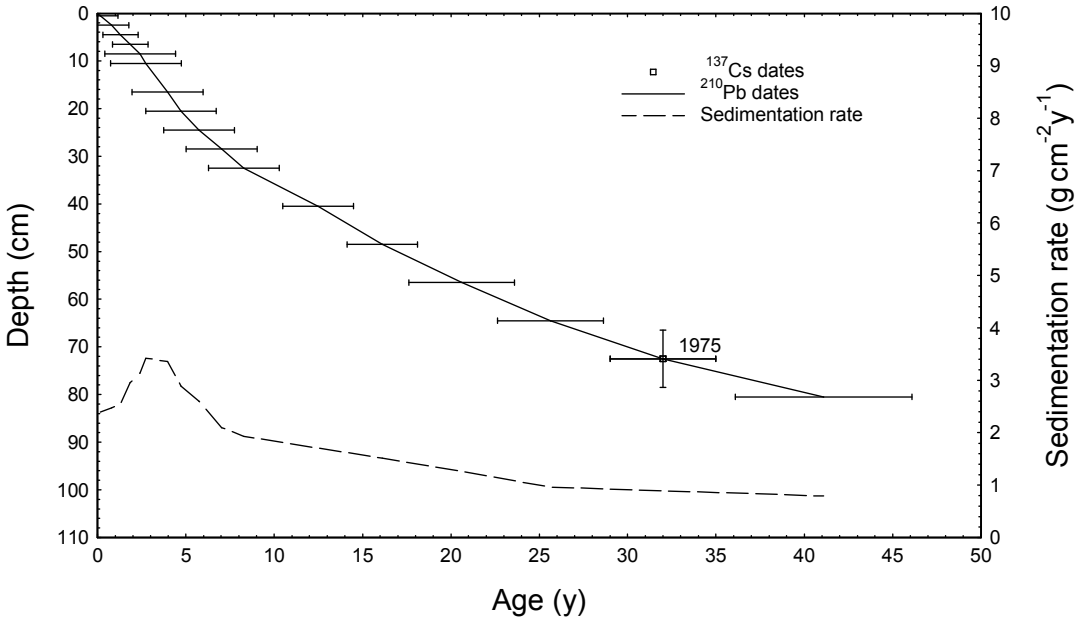

Figure 5.28 Radiometric chronology of OB5.

Decoy Marsh

As the depth of the ^{137}Cs and ^{241}Am peak is much higher in DMC1 than for OB5 it reveals that the sediment is much older, and therefore, the sedimentation rate is much lower. Samples 11-13 cm contain the highest ^{137}Cs and ^{241}Am concentrations and therefore most likely date from the period 1974-1978 giving a mean sedimentation rate of 0.35 cm y^{-1} since the mid-1970s. High ^{137}Cs and ^{241}Am concentrations at 18-19 cm suggest that sediments at this depth post-date the onset of high Sellafield discharges in the late 1960s, therefore implying that accumulation rates in the preceding decade were significantly higher (Appleby and Piliposyan, 2010).

The ^{210}Pb record from DMC1 indicates a mean sedimentation rate in recent decades of between 0.17 g cm^2 $year^1$ (constant rate of supply model (CRS)) and 0.21 g cm^2 $year^1$ (constant initial concentration model (CIC)) which is consistent with the ^{137}Cs/^{241}Am chronology. The lower value given by the CRS model may be due to uncertainties in the calculation of the ^{210}Pb inventory, possibly due to the suggested higher sedimentation rate in the earlier part of the record (Appleby and Piliposyan, 2010). CRS model calculations were revised using ^{137}Cs/^{241}Am date as a reference point (Appleby, 2001), date the 18-19 cm sample to the early 1960s (Appleby and Piliposyan, 2010). The results of these calculations are shown in figure 5.29 and table 5.7. Figure 5.29 shows the 1976

stratigraphic date determined from the $^{137}Cs/^{241}Am$ records and also the CRS model ^{210}Pb calculated using the $^{137}Cs/^{241}Am$ date as a reference point. The feature in the ^{210}Pb record between 12-16 cm is associated with a brief episode of more rapid accumulation. There was found to be very low concentrations of ^{210}Pb below 20cm and therefore it was not possible to date the sediments from the lower part of the core.

Table 5.7 ^{210}Pb chronology of DMC1.

Depth		Chronology			Sedimentation Rate	
		Date	Age			
Cm	g cm^{-2}	AD	y	±	g cm^{-2} y^{-1}	cm y^{-1}
0.0	0.00	2010	0	0		
3.5	2.28	1999	11	2	0.21	0.39
6.5	3.61	1993	17	3	0.21	0.42
8.5	4.83	1988	22	3	0.21	0.32
9.5	5.62	1984	26	3	0.21	0.29
11.5	7.09	1977	33	4	0.21	0.34
12.5	7.86	1975	35	5	0.51	0.57
15.5	10.69	1970	40	6	0.46	0.50
18.5	13.43	1963	47	8	0.29	0.39
20.0	14.72	1959	51	9		

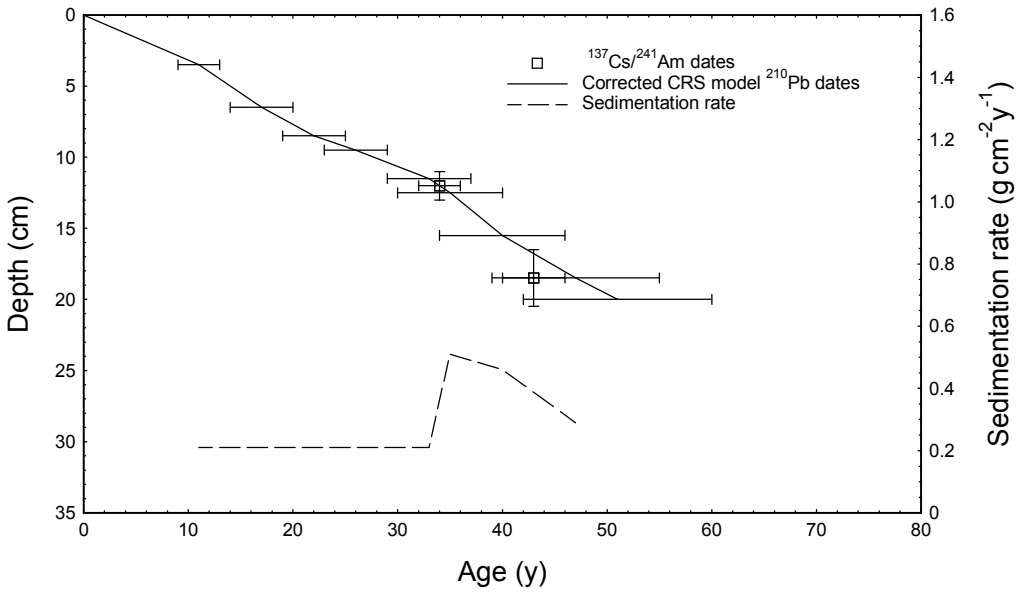

Figure 5.29 Radiometric chronology of DMC1.

Comparisons with other studies and saltmarshes in the area reveal that the sedimentation rates are not out of the ordinary. Jemmett (1991) used ^{241}Am and ^{137}Cs to date a stratified sediment profile from Hale Head Marsh, concluding that the stratifications were annual formations and therefore the annual rate of sedimentation rate per strata was calculated. It was concluded that the rate of accretion varied between 0.9 cm to 4.0 cm year^{-1}, with accretion rates decreasing after 1975. Jemmett (1991) found that from 1911 to 1985 the average sedimentation rate was 1.9 cm year^{-1}, similar to that found at Oglet Bay. Fox et al. (1999) used DDT and ^{137}Cs to determine accretion rates for cores from the Inner Estuary saltmarshes Widnes Warth and Ince Banks. It was found that Ince Banks sediment accreted at ≈0.8 cm year^{-1} from 1968-1922 for the upper part of the core when the marsh was stable and vegetated, and at ≈3 cm year^{-1} from 1945-1968 for the lower part, that developed more rapidly as a mud. The sedimentation rate for the Widnes Warth core was found to remain constant at ≈0.6 cm year^{-1} from 1945-1992.

Therefore, the seemingly fast accumulation of Oglet Bay Marsh fits in with these estimates of accumulation rates elsewhere in the estuary. Fox et al. (1999) stated that these accumulation rates of up to 3 cm year $^{-1}$ for Ince Banks Marsh cannot be explained by sea-level rise alone during this period, as Shennan (1986) and Zong and Tooley (1996) reported little rise in sea-level for the Mersey Estuary. In contrast the sedimentation rates from Decoy Marsh are more similar to those of Widnes Warth than the other saltmarshes, however, Decoy Marsh has still accumulated at half the rate of that of Widnes.

5.5. Discussion of chronology

In light of the chronology assigned from the radionuclides, the geochemical data from the cores can be re-examined, particularly for Oglet Bay, in order to develop and combine the chronology. The peak in the ^{137}Cs occurs at 72-73 cm giving a date between 1974 and 1978. This is close to the depth of the peaks in heavy metals which is approximately 70 cm. This indicates that these peaks may be related to the peak in emissions in mid 1970s (Fox, et al., 1999) and not related to any of the other peaks in emissions occurring around the years 1905, 1927, 1938 for Hg in particular. Unfortunately, as the peak ^{137}Cs occurs very close to the peaks in heavy metals, it does not allow us to distinguish any other dates at different depths which can be used to build up a more constrained chronology up the core.

There are limited data and information regarding changes in industrial activity and emissions during this time period of 1970 onwards, however, Harland et al. (2000) have been monitoring the heavy metals in surface sediments in the Mersey Estuary since 1974. Figure 5.30 shows some of the heavy metals normalised with silt from Harland et al. (2000). The Pb, Zn, Ni and Cd profiles all show that the highest concentrations occurring at 1975-1976, and a consistent trend of a decline in concentration since. Therefore, it is likely that this is the same point as the peaks in heavy metals concentrations in Oglet Bay. This date can be used to add another point in the chronology.

There are also some limited data available of emissions and inputs of Hg from the two chlor-alkali factories on the estuary. Emissions from 1999-2008 are reported from the OSPAR commission from the "Hazardous Substances Series" reporting Hg losses from the chlor-alkali industry from Europe. Passant et al. (2002) from the Department for Environment, Food and Rural Affairs, the National Assembly for Wales, the Scottish Executive and the Department of the Environment on Northern Ireland, have data from 1996-1999, and, Harland et al. (2000) have input loads from 1990-1997, these can all be seen in figure 5.31. The Runcorn data from OSPAR Commission (2010) shows that there was an increase in Hg at 1990 this may be why there is an increase in concentrations in Hg near the surface of the core.

Using the ^{137}Cs age along with the pollution marker and including the present day (table 5.8), a linear fit was plotted using depth, not mass accumulation rate, to interpolate the dates between the assigned dates. The results of this can be seen in figure 5.32.

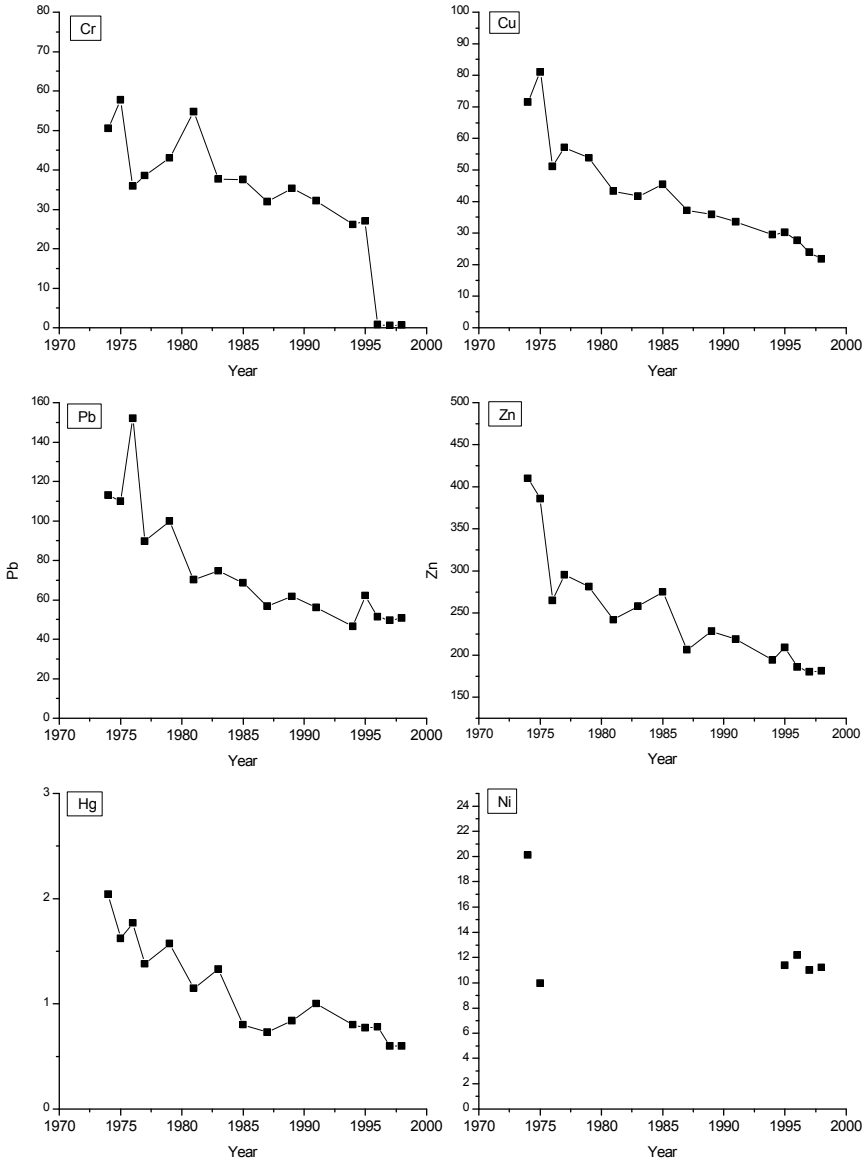

Figure 5.30 Arithmetic mean values for metals monitored from at least 50 surface sediment stations over 25 years, normalised with silt (ppm) taken from Harland et al. (2000).

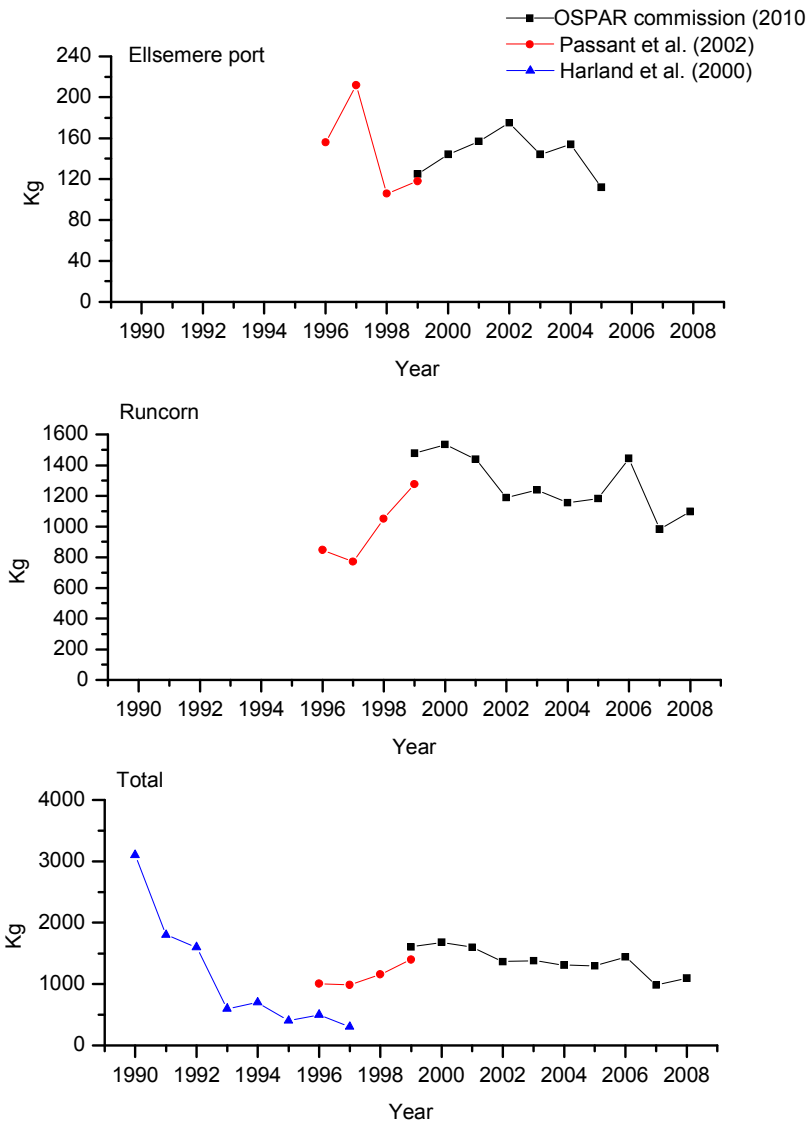

Figure 5.31 Input loads and emissions of Hg. OSPARCommission (2010) Hg losses from the chloralkali plants through product, waste water and Air. Passant et al. (2002) Hg emissions from the chloralkali plants. Harland et al. (2000) Hg input loads to the Mersey.

Table 5.8 Summary of potential age markers, their depths and possible ages for OB5 and DMC1.

Core	Age Marker	Depth	Approximate ages
OB5	^{137}Cs peak	72-73 cm	1974-1978
OB5	Heavy metal emissions peak	70 cm	1975-1976
DMC1	Hg take-off	36 cm	1887-1907
DMC1	Hg peak	28-32 cm	1914-1919
DMC1	Hg decline	25.5-29.5 cm	1920-1930
DMC1	Heavy metal increase	20.5-24.5 cm	1939-1945
DMC1	Cu decline	17-21 cm	1959-1961
DMC1	Hg decline	10.5-12.5 cm	Late 1970s

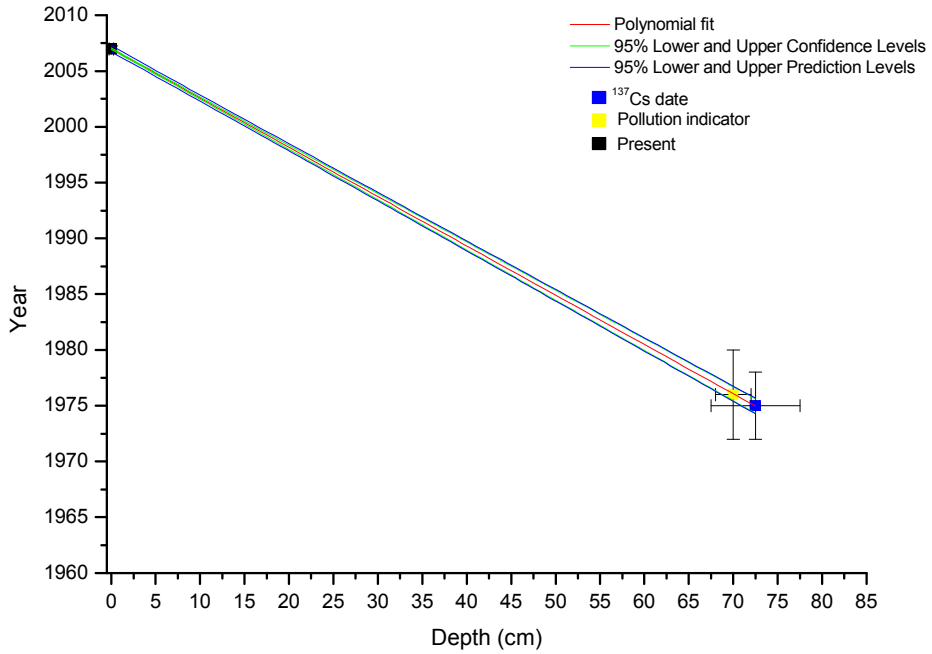

Figure 5.32 Chronology of OB5, showing the ^{137}Cs date, and pollution marker with linear fit with depth.

For DMC1 the radionuclide data supports the ages inferred from the geochemical data. The peak in ^{137}Cs occurs at a much shallower depth than in OB5 indicating it is much older in age. This also means that another date related to ^{137}Cs and ^{241}Am can be assigned from the date of the onset of Sellafield discharge. Although two dates from the ^{137}Cs and ^{241}Am data, along with a better ^{210}Pb record, can be assigned, dates below 20 cm still cannot be established using the radionuclides. As the record is longer, however, it is possible to use the geochemical data to add more markers and dates to the core. These include: 1) 1897, the take-off point for Hg emissions from the chemical factory at Runcorn; 2) 1914-1919, peak in chlorine production and therefore Hg pollution; 3) 1920-1930, decline in industries including the copper industry and chorine production; 4) 1939-1945, increase in demand and emissions from industries; 5) 1959-1961 decline in Cu industry; 6) late 1970s, introduction of new technology to clean-up Hg effluents (table 5.8). These dates can be used along with those established from the radionuclides to build upon the established chronology. The chronology using all of the data can be seen in figure 5.33, which shows an interpolation of dates using a 3rd order polynomial fit. The heavy metal data can now be plotted against the dates established for each depth and can be seen in figure 5.34 and 5.35.

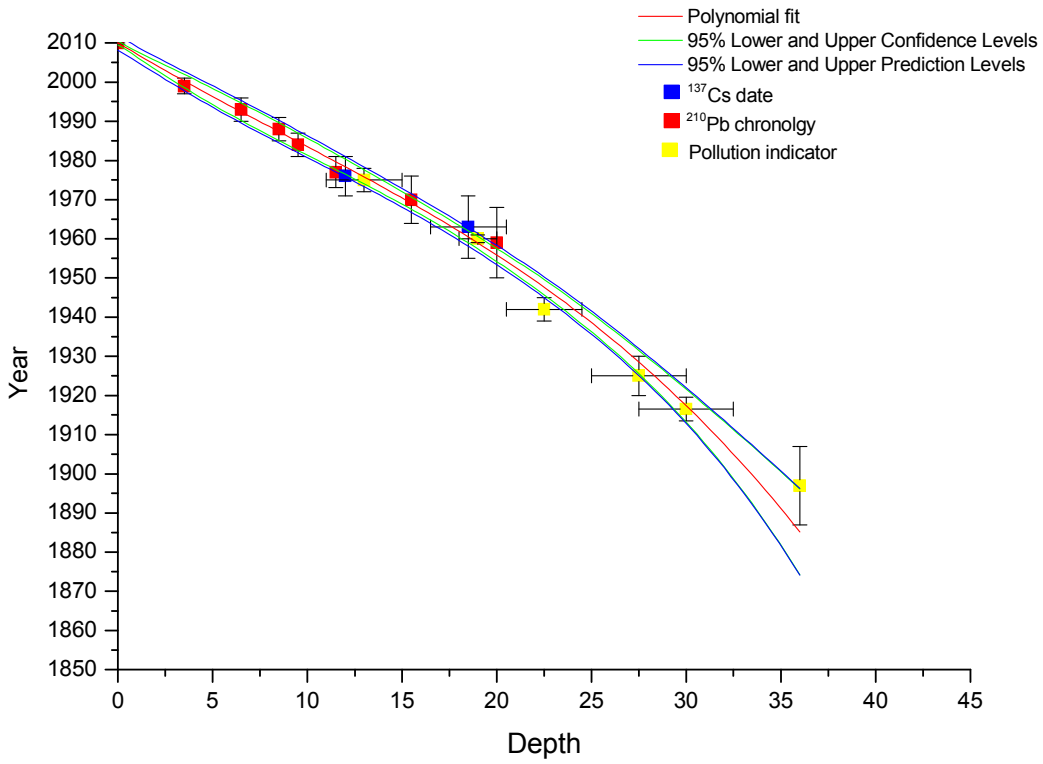

Figure 5.33 Chronology of DMC1 showing the ^{137}Cs date, the ^{210}Pb chronology, and the pollution markers with a 3rd order polynomial fit with depth.

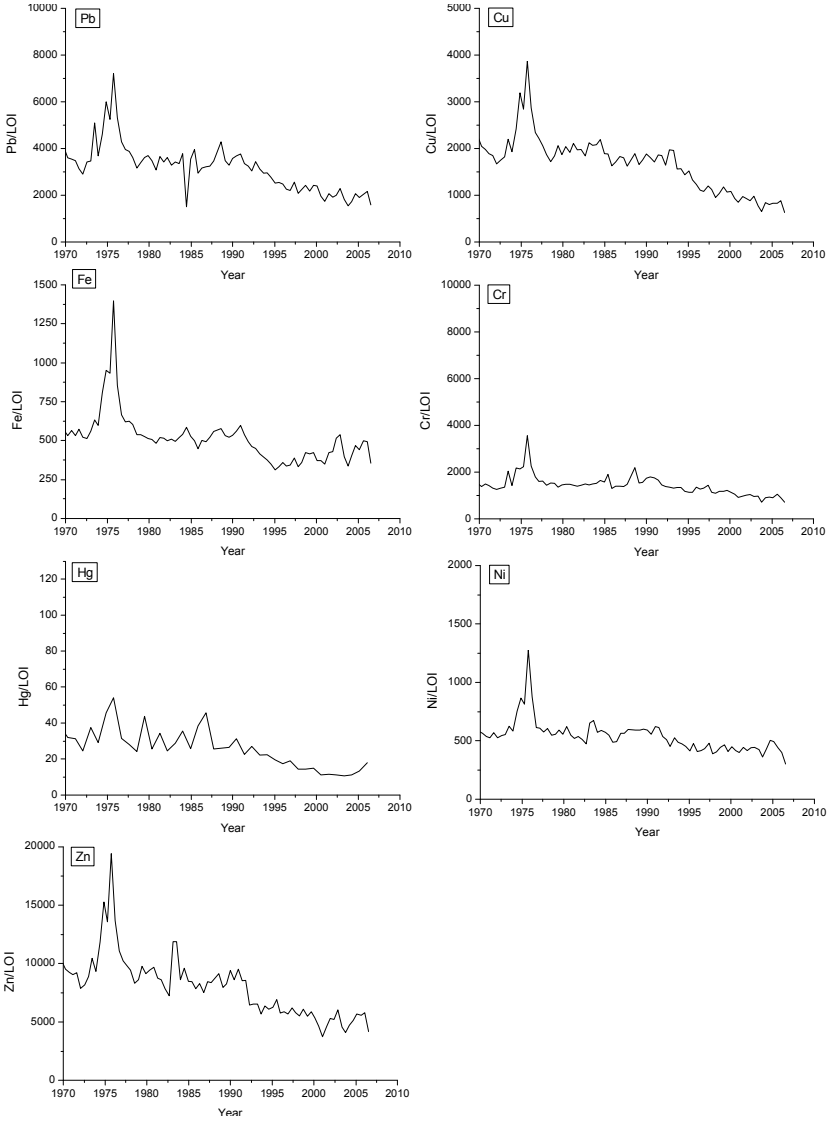

Figure 5.34 Heavy metals (normalised) from OB5 against the chronology.

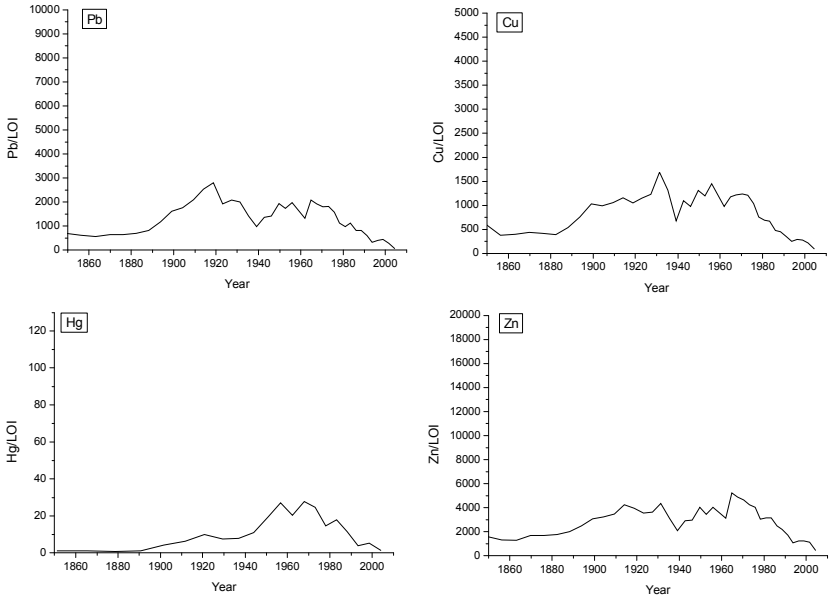

Figure 5.35 Heavy metals (normalised) from DMC1 against the chronology.

It was then possible to plot both DMC1 and OB5 metals against chronology on the same scale to see if there is any overlap between the two. As the two scales and lengths of cores are different, in order to interpret the profiles, the OB5 results were smoothed using 2-point adjacent-averaging. The DMC1 chronology could also be then used to try and tie the OB5 chronology down further, if there were similar features in each cores. It was found that a peak in Hg in DMC1 could be related to a peak in OB5. The yearly range of this peak was taken from the chronology of DMC1 and the depth range of the peak in OB5, this was added to chronology of OB5 (figure 5.36). The date was found to fit with the other dates assigned. The updated profiles of OB5 with the new chronology can be seen in figure 5.38. It can be seen that the two cores compare quite well, particularly the Hg profiles, although there is still about a 5-year offset between the two cores were they overlap, but this is within errors.

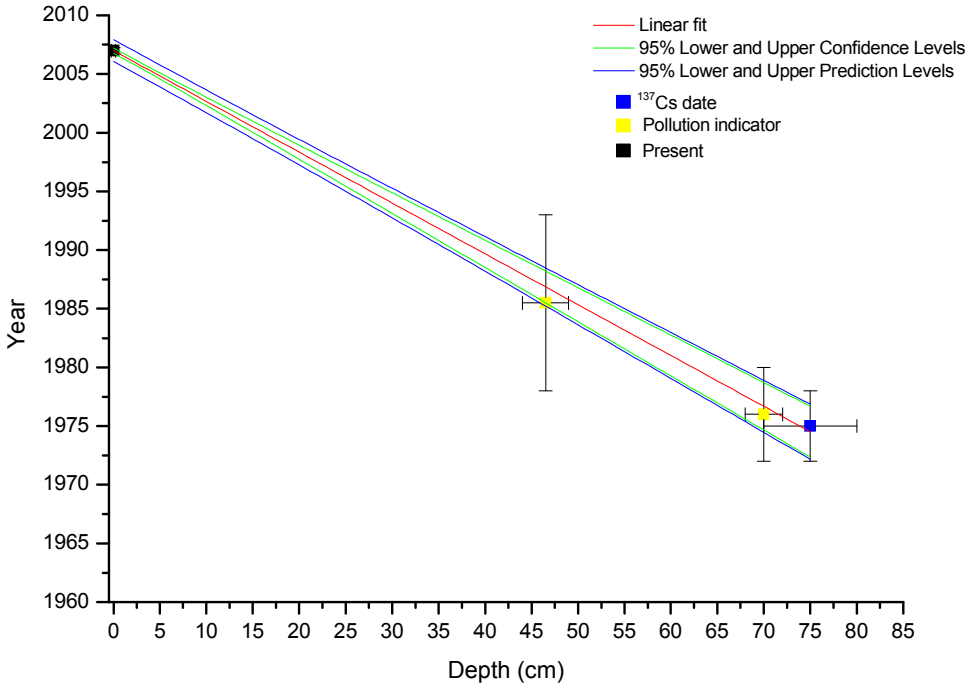

Figure 5.36 Chronology of OB5 with added pollution marker from Hg from DMC1 chronology.

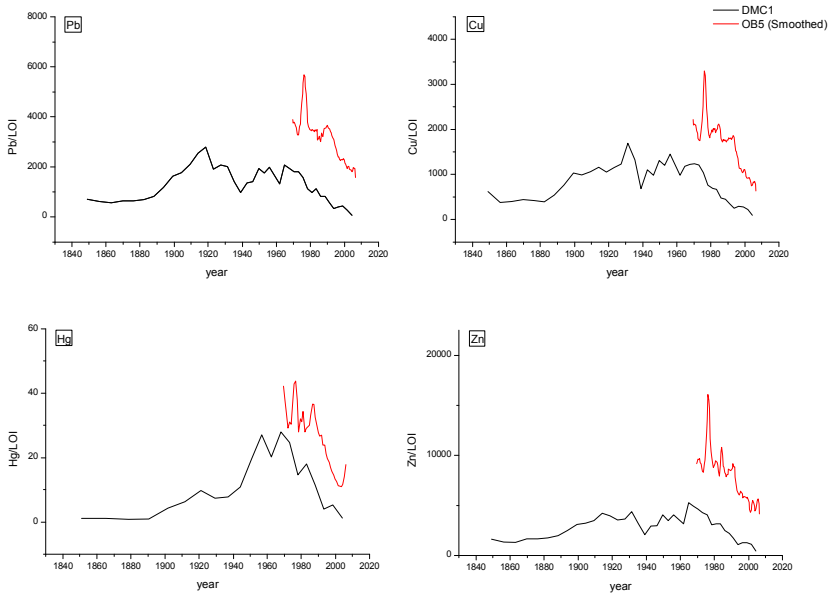

Figure 5.37 Heavy metals (normalised) from DMC1 and OB5 against the updated chronology.

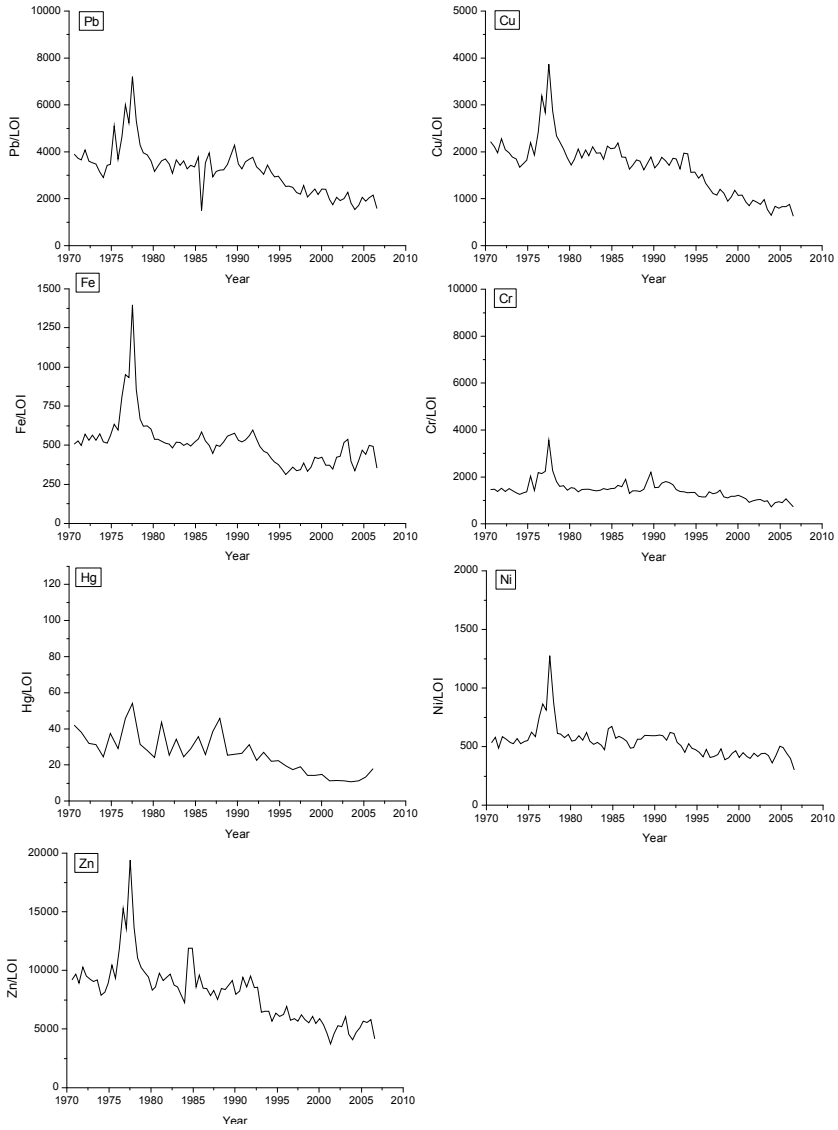

Figure 5.38 Heavy metals (normalised) from OB5 against updated chronolgy.

As other cores from Oglet Bay contain the peaks in heavy metals at a depth of approximately 70 cm, which we can now say may relate to a date of 1976, the average accumulation rate could be calculated using this date. Those cores which contain the upper peak ≈50 cm depth which have now been assigned a date of approximately 1985 can be used instead of the lower peak. The plots of these can be seen in figures 5.40 to 5.42.

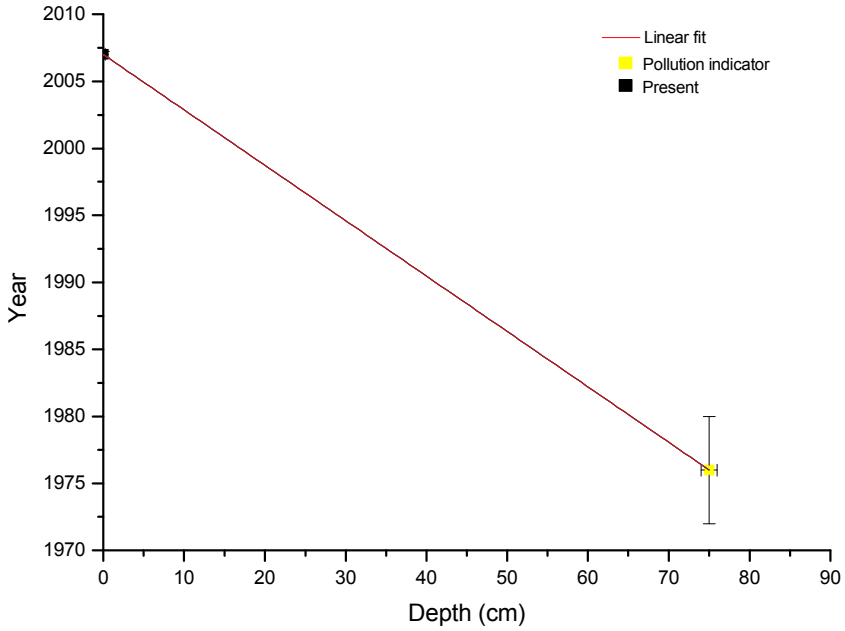

Figure 5.39 Chronology of OB1 using pollution marker from OB5 chronology.

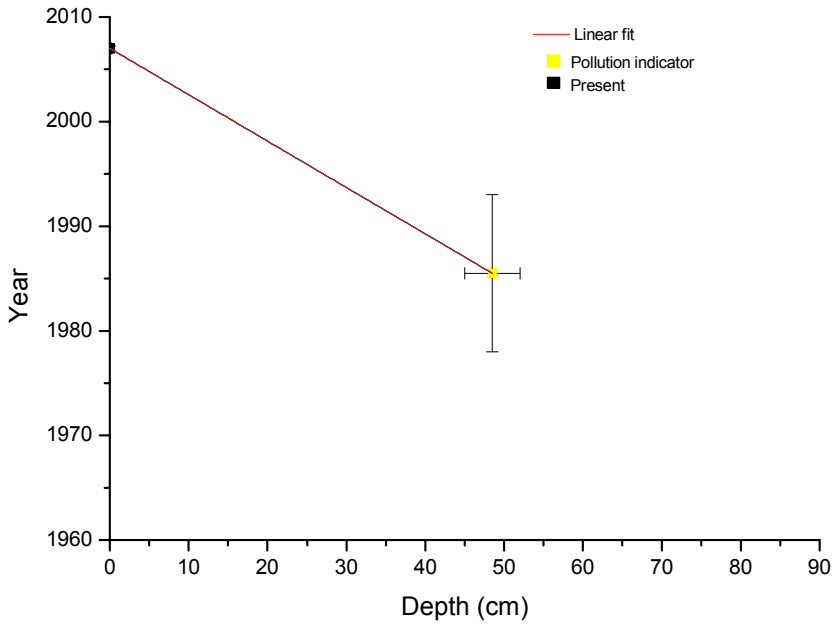

Figure 5.40 Chronology of OB4 using pollution marker from OB5 chronology.

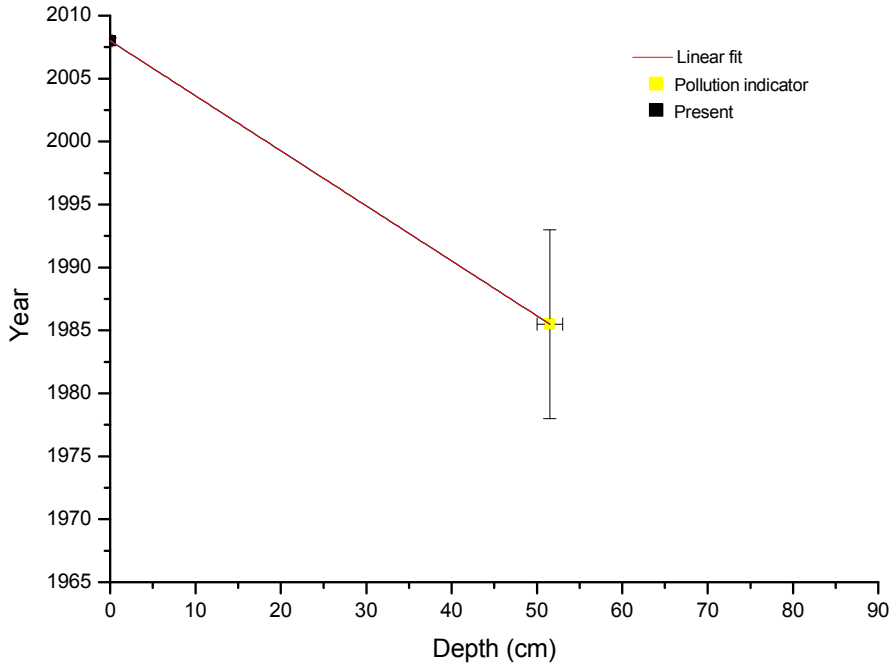

Figure 5.41 Chronology of PB1 using pollution marker from OB5 chronology.

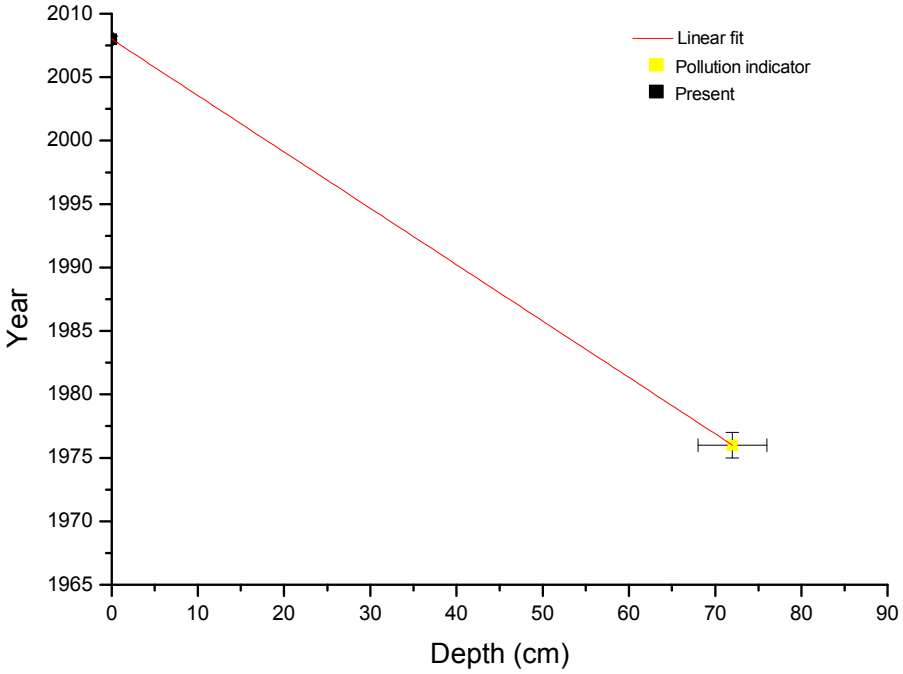

Figure 5.42 Chronology of PB3 using pollution marker from OB5 chronology.

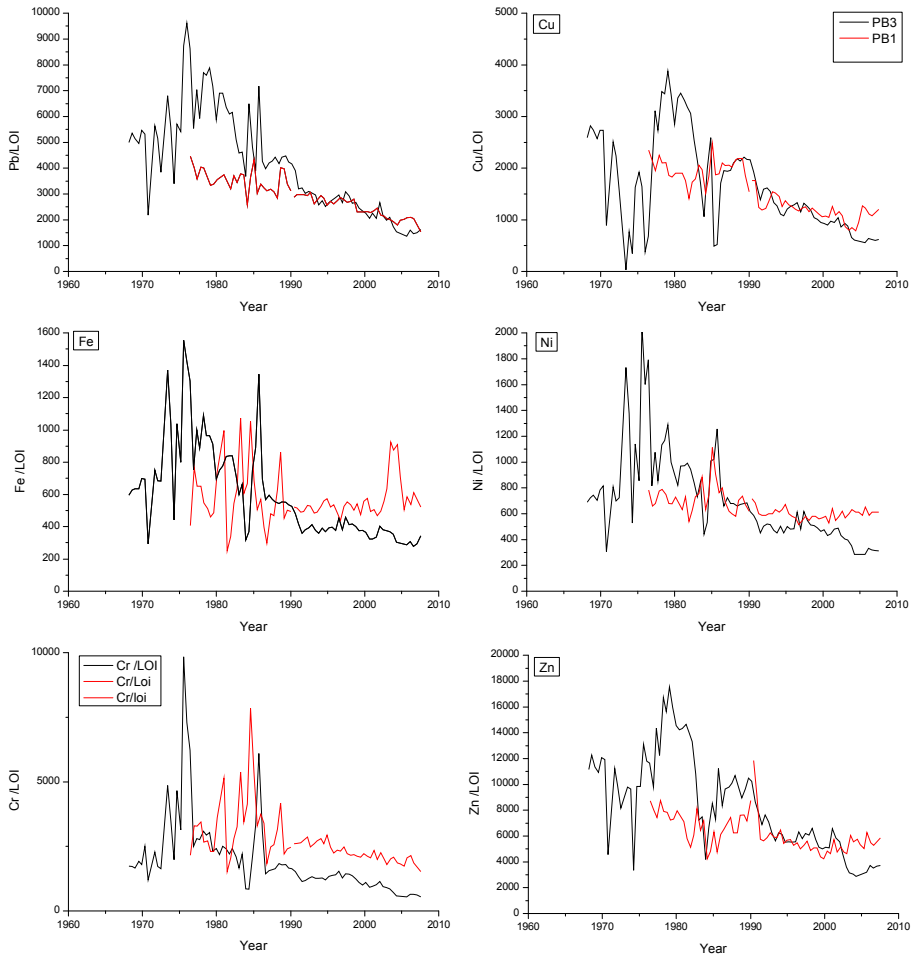

Figure 5.43 Heavy metal profiles of PB1 and PB3 against chronology.

The average accumulation rates for each core are as follows: OB1, 2.42 cm year^{-1} from 1976 to 2007; OB4, 2.26 cm year^{-1} from 1985 to 2007; OB5, 2.34 cm year^{-1} from 1975 to 2007; PB1, 2.22 cm year^{-1} from 1985 to 2008; and, PB3, 2.22 cm year^{-1} from 1976 to 2008. All accumulation rates are very similar ranging from 2.2 cm to 2.42 cm as all the peaks occur at similar depths. The highest accumulation rate is found in core OB1, this is the core which was taken at the lowest altitude and would be expected to have a much greater accumulation rate as its flood frequency and duration (hydroperiod) will be greater. DMC1 had an average accumulation rate of 0.32 cm year^{-1} from 1897 to 2010.

Oglet Bay has very young sediments with a very rapid accumulation rate, with all areas of the marsh accreting at the same or similar time. The mean sea-level record from 1850 to 1999 from Woodworth (1999b) indicates that the average rate of rise was 1.23 +/- 0.12 mm year^{-1}. As the accumulation rate from Oglet Bay is much higher than the average sea-level rise the accumulation cannot be explained by sea-level rise alone. Generally, developing

saltmarshes accumulate more rapidly at first, then once the accommodation space has been filled with limits of the tidal frame, the saltmarsh will accumulate due to a rise in sea-level which will increase the tidal frame. The accumulation rate also decreases as the saltmarsh develops as it ascends higher in the tidal frame and is therefore inundated less frequently, although increased organic matter accumulation may counter this (Cahoon et al., 2000).

Although only one core is available for Decoy Marsh, DMC1 shows the accumulation to be much slower at Decoy Marsh and contains a much longer record than Oglet Bay. The marsh is more likely to have accreted due to changes in sea-level. However, the accumulation rate for Decoy Marsh is much lower than the rate of sea level rise, therefore, the marsh is not keeping pace with sea level. It is likely that this is due to the amount of inundation the marsh receives as it is much higher in altitude than Oglet Bay and is also higher up in the tidal frame.

Although both marshes are within the Mersey Estuary and located within the Inner Estuary, they both show very contrasting records. The reason for the difference in age and accumulation may be related to the changes in the low water channels within the estuary. Blott et al. (2006) have documented the history of the movement of these channels within the Inner Estuary using the Mersey Docks and Harbour surveys. Figures 2.4 to 2.7 also shows the digitised low water channels from aerial photographs. Gifford and Partners (2004) found that the historic maps do not accurately record the position of sedimentary features within the permanent banks of the estuary and, therefore, the locations of the low water channels. As such, only aerial photographs and bathymetric surveys of the estuary will be considered.

Allison (1949) found that in 1738 the Inner Estuary contained only two main channels in the west of the Inner Estuary, one in the north and one in the south, by 1842 three main deep channels (Eastham, Garston and the Middle Deep) had developed in the west and still persist today. The Mersey Docks and Harbour surveys are available for the years 1906, 1936, 1956, 1977, and 1997. The survey from 1906 shows the three main channels and between these, extensive inter-tidal flats, saltmarshes at Stanlow, Ince and Score on the southern banks and Dungeon (Oglet Bay) in the north. The 1936 survey shows that the deep channels have become more distinct, the Eastham channel had deepened, the Garston channel had narrowed and the Middle Deep Channel had moved to the south. In the east of the Inner Estuary the main channel had moved northwards eroding Dungeon

Bank in the north and causing greater accretion of Stanlow and Ince Banks in the south. This continued up until 1956 at least, with continued erosion of Dungeon Banks and accretion of Ince Banks as well as Eastham Sands. The 1977 survey shows that between 1956 and 1977 the main channel in the eastern Inner Estuary had migrated south causing the erosion of Stanlow and Ince Banks although the marshes still continued to accrete, and allowing accretion of Dungeon Banks, as well as continued accretion of Eastham Sands. By the 1997 survey, Eastham Sands had been substantially eroded and accretion of Stanlow Bank had occurred. The Middle Deep channel in the western Inner Estuary had infilled and the Garston channel had enlarged.

Digitised aerial photographs from 1971, 1983, 1997, 2000 and 2006 can be seen in figures 2.4 and 2.5. This shows that since 1971 Oglet Bay saltmarsh (Dungeon Banks) has been eroding and is still presently eroding. Figure 2.5 shows the location of the low water channels for the same years (except 2006 where the channels cannot be seen). Figure 2.5 not only shows the main channels but also smaller channels through the mudflat. In 1971 the channel seen in figure 4.5 is only a small channel which has developed, with the larger main channel located further south (cannot be seen in figure 2.5) which is in agreement with the Mersey Docks and Harbour survey. Following this, the 1983 aerial photograph shows the main channel had migrated northwards, which can be seen in figure 2.5. By 1997 it appears that the main channel had migrated southwards again, but leaving behind a smaller channel in the north. In the 2000 aerial photograph the smaller channel similar to that seen in 1997 now appears to be joined to the main channel which is still further south. These show that the channel migration and development within the estuary is much more complicated than that shown in the bathymetry surveys, as the scale of these are much larger both spatially and temporally compared to the photographs. The erosion and accretion of the saltmarsh may be effected by the movement of the main low water channel but also the development of smaller channels through the mudflats.

Ince Banks is located on the opposite side of the estuary of Oglet Bay in the Inner Estuary and therefore has also been affected by the migration of the low water channel. The Mersey Docks and Harbour surveys show that by 1936 the main channel had moved northwards allowing Ince Banks to accumulate this may be why the record can be obtained from this time period. Similarly, by 1977 the channel had migrated southwards allowing Oglet Bay to accumulate which may be the reason for the record covering this time period.

The tidal channel is currently located in the north in the Inner Estuary and consequently, Oglet Bay saltmarsh is currently experiencing rapid erosion. The radionuclides and metal pollution indicators not only established the chronology for Oglet Bay but also revealed the extremely high pollution of radionuclides (^{137}Cs and ^{241}Am) where the inventory was much greater than the nearby Dee estuary. As the saltmarsh is undergoing rapid erosion, these radionuclides which are currently buried within the sediments may become released into the environment and transported and deposited elsewhere within the estuary. The location of the channel in the north allows accretion of the southern saltmarshes (Ince Banks) (Blott et al., 2006), therefore these sediments may be deposited on these marshes.

In contrast to Oglet Bay, Decoy Marsh seems not to be effected by the movement of the channels, with the low water channel and the saltmarsh remaining in the same location. Hence, it has not experienced erosion, despite not keeping pace with sea-level rise. The Mersey Docks and Harbour surveys show that there is little change in location, with only the size in the channel changing over time. There appears to be a large channel in the surveys 1906 and 1936 but by 1956 the channel has reduced in size and remained at this size up until present. The aerial photographs (figures 2.6 and 2.7) also show that the channel and saltmarsh have been consistent over the time period 1971 to 2000.

5.6. Summary of chronology

Oglet Bay saltmarsh underwent a thorough investigation of the stratigraphy and geochemistry. The information gathered from this investigation allowed the selection of a representative core from the marsh. This core was then examined further with chronological analysis of radionuclides. Decoy Marsh was subject to a less extensive investigation, with the collection and examination of one core (DMC1) for stratigraphy, geochemistry and radionuclides. Both selected cores were examined to determine the age and sedimentation history. Radionuclides ^{137}Cs and ^{241}Am along with the determination of a pollution history, allowed the chronology for both cores to be established. ^{137}Cs and ^{241}Am derived from the Sellafield nuclear reprocessing plant were demonstrated to be successful in dating both saltmarsh cores and were reliable benchmark dates. ^{210}Pb was found only to be successful in the older sediments of Decoy Marsh, however not for the younger sediments of Oglet Bay. Hg pollution was found to be particular valuable in determining ages within the record, as two out of the three chlor-alkali factories within the UK are located on the estuary which release large amount of Hg emissions into the environment.

Before exploration of the heavy metals for the pollution history, different correction techniques were examined, and it was concluded that the best procedure was to use LOI% to normalise the heavy metals for organic matter content in order to create heavy metals profiles which were related to pollution input and not reflecting changes composition. Unlike other studies carried out on sediments within the estuary, the heavy metals did not seem to be related significantly with grain size but mainly related to organic matter content, particularly for cores taken from Oglet Bay saltmarsh.

It was found that the two saltmarshes were considerably different, with different sedimentation histories and ages. DMC1 shows a pollution history from the start of the 20th century onwards, using the heavy metals Hg, Zn, Cu, and Pb. This was found to be similar to the record found from Widnes Warth from Fox et al. (1999). DMC1 was also found to have a very long record of up to 166 years at the bottom of the core and had a low average accumulation rate of 0.32 cm year^{-1} from 1916 to 2010. The low accumulation may be related to low frequency and duration of tidal inundation and may also be the explanation for the accumulation rate being less than that of the average change in sea-level for a similar time period. Hence, the sediment record has the potential to preserve rising tidal levels and to detect the onset of these over the past c 150 years.

Oglet Bay did not show a long and detailed history of pollution, with only one or possibly two distinct peaks in concentrations of Hg, Cu, Pb, Zn, Fe and Cr. The sediments collected were very young in age, being no more than 40 years old. The accumulation rates were consistent across the marsh ranging from 2.2 cm to 2.42 cm $year^{-1}$. The highest accumulation rate was found in core OB1; this core was taken at the lowest altitude and would be expected to have a much greater accumulation rate as its flood frequency and duration (hydroperiod) will be greater. This fast accumulation rate is not out of the ordinary with accumulation rates ranging from 0.6 to 4 cm $year^{-1}$ in other locations in the estuary. Although the OB5 contained a limited amount of record, the core does overlap the DMC1 to some extent, with peaks in heavy metals in the 1970s followed by a general decline in concentrations.

The difference in age and accumulation rates is also likely to have affected the Ca concentrations down-core with greater de-calcification taking place in DMC1 due to the greater age of the sediments but also the slower rate of accumulation and higher elevation within the tidal frame. In contrast, the sediments at Oglet Bay have greater variability in Ca concentrations with large falls in Ca resulting from some but not complete de-calcification in the cores.

It is likely that Oglet Bay contains only a very short record of estuary sedimentation due to the changes in local hydrodynamics and sedimentation patterns due to the migration of low water channels within the estuary. Movement of the channel southwards between 1956 and 1977 may have increased the accommodation space via shoreward erosion in the northern side of the estuary allowing the development of the marsh after the erosion which occurred between 1936 and 1956. In contrast Decoy Marsh has a very long record which is likely to be due to the constant and continued upward accretion of sediment with no obvious affects arising from migration of low water channels.

6. Sea level reconstructions

6.1. Introduction

From analysis of the modern foraminifera surface data, in chapter 4, it was concluded that as elevation is a key control on assemblage distribution and other environmental variables are correlated with elevation, the foraminiferal assemblages have the potential to be used for a quantitative sea-level reconstruction. However, some caution should be taken when carrying out a reconstruction because the distributions were also found to reflect intra- and inter-site variability relating to changes in salinity and vegetation cover in addition to elevation.

In the following chapter the foraminiferal datasets will be used to reconstruct the local relative sea level from two different saltmarshes within the Inner Mersey Estuary. Different combinations of the modern transect data will be tested in order to determine which dataset proves to be the most successful, based upon performance measures. Furthermore, tests will be undertaken on different models to establish the most appropriate transfer function. A local transfer function based upon these data will be developed and applied to the cores OB5 and DMC1, and comparisons made between the two cores and the tide gauge data from Liverpool. A regional transfer function will also be developed and applied to the fossil record using data from Horton and Edwards (2006). Lastly, the local data will be combined with the regional to create a third, intermediate transfer function. Each of the transfer functions will be tested for their performance, based upon their predictive ability; reliability, based upon comparisons between the modern and fossil data and between complementary models; and significance, based upon the amount of variance in the fossil data explained by the transfer function. Only the most appropriate datasets and models based upon these tests will be used to calculate the final reconstruction of MTL.

6.2. Statistical analysis

The species data were converted into percentages before representing the data in species diagrams and carrying out any statistical analysis. Species which contributed less than 5% to the sample were removed following Fatela and Taborda (2002). The percentages of agglutinated and calcareous species were presented in the diagrams along with abundance, which was calculated using the same method described in 4.2.

Similar to the ordination techniques described in chapter 4.2, the regression analysis used to create the transfer function may assume unimodal or linear data distributions (discussed further in chapter 1.4.1). To determine whether the data are unimodal or linear, and therefore which statistical method should be used, DCCA using elevation as the only environmental variable was carried out, following Horton et al. (1999), Gehrels et al. (2001), Sawai et al. (2004), Massey et al. (2006a), Szkornik et al. (2006), Engelhart et al. (2007), Hill et al. (2007), Kemp et al. (2009a), Woodroffe and Long (2009), Leorri et al. (2011), and Rossi et al. (2011). As discussed in chapter 4.2 there are different values which are used by different authors to determine whether the data are unimodal or not; linear values range from 0-3 SD in gradient length, unimodal values range from >2 to >4 SD, and values which may be either unimodal or linear range from 1.5-4 SD (Birks, 1995; ter Braak, 1995; Leps and Smilauer, 2003). Therefore, a similar method that was established in chapter 4.2 was used, whereby if the DCCA gradient values were not clearly linear (<1.5 SD) or clearly unimodal (>4 SD), both methods were carried out and performance statistics used to determine which methods were most appropriate. The methods used include the unimodal techniques WA, WA tol, and ML, the linear technique PLS as well as WAPLS, and the analogue-based method MAT. More details of these statistical methods can be found in chapter 1.4.1.

As all quantitative palaeoenvironmental reconstructions will produce a result no matter what data are used, the transfer functions reliability was tested. Imbrie and Webb (1981) stated that there is no simple means of evaluating how reliable the results are. However, there are statistical methods available which can be used to provide some information about the performance and may be useful in making comparisons between the different methods. The performance tests used were r^2_{jack} and $RMSEP_{jack}$, which determine the predictive ability of the transfer function. Cross-validation results from jack-knifing were used as they provide more reliable measures of the predictive ability than those without the split-sampling which over- and under-estimate the results (ter Braak and Juggins, 1993)

(see chapter 1.4.1 for more details on the transfer function construction and performance tests). These measures allow the comparison of performances between models and previous studies, and allow the most appropriate model to be chosen. Models were selected as being the most appropriate and reliable where there was found to have a low RMSEP and a high r^2 (Birks, 1995, 1998).

In addition, the r^2 value, which shows the relationship between the observed and predicted values, was utilised for the identification of outliers. Samples which have a poor fit will have a high residual distance from the elevation gradient (Horton and Edwards, 2006). Outliers were identified as those samples which had an absolute residual value (observed-predicted values) greater than that of the standard deviation of the elevation gradient (e.g. Jones and Juggins, 1995; Edwards et al., 2004; Horton and Edwards, 2006; Engelhart et al., 2007) or ¼ of the gradient (e.g. Woodroffe and Long, 2009; Woodroffe and Long, 2010). The approach used depended on which removed the most outliers. In large datasets it is common that some samples show a poor relationship to elevation compared with the majority of the samples as these may have been affected by transport, differential preservation or other environmental variables may be influencing the sample more (Horton and Edwards, 2006). These outliers may strongly influence the transfer function performance and predictive ability (Martens and Naes, 1989), and the potential to produce erroneous reconstruction (Horton and Edwards, 2006). They, therefore, should be removed from the training set (Jones and Juggins, 1995; Gasse et al., 1997; Horton and Edwards, 2006) and it is normal practice to do so in order to improve the model performance and predictive power (e.g. Edwards et al., 2004; Engelhart et al., 2007; Woodroffe and Long, 2010). The removal of outliers was performed for each of the models, as samples which appear as outliers in one statistical model may not appear so in another. There may be several iterations of models before a final model and dataset is chosen.

Whilst $RMSEP_{jack}$ and r^2_{jack} were used to determine the predictive ability of the transfer functions, other methods should be used to determine whether the estimates which they produce are reliable. Therefore, the reliability of the transfer function was evaluated in several ways. Firstly, the MAT approach was carried out as it is considered a standard method to assess the reliability of reconstructions (Guiot and de Vernal, 2007). MAT can be used to predict values of elevation, however, in this case it is used to identify fossil assemblages without modern equivalents to provide an independent assessment of the reliability of predictions (Edwards and Horton, 2000). A dissimilarity coefficient is produced

from the MAT results based upon the squared chord distance (Prentice, 1980; Overpeck et al., 1985). The fossil samples with coefficients below the 10th percentile were considered to have good analogues in the training set, and samples above the 20th percentile were considered as poor (Birks et al., 1990).

Another test of reliability used in this study was to use an additional numerical model on the same data to reconstruct the elevation. The similarity of the results from each transfer function, tests whether or not the statistical technique used is significantly determining the outcome (Edwards and Horton, 2000). ML was used to produce a second transfer function as it is regarded as the most 'statistically rigorous approach to environmental reconstruction' (Birks, 1985). ML is a unimodal classical approach so it will complement any inverse unimodal method, WAPLS for example. ML models ecological response curves for each species, which are then used to calculate the probability that an elevation value would occur for a particular foraminiferal assemblage. The elevation value is calculated as the value which is associated with highest probability and is the 'maximum likelihood' estimate (Horton and Edwards, 2006).

Finally, there is still no guarantee that a variable can be meaningfully reconstructed at a specific site; even after using statistical cross-validation reliability tests, the results of the reconstruction may still not be significant and meaningful. Telford and Birks (2011) created a statistical method to test the statistical significance of reconstructions. This was applied to different reconstruction models and datasets in this study. Firstly, the proportion of variance in the fossil data explained by the reconstruction was estimated using constrained ordination (RDA). A 'random value transfer function' was then created with the same species data but with randomly generated variables. The proportion of variance in the fossil data explained by this reconstruction was then determined. For the reconstruction to be significant, Telford and Birks (2011) stated that the transfer function should explain more of the variance in the fossil data in a constrained ordination than a transfer function trained on random data for the same fossil data. If the 'random value transfer function' explains as much variance of the fossil data as the transfer function based upon actual environmental data, then the reconstruction is no better than random data. 999 random environmental variables were created to produce a null distribution and this was used to produce significance values which were calculated as the fraction of the random variables that explain as much as or more of the fossil data than the transfer function trained on real

data. These statistical methods were carried out using the package *PalaeoSig* (Telford, 2011) in *R*.

In addition to these statistical analyses, as sea-level data are available for Liverpool, another independent test of reliability is available, and thus the estimates were compared to the known tide gauge records. This method was used to provide some validation for the reconstruction, however, differences in site location relative to the tide gauge and estuarine dynamics should be considered when comparing the fossil reconstructions and tide gauge records.

Once a transfer function method was deemed the most suitable, it was applied to the fossil data and a reconstruction of palaeo-marsh elevation (PME) was produced using *C2* (Juggins, 2007). Some transfer functions produce different components in their results, each one increasing in complexity. The lowest component possible that gave acceptable results was chosen based upon the 'principle of parsimony' (Horton et al., 2003). This was then converted into MTL by subtracting the PME from the altitude of the fossil sample.

MTL = Sample depth (altitude) - PME

As discussed in 2.2 the tidal constituents change up-estuary, consequently the Liverpool tidal data may be inappropriate to use for the study sites. Hence, tidal constituents from the secondary port of Hale Head were used. Hale Head is located in between the two study sites (figure 1. 20) and, therefore, should provide the most appropriate tidal data to use.

In addition to the data collected and analysed from the two sites in this study, a regional transfer function was produced using UK data taken from Horton and Edwards (2006). In order to combine data with different tidal ranges, elevation was converted into a Standardised Water Level Index (SWLI) following Horton and Edwards (2005). The following equation was used to calculate the SWLI for each site.

SWLI = [(Altitude of sample-MLWST)/(MHWST-MLWST)]*100

The SWLI was developed by Horton (1997) in order to normalise the elevations of different saltmarshes for their tidal ranges so the data could be combined. The original SWLI equation used MTL and this was updated to MLWST by Horton and Edwards (2005). The above equation converts the altitude difference between the sample and MLWST to a percentage of the range, therefore 100 will equal MHWST and 0 will equal MLWST, whilst

50 will equal MTL, these values will be consistent for each saltmarsh. Gehrels et al. (2001) also found that normalising height was an acceptable method to use.

As SWLI is an expression of elevation, and elevation in itself it not an environmental variable but is a representation of flooding duration, the SWLI must demonstrate a relationship with flooding duration. This was demonstrated by Horton (1997) where a strong linear relationship was found between the SWLI and flood duration.

To calculate the MTL when using the SWLI, the equation was rearranged and same method applied as for the PME, i.e.

Palaeo-marsh altitude = (SWLI/100) * (MHWST-MLWST)] + MLWST

MTL = Sample depth (altitude) – PME

MTL will be reconstructed in this study (following Horton and Edwards, 2006; Woodroffe et al., 2010) as sample elevation is referenced to the present local MTL, and not MSL which is unknown. MTL and MSL are calculated differently; MTL is the mean of high and low waters only, and MSL is the mean of all tides measured over a length of time. The difference between MSL and MTL is usually very small in most areas (Pugh, 2004; Woppelmann et al., 2006). However, it is possible that up to 20 cm difference can occur in some locations due to shallow water effects (Lassen, 1989; Wahl et al., 2010). Within the Mersey Estuary therefore the MTL and MSL may not be the same and therefore the reconstructed MTL cannot be assumed to be MSL. The tide gauge for Liverpool is located in the Outer Estuary and therefore the difference between MTL and MSL is negligible.

To determine the errors for all the reconstructions, bootstrapping was used as it provides standard error of prediction (SE_{pred}) (Birks et al., 1990) for individual samples, determining confidence intervals (Dixon, 2003). The errors for the reconstructions using multiple sites and SWLI were taken as a percentage and were converted to errors for the site using the appropriate tidal values.

SE_{pred} (altitude) = (SE_{pred} (SWLI)/100) * max SWLI value]/100 * (MHWST-MLWST)

Finally, to create the sea-level record, the reconstruction was plotted against the chronology as established in chapter 5. Errors for the chronology were calculated for each sample in the reconstruction by interpolating between the errors assigned to the samples for which dates had been established.

6.3. Results of foraminiferal data

Figures 6.1 and 6.2 show the foraminiferal assemblages for the two cores OB5 and DMC1 including the ages which were estimated from the chronology establish from the radionuclide and geochemical analysis discussed in chapter 5.

A total of 38 samples from OB5 contained foraminifera, with the abundance declining rapidly down-core from up to 2856 individuals per 5 cm^2 in the top half of the core, falling to only 27 individuals per 5 cm^2 in the lower half of the core (23-55 cm). Samples 26-32 cm contained the least foraminiferal tests, containing an average of 55 individuals per 5 cm^2, below which the foraminifera abundance increased to an average of 270 individuals per 5 cm^2. At least 150 individual foraminifera tests were attempted to be counted for each sample, however, in 6 samples less than 100 individuals were counted (samples 26-32). In total 15,048 individuals and 26 species were identified for this core.

The OB5 foraminiferal assemblage (figure 6.1) shows the majority of species from 0-25 cm depth are agglutinated species but below this depth increasing numbers of calcareous species are present. The agglutinated species dominating the top half the core are *Haplophragmoides* spp*., J. macrescens* and *M. fusca.* Near the surface of the core *T. inflata* was found to dominate between 1 and 8 cm depth. From 26 to 32 cm there is an increase in the agglutinated species *T. ochracea*, although there are low foraminifera numbers at this depth. Below this depth the assemblages are dominated by calcareous species, particularly *Elphidium* spp*.* Samples were counted to a depth of 51 cm, below which it was found that too few foraminifera were present, with the majority of the remaining species being calcareous, in particular *Elphidium* spp*.*

For DMC1 (figure 6.2) only 11 samples contained foraminifera. Unlike OB5, the abundance increased with depth, although it remained more stable than that of OB5. There was also little change in the foraminifera assemblage downcore. A total of only 1,636 individuals were counted, with samples containing fewer individual tests than OB5, having an average of 200 tests per 5 cm^2. All samples were dominated by *B. pseudomacrescens*, *Haplophragmoides* spp. and *J. macrescens*. Near the surface of the core (2-3 cm) *M. fusca* dominated with some *T. inflata* present.

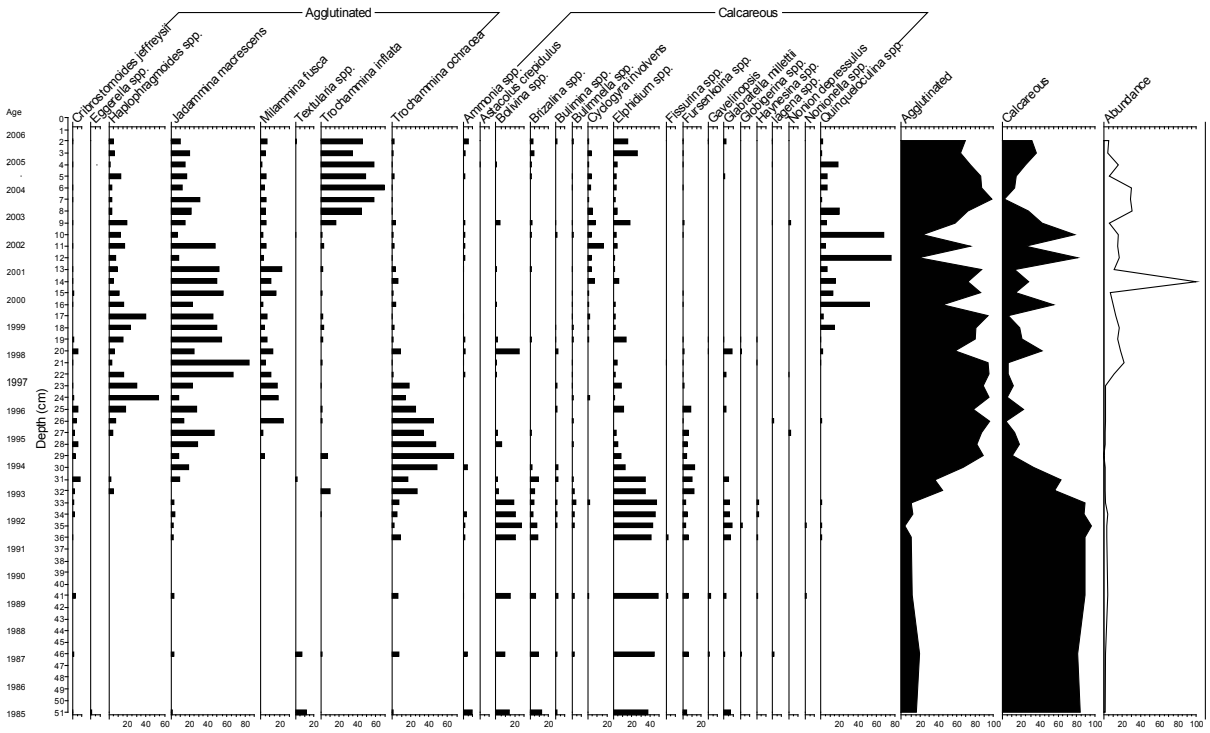

Figure 6.1 Relative percentages of foraminifera abundance for OB5, by depth and including the ages from chapter 5.

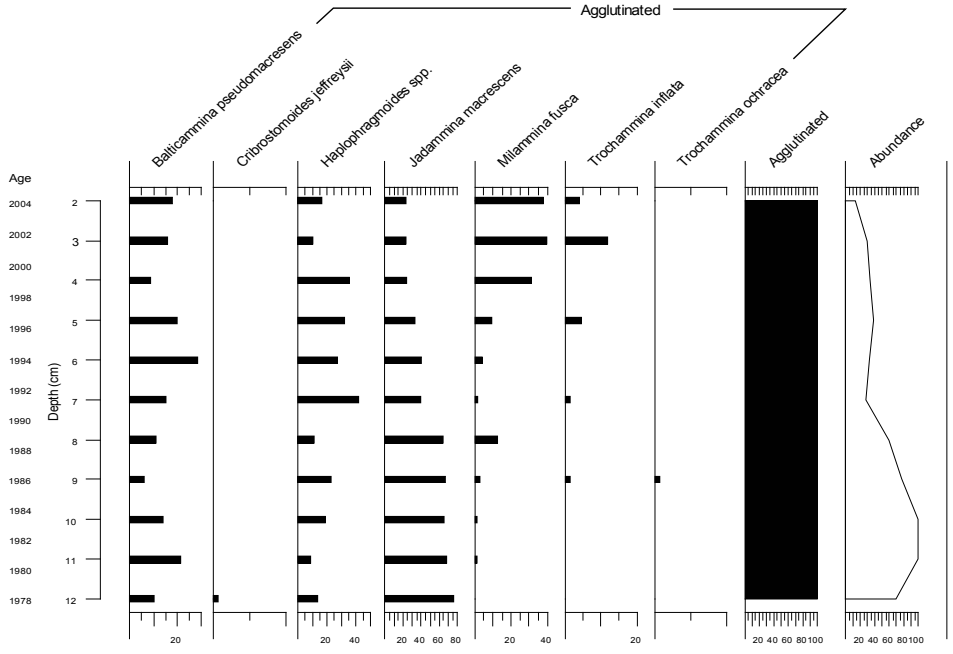

Figure 6.2 Relative percentages of foraminifera abundance for DMC1, by depth and including the ages from chapter 5.

The environmental variables, organic matter content, grain size and dry bulk density (DBD), were analysed along with the foraminifera for both cores. The results of these analyses can be seen in figures 6.3 to 6.5. Figures 6.3 and 6.4 show the grain size data in phi for OB5. The figures show little change in grain size up-core, with the most common grain size being medium to fine silt (6-8 ϕ) which accounts for 20% of the sample with little coarse sediment in the core, i.e. the largest grain size being fine to very fine sand. The only perturbation from this trend is between 30-40 cm depth where there is a fall and a coarsening in phi size down to 5 ϕ. This can be seen in figure 6.3 were there is an increase in the 4-5 ϕ fraction. At 30 and 44 cm there is also an increase in the percentage of fine to medium silt, which can be seen in the 6-8 ϕ size fraction. Figure 6.4 also shows there are clear high frequency changes in the grain size throughout the core, which is also obvious in figure 6.3 where it shows frequent switches in the sand and clay content.

Figure 6.3 also includes the percentage organic matter and shows there is a slight increase in organic matter content up-core, ranging from as low as 2% up to 12%. At depths of 35 cm and 70 cm there are also decreases observed in organic matter.

Figure 6.5 shows the dry bulk density (DBD) results for both cores, it shows there is little change up-core for OB5, although there is an increase in DBD at a depth between 30 and 45 cm. Correlations between DBD with organic matter content, and also sand content can be seen in figure 6.6 (correlation matrices are given in appendix 2). It shows that the DBD is strongly negatively correlated with organic matter (figure 6.6b). It also shows some positive correlation with sand (r^2= 0.47) (figure 6.6a) although the correlations reveal that the size fraction 6-7 (medium silt) is related to DBD the most (r^2= -0.525) (figure 6.6c).

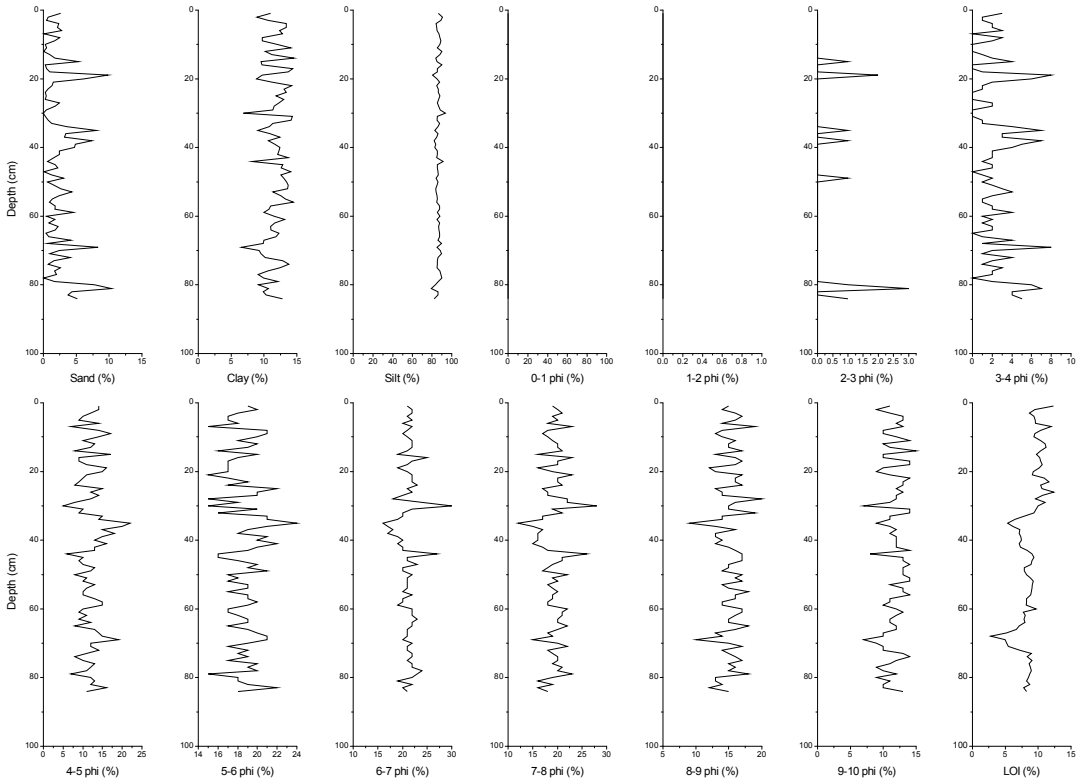

Figure 6.3 OB5 grain size fraction and LOI % by depth.

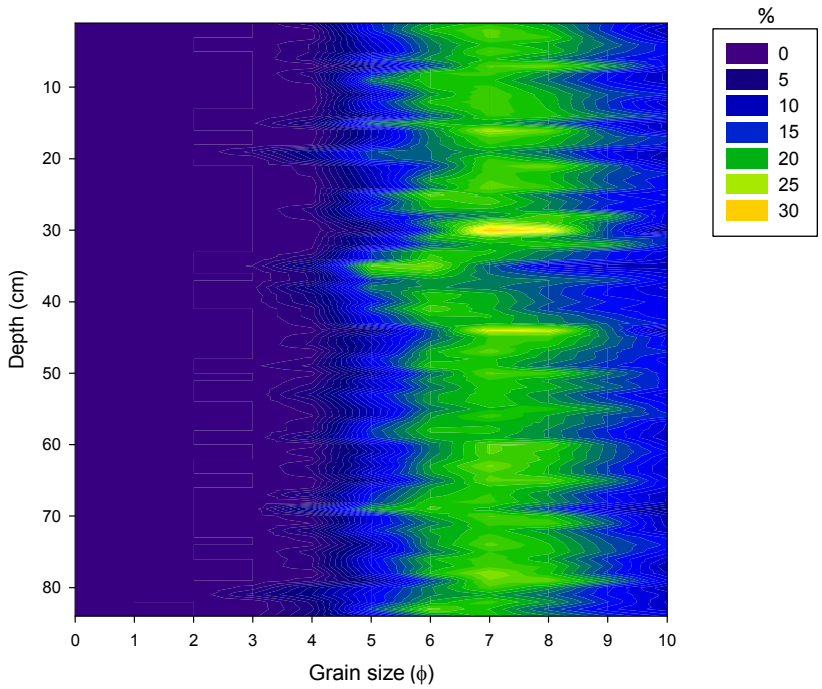

Figure 6.4 Contour plot of OB5 grain size fractions as percentages expressed in colour by depth.

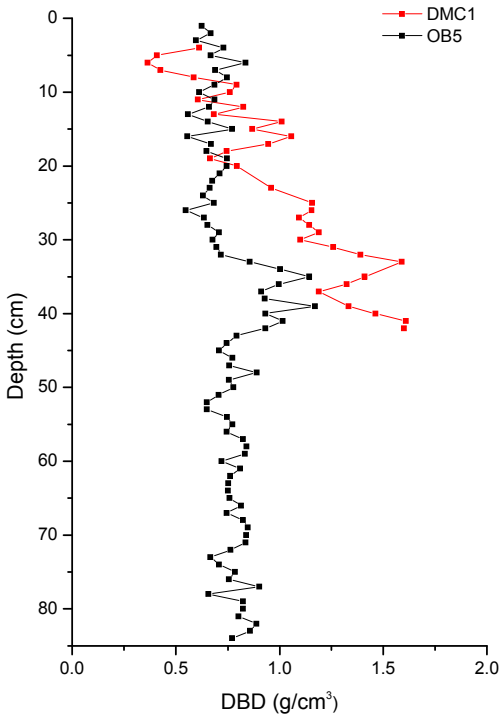

Figure 6.5 Dry Bulk Density results for cores OB5 and DMC1.

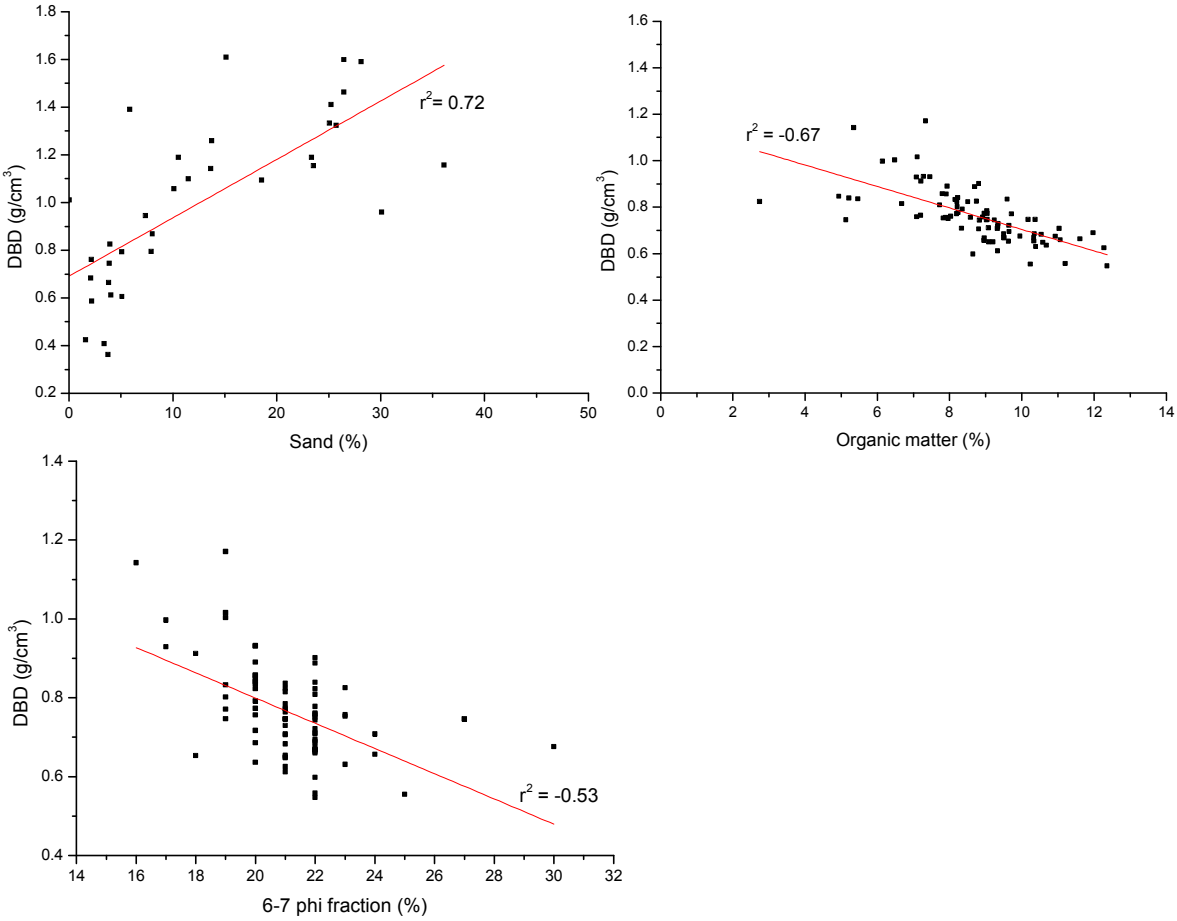

Figure 6.6 Correlations between DBD and a) sand % b) organic matter content c) 6-7 ϕ content for OB5.

Figures 6.7 and 6.8 show the grain size data in phi for DMC1. Both figures show a general trend in increasing phi sizes up-core, i.e. fining upwards, from 3-8 ϕ between 42-25 cm to 6-9 ϕ between 25 and 0 cm. There is a decrease in the percentages of the 0-6 phi sizes up-core and an increase in percentages of 6-10 phi sizes. At depths of 24, 26 and 34 cm there are decreases in high phi sizes (6-10 ϕ) and increases in low phi sizes (0-4 ϕ). Between 35-42 cm, the phi size remains low between 4-6 ϕ. In contrast to the core OB5 were there are high frequency changes in grain size, there are few such changes in the core DMC1.

Figure 6.7 shows the percentage organic matter content for DMC1 and shows there is a greater amount of organic matter content in this core than OB5, with percentages ranging from 3% at the bottom of the core up to 58 % at the top of the core. There is a clear trend of increasing organic matter content up-core. Figure 6.5 shows the DBD for DMC1 showing there is a general decrease in density up-core, with an increase between 12 and 20 cm. Correlations between DBD with organic matter content and sand content are shown in figure 6.9 (correlation matrices can be seen in appendix 2). It shows that DBD is highly correlated with the variables organic matter (r^2= -0.91) (figure 6.9b) and sand content (r^2= 0.72) (figure 6.9a) as well as strongly negative correlation with the particular size fraction 8-9 ϕ (r^2= -0.85) (figure 6.9c).

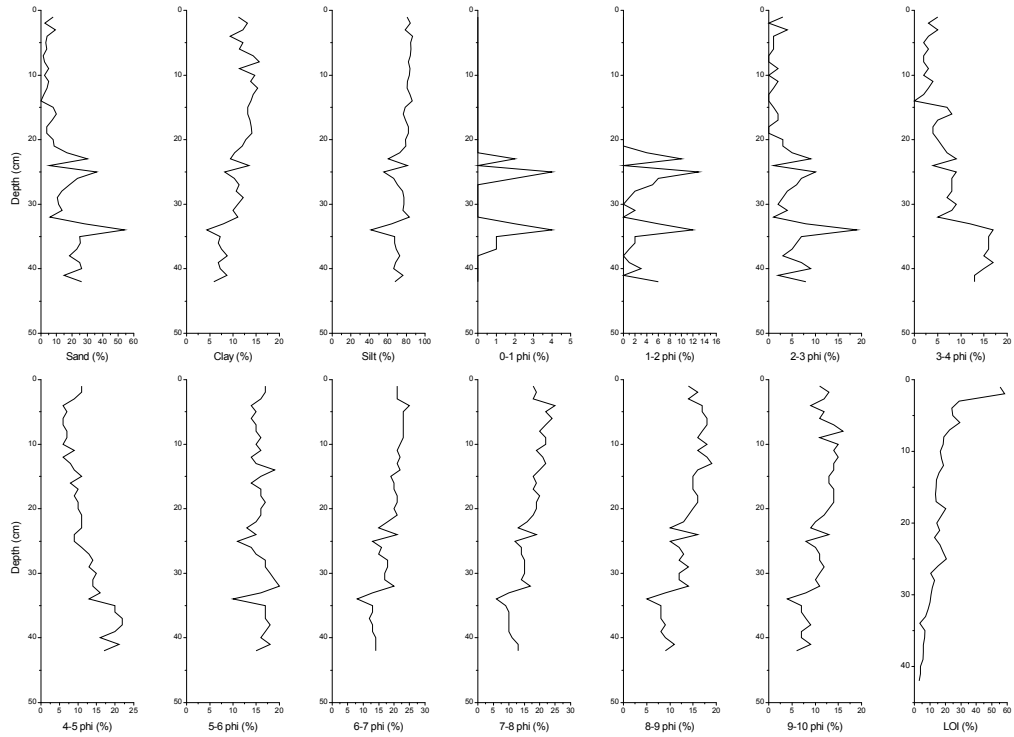

Figure 6.7 DMC1 grain size fraction and LOI% by depth.

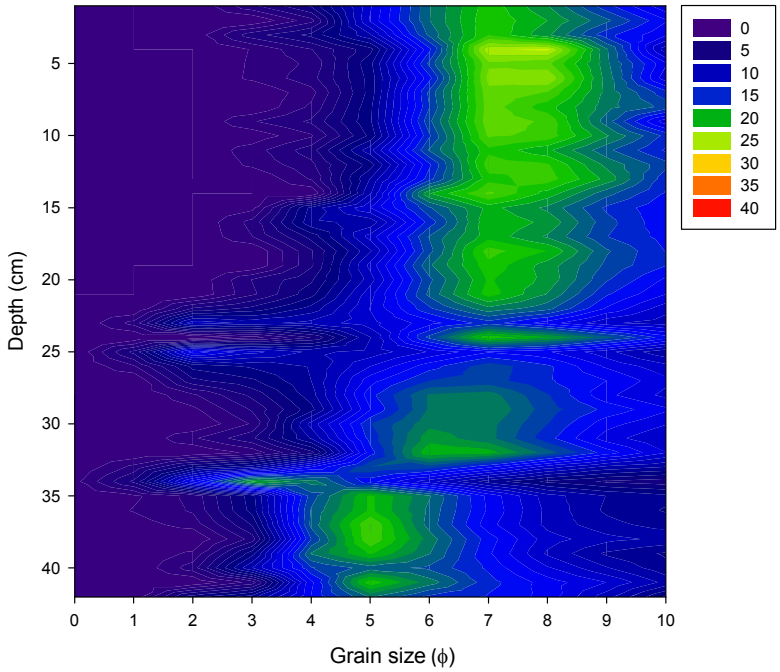

Figure 6.8 Contour plot of DMC1 grain size fractions as percentages expressed in colour by depth.

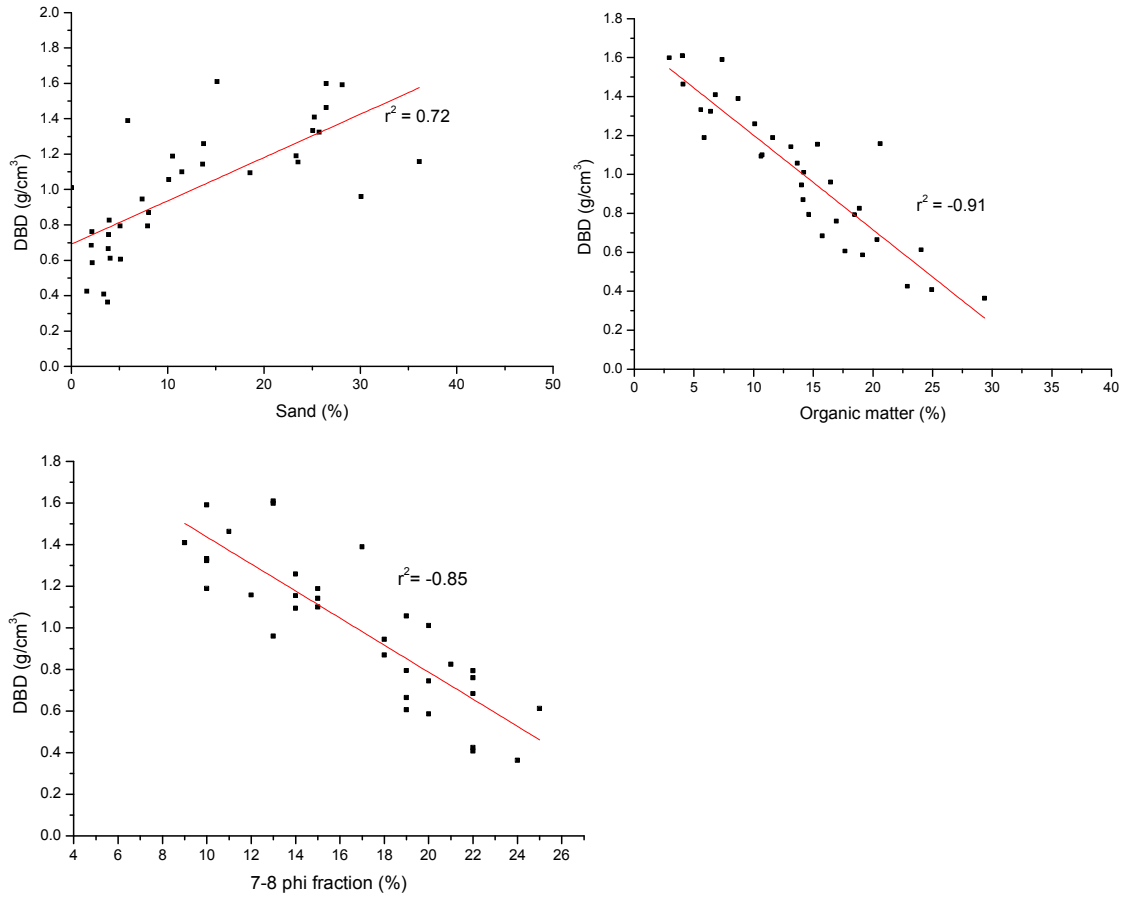

Figure 6.9 Correlations between DBD and a) sand % b) organic matter content c) 7-8 ϕ content for DMC1.

6.3.1. Model selection

Statistical analyses of different combinations of modern data using different models were carried out. This was done in order to create the best performing training set, including only the best performing transect data, and to determine if all modern transects should be included in the training set or whether including certain transects causes a deterioration of the transfer function performance. This was thought of as a method of 'pruning', reducing the number of transects included in the training set to increase the overall model performance. There are however potential problems with reducing the number of samples which are included in the training set as this reduces the number of modern analogues leading to fossil samples without modern analogues. The training set may also be less representative of the full extent of contemporary saltmarsh environments. The aim of this 'pruning' was to create the best performing model to produce the most accurate and precise reconstruction and is routinely carried out in most sea-level reconstruction (e.g. Edwards et al., 2004; Engelhart et al., 2007; Woodroffe and Long, 2010). In addition, it allows the selection of other UK saltmarshes to be included in the training set, and is a method of choosing the sites which may be more closely related to the sites in this study.

The performance of the models was evaluated based upon measures of predicative ability (r^2_{jack} and $RMSEP_{jack}$). r^2_{jack} shows the relationship between the observed and predicted elevation, therefore when this value is high (>0.6) a strong relationship between elevation and the distribution of foraminifera species can be inferred (Rossi et al., 2011). $RMSEP_{jack}$ shows the errors associated with the reconstructed data as a whole, therefore a low $RMSEP_{jack}$ indicates smaller errors. In addition to these performance measures, one of the most important criteria for judging whether a dataset should be included in the training set or not, is based upon whether including the dataset improves the number of modern analogues the fossil record has in the training set.

Table 6.6 is a comprehensive list of the different datasets examined in the model selection process and describes which data are included within the datasets.

Local data

Tables 6.1 to 6.5 show the results of the DCCA statistical analysis for modern species data with only elevation as the environmental variable for different datasets. The length of the gradient is in SD units and shows whether the data are unimodal or linear. Both the

individual transects (tables 6.1 to 6.3) and grouped datasets (tables 6.4 to 6.5) have values between 1.5 and 3 SD, indicating both statistical methods may be appropriate to use.

Table 6.1 DCCA for OBSS1 with only elevation.

Axes	1	2	3	4	Total inertia
Eigenvalues	0.404	0.158	0.023	0.009	1.270
Lengths of gradient	2.587	2.024	0.935	1.314	
Species-environment correlations	0.911	0.000	0.000	0.000	
Cumulative percentage variance					
of species data	31.8	44.3	46.1	46.8	
of species-environment relation	99.8	99.7	0.0	0.0	
Sum of all eigenvalues					1.270
Sum of all canonical eigenvalues					0.404

Table 6.2 DCCA for OBSS2 with only elevation.

Axes	1	2	3	4	Total inertia
Eigenvalues	0.233	0.217	0.049	0.032	0.873
Lengths of gradient	1.616	1.954	1.894	1.751	
Species-environment correlations	0.789	0	0	0	
Cumulative percentage variance					
of species data	26.7	51.6	57.2	60.8	
of species-environment relation	91.4	98.6	0	0	
Sum of all eigenvalues					0.873
Sum of all canonical eigenvalues					0.233

Table 6.3 DCCA for OBSS3 with only elevation.

Axes	1	2	3	4	Total inertia
Eigenvalues	0.287	0.148	0.032	0.023	0.948
Lengths of gradient	1.634	1.837	0.976	0.796	
Species-environment correlations	0.92	0	0	0	
Cumulative percentage variance					
of species data	30.2	45.9	49.3	51.6	
of species-environment relation	100.1	99.7	0	0	
Sum of all eigenvalues					0.948
Sum of all canonical eigenvalues					0.287

Table 6.4 DCCA for all Oglet Bay with only elevation.

Axes	1	2	3	4	Total inertia
Eigenvalues	0.224	0.377	0.111	0.072	1.604
Lengths of gradient	2.01	3.081	1.931	2.633	
Species-environment correlations	0.766	0	0	0	
Cumulative percentage variance					
of species data	13.9	37.5	44.4	48.9	
of species-environment relation	101.1	99.3	0	0	
Sum of all eigenvalues					1.604
Sum of all canonical eigenvalues					0.224

Table 6.5 DCCA for all of Oglet Bay and Decoy Marsh data with only elevation.

Axes	1	2	3	4	Total inertia
Eigenvalues	0.373	0.372	0.169	0.093	2.254
Lengths of gradient	2.006	2.818	2.784	1.742	
Species-environment correlations	0.834	0	0	0	
Cumulative percentage variance					
of species data	16.6	33.1	40.5	44.7	
of species-environment relation	101.3	99	0	0	
Sum of all eigenvalues					2.254
Sum of all canonical eigenvalues					0.373

Table 6.6 Description of foraminiferal data included within the different datasets.

Dataset name	Data included
OB1	OBSS1 (Oglet Bay transect 1).
OB2	OBSS2 (Oglet Bay transect 2).
OB3	OBSS3 (Oglet Bay transect 3).
DM1	All Decoy Marsh (live).
OB4	OBSS1 and OBSS2.
OB5	OBSS1 and OBSS3.
OB6	OBSS2 and OBSS3.
OB a	All Oglet Bay data.
OBDM1	OBSS1 and DMSS1.
OBDM2	OBSS3 and DMSS2.
OBDM3a	OBSS1, OBSS3, DMSS1 and DMSS2.
OBDM3b	OBSS1, OBSS3, DMSS1 and DMSS2 pruned for WATOL.
OBDM3c	OBSS1, OBSS3, DMSS1 and DMSS2 pruned for WAPLS.
OBDM3d	OBSS1, OBSS3, DMSS1 and DMSS2 pruned for MAT.
OBDMa	OBSS1, OBSS2, OBSS3, DMSS1 and DMSS2.
OBDMb	OBSS1, OBSS2, OBSS3, DMSS1 and DMSS2 pruned for WATOL.
OBDMc	OBSS1, OBSS2, OBSS3, DMSS1 and DMSS2 pruned for WAPLS.
OBDMd	OBSS1, OBSS2, OBSS3, DMSS1 and DMSS2 pruned for MAT.
H&E a	All UK sites from Horton and Edwards (2006).
H&E b	All UK sites from Horton and Edwards (2006) pruned for WAPLS.
H&E NW	North West sites Horton and Edwards (2006) (Kentra Marsh, Tramaig Bay and Roudsea Marsh).
H&E S1 to S10	Individual sites from Horton and Edwards (2006). See table 6.15.
H&E 7a	7 sites Horton and Edwards (2006) (Alnmouth Marsh, Arne Peninsular, Brancaster Marsh, Keyhaven Marsh, Nith Estuary, Roudsea Marsh and Thornham Marsh).
H&E 7b	7 sites Horton and Edwards (2006) (Alnmouth Marsh, Arne Peninsular, Brancaster Marsh, Keyhaven Marsh, Nith Estuary, Roudsea Marsh and Thornham Marsh) pruned for WAPLS.
OBDMH&E A	All Oglet Bay and Decoy Marsh data with all UK sites from Horton and Edwards (2006).
OBDMH&E B	All Oglet Bay and Decoy Marsh data with all UK sites from Horton and Edwards (2006) pruned for WAPLS.
OBDM3H&E A	OBSS1, OBSS3, DMSS1, DMSS2 with all UK sites from Horton and Edwards (2006).
OBDM3H&E B	OBSS1, OBSS3, DMSS1, DMSS2 all UK sites from Horton and Edwards (2006) pruned for WAPLS.
OBDM3H&E 1 to 13	OBSS1, OBSS3, DMSS1 and DMSS2 with individual sites from Horton and Edwards (2006). See table 6.17.
OBDM3H&E 4a	OBSS1, OBSS3, DMSS1 and DMSS2 with Alnmouth Marsh, Kentra Marsh, Thornham Marsh and Roudsea Marsh from Horton and Edwards (2006).
OBDM3H&E 4b	OBSS1, OBSS3, DMSS1 and DMSS2 with sites Alnmouth Marsh, Kentra Marsh, Thornham Marsh and Roudsea Marsh from Horton and Edwards (2006) pruned for WAPLS.
OBDM3H&E NW	OBSS1, OBSS3, DMSS1 and DMSS2 with North West sites Horton and Edwards (2006) (Kentra Marsh, Tramaig Bay and Roudsea Marsh).
OBDM3H&E NWb	OBSS1, OBSS3, DMSS1 and DMSS2 with North West sites (Kentra Marsh, Tramaig Bay and Roudsea Marsh) from Horton and Edwards (2006) pruned for WAPLS.

The performance results of different combinations of modern data using different models can be seen in table 6.7 for all transects, table 6.8 for Oglet Bay transects alone, and table 6.9 for results using data from both sites. Table 6.7 shows that the highest r^2_{jack} and lowest $RMSEP_{jack}$ was produced using the model WMAT (Weighted Modern Analogue Technique) followed by the WAPLS model. Transect OBSS3 was found to have the highest r^2_{jack} and lowest $RMSEP_{jack}$ as well as having the largest number of samples in the cores which had good and fair modern analogues based upon samples with coefficients below the 20th percentile (Birks et al., 1990). Both OBSS2 and DMSS have much lower r^2_{jack} and higher $RMSEP_{jack}$ with only 1 sample for each of the cores having modern analogues from OBSS2 and zero modern analogues for both cores from DMSS. It also shows that OBSS1 and OBSS2 in combination have the lowest r^2_{jack} and highest $RMSEP_{jack}$, as well as having the lowest modern analogues for the fossil data. The dataset which has the highest r^2_{jack} and lowest $RMSEP_{jack}$ are the transects OBSS1 and OBSS3. This dataset also has the most modern analogues for the fossil data. The dataset containing all three transects from Oglet Bay contains the same number of modern analogues for the fossil data, but has lower r^2_{jack} and higher $RMSEP_{jack}$ than the OBSS1 and OBSS3 dataset.

The data from Oglet Bay were then combined with the data from Decoy Marsh and analysed again using different models, the results of which can be seen in table 6.9. The highest r^2_{jack} and $RMSEP_{jack}$ values were found to be from the dataset OBSS1 and DMSS (OBDM1) although the samples from the fossil records have few modern analogues in this contemporary dataset. Other datasets also have high r^2_{jack} values and low $RMSEP_{jack}$ values with the dataset containing OBSS1, OBSS3 and DMSS (OBDM3a) having the most modern analogues for the fossil data. As the dataset OBDM3a has the largest number of fossil data with modern analogues, these data were pruned and the results can be seen in table 6.12. The results of the DCCA with this dataset can be seen in table 6.10. In addition, the dataset OBDM was also pruned as it also performs well, having a high r^2_{jack} and low $RMSEP_{jack}$, although the fossil record has fewer modern analogues in this dataset. The pruned results can be seen in table 6.13. DCCA was also performed for this dataset and can be seen in table 6.11.

Table 6.10 shows that the length of the elevation gradient for OBDM3 to be 2 SD, which is in the 'ambiguous zone'. Therefore, different models which gave the 'best' results in table 6.9 can be seen in table 6.12 with pruned data. The results show that MAT and WMAT have the highest r^2_{jack} and a low $RMSEP_{jack}$. WA tol and WAPLS pruned models have similar

performances. Table 6.5 shows the results of the DCCA for the Oglet Bay and Decoy Marsh data (OBDM) and shows that the length of the gradient to be 2 SD also. Table 6.14 shows the performance results of the OBDM data with different models. MAT and WMAT were found to have the highest r^2_{jack} and lowest $RMSEP_{jack}$. Second to this was the model WAPLS C2 (component 2) which performed similarly well.

Although the OBDM3 data performed better than the OBDM data (table 6.8), after the data were pruned (tables 6.12 and 6.13) the OBDM dataset was found to perform better than the OBDM3 dataset. The OBDMc (pruned) data have a slightly higher r^2_{jack} value, lower $RMSEP_{jack}$ value and more modern analogues for the fossil data; it also contains more samples than the OBDM3c data (pruned). Therefore this dataset was chosen to be the most appropriate for performing a reconstruction. The model WAPLS C2 was chosen as the most appropriate model as it has high r^2_{jack} and low $RMSEP_{jack}$ values as well as large numbers of fossil record samples with modern analogues. Although MAT and WMAT model performances were better, these were not selected to be the most appropriate as Telford and Birks (2005) deemed MAT and WMAT to be the most over-optimistic models. Furthermore, MAT is not as robust to autocorrelation compared to other models as it may find local relationships between species and the environment as opposed to more global relationships (Telford and Birks, 2009). Telford and Birks (2005) also argued global response models (e.g. WA) are more robust to autocorrelation over those which find local structure in assemblage data (e.g. MAT).

Table 6.7 Results of different models for individual transects.

			Model Performance			Cross-validation						Samples with MA	
Data	Dataset name	Model	RMSE	R^2	Max bias	r^2_{jack}	Max $bias_{jack}$	$RMSEP_{jack}$	r^2_{boot}	Max $bias_{boot}$	$RMSEP_{boot}$	OB5	DMC1
OBSS1	OB1	WA_Inv	0.098	0.838	0.246	0.751	0.355	0.122	0.753	0.356	0.130	2	5
		WA_Cla	0.108	0.838	0.173	0.761	0.299	0.128	0.761	0.303	0.136		
		WA tol Inv	0.098	0.838	0.246	0.751	0.355	0.122	0.753	0.356	0.130		
		WA tol Cla	0.108	0.838	0.173	0.761	0.299	0.128	0.761	0.303	0.136		
		WAPLS C1	0.098	0.838	0.246	0.751	0.355	0.122	0.754	0.360	0.132		
		WAPLS C2	0.078	0.898	0.153	0.762	0.296	0.121	0.760	0.330	0.139		
		PLSC1	0.142	0.665	0.298	0.548	0.371	0.165	0.553	0.383	0.177		
		PLS C2	0.101	0.831	0.246	0.727	0.345	0.128	0.724	0.355	0.148		
		MAT	0.159	0.748	0.516	0.748	0.516	0.159	0.710	0.528	0.173		
		WMAT	0.102	0.864	0.283	0.864	0.283	0.102	0.843	0.352	0.131		
OBSS2	OB2	WA_Inv	0.124	0.598	0.201	0.479	0.228	0.142	0.473	0.216	0.150	1	1
		WA_Cla	0.160	0.598	0.249	0.522	0.276	0.184	0.516	0.227	0.182		
		WA tol Inv	0.119	0.629	0.183	0.479	0.227	0.141	0.482	0.243	0.152		
		WA tol Cla	0.150	0.629	0.220	0.524	0.250	0.169	0.514	0.228	0.174		
		WAPLS C1	0.124	0.598	0.201	0.479	0.228	0.142	0.473	0.216	0.150		
		WAPLS C2	0.103	0.721	0.148	0.589	0.175	0.126	0.611	0.163	0.138		
		PLSC1	0.126	0.583	0.200	0.445	0.228	0.146	0.420	0.243	0.162		
		PLS C2	0.105	0.708	0.174	0.553	0.209	0.131	0.472	0.224	0.158		
		MAT	0.170	0.362	0.276	0.362	0.276	0.170	0.365	0.275	0.182		
		WMAT	0.142	0.555	0.221	0.555	0.221	0.142	0.532	0.228	0.159		
OBSS3	OB3	WA_Inv	0.100	0.841	0.218	0.793	0.250	0.114	0.790	0.257	0.124	6	7
		WA_Cla	0.109	0.841	0.177	0.801	0.217	0.120	0.794	0.224	0.131		
		WA tol Inv	0.067	0.928	0.224	0.854	0.277	0.097	0.881	0.296	0.117		
		WA tol Cla	0.070	0.928	0.207	0.853	0.269	0.098	0.880	0.287	0.121		
		WAPLS C1	0.100	0.841	0.218	0.794	0.250	0.114	0.789	0.259	0.124		
		WAPLS C2	0.077	0.905	0.201	0.818	0.243	0.110	0.819	0.248	0.123		
		PLSC1	0.111	0.802	0.268	0.734	0.303	0.129	0.731	0.280	0.138		
		PLS C2	0.090	0.870	0.170	0.754	0.253	0.126	0.752	0.269	0.142		
		MAT	0.123	0.874	0.241	0.874	0.241	0.123	0.872	0.257	0.147		
		WMAT	0.095	0.928	0.213	0.928	0.213	0.095	0.923	0.223	0.115		
DMSS	DM1	WA_Inv	0.028	0.730	0.061	0.466	0.111	0.043	0.574	0.095	0.044	0	0
		WA_Cla	0.033	0.730	0.103	0.538	0.159	0.048	0.671	0.151	0.057		
		WA tol Inv	0.035	0.589	0.097	0.317	0.250	0.071	0.431	0.115	0.057		
		WA tol Cla	0.046	0.589	0.159	0.366	0.341	0.087	0.505	0.168	0.065		
		WAPLS C1	0.028	0.730	0.061	0.466	0.111	0.043	0.541	0.098	0.044		
		WAPLS C2	0.020	0.863	0.030	0.546	0.103	0.041	0.710	0.082	0.043		
		PLSC1	0.031	0.685	0.075	0.481	0.107	0.043	0.518	0.104	0.045		
		PLS C2	0.025	0.788	0.034	0.469	0.149	0.053	0.570	0.059	0.054		
		MAT	0.564	0.156	0.523	0.156	0.049	0.546	0.156	0.051	0.049		
		WMAT	0.592	0.150	0.592	0.150	0.043	0.598	0.151	0.046	0.043		

Table 6.8 Results of different models with different datasets for Oglet Bay transects.

			Model Performance					Cross-validation				Samples with MA	
Data	Dataset name	Model	RMSE	R^2	Max bias	r^2_{jack}	Max $bias_{jack}$	$RMSEP_{jack}$	r^2_{boot}	Max $bias_{boot}$	$RMSEP_{boot}$	OB5	DMC1
OBSS 1 & 2	OB4	WA_Inv	0.153	0.539	0.439	0.428	0.521	0.171	0.432	0.536	0.176	3	5
		WA_Cla	0.208	0.539	0.253	0.466	0.394	0.224	0.462	0.429	0.217		
		WA tol Inv	0.137	0.629	0.380	0.517	0.472	0.157	0.528	0.498	0.162		
		WA tol Cla	0.173	0.629	0.218	0.552	0.347	0.186	0.551	0.401	0.183		
		WAPLS C1	0.153	0.539	0.439	0.428	0.521	0.171	0.435	0.525	0.175		
		WAPLS C2	0.133	0.651	0.326	0.437	0.508	0.173	0.457	0.508	0.184		
		PLSC1	0.179	0.371	0.490	0.249	0.550	0.197	0.256	0.551	0.201		
		PLS C2	0.160	0.495	0.472	0.306	0.581	0.192	0.308	0.585	0.204		
		MAT	0.152	0.555	0.473	0.555	0.473	0.152	0.518	0.491	0.167		
		WMAT	0.134	0.653	0.322	0.653	0.322	0.134	0.624	0.366	0.150		
OBSS 1 & 3	OB5	WA_Inv	0.136	0.725	0.390	0.665	0.429	0.151	0.666	0.446	0.156	20	11
		WA_Cla	0.160	0.725	0.270	0.674	0.329	0.172	0.674	0.351	0.177		
		WA tol Inv	0.114	0.809	0.363	0.760	0.409	0.128	0.748	0.440	0.148		
		WA tol Cla	0.127	0.809	0.282	0.765	0.341	0.134	0.752	0.374	0.157		
		WAPLS C1	0.136	0.725	0.390	0.665	0.429	0.151	0.664	0.448	0.158		
		WAPLS C2	0.126	0.767	0.392	0.683	0.434	0.147	0.685	0.438	0.157		
		PLSC1	0.156	0.640	0.339	0.575	0.368	0.170	0.578	0.393	0.177		
		PLS C2	0.131	0.746	0.331	0.690	0.371	0.145	0.684	0.389	0.153		
		MAT	0.139	0.741	0.510	0.741	0.510	0.139	0.737	0.510	0.157		
		WMAT	0.125	0.780	0.445	0.780	0.445	0.125	0.772	0.466	0.143		
OBSS 2 & 3	OB6	WA_Inv	0.144	0.616	0.226	0.536	0.254	0.158	0.547	0.253	0.162	17	11
		WA_Cla	0.183	0.616	0.312	0.555	0.323	0.194	0.565	0.297	0.195		
		WA tol Inv	0.128	0.693	0.206	0.641	0.232	0.140	0.660	0.226	0.143		
		WA tol Cla	0.154	0.693	0.184	0.654	0.187	0.148	0.671	0.191	0.154		
		WAPLS C1	0.144	0.616	0.226	0.536	0.254	0.158	0.536	0.263	0.165		
		WAPLS C2	0.113	0.761	0.181	0.607	0.215	0.149	0.598	0.223	0.171		
		PLSC1	0.170	0.461	0.279	0.345	0.317	0.188	0.348	0.325	0.196		
		PLS C2	0.149	0.586	0.224	0.444	0.244	0.176	0.455	0.256	0.186		
		MAT	0.130	0.705	0.261	0.705	0.261	0.130	0.682	0.283	0.149		
		WMAT	0.112	0.785	0.197	0.785	0.197	0.112	0.763	0.220	0.129		
OB	OB a	WA_Inv	0.155	0.589	0.479	0.524	0.512	0.167	0.522	0.516	0.173	20	11
		WA_Cla	0.203	0.589	0.323	0.540	0.382	0.213	0.533	0.399	0.219		
		WA tol Inv	0.138	0.678	0.445	0.617	0.482	0.150	0.613	0.497	0.159		
		WA tol Cla	0.167	0.678	0.323	0.629	0.379	0.175	0.621	0.406	0.185		
		WAPLS C1	0.155	0.589	0.479	0.524	0.512	0.168	0.524	0.514	0.172		
		WAPLS C2	0.149	0.625	0.494	0.529	0.536	0.167	0.533	0.531	0.176		
		PLSC1	0.180	0.450	0.474	0.369	0.512	0.193	0.376	0.518	0.198		
		PLS C2	0.166	0.532	0.487	0.437	0.528	0.183	0.444	0.512	0.190		
		MAT	0.147	0.641	0.510	0.641	0.510	0.147	0.647	0.497	0.158		
		WMAT	0.133	0.708	0.445	0.708	0.445	0.133	0.703	0.439	0.146		

Table 6.9 Results of different models with different datasets for both sites.

			Model Performance			Cross-validation						Samples with MA	
Data	Dataset name	Model	RMSE	R^2	Max bias	r^2_{jack}	Max $bias_{jack}$	$RMSEP_{jack}$	r^2_{boot}	Max $bias_{boot}$	$RMSEP_{boot}$	OB5	Dmc1
OBSS1 & DM1	OBDM1	WA_Inv	0.098	0.892	0.200	0.863	0.229	0.111	0.858	0.243	0.119	9	11
		WA_Cla	0.104	0.892	0.162	0.864	0.207	0.116	0.859	0.223	0.124		
		WA tol Inv	0.077	0.934	0.156	0.913	0.194	0.089	0.912	0.204	0.097		
		WA tol Cla	0.080	0.934	0.136	0.913	0.179	0.090	0.912	0.190	0.099		
		WAPLS C1	0.098	0.892	0.200	0.863	0.229	0.111	0.856	0.243	0.119		
		WAPLS C2	0.079	0.930	0.112	0.898	0.144	0.096	0.896	0.162	0.106		
		PLSC1	PLSC1	0.179	0.644	0.411	0.597	0.431	0.191	0.604	0.427		
		PLS C2	PLS C2	0.130	0.813	0.311	0.727	0.344	0.157	0.726	0.337		
		MAT	0.098	0.906	0.222	0.905	0.222	0.098	0.906	0.223	0.109		
		WMAT	0.080	0.935	0.189	0.935	0.189	0.080	0.930	0.201	0.096		
OBSS3 & DM1	OBDM2	WA_Inv	0.111	0.910	0.092	0.899	0.105	0.117	0.897	0.126	0.128	12	11
		WA_Cla	0.116	0.910	0.115	0.899	0.118	0.120	0.898	0.123	0.128		
		WA tol Inv	0.111	0.910	0.092	0.899	0.105	0.117	0.897	0.126	0.128		
		WA tol Cla	0.116	0.910	0.115	0.899	0.118	0.120	0.898	0.123	0.128		
		WAPLS C1	0.111	0.910	0.091	0.898	0.105	0.118	0.897	0.121	0.129		
		WAPLS C2	0.099	0.928	0.163	0.824	0.156	0.168	0.857	0.110	0.158		
		PLSC1	0.217	0.653	0.610	0.598	0.672	0.234	0.591	0.673	0.241		
		PLS C2	0.125	0.884	0.128	0.801	0.480	0.165	0.795	0.489	0.192		
		MAT	0.127	0.905	0.265	0.905	0.265	0.127	0.903	0.296	0.144		
		WMAT	0.114	0.918	0.249	0.918	0.249	0.114	0.917	0.278	0.126		
OBSS1, 3 & DM1	OBDM3a	WA_Inv	WA_Inv	0.164	0.761	0.223	0.729	0.250	0.174	0.734	0.238	25	11
		WA_Cla	WA_Cla	0.187	0.761	0.177	0.732	0.185	0.196	0.737	0.188		
		WA tol Inv	0.1312	0.8465	0.1774	0.8144	0.1950	0.1444	0.8238	0.1949	0.1520		
		WA tol Cla	0.1426	0.8465	0.1295	0.8164	0.1479	0.1526	0.8252	0.1394	0.1602		
		WAPLS C1	0.1636	0.7615	0.2224	0.7286	0.2502	0.1745	0.7214	0.2560	0.1823		
		WAPLS C2	0.1410	0.8227	0.1735	0.7722	0.1850	0.1605	0.7655	0.1864	0.1719		
		PLSC1	0.239	0.490	0.527	0.446	0.559	0.249	0.451	0.547	0.252		
		PLS C2	0.164	0.759	0.295	0.681	0.429	0.189	0.687	0.455	0.199		
		MAT	0.143	0.826	0.370	0.826	0.370	0.143	0.834	0.371	0.153		
		WMAT	0.131	0.849	0.334	0.849	0.334	0.131	0.853	0.340	0.141		
OBDM	OBDMa	WA_Inv	0.166	0.720	0.231	0.690	0.252	0.175	0.689	0.254	0.180	20	11
		WA_Cla	0.196	0.720	0.137	0.693	0.161	0.203	0.693	0.163	0.210		
		WA tol Inv	0.142	0.794	0.162	0.761	0.215	0.153	0.765	0.213	0.159		
		WA tol Cla	0.160	0.794	0.093	0.763	0.119	0.168	0.767	0.120	0.175		
		WAPLS C1	0.166	0.720	0.231	0.690	0.252	0.175	0.690	0.254	0.179		
		WAPLS C2	0.147	0.781	0.145	0.734	0.156	0.162	0.734	0.160	0.169		
		PLSC1	PLSC1	0.180	0.450	0.474	0.369	0.512	0.193	0.376	0.518		
		PLS C2	PLS C2	0.166	0.532	0.487	0.437	0.528	0.183	0.444	0.512		
		MAT	0.147	0.641	0.510	0.641	0.510	0.147	0.647	0.497	0.158		
		WMAT	0.133	0.708	0.445	0.708	0.445	0.133	0.703	0.439	0.146		

Table 6.10 DCCA OBSS1, OBSS3, OBSS6 with elevation only.

Axes	1	2	3	4	Total inertia
Eigenvalues	0.405	0.338	0.167	0.094	2.255
Lengths of gradient	2.003	2.933	3.238	1.736	
Species-environment correlations	0.857	0	0	0	
Cumulative percentage variance					
of species data	17.9	32.9	40.3	44.5	
of species-environment relation	100.9	98.9	0	0	
Sum of all eigenvalues					2.255
Sum of all canonical eigenvalues					0.405

Analysis of local transfer function reconstruction

Figure 6.10 shows the MAT reconstruction diagnosis for OB5 using the dataset OBDMc and model WAPLS C2, showing the samples which have poor or no modern analogues in the dataset. It shows that 12 samples have poor analogues with the modern data and only 3 samples have good analogues. Figure 6.11 shows the reconstructed palaeo-marsh elevation (PME) using the model WAPLS C2 showing the error bars from the bootstrapped SE_{pred} results as well as the poor analogue samples. Figure 6.11 shows a general increase in marsh elevation up-core until a depth of 22 cm, after which there is a decline in surface elevation. The marsh surface elevation was then converted into past MTL, which can be seen in figure 6.12 plotted against depth. Figure 6.13 shows the same MTL reconstruction plotted against the estimated chronology which was establish in chapter 5, and includes the errors associated with the MTL reconstruction as well as the errors associated with the chronology. It is also plotted along with the available tide gauge data from Liverpool. It shows that from 1985 to 1993 there is an increase in MTL, followed by a decrease in MTL between 1993 and 1998. From 1998 to 2006 there is again an increase but this time is rather rapid (max of 11.8 cm $year^{-1}$). Figure 6.13 also illustrates that the reconstructed MTL is not comparable with that recorded by the Liverpool tide gauge.

Table 6.11 DCCA for OBDM with elevation only.

Axes	1	2	3	4	Total inertia
Eigenvalues	0.373	0.372	0.169	0.093	2.254
Lengths of gradient	2.006	2.818	2.784	1.742	
Species-environment correlations	0.834	0	0	0	
Cumulative percentage variance					
of species data	16.6	33.1	40.5	44.7	
of species-environment relation	101.3	99	0	0	
Sum of all eigenvalues					2.254
Sum of all canonical eigenvalues					0.373

Table 6.12 Results of different models with different pruned OBDM3 datasets.

			Model Performance					Cross-validation				Samples with MA	
Data	Dataset Name	Model	RMSE	R^2	Max bias	r^2_{jack}	Max $bias_{jack}$	$RMSEP_{jack}$	r^2_{boot}	Max $bias_{boot}$	$RMSEP_{boot}$	OB5	DMC1
OBSS1, 3 and DM Pruned 2	OBDM3b	WATOL Inv	0.119	0.868	0.152	0.836	0.171	0.133	0.843	0.171	0.139	24	11
		WATOL Clas	0.131	0.865	0.130	0.815	0.150	0.153	0.835	0.151	0.152	19	11
OBSS1, 3 and DM Pruned 2	OBDM3c	WAPLS C1	0.132	0.826	0.214	0.794	0.251	0.144	0.791	0.253	0.150	25	11
OBSS1, 3 and DM Pruned 6		WAPLS C2	0.110	0.879	0.118	0.830	0.132	0.131	0.827	0.132	0.142		
	OBDM3d	MAT	0.119	0.876	0.170	0.876	0.170	0.119	0.873	0.197	0.136	25	11
OBSS1, 3 and DM Pruned 3		WMAT	0.113	0.881	0.163	0.881	0.163	0.113	0.878	0.181	0.126		

Table 6.13 Results of different models with different pruned OBDM datasets.

			Model Performance					Cross-validation				Samples with MA	
Data	Dataset Name	Model	RMSE	R^2	Max bias	r^2_{jack}	Max $bias_{jack}$	$RMSEP_{jack}$	r^2_{boot}	Max $bias_{boot}$	$RMSEP_{boot}$	OB5	DMC1
OBDM Pruned 5	OBDMb	WATOL Inv	0.132	0.817	0.149	0.783	0.173	0.143	0.783	0.177	0.152	26	11
OBDM Pruned 6		WATOL Clas	0.144	0.823	0.106	0.792	0.118	0.153	0.791	0.129	0.160	25	11
OBDM Pruned 12	OBDMc	WAPLS C1	0.117	0.835	0.186	0.810	0.209	0.125	0.810	0.210	0.129	26	11
		WAPLS C2	0.097	0.887	0.132	0.853	0.144	0.111	0.850	0.142	0.118		
OBDM Pruned 4	OBDMd	MAT	0.118	0.847	0.259	0.847	0.259	0.118	0.856	0.253	0.126	25	11
		WMAT	0.107	0.866	0.217	0.866	0.217	0.107	0.867	0.225	0.116		

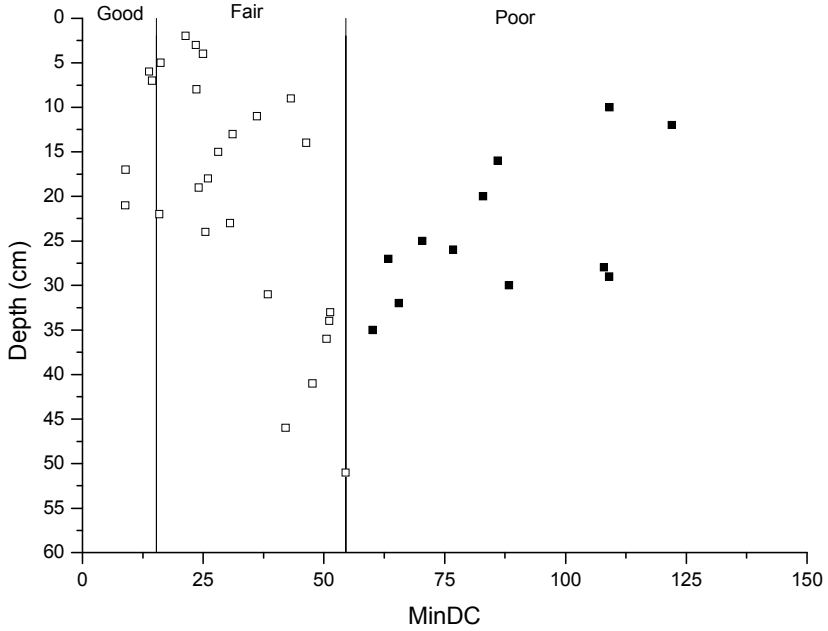

Figure 6.10 MAT reconstruction diagnosis results for OB5 using dataset OBDMc and model WAPLS C2. Open squares show samples which have good to fair modern analogues. Black squares show samples which have poor modern analogues.

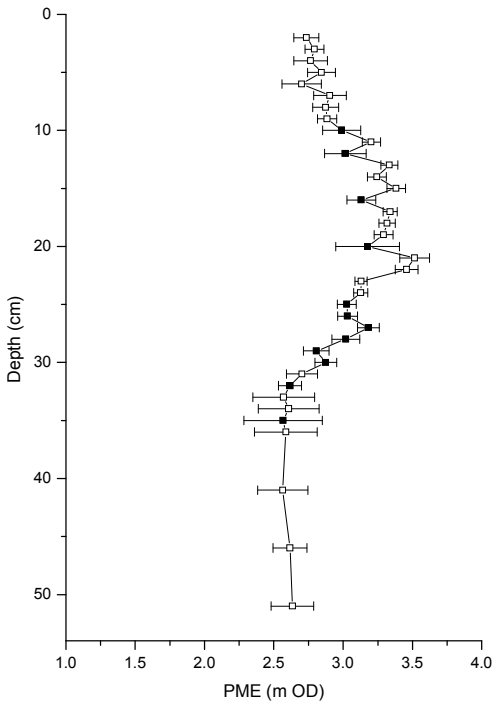

Figure 6.11 Reconstructed palaeo-marsh elevation of OB5, using dataset OBDMc and model WAPLS C2. Open squares show samples which have good to fair modern analogues. Black squares show samples which have poor modern analogues.

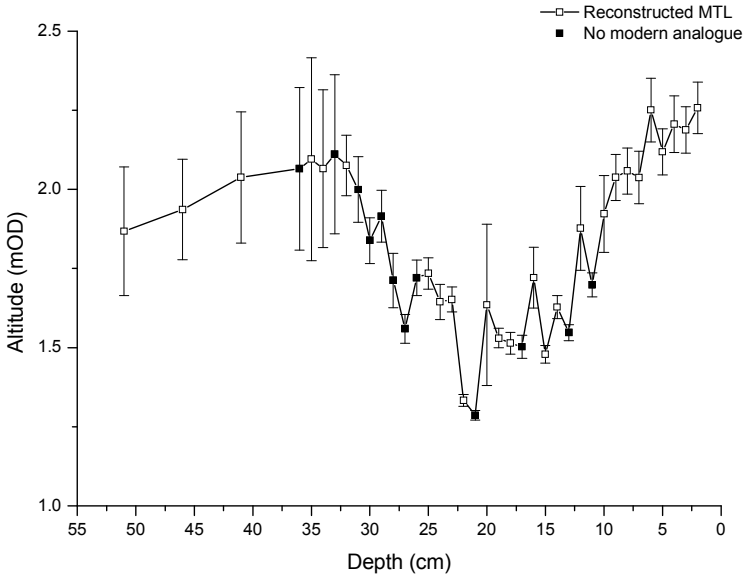

Figure 6.12 Reconstructed MTL for OB5 using dataset OBDMc and model WAPLS C2 plotted against depth. Open squares show samples which have good to fair modern analogues.

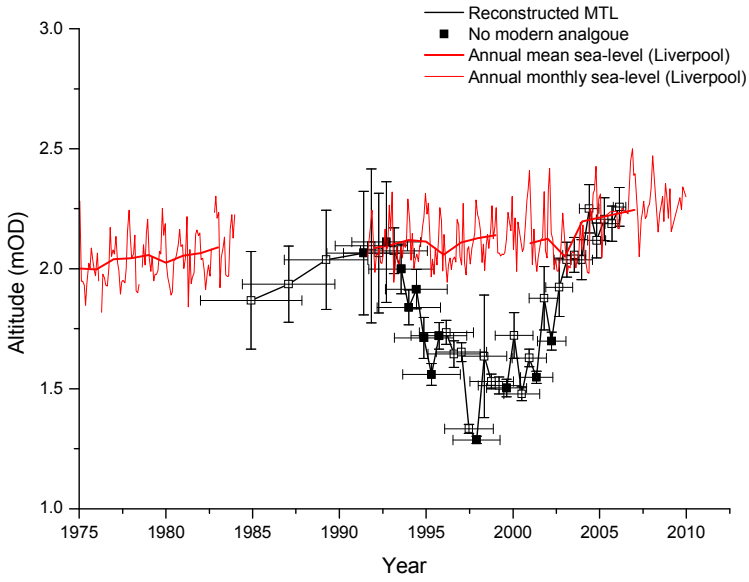

Figure 6.13 Reconstructed MTL for OB5 using dataset OBDMc and model WAPLS C2, plotted against chronology. Open squares show samples which have good to fair modern analogues. The annual and monthly mean sea-level from Liverpool tide gauge (PSMSL) are included. As MTL is different at the study site and tide gauge site, 1.725 m was added to the instrumental data in order for the records to be compared more easily.

Figure 6.14 shows the MAT reconstruction diagnosis for DMC1 using the dataset OBDMc and the WAPLS C2 model, showing that all samples have good to fair modern analogues, with 7 samples being classified as 'good' and 4 classified as 'fair'. Figure 6.15 shows the reconstructed palaeo-marsh elevation using the same model and dataset. The figure shows a general decrease in marsh elevation up-core, with a slight dip in marsh elevation between 6 and 3 cm. The marsh surface elevation was then converted into palaeo-MTL, which can be seen in figure 6.16. It shows a general trend of increasing MTL with a slight decrease in MTL at a depth of 2 cm. Figure 6.17 shows the same data plotted against the estimated chronology established from chapter 6, with the addition of the available tide gauge data from Liverpool. The errors associated with the MTL reconstruction and chronology are also included. It shows that the MTL generally increases up until 2002, were it decreases slightly. The MTL reconstruction compares well with the tide gauge data.

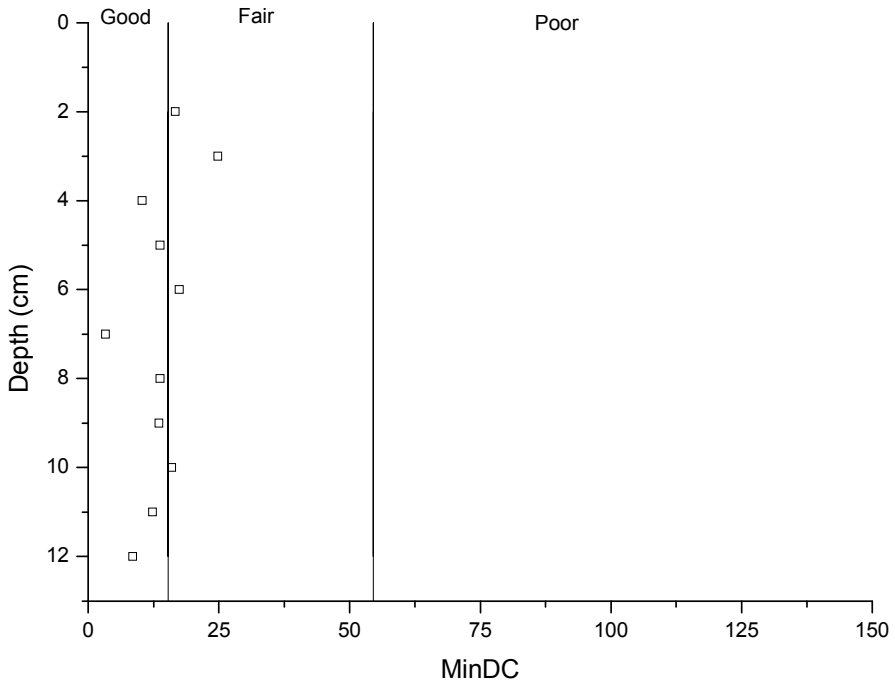

Figure 6.14 MAT reconstruction diagnosis results for DMC1 using dataset OBDMc and model WAPLS C2.

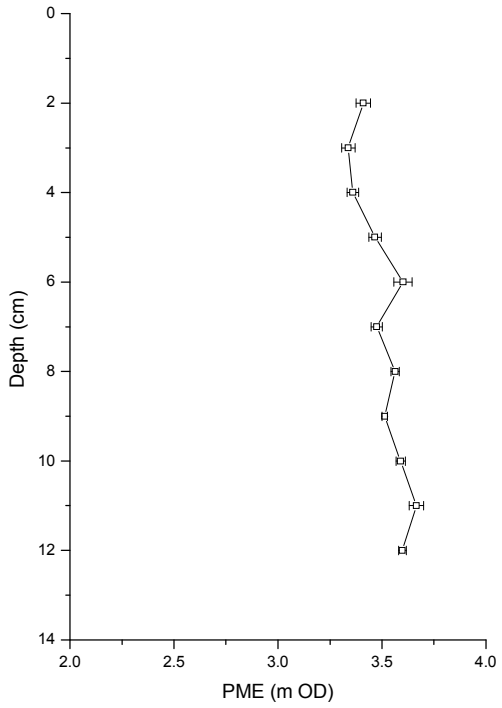

Figure 6.15 Reconstructed palaeo-marsh elevation of DMC1, using dataset OBDMc and model WAPLS C2.

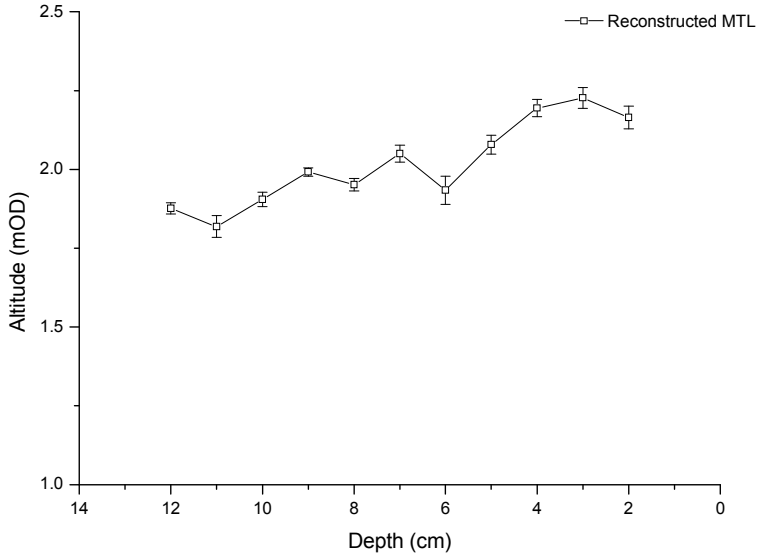

Figure 6.16 Reconstructed MTL for DMC1 using dataset OBDMc and model WAPLS C2 plotted against depth. Open squares show samples which have 'good' to 'fair' modern analogues.

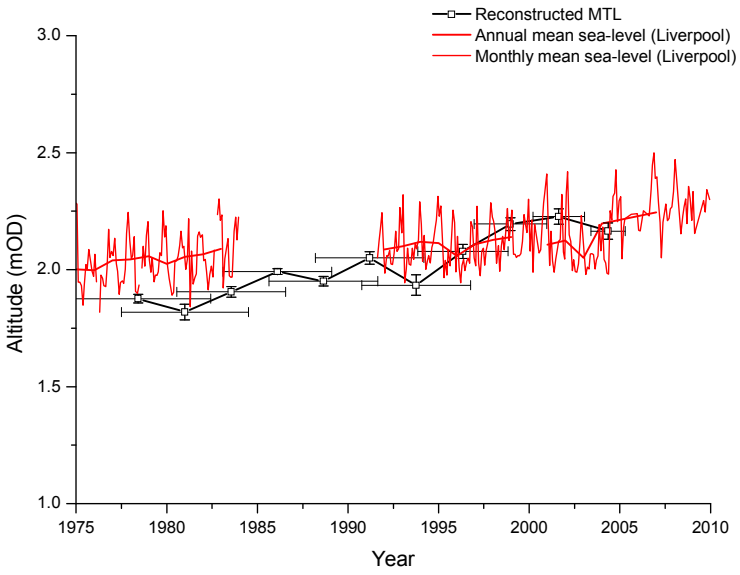

Figure 6.17 Reconstructed MTL for DMC1 using dataset OBDMc and model WAPLS C2, plotted against chronology and with annual and monthly mean sea-level from Liverpool tide gauge.

UK sites

As the OB5 core still contains 12 samples out of 28 which have no modern analogue in the modern dataset (OBDMc), additional data for UK sites taken from Horton and Edwards (2006) were used to create a regional transfer function, which was applied to the two cores from this study. Analysis was carried out similar to the Oglet Bay and Decoy Marsh data with different datasets and models being tested and the most appropriate chosen. Table 6.14 shows the results of the DCCA for all the Horton and Edwards (2006) (H&E) sites, and shows the gradient length to be 2.55 SD, which is on the unimodal end of the scale but both statistical analyses may still be applied. The results of the different model analysis can be seen in table 6.15. It shows that using all the H&E data produces comparatively low r^2_{jack} values and high $RMSEP_{jack}$ values. It is important, however, to keep in mind that the $RMSEP_{jack}$ is a proportion of the SWLI, which was standardised to 100, therefore the RMSEP will be much greater than for the local dataset. The 'best' models were WA, WA tol, WAPLS and MAT and WMAT. The data were pruned individually for these models to remove outliers, and the results can be seen in table 6.15 also. It shows that the data improved greatly, with much higher r^2_{jack} and lower $RMSEP_{jack}$, although the number of good to fair analogues for the fossil data using this dataset remained the same, which was less than that which was achieved from the present study's data alone (OBDMc). Since the two cores were collected from North West England, the analysis was repeated with only North West

UK sites included (Kentra Marsh, Tramaig Bay and Roudsea Marsh, (see figure 1.4)), with the aim being to reduce the dataset to a more regional dataset which may be more appropriate. The results were found to be very poor (table 6.15), except for the r^2_{jack} of WAPLS C2; the number of samples having no modern analogues in the fossil data also increased.

As the UK dataset included 13 sites, each of these was tested individually to determine which were the most appropriate to improve the transfer functions' performance. As the WAPLS model was found to perform the 'best', excluding MAT, this was the only analysis used to test the sites. The results of this can be seen in table 6.16. As several of the sites contain fewer than 10 samples the results were not included in the table as performance tests using jack-knifing and bootstrapping cannot be carried out. The number of modern analogues the data have for the fossil record is very low for the sites, similar to the results for the individual transects for the data from the present study (table 6.7). Many of the sites had high r^2_{jack} and low $RMSEP_{jack}$. The 'best' sites were chosen to be the sites with higher r^2_{jack}, lower $RMSEP_{jack}$ and/or higher numbers of modern analogues for the fossil record. These were found to be Alnmouth Marsh, Arne Peninsula, Brancaster and Thornham Marshes, Keyhaven Marsh, Nith Estuary and Roudsea Marsh. These were used to create a new regional transfer function (H&E 7a) (table 6.16). The performance tests showed that the data performed well with high r^2_{jack} (0.853), low $RMSEP_{jack}$ (6.714) and had 19 modern analogues in the OB5 fossil dataset.

Table 6.14 DCCA for H&E (2006) with only elevation.

Axes	1	2	3	4	Total inertia
Eigenvalues	0.3	0.812	0.575	0.286	4.402
Lengths of gradient	2.55	4.315	3.259	3.788	
Species-environment correlations	0.659	0	0	0	
Cumulative percentage variance					
of species data	6.8	25.3	38.3	44.8	
of species-environment relation	98	93.9	0	0	
Sum of all eigenvalues					4.402
Sum of all canonical eigenvalues					0.3

Table 6.15 Results of different models with different UK datasets from Horton and Edwards (2006).

			Model Performance					Cross-validation				Samples with MA	
Data	Dataset name	Model	RMSE	R^2	Max bias	r^2_{jack}	Max $bias_{jack}$	$RMSEP_{jack}$	r^2_{boot}	Max $bias_{boot}$	$RMSEP_{boot}$	OB5	Dmc1
H&E 13 sites	H&E a	WA_Inv	15.649	0.467	65.216	0.439	66.716	16.051	0.438	66.659	16.237	21	11
		WA_Cla	22.899	0.467	54.913	0.447	57.835	23.281	0.447	58.205	22.888		
		WATOL Inv	15.388	0.485	67.527	0.454	68.903	15.835	0.451	69.398	16.173		
		WATOL Cla	22.104	0.485	60.385	0.462	62.930	22.365	0.459	64.092	22.122		
		WAPLS C1	15.649	0.467	65.205	0.439	66.714	16.052	0.437	67.071	16.265		
		WAPLS C2	14.650	0.533	61.539	0.475	65.621	15.579	0.473	66.499	16.375		
		PLSC1	16.917	0.377	66.095	0.354	67.205	17.229	0.358	67.258	17.276		
		PLS C2	16.085	0.437	63.331	0.399	65.699	16.621	0.400	66.022	16.802		
		MAT	15.229	0.498	61.918	0.497	61.918	15.236	0.500	62.498	16.023		
		WMAT	13.999	0.559	72.326	0.559	72.326	13.999	0.550	75.326	14.920		
H&E a Pruned 19	H&E b	WAPLS C1	9.081	0.703	13.340	0.674	13.704	9.525	0.678	13.875	9.617	21	11
		WAPLS C2	8.540	0.738	13.073	0.697	13.579	9.183	0.703	13.388	9.657		
H&E NW sites	H&E NW	WA_Inv	19.138	0.568	49.784	0.116	86.971	28.231	0.113	87.419	30.210	17	11
		WA_Cla	25.403	0.568	53.243	0.172	82.784	31.730	0.136	77.189	36.423		
		WATOL Inv	20.893	0.485	57.476	0.010	105.793	33.527	0.020	104.751	32.291		
		WATOL Cla	30.014	0.485	41.009	0.000	149.285	47.959	0.020	108.807	41.737		
		WAPLS C1	19.139	0.568	49.641	0.116	87.010	28.228	0.145	85.332	30.033		
		WAPLS C2	10.924	0.859	31.389	0.576	64.869	19.600	0.494	67.180	25.602		
		PLSC1	26.536	0.169	81.283	0.007	96.736	30.456	0.014	95.969	31.638		
		PLS C2	17.956	0.619	40.908	0.030	93.515	30.587	0.099	89.474	31.159		
		MAT	30.772	0.023	104.101	0.024	104.101	30.791	0.000	101.893	31.098		
		WMAT	27.444	0.169	99.509	0.169	99.509	27.444	0.216	98.002	27.910		

Table 6.16 Results of different models with different UK sites from Horton and Edwards (2006).

			Model Performance					Cross-validation				Samples with MA	
Data	Dataset name	Model	RMSE	R^2	Max bias	r^2_{jack}	Max bias $_{jack}$	RMSEP $_{jack}$	r^2_{boot}	Max bias $_{boot}$	RMSEP $_{boot}$	OB5	Dmc1
Alnmouth	H&E S1	WAPLS C1	6.583	0.868	9.102	0.816	10.738	7.775	0.819	10.628	8.138	3	1
		WAPLS C2	5.211	0.917	6.194	0.866	7.470	6.632	0.872	7.640	7.257		
Cowpen	H&E S2	WAPLS C1	11.298	0.702	22.125	0.650	24.032	12.244	0.655	24.674	12.486	0	0
		WAPLS C2	5.591	0.927	9.551	0.819	21.719	8.817	0.796	19.907	10.987		
Welwick	H&E S3	WAPLS C1	5.011	0.471	8.871	0.375	9.62759	5.45586	0.350	9.766	5.978	0	0
		WAPLS C2	4.128	0.641	7.469	0.375	8.71491	5.77152	0.366	8.804	6.714		
Thornham	H&E S4	WAPLS C1	6.706	0.790	12.677	0.716	17.090	7.793	0.705	17.234	8.392	1	1
		WAPLS C2	5.918	0.836	10.925	0.702	19.759	8.353	0.716	19.456	9.067		
Brancaster	H&E S5	WAPLS C1	1.488	0.946	2.142	0.923	3.380	1.791	0.922	4.738	2.287	1	0
		WAPLS C2	1.218	0.964	1.609	0.922	2.103	1.790	0.925	3.141	2.309		
Bury	H&E S6	WAPLS C1	15.865	0.637	43.338	0.432	51.752	20.447	0.431	49.570	23.622	0	2
		WAPLS C2	14.732	0.687	42.346	0.465	52.501	19.914	0.447	50.720	25.007		
Keyhaven	H&E S7	WAPLS C1	2.494	0.980	2.412	0.963	5.912	3.833	0.956	12.663	7.809	0	0
		WAPLS C2	1.858	0.989	0.352	0.970	1.324	3.130	0.974	5.458	5.878		
Arne Peninsula	H&E S8	WAPLS C1	10.823	0.836	18.220	0.672	24.753	15.656				3	4
		WAPLS C2	8.324	0.903	13.046	0.604	38.426	20.697					
Roudsea	H&E S9	WAPLS C1	2.666	0.859	5.918	0.781	7.869	3.322	0.788	7.420	3.518	7	5
		WAPLS C2	1.017	0.979	2.545	0.935	3.531	1.826	0.906	4.415	2.826		
Nith	H&E S10	WAPLS C1	3.878	0.782	5.720	0.202	21.609	7.677	0.224	21.546	7.651	4	4
		WAPLS C2	3.002	0.869	4.709	0.137	24.622	8.314	0.192	23.097	8.134		
7 sites (Alnmouth, Arne Peninsular, Brancaster, Keyhaven, Nith, Roudsea, Thornham)	H&E 7a	WAPLS C1	8.050	0.802	12.608	0.781	13.167	8.466	0.774	13.484	8.840	19	11
		WAPLS C2	6.410	0.874	11.141	0.842	12.366	7.195	0.848	13.064	7.887		
	H&E 7b (Pruned 2)	WAPLS C1	7.091	0.835	9.516	0.798	11.691	7.862	0.797	12.406	8.114	19	11
		WAPLS C2	5.547	0.899	7.818	0.853	8.501	6.714	0.853	9.344	7.160		

Local and UK datasets

As the data H&E b (all Horton and Edwards (2006) sites) or H&E 7b (7 sites from Horton and Edwards (2006)) did not improve the number of analogues compared with the OBDMc dataset, the statistical analysis was repeated with H&E added to OBDMc and OBDM3c data to investigate whether this improves the performance and which dataset was the most appropriate to use. The results of which can be seen in table 6.17 and shows the pruned dataset OBDM3c along with H&E (OBDM3c H&E) to have the 'best' performance and greatest number of modern analogues.

To try and improve the dataset further, statistical analysis for the individual H&E sites along with the modern foraminifera dataset OBDM3c was repeated in order to choose which sites were most appropriate for this study. The WAPLS model was chosen for the analysis as it was found to perform the 'best' in the previous results. Table 6.18 shows the results of the WAPLS models showing that some sites perform better than others in their relationship with elevation (r^2_{jack}), their errors ($RMSEP_{jack}$) and their modern analogues for the fossil data. For example r^2_{jack} is high, $RMSEP_{jack}$ low, and the greatest number of modern analogues for the fossil data can be seen in the Alnmouth and OBDM3c data.

The OBDM3c data were combined with all the H&E data, the North West sites and with the 'best' performance sites from table 6.18. The individual UK sites were chosen based upon those which had a greater r^2_{jack} than OBDM3c, a low $RMSEP_{jack}$ and a greater number of modern analogues for the fossil record than OBDM3c, resulting in 4 sites being chosen (Alnmouth, Kentra Marsh, Thornham Marsh and Roudsea Marsh). The data were also pruned individually to remove any outliers to see if this improved the models performance. The results of this can be seen in table 6.19 where it shows that OBDM3c with all H&E data pruned (OBDM3 H&Eb) and the smaller dataset of OBDM3c with the 4 chosen sites pruned (OBDM3H&E 4b) had the 'best' performance.

Table 6.17 Results of different models with different UK pruned datasets from Horton and Edwards (2006).

			Model Performance					Cross-validation				Samples with MA	
Data	Dataset Name	Model	RMSE	R^2	Max bias	r^2_{jack}	Max bias $_{jack}$	RMSEP $_{jack}$	r^2_{boot}	Max bias $_{boot}$	RMSEP $_{boot}$	OB5	Dmc1
OBDMa H&E	OBDMH&E A	WAPLS C1	13.914	0.486	67.816	0.463	69.141	14.225	0.462	69.205	14.384	30	11
		WAPLS C2	13.181	0.539	64.736	0.490	67.884	13.893	0.490	67.899	14.681		
OBDMa H&E Pruned 22	OBDMH&E B	WAPLS C1	8.013	0.693	13.634	0.664	15.520	8.388	0.662	16.050	8.539	30	11
		WAPLS C2	7.613	0.723	12.576	0.680	13.599	8.189	0.680	13.794	8.512		
OBDM3a H&E	OBDM3H&E A	WAPLS C1	8.394	0.692	14.203	0.660	16.198	8.813	0.660	16.393	8.955	29	11
		WAPLS C2	7.917	0.726	12.289	0.677	14.015	8.592	0.682	14.144	8.921		
OBDM3a H&E Pruned 21	OBDM3H&E B	WAPLS C1	5.494	0.855	6.899	0.838	7.669	5.800	0.840	7.961	5.908	33	11
		WAPLS C2	4.416	0.906	4.160	0.875	4.867	5.108	0.879	5.008	5.251		

Table 6.18 Different models with different UK sites from Horton and Edwards (2006) and OBDM3c.

			Model Performance				Cross-validation					Samples with MA	
Data	Dataset name	Model	RMSE	R^2	Max bias	r^2_{jack}	Max bias $_{jack}$	RMSEP $_{jack}$	r^2_{boot}	Max bias $_{boot}$	RMSEP $_{boot}$	OB5	DMC1
OBDM3a Alnmouth	OBDM3H&E 1	WAPLS C1	3.784	0.944	7.133	0.934	8.655	4.122	0.933	8.698	4.351	30	11
		WAPLS C2	3.230	0.959	3.975	0.943	5.304	3.833	0.943	5.448	4.101		
OBDM3a Cowpen	OBDM3H&E 2	WAPLS C1	7.654	0.784	24.383	0.759	26.080	8.086	0.756	26.776	8.343	23	11
		WAPLS C2	6.817	0.829	20.787	0.793	23.047	7.509	0.794	23.506	7.786		
OBDM3a Welwick	OBDM3H&E 3	WAPLS C1	5.937	0.363	18.892	0.301	19.737	6.224	0.293	19.639	6.398	23	11
		WAPLS C2	5.524	0.448	16.266	0.338	18.254	6.098	0.345	18.127	6.365		
OBDM3a Thornham	OBDM3H&E 4	WAPLS C1	6.368	0.708	20.505	0.658	23.012	6.896	0.664	22.721	7.030	29	11
		WAPLS C2	5.131	0.810	17.400	0.736	21.661	6.080	0.742	20.708	6.452		
OBDM3a Brancaster	OBDM3H&E 5	WAPLS C1	2.613	0.795	3.839	0.765	5.140	2.797	0.760	5.759	2.977	23	11
		WAPLS C2	2.342	0.835	3.183	0.793	3.415	2.626	0.793	3.228	2.786		
OBDM3a Bury	OBDM3H&E 6	WAPLS C1	11.643	0.429	68.451	0.329	73.628	12.674	0.321	73.690	13.453	22	11
		WAPLS C2	9.350	0.632	55.574	0.484	62.876	11.230	0.485	64.007	12.410		
OBDM3a Keyhaven	OBDM3H&E 7	WAPLS C1	5.572	0.606	15.936	0.464	23.430	6.516	0.458	24.802	6.872	26	11
		WAPLS C2	4.632	0.728	7.458	0.567	17.044	5.847	0.565	20.593	6.716		
OBDM3a Newton	OBDM3H&E 8	WAPLS C1	4.087	0.566	19.201	0.522	19.882	4.291	0.522	19.745	4.425	22	11
		WAPLS C2	3.729	0.639	18.115	0.557	19.104	4.162	0.561	18.905	4.352		
OBDM3a Arne Peninsular	OBDM3H&E 9	WAPLS C1	5.878	0.746	8.918	0.663	13.241	6.791	0.620	15.111	8.010	26	11
		WAPLS C2	4.942	0.821	8.546	0.685	26.737	6.945	0.701	12.546	7.815		
OBDM3a Rousdsea	OBDM3H&E 10	WAPLS C1	3.036	0.730	5.370	0.694	6.771	3.236	0.694	6.764	3.320	26	11
		WAPLS C2	2.548	0.810	5.761	0.743	8.122	2.975	0.751	7.897	3.098		
OBDM3a NIth	OBDM3H&E 11	WAPLS C1	3.203	0.723	8.448	0.568	19.449	4.015	0.606	18.780	3.203	22	11
		WAPLS C2	2.908	0.772	5.703	0.551	21.293	4.127	0.617	19.124	2.908		
OBDM3a Tramiag	OBDM3H&E 12	WAPLS C1	12.458	0.656	57.839	0.572	63.415	13.898	0.535	62.881	15.920	25	11
		WAPLS C2	10.364	0.762	43.471	0.576	60.960	14.970	0.557	60.251	17.025		
OBDM3a Kentra	OBDM3H&E 13	WAPLS C1	4.335	0.751	17.471	0.719	17.976	4.615	0.720	17.972	4.741	26	11
		WAPLS C2	3.798	0.809	17.261	0.774	18.318	4.137	0.777	18.084	4.350		

Table 6.19 Different models with different UK datasets from Horton and Edwards (2006) and OBDM3c.

			Model Performance					Cross-validation				Samples with MA	
Data	Dataset name	Model	RMSE	R^2	Max bias	r^2_{jack}	Max bias $_{jack}$	RMSEP $_{jack}$	r^2_{boot}	Max bias $_{boot}$	RMSEP $_{boot}$	OB5	Dmc1
OBDM3a Alnmouth Kentra Thornham Roudsea	OBDM3H&E 4a	WAPLS C1	7.341	0.770	14.416	0.743	15.905	7.757	0.742	16.322	7.984	32	11
		WAPLS C2	5.828	0.855	9.570	0.807	12.369	6.738	0.813	12.329	7.061		
OBDM3H&E 4a Pruned 6	OBDM3H&E 4b	WAPLS C1	5.494	0.855	6.899	0.838	7.669	5.800	0.840	7.961	5.908	32	11
		WAPLS C2	4.416	0.906	4.160	0.875	4.867	5.108	0.879	5.008	5.251		
OBDM3a H&E NW	OBDM3H&E NW	WAPLS C1	14.316	0.458	59.382	0.236	92.304	17.219	0.236	90.438	17.814	27	11
		WAPLS C2	10.973	0.682	49.897	0.432	62.523	14.688	0.424	68.316	16.211		
OBDM3a H&E NW Pruned 6	OBDM3H&E NWb	WAPLS C1	4.785	0.687	14.870	0.650	15.702	5.069	0.655	15.729	5.215	27	11
		WAPLS C2	4.330	0.744	13.369	0.696	14.802	4.720	0.698	14.807	5.106		

Analysis of all transfer function reconstructions

Figure 6.18 shows the reconstructed marsh elevation for OB5 and figure 6.19 for DMC1, comparing different datasets (local: OBb, OBDMc, OBDM3c, regional: H&Eb, H&E 7b, and combined: OBDM3H&Eb, OBDM3H&E 4b) using the WAPLS C2 model. Figure 6.18 shows that each of the models gives slightly different reconstructions with different analogues and errors associated with them. OBDM and OBDM3c have similar trends in PME up-core, with little change up until 35 cm. This is followed by an increase in PME up until 20 cm where there is then an up-core decrease in PME. The OBDM3c model, however, has a sharp fall in PME at 20 cm which is not seen in OBDMc but is in OBb; it also increases more greatly then OBDMc. The other transfer functions OB, OBDM3 H&E and OBDM3 H&E 4b show similar models all differing from OBDMc and OBDM3c, with a fall in PME/SWLI between 50 and 35 cm. Transfer functions H&Eb and H&E 7b have similar reconstructions with larger changes in elevation than the other transfer functions. The two differ slightly in the lower half of the core with transfer function H&Eb having an increase in SWLI between 35 and 50 cm whereas H&E 7b is more similar to the other transfer functions OBDM3H&Eb and OBDM3H&E 4b. The H&Eb transfer function also has larger errors but has more modern analogues.

Figure 6.19 shows the models for DMC1, where there is much less change in the PME/SWLI than for OB5. All models are similar, excluding model H&Eb which has larger changes than the other models. The trend from this dataset also appears to be opposite to the other models, for example it has a fall in SWLI at 8 cm depth where other models show a slight increase. H&Eb also has greater errors. H&E 7b also has much fewer changes in SWLI than the other transfer functions, but has similar errors to H&Eb.

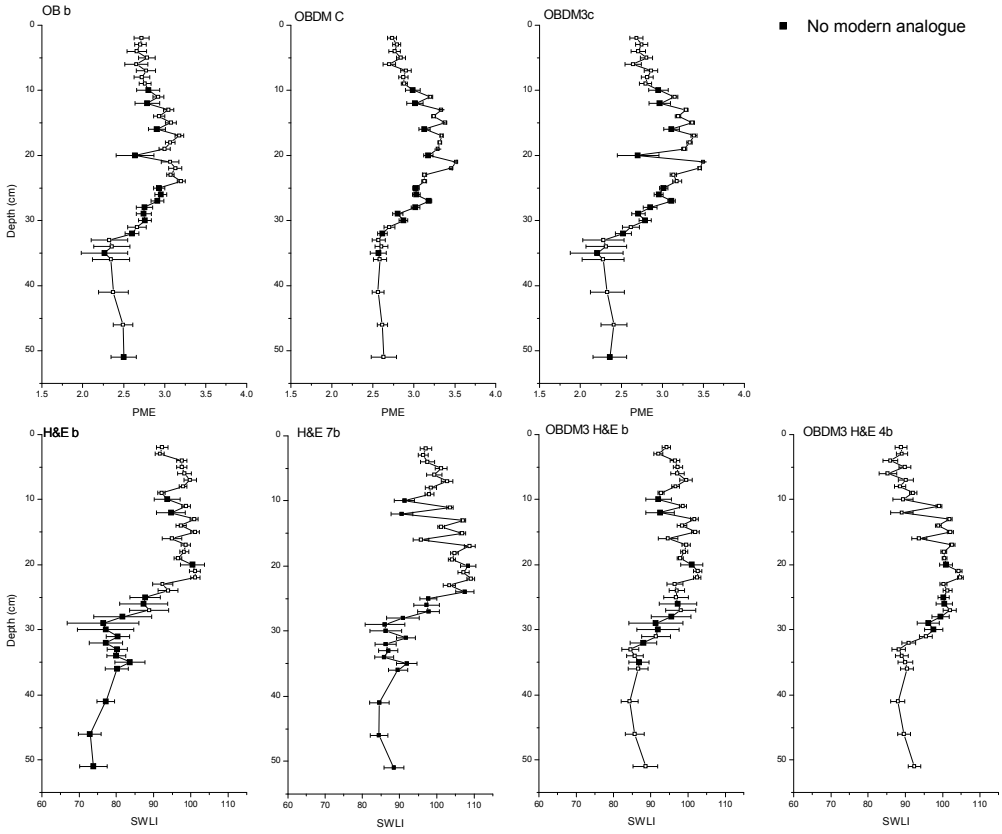

Figure 6.18 Reconstructed marsh elevation and SWLI of OB5, with different datasets with the model WAPLS c2. Open squares show samples which have 'good' to 'fair' modern analogues. Black squares show samples which have poor modern analogues

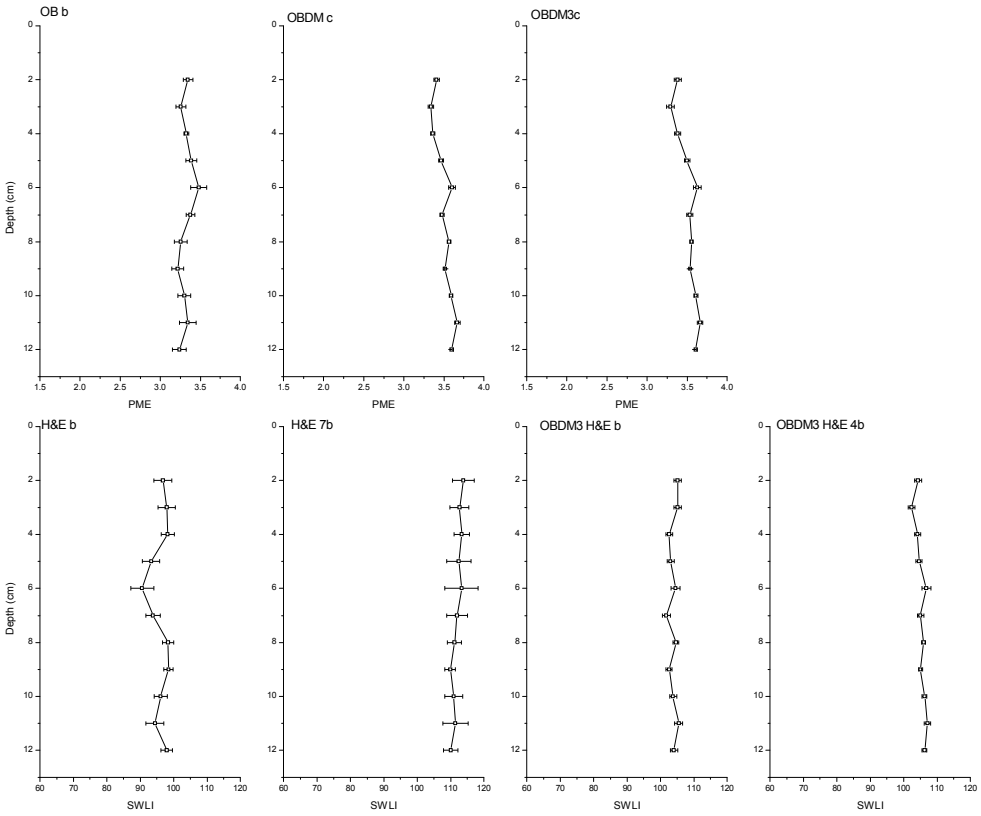

Figure 6.19 Reconstructed marsh elevation and SWLI of DMC1 with different datasets with the model WAPLS c2.

To identify which of the datasets may be more reliable, the WAPLS reconstructions were compared with ML reconstructions in order to determine if the selection of the statistical technique is controlling the outcome. This comparison will provide some verification of the statistical reliability of the transfer functions (Horton and Edwards, 2006). As WAPLS is an inverse statistical method, ML is used for the comparison as it is complementary to this method (e.g. Edwards and Horton, 2000; Horton and Edwards, 2006). The results of comparisons between WAPLS with ML reconstructions can be seen in table 6.20 and figures 6.20 and 6.21.

Figure 6.20 shows both sets of reconstructions (WAPLS and ML) for OB5. It shows that some of the datasets have greater consistency between the two transfer functions than others. The ML reconstructions in general have larger errors, particularly for OBb, OBDMc, OBDM3c and H&Eb. The ML reconstructions also have additional and more exaggerated peaks than the WAPLS reconstructions for the OBb, OBDMc and OBDM3c datasets. For the lower half of the H&E dataset, the ML has a much lower SWLI than the WAPLS reconstruction. There is some overlap between ML and WAPLS models for OBDMH&Eb, although there are sharper peaks in ML and a larger SWLI in the lower half of the core than

for WAPLS. The H&E 7b and OBDM3H&E 4b SWLI reconstructions using WAPLS and ML appear the most similar, with greater overlap between the models and similar trends.

Figure 6.21 shows the results of the reconstructed marsh elevation of DMC1 with the two methods (ML and WAPLS). The OBb dataset using the model ML can be seen to have a completely different trend to the WAPLS model and also to the other ML models with the different datasets. The ML OBb model seems to have opposite trends in PME in the lower half of the core but a similar trend in the upper part. The H&Eb and OBDM3c H&Eb ML reconstructions show similar trends to each other and to the WAPLS models, but have generally high SWLI for the lower half of the core. Datasets OBDMc, OBDM3c, H&E 7b and OBDM3H&E 4b show very similar trends in the WAPLS and ML PME/SWLI reconstructions with OBDMc and OBDM3c models mostly overlapping, and the OBDM3H&E 4b ML model having slightly higher SWLI than the WAPLS model.

Table 6.20 Results of ML model with different datasets.

			Model Performance					Cross-validation				Samples with MA	
Data	Dataset name	Model	RMSE	R^2	Max bias	r^2_{jack}	Max bias $_{jack}$	RMSEP $_{jack}$	r^2_{boot}	Max bias $_{boot}$	RMSEP $_{boot}$	OB5	Dmc1
OB	OB a	ML	0.219	0.612	0.192	0.561	0.195	0.230	0.591	0.207	0.233	20	11
OB Pruned 12	OB (ML b)	ML	0.144	0.784	0.126	0.723	0.154	0.159	0.778	0.134	0.154		
OBDM	OBDM	ML	0.673	0.074	1.474	0.097	1.481	0.686	0.078	1.890	1.933	25	11
OBDM Pruned 7	OBDM (ML b)	ML	0.130	0.851	0.165	0.832	0.231	0.137	0.805	0.262	0.168		
OBDM3	OBDM3 a	ML	0.154	0.829	0.202	0.799	0.287	0.163	0.799	0.293	0.270	25	11
OBDM3 Pruned 4	OBDM (ML b)	ML	0.123	0.879	0.173	0.860	0.213	0.130	0.123	0.879	0.173		
H&E	H&E	ML	18.507	0.482	56.400	0.442	59.872	19.131	0.458	62.734	19.179	20	11
H&E 4 Pruned 7	H&E (ML b)	ML	9.809	0.786	17.295	0.732	19.182	10.977	0.490	29.175	55.058		
H&E 7	H&E 7 (ML a)	ML	24.164	0.478	101.908	0.551	21.018	16.961	0.739	35.545	17.760	19	11
H&E 7 Pruned 2	H&E 7 (ML b)	ML	7.971	0.827	19.633	0.780	21.133	8.920	0.799	20.789	9.523		
OBDM3 H&E	OBDM3H&E (ML a)	ML	17.131	0.489	56.581	0.454	60.706	17.636	0.462	61.872	17.824	29	11
OBDM3 H&E Pruned 59	OBDMSH&E (ML b)	ML	9.399	0.775	14.953	0.753	17.026	9.669	0.703	16.446	22.176		
OBDM3 H&E 4 sites	OBDMH&E 4 (ML a)	ML	195.046	0.071	179.773	0.058	80.956	141.526	0.142	35.129	86.309	33	11
OBDM3 H&E 4 sites Pruned 12	OBDMH&E 4 (ML b)	ML	5.550	0.871	10.041	0.828	11.028	6.334	0.824	11.067	6.960		

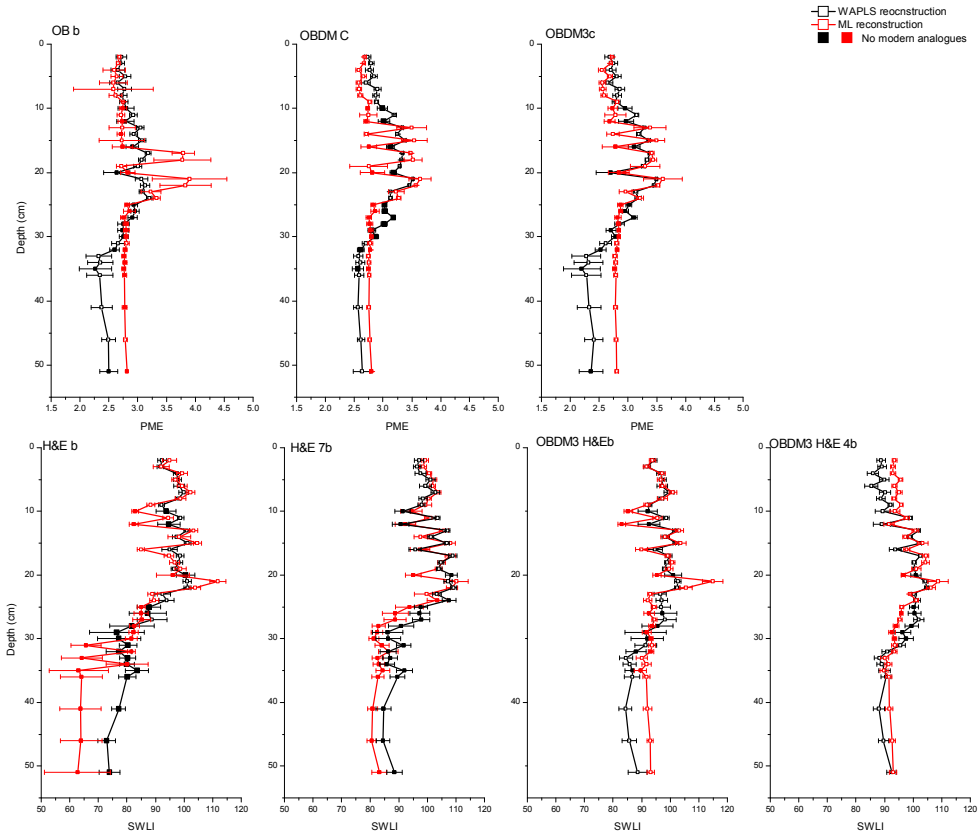

Figure 6.20 Reconstructed marsh elevation and SWLI of OB5 with different datasets with WAPLS and ML models.

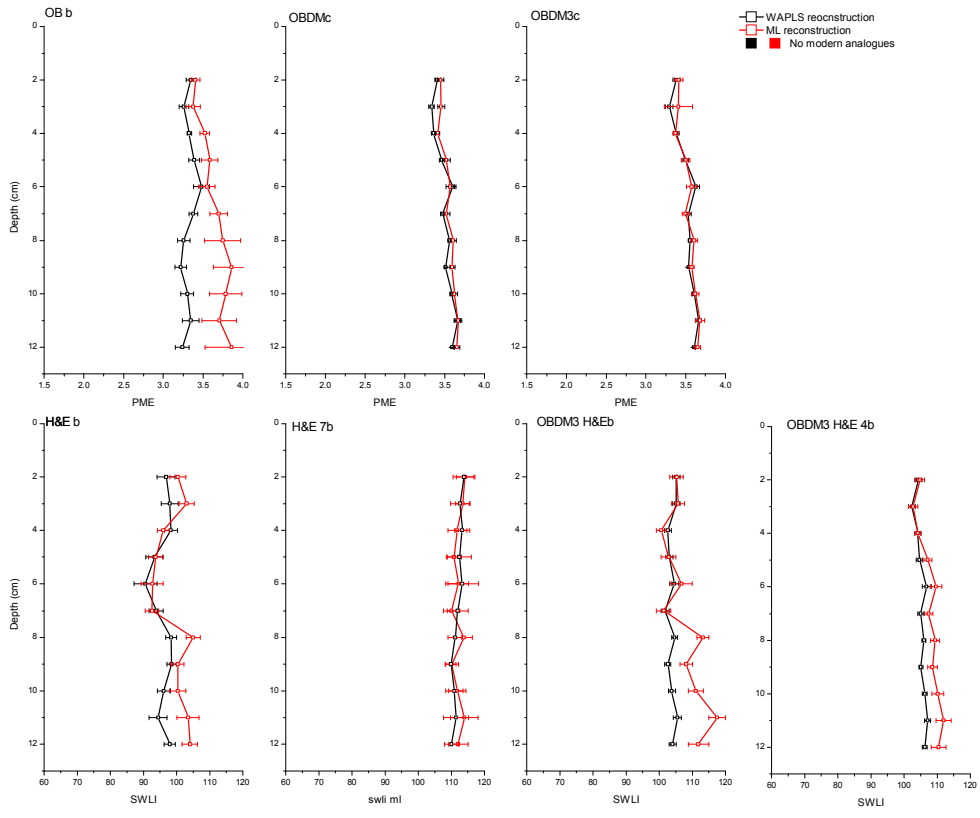

Figure 6.21 Reconstructed marsh elevation and SWLI of DMC1 with different datasets with WAPLS and ML models.

The statistical significance of the different reconstructions has been tested, and the results of this can be seen in figures 6.22 to 6.28 (additional results for different datasets in appendix 5). WAPLS and MAT transfer functions were used for the Oglet Bay and Decoy Marsh data alone, as Telford (2011) stated that if there are few species in the modern data then MAT reconstructions have more statistical power than those based upon WA methods. When the Horton and Edwards (2006) data were included, there were more species and therefore only WAPLS were included.

The histograms show the proportion of variance explained in the fossil record by the 999 transfer functions trained on random data. It shows the difference in how much variance is explained using the different random transfer functions. The mean and median given in the centre of the histogram are the average variances explained by the 999 random transfer functions. The dotted line shows the variance explained by the first axis of a PCA which is the most variance that could possibly be explained by any data, as this is a theoretical variable. The black line is the variance explained by the data from this study. How significant the transfer functions from this study are, is based upon how much variance explained overlaps with the variance explained by the random transfer function. The less overlap and the closer it is to the results from those results of the PCA, the more significant it will be.

Figures 6.22 and 6.23 show the results of the significance tests for the dataset OBDM for the models WAPLS (figure 6.22) and MAT models (figure 6.23). Both reconstructions (figure 6.24) were found to be significant, with the pruned data (figure 6.22 b) having a slightly larger p-value than the un-pruned (figure 6.22 a). The MAT OBDM model (figure 6.23) can also be seen to be significant, with a low p-value (0.004). This shows that all models using the dataset OBDM produce a statistically significant transfer function.

Figures 6.24 and 6.25 show the results for OBDM3a and OBDM3c for WAPLS (figure 6.24) and MAT (figure 6.25). They illustrate that all three models produce a significant transfer function with the WAPLS models being more significant than the MAT model.

Figure 6.26 shows the results for the model H&E and H&Eb using WAPLS. It shows that the un-pruned model (figure 6.26a) is of reduced significance (p=0.056) but the pruned model (figure 6.26b) does produces a more significant transfer function, with a p-value of 0.002.

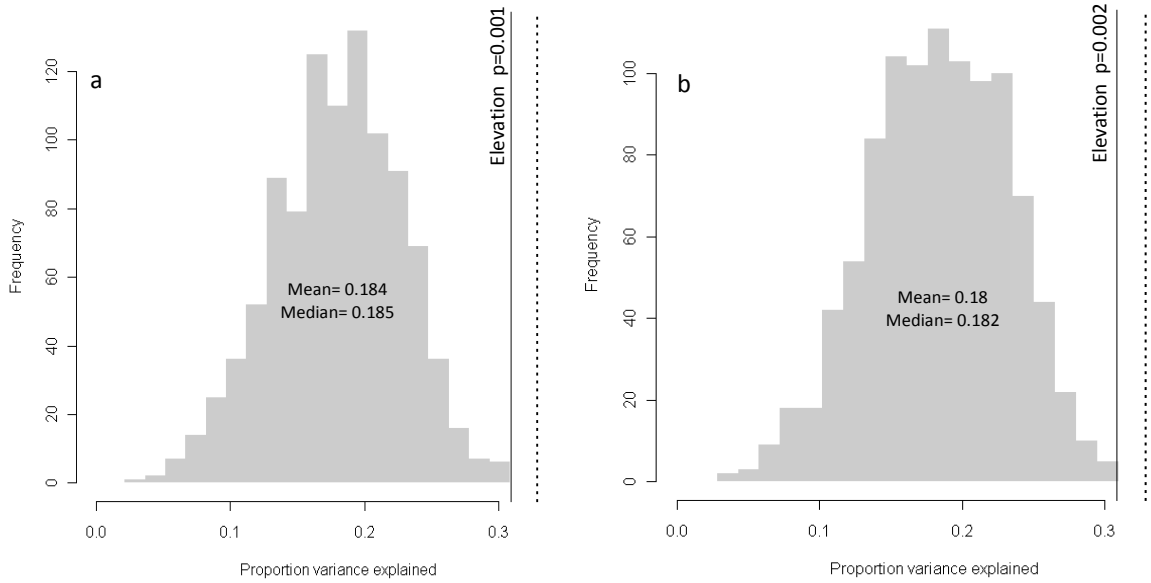

Figure 6.22 Histogram of the proportion of variance in the OB5 record explained by 999 WAPLS transfer functions trained by random data. Solid black line is the proportion of variance explained by transfer functions trained by a) OBDM 4 b) OBDM c datasets. Dotted black line is the proportion of the variance explained by the 1st axis of a PCA of OB5.

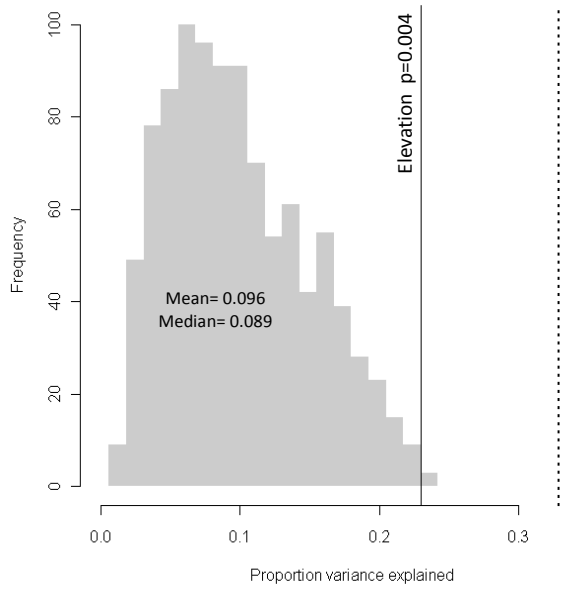

Figure 6.23 Histogram of the proportion of variance in the OB5 record explained by 999 MAT transfer functions trained by random data. Solid black line is the proportion of variance explained by transfer functions trained by OBDM dataset. Dotted black line is the proportion of the variance explained by the 1st axis of a PCA of OB5.

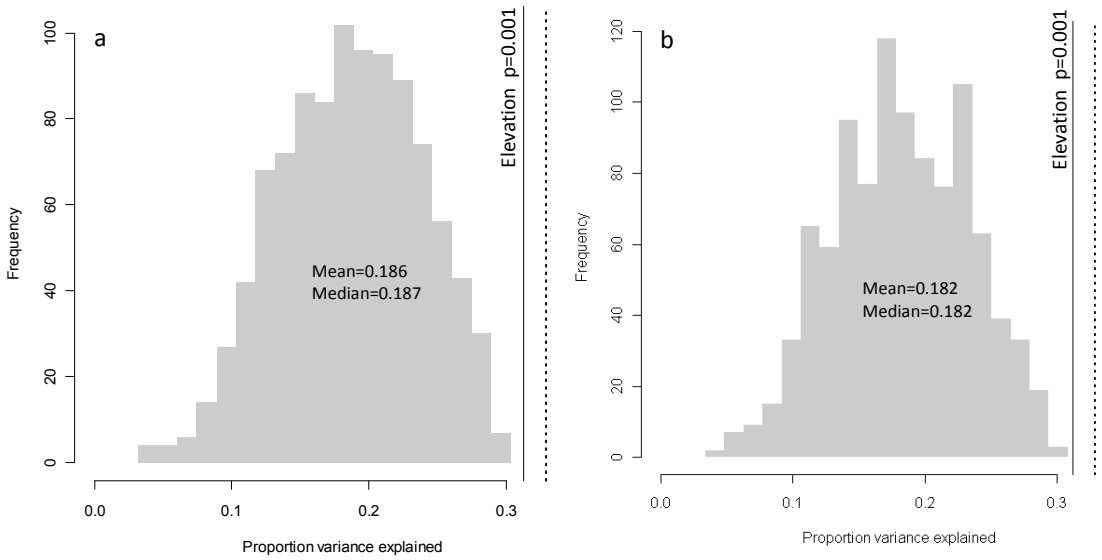

Figure 6.24 Histogram of the proportion of variance in the OB5 record explained by 999 WAPLS transfer functions trained by random data. Solid black line is the proportion of variance explained by transfer functions trained by a) OBDM3a b) OBDM3c datasets. Dotted black line is the proportion of the variance explained by the 1st axis of a PCA of OB5.

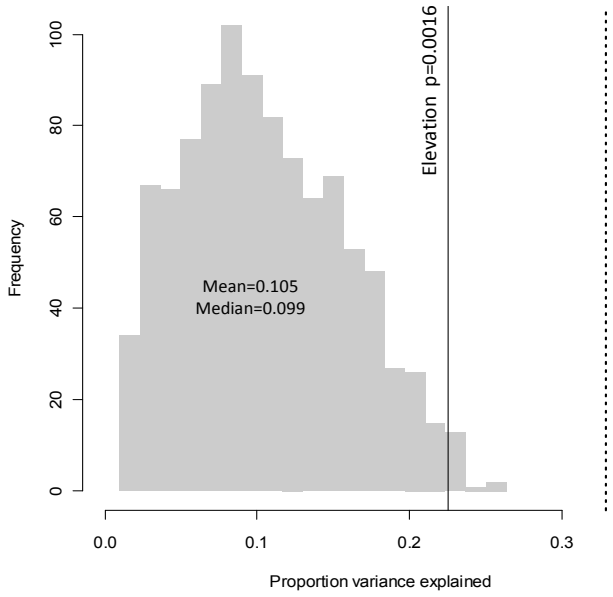

Figure 6.25 Histogram of the proportion of variance in the OB5 record explained by 999 MAT transfer functions trained by random data. Solid black line is the proportion of variance explained by transfer functions trained by OBDM3a dataset. Dotted black line is the proportion of the variance explained by the 1st axis of a PCA of OB5.

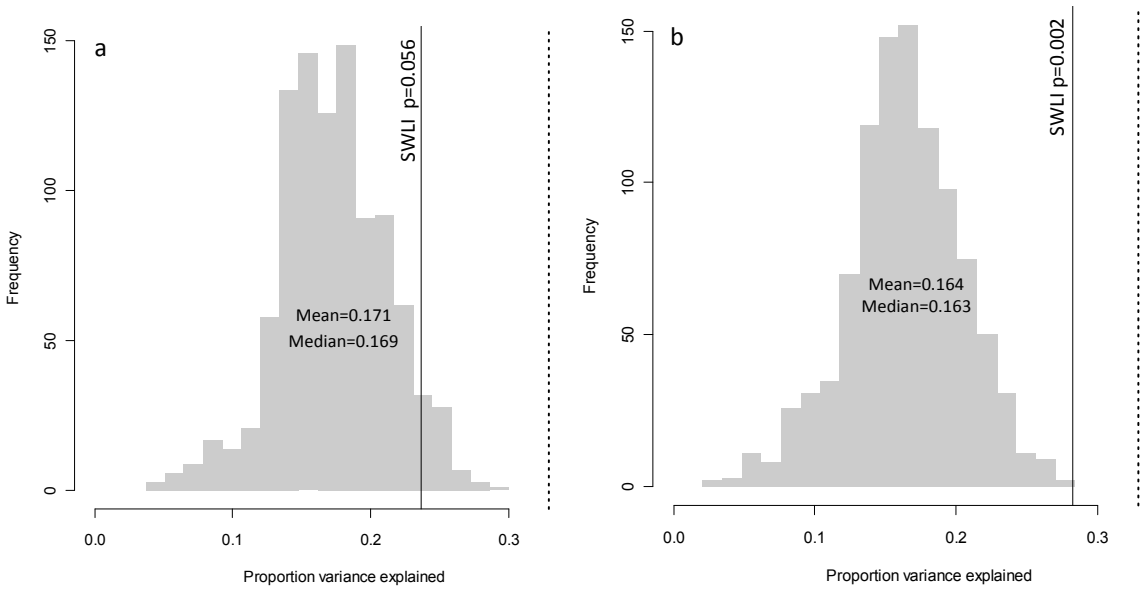

Figure 6.26 Histogram of the proportion of variance in the OB5 record explained by 999 WAPLS transfer functions trained by random data. Solid black line is the proportion of variance explained by transfer functions trained by a) H&E b) H&E b datasets. Dotted black line is the proportion of the variance explained by the 1st axis of a PCA of OB5.

Figure 6.27 shows the results of the models OBDM3H&E (figure 6.27a) and OBDMH&Eb (figure 6.27b) using WAPLS. The un-pruned model (figure 6.27a) was found produce a less statistically significant transfer function (p=0.118), whereas the pruned dataset (figure 6.27b) was found to produce a significant transfer function (p=0.01).

The results of the dataset OBDM3H&E 4 and OBDM3H&E 4b can be seen in figure 6.28. It shows that the un-pruned dataset OBDM3H&E 4 (figure 6.28a) did not produce a significant transfer function to 95% confidence, whereas the pruned dataset OBDM3H&E 4b (figure 6.28b) was found to produce a more significant (p=0.02) transfer function.

Table 6.21 shows a summary of the results and shows that all of the pruned datasets with WAPLS produced significant transfer functions. It also shows that the pruned dataset performs better for the H&E datasets than the non-pruned datasets. However, the opposite is true for OBDM data which may be due to the fewer samples remaining after pruning.

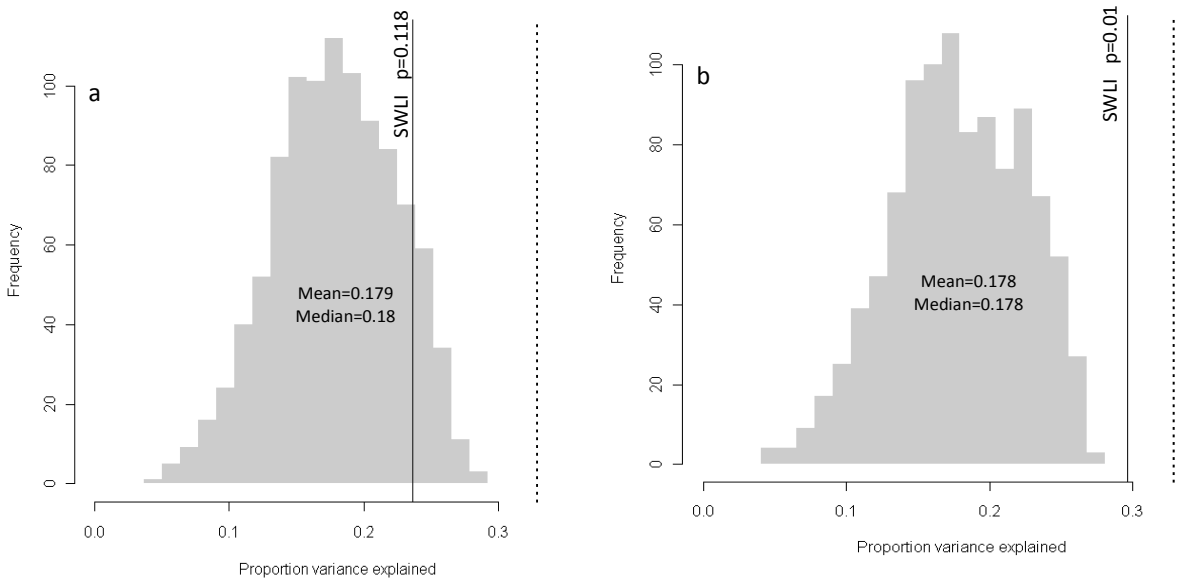

Figure 6.27 Histogram of the proportion of variance in the OB5 record explained by 999 WAPLS transfer functions trained by random data. Solid black line is the proportion of variance explained by transfer functions trained by a) OBDM3H&E b) OBDM3H&Eb datasets. Dotted black line is the proportion of the variance explained by the 1st axis of a PCA of OB5.

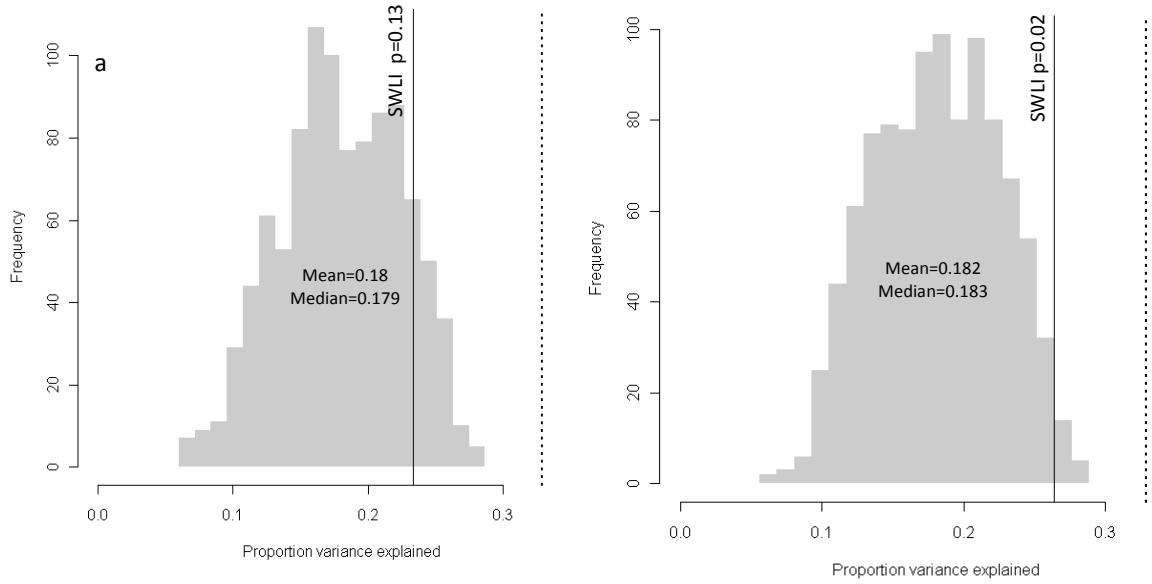

Figure 6.28 Histogram of the proportion of variance in the OB5 record explained by 999 WAPLS transfer functions trained by random data. Solid black line is the proportion of variance explained by transfer functions trained by a) OBDM3H&E 4 b) OBDM3H&E 4b datasets. Dotted black line is the proportion of the variance explained by the 1st axis of a PCA of OB5.

Table 6.21 Summary of 'random transfer function' statistical tests.

Dataset	No. of samples	Transfer function	Significance
OBDM	81	WAPLS	0.001
OBDM c	76	WAPLS	0.002
OBDM	81	MAT	0.004
OBDM3 a	62	WAPLS	0.001
OBDM3 c	56	WAPLS	0.001
OBDM3 a	62	MAT	0.0016
H&E	204	WAPLS	0.056
H&E b	185	WAPLS	0.002
OBDM3 H&E	266	WAPLS	0.118
OBDM3 H&E b	245	WAPLS	0.01
OBDM3 H&E 4	126	WAPLS	0.13
OBDM3 H&E 4b	120	WAPLS	0.02

Table 6.22 shows a summary of transfer function performance and significance. It shows that from the Oglet Bay and Decoy Marsh data alone (OBDMb) using model WAPLS C2 performs the 'best' compared with the others. It has a high r^2_{jack} (0.853), low $RMSEP_{jack}$ (0.111), high significance (p=0.002), it has the largest number of modern analogues for the fossil data, and the OBDMb ML and WAPLS also compare well (figures 6.20 and 6.21).

For the regional data, the dataset H&E 7b performs the 'best' with a higher r^2_{jack} (0.853), lower $RMSEP_{jack}$ (6.714) and the ML and WAPLS compare very well. However, H&E b has a higher significance and also has the most modern analogues for the OB5 fossil data.

For the data combined, the OBDM3H&Eb and OBDM3H&E 4b datasets perform similarly well with the same r^2_{jack} (0.875) and $RMSEP_{jack}$ (5.108), and both were found to be significant. The transfer function derived from OBDM3H&Eb has a larger number of modern analogues for the fossil record than OBDM3H&E 4b. However, the ML and WAPLS comparisons show that OBDM3H&E 4b performs more consistently compared with OBDM3H&Eb where different reconstructions are produced for the different techniques (WAPLS and ML).

Table 6.22 Summary of transfer function performance. (WAPLS results are from component 2).

Dataset	No. of samples	Transfer function	r^2_{jack}	$RMSEP_{jack}$	MA		Significance
					OB5	DMC1	
OB	63	WAPLS	0.536	0.167	20	11	0.011
OB b	56	WAPLS	0.656	0.129	22	11	0.017
OB	63	MAT	0.641	0.147	20	11	0.068
OBDM	81	WAPLS	0.734	0.162	20	11	0.001
OBDM b	76	WAPLS	0.853	0.111	26	11	0.002
OBDM	81	MAT	0.641	0.147	20	11	0.004
OBDM3 a	62	WAPLS	0.772	0.161	25	11	0.001
OBDM3 c	56	WAPLS	0.830	0.131	25	11	0.001
OBDM3 a	62	MAT	0.826	0.143	25	11	0.0016
H&E	204	WAPLS	0.475	15.579	21	11	0.056
H&E b	185	WAPLS	0.697	9.183	21	11	0.002
H&E 7	116	WAPLS	0.842	7.195	19	11	0.142
H&E 7b	114	WAPLS	0.853	6.714	19	11	0.011
OBDM3 H&E	266	WAPLS	0.677	8.592	29	11	0.118
OBDM3 H&E b	245	WAPLS	0.875	5.108	33	11	0.01
OBDM3 H&E 4	126	WAPLS	0.807	6.738	32	11	0.13
OBDM3 H&E 4b	120	WAPLS	0.875	5.108	32	11	0.02

Figures 6.29 and 6.31 show the reconstructed MTL of OB5 and DMC1, respectively, using the combined transfer function compared with the available Liverpool tide gauge record. Figure 6.29 shows the reconstructed MTL for OB5 using the transfer function OBDM3H&E 4b plotted against the established chronology. It shows the same trends in MTL as the reconstruction made using the transfer function OBDMc (figure 6.13). Comparisons of the two reconstructions can be seen in figure 6.30. The OBDM3H&E 4b reconstruction shows the MTL increasing to a higher level during the 2000s compared with the OBDMc reconstruction (and with the tide gauge data) which has smaller errors, but fewer modern analogue samples. It also shows the OBDMc reconstruction to be more similar to the tidal record than the OBDM3H&E 4b reconstruction.

Figure 6.33 shows the DMC1 reconstructed MTL using the combined transfer function OBDM3H&E 4b against the established chronology and compared with the Liverpool tide gauge record. It shows similar results to the OBDMb reconstruction (figure 6.17). Figure 6.32 shows a comparison between the two reconstructions. The reconstructions are more similar to each other than those for OB5 reconstructions, and also have smaller errors associated with them. When comparing these with the instrumental sea-level record it shows that both reconstructions compare well to the tide gauge record. It shows that there is an overlap between the two reconstructions from the two sites, except between 1993 and 2003 when there is a fall in MTL in the Oglet Bay reconstruction.

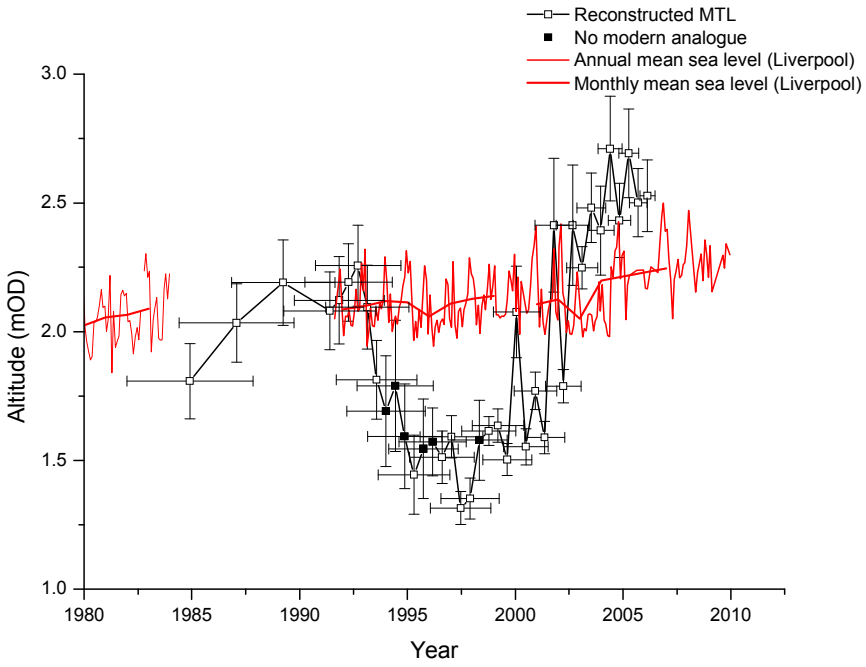

Figure 6.29 Reconstructed MTL for OB5 using dataset OBDM3H&E 4b (combined transfer function) and model WAPLS C2, compared with Liverpool tide gauge data.

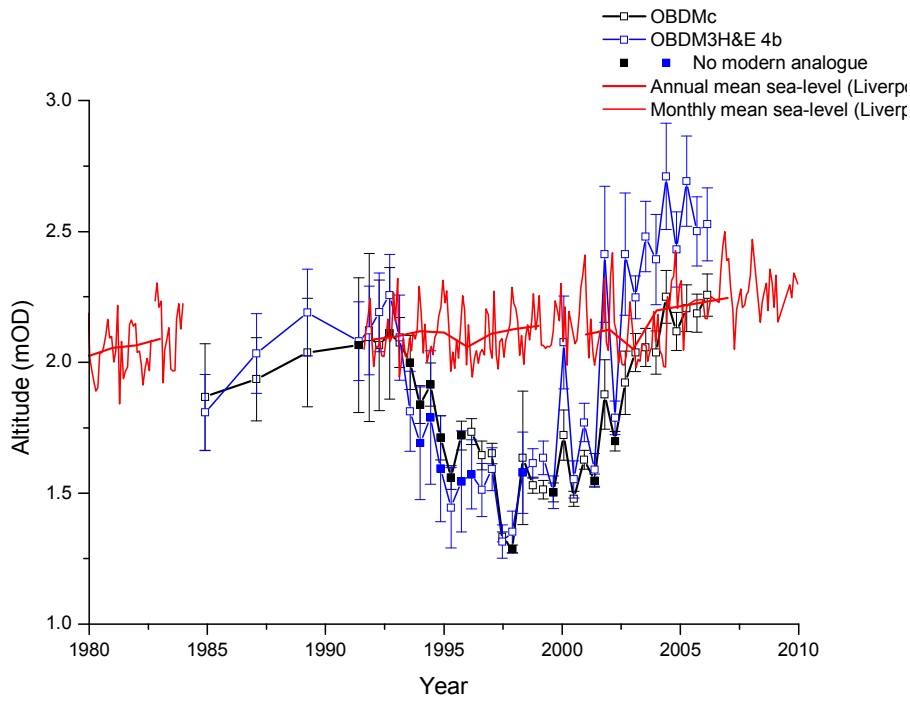

Figure 6.30 Reconstructed MTL for OB5 using dataset OBDM3H&E 4b (combined transfer function) and model WAPLS C2, compared with dataset OBDMc (local transfer function) and model WAPLS C2 compared with Liverpool tide gauge data.

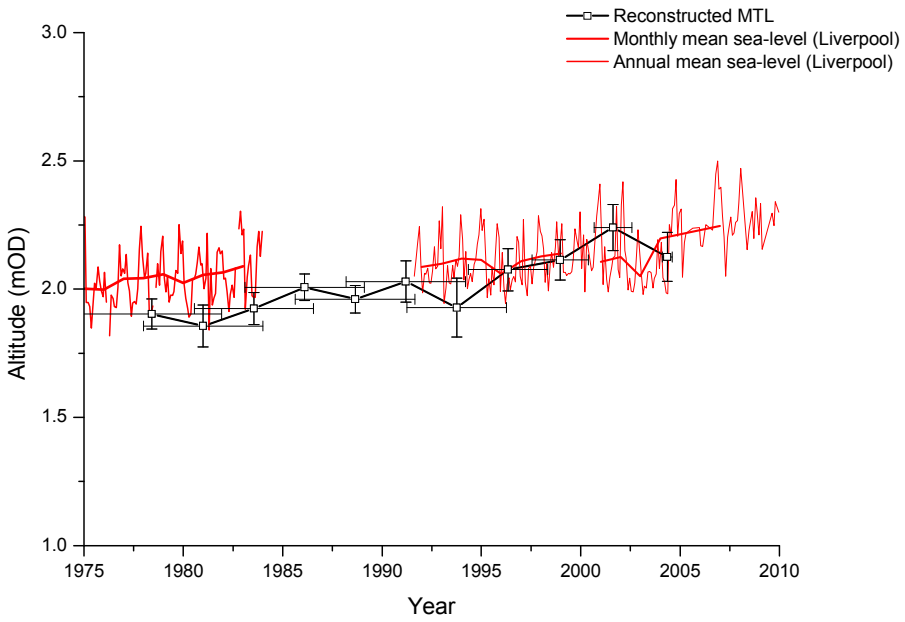

Figure 6.31 Reconstructed MTL of DMC1 using dataset OBDM3H&E 4b (combined transfer function) and model WAPLS C2 compared with Liverpool tide gauge data.

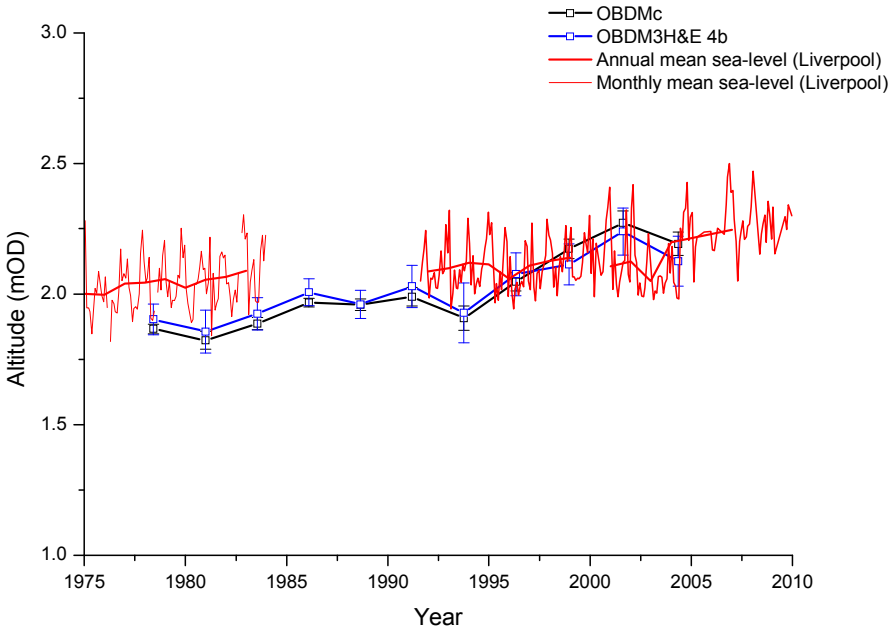

Figure 6.32 Reconstructed MTL for DMC1 using dataset OBDM3H&E 4b (combined transfer function) and model WAPLS C2, compared with dataset OBDMc (local transfer function) and model WAPLS C2 compared with Liverpool tide gauge data.

6.4. Interpretation of fossil records

6.4.1. OB5

The fossil assemblages of OB5 (figure 6.1) show a change from calcareous species to agglutinated species up-core, revealing a significant change in the environment. Between 51 and 29 cm depth, the samples are dominated by *Elphidium* spp., along with other calcareous species *Bolivina* spp., *Fursenkoina* spp. and *Brizalina* spp. The different species of *Elphidium* spp. found included *E. excacatum* and *E. incertum* which are both inner shelf species; inhabiting estuary mouths and nearshore areas (Murray, 1979). The additional species of *Bolivina* spp., *Fursenkoina* spp. and *Brizalina* spp. also inhabit the inner shelf. Between 30 and 23 cm depth there is a large increase in the species *T. ochracea,* an agglutinated species, which also inhabits the inner shelf. At the same depth there are increasing numbers of high marsh species *J. macrescens* and *Haplophragmoides* spp. Between 51 and 23 cm the species present indicate a low marsh/mudflat environment inferred from the presence of many marine and inwashed species, or may be due to foraminifera redistribution and mixing.

Up-core, there are increasing numbers of *J. macrescens* and between 22 and 9 cm the assemblage is dominated by *J. macrescens* along with *Haplophragmoides* spp. and small numbers of *M. fusca*. These species indicate a high marsh environment, with the presence of *Haplophragmoides* spp. also indicating lower salinities (see discussion in chapter 4.5). Nearer the surface of the core, between 9 and 2 cm, the samples are dominated by *T. inflata* and between 17 and 3 cm increasing numbers of *Quinqueloculina* spp. This may indicate a subtle lowering in the marsh environment to a more high to mid-marsh because of the presence of *T. inflata* and *Quinqueloculina* spp. but there is still the presence of *Haplophragmoides* spp. and *J. macrescens.*

The grain size distributions do not show any overall changes up-core, there is a slight decrease in grain sizes in general (figure 6.3) and between 30 and 45 cm there is an increase in more coarse grain size (figure 6.4), at the same time there is low organic matter content (figure 6.3). The DBD also increases at the same depth indicating that is likely to be the result of the change in composition from organic to mineral. This indicates a lower marsh environment with higher energy and less organic matter. The foraminiferal assemblage at this depth also reflects this, with the presence of low marsh-mudflat species (figure 6.1).

The high frequency changes in grain size from sand to clay can also be seen in figures 6.3 and 6.4, showing clear laminations in the sediment core. The samples are 1 cm in thickness and the chronology demonstrated that each 1 cm probably represents less than one year, therefore, the grain size results may be capturing seasonal variations. Neap and spring tides change over semi-annual and annual periods due to the changing alignment of the earth, sun and moon causing larger equinoctial tides to occur twice a year (Pugh, 2004) and this may be reflected in the sediment. These changes are not captured by the foraminiferal assemblages in the core as these are infrequent short term-events of higher energy, whereas, the foraminifera respond to longer environmental changes (e.g. inundation duration and salinity). The high frequency of the laminations and the limited overall change in grain size up-core indicates rapid sedimentation and supports the established chronology (chapter 5). This is also in support of the stratigraphy which was described in chapter 5.2 were laminated deposits of heterolithic tidal rythmites were found, recording changes in tidal cyclicity during a phase a rapid tidal sedimentation (Stupples and Plater, 2007). throughout the Oglet Bay Marsh

The reconstructions of changes in MTL for OB5 using the most appropriate transfer functions can be seen in figure 6.33. OBDMc WAPLS C2 (local transfer function) and OBDM3H&E 4b WAPLS C2 (combined transfer function) were chosen as the most appropriate as they were found to have the greatest predictive ability, with the highest r^2_{jack} values and the lowest $RMSEP_{jack}$ values. The MAT statistical technique also revealed that these transfer functions also had the greatest number of modern analogues in the fossil record and, therefore, may be more reliable. Comparisons of the WAPLS and ML transfer functions also tested the reliability of the reconstructions and demonstrated that using OBDMc and OBDM3H&E 4b datasets performed consistently, showing similar trends independent of the statistical method used. The OBDMc transfer functions do have slight disparities in their reconstructions (WAPLS and ML), reflecting the differences in how the techniques interpret samples which have few modern analogues in the data. Lastly, the proportion of variance in the fossil data explained by the transfer functions was calculated and compared with 999 WAPLS transfer functions trained on random data, and this demonstrated that the two transfer functions were significant at the 95% confidence level (table 6.21). As both of these transfer functions show similar reconstructions this also gives greater confidence that the transfer functions are reliable.

A noticeable fall in sea level between 1993 (+/-2) and 1998 (+/-1) is shown in both Oglet Bay reconstructions. This fall in MTL seems to reflect the increasing numbers of high marsh species *Haplophragmoides* spp. and *J. macrescens* and a fall in *Elphidium* spp., (figure 6.1) resulting in an increase in marsh elevations and therefore causing a negative sea-level tendency. Between 2002 and 2006 (+/-0.5) there is a rapid increase in MTL which is related to the increasing numbers of *Quinqueloculina* spp. and *T. inflata* showing a fall in marsh environment elevation resulting in a fall in marsh elevation and a positive sea-level tendency. The spikes in the MTL are also caused by the changes in abundance in of *Quinqueloculina* spp. (figure 6.1).

Comparing the two reconstructions with the tide gauge data from Liverpool shows that there are similarities between the reconstruction and instrumental record before and after the fall and recovery in MTL in the reconstructions. Figure 6.30 also reveals that the combined regional model (OBDM3 H&E 4b) over-estimates the increase in MTL and positive sea-level tendency between years 2000 and 2006. This may be because the elevations which the species occupy in the other UK sites are different from those of Oglet Bay. There are also greater errors associated with the regional model than the local as the regional model contains several sites with species occupying slightly different altitudes. Therefore, when the data are combined this leads to wider elevational ranges that each species occupies.

As the substantial fall in MTL apparent in the reconstruction has not been recorded by the tide gauge at Liverpool, this suggests that the fall in the reconstruction is either unreliable or inaccurate, or is reflecting changes associated specifically with the location of the study site within the Inner Estuary.

Before the changes in MTL can be interpreted as real changes it is important to consider whether they have modern analogues in the contemporary data and also whether the fossil data is reliable. All of the no modern analogue samples (5) using the regional transfer function (OBDM3H&E 4b) are within the fall in reconstructed MTL, and 8 out of 12 using the local transfer function (OBDMc) have no modern analogues, and therefore should be treated with caution. This is due to the high numbers of *T. ochracea* which are not found in the same high numbers in the modern data. In addition, several of the samples contain low numbers of foraminifera, with less than 100 tests; therefore, the assemblages in these fossil samples may also not be reliable. These samples were removed and the results of the record without these can be seen in figure 6.34. This plot shows the same results with the

samples removed; it shows the fall in MTL is still present, indicating that the results from the transfer functions are reliable, and may be interpreted as such but with considerable caution.

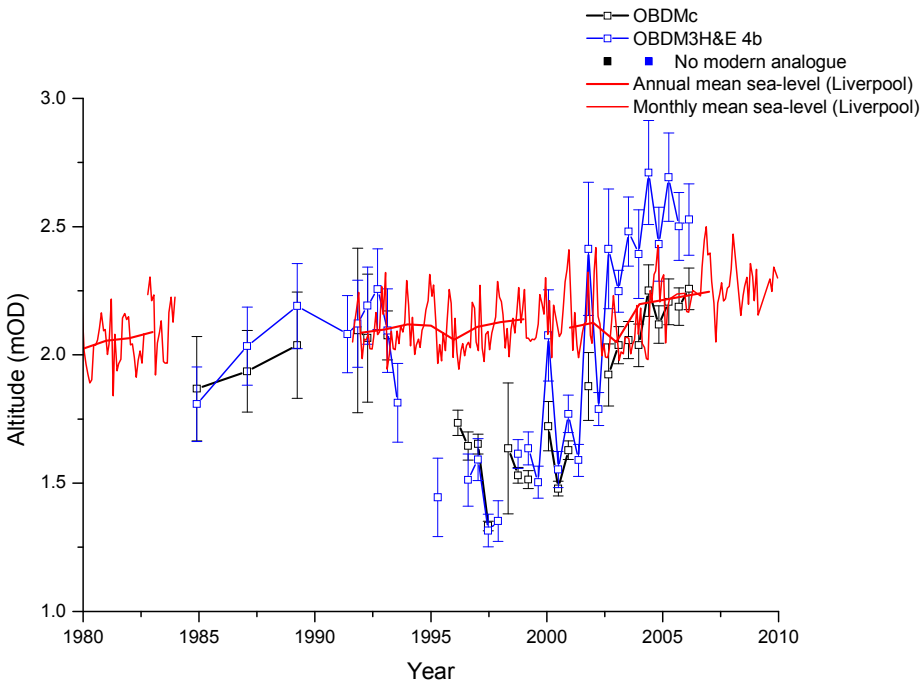

Figure 6.33 Reconstructed MTL for OB5 using dataset OBDM3H&E 4b and model WAPLS C2, compared with dataset OBDMc and model WAPLS C2 with samples removed with low numbers.

The rate of sea-level change using the OBDMc (local) transfer function between 1985 and 2006 is 1.836 cm year^{-1}. This is the average rate, but including errors the maximum rate in sea-level change is 3.177 cm year^{-1} and the minimum rate is 0.495 cm year^{-1}. The average rate of sea-level change using OBDM3H&E 4b (combined) transfer function between 1985 and 2006 is 3.392 cm year^{-1}. With errors, the maximum sea-level change is 4.735 cm year^{-1} and the minimum is 2.05 cm year^{-1}. The monthly mean rate of sea-level rise from the tide gauge record from Liverpool between 1983 and 2007 is 1.04 cm year^{-1} (figure 6.33). This covers a similar time period yet the average local transfer function reconstruction has a greater rate than tide gauge. However, the instrumental rate of change does fit within the errors associated with the reconstruction using the local transfer function but not for the combined transfer function. This demonstrates that the OBDM3& 4b is less realistic in its reconstruction as it has a much greater rate of sea-level change compared with the OBDMc reconstruction and the tide gauge record. This is considered to be due to the large over-estimation in MTL in the very recent time period, which may be because the elevations

which the species occupy in the other UK sites are different from those of Oglet Bay, particularly *T. Inflata.*

6.4.2. DMC1

The foraminiferal fossil data for DMC1 can be seen in figure 6.2 and shows little change in foraminiferal assemblages up-core. *J. macrescens* dominates all samples along with a great presence of *Haplophragmoides* spp. and *B. pseudomacrescens*. There is a slight fall in *J. macrescens* up-core along with an increase in *M. fusca* and *T. inflata*. These species illustrate a high, high marsh environment due to the presence of *B. pseudomacrescens* (see discussion in chapter 4.5.1). The fall in *J. macrescens* and *M. fusca* between 4 and 2 cm indicates a slight change in the environment.

The most significant feature of the foraminifera assemblage of this core is the lack of foraminifera below 12 cm depth. The most likely explanation for this is dissolution of foraminifera. Calcareous species are more susceptible to dissolution (e.g. Edwards and Horton, 2000) and as there are no calcareous species present in the core it may be possible that these species have been removed due to dissolution. This is more likely in this core than the core OB5 from Oglet Bay as the core is older in age. If this was the case then there are two possible situations that may have occurred. Firstly, it may be possible that calcareous species may have been present in the top half of the core in addition to the agglutinated species found, and the calcareous species have been removed throughout due to post-depositional dissolution. This is supported by the reduction in *M. fusca* down-core which is the most susceptible agglutinated species to destruction (e.g. Culver and Horton, 2005). A more likely situation is that only agglutinated species are present in the top half of the record due to the high position of the core on the marsh and the high altitude of the marsh within the tidal frame, hence only agglutinated species occupying the marsh. This is reflected in the surface samples collected from the marsh were the live and dead DMSS1 and the live DMSS2 show almost exclusively agglutinated species (chapter 4.3.2). When the foraminifera disappear below the depth of 12 cm it may be that the calcareous species which were present have been removed through dissolution.

The grain size distributions (figures 6.7 and 6.8) show a decrease in grain size up-core, with a fining of sediments, and the modal grain size decreasing up-core. DMC1 was also found to be less clearly laminated than OB5, reflecting the greater time captured by each 1 cm and so not recording any sub-annual tidal changes. The fining of sediments up-core, along with the increase in organic matter, indicate a fall in the energy in the environment and

increased vegetation, suggesting a change to a higher saltmarsh setting. This fining of sediments up-core and less obvious laminations indicates the more gradual development of a saltmarsh from a tidal flat was much slower than OB5.

The reconstructions of the change in MTL for DMC1 using the most appropriate transfer functions (OBDMc WAPLS C2 and OBDM3H&E 4b WAPLS) can be seen in figure 6.35. Both reconstructions were found to be very similar and show a general increase in MTL. There are no dramatic changes in MTL, and this can also be seen in figure 6.19 were there is little change in marsh elevation, reflecting the consistent high marsh species throughout the core. Figure 6.32 shows both reconstructions compared with the tide gauge record from Liverpool. It shows that both are similar to the record, although between 1977 and 1995 both reconstructions under-estimate the MTL compared with the tide gauge record.

The rate of sea-level change using OBDMc (local) transfer function between 1978 and 2004 is an average of 1.12 cm $year^{-1}$. The rate of change including the associated errors has a maximum rate of 1.319 cm $year^{-1}$ and a minimum rate of 0.906 cm $year^{-1}$. The rate of sea-level change using OBDM3H&E 4b (combined) transfer function between 1978 and 2004 is on average 0.857 cm $year^{-1}$. The maximum rate including errors is 1.45 cm $year^{-1}$ and minimum rate of 0.264 cm $year^{-1}$. The monthly mean rate of sea-level rise from the tide gauge record from Liverpool between 1978 and 2004 is 1.04 cm $year^{-1}$. This covers the same period the OBDMc (local) reconstruction and has a very similar rate of change. The OBDM3H&E 4b (combined) gives a much slower sea-level rise compared with the tide gauge record but is within errors of the instrumental data.

6.5. Discussion of fossil records

6.5.1. Transfer function assessment

The model WAPLS was found to be the most appropriate model to create a transfer function in this study as performance measures revealed the predictive ability to be greater for this model than other techniques, not including MAT and WMAT as these are considered to give over-optimistic results (Telford and Birks, 2005). WAPLS is likely to have performed well as it incorporates residual correlations so effectively considers the additional environmental variables which may also be influencing the foraminiferal assemblage distributions to a lesser extent (ter Braak and Juggins, 1993). ter Braak et al. (1993) recommended WAPLS as a simple and robust method to be used until a more

sophisticated method is developed and is still the most common method used in palaeo-sea-level reconstructions (e.g. Sawai et al., 2004; Edwards et al., 2004; Gehrels et al., 2006; Horton and Edwards, 2006; Szkornik et al., 2006; Massey et al., 2006a; Kemp et al., 2009b; Woodroffe and Long, 2010; Leorri et al., 2011).

The performance of the transfer function in the present study varied greatly depending upon which data were included in the model. The r^2_{jack} value varied from 0.48 to 0.81 for un-pruned data, to 0.66 to 0.88 for the pruned data (table 6.22). The $RMSEP_{jack}$ for the un-pruned data varied from 1.2 to 0.14 m and for the pruned data from 0.70 to 0.11 m. Removing outlying samples through pruning was carried out in order to improve the predictive ability of the transfer functions and it was found to significantly improve some of the models results, particularly the regional transfer function (H&E) where the r^2_{jack} value improved from 0.48 to 0.7 by removing 19 samples (predominantly from the low marshes of Roudsea and Brancaster Marshes and most of Tramaig Marsh) and improved the $RMSEP_{jack}$ value from 1.19 to 0.70 m. The significance of the combined regional and local transfer functions also improved when the pruned data were used, resulting in some transfer functions which were not significant (to 95% confidence) with all data included becoming significant with the pruned dataset (table 6.21). For example, the transfer function OBDM3 H&E 4b (combined transfer function) was found to have a low significance when all samples were included (p-value=0.13) but this improved to a p-value of 0.02 when 6 samples were removed.

This demonstrates the consequences of pruning in reconstructions and how it can have a significant effect on the results. The aim of pruning is to improve the predictive ability of the transfer function but the remaining data should still be representative of the natural environmental conditions. Removing large numbers of samples to leave the 'best' samples may remove the natural variability in the dataset and the result may be a less realistic reconstruction as this will reduce the error margins in the reconstruction.

The Oglet Bay data alone were found to perform the least well, with an r^2_{jack} of 0.66 and an $RMSEP_{jack}$ of 0.13 m for the pruned data (OBb). Similar results were found for the pruned H&E data alone (H&Eb), with an r^2_{jack} value of 0.7 and an RMSEP value of 0.70 m. The best performing datasets were found to be the combined Oglet Bay and Decoy Marsh dataset (OBDMc) as well as this local dataset combined with selected H&E data (OBDM3 H&E b and OBDM3 H&E 4b) (table 6.22).

The highest performing transfer functions in the present study were found to compare well with the performance of transfer functions from previous studies. Former studies have found r^2 values varying between 0.72 (Edwards et al., 2004) for foraminifera in Connecticut, to as high as 0.90 for diatoms in western Denmark (Szkornik, et al., 2006). The best performing transfer functions in the present study were found to have an r^2_{jack} between 0.83 to 0.88, which are on the higher end of values from previous studies (e.g. Edwards et al., 2004; Sawai et al., 2004; Horton and Edwards, 2005, 2006; Szkornik et al., 2006; Engelhart et al., 2007; Hill et al., 2007; Leorri et al., 2011; Rossi et al., 2011).

The $RMSEP_{jack,}$ (the vertical error of the SLIP in metres) for the best performing local transfer functions varied from 0.11 m to 0.13 m. Although these values are not very precise, these compare well with previous studies which vary between 0.88 m (Hill et al., 2007) to 0.05 m (Kemp et al., 2009b), with most precisions being between 0.1 and 0.2 m (Edwards et al., 2004; Sawai et al., 2004; Szkornik et al., 2006; Massey et al., 2006a; Gehrels et al., 2006; Engelhart et al., 2007; Hill et al., 2007; Kemp et al., 2009b; Woodroffe and Long, 2009; Woodroffe and Long, 2010; Leorri et al., 2011; Rossi et al., 2011). The highest precisions are usually achieved for microtidal settings which have errors below 0.1 m, e.g. 0.09 m from Edwards et al. (2004), 0.07 m from Horton et al. (2003) and 0.06 m from Gehrels et al. (2005) or have a multiproxy approach e.g. 0.05 m from Gehrels et al. (2001) and 0.05 m from Kemp et al. (2009b). The lowest precisions are usually found in macrotidal environments, e.g. 0.6 m from Edwards and Horton (2006) and 0.88 m from Hill et al. (2007). For the combined transfer function OBDMH&E 4b from the present study using the SWLI, the $RMSEP_{jack}$ has a value of 0.37 m which is much higher than the $RMSEP_{jack}$ for the local transfer function but still of high precision in comparison to other studies from macrotidal environments.

Bootstrapped errors of prediction provide errors for individual samples. The SE_{pred} for samples using the local transfer function (OBDMc) from OB5 were found to vary between 0.02 m to 0.32 m. Most samples, however, were found to have errors between 0.02 and 0.1 m which are very precise, although several samples (including the bottom 9) have much larger errors between 0.1 to 0.32 m. The SE_{pred} for samples from DMC1 have much smaller bootstrapped errors associated with them than those from OB5, and vary between 0.01 to 0.04 m. This is likely to be due to the more constrained high marsh species present throughout DMC1, in particular the presence of *B. pseudomacrescens* which has a small altitudinal range in the modern data (see chapter 6.5.2) in this study. In contrast, OB5

samples have larger bootstrapped errors associated with them, particularly for the lower samples due to the presence of calcareous species which are less constrained in relation to elevation.

The reconstructions using the combined transfer function (OBDM3H&E 4b) were found to have larger bootstrapped errors for samples. SE_{pred} for OB5 samples varied between 0.06 to 0.26 m; samples from DMC1 had lower SE_{pred} errors varying between 0.05 to 0.11 m. The errors are larger for the datasets combining different sites with different tidal ranges, as when the data are added together this results in wider elevational ranges in which a species occupies.

6.5.2. Final MTL reconstruction and summary

The transfer function OBDMc WAPLS C2 (local) was chosen as the best dataset and model to perform the reconstruction as r^2_{jack}, and $RMSEP_{jack}$ showed it performed well and it produced significant results over a random transfer function. It was also chosen over the transfer function OBDM3H&E 4b WAPLS C2 (combined) because although OBDMc WAPLS C2 (local) had less modern analogues in the fossil data, it had smaller errors associated with it, and also compared more consistently with the tide gauge record. In addition the significance of the transfer function remained high before and after pruning and therefore the results produced may be more reliable.

The results of the reconstruction for the OB5 core can be seen in figure 6.34 with all errors included and the samples which had poor modern analogues removed. The reconstruction itself is very short in length dating back to 1985 only, however, it does provide a high resolution record, with each sample representing approximately 6-months, and therefore can be compared with the tide gauge record from Liverpool at comparatively high resolution.

The comparison shows a large discrepancy between the reconstruction and the tide gauge data, with a fall in the MTL reconstruction between 1993 and 1997. This fall is related to the presence of *T. ochracea* as well as *Elphidium* spp*., Brizalina* spp. and *Bolivina* spp*.* and increasing numbers of high marsh species *J. macrescens* and *Haplophragmoides* spp*.* reflecting a negative sea-level tendency. From 2002 to 2006 there is a marked positive sea-level tendency, which may be due to the increasing numbers of lower marsh species of *Quinqueloculina* spp. and *T. inflata.*

The fall in MTL is considered to be based upon reliable data and is reflecting real changes in the foraminifera data. As this is not reflected in the tide gauge data from Liverpool or the DMC1 core from Decoy Marsh (figure 6.35) it is most likely that the core OB5, and the sediment record overall, is reflecting local factors which are not representative of the wider estuary environment.

In contrast to OB5 and Oglet Bay, the sea-level record from Decoy Marsh shows a different MTL reconstruction. The record is of a similar timeframe to OB5, dating back to 1978, however the record is of a lower resolution because the data are from a sediment record that is only 12 cm in length and each sample therefore encompasses approximately 2 to 3 years. There is little change in the species throughout the core and this is reflected in the reconstruction which shows little change in MTL. The reconstruction is also very similar to the tide gauge data from Liverpool (figure 6.35).

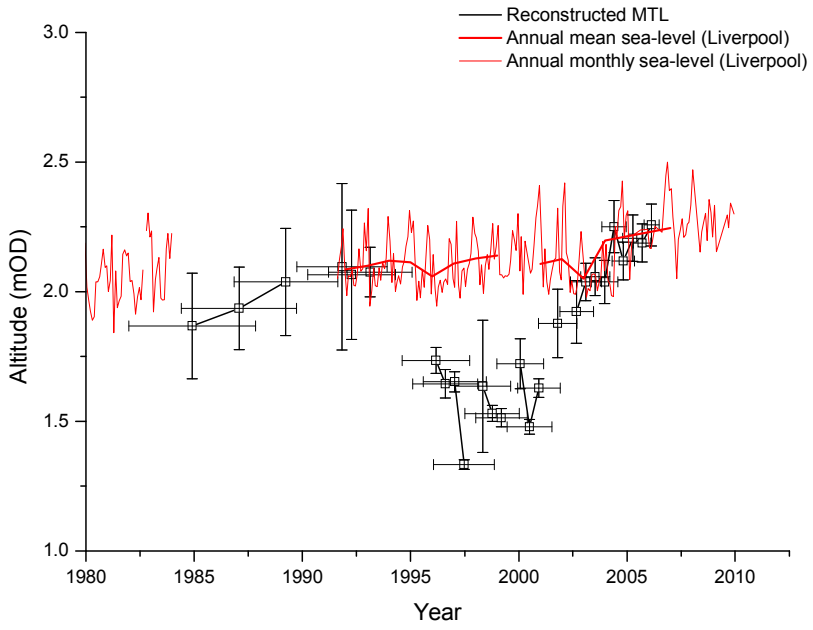

Figure 6.34 Reconstructed MTL for OB5 using dataset OBDMc and model WAPLS C2, compared with Liverpool tide gauge data, including chronology errors. Poor modern analogues removed.

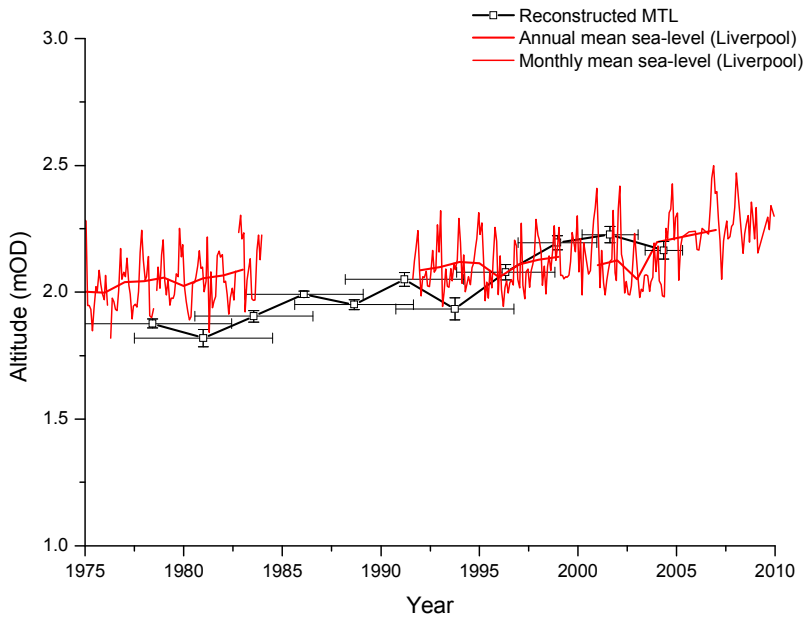

Figure 6.35 Reconstructed MTL for DMC1 using dataset OBDMc and model WAPLS C2, compared with Liverpool tide gauge data including chronology errors.

7. Discussions and further work

Oglet Bay saltmarsh was found to be a very dynamic marsh with periods of rapid erosion and accretion. Between 1936 and 1956 the marsh had eroded due to the migration of a channel northwards, and between 1956 and 1977 the marsh began accreting again due to the migration of the channel southwards (Blott et al., 2006). At present it is in a phase of rapid frontal erosion. The 84 cm core from Oglet Bay (OB5) showed rapid sedimentation during the period from the mid 1970s onwards. This was reflected in the chronology of the core, established from the peak in ^{137}Cs and ^{241}Am are related to peak Sellafield discharge in the mid-1970s and supported by the pollution record. The stratigraphic survey of Oglet Bay marsh also provided evidence for rapid accretion, with laminated deposits of heterolithic tidal rhythmites (figure 5.2), which were also reflected in the grain size data from the core (figures 6.3 and 6.4). The geochemical analysis also revealed that the saltmarsh had developed synchronously, with similar trends in heavy metals in different saltmarsh cores, as well as very similar sedimentation rates (2.2 cm to 2.42 cm year^{-1}), demonstrating rapid accretion of the marsh due to infilling (Model 1, figure 5.1).

In contrast Decoy Marsh was found to be more stable, and less affected by tidal channels within the estuary (figures 2.6 and 2.7). It was found to have a much lower accumulation rate (0.32 cm year^{-1}), established from the chronology which was based on ^{137}Cs, ^{241}Am, ^{210}Pb, as well as several pollution markers. Due to the older age of the Decoy Marsh core, many more pollution indictors were able to be utilised, resulting in a much better constrained chronology dating back to 1897. However, foraminifera preservation problems limited the length of the sea-level record which could be reconstructed. Stratigraphic and geochemical analyses were not available across the marsh, and only one principal core was able to be collected. The slow accumulation record established from the chronology is reflected in the grain size data from the core, where laminated tidal rythmites were barely present.

Transects of modern surface samples collected from both marshes showed the foraminifera assemblages to be related mostly to elevation and distance from the tidal influence, although both inter- and intra-site differences were apparent. The intra-site variability within Oglet Bay seemed to be mostly related to the presence of *Phragmites* spp. and freshwater input onto the marsh. *Haplophragmoides* spp. was found to be present where there was lower salinity and greater *Phragmites* spp. present (transects OBSS1 and

OBSS2) whilst *J. macrescens* was more abundant were *Phragmites* spp. was absent on the marsh reflecting higher salinities (OBSS3).

Ammonia beccarii spp. was also found to occupy different locations across Oglet Bay, with higher abundance at OBSS1 (figure 4.4). Other calcareous species were found throughout all the Oglet Bay transects (although in lower numbers at higher elevations) (figures 4.4 to 4.6). These occurrences are most likely to be related to mixing and redistribution of sediments due to the current erosion of the saltmarsh front. This is reflected in the live foraminifera assemblages where less calcareous species are present (figures 4.8 to 4.10) (Murray and Alve, 1999).

The inter-site variability between Oglet Bay and Decoy Marsh was found to be related to the elevation of the sites, as Decoy Marsh is located much higher within the tidal frame. Decoy Marsh was much more dominated by *J. macrescens* with less *Haplophragmoides* spp. indicating a higher salinity environment, but also had more *B. pseudomacrescens* indicating higher elevations (figures 4.11 to 4.13).

Decoy Marsh foraminifera also differed dramatically between transects in their dead assemblages, reflecting a large component of allochthonous foraminifera (figures 4.14 to 4.16 see section 4.3.2). To overcome this problem, the live data were used, as these were found to be more representative of the marsh environment.

These intra-site differences highlight the different environments and foraminifera assemblages which may be occurring on a saltmarsh within short distances. Most of the UK saltmarshes studies are based upon the collection of one transect, e.g. Horton and Edwards (2006). Therefore, if only one saltmarsh transect is being used for a site, it is important to choose a location on the marsh which is representative. More recent studies, sample along one transect also, but more often from several saltmarshes within a local area (i.e. same tidal range) e.g. Szkornik et al. (2006), Roe et al. (2009), Woodroffe and Long (2010) and Leorri et al. (2010). As the fossil record may contain all environmental conditions which are occurring on the marsh surface, it is important to sample all environments across the contemporary marsh. In addition, over longer timescales there may be changes in the environment, for example changes in vegetation, salinity, freshwater input etc. which need to be captured in the modern environment.

The present study used the modern surface foraminiferal assemblages which were documented for Oglet Bay and Decoy Marsh in order to produce a local transfer function. In

addition, data from the UK dataset (Horton and Edwards, 2006) were also used to develop a regional transfer function as well as a combined transfer function using both the local and regional data. The best performing transfer function model was WAPLS and this was chosen as the method of transfer function for all reconstructions.

The local transfer function was found to outperform the regional transfer function and was also found to be more reliable and accurate than the combined transfer function. The local transfer function had a high predictive ability (r^2_{jack} = 0.85), low errors ($RMSEP_{jack}$ = 0.11 m) and was significant (p=0.002) compared to a random data-trained transfer function, and it compared well with a ML based reconstruction. The local transfer function reconstruction also compared more favourably with the instrumental record. However, it did suffer the problems of having several samples which did not have modern analogues for the Oglet Bay core.

Although the OB5 core was 84 cm in length, the sea-level record established from the sediments using the local transfer function, OBDMc WAPLS C2, dated back only 25 years (chapter 5) due to the sediments being very young in age, and low foraminifera abundance (chapter 6). The core, however, did produce a high resolution reconstruction that was considered to be reliable, which could be compared to the tide gauge record from Liverpool (figure 6.34). The comparison shows a large discrepancy between the reconstruction and the tide gauge data, with a fall in the MTL reconstruction between 1993 and 1997 followed by a marked increase from 2002 to 2006. As this fall is not reflected in the instrumental data nor in the Decoy Marsh reconstruction, it is most likely that it is influenced by local changes.

The DMC1 reconstruction covered a similar time period to the record from OB5. Although the core was shorter in length (42 cm), the accumulation rate was much lower and the core was much older, dating back to 1845. Similarly to OB5, the limit of the foraminifera preservation restricted the timescale of the sea-level reconstruction, therefore the core produced a record spanning only 32 years, dating back to 1978. The core also produced a high resolution reconstruction that was considered to be reliable, which could be compared to the tide gauge record from Liverpool. DMC1 proved to be successful in reconstructing MTL with a record that compared well with the tide gauge data from Liverpool (figure 6.35).

The rate of sea-level change from the Decoy Marsh reconstruction between 1978 and 2004 was an average of 1.12 cm $year^{-1}$. Including the associated errors, the rate had a maximum

of 1.319 cm year^{-1} and a minimum rate of 0.906 cm year^{-1} with the monthly mean sea-level rate from the tide gauge record from Liverpool between 1978 and 2004 being 1.04 cm year^{-1}.

The average rate of sea-level rise from the Oglet Bay reconstruction was found to be is 1.836 cm year^{-1} between 1985 and 2006. This compares with the monthly mean sea-level rise from the Liverpool tide gauge record between 1983 and 2007 of 1.04 cm year^{-1}.

The sea-level reconstructions from both Oglet Bay and Decoy Marsh were found to be comparable to the monthly mean of the instrumental record, although the Oglet Bay rate is much higher. The rates, however, are less comparable with longer records of sea-level change. The annual mean of the instrumental record for the period covering the reconstructions is 0.6 cm year^{-1}. Woodworth (1999a) found the rate of sea-level change during the 20th century for Liverpool to have an average trend of 1.39 +/- 0.19 mm year^{-1}. The difference between the long-term and short-term rates in sea-level change may be because the short-term records are reflecting short-term variability which may be averaged out the longer record or may be that the rate of sea-level rise is increasing in the recent period.

7.1. Considerations

There are several factors which may have impacted on the two sea-level reconstructions. A discussion of each of these will follow along with the implications these may also have on other sea-level reconstructions.

7.1.1. Tidal range changes

As discussed in the chapter 4.3.2 the tidal constituents have changed in the past due to changes in the bathymetry of the estuary. Lane (2004) modelled the tidal amplitude of different tidal constituents M_2, M_4, and Z_0 (figure 2.3) and suggested there to be a 1.5 m increase in M_2 amplitude between the dates 1956 and 1977 at Hale in the Inner Estuary, with a decrease in the Z_0 component (1.5 m) over the same period. From 1977 to 1997 there is a decrease in the M_2 component by over 1 m and an increase in Z_0 (1 m). These changes are consequential on changes in the bathymetry of the Inner Estuary, related to changes in sedimentation, dredging and the relocation of low water channels. Between 1936 and 1977 there was a reduction in the tidal volume of the estuary due to a fall in dredging and increased sedimentation, this was followed by a smaller increase in tidal volume between 1977 and 1997 (Lane, 2004; Blott et al., 2006). A discussion of the changes in low water channels can also be found in the discussion in chapter 2.3.

It is important to note that these major changes in tidal constituents have been modelled for Hale which is 3 km up-estuary from Oglet Bay and this difference in location may affect the tidal components significantly. For example at Widnes, which is 4 km up-estuary from Hale, there are no dramatic historical changes in the tidal constituents, due to changing estuary bathymetry or volume with Z_0 and M_2 remaining constant between the years 1956 and 1997 (Lane, 2004).

The M_2 tide is the main lunar component of the tide and the Z_0 constituent represents MSL (essentially MTL) and it would be expected that the M_2 and Z_0 constituents change together, as opposed to being negatively correlated, which is seen in Lane (2004). When there are decreases in M_2 amplitude equally, this does not cause a change in MSL, as demonstrated in figure 7.1a. The constituents have opposite trends in Lane's (2004) model output suggesting that there are asymmetrical decreases/increases in the tidal range. These changes are demonstrated in figure 7.1a and b. Scenario 2 (figure 7.1b) shows the effects of lowering the high waters only which results in a decrease in the tidal range and a decrease in the MSL. Scenario 3 (figure 7.1c) shows the effects of raising the low waters only which

results in a decrease in tidal range but causes an increase in MSL. This demonstrates that the changes shown in Lane (2004) of opposite trends in amplitude (M_2) and MSL (Z_0) are related to changes in the low tides. Intuitively, a decrease in tidal volume, increasing the height of the bottom of the channel may lead to the rise of low waters, however, there is in fact an increase in tidal volume at the time this occurs (Lane, 2004).

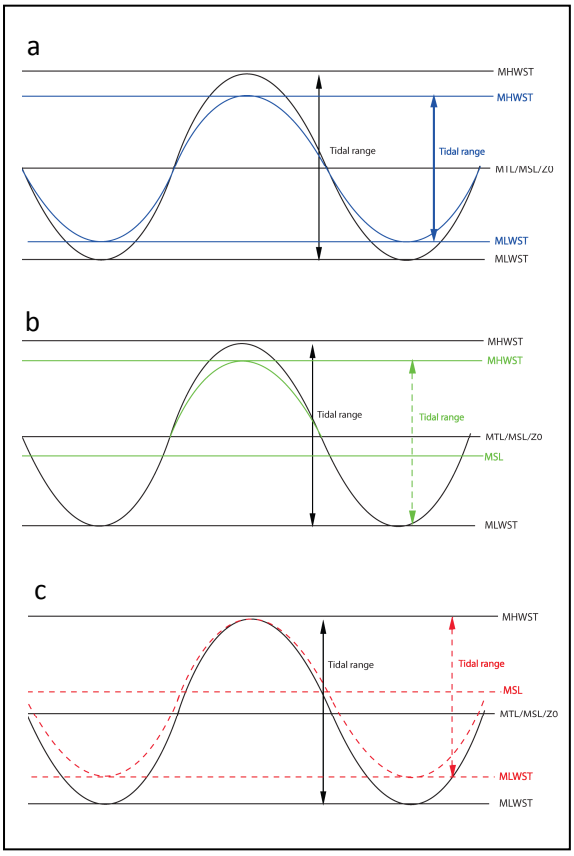

Figure 7.1 Simple schematic representation of a tidal curve with the effects of decreasing tidal amplitude. a) scenario 1 = a symmetrical decrease in tidal amplitude. b) scenario 2 = an asymmetrical decrease in amplitude in the high waters only. c) scenario 3 = an asymmetrical decrease in amplitude in the low waters only.

Reconstructions of OB5 were carried out using the local transfer function (OBDMc) using the SWLI in order to test the outcome of changing the tidal levels MHWST, MLWST and MTL. The SWLI was used as a mechanism by which different components were able to be changed. The results of decreasing the amplitude of the tide in different ways can be seen in figure 7.1, and shows the three different scenarios as described above with an overall 1 m decrease in tidal range (approximately 10% of the tidal range at Liverpool). Scenario 1 raises the MLWST and lowers the MHWST, and this decreases the range. This results in the raising of the SWLI (figure 7.2.a) and when this is back transformed to produce the MTL, the MTL remains unchanged from the present MTL (figure 7.2a). Scenario 2 which lowers the

MHWS by 1.0 m, does not change the MLWS but does decrease the range, therefore, this raises the SWLI greatly (figure 7.2). When this is transformed to produce the MTL, the MTL decreases below the present MTL (figure 7.2b). Scenario 3 raises the MLWS and also decreases the range, and therefore this decreases the SWLI slightly (figure 7.2a). When this is back transformed to a MTL, the MTL increases above the present MTL (figure 7.2b).

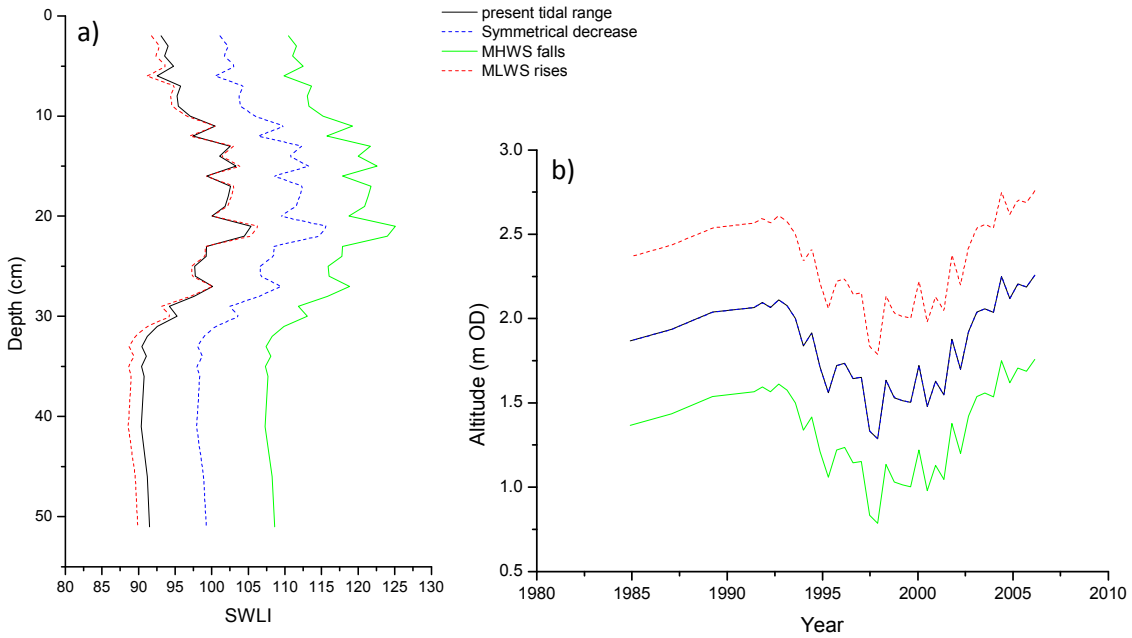

Figure 7.2 Reconstructed a) SWLI and b) MTL of OB5 using dataset OBDMc and model WAPLS c2 with different decreases in tidal range. Scenario 1 = an symmetrical decrease in tidal amplitude. Scenario 2 = an asymmetrical decrease in amplitude in the high waters only. Scenario 3 = an asymmetrical decrease in amplitude in the low waters only.

This demonstrates that the fall between 1993 to 1996 in the reconstruction from Oglet Bay may potentially be related to a decrease in amplitude of 1 m, i.e. if the correct tidal data (lower range and higher MTL) was included in the reconstruction for the period 1993 to 2002 this would correct for the fall. The model results of Lane (2004) suggested a fall in M_2 amplitude and an increase in Z_0 of 1 m between 1977 and 1997 due to increase in tidal volume and the migration of low water channels, therefore this apparent fall in MTL may be related to this. From 2005 onwards the amplitude would have to reverse back to the previous amplitude to correct the fall completely. There are no model results available from 1997 onwards therefore it is not possible to verify or refute this change in amplitude.

The fall in the Oglet Bay reconstruction occurs between 1993 onwards, however Lane's (2004) results shows a fall from 1977. However, the exact timing of the changes is not known as the bathymetries and sea-level data used in the study are from 1977 and 1997 only. Therefore, the changes have occurred somewhere between 1977 and 1997 and may

not have occurred until 1993. Alternatively, the location of the study site may be reflecting different changes in tidal regime compared to the location modelled by Lane (2004) resulting in different timings.

The fall seen in OB5 is not present in DMC1 and shows that the whole of the Inner Estuary is not affected by the same estuarine processes, as shown in figures 2.6 and 2.7. Decoy Marsh does not appear to be affected by changes in low water channels. The reconstruction is similar to the tide gauge record. However, the reconstruction does appear to be lower than the tide gauge record between 1978 and 1996. This small difference between the reconstruction and tide gauge record again has the potential to be related to small changes in tidal constituents within the Inner Estuary.

7.1.2. Errors

Although the local and combined transfer functions for DMC1 shows very similar trends which are within errors of each other, the minimum and maximum rates of changes for the reconstructions differ greatly. Bootstrapped errors which are used to determine the sample errors only include uncertainty in the relationship between modern assemblages and measured elevation. They assume the relationship between fossil assemblages and palaeo-elevation is the same. As the reconstruction and instrumental records do not match completely within errors, this suggests that the relationship between the assemblages and elevation may not have remained the same in the past or the effects of changing tidal regimes, disturbance, taphonomy, preservation etc. may have influenced the observed assemblage and these are not included within the bootstrapped errors. The errors associated with the reconstruction are a reasonable estimate of average errors but may be on the conservative side, particularly as it does not account for any post-depositional changes, compaction for example (Charman et al., 2010).

7.1.3. Compaction and volume loss

The underestimation of MTL in the earliest part the DMC1 record compared to the instrumental record may be due to the effects of autocompaction. Compaction is not equal through sedimentary sequence, with older sediments experiencing more compaction, resulting in the reconstructed sea-level being under-estimated for older sediments and would also lead to over-estimated rates of sea-level change (Edwards and Horton, 2006).

Most investigations related to compaction are commonly carried out on minerogenic sediments and are related to the compression of sediments due to the weight and pressure of the overlying sediments (autocompaction), or very organic sediments related to the de-watering of peat, all of which consider long sedimentary sequences between 5 m to 3 km plus (Pizzuto and Schwendt, 1997; Allen, 1999; Edwards, 2006; Brain, 2006). It is usually assumed that the cores which are short in length and are located in the high marsh are unaffected by autocompaction (e.g. Edwards and Horton, 2000). Although, Kearney et al. (1994) suggested that early autocompaction (and dewatering) can begin even within sediments buried less than 1 m below the modern substrate. In addition, Vranken et al. (1990) found that 1.2 cm subsidence occurred in the top 5 cm of a high marsh core in S W Netherlands for the period 1984 and 1987, suggesting that shallow sediments can suffer from compaction due to sediment volume loss over a short time period.

Sediment volume loss may also take place due to diagenetic factors. Organic soils are prone to decomposition, humification, physical, chemical and biological processes which may affect the volume of the sediments. Oxygenation of organic matter results in the decay of organic matter reducing sediment volume. In addition, saltmarshes have root networks which create high porosity which may result in structural collapse upon death further reducing the volume (Brain, 2006). Furthermore, other diagenetic factors may reduce the volume. Chemical processes can affect autocompacting sediments including chemical dissolution and precipitation (Brain, 2006). Dissolution of mineral phases (e.g. calcium carbonate) can cause a decrease in the void ratio and can result in closer packing of the grain structure which may change the sediment volume (Bjørlykke and Høeg, 1997). Dissolution of calcium carbonate is typical in elevated saltmarsh environments (Spencer et al., 2008) and is much more pronounced in saltmarsh sediments than in tidal flat sediments or permanently submerged sediments (Kooistra, 1978).

The sediments from DMC1 are very shallow (42 cm), with a reconstruction based upon 12 cm of sediments only. Even so the DBD which is used as proxy for compaction, increases dramatically down-core along with a decrease in organic matter content from 60 to 20% during the same time (figure 7.3a) indicating some loss of volume possibly related to the decay of organic matter. In addition figure 7.3a, shows the Ca profile for the same depth, which shows that there has also been a decrease in Ca indicating that further sediment loss and compaction may have occurred as a result of decalcification.

The DBD and organic matter content for OB5 does not change significantly down-core with the only increase between 30 and 40 cm which is likely to be reflecting the increase in coarse grain sizes (figure 7.3b) In addition, most of the foraminifera are also above this depth.

DMC1 is likely to have experienced more compaction as it is much older in age, it also has much lower accretion rate, which results in greater carbonate loss (Vranken et al., 1990). The elevation of the marsh is also higher than Oglet Bay, therefore it experiences greater sub-aerial exposure resulting in greater biodegradation of organic matter and increased decalcification (Vranken et al., 1990). This may also explain the absence of calcareous foraminifera in DMC1.

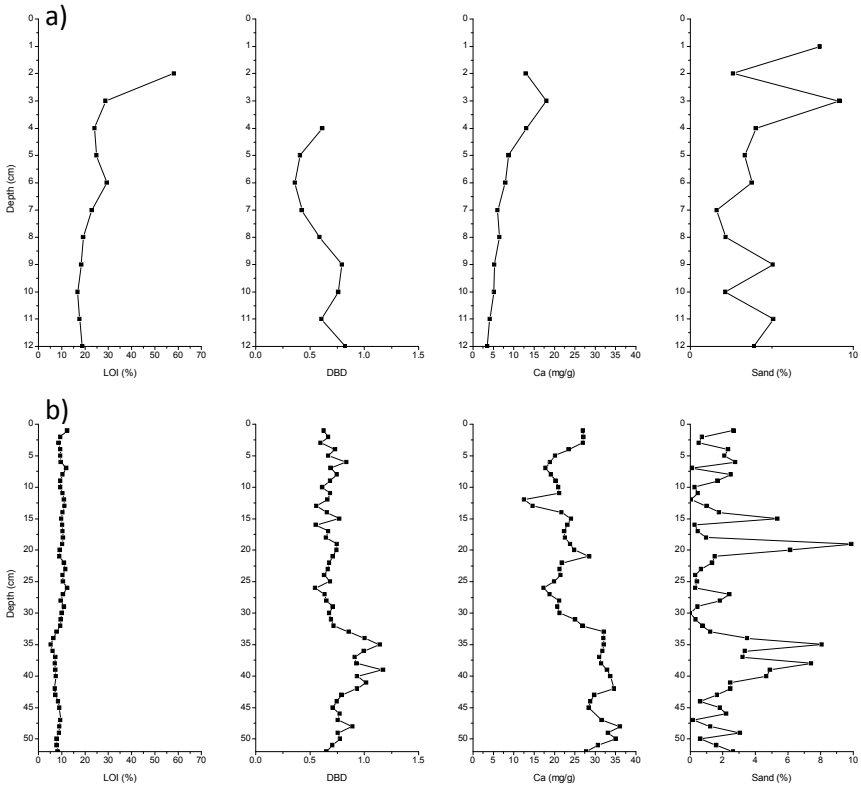

Figure 7.3 Changes in organic matter, dry bulk density and calcium, down core for the length of the reconstructions for a) DMC1 and b) OB5.

7.1.4. Calcareous dissolution

The dissolution of calcareous foraminifera is obvious in DMC1 due to the complete absence of calcareous species below 13 cm depth. The destruction of the calcareous tests is caused by carbonate dissolution and is attributed to the reducing conditions below the oxidized the sediment layer (Murray, 1973). This may be caused by several processes including corrosive bottom or sediment pore waters which may be brought about by metabolisation of organic matter and bacterial destruction (Murray and Alve, 1999). Therefore, as discussed above, the high elevation of Decoy Marsh may result in greater biodegradation of organic matter and decalcification. In addition, calcareous dissolution of shells often occurs in areas which have slow sediment accumulation.

Oglet Bay saltmarsh is lower in the tidal frame and also has a slower accumulation rate, however, the OB5 fossil record may also have experienced some dissolution of foraminifera, although it appears to be less obvious than in Decoy Marsh. Figure 7.4 shows the abundance of calcareous and agglutinated foraminifera per 1 cm^3 compared with Ca profile. It shows where there is a dramatic fall in calcareous species there is also a dramatic fall in Ca content (22-32 cm), at the same time there are also decreases in the abundance of agglutinated species (Sr content also decreases in concentration with Ca). When the Ca content increases, however, the abundance of calcareous foraminifera also increases but the abundance of agglutinated species remains low. A simple comparison between two samples shows that the difference between Ca content at a depth of 35 cm and a depth of 25 cm is 12239 ppm. It is estimated that the amount of Ca the foraminifera contribute to the sediment is 120 ppm at 35 cm, and 40 ppm at 25 cm (estimated from the average volume and mass of calcareous foraminifera (Fok-Pun and Komar, 1983), the abundance of foraminifera per 1 cm^3, and the sediment mass per 1 cm^3). Therefore, the decrease in calcareous foraminifera abundance is not sufficient to account for the observed difference in Ca content between these two levels. Hence, the loss of calcareous foraminifera is likely to be a consequence of decalcification rather than the reason for the difference in Ca content. The increased decalcification in the core was found to be greatest between 20 and 30 cm and this interval was found to be a zone of extensive geochemical activity that can potentially alter assemblages and is subject to relatively deep bioturbation by invertebrates (Hippensteel et al., 2000).

The dominant calcareous species in the fossil record is *Elphidium* spp. and this can be seen to decrease in abundance between 32 and 22 cm depth (figure 6.1), resulting in increased relative abundance of high marsh species (*J. macrescens)* and consequently resulting in increased marsh elevation and a negative sea-level tendency. *Elphidium* spp. is particularly prone to dissolution and therefore this species is less likely to be preserved (Hippensteel et al., 2000). The fall in *Elphidium* spp. therefore may be the result of dissolution, with the fall in MTL reflecting taphonomic change rather than sea-level changes. In addition, if the *Quinqueloculina* spp. which increases between 18 and 10 cm has been dissolved below this depth (20 cm) the increase in MTL may also not be reflecting real changes in sea-level. It is possible that if *Elphidium* spp. did not actually fall in numbers at this depth (at the time of deposition) and at the same time there were greater abundances of *Quinqueloculina* spp., resulting in consistent calcareous species throughout the core, it would result in less change in the MTL reconstruction, possibly removing the reconstructed fall. For example, Hippensteel et al. (2000) in Delaware Bay found that differential preservation of foraminifera could produce an apparent palaeoenvironmental change which could potentially be misinterpreted. Dissolution of calcareous foraminifera resulted in a reconstruction with a rapid fall in sea level over the last 100-200 years which was not reflected real changes in sea-level.

It is unlikely that any correction for the dissolution of calcareous species would completely remove the reconstructed decrease in MTL in the reconstruction however, as the *Elphidium* spp. abundance cannot be seen to increase again near the surface of the core, when abundance of calcareous species increases. Further, the decrease is calcareous foraminifera is accompanied by a change in the relative proportions of different calcareous species. It is therefore likely that there has been a real change in the environment, but possibly less extreme than the decalcified foraminifera assemblage indicates.

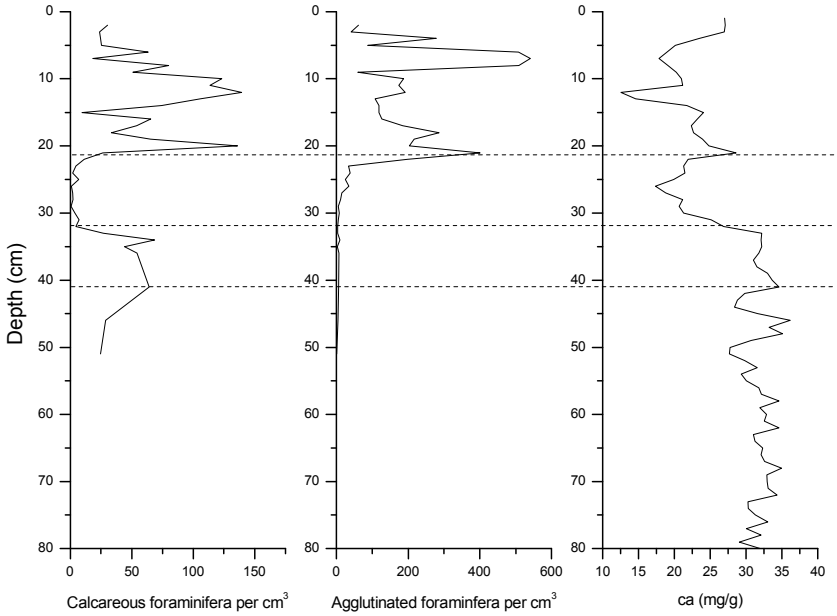

Figure 7.4 Abundance of calcareous and agglutinated foraminifera per 1 cm^3 for OB5 compared with Ca profile.

7.1.5. Asymmetry

Changes in the tidal curve occur up the Mersey Estuary, with changes in the MHWS, MLWS, MTL and tidal range, as well as increasing asymmetry (see figure 2.2). As Oglet Bay and Decoy Marsh are located within the Inner Estuary, they are likely to experience tidal asymmetry. Unfortunately, as there are no temporary tide gauges which have been installed at the study sites, the real tidal constituents and asymmetry are unknown but the data available from Hale suggests that both sites are likely to have asymmetrical tides.

Tidal asymmetry may have an effect on the reconstruction as asymmetry will affect the hydroperiod in relation to elevation. Flooding duration has been found to have a strong relationship with elevation (e.g. Horton, 1997). However, this relationship may change when the tidal curve is not symmetrical. As a result a sample elevation will appear higher than it is in reality in relation to flooding duration. This may have implications for the reconstructions which may be over-estimated. This is demonstrated by figure 7.5 which compares examples of two tidal curves, Princes Pier (symmetrical) and Hale (asymmetrical) (figure 7.5a) and also shows the relationship between elevation and duration of flooding based upon the tidal curves (figure 7.5b). The asymmetry may also affect the rate of sea-level change from the reconstruction. As the gradient of an asymmetrical curve may be less steep in relation to flood duration, this may result in the SWLI overestimating the high elevations and under-estimating the low elevations (figure 7.5b)

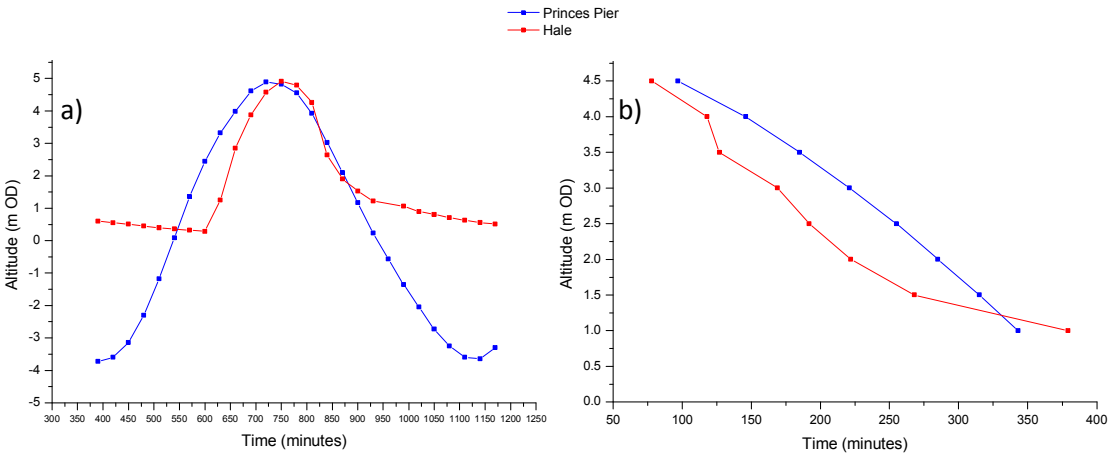

Figure 7.5 An example of the differences between a symmetrical and asymmetrical tidal curves, an example from Princes Pier and Hale. The height of the Princes Pier high water was decreased by 0.5 m in order for the two curves to be compared. a) tidal curves from Princes Pier and Hale over one rise and fall b) inundation duration at different altitudes estimated from the tidal curves (a) (Values taken from Rossiter et al., 1956).

When using a local transfer function these problems are circumvented as the reconstruction is trained on modern data from the area in which the core is collected. Therefore, as it is presumed that the modern and fossil data are and have been responding to the same environmental parameters, the asymmetry of the tide will be included in the local transfer function inherently. Problems may only arise when data from different sites are combined and the SWLI is used, as this does not consider the shape of the tidal curves from the different sites. Consequently, combining sites with different tidal shapes in a SWLI may be problematic. This may be a possible explanation for the difference between the local and combined transfer functions, particularly for the OB5 record as the asymmetrical data from Oglet Bay and Decoy Marsh are combined with sites which have symmetrical tides.

Several contemporary saltmarsh studies for the UK have also been undertaken in locations which may not have symmetrical tidal curves and therefore may be affected. For example, Edwards and Horton (2006) utilise surface samples from 12 study sites from the British Isles and Ireland. These sites include Bury Farm which is located within Southampton Water, along with Keyhaven Marsh, Newton Bay and Arne Peninsular all of which may experience double high waters and asymmetrical tides (Pugh, 2004). The River Nith may also have an asymmetric tide as it experiences a tidal bore (Davies, 1988), and lastly, Roudsea Marsh which is located within Morecombe Bay which experiences tidal asymmetry (Mason et al., 2010).

Using a local transfer function does overcome any problems that may arise due to differential asymmetry and, consequently, should be more reliable. However, this method is also not without its problems. Asymmetry affects the flooding duration of a saltmarsh and the local transfer function assumes that these conditions have not changed over time. However, as demonstrated above (section 7.1.1), tidal constituent changes can occur over very short time scales within estuaries. A tide becomes asymmetric up-estuary due to changes in topography and bottom friction, therefore changes in these will not only cause changes in the tidal amplitude but also the shape of the tide.

If the tide is amplified by lowering the low waters, this would make the tide more asymmetrical. To account for the fall in MTL for the Oglet Bay reconstruction this suggests that the present day tidal change may be overly asymmetric which is why the MTL is being lowered. Therefore, during this period the tidal curve may have been more symmetrical. If this was accounted for in the reconstruction this would counter-act the fall. A reduction in asymmetry is likely to occur when there is a fall in tidal amplitude in the low waters, which also supports the previous theory and discussion above.

7.1.6. Reference water levels

There are several problems related to using the correct reference water levels for both local and regional transfer functions. Firstly, obtaining the correct tidal measurements for the study site is important and may be more difficult for sites located within estuaries. Secondly, there are problems relating to reference water levels when the tidal regime is asymmetric. Thirdly, the correct reference water levels must be used when standardising elevation using the SWLI method. The three problems will be discussed in turn below.

Correct water levels

Determining the correct tidal data may be problematic if using sites located within estuaries. Tide gauges which provide reference levels are often not available for inner estuary locations (where suitable conditions for growth of saltmarshes tend to exist), therefore data from secondary ports which may be located in estuaries (e.g. Hale) may be used. Secondary port tidal data are usually calculated by applying time and height differences to predictions at a standard port (e.g. Liverpool) or by using the harmonic constants and the Simplified Harmonic Method of Tidal Prediction (Admiralty, 2010). Consequently, these data may not be completely accurate, and furthermore, these secondary ports may still not be located close enough to the study site.

Studies by Zong et al. (2003) and Hamilton and Shennan (2005a) can be used as an example of how using inaccurate tidal information can affect results. Zong et al. (2003) collected samples from an inner estuary saltmarsh and were levelled to the height of MLLW (Mean Low Low Water) with the altitudes calculated based on the published predicted tidal height. A diatom transfer function was created to determine earthquake history of the area. However, following the study, Hamilton and Shennan (2005a) measured the high and low water levels from the same site, and compared these with the nearest tide gauge (20 km north of the river entrance), revealing that there was a 16% increase in high water upstream in comparison to the tide station. This had implications for the resulting subsidence reconstruction. Zong et al. (2003) estimated the magnitude of subsidence as 0.17 +/- 0.12 m, but the amplification of the tide was not taken into account (an omission in their calculation of the error was also made) resulting in an under-estimation. Recalculations by Hamilton and Shennan (2005a) estimated the subsidence to be 0.3 m, demonstrating how important using correct tidal reference levels is, particularly when sites are not located on the coast.

Asymmetry

Using the constituents MHWST, MTL and MLWST is also misleading for an asymmetrical tide. If it is possible to calculate the MHWST or MLWST for the data, these values will only incorporate the mean heights as opposed to the mean time (duration), which is also incorporated into the values for a symmetrical tide. The MTL is the difference between the MHWST and MLWST and it is the same as the mean in time for a symmetrical tide (figure 7.6). However, in an asymmetrical tide the altitudinal mean between MHWST and MLWST is not the same as mean in time which is much lower for an asymmetrical tide (figure 7.6). This may be more problematic when using the SWLI, in particular due to combining different sites together.

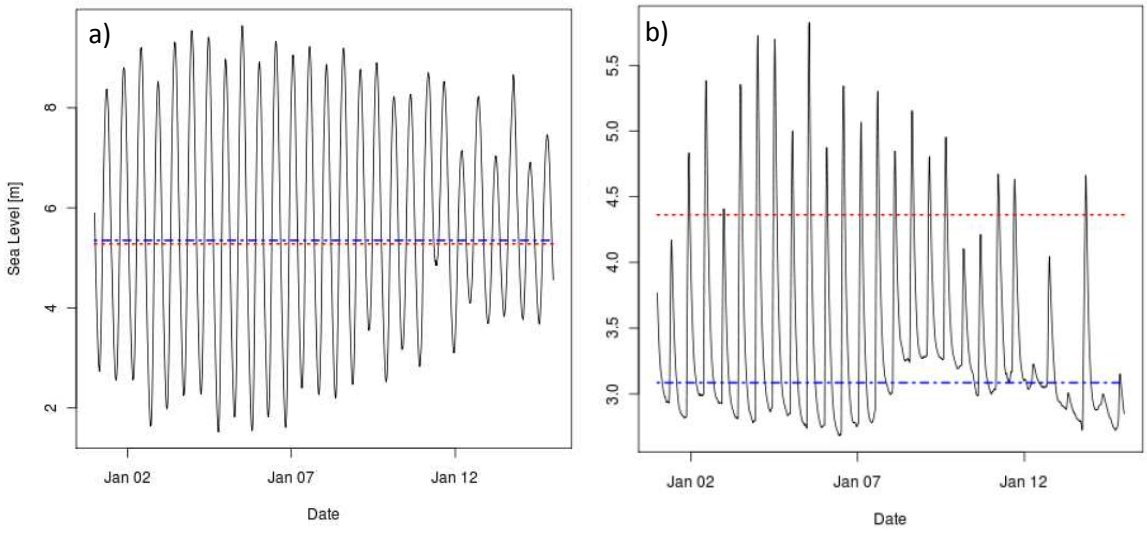

Figure 7.6 Fortnight of tidal time-series data from a) Gladstone Dock and b) Fiddlers Ferry (located approximately 6 km upstream from Hale Head). The mean of the time-series is shown in blue and the mean of the range is shown in red.

SWLI

The SWLI method developed by Horton (1997) was originally based upon MTL and MHWST. Horton (1997) chose these tidal levels over other tidal levels due to the availability of the data, the height in which the samples are taken (usually between MTL and MHWST) and these levels were found to perform more consistently for different marshes. This method was applied for modern studies and reconstructions (e.g. Horton et al., 1999; Edwards et al., 2004) up until 2005 when the SWLI was based upon MLWST and MTL (Horton and Edwards, 2005), which was then applied (e.g. Boomer and Horton, 2006; Horton and Edwards, 2006).

Since then, variations of this method have been established. The Hamilton and Shennan (2005b) study is an example of how the SWLI method has and can be adapted for different studies. In order to overcome the difference in tidal amplitude between the tide gauge and the study site, Hamilton and Shennan (2005b) used MHHW (Mean High High Water) to standardise the elevations. Tidal range differences between sites were converted into SWLI values were therefore based upon MHHW and MTL. MHHW was used as this could be measured in the field and compared with the tide gauge, as MLLW was found not be suitable as the base flow of the river dampens out the effect of the low tide. Leorri et al. (2008, 2009, 2010, 2011) also used MHHW and MTL and Rossi et al. (2011) used MHHW along with MLLW.

It is important to choose the correct and most reliable reference water levels when using the SWLI method as there can be disparities between the different values used, and therefore this may affect the results of the reconstruction. For example, Woodroffe and Long (2010) used HAT and MTL for standardisation as there was found to be a significant disparity in the SWLI values close to HAT for two sites when using MLWST and MHWST. The reference water levels HAT and MTL were used and this resulted in only a small disparity in the SWLI value for MHWST between the two sites (0.70 SWLI units and 0.63 SWLI units) (Woodroffe and Long, 2010). This demonstrates how it is important to use the correct reference water levels.

7.1.7. Macro-tidal setting

As the Mersey Estuary is macrotidal it does have some disadvantages over microtidal study sites. First, the greater tidal range results in a more energetic and dynamic environment which can cause greater mixing and in-washing of sediments and foraminifera. There were some problems with in-washing of exotic species onto the marsh at both sites, this was limited mostly to the lower elevation in Oglet Bay and did not affect the relationship of the foraminiferal assemblages with elevation. In contrast, there was a large allochthonous component of dead exotic species in Decoy Marsh due to the high equinoctial tide however this was resolved by using the live assemblage component. Secondly, a large tidal range can cause greater asymmetry within the estuary, resulting in problems relating to the use of a regional transfer function using the SWLI approach as described above.

Thirdly, the more extensive water level movements and considerable elevational difference between the high and low waters causes greater dewatering (wetting and drying) during low tide and greater duration of the flood waters, this optimises the conditions for carbonate dissolution (de la Paz et al., 2007). Consequently, this can cause considerable decalcification and loss of calcareous foraminifera. This is likely to have caused the loss of foraminifera in the Decoy Marsh core, constraining the length of the sea-level record, but may also have resulted in compaction (or mass loss) of the core as discussed above. In addition, the calcium dissolution varies through the sediments as a result of the fast accumulation. In Oglet Bay, for example, this may result in an inaccurate sea-level reconstructions as a fall in calcareous species caused by dissolution may be interpreted as a change in environment. This may have caused or at least contributed to the substantial fall in MTL in the reconstruction.

Fourthly, the macrotidal estuary appears to be very sensitive to changes in bathymetry, mostly in the inner estuary, which may have resulted in large changes in tidal range and asymmetry over short time periods. The dynamic migration of channels within the Inner Estuary may have significantly affected the reconstruction from Oglet Bay. Channel migration has not only affected the erosion and accretion of the marsh but may have caused changes in the tidal regime, changing the tidal range and probably the asymmetry of the tide. These changes are likely to be the cause of the dramatic fall in MTL between 1993 and 1997.

Lastly, the tidal distortion which occurs in a macrotidal estuary up-stream results in different tidal regimes in the outer and inner estuary, and consequently the primary tidal gauge is not appropriate to use. Secondary ports may be available within the estuary and these are more suitable. However, as discussed above, these may also have problems with their use.

In spite of these shortcomings, the local transfer function in the Mersey Estuary performs well in comparison to other macro-tidal studies. For example, Hill et al. (2007) demonstrated, using diatoms, that a prediction error of 0.876 m is acceptable in the context of a macro-tidal setting. This is of low precision in comparison to the local transfer function established in this study, which was found to have a prediction error of 0.11 m. Gehrels et al. (2001) studied the distributions of foraminifera, diatoms and testate amoebae over three macrotidal (4.47 to 6.6 m) saltmarshes and found a maximum precision of 0.13 m using all proxies for a regional dataset, to as low as 0.10 m for a local diatom dataset only, both are comparable to the results of the present study.

7.2. Further work

The main focus of further work highlighted by this study, and the above discussion are issues related to the location of the study sites within the inner estuary, particularly relating to the effects of tidal asymmetry. This is an important issue as inner estuaries are often suitable locations of saltmarsh growth, and, in addition, modern saltmarsh studies may have already been conducted in locations which are subjected to asymmetrical tides.

The effects of asymmetry needs further exploration in relation to standardising elevations when combining sites with different tidal regimes and curves, and the impacts of this on sea-level reconstructions. It may be that tidal asymmetry has a little impact on the reconstruction within errors, and therefore the present method is applicable, or it may have a greater impact which must be corrected for. The above discussion theorises the effects tidal asymmetry may have on using a SWLI, but in order to examine this further and quantify the effects, further investigation must be carried out.

The first step could be to further examine the relationship between flooding duration and elevation for an asymmetrical tide. Temporary tide gauges could be installed at the study sites in order to determine the extent of the asymmetry over a monthly cycle and this can be compared with measurements of the symmetrical tide at Liverpool. Correlation coefficients will reveal how good elevation is as a proxy for tidal flooding for an asymmetrical tide which has only be previously conducted for symmetrical tides (e.g. Horton, 1997; Gehrels et al., 2001). The two can then be compared to reveal whether there is a difference between the relationships for the two different tidal regimes.

Once this relationship has been established it may be possible that a correction method can be calculated which can be applied to the SWLI results. Alternatively, a new standardisation method could be developed, with emphasis on tidal inundation time rather than altitude. This may be a tidal flooding standardisation such as that carried out in Gehrels (2000), but using a flood duration calculation for an asymmetrical tide instead.

A second important issue is related to using the correct tidal reference levels for the study sites. This study presently uses values from the secondary port of Hale. If possible, further work could involve establishing observed tidal measurements from Hale in order to compare the two, and establish whether the values supplied by Admiralty (Admiralty, 2010) are accurate enough to be used. Additionally, temporary tide gauges could be installed on

the saltmarsh sites in order to determine if the tidal data from Hale is accurate enough to use for both sites.

Following the above, several new sea-level reconstructions may be developed. Firstly, a reconstruction based upon flooding duration which could be compared with those established from this study based upon elevation. Secondly, a new reconstruction based upon new standardisation method developed (which can be used for UK sites) could be compared to the previous SWLI reconstructions in this study. Thirdly, if the tide is measured on the saltmarshes in this study, then a further reconstruction based upon these tide levels may be developed and compared with the previous reconstructions. Errors from using incorrect or inaccurate tidal levels may be established so in future studies these may be incorporated into the reconstruction.

Lastly, due to the uncertainties related to the cause of the substantial fall in MTL at Oglet Bay between 1993 (+/-2) and 1998 (+/-1) and whether this is related to changes in tidal amplitude and asymmetry as a consequence of tidal channel migration, or related to the fluctuating dissolution of calcareous foraminifera in the core, the data could be re-presented in terms of concentration data rather than relative percentages and the calcareous species removed. Alternatively, the calcareous species could be removed and the percentages re-calculated based upon the agglutinated species only and a 'dissolved' transfer function reconstruction carried out. This may remove the increase in agglutinated species in relation to the calcareous species decline, and may alter the MTL reconstruction. In addition, a second proxy which is less susceptible to dissolution by decalcification could be utilised. The proxy could be used to create a second reconstruction from the same location and comparisons made with the foraminifera-based reconstruction, with the potential to differentiate between the potential causes of the apparent sea-level fall.

8. Conclusions and implications

A total of 82 surface samples from two saltmarshes in the Inner Mersey Estuary, Oglet Bay and Decoy Marsh, were analysed for foraminifera along with several environmental variables (organic matter content, salinity, pH, and grain size). Species assemblages were found to be similar to other studies in the UK and elsewhere, with two main zonations across the marsh: a high-to-middle marsh zone occupied by *Haplophragmoides* spp*., J. macrescens* and *M. fusca;* and a low marsh zone composed of similar agglutinated species with increasing numbers of calcareous species, including *Brizalina* spp*., Elphidium* spp*.* and *Haynesina* spp*.* There was intra-site variability across Oglet Bay saltmarsh which also differed from previous studies, with a greater abundance of *Haplophragmoides* spp. reflecting the low salinity of the marsh and estuary, and the dense *Phragmites* spp. vegetation. In addition, a large input of allochthonous calcareous species were found to dominate a dead assemblage from Decoy Marsh causing discrepancies between the two transects. This latter problem was overcome by using the live data from Decoy Marsh which were consistent for both transects*.*

All foraminiferal distributions along the individual transects were found to be controlled predominantly by elevation and distance from tidal influence, whilst the combined data's main control was related to the site at which the transect was carried out, reflecting the intra- and inter-site variability in the assemblages. Elevation was also found have an important control when the data were combined, explaining 4% of the total inertia when transect number was included as a variable, and 20% when this was removed. The amount of variance explained by elevation in previous studies varies from 3% to 32% with all studies concluding that the data was able to be used for a reconstruction. Therefore the dataset within this study compares well in comparison.

The modern foraminifera distribution data from this study highlights the importance of sampling location and sampling time when collecting contemporary foraminiferal data to form part of a training set. Therefore future studies should take more than one transect across the marsh if possible, which will add to the modern local transect, capturing more environments and providing more modern analogues for the reconstruction. If only one transect is sampled, a representative area should be chosen. Alternatively, samples could be randomly collected across the marsh at different elevations capturing all environments (e.g. Leorri et al., 2008).

The modern distribution data from this study was used to reconstruct former sea level from the two study sites as there was a reasonable relationship between species and elevation and a large enough dataset. Before the reconstructions were undertaken, the saltmarsh sediments, particularly from Oglet Bay, were examined. Cores for sea-level reconstructions were taken and a chronological framework established. These methods allowed the sediment accretion process to be established for each of the marshes.

Oglet Bay was found to have rapid sedimentation rate (2.2 to 2.42 cm $year^{-1}$) due to infilling. The sediment core covered a short time-period of approximately 35 years, based upon the ^{137}Cs and ^{241}Am radionuclide peak activities. Only two pollution indicators based upon Hg pollution could be used to further constrain the chronology. The saltmarsh was found to be very dynamic, with periods of rapid erosion and accretion due to the changes in local hydrodynamics and sedimentation patterns due to the migration of low water channels within the estuary.

Decoy Marsh was determined to have a slower sedimentation rate (0.32 cm $year^{-1}$) compared to Oglet Bay, and is more likely to reflect sea-level rise. The sediment core covered a longer time period of approximately 110 years. The chronology was based upon ^{137}Cs, ^{241}Am and ^{210}Pb, and as the core covered a period of higher industrial activity, more pollution indicators could to be used, allowing older sediments to be further constrained. The saltmarsh was found to be more stable than Oglet Bay and seemed to be less affected by channel migration.

Although the Decoy Marsh sediments are much older in age than Oglet Bay and had the potential to reconstruct a sea-level record from the late 17^{th} century onwards, unfortunately, the foraminifera preservation, caused by decalcification of the sediments, only allowed the sea-level record to be reconstructed from 1978 onwards. The sediment accumulation rate implied that the marsh accretion reflects sea-level change, however the foraminifera-based reconstruction was found to have a rate of change (1.12 cm $year^{-1}$) which was much greater than the annual instrumental record for the same time period of 0.6 cm $year^{-1}$, although it was similar to the mean monthly record of change from Liverpool of 1.04 cm $year^{-1}$). The earliest part of the reconstruction also under-estimated the instrumental record. This is most likely to be due to compaction which has occurred in the sediments related to volume loss due to decomposition of organic matter as well as decalcification.

The Oglet Bay reconstruction had an average rate of sea-level change (1.84 cm $year^{-1}$), which was also greater than the instrumental record but was comparable within errors.

The sea-level trend from Oglet Bay did not compare well with the tide gauge record as it had a large fall in MTL, which was not recorded in the instrumental record. Therefore it appears to be is unrelated to any real changes in sea level. It is possible that the fall in MTL is reflecting changes in tidal amplitude in the low waters, and decreasing the asymmetry within the inner estuary only, which were not corrected for in the reconstruction. It is also possible that it is related to the variable decalcification through the core causing the loss of calcareous species which occurred at the same depth as MTL the fall.

In order to overcome the potential problems related to foraminifera loss and compaction related to decalcification and possible organic decomposition, future studies should examine the Ca, Sr, organic matter content along with dry bulk density profiles to try and identify these problems before a reconstruction is attempted.

In addition, this study also demonstrates the problems associated with changes in tidal range over very short periods of time. Although these changes are most likely to be related to human impacts in this study, natural processes alone may result in changes in the tidal regime within an estuary, particularly if it is macrotidal, e.g. storms may reconfigure tidal channels. Therefore, future studies should not assume that tidal ranges have remained unchanged, particularly if studies are within estuaries.

Both sea-level reconstructions in this study were made using the local modern foraminifera relationship with elevation, and the WAPLS model, using component 2. This proved to have the best predictive ability (r^2_{jack} = 0.8), lowest errors ($RMSEP_{jack}$ = 0.11 m) and was more reliable than other reconstructions based on multiple sites. The regional transfer function alone was found not to perform as well, and the combined local and regional dataset was thought to potentially have problems related to combined sites with different asymmetry.

As the tide propagates up-estuary in the Mersey it becomes increasing asymmetrical, therefore as the sites in this study are located within the Inner Estuary, they subjected to an asymmetrical tide. Adding these sites to foraminifera data from saltmarshes which have symmetrical tides may be problematic when standardising for elevation. This may have implications for sea-level reconstruction and needs to be explored further.

To conclude, the study found that a foraminifera-based sea-level reconstruction using sediments from the Mersey Estuary is possible to +/- 0.11 m errors. A local transfer function based upon foraminifera assemblages collected from the Inner Estuary was developed and was used to reconstruct the sea-level from two cores. Although the estuary is strongly macro-tidal it was demonstrated that it is possible to achieve good model prediction error in comparison to other macrotidal studies, and to produce two reconstructions which could be compared with the instrumental record. However, the records were very short in duration and were unable to meet the length of the instrumental record nor pre-date it. This was a consequence of decalcification in the cores causing the loss of foraminifera with depth. This also proved to be problematic in Oglet Bay were it may have resulted in an unreliable sea-level reconstruction. There were also problems relating to the dynamic nature and movement of tidal changes within the Inner Estuary which may also have dramatically affected the reconstruction from Oglet Bay. In addition, the high tidal range and high equinox tide disturbed the foraminiferal assemblage at Decoy Marsh at the time of collection. The Mersey Estuary's substantial anthropogenic activity did however prove to be beneficial in establishing pollution indictors to provide a well constrained chronology for Decoy Marsh. Overall, the study highlights the problems which may arise when conducting sea-level research in an inner estuary which is strongly macrotidal as well as drawing attention to some of the issues relating to the transfer function technique, and demonstrates some potential problems which should be considered in all future sea-level reconstructions.

9. References

Adam, P. (1990) *Saltmarsh ecology*, Cambridge University Press, Cambridge.

Adams, D.A. (1963) 'Factors Influencing Vascular Plant Zonation in North Carolina Salt Marshes', *Ecology*, vol. 44, no. 3, pp. 445-456.

Admiralty (2010) *Admiralty tide tables NP 201-07*, United Kingdom hydrographic office, Taunton.

Alexander, C., Smith, R., Calder, F., Schropp, S. and Windom, H. (1993) 'The historical record of metal enrichment in two Florida estuaries', *Estuaries and Coasts*, vol. 16, no. 3, pp. 627-637.

Allen, J.R.L. (1990) 'Salt-marsh growth and stratification - a numerical-model with special reference to the Severn Estuary, Southwest Britain', *Marine Geology*, vol. 95, no. 2, pp. 77-96.

Allen, J. R. L. (1991). 'Salt-marsh accretion and sea-level movement in the inner Severn Estuary, southwest Britain: The archaeological and historical contribution.' *Journal of the Geological Society,* vol. 148, no. 3, pp. 485-494.

Allen, J.R.L. (1999) 'Geological impacts on coastal wetland landscapes: some general effects of sediment autocompaction in the Holocene of northwest Europe', *Holocene*, vol. 9, no. 1, pp. 1-12.

Allen, J.R.L. (2000) 'Holocene coastal lowlands in NW Europe: autocompaction and the uncertain ground', In: Pye K. and Allen J.R.L. (eds), *Coastal and Estuarine Environments: sedimentology, geomorphology and geoarchaeology*, vol. 175, Special Publication, Geological Society of London, pp. 239-252.

Allen, J.R.L. and Haslett, S.K. (2002) 'Buried salt-marsh edges and tide-level cycles in the mid-Holocene of the Caldicot Level (Gwent), South Wales, UK', *Holocene*, vol. 12, no. 3, pp. 303-324.

Aller, R.C. (1982) 'Carbonate dissolution in nearshore terrigenous muds - the role of physical and biological reworking', *Journal of Geology*, vol. 90, no. 1, pp. 79-95.

Allison, J.E. (1949) *The Mersey estuary,* Liverpool University Press, Liverpool.

Alloway, B.J. (1995) *Heavy metals in soils*, (2nd ed), Blackie Academic and Professional, London.

Alve, E. and Murray, J.W. (1995) 'Benthic foraminiferal distribution and abundance changes in Skagerrak surface sediments: 1937 (Hoglund) and 1992/1993 data compared', *Marine Micropaleontology*, vol. 25, no. 4, pp. 269-288.

Alve, E. and Murray, J.W. (2001) 'Temporal variability in vertical distributions of live (stained) intertidal foraminifera, southern England', *Journal of Foraminiferal Research*, vol. 31, no. 1, pp. 12-24.

Andersen, T.J., Mikkelsen, O.A., Moller, A.L. and Pejrup, M. (2000) 'Deposition and mixing depths on some European intertidal mudflats based on Pb-210 and Cs-137 activities', *Continental Shelf Research*, vol. 20, no. 12-13, pp. 1569-1591.

Anderson, N.J., Bugmann, H., Dearing, J.A. and Gaillard, M.J. (2006) 'Linking palaeoenvironmental data and models to understand the past and to predict the future', *Trends in Ecology and Evolution*, vol. 21, no. 12, pp. 696-704.

Appleby, P.G., Nolan, P.J., Gifford, D.W., Godfrey, M.J., Oldfield, F., Anderson, N.J. and Battarbee, R.W. (1986) '210Pb dating by low background gamma counting.', *Hydrobiologia*, vol. 141, pp. 21-27.

Appleby, P.G., Richardson, N. and Nolan, P.J. (1991) '241AM dating of lake-sediments', *Hydrobiologia*, vol. 214, pp. 35-42.

Appleby, P.G., Richardson, N. and Nolan, P.J. (1992) 'Self-absorption corrections for well-type germaniun detector', *Nuclear Instruments and Methods*, vol. 71, pp. 228-233.

Appleby, P.G. (2001) 'Chronostratigraphic techniques in recent sediments', In: Last W.M. and Smo J.P. (eds), *Tracking Environmental Change Using Lake Sediments*, vol. 1: Basin Analysis, Coring, and Chronological Techniques, Kluwer Academic, Dordrecht, pp. 171-203.

Appleby, P.G. and Piliposyan, G.T. (2010) *Report on the radiometric analysis of a sediment core from Oglet Bay in the Mersey Estuary*, Environmental Radioactivity Research Centre, University of Liverpool.

Archer, A. and Barratt, R.S. (1976) 'Lead levels in Birmingham England dust', *Science of the Total Environment*, vol. 6, no. 3, pp. 275-286.

Aston, S.R. and Stanners, D.A. (1979) 'Determination of estuarine sedimentation-rates by Cs-134-Cs-137 and other artificial radionuclide profiles', *Estuarine and Coastal Marine Science*, vol. 9, no. 5, pp. 529-541.

Aston, S.R., Assinder, D.J. and Kelly, M. (1985) 'Plutonium in intertidal coastal and estuarine sediments in the Northern Irish sea', *Estuarine Coastal and Shelf Science*, vol. 20, no. 6, pp. 761-771.

Beeftink, W.G. (1966) 'Vegetation and habitat of the salt marshes and beach plains in the south-western part of the Netherlands', *Wentia*, vol. 15, pp. 83-108.

Belknap, D.F. and Kraft, J.C. (1977) 'Holocene relative sea-level changes and coastal stratigraphic units on northwest flank of Baltimore canyon through geosyncline', *Journal of Sedimentary Petrology*, vol. 47, no. 2, pp. 610-629.

Bell, G. (2000) 'The distribution of abundance in neutral communities', *American Naturalist*, vol. 155, no. 5, pp. 606-617.

Belyea, L.R. (2007) 'Revealing the Emperor's new clothes: niche-based palaeoenvironmental reconstruction in the light of recent ecological theory', *Holocene*, vol. 17, no. 5, pp. 683-688.

Bentley, S.J., Sheremet, A. and Jaeger, J.M. (2006) 'Event sedimentation, bioturbation, and preserved sedimentary fabric: Field and model comparisons in three contrasting marine settings', *Continental Shelf Research*, vol. 26, no. 17-18, pp. 2108-2124.

Berry, A. and Plater, A.J. (1998) 'Rates of tidal sedimentation from records of industrial pollution and environmental magnetism: The Tees Estuary, North-East England', *Water Air and Soil Pollution*, vol. 106, no. 3-4, pp. 463-479.

Birks, H.J.B. (1995) 'Quantitative palaeoenvironemtal reconstructions', In: Maddy D. and Brew J. (eds), *Statistical modelling of Quaternary science data, Technical guide No. 5.,* Quaternary Research Association Cambridge, pp. 161-236.

Birks, H.J.B., Line, J.M., Juggins, S., Stevenson, A.C. and Terbraak, C.J.F. (1990) 'Diatoms and ph reconstruction', *Philosophical Transactions of the Royal Society B-Biological Sciences*, vol. 327, no. 1240, pp. 263-278.

Blanchet, F.G., Legendre, P. and Borcard, D. (2008) 'Forward selection of explanatory variables', *Ecology*, vol. 89, pp. 2623-2632.

Bloom, A.L. (1964) 'Peat accumulation and compaction in a Connecticut coastal marsh', *Journal of Sedimentary Petrology*, vol. 34, no. 599-603.

Blott, S. (2000) *GRADISTAT* version 4.0, Univeristy of London, Surrey.

Blott, S.J., Pye, K., van der Wal, D. and Neal, A. (2006) 'Long-term morphological change and its causes in the Mersey Estuary, NW England', *Geomorphology*, vol. 81, no. 1-2, pp. 185-206.

Boomer, I. (1998) 'The relationship between meiofauna (Ostracoda, Foraminifera) and tide levels in modern intertidal environments of North Norfolk: A tool for palaeoenvironmental reconstruction' *Bulletin of the Geological Society of Norfolk*, vol. 46, pp. 17-29.

Boomer, I. and Horton, B.P. (2006) 'Holocene relative sea-level movements along the North Norfolk Coast, UK', *Palaeogeography Palaeoclimatology Palaeoecology*, vol. 230, no. 1-2, pp. 32-51.

Boorman, L., Hazelden, J. and Brooman, M. (2002) 'New salt marshes for old: salt marsh creation and management', In: *The changing Coast*, EUROCAST/ EUCC, EUROCOAST Litora, Porto, Portugal, pp. 35-45.

Bjørlykke, K. and Høeg, K. (1997) 'Effects of burial diagenesis on stresses, compaction and fluid flow in sedimentary basins:' *Marine and Petroleum Geology*, vol. 14, pp. 267 -276.

Bradshaw, J.S. (1968) 'Environmental parameter and marsh foraminifera', *Limnology and Oceanography*, vol. 13, pp. 26-38.

Brain, M. (2006) '*Autocompaction of Mineralogenic Intertidal Sediments'*, Thesis Ph.D, University of Durham, Durham, UK.

Brasier, M.D. (1981) 'Microfossil transport in the tidal Humber Basin', Neale J.W. and M.D. Brasier (eds), *Microfossils from Recent and Fossil Shelf Seas*, Ellis Horwood, Chichester, pp. 314-322.

Bronnimann, P., van Dover, C.L. and Whittaker, J.E. (1989) 'Abyssotherma pacifica n. gen n. sp. A recent remaneicid (Foraminifera: Remaneicacea) from the East Pacific Rise', *Micropaleontology,* vol. 35 no. 2 pp. 142-149.

Buzas, M.A. (1968) 'On the spatial distribution of foraminifera', *Contributions from the Cushman Foundation for Foraminiferal Research*, vol. 19, pp. 1-11.

Buzas, M.A., Smith, R.K. and Beem, K.A. (1977) 'Ecology and systematics of foraminifera in 2 thalassia habitats jamaica west-indies', *Smithsonian Contributions to Paleobiology*, no. 31, pp. 1-139.

Buzas, M.A., Hayer, L.A.C., Reed, S.A. and Jett, J.A. (2002) 'Foraminiferal densities over five years in the Indian River Lagoon, Florida: A model of pulsating patches', *Journal of Foraminiferal Research*, vol. 32, no. 1, pp. 68-92.

Cahoon, D.R., French, J.R., Spencer, T., Reed, D. and Moller, I. (2000) 'Vertical accretion versus elevational adjustment in UK saltmarshes: an evaluation of alternative methodologies', *Coastal and Estuarine Environments: Sedimentology, Geomorphology and Geoarchaeology*, vol. 175, pp. 223-238.

Camill, P. and Clark, J.S. (2000) 'Long-term perspectives on lagged ecosystem responses to climate change: Permafrost in boreal peatlands and the Grassland/Woodland boundary', *Ecosystems*, vol. 3, no. 6, pp. 534-544.

Carpenter, R., Beasley, T.M., Zahnle, D. and Somayajulu, B.L.K. (1987) 'Cycling of fallout (Pu, Am-241, Cs-137) and natural (U, Th, Pb-210) radionuclides in washington continental-slope sediments', *Geochimica Et Cosmochimica Acta*, vol. 51, no. 7, pp. 1897-1921.

Carter, N. (1933) 'Comparative study of the alga flora of two salt marshes. Part III', *Journal of Ecology*, vol. 21, no. 2, pp. 385-403.

Carter, R.W.G. (1988) *Coastal Environments*. Academic Press, London, 617 pp.

Chapman, V.J. (1938) 'Studies in salt-marsh ecology sections I to III', *Journal of Ecology*, vol. 26, pp. 144-179.

Charman, D.J., Roe, H.M. and Gehrels, W.R. (1998) 'The use of testate amoebae in studies of sea-level change: a case study from the Taf Estuary, south Wales, UK', *Holocene*, vol. 8, no. 2, pp. 209-218.

Charman, D.J., Roe, H.M. and Gehrels, W.R. (2002) 'Modern distribution of saltmarsh testate amoebae: regional variability of zonation and response to environmental variables', *Journal of Quaternary Science*, vol. 17, no. 5-6, pp. 387-409.

Chave, J., Muller-Landau, H.C. and Levin, S.A. (2002) 'Comparing classical community models: Theoretical consequences for patterns of diversity', *American Naturalist*, vol. 159, no. 1, pp. 1-23.

Church, J.A., Gregory, J.M., Huybrechts, P., Kuhn, M., Lambeck, K., Nhuan, M.T., Qin, D. and Woodworth, P.L. (2001) 'Changes in sea-level', In: *The scientific basis. IPCC third assessment report - climate change 2001*, Cambridge University Press, New York.

Clark, C.H. (2007) *Elements of tidal-electric engineering*, Wiley and sons, Canada.

Clarke, J.A., Farrell, W.E., and Peltier, W.R. (1978) 'Global changes in postglacial sea level: a numerical calculation' *Quaternary Research,* vol. 9, pp. 265–287.

Coe, A.L. and Church, K.D. (2003) 'Sequence stratigraphy and sea-level change', In: A.L Coe. (ed.), *The sedimentary record of sea-level change*, The Open Univeristy, Cambridge.

Coles, B.P.L., and Funnell, B.M. (1981) 'Holocene palaeoenvironments of Broadland, England' *Special Publication of the International Association of Sedimentologists*, vol. 5, pp. 123-131.

Cook, G.T., MacKenzie, A.B., McDonald, P. and Jones, S.R. (1997) 'Remobilization of Sellafield-derived radionuclides and transport from the north-east Irish Sea', *Journal of Environmental Radioactivity*, vol. 35, no. 3, pp. 227-241.

Covelli, S. and Fontolan, G. (1997) 'Application of a normalization procedure in determining regional geochemical baselines', *Environmental Geology*, vol. 30, no. 1-2, pp. 34-45.

Croudace, I.W. and Cundy, A.B. (1995) 'Heavy-metal and hydrocarbon pollution in recent sediments from southampton water, Southern England - a geochemical and isotopic study', *Environmental Science and Technology*, vol. 29, no. 5, pp. 1288-1296.

Culver, S.J. and Horton, B.P. (2005) 'Infaunal marsh foraminifera from the outer banks, North Carolina, USA', *Journal of Foraminiferal Research*, vol. 35, no. 2, pp. 148-170.

Cundy, A.B. and Croudace, I.W. (1996) 'Sediment accretion and recent sea-level rise in the solent, Southern England: Inferences from radiometric and geochemical studies', *Estuarine Coastal and Shelf Science*, vol. 43, no. 6, pp. 819-819.

Cundy, A.B., Croudace, I.W., Thomson, J. and Lewis, J.T. (1997) 'Reliability of salt marshes as ''geochemical recorders'' of pollution input: A case study from contrasting estuaries in southern England', *Environmental Science and Technology*, vol. 31, no. 4, pp. 1093-1101.

Cundy, A.B., Croudace, I.W., Cearreta, A. and Irabien, M.J. (2003) 'Reconstructing historical trends in metal input in heavily-disturbed, contaminated estuaries: studies from Bilbao, Southampton Water and Sicily', *Applied Geochemistry*, vol. 18, no. 2, pp. 311-325.

Davies, C. (1988) 'Tidal river bores' a dissertation submitted to the University of Lancaster in partial fulfillment for the award of the degree of Bachelor of Arts, Lancaster University.

de Rijk, S. (1995) 'Salinity control on the distribution of salt-marsh foraminifera (Great-marshes, Massachusetts)', *Journal of Foraminiferal Research*, vol. 25, no. 2, pp. 156-166.

de Rijk, S. and Troelstra, S.R. (1997) 'Salt marsh foraminifera from the Great Marshes, Massachusetts: Environmental controls', *Palaeogeography Palaeoclimatology Palaeoecology*, vol. 130, no. 1-4, pp. 81-112.

de Rijk, S. and Troelstra, S. (1999) 'The application of a foraminiferal actuo-facies model to salt-marsh cores', *Palaeogeography Palaeoclimatology Palaeoecology*, vol. 149, no. 1-4, pp. 59-66.

De Vos, W., Tarvainen, S., Salminen, R., Reeder, S., De Vivo, B., Demetriades, A., Pirc, S., Batista, M.J., Marsina, K., Ottesen, R.T., O'Connor, P.J., Bidovec, M., Lima, A., Siewers, U., Smith, B., Taylor, H., Shaw, R., Salpeteur, I., Gregorauskiene, V., Halamic, J., Slaninka, I., Lax, K., Gravesen, P., Birke, M., Breward, N., Ander, E.L., Jordan, G., Duris, M., Klein, P., Locutura, J., Bel-lan, A., Pasieczna, A., Lis J., Mazreku, A., Gilucis, A., Heitzmann, P., Klaver, G. and Petersell, 27. (2006) *Geochemical Atlas of Europe*, Geological Survey of Finland.

Delaune, R.D., Patrick, W.H. and Buresh, R.J. (1978) 'Sedimentation-rates determined by Cs-137 dating in a rapidly accreting salt-marsh', *Nature*, vol. 275, no. 5680, pp. 532-533.

Dixon, G.E. (2003) Essential FVS: A User's Guide to the Forest Vegetation Simulator.U.S. Department of Agriculture, Forest Service, Forest Management Service Center, vol. 193, Fort Collins, CO, USA.

Donnelly, J.P., Cleary, P., Newby, P. and Ettinger, R. (2004) 'Coupling instrumental and geological records of sea-level change: Evidence from southern New England of an increase in the rate of sea-level rise in the late 19th century', *Geophysical Research Letters*, vol. 31, no. 5.

Douglas, B.C. (1992) 'Global sea-level acceleration', *Journal of Geophysical Research-Oceans*, vol. 97, no. C8, pp. 12699-12706.

Duchemin, G., Jorissen, F.J., Redois, F. and Debenay, J.P. (2005) 'Foraminiferal microhabitats in a high marsh: Consequences for reconstructing past sea levels', *Palaeogeography Palaeoclimatology Palaeoecology*, vol. 226, no. 1-2, pp. 167-185.

Edwards, R.J. and Horton, B.P. (2000) 'Reconstructing relative sea-level change using UK salt-marsh foraminifera', *Marine Geology*, vol. 169, pp. 41-56.

Edwards, R.J. (2001) 'Mid- to late Holocene relative sea-level change in Poole Harbour, southern England', *Journal of Quaternary Science*, vol. 16, pp. 221-235.

Edwards, R.J., van de Plassche, O., Gehrels, W.R. and Wright, A.J. (2004a) 'Assessing sea-level data from Connecticut, USA, using a foraminiferal transfer function for tide level', *Marine Micropaleontology*, vol. 51, no. 3-4, pp. 239-255.

Edwards, R.J., Wright, A. and Van de Plassche, O. (2004b) 'Surface distributions of salt-marsh foraminifera from Connecticut, USA: modem analogues for high-resolution sea level studies', *Marine Micropaleontology*, vol. 51, no. 1-2, pp. 1-21.

Edwards, R.J. and Horton, B.P. (2006) 'Developing detailed records of relative sea-level change using a foraminiferal transfer function: an example from North Norfolk, UK', *Philosophical Transactions of the Royal Society A: Mathematical, Physical and Engineering Sciences*, vol. 364, no. 1841, pp. 973-991.

Edwards, R.J. (2006) 'Mid to late Holocene relative sea-level change in southwest Britain and the influence of sediment compaction', *The Holocene*, vol. 16, pp. 575-587.

Ekman, M. (2003) 'The World's longest sea-level series and a winter oscillation index for Northern Europe, 1774-2000', *Small Publications in Historical Geophysics*, vol. 12, pp. 1-29.

Engelhart, S.E., Horton, B.P., Roberts, D.H., Bryant, C.L. and Corbett, D.R. (2007) 'Mangrove pollen of Indonesia and its suitability as a sea-level indicator', *Marine Geology*, vol. 242, no. 1-3, pp. 65-81.

English Nature, (2001) *English Nature's advice given under Regulation 33(2) of the Conservation,* English Nature.

Fairbanks, R.G. (1989) 'A 17,000-year glacio-eustatic sea level record: influence of glacial melting rates on the Younger Dryas event and deep-ocean circulation', *Nature*, vol. 342, no. 6250, pp. 637-642.

Fairbridge, R.W. (1961) Eustatic changes in sea level, in L.H. Ahrens, Press, F., Runcorn, S. K., Urey, H. C. (ed.), *Physics and chemistry of the Earth*, Pergamon Press, London.

Farmer, J.G. and Lovell, M.A. (1984) 'Massive diagenetic enhancement of manganese in Loch Lomond sediments', *Environmental Technology Letters*, vol. 5, pp. 257-262.

Fatela, F. and Taborda, R. (2002) 'Confidence limits of species proportions in microfossil assemblages', *Marine Micropaleontology*, vol. 45, no. 2, pp. 169-174.

Faure, G., Mensing, T.M. and Faure, G.P.o.i.g. (2005) *Isotopes: principles and applications*, (3rd ed), Hoboken, Wiley.

Fokpun, L. and Komar, P.D. (1983) 'Settling velocities of planktonic-foraminifera - density variations and shape effects', *Journal of Foraminiferal Research*, vol. 13, no. 1, pp. 60-68.

Forshaw, R. (1990) *Hale Cliff Wharf*, Interim Survey and Excavation Report Liverpool, North Western Society for Industrial Archaeology and History.

Fox, W.M., Johnson, M.S., Jones, S.R., Leah, R.T. and Copplestone, D. (1999) 'The use of sediment cores from stable and developing salt marshes to reconstruct historical contamination profiles in the Mersey Estuary, UK', *Marine Environmental Research*, vol. 47, no. 4, pp. 311-329.

Freiwald, A. and Schonfeld, J. (1996) 'Substrate pitting and boring pattern of Hyrrokkin sarcophaga Cedhagen, 1994 (Foraminifera) in a modern deep-water coral reef mound', *Marine Micropaleontology*, vol. 28, no. 2, pp. 199-207.

French, J. (2006) 'Tidal marsh sedimentation and resilience to environmental change: Exploratory modelling of tidal, sea-level and sediment supply forcing in predominantly allochthonous systems', *Marine Geology*, vol. 235, no. 1-4, pp. 119-136.

Freund, H., Gerdes, G., Streif, H., Dellwig, O. and Watermann, F. (2004) 'The indicative meaning of diatoms, pollen and botanical macro fossils for the reconstruction of palaeoenvironments and sea-level fluctuations along the coast of Lower Saxony; Germany', *Quaternary International*, vol. 112, pp. 71-87.

Fuller, W.H. (1977) *Movement of selected metals, asbestos, and cyanide in soil: Applications to waste disposal problems*, Environmental Protection Agency, Solid and Hazardous Waste Research Division, Cincinnati, Ohio.

Galloway, J.N., Thornton, J.D., Norton, S.A., Volchok, H.L. and McLean, R.A.N. (1982) 'Trace-metals in atmospheric deposition - a review and assessment', *Atmospheric Environment*, vol. 16, no. 7, pp. 1677-1700.

Garnett, M.H. and Stevenson, A.C. (2004) 'Testing the use of bomb radiocarbon to date the surface layers of blanket peat', *Radiocarbon*, vol. 46, no. 2, pp. 841-851.

Gasse, F., Barker, P., Gell, P.A., Fritz, S.C. and Chalie, F. (1997) 'Diatom-inferred salinity in palaeolakes: An indirect tracer of climate change', *Quaternary Science Reviews*, vol. 16, no. 6, pp. 547-563

Gehrels, W.R. (1994) 'Determining relative sea-level change from salt-marsh foraminifera and plant zones on the coast of maine, usa', *Journal of Coastal Research*, vol. 10, no. 4, pp. 990-1009.

Gehrels, W.R., Belknap, D.F., Pearce, B.R. and Gong, B. (1995) 'Modeling the contribution of m(2) tidal amplification to the holocene rise of mean high water in the gulf of maine and the bay of fundy', *Marine Geology*, vol. 124, no. 1-4, pp. 71-85.

Gehrels, W.R. (1999) 'Middle and late holocene sea-level changes in Eastern Maine reconstructed from foraminiferal saltmarsh stratigraphy and AMS C-14 dates on basal peat', *Quaternary Research*, vol. 52, no. 3, pp. 350-359.

Gehrels, W.R. and Van De Plassche, O. (1999) 'The use of Jadammina macrescens (Brady) and Balticammina pseudomacrescens Bronnimann, Lutze and Whittaker (Protozoa: Foraminiferida) as sea-level indicators', *Palaeogeography, Palaeoclimatology, Palaeoecology*, vol. 149, no. 1-4, pp. 89-101.

Gehrels, W.R. (2000) 'Using foraminiferal transfer functions to produce high-resolution sea-level records from salt-marsh deposits, Maine, USA', *Holocene*, vol. 10, no. 3, pp. 367-376.

Gehrels, W.R., Roe, H.M. and Charman, D.J. (2001) 'Foraminifera, testate amoebae and diatoms as sea-level indicators in UK saltmarshes: a quantitative multiproxy approach', *Journal of Quaternary Science*, vol. 16, no. 3, pp. 201-220.

Gehrels, W.R. (2002) 'Intertidal foraminifera as palaeoenvironmental indicators', In: S.K. Haslett (ed.), *Quantitative Environmental Micropalaeontology*, Arnold, London, pp. 91-114.

Gehrels, W.R., Belknap, D.F., Black, S. and Newnham, R.M. (2002) 'Rapid sea-level rise in the Gulf of Maine, USA, since AD 1800', *Holocene*, vol. 12, no. 4, pp. 383-389.

Gehrels, W.R. and Newman, S.W.G. (2004) 'Salt-marsh foraminifera in Ho Bugt, western Denmark, and their use as sea-level indicators', *Danish Journal of Geography*, no. 104, pp. 97-106.

Gehrels, W.R., Kirby, J.R., Prokoph, A., Newnham, R.M., Achterberg, E.P., Evans, H., Black, S. and Scott, D.B. (2005) 'Onset of recent rapid sea-level rise in the western Atlantic Ocean', *Quaternary Science Reviews*, vol. 24, no. 18-19, pp. 2083-2100.

Gehrels, W.R., Marshall, W.A., Gehrels, M.J., Larsen, G., Kirby, J.R., Eiriksson, J., Heinemeier, J. and Shimmield, T. (2006) 'Rapid sea-level rise in the North Atlantic Ocean since the first half of the nineteenth century', *Holocene*, vol. 16, no. 7, pp. 949-965.

Gehrels, W.R. (2007) 'Sea level studies, Microfossil Reconstructions', In: A.E. Scott (ed.), *Encyclopaedia of Quaternary Science*, Elsevier, Oxford, pp. 3015-3024.

Gehrels, W.R., Hayward, B., Newnham, R.M. and Southall, K.E. (2008) 'A 20th century acceleration of sea-level rise in New Zealand', *Geophysical Research Letters*, vol. 35, no. 2.

Ghosh, S.N. (1998) *Tidal hydraulic engineering*, Balkema, Brookfield, USA.

Gifford and Partners (2004) *Morpholgy Desk Study*, Chester.

Godwin, H. (1940) 'Pollen analysis and forest history of England and Wales', *New Phytologist*, pp. 39.

Goldstein, S.T., Watkins, G.T. and Kuhn, R.M. (1995) 'Microhabitats of salt marsh foraminifera: St Catherines Island, Georgia, USA', *Marine Micropaleontology*, vol. 26, no. 1-4, pp. 17-29.

Gonzalez-Regalado, M.L., Ruiz, F., Baceta, J.I., Gonzalez-Regalado, E. and Munoz, J.M. (2001) 'Total benthic foraminifera assemblages in the southwestern Spanish estuaries', *Geobios*, vol. 34, no. 1, pp. 39-51.

Goodman, J.E., Wood, M.E. and Gehrels, W.R. (2007) 'A 17-yr record of sediment accretion in the salt marshes of Maine (USA)', *Marine Geology*, vol. 242, no. 1-3, pp. 109-121.

Grimm, E.C. (1991) *Tilia 1.5.12*, Illinois state museum.

Gubala, C.P., Engstrom, D.R. and White, J.R. (1990) 'Effects of iron cycling on Pb-210 dating of sediments in an adirondack lake, usa', *Canadian Journal of Fisheries and Aquatic Sciences*, vol. 47, no. 9, pp. 1821-1829.

Guilbault, J.P., Clague, J.J. and Lapointe, M. (1995) 'Amount of subsidence during a late holocene earthquake - evidence from fossil tidal marsh foraminifera at vancouver-island, west-coast of Canada', *Palaeogeography Palaeoclimatology Palaeoecology*, vol. 118, no. 1-2, pp. 49-71.

Guiot, J. and de Vernal, A. (2007) 'Chapter Thirteen Transfer Functions: Methods for Quantitative Paleoceanography Based on Microfossils', In: H.M. Claude and V. Anne De (eds), *Developments in Marine Geology*, Elsevier, vol. 1, pp. 523-563.

Haghiri, F. (1974) 'Plant uptake of cadmium as influenced by cation exchange capacity, organic matter, zinc and soil temperature', *Journal of Environmental Quality*, vol. 3, p. 180.

Hamilton, S. and Shennan, I. (2005a) 'Late Holocene great earthquakes and relative sea-level change at Kenai, southern Alaska', *Journal of Quaternary Science*, vol. 20, no. 2, pp. 95-111.

Hamilton, S. and Shennan, I. (2005b) 'Late Holocene relative sea-level changes and the earthquake deformation cycle around upper Cook Inlet, Alaska', *Quaternary Science Reviews*, vol. 24, no. 12-13, pp. 1479-1498.

Hammer, O. and Harper, D.A.T. (2004) *Past, Version 1.28, http//folk.uio.no/ohammer/past*

Handley, J.F. and Wood, R.W.S. (1999) 'The consequences of landscape change: principles and practice, problems and opportunities' In: E.F. Greenwood (ed.), *Ecology and landscape development: a history of the Mersey Basin*, Liverpool University Press.

Hardie, D.W.F. (1950) *A history of the chemical industry in Widnes*, Imperial Chemical Industries General Chemicals Division, Widnes.

Harland, B.J., Taylor, D. and Wither, K. (2000) 'The distribution of mercury and other trace metals in the sediments of the Mersey Estuary over 25 years 1974-1998', *Science of the Total Environment*, vol. 253, no. 1-3, pp. 45-62.

Harvey, M.M., Hansom, J.D. and MacKenzie, A.B. (2007) 'Constraints on the use of anthropogenic radionuclide-derived chronologies for saltmarsh sediments', *Journal of Environmental Radioactivity*, vol. 95, no. 2-3, pp. 126-148.

Haslett, S.K., Davies, P., and Strawbridge, F. (1997) 'Reconstructing Holocene sea-level change in the Severn Estuary and Somerset Levels: The foraminifera connection' *Archaeology in the Severn Estuary,* vol. 8, pp. 29-40.

Haslett, S.K., Davies, P., Curr, R.H.F., Davies, C.F.C., Kennington, K., King, C.P. and Margetts, A.J. (1998) 'Evaluating late-Holocene relative sea-level change in the Somerset Levels, southwest Britain', *Holocene*, vol. 8, no. 2, pp. 197-207.

Hastie, T. and Tibshirani, R. (1986) 'Generalized Additive Models', *Statistical Science*, vol. 1, no. 3, pp. 297-310.

Hayes, M.O. (1976) 'Morphology of sand accumulation in estuaries. An introduction to the symposium' In: L.E. Cronin (ed) *Estuarine Research, 2, Geology and Engineering Academic Press*, London, pp. 3-22.

Haynes, J.R. (1973) 'Cardigan Bay recent foraminifera (cruises of the R.V. Antur, 1962–1964). Bulletin of the British Museum (Natural History)' *Zoology*, Supplement 4.

Hayward, B.W., Holzmann, M., Grenfell, H.R., Pawlowski, J. and Triggs, C.M. (2004a) 'Morphological distinction of molecular types in Ammonia - towards a taxonomic revision of the world's most commonly misidentified foraminifera', *Marine Micropaleontology*, vol. 50, no. 3-4, pp. 237-271.

Hayward, B.W., Scott, G.H., Grenfell, H.R., Carter, R. and Lipps, J.H. (2004b) 'Techniques for estimation of tidal elevation and confinement (similar to salinity) histories of sheltered harbours and estuaries using benthic foraminifera: examples from New Zealand', *Holocene*, vol. 14, no. 2, pp. 218-232.

Hayward, B.W., Grenfell, H.R., Sabaa, A.T. and Kay, J. (2010) 'Using foraminiferal faunas as proxies for low tide level in the estimation of Holocene tectonic subsidence, New Zealand', *Marine Micropaleontology*, vol. 76, no. 1-2, pp. 23-36.

Herut, B. and Sandler, A. (2006), Normalization methods for pollutants in marine sediments: review and recommendations for the Mediterranean' *Israel Oceanographic and Limnological Research, and Geological Survey of Israel IOLR Report H18/2006, submitted to UNEP/MAP.*

Hill, M.O. and Gauch, H.G. (1980) 'Detrended correspondence analysis: An improved ordination technique ', *Plant Ecology* vol. 42,, no. 1-3, pp. 47-58.

Hill, T.C.B., Woodland, W.A., Spencer, C.D. and Marriott, S.B. (2007) 'Holocene sea-level change in the Severn Estuary, southwest England: a diatom-based sea-level transfer function for macrotidal settings', *Holocene*, vol. 17, pp. 639-648.

Hippensteel, S.P., Martin, R.E., Nikitina, D. and Pizzuto, J.E. (2000) 'The formation of holocene marsh foraminiferal assemblages, middle Atlantic Coast, USA: Implications for Holocene sea-level change', *Journal of Foraminiferal Research*, vol. 30, no. 4, pp. 272-293.

Hippensteel, S.P., Martin, R.E., Nikitina, D. and Pizzuto, J.E. (2002) 'Interannual variation of marsh foraminiferal assemblages (Bombay Hook National Wildlife Refuge, Smyrna, DE): Do

foraminiferal assemblages have a memory?', *Journal of Foraminiferal Research*, vol. 32, no. 2, pp. 97-109.

Horowitz, A.J., Elrick, K.A. and Hooper, R.P. (1989) 'The prediction of aquatic sediment-associated trace element concentrations using selected geochemical factors', *Hydrological Processes*, vol. 3, no. 4, pp. 347-364.

Horton, B.P. (1997) '*Quantification of the indicative meaning of a range of Holocene sea-level index points from the western North Sea'*, Thesis Ph.D, University of Durham, Durham, UK.

Horton, B.P. (1999) 'The distribution of contemporary intertidal foraminifera at Cowpen Marsh, Tees Estuary, UK: implications for studies of Holocene sea-level changes', *Palaeogeography Palaeoclimatology Palaeoecology*, vol. 149, no. 1-4, pp. 127-149.

Horton, B.P., Edwards, R.J. and Lloyd, J.M. (1999a) 'A foraminiferal-based transfer function: implications for sea-level studies.', *Journal of Foraminiferal Research*, vol. 29, no. 2, pp. 117-129.

Horton, B.P., Edwards, R.J. and Lloyd, J.M. (1999b) 'UK intertidal foraminiferal distributions: implications for sea-level studies', *Marine Micropaleontology*, vol. 36, no. 4, pp. 205-223.

Horton, B.P., Edwards, R.J. and Lloyd. J. M. (1999c) 'Reconstruction of former sea levels using a foraminifera-based transfer function', *Journal of Foraminiferal Research*, vol. 29, no. 2, pp. 117-129.

Horton, B.P., Edwards, R.J. and Lloyds, J.M. (2000) 'Implications of a microfossil transfer function in Holocene sea-level studies', In: I. Shennan, and Andrews J.E. (ed.), *Holocene Land-Ocean Interaction and Environmental Change around the Western North Sea*, vol. 166, Geological Society of London, Special publications, London, pp. 41-54.

Horton, B.P. and Edwards, R.J. (2003) 'Seasonal distributions of foraminifera and their implications for sea-level studies', *SEPM Special Publication*, vol. 75, pp. 21-30.

Horton, B.P., Larcombe, P., Woodroffe, S.A., Whittaker, J.E., Wright, M.R. and Wynn, C. (2003) 'Contemporary foraminiferal distributions of a mangrove environment, Great Barrier Reef coastline, Australia: implications for sea-level reconstructions', *Marine Geology*, vol. 198, no. 3-4, pp. 225-243.

Horton, B.P. and Edwards, R.J. (2005) 'The application of local and regional transfer functions to the reconstruction of Holocene sea levels, north Norfolk, England', *Holocene*, vol. 15, no. 2, pp. 216-228.

Horton, B.P., Whittaker, J.E., Thomson, K.H., Hardbattle, M.I.J., Kemp, A., Woodroffe, S.A. and Wright, M.R. (2005) 'The development of a modern foraminiferal data set for sea-level reconstructions, Wakatobi Marine National Park, Southeast Sulawesi, Indonesia', *Journal of Foraminiferal Research*, vol. 35, no. 1, pp. 1-14.

Horton, B.P. and Edwards, R.J. (2006) 'Quantifying Holocene sea-level change using intertidal foraminifera: Lessons from the British Isles', *Cushman Foundation for Foraminiferal Research Special Publication*, no. 40, pp. 3-97.

Horton, B.P. and Murray, J.W. (2006) 'Patterns in cumulative increase in live and dead species from foraminiferal time series of Cowpen Marsh, Tees Estuary, UK: Implications for sea-level studies', *Marine Micropaleontology*, vol. 58, no. 4, pp. 287-315.

Horton, B.P., Corbett, R., Culver, S.J., Edwards, R.J. and Hillier, C. (2006) 'Modern saltmarsh diatom distributions of the Outer Banks, North Carolina, and the development of a transfer function for high resolution reconstructions of sea level', *Estuarine Coastal and Shelf Science*, vol. 69, no. 3-4, pp. 381-394.

Horton, B.P., Culver, S.J., Hardbattle, M.I.J., Larcombe, P., Milne, G.A., Morigi, C., Whittaker, J.E. and Woodroffe, S.A. (2007) 'Reconstructing holocene sea-level change for the central great barrier reef (Australia) using subtidal foraminifera', *Journal of Foraminiferal Research*, vol. 37, no. 4, pp. 327-343.

Horton, B.P. and Murray, J.W. (2007) 'The roles of elevation and salinity as primary controls on, living foraminiferal distributions: Cowpen Marsh, Tees Estuary, UK', *Marine Micropaleontology*, vol. 63, no. 3-4, pp. 169-186.

Horton, B.P. and Culver, S.J. (2008) 'Modern intertidal foraminifera of the Outer Banks, North Carolina, USA, and their applicability for sea-level studies', *Journal of Coastal Research*, vol. 24, no. 5, pp. 1110-1125.

Hubbell, S.P. (2001) *The unified neutral theory of biodiversity and biogeography*, Princeton NJ, Princeton University Press.

Huisman, J., Olff, H. and Fresco, L.F.M. (1993) 'A hierarchical set of models for species response analysis. ', *Journal of Vegetation Science*, vol. 4, pp. 37-46.

Imbrie, J. and Kipp, N.G. (1971) 'A new micropaleontological method for quantitative paleoclimatology: Applications to late Pleistocene Caribbean core', In: K.K. Turekian (ed.), *The Late Cenozoic Glacial Ages*, Yale University Press, New Haven, pp. 71-181.

Imbrie, J. and Webb, T.I. (1981) 'Transfer functions: Calibrating micropaleontological data in climatic terms', In: Berger A. (ed.), *Climate Variations and Variability: Facts and Theories*, Reidel, Dordrecht,, pp. 125-134.

ICRCL (1987) 'Interdepartmental Committee on the Redevelopment of Contaminated Land. Guidance on the assessment and redevelopment of contaminated land' *Guidance Note ICRCL 59/83 (2nd ed),* Department of the Environment, London UK.

Jelgersma, S. (1961) *Holocene Sea Level Changes in the Netherlands,* Thesis Ph.D. Leiden. Mededelingen Geologische Stichting, CVI-7.

Jemmett, A.W.L. (1991) *'An investigation into the heavy metals, sediment and vegetation of a mersey estuary salt marsh'*, Thesis Ph.D., University of Liverpool, Liverpool UK.

Jennings, A.E., Nelson, A.R., Scott, D.B. and Aravena, J.C. (1995) 'Marsh foraminiferal assemblages in the valdivia estuary, south-central Chile, relative to vascular plants and sea-level', *Journal of Coastal Research*, vol. 11, no. 1, pp. 107-123.

Jevrejeva, S., Moore, J.C., Grinsted, A. and Woodworth, P.L. (2008) 'Recent global sea level acceleration started over 200 years ago?', *Geophysical Research Letters*, vol. 35, no. 8.

Jickells, T.D. and Rae, J.E. (1997) *Biogeochemistry of intertidal sediments*, Cambridge university press, Cambridge.

Jonasson, K.E. and Patterson, R.T. (1992) 'Preservation potential of salt-marsh foraminifera from the fraser-river delta, british-columbia', *Micropaleontology*, vol. 38, no. 3, pp. 289-301.

Jones, G.D. and Ross, C.A. (1979) 'Seasonal distribution of foraminifera in samish bay, washington', *Journal of Paleontology*, vol. 53, no. 2, pp. 245-257.

Jones, V.J. and Juggins, S. (1995) 'The construction of a diatom-based chlorophyll a transfer function and its application at three lakes on Signy Island (maritime Antarctic) subject to differing degrees of nutrient enrichment', *Freshwater Biology*, vol. 34, no. 3, pp. 433-445.

Juggins, S. (1992) 'Bibliotheca Diatomologica, Diatoms in the Thames estuary, England: Ecology, palaeoecology, and salinity transfer function', *Bibliotheca Diatomologica; Diatoms in the Thames estuary, England: Ecology, palaeoecology, and salinity transfer function*, vol. 6 pp. 216.

Juggins, S. (2007) *C2, version 1.5.1. University of Newcastle.*

Kaye, C.A. and Barghoorn, E.S. (1964) 'Late quaternary sea-level change and crustal rise at boston, massachusetts, with notes on the autocompaction of peat', *Geological Society of America Bulletin*, vol. 75, no. 2, pp. 63-80.

Kearney, M.S. and Stevenson, J.C. (1991) 'Island land loss and marsh vertical accretion rate evidence for historical sea-level changes in Chesapeake Bay', *Journal of Coastal Research*, vol. 7, no. 2, pp. 403-415.

Kearney, M.S., Stevenson, J.C. and Ward, L.G. (1994) 'Spatial and Temporal Changes in Marsh Vertical Accretion Rates at Monie Bay: Implications for Sea-Level Rise', *Journal of Coastal Research*, vol. 10, no. 4, pp. 1010-1020.

Keitt, T.H., Bjornstad, O.N., Dixon, P.M. and Citron-Pousty, S. (2002) 'Accounting for spatial pattern when modeling organism-environment interactions', *Ecography*, vol. 25, no. 5, pp. 616-625.

Kemp, A.C., Horton, B.P. and Culver, S.J. (2009a) 'Distribution of modern salt-marsh foraminifera in the Albemarle-Pamlico estuarine system of North Carolina, USA: Implications for sea-level research', *Marine Micropaleontology*, vol. 72, no. 3-4, pp. 222-238.

Kemp, A.C., Horton, B.R., Corbett, D.R., Culver, S.J., Edwards, R.J. and van de Plassche, O. (2009b) 'The relative utility of foraminifera and diatoms for reconstructing late Holocene sea-level change in North Carolina, USA', *Quaternary Research*, vol. 71, no. 1, pp. 9-21.

Kersten, M. and Forstner, U. (1986) 'Chemical fractionation of heavy-metals in anoxic estuarine and coastal sediments', *Water Science and Technology*, vol. 18, no. 4-5, pp. 121-130.

Kim, G., Hussain, N., Chureh, T.M. and Carey, W.L. (1997) 'The fallout isotope 207Bi in a Delaware salt marsh: a comparison with 210Pb and 137Cs as a geochronological tool', *Science of The Total Environment*, vol. 196, no. 1, pp. 31-41.

Kirkham, M.B. (1977) 'Trace elements sludge on land: Effect on plants, soils, and ground water', In: R.C. Laehr (ed.), *Land as waste management alternative* Ann Arbor Science Publishers, Ann Arbor, pp. 209-247.

Kooistra, M.J. (1978) *Soil Development in Recent Marine Sediments of the Intertidal Zone in the Oosterschelde,* The Netherlands, Netherlands Soil Survey Institute.

Krey, PW, Hardy, EP, Pachucky, C, Rourke, F, Coluzza, J. and Benson, W.K. (1976) 'Mass isotopic composition of global fall-out plutonium in soil', In: *Transuranium nuclides in the environment IAEA-SM-199/39*, IAEA, Vienna, pp. 671–678.

Lambeck, K. (1993) 'Glacial rebound of the british-isles .1. preliminary model results', *Geophysical Journal International*, vol. 115, no. 3, pp. 941-959.

Lambeck, K. (1995) 'Late devensian and holocene shorelines of the British-Isles and north-sea from models of glacio-hydro-isostatic rebound', *Journal of the Geological Society*, vol. 152, pp. 437-448.

Lambeck, K. (1996) 'Glaciation and sea-level change for Ireland and the Irish Sea since Late Devensian/Midlandian time', *Journal of the Geological Society*, vol. 153, pp. 853-872.

Lane, A. (2004) 'Bathymetric evolution of the Mersey Estuary, UK, 1906-1997: causes and effects', *Estuarine Coastal and Shelf Science*, vol. 59, no. 2, pp. 249-263.

Le, J. and Shackleton, N.J. (1994) 'Estimation of palaeoenvironment by transfer functions: simulation with hypothetical data', *Marine Micropaleontology*, vol. 24, pp. 187-199.

Legendre, P. (1993) 'Spatial autocorrelation - trouble or new paradigm', *Ecology*, vol. 74, no. 6, pp. 1659-1673.

Legendre, P. (2007) *Program 'varpart' in the package 'vegan' in 'R'* in J. Adapted to vegan by Oksanen (ed.)Departement de Sciences Biologiques. Universite de Montreal, Canada.

Leorri, E., Horton, B.P. and Cearreta, A. (2008) 'Development of a foraminifera-based transfer function in the Basque marshes, N. Spain: Implications for sea-level studies in the Bay of Biscay', *Marine Geology*, vol. 251, no. 1-2, pp. 60-74.

Leorri, E. and Cearreta, A. (2009) 'Recent sea-level changes in the southern Bay of Biscay: transfer function reconstructions from salt-marshes compared with instrumental data', *Scientia Marina*, vol. 73, no. 2, pp. 287-296.

Leorri, E., Martin, R.E. and Horton, B.P. (2009) 'Field experiments on bioturbation in salt marshes (Bombay Hook National Wildlife Refuge, Smyrna, DE, USA): implications for sea-level studies', *Journal of Quaternary Science*, vol. 24, no. 2, pp. 139-149.

Leorri, E., Gehrels, W.R., Horton, B.P., Fatela, F. and Cearreta, A. (2010) 'Distribution of foraminifera in salt marshes along the Atlantic coast of SW Europe: Tools to reconstruct past sea-level variations', *Quaternary International*, vol. 221, no. 1-2, pp. 104-115.

Leorri, E., Fatela, F., Cearreta, A., Moreno, J., Antunes, C. and Drago, T. (2011) 'Assessing the performance of a foraminifera-based transfer function to estimate sea-level changes in northern Portugal', *Quaternary Research*, vol. 75, no. 1, pp. 278-287.

Leps, J. and Smilauer, P. (2003) *Multivariate analysis of ecological data using CANOCO*, Cambridge, Cambridge University Press.

Loring, D.H. and Prosi, F. (1986) 'Cadmium and Lead cycling between water, sediment, and biota in an artificially contaminated mud flat on borkum (frg)', *Water Science and Technology*, vol. 18, no. 4-5, pp. 131-139.

Loring, D.H. (1990) 'Lithium - a new approach for the granulometric normalization of trace metal data', *Marine Chemistry*, vol. 29, pp. 155-168.

Madsen, A.T., Murray, A.S., Andersen, T.J., Pejrup, M. and Breuning-Madsen, H. (2005) 'Optically stimulated luminescence dating of young estuarine sediments: a comparison with Pb-210 and Cs-137 dating', *Marine Geology*, vol. 214, no. 1-3, pp. 251-268.

Marshall, W.A., Gehrels, W.R., Garnett, M.H., Freeman, S., Maden, C. and Xu, S. (2007) 'The use of 'bomb spike' calibration and high-precision AMS C-14 analyses to date salt-marsh sediments deposited during the past three centuries', *Quaternary Research*, vol. 68, pp. 325-337.

Martens, H. and Naes, T. (1989) *Multivariate calibration*, Wiley and Sons , Chichester.

Martin, R.E. (1999) *Taphonomy. A process approach*, Cambridge University Press, Cambridge.

Martin, R.E., Hippensteel, S.P., Nikitina, D. and Pizzuto, J. (2003) 'Taphonomy and artificial time-averaging of marsh foraminiferal assemblages (Bombay Hook National Wildlife Refuge, Smyrna, DE): implications for rates and magnitudes of late Holocene sea-level change', *SEPM (Society for Sedimentary Geology) Special Publication*, vol. 75, pp. 31-49.

Mason, D.C., Scott, T.R. and Dance, S.L. (2010) 'Remote sensing of intertidal morphological change in Morecambe Bay, UK, between 1991 and 2007', *Estuarine Coastal and Shelf Science*, vol. 87, no. 3, pp. 487-496.

Massey, A.C., Gehrels, W.R., Charman, D.J. and White, S.V. (2006a) 'An intertidal foraminifera-based transfer function for reconstructing Holocene sea-level change in southwest England', *Journal of Foraminiferal Research*, vol. 36, no. 3, pp. 215-232.

Massey, A.C., Paul, M.A., Gehrels, W.R. and Charman, D.J. (2006b) 'Autocompaction in Holocene coastal back-barrier sediments from south Devon, southwest England, UK', *Marine Geology*, vol. 226, no. 3-4, pp. 225-241.

Massey, A.C., Gehrels, W.R., Charman, D.J., Milne, G.A., Peltier, W.R., Lambeck, K. and Selby, K.A. (2008) 'Relative sea-level change and postglacial isostatic adjustment along the coast of south Devon, United Kingdom', *Journal of Quaternary Science*, vol. 23, no. 5, pp. 415-433.

Matera, N.J. and Lee, J.J. (1972) 'Environmental factors affecting standing crop of foraminifera in sublittoral and psammolittoral communities of a long-island salt marsh', *Marine Biology*, vol. 14, no. 2, pp. 89-103.

McCaffrey, R.J. and Thomas, J. (1980) 'A record of the accumulation of sediments and trace metals in a Connecticut salt marsh,' *Advances in Geophysics*, vol. 22, pp. 165-236.

Michel, H., Barci-Funel, G., Dalmasso, J., Ardisson, G., Appleby, P.G., Haworth, E. and El-Daoushy, F. (2001) 'Plutonium, americium and caesium records in sediment cores from Blelham Tarn Cumbria (UK)', *Journal of Radioanalytical and Nuclear Chemistry*, vol. 247, pp. 107-110.

Milan, C.S., Swenson, E.M., Turner, R.E. and Lee, J.M. (1995) 'Assessment of the Cs-137 method for estimating sediment accumulation rates - Louisiana salt marshes', *Journal of Coastal Research*, vol. 11, no. 2, pp. 296-307.

Miller, L. and Douglas, B.C. (2006) 'On the rate and causes of twentieth century sea-level rise', *Philosophical Transactions of the Royal Society a-Mathematical Physical and Engineering Sciences*, vol. 364, no. 1841, pp. 805-820.

Milne, G.A., Shennan, I., Youngs, B.A.R., Waugh, A.I., Teferle, F.N., Bingley, R.M., Bassett, S.E., Cuthbert-Brown, C. and Bradley, S.L. (2006) 'Modelling the glacial isostatic adjustment of the UK region', *Philosophical Transactions of the Royal Society a-Mathematical Physical and Engineering Sciences*, vol. 364, no. 1841, pp. 931-948.

Moodley, L. and Hess, C. (1992) 'Tolerance of infaunal benthic foraminifera for low and high oxygen concentrations', *Biological Bulletin*, vol. 183, no. 1, pp. 94-98.

Moore, R.D., Wolf, J., Souza, A.J. and Flint, S.S. (2009) 'Morphological evolution of the Dee Estuary, Eastern Irish Sea, UK: A tidal asymmetry approach', *Geomorphology*, vol. 103, no. 4, pp. 588-596.

Morris, K., Butterworth, J.C. and Livens, F.R. (2000) 'Evidence for the Remobilization of Sellafield Waste Radionuclides in an Intertidal Salt Marsh, West Cumbria, U.K', *Estuarine, Coastal and Shelf Science*, vol. 51, no. 5, pp. 613-625.

Murray, J.W. (1967) 'Production in benthic foraminiferids', *Journal of Natural History*, vol. 1, no. 1, pp. 61-and.

Murray, J.W. and Wright, C.A. (1970) 'Surface textures of calcareous foraminiferids', *palaeontology (Oxford)*, vol. 13, no. 2, pp. 184-187.

Murray, J.W. (1971) 'Living foraminiferainiferids of tidal marshes; a review', *The Journal of Foraminiferal Research*, vol. 1, pp. 153-161.

Murray, J.W. (1973) *Distribution and ecology of living benthic foraminiferids by John W. Murray*, Heinemann Educational, London.

Murray, J.W. and Hawkins, A.B. (1976) 'Sediment transport in the Severn Estuary during the past 8000-9000 years', vol. 132, pp. 385-389.

Murray, J.W. (1979) *British nearshore Foraminiferids: keys and notes for the identification of the species by John W. Murray*, for Linnean Society of London and Estuarine and Brackish-Water Sciences Association by Academic Press, London.

Murray, J.W. (1982) 'Benthic foraminifera: the validity of living, dead or total assemblages for the interpretation of paleaecology', *Journal of Micropalaeontology*, vol. 1, pp. 137-140.

Murray, J.W. (1991) *Ecology and palaeoecology of benthic foraminifera*, Harlow, New York, Longman Scientific and Technical, Wiley.

Murray, J.W. and Alve, E. (1999) 'Natural dissolution of modern shallow water benthic foraminifera: taphonomic effects on the palaeoecological record', *Palaeogeography Palaeoclimatology Palaeoecology*, vol. 146, no. 1-4, pp. 195-209.

Murray, J.W. (2000) 'The enigma of the continued use of total assemblages in ecological studies of benthic foraminifera', *Journal of Foraminiferal Research*, vol. 30, no. 3, pp. 244-245.

Murray, J.W. and Bowser, S.S. (2000) 'Mortality, protoplasm decay rate, and reliability of staining techniques to recognize 'living' foraminifera: A review.', *Journal of Foraminiferal Research*, vol. 30, pp. 66-70.

Murray, J.W. (2003) 'Patterns in the cumulative increase in species from foraminiferal time-series', *Marine Micropaleontology*, vol. 48, no. 1-2, pp. 1-21.

Nelder, J.A. and Wedderburn, R.W.M. (1972) ' ‘‘Generalized linear models".', *Journal of the Royal Statistical Society, ,* vol. Series A, no. 135, pp. 370—384.

Nelson, A.R. and Kashima, K. (1993) 'Diatom zonation in southern oregon tidal marshes relative to vascular plants, foraminifera, and sea-level', *Journal of Coastal Research*, vol. 9, no. 3, pp. 673-697.

New Dutchlist, (1999) Contaminatedland.co.uk.

Ng, S.L. and Sin, F.S. (2003) 'A diatom model for inferring sea level change in the coastal waters of Hong Kong', *Journal of Paleolimnology*, vol. 30, no. 4, pp. 427-440.

Nichols, M.M. and Briggs, R.B. (1985) ‘Estuaries’, In: R.A. Davis (ed.), *Coastal sedimentary environments*, Springer-Verlag, New York, pp. 75-186.

Nikitina, D.L., Pizzuto, J.E., Schwimmer, R.A. and Ramsey, K.W. (2000) 'An updated Holocene sea-level curve for the Delaware coast', *Marine Geology*, vol. 171, no. 1-4, pp. 7-20.

NRA (1995) *The Mersey Estuary: A report on environmental water quality* National Rivers Authority, Bristol.

O'Connor, B.A. (1987) 'Short and long term changes in estuary capacity', *Journal of the Geological Society*, vol. 144, no. 1, pp. 187-195.

Ogichi, T., Jarvie, H.P., Neal, C. (2000) ‘River water quality in the Humber catchment: an introduction using GIS-based mapping analysis’ *Science and the Total Environment,* vol. 251, pp. 9-26.

Oksanen, J. (2011) *Multivariate Analysis of Ecological Communities in R: vegan tutorial* [Online], Available from: http://cc.oulu.fi/~jarioksa/opetus/metodi/vegantutor.pdf

Oksanen, J., Blanchet, F.G., Kindt, R., Legendre, P., O'Hara, R.B., Simpson, G.L., Solymos, P., Stevens, M.H.H. and Wagner, H. (2011) *Vegan*, Ordination methods, diversity analysis and other functions for community and vegetation ecologists.

Oldfield, F. and Appleby, P. (1984) ‘Empirical testing of 210Pb dating models for lake sediments’ In: E.Y. Haworth, and Lund, J.W.G. (eds) *Lake sediments and environmental history,* University of Leicester Press, 93–124.

Oldfield, F., Richardson, N., Appleby, P.G. and Yu, L. (1993) 'Am-241 and Cs-137 activity in fine-grained salt-marsh sediments from parts of the NE Irish sea shoreline', *Journal of Environmental Radioactivity*, vol. 19, no. 1, pp. 1-24.

OSPAR Commission (2010) *Mercury losses from the chlor-alkali industry in 2008.*

Ozarko, D.L., Patterson, R.T. and Williams, H.F.L. (1997) 'Marsh foraminifera from Nanaimo, British Columbia (Canada): Implications of infaunal habitat and taphonomic biasing', *Journal of Foraminiferal Research*, vol. 27, no. 1, pp. 51-68.

Palmer, A.J.M. and Abbott, W.H. (1986) 'Diatoms as indicators of sea-level change', In: O. van de Plassche, (ed.), *Sea-level research: A Manual for the collection and evaluation of data*, Geobooks, Norwich, pp. 457-488.

Parker, F.L. and Athearn, W.D. (1959) 'Ecology of marsh foraminifera in Poponesset Bay, Massachusetts', *Journal of Paleontology*, vol. 33, no. 2, pp. 333-343.

Passant, N.R., Peirce, M., Rudd, H.J., Scott, W.D., Marlowe, I. and Watterson, J.D. (2002.) *UK particulate and heavy metal emissions from industrial processes,* Industrial Processes. AEAT-6270 Issue 2.

Patterson, R.T. (1990) 'Intertidal benthic foraminifera biofacies on the Fraser River Delta, British Columbia', *Micropaleontology*, vol. 36, pp. 229-244.

Patterson, R.T., Dalby, A.P., Roe, H.M., Guilbault, J.P., Hutchinson, I. and Clague, J.J. (2005) 'Relative utility of foraminifera, diatoms and macrophytes as high resolution indicators of paleo-sea level in coastal British Columbia, Canada', *Quaternary Science Reviews*, vol. 24, no. 18-19, pp. 2002-2014.

Paul, M.A. and Barras, B.F. (1998) 'A geotechnical correction for post-depositional sediment compression: examples from the Forth valley, Scotland', *Journal of Quaternary Science*, vol. 13, no. 2, pp. 171-176.

Peltier, W.R., Shennan, I., Drummond, R. and Horton, B. (2002) 'On the postglacial isostatic adjustment of the British Isles and the shallow viscoelastic structure of the Earth', *Geophysical Journal International*, vol. 148, no. 3, pp. 443-475.

Perillo, G.M.E. (1996) *Geomorphology and Sedimentology of Estuaries*, Elsevier science, Netherlands.

Peres-Neto, P.R., Legendre, P., Dray, S. and Borcard, D. (2006) 'Variation partitioning of species data matrices: Estimation and comparison of fractions', *Ecology*, vol. 87, no. 10, pp. 2614-2625.

Peters, D.P.C., Gosz, J.R., Pockman, W.T., Small, E.E., Parmenter, R.R., Collins, S.L. and Muldavin, E. (2006) 'Integrating patch and boundary dynamics to understand and predict biotic transitions at multiple scales', *Landscape Ecology*, vol. 21, no. 1, pp. 19-33.

Pethick, J.S. (1981) 'Long-term accretion rates on tidal salt marshes', *Journal of Sedimentary Research*, vol. 51, no. 2, pp. 571-577.

Phleger, F.B. and Walton, W.R. (1950) 'Ecology of marsh and bay foraminifera, Barnstable, Massachusetts', *American Journal of science*, vol. 248, pp. 274-294.

Phleger, F.B. (1965) 'Patterns of marsh foraminifera, Galveston Bay Texas', *Limnology Oceanography supplement*, vol. 10, pp. 169-184.

Pirazzoli, P.A. (1996) *Sea-level changes : The last 20,000 years*, Wiley, New York.

Pizzuto, J.E. and Schwendt, A.E. (1997) 'Mathematical modeling of autocompaction of a Holocene transgressive valley-fill deposit, Wolfe Glade, Delaware', *Geology*, vol. 25, no. 1, pp. 57-60.

Plater, A.J. and Appleby, P.G. (2004) 'Tidal sedimentation in the Tees estuary during the 20th century: radionuclide and magnetic evidence of pollution and sedimentary response', *Estuarine, Coastal and Shelf Science*, vol. 60, no. 2, pp. 179-192.

Plater, A., Boyle, J., Mayers, C., Turner, S. and Stroud, R. (2006) 'Climate and human impact on lowland lake sedimentation in Central Coastal California: the record from c. 650, *Regional Environmental Change*, vol. 6, no. 1, pp. 71-85-85.

Plater, A.J. and Kirby, J.R. (in press) 'Sea-level variation and coastal response' In: J. Hansom (ed.) *Treatise on Coastal and Estuarine Science*, Elsevier.

Pugh, D.T. (2004) *Changing sea levels: effects of tides, weather, and climate*, Cambridge University Press, Cambridge.

Pulford, I.D., Allan, R.L., Cook, G.T. and MacKenzie, A.B. (1998) 'Geochemical associations of Sellafield-derived radionuclides in saltmarsh deposits of the Solway Firth', *Environmental Geochemistry and Health*, vol. 20, no. 2, pp. 95-101.

Puntí, T., Rieradevall, M. and Prat, N. (2009) 'Environmental factors, spatial variation, and specific requirements of Chironomidae in Mediterranean reference streams', *Journal of the North American Benthological Society*, vol. 28, no. 1, pp. 247-265.

Rahman, R. (2010) *Radioactive pollution and potential redistribution, exposure and health risks from Sellafield-contaminated saltmarshes in north-west England, UK.*, Thesis Ph.D. Liverpool University.

Rees, P. (1991) *A guide to Merseyside's industrial past* Countywise, Birkendhead.

Reiter, M. (1959) 'Seasonal variations in intertidal foraminifera of Santa-Monica Bay, California', *Journal of Paleontology*, vol. 33, no. 4, pp. 606-630.

Ridgway, J. and Shimmield, G. (2002) 'Estuaries as repositories of historical contamination and their impact on shelf seas', *Estuarine Coastal and Shelf Science*, vol. 55, no. 6, pp. 903-928.

Riveiros, N.V., Babalola, A.O., Boudreau, R.E.A., Patterson, R.T., Roe, H.M. and Doherty, C. (2007) 'Modern distribution of salt marsh foraminifera and thecamoebians in the Seymour-Belize Inlet Complex, British Columbia, Canada', *Marine Geology*, vol. 242, no. 1-3, pp. 39-63.

Roe, H.M., Doherty, C.T., Patterson, R.T. and Swindles, G.T. (2009) 'Contemporary distributions of saltmarsh diatoms in the Seymour-Belize Inlet Complex, British Columbia, Canada: Implications for studies of sea-level change', *Marine Micropaleontology*, vol. 70, no. 3-4, pp. 134-150.

Rossi, V., Horton, B.P., Corbett, D.R., Leorri, E., Perez-Belmonte, L. and Douglas, B.C. (2011) 'The application of foraminifera to reconstruct the rate of 20th century sea level rise, Morbihan Golfe, Brittany, France', *Quaternary Research*, vol. 75, no. 1, pp. 24-35.

Rossiter, J.R., Liverpool, O. and Tidal, I. (1956) *Tidal reduction tables for the River Mersey Prepared by the Liverpool Observatory and Tidal Institute for the Mersey Docks and Harbour Board*, Unpublished manuscript.

Salomons, W. and Forstner, U. (1984) *Metals in the Hydrocyle*, Springer-Verlag.

Sawai, Y., Horton, B.P. and Nagumo, T. (2004) 'The development of a diatom-based transfer function along the Pacific coast of eastern Hokkaido, northern Japan - An aid in paleoseismic studies of the Kuril subduction zone', *Quaternary Science Reviews*, vol. 23, no. 23-24, pp. 2467-2483.

Schafer, C.T. (1968) *Ecology of benthic foraminifera in western Long Island Sound and adjacent nearshore waters*, vol. 27, Dartmouth, Nova Scotia.

Schoer, J. (1985) Iron-oxi-hydroxides and their significance to the behaviour of heavy metals in estuaries, *Heavy Metals in the Environment*, Proceedings International Conference.

Schroder, C.J. (1988) 'Subsurface preservation of agglutinated foraminifera in the northwest Atlantic Ocean', In: Rögel F. and F.M. Gradstein (eds), *Proceedings, 2nd Workshop on Agglutinated Foraminifera*, vol. 41, Abhandlungen Geologische Bundesansalt, Vienna, Austria, pp. 325-336.

Scott, D.B. and Medioli, F.S. (1978) 'Vertical zonation of marsh foraminifera as accurate indicators of former sea-levels', *Nature*, vol. 272, pp. 538-541.

Scott, D.B. and Medioli, F.S. (1980a) 'Living vs total foraminiferal populations - their relative usefulness in paleoecology', *Journal of Paleontology*, vol. 54, no. 4, pp. 814-831.

Scott, D.B. and Medioli, F.S. (1980b) 'Quantitative studies of marsh foraminiferal distributions in Nova-Scotia Canada implications for sea level studies', *Cushman Foundation for Foraminiferal Research Special Publication*, no. 17, pp. 1-58.

Scott, D.B. and Medioli, F.S. (1986) 'Foraminifera as sea-level indicators', In: O. Van de Plassche, (ed.), *Sea-level research: a manual for the collection and evaluation of data*, Geo Books, Norwich.

Scott, D.B. and Leckie, R.M. (1990) 'Foraminiferal zonation of Great Sippewissett salt marsh (Falmouth, Massachusetts)', *Journal of Foraminiferal Research*, vol. 20, pp. 248-266.

Scott, D.B. and Hermelin, J.O.R. (1993) 'A device for precision splitting of micropaleontological samples in liquid suspension', *Journal of Paleontology*, vol. 67, no. 1, pp. 151-154.

Scott, D.B., Brown, K., Collins, E.S. and Medioli, F.S. (1995) 'A new sea-level curve from Nova Scotia: Evidence for a rapid acceleration of sea level rise in the late mid-Holocene', *Canadian Journal of Earth Sciences*, vol. 32, no. 12, pp. 2071-2080.

Scott, D.B., Medioli, F.S. and Schafer, C.T. (2001) *Monitoring in coastal environments using Foraminifera and Thecamoebian indicators*, Cambridge University Press, Cambridge.

Segurado, P., Araujo, M.B. and Kunin, W.E. (2006) 'Consequences of spatial autocorrelation for niche-based models', *Journal of Applied Ecology*, vol. 43, no. 3, pp. 433-444.

Sevilla, A.M. (2009) *Study of heavy metal concentraion of the last 150 years in sediments of Oglet Bay in relation with Mersey History.*, [unpublished], University of Liverpool.

Sharma, P., Gardner, L.R., Moore, W.S. and Bollinger, M.S. (1987) 'Sedimentation and bioturbation in a salt-marsh as revealed by Pb-210, Cs-137, and Be-7 studies', *Limnology and Oceanography*, vol. 32, no. 2, pp. 313-326.

Shaw, J. and Ceman, J. (1999) 'Salt-marsh aggradation in response to late-Holocene sea-level rise at Amherst Point, Nova Scotia, Canada', *Holocene*, vol. 9, no. 4, pp. 439-451.

Shennan, I. (1982). 'Interpretation of Flandrian sea-level data from the Fenland, England.' *Proceedings Geologists Association,* vol. 93, no. 1, pp. 53-63.

Shennan, I. (1986) 'Flandrian sea-level changes in the Fenland, II: Tendencies of sea level movement, altitudinal changes and local and regional factors', *Journal of Quaternary Science*, vol. 1, pp. 155-179.

Shennan, I., Lambeck, K., Horton, B.P., Innes, J.B., Lloyd, J.M., McArthur, J.J. and Rutherford, M.M. (2000) 'Holocene isostasy and relative sea-level changes on the east coast of England', In: I. Shennan, and Andrews, J., (ed.), *Holocene Land-Ocean Interaction and Environmental Change around the North Sea*, vol. Geological Society Special Publication 166, Bath, Geological Society Publishing House, pp. 275-298.

Shennan, I. and Horton, B. (2002) 'Holocene land- and sea-level changes in Great Britain', *Journal of Quaternary Science*, vol. 17, no. 5-6, pp. 511-526.

Shennan, I., Peltier, W.R., Drummond, R. and Horton, B. (2002) 'Global to local scale parameters determining relative sea-level changes and the post-glacial isostatic adjustment of Great Britain', *Quaternary Science Reviews*, vol. 21, no. 1-3, pp. 397-408.

Shennan, I., Bradley, S., Milne, G., Brooks, A., Bassett, S. and Hamilton, S. (2006) 'Relative sea-level changes, glacial isostatic modelling and ice-sheet reconstructions from the British Isles since the Last Glacial Maximum', *Journal of Quaternary Science*, vol. 21, no. 6, pp. 585-599.

Shennan, I. and Woodworth, P.L. (1992) 'A comparison of late holocene and 20th-century sea-level trends from the uk and North-sea region', *Geophysical Journal International*, vol. 109, no. 1, pp. 96-105.

Sherrod, B.L. (1999) 'Gradient analysis of diatom assemblages in a Puget Sound salt marsh: can such assemblages be used for quantitative paleoecological reconstructions?', *Palaeogeography Palaeoclimatology Palaeoecology*, vol. 149, no. 1-4, pp. 213-226.

Shotyk, W., Goodsite, M.E., Roos-Barraclough, F., Frei, R., Heinemeier, J., Asmund, G., Lohse, C. and Hansen, T.S. (2003) 'Anthropogenic contributions to atmospheric Hg, Pb and As accumulation recorded by peat cores from southern Greenland and Denmark dated using the 14C "bomb pulse curve', *Geochimica Et Cosmochimica Acta*, vol. 67, no. 21, pp. 3991-4011.

Sissons, J.B. (1983) 'Shorelines and isostasy in Scotland', In: Smith D.A.G (ed.), *shorelines and isostasy*, Academic Press, London, pp. 209-225.

Smith, J.N. (2001) 'Why should we believe Pb-210 Sediment geochronologies?', *Journal of Environmental Radioactivity*, vol. 55, no. 2, pp. 121-123.

Smoak, J.M. and Patchineelam, S.R. (1999) 'Sediment mixing and accumulation in a mangrove ecosystem: Evidence from 210Pb, 234Th and 7Be', *Mangroves and Salt Marshes*, vol. 3, no. 1, pp. 17-27.

Society of the Chemical Industry (1980) *Site investigation and materials problems,* proceeding conference of contaminated land, London.

Solomon, S., Qin, D., Manning, M., Chen, Z., Marquis, M., Averyt, K.B., Tignor, M. and Miller, H.L. (2007) *Contribtion of workinh group 1 to the fourth assessment respor to the Intergovernment Panel on Climate Change,* Cambridge University Press, Cambridge, UK.

Southall, K.E., Gehrels, W.R. and Hayward, B.W. (2006) 'Foraminifera in a New Zealand salt marsh and their suitability as sea-level indicators', *Marine Micropaleontology*, vol. 60, no. 2, pp. 167-179.

Spencer, K.L., Cundy, A.B. and Croudace, I.W. (2003) 'Heavy metal distribution and early-diagenesis in salt marsh sediments from the Medway Estuary, Kent, UK', *Estuarine Coastal and Shelf Science*, vol. 57, no. 1-2, pp. 43-54.

Spencer, K.L., Cundy, A.B., Davies-Hearn, S., Hughes, R., Turner, S. and MacLeod, C.L. (2008) 'Physicochemical changes in sediments at Orplands Farm, Essex, UK following 8 years of managed realignment', *Estuarine Coastal and Shelf Science*, vol. 76, no. 3, pp. 608-619.

Steele, J.H., Thorpe, S. H., Turekian, K. K. (2009) *Ocean Currents: A derivative of the Encyclopaedia of Ocean Sciences*, Elsevier, London.

Steineck, P.L. and Bergstein, J. (1979) 'Foraminifera from hommocks salt marsh larchmont harbor new-york usa', *Journal of Foraminiferal Research*, vol. 9, no. 2, pp. 147-158.

Stocchi, P. and Spada, G. (2009) 'Influence of glacial isostatic adjustment upon current sea level variations in the Mediterranean' *Tectonophysics* vol. 474, pp. 56–68.

Stuiver, M., Reimer, P.J. and Braziunas, T.F. (1998) 'High-precision radiocarbon age calibration for terrestrial and marine samples', *Radiocarbon*, vol. 40, no. 3, pp. 1127-1151.

Stupples, P. and Plater, A.J. (2007) 'Statistical analysis of the temporal and spatial controls on tidal signal preservation in late-Holocene tidal rhythmites, Romney Marsh, Southeast England', *International Journal of Earth Sciences*, vol. 96, pp. 957-976.

Szkornik, K., Gehrels, W.R. and Kirby, J.R. (2006) 'Salt-marsh diatom distributions in Ho Bugt (western Denmark) and the development of a transfer function for reconstructing Holocene sea-level changes', *Marine Geology*, vol. 235, no. 1-4, pp. 137-150.

Tam, N.F.Y. and Yao, M.W.Y. (1998) 'Normalisation and heavy metal contamination in mangrove sediments', *Science of the Total Environment*, vol. 216, no. 1-2, pp. 33-39.

Taylor, S.R. (1964) 'Abundance of chemical elements in the continental crust - a new table', *Geochimica Et Cosmochimica Acta*, vol. 28, pp. 1273-1285.

Telford, R.J. (2011) *palaeoSig*, 1.0.

Telford, R.J., Andersson, C., Birks, H.J.B. and Juggins, S. (2004) 'Biases in the estimation of transfer function prediction errors', *Paleoceanography*, vol. 19, no. 4.

Telford, R.J. and Birks, H.J.B. (2005) 'The secret assumption of transfer functions: problems with spatial autocorrelation in evaluating model performance', *Quaternary Science Reviews*, vol. 24, no. 20-21, pp. 2173-2179.

Telford, R.J. and Birks, H.J.B. (2009) 'Evaluation of transfer functions in spatially structured environments', *Quaternary Science Reviews*, vol. 28, no. 13-14, pp. 1309-1316.

Telford, R.J. and Birks, H.J.B. (2011) 'A novel method for assessing the statistical significance of quantitative reconstructions inferred from biotic assemblages', *Quaternary Science Reviews*, vol. 30, no. 9-10, pp. 1272-1278.

Temmerman, S., Govers, G., Wartel, S. and Meire, P. (2004) 'Modelling estuarine variations in tidal marsh sedimentation: response to changing sea level and suspended sediment concentrations', *Marine Geology*, vol. 212, no. 1-4, pp. 1-19.

ter Braak, C.J.F. and Looman, C.W.N. (1986) 'Weighted Averaging Logistic regression and the gaussian response model', *Vegetation*, vol. 65, no. 1, pp. 3-12.

ter Braak, C.J.F. and Prentice, I.C. (1988) 'A Theory of Gradient Analysis', *Advances in Ecological Research*, vol. 18, pp. 271-317.

ter Braak, C.J.F. and Juggins, S. (1993) 'Weighted Averaging Partial Least-Squares Segression (WA-PLS) - an improved method for reconstructing environmental variables from species assemblages', *Hydrobiologia*, vol. 269, pp. 485-502.

ter Braak, C.J.F. (1995) 'Nonlinear methods for multivariate statistical calibration and their use in paleoecology - a comparison of inverse (k-nearest neighbors, partial least-squares and weighted averaging partial least-squares) and classical approaches', *Chemometrics and Intelligent Laboratory Systems*, vol. 28, no. 1, pp. 165-180.

Theisen, R. and Vollath, D. (1969) *Tables of x-ray mass attenuation coefficients.*, Dussekdorf.

Thomas, C., (2002), 'The application of historical data and computational methods for investigating causes of long term morphological change in estuaries: A case study of the Mersey Estuary', UK, PhD Thesis, Oxford Brookes University.

Thomas, C.G., Spearman, J.R. and Turnbull, M.J. (2002) 'Historical morphological change in the Mersey Estuary', *Continental Shelf Research*, vol. 22, no. 11-13, pp. 1775-1794.

Thomas, E., Nydick, K., Scholand, S.J. and Varekamp, J.C. (1993) 'Accelerated sea-level rise over the last 200 years?', *Geological Society of American Abstracts programs*, vol. 6, no. A, p. 60.

Tobin, R., Scott, D.B., Collins, E.S. and Medioli, F.S. (2005) 'Infaunal benthic foraminifera in some North American marshes and their influence on fossil assemblages', *Journal of Foraminiferal Research*, vol. 35, no. 2, pp. 130-147.

Tooley, M.J. (1974) 'Sea-level changes during last 9000 years in Northwest England', *Geographical Journal*, vol. 140, pp. 18-and.

Tooley, M.J. (1978) *Sea-level changes: north-west England during the Flandrian Stage*, Clarendon Press, Oxford.

Troels-Smith, J. (1955) 'Karakterisering af løse jordarter (Characterization of unconsolidated sediments)', *Danmarks Geologiske Undersøgelse IV*, vol. vol. 3, no. 10.

Turekian, K.K. and Wedepohl, K.H. (1961) 'Distribution of the elements in some major units of the Earths crust', *Geological Society of America Bulletin*, vol. 72, no. 2, pp. 175-191.

Valette-Silver, N.J. (1993) 'The use of sediment cores to reconstruct historical trends in contamination of estuarine and coastal sediments', *Estuaries*, vol. 16, no. 3B, pp. 577-588.

Valette-Silver, N., Bricker, S. and Salomons, W. (1993) 'Historical trends in contamination of estuarine and coastal sediments: An introduction to the dedicated issue', *Estuaries and Coasts*, vol. 16, no. 3, pp. 575-576.

van de Plassche, O. (1979) Sea-level research in the provinces of south Holland, Netherlands, *1978 international symposium of coastal evolution in the Quaternary*, vol. 534-551, Sao Paulo, Brazil.

van de Plassche, O., van der Borg, K. and de Jong, A.F.M. (1998) 'Sea level-climate correlation during the past 1400 yr', *Geology*, vol. 26, no. 4, pp. 319-322.

Vane, C.H., Jones, D.G. and Lister, T.R. (2009) 'Mercury contamination in surface sediments and sediment cores of the Mersey Estuary, UK', *Marine Pollution Bulletin*, vol. 58, no. 6, pp. 940-946.

Varekamp, J.C., Thomas, E. and Vandeplassche, O. (1992) 'Relative sea-level rise and climate change over the last 1500 years', *Terra Nova*, vol. 4, no. 3, pp. 293-304.

Vranken, M., Oenema, O. and Mulder, J. (1990) 'Effects of tide range alterations on salt marsh sediments in the Eastern Scheldt, S. W. Netherlands', *Hydrobiologia*, vol. 195, no. 1, pp. 13-20.

Wahl, T., Jensen, J. and Frank, T. (2010) 'On analysing sea level rise in the German Bight since 1844', *Natural Hazards and Earth System Sciences*, vol. 10, no. 2, pp. 171-179.

Walton, W.R. (1952) 'Techniques for recognition of living foraminifera.', *Contributions from Cushman Foundation for Foraminfera Research*, vol. 3, pp. 56-60.

Wang, P., Min, Q. and Bian, Y. (1985) 'On marine continental transitional faunas in Cenozoic deposits of East China', In: P. Wang (ed.), *Marine Micropaleontology of China. China Ocean Press, Beijing*, Springer-Verlag, Berlin, pp. 15-33.

Wang, P. and Murray, J.W. (1983) 'The use of foraminifera as indicators of tidal effects in estuarine deposits', *Marine Geology*, vol. 51, no. 3-4, pp. 239-250.

Wang, P.X. and Chappell, J. (2001) 'Foraminifera as Holocene environmental indicators in the South Alligator River, Northern Australia', *Quaternary International*, vol. 83-5, pp. 47-62.

Wen, L. S., Shiller, A., Santschi, P.H., Gill, G. (1999) 'Trace elements behaviour in Gulf of Mexico estuaries', In: T.S Bianchi, Pennock, J.R., Twilley, R.R., (eds.). Biogeochemistry of Gulf of Mexico Estuaries, John Wiley and Sons, New York.

Wenk, H. and Bulakh, A. (2004) *Minerals. Their constitution and origin.*, Cambridge Univeristy Press., Cambridge.

Whiting, M.C. and McIntire, C.D. (1985) 'An investigation of distributional patterns in the diatom flora of netarts bay, oregon, by correspondence-analysis', *Journal of Phycology*, vol. 21, no. 4, pp. 655-661.

Williams, H.F.L. (1999) 'Foraminiferal distributions in tidal marshes bordering the Strait of Juan de Fuca: Implications for paleoseismicity studies', *Journal of Foraminiferal Research*, vol. 29, no. 3, pp. 196-208.

Williams, T.B., Bubb, J.M. and Lester, J.N. (1994) 'Metal accumulation within saltmarsh environments: a review. ', *Marine pollution bulletin*, vol. 28, pp. 277-290.

Wilson, G.P., Lamb, A.L., Leng, M.J., Gonzalez, S. and Huddart, D. (2005a) 'delta C-13 and C/N as potential coastal palaeoenvironmental indicators in the Mersey Estuary, UK', *Quaternary Science Reviews*, vol. 24, no. 18-19, pp. 2015-2029.

Wilson, G.P., Lamb, A.L., Leng, M.J., Gonzalez, S. and Huddart, D. (2005b) 'Variability of organic delta C-13 and C/N in the Mersey Estuary, UK and its implications for sea-level reconstruction studies', *Estuarine Coastal and Shelf Science*, vol. 64, no. 4, pp. 685-698.

Woodroffe, C.D. (2003) *Coasts: Form, Process and Evolution*, Cambridge University Press, Cambridge.

Woodroffe, S.A. and Long, A.J. (2009) 'Salt marshes as archives of recent relative sea level change in West Greenland', *Quaternary Science Reviews*, vol. 28, no. 17-18, pp. 1750-1761.

Woodroffe, S.A. and Long, A.J. (2010) 'Reconstructing recent relative sea-level changes in West Greenland: Local diatom-based transfer functions are superior to regional models', *Quaternary International*, vol. 221, no. 1-2, pp. 91-103.

Woodworth, P.L. (1999a) *A study of changes in high water levels and tides at Liverpool during the last two hundred and thirty years wuth some historical background.*, Proudman Oceanographic Laboratory, Liverpool, document 56.

Woodworth, P.L. (1999b) 'High waters at liverpool since 1768: the UK's longest sea level record', *Geophysical Research Letters*, vol. 26, no. 11, pp. 1589-1592.

Woodworth, P.L., Tsimplis, M.N., Flather, R.A. and Shennan, I. (1999) 'A review of the trends observed in British Isles mean sea level data measured by tide gauges', *Geophysical Journal International*, vol. 136, no. 3, pp. 651-670.

Woodworth, P.L. and Blackman, D.L. (2002) 'Changes in extreme high waters at Liverpool since 1768', *International Journal of Climatology*, vol. 22, no. 6, pp. 697-714.

Woodworth, P.L. (2006) 'Some important issues to do with long-term sea level change', *Philosophical Transactions of the Royal Society a-Mathematical Physical and Engineering Sciences*, vol. 364, no. 1841, pp. 787-803.

Zong, Y. and Horton, B.P. (1998) 'Diatom zones across intertidal flats and coastal saltmarshes in Britain', *Diatom Research*, vol. 13, no. 2, pp. 375-394.

Zong, Y.Q. and Horton, B.P. (1999) 'Diatom-based tidal-level transfer functions as an aid in reconstructing Quaternary history of sea-level movements in the UK', *Journal of Quaternary Science*, vol. 14, no. 2, pp. 153-167.

Zong, Y., Shennan, I., Combellick, R.A., Hamilton, S.L. and Rutherford, M.M. (2003) 'Microfossil evidence for land movements associated with the AD 1964 Alaska earthquake', *Holocene*, vol. 13, no. 1, pp. 7-20.

Zwolsman, J.J.G., Berger, G.W. and Van Eck, G.T.M. (1993) 'Sediment accumulation rates, historical input, postdepositional mobility and retention of major elements and trace metals in salt marsh sediments of the Scheldt estuary, SW Netherlands', *Marine Chemistry*, vol. 44, no. 1, pp. 73-94.

Table A1.1 Dead foraminifera percentages for transect OBSS1.

OBSS1	1	2	3	4	5	6	7	8	9	10	11	12	13	14	15	16	17	18	19	20	21	22
B. pseudomacresens	0.0	0.0	3.9	0.0	0.0	0.0	0.0	0.0	0.0	0.0	0.0	0.0	0.0	0.0	0.7	1.8	4.0	5.9	11.8	0.0	0.0	0.0
Cribrostomoides jeffreysii	2.3	2.8	0.0	1.5	0.0	0.0	2.7	0.0	1.2	0.0	0.7	0.4	0.0	0.0	0.0	0.0	0.0	0.0	0.0	0.0	0.0	0.0
Haplophragmoides spp.	3.0	1.1	0.8	7.6	1.7	2.4	0.9	0.0	7.8	8.4	22.2	21.8	10.1	1.0	0.0	33.9	59.4	26.9	56.1	67.5	67.9	60.9
J. macrescens	12.1	7.4	13.1	6.1	6.9	2.4	3.6	1.4	3.6	0.7	2.2	3.6	0.9	0.0	0.7	5.2	6.3	9.2	3.3	0.4	19.6	26.4
M. fusca	9.9	6.3	11.5	30.3	35.3	12.9	18.9	8.0	31.3	49.0	50.4	45.6	45.0	44.8	8.4	21.5	23.7	50.4	21.7	25.1	12.5	10.3
Textularia spp.	6.1	0.0	3.1	0.0	0.0	0.0	0.0	0.0	0.0	0.0	0.0	0.0	0.0	0.0	0.0	0.0	0.0	0.0	0.0	0.0	0.0	0.0
Tiphotrocha comprimata	0.0	2.3	0.0	0.0	0.0	0.0	0.0	0.0	0.0	0.0	0.0	0.0	0.9	0.0	0.0	0.0	0.0	0.0	0.0	0.0	0.0	0.0
T. inflata	0.8	2.3	0.8	1.5	0.0	0.0	0.0	0.0	0.0	0.0	0.0	0.0	0.0	0.0	0.0	0.0	0.0	1.7	0.0	1.3	0.0	2.3
Trochammina ochracea	3.8	4.6	3.9	2.3	0.0	4.8	0.0	0.9	3.6	1.4	2.2	0.8	0.9	0.0	0.0	0.0	0.0	0.0	0.0	0.0	0.0	0.0
Ammonia beccarii beccarii spp.	27.3	4.6	15.4	10.6	39.7	66.1	57.7	87.8	42.8	35.7	18.5	24.6	37.6	45.7	90.3	36.1	6.3	0.0	1.4	2.6	0.0	0.0
Astacolus crepidulus	0.0	0.0	0.0	0.8	0.0	0.0	0.0	0.0	0.0	0.0	0.0	0.0	0.0	0.0	0.0	0.0	0.0	0.0	0.0	0.0	0.0	0.0
Brizalina spp.	6.1	17.6	9.2	6.1	5.2	3.2	1.8	0.5	3.0	1.4	0.7	1.6	0.0	1.0	0.0	0.3	0.0	0.0	0.0	0.0	0.0	0.0
Bulimina spp.	0.8	0.0	1.5	0.0	0.0	0.0	0.0	0.0	0.0	0.0	0.0	0.0	0.0	0.0	0.0	0.0	0.0	0.0	0.0	0.0	0.0	0.0
Bulimnella spp.	0.0	0.0	0.0	0.0	0.0	0.0	0.0	0.0	0.0	0.0	0.0	0.4	0.0	0.0	0.0	0.0	0.0	0.0	0.0	0.0	0.0	0.0
Cyclogyra involvens	0.0	2.3	0.8	0.0	1.7	2.4	0.0	0.0	0.6	0.7	0.7	0.0	0.0	0.0	0.0	0.2	0.5	0.0	0.0	0.0	0.0	0.0
Elphidium spp.	18.2	33.5	27.7	20.5	5.2	0.0	1.8	0.5	1.8	2.1	2.2	0.0	0.0	0.0	0.0	0.3	0.0	0.0	0.0	0.0	0.0	0.0
Fissurina spp.	0.8	0.0	0.0	0.0	0.0	0.0	0.0	0.0	0.0	0.0	0.0	0.0	0.0	0.0	0.0	0.0	0.0	0.0	0.0	0.0	0.0	0.0
Fursenkoina spp.	4.6	4.6	3.1	0.0	0.9	0.8	2.7	0.5	0.0	0.0	0.0	0.0	0.0	0.0	0.0	0.3	0.0	0.0	0.0	0.0	0.0	0.0
Gavelinopsis	0.0	0.0	0.0	0.0	0.0	0.0	2.7	0.0	0.0	0.0	0.0	0.0	0.0	0.0	0.0	0.0	0.0	0.0	0.0	0.0	0.0	0.0
Glabratella millettii	0.0	4.6	0.0	0.0	0.0	0.0	4.5	0.0	0.0	0.0	0.0	0.0	0.0	0.0	0.0	0.0	0.0	0.0	0.0	0.0	0.0	0.0
Haynesina spp.	1.5	0.0	3.1	11.4	0.0	3.2	0.0	0.0	0.6	0.0	0.0	0.0	0.0	0.0	0.0	0.0	0.0	0.0	0.5	0.0	0.0	0.0
Massilina secans	0.0	1.7	0.0	0.0	0.0	0.0	0.0	0.0	0.0	0.0	0.0	0.0	0.0	0.0	0.0	0.0	0.0	0.0	0.0	0.0	0.0	0.0
Quinqueloculina spp.	3.0	4.6	2.3	1.5	3.5	1.6	2.7	0.5	3.6	0.7	0.0	1.2	4.6	7.6	0.0	0.6	0.0	1.7	5.2	3.0	0.0	0.0
Turrispirillina spp.	0.0	0.0	0.0	0.0	0.0	0.0	0.0	0.0	0.0	0.0	0.0	0.0	0.0	0.0	0.0	0.0	0.0	4.2	0.0	0.0	0.0	0.0
Total	87	56	231	212	119	224	676	154	105	109	252	135	143	166	111	213	124	116	132	130	176	132

Table A1.2 Dead foraminifera percentages for transect OBSS2.

OBSS2	1	2	3	4	5	6	7	8	9	10	11	12	13	14	15	16	17	18	19
B.pseudomacresens	0.0	0.0	0.0	0.0	0.0	0.0	0.0	0.0	0.0	0.0	4.3	0.0	0.0	2.8	1.4	4.0	1.5	4.2	4.9
Haplophragmoides spp.	2.6	11.1	5.2	7.0	5.4	32.4	56.3	41.5	90.6	6.0	10.7	70.6	32.4	31.9	23.4	43.7	5.9	23.2	32.4
J. macrescens	4.7	8.1	13.5	9.0	9.5	0.0	0.6	0.0	0.2	8.0	2.1	0.5	0.0	0.0	2.1	11.9	2.2	2.8	4.9
M. fusca	5.8	29.6	7.2	25.0	25.7	64.1	24.7	47.4	6.5	35.3	72.1	25.3	57.6	40.4	57.9	37.1	73.3	67.6	57.0
Textularia spp.	4.7	0.7	8.5	4.0	3.4	0.0	1.7	1.5	0.0	11.3	0.0	0.0	0.0	7.8	5.5	0.0	0.0	0.0	0.0
Tiphotrocha comprimata	0.0	0.0	0.8	0.0	0.0	0.0	0.0	0.0	0.0	0.0	0.0	0.0	1.4	0.7	0.7	0.0	0.0	0.0	0.0
T. inflata	2.1	5.9	1.9	7.5	4.7	0.0	0.0	0.0	0.0	4.0	0.0	0.0	0.0	0.0	0.7	0.0	1.5	0.0	0.0
Trochammina ochracea	3.7	0.7	1.7	0.5	0.7	1.4	4.0	1.5	0.0	4.0	0.0	0.5	0.0	1.4	2.1	0.0	1.5	2.1	0.7
Ammonia beccarii beccarii spp.	18.8	14.1	14.3	24.0	7.4	0.0	4.0	0.0	0.4	4.0	3.6	0.0	2.2	0.7	0.0	1.3	3.0	0.0	0.0
Astacolus crepidulus	0.0	0.7	0.0	0.0	0.0	0.0	0.0	0.0	0.0	0.0	0.0	0.0	0.0	0.0	0.0	0.0	0.0	0.0	0.0
Brizalina spp.	11.0	0.7	17.4	8.5	9.5	0.0	0.0	1.5	0.0	5.3	2.1	0.9	1.4	4.3	5.5	0.7	3.0	0.0	0.0
Bulimina spp.	0.0	0.0	0.6	0.0	0.0	0.0	0.0	0.0	0.0	0.0	0.0	0.0	0.0	0.0	0.0	0.0	0.0	0.0	0.0
Cyclogyra involvens	3.7	1.5	3.0	1.5	0.0	0.0	1.1	0.0	0.0	4.7	0.0	0.0	0.0	1.4	0.0	0.0	0.0	0.0	0.0
Elphidium spp.	28.3	18.5	15.2	4.0	6.1	0.0	2.3	0.0	0.2	1.3	1.4	0.0	3.6	1.4	0.0	0.0	3.0	0.0	0.0
Fursenkoina spp.	3.7	0.7	1.7	2.5	5.4	2.1	1.1	3.7	0.2	4.7	0.0	1.8	1.4	0.0	0.0	0.0	0.0	0.0	0.0
Globigerina spp.	0.5	0.0	0.0	1.5	0.0	0.0	0.0	0.0	0.2	0.0	0.0	0.0	0.0	0.0	0.0	0.0	0.0	0.0	0.0
Haynesina spp.	5.2	5.9	6.6	3.0	17.6	0.0	2.9	0.0	1.3	8.0	2.1	0.5	0.0	5.7	0.7	0.7	3.0	0.0	0.0
Nonionella spp.	0.5	0.0	0.0	0.0	0.0	0.0	0.0	0.0	0.0	0.0	0.0	0.0	0.0	0.0	0.0	0.0	0.0	0.0	0.0
Quinqueloculina spp.	4.7	1.5	2.5	2.0	2.7	0.0	1.1	3.0	0.2	3.3	1.4	0.0	0.0	1.4	0.0	0.7	2.2	0.0	0.0
Rosalina spp.	0.0	0.0	0.0	0.0	2.0	0.0	0.0	0.0	0.0	0.0	0.0	0.0	0.0	0.0	0.0	0.0	0.0	0.0	0.0
Total	191	135	363	200	148	145	174	135	446	150	140	221	139	141	145	151	135	142	142

Table A1.3 Dead foraminifera percentages for transect OBSS3.

OBSS3	1	2	3	4	5	6	7	8	9	10	11	12	13	14	15	16	17	18	19	20	21	22
B. pseudomacresens	0.0	0.0	0.0	0.0	0.0	0.0	0.4	0.0	0.0	0.0	0.0	0.0	0.0	0.0	0.0	0.0	0.0	0.0	4.8	9.6	8.3	0.0
Cribrostomoides jeffreysii	0.0	0.0	0.0	0.0	0.0	0.0	0.0	0.0	0.0	0.0	0.0	0.0	0.0	0.0	0.0	0.0	0.0	0.0	0.0	0.0	0.0	0.0
Eggerelloides spp.	0.0	0.0	0.7	0.0	0.0	0.0	0.0	0.0	0.0	0.0	0.0	0.0	0.0	0.0	0.0	0.0	1.5	0.0	0.0	0.0	0.0	0.0
Haplophragmoides spp.	0.0	0.0	2.8	3.8	0.0	1.9	12.9	23.0	14.7	17.5	28.4	14.1	39.0	31.4	42.2	41.0	32.5	66.0	34.7	26.9	45.8	34.7
J. macrescens	33.0	19.8	11.7	26.0	44.2	23.4	28.4	18.1	11.6	21.1	19.6	17.6	31.5	35.4	28.9	29.7	31.5	28.3	45.4	46.2	41.7	50.3
M. fusca	3.0	4.3	4.1	19.8	8.7	35.5	17.0	33.9	38.8	38.6	30.4	11.1	14.7	14.3	19.4	17.0	19.7	4.0	12.4	8.7	2.8	13.2
Textularia spp.	2.0	0.0	0.0	0.0	0.0	0.0	1.5	0.0	0.0	0.0	0.0	0.0	0.0	0.0	0.3	0.5	0.0	0.0	0.0	0.0	0.0	0.0
Tiphotrocha comprimata	0.0	1.7	0.0	0.0	0.0	0.0	0.0	0.0	0.0	0.0	0.0	0.0	0.0	0.0	0.0	0.0	0.0	0.0	0.0	0.0	0.0	0.0
T. inflata	11.0	6.0	53.8	14.5	15.4	13.1	13.7	16.5	14.7	7.0	14.4	56.0	14.5	18.9	6.5	6.1	13.3	1.2	1.7	1.0	0.7	1.2
Trochammina ochracea	1.0	1.7	0.0	1.5	2.9	0.9	0.4	0.4	2.3	0.9	0.0	0.5	0.0	0.0	0.0	0.0	0.0	0.0	0.0	0.0	0.0	0.6
Ammobaculites diloctatus	0.0	0.0	0.0	0.0	0.0	0.0	0.0	0.0	0.0	0.0	0.0	0.0	0.0	0.0	0.0	0.0	0.0	0.0	0.0	0.0	0.0	0.0
Ammonia spp.	1.0	6.0	0.7	2.3	0.0	1.9	10.0	0.4	0.0	3.5	0.0	0.0	0.0	0.0	0.0	0.0	1.0	0.0	0.0	1.0	0.0	0.0
Astacolus crepidulus	0.0	0.0	0.0	0.0	0.0	0.0	0.4	0.0	0.0	0.0	0.0	0.0	0.0	0.0	0.0	0.0	0.0	0.0	0.0	0.0	0.0	0.0
Bolivina spp.	2.0	0.0	0.0	0.0	0.0	0.0	0.0	0.0	0.0	0.0	0.0	0.0	0.0	0.0	0.0	0.0	0.0	0.0	0.0	0.0	0.0	0.0
Brizalina spp.	10.0	12.9	4.8	3.1	3.8	1.9	3.7	0.8	3.1	0.9	0.0	0.3	0.0	0.0	0.3	1.4	0.5	0.0	0.0	1.0	0.7	0.0
Bulimina spp.	1.0	0.0	0.0	0.0	0.0	0.0	0.0	0.0	0.0	0.0	0.0	0.0	0.0	0.0	0.0	0.0	0.0	0.0	0.0	0.0	0.0	0.0
Cassidulina obtusa	0.0	0.0	0.0	0.0	0.0	0.0	0.0	0.0	0.0	0.0	0.0	0.0	0.0	0.0	0.0	0.0	0.0	0.0	0.0	0.0	0.0	0.0
Cyclogyra involvens	2.0	1.7	4.8	16.0	1.0	3.7	2.2	1.6	2.3	1.8	6.2	0.0	0.0	0.0	0.0	0.0	0.0	0.0	0.0	0.0	0.0	0.0
Elphidium spp.	19.0	14.7	8.3	8.4	21.2	13.1	8.5	2.0	6.2	7.0	1.0	0.4	0.3	0.0	2.4	4.2	0.0	0.0	0.0	4.8	0.0	0.0
Fursenkoina spp.	0.0	5.2	2.1	0.8	1.0	0.9	0.0	0.4	0.0	0.0	0.0	0.0	0.0	0.0	0.0	0.0	0.0	0.0	0.0	0.0	0.0	0.0
Gavelinopsis	0.0	0.0	0.0	0.0	0.0	0.0	0.0	0.0	0.0	0.0	0.0	0.0	0.0	0.0	0.0	0.0	0.0	0.0	0.0	1.0	0.0	0.0
Glabratella millettii	2.0	1.7	0.0	0.0	0.0	0.0	0.0	0.0	0.0	0.0	0.0	0.0	0.0	0.0	0.0	0.0	0.0	0.0	0.0	0.0	0.0	0.0
Globigerina spp.	0.0	0.0	0.0	0.0	0.0	0.0	0.0	0.0	0.0	0.0	0.0	0.0	0.0	0.0	0.0	0.0	0.0	0.0	0.0	0.0	0.0	0.0
Haynesina spp.	5.0	20.7	1.4	0.8	1.0	0.0	0.0	0.8	1.6	0.0	0.0	0.0	0.0	0.0	0.0	0.0	0.0	0.5	1.0	0.0	0.0	0.0
lagena spp.	0.0	0.0	0.0	0.0	0.0	0.0	0.0	0.0	0.0	0.0	0.0	0.0	0.0	0.0	0.0	0.0	0.0	0.0	0.0	0.0	0.0	0.0
Quinqueloculina spp.	8.0	3.4	4.8	3.1	1.0	3.7	1.1	2.2	4.7	1.8	0.0	0.0	0.0	0.0	0.0	0.0	0.0	0.0	0.0	0.0	0.0	0.0
Total	100	116	145	131	104	107	271	508	129	114	194	731	387	328	294	212	203	424	291	104	144	167

Table A1.4 Dead foraminifera percentages for transects from Decoy Marsh.

Deocy Marsh	1	2	3	4	5	6	7	8	9	10	11	12	13	14	15	16	17	18	19
B. pseudomacresens	0.0	0.0	0.0	0.0	1.5	1.8	0.0	0.0	0.0	1.6	19.0	4.4	0.0	0.0	0.0	0.0	1.1	20.0	22.3
Cribrostomoides jeffreysii	0.0	0.0	0.0	0.0	0.0	3.7	0.0	0.0	0.0	0.0	0.0	0.0	0.0	0.0	0.0	1.6	0.0	0.0	0.0
Haplophragmoides spp.	5.9	0.0	0.0	0.0	4.5	17.9	4.3	6.5	0.0	0.0	6.9	5.3	1.8	0.0	0.0	6.4	5.6	8.6	24.3
J. macrescens	75.0	6.9	28.4	24.4	54.5	76.1	57.1	19.4	13.8	63.5	22.4	46.0	42.3	36.7	12.3	17.6	40.4	15.7	5.8
M. fusca	13.3	0.0	0.0	0.0	14.9	0.0	2.9	5.8	0.0	3.1	46.6	3.5	0.9	0.0	0.0	18.4	3.4	52.9	46.6
Textularia spp.	0.0	0.5	0.0	0.0	0.0	0.0	4.3	2.2	1.2	0.0	0.0	0.0	3.6	1.8	2.3	1.6	0.0	0.0	0.0
Trochammina inflata	3.2	1.0	0.0	0.0	0.0	0.0	0.0	2.2	0.0	0.0	0.0	0.0	0.0	0.0	0.0	1.6	0.0	0.0	0.0
Ammonia beccarii spp.	0.0	0.0	0.0	0.0	3.7	0.0	0.0	8.6	0.0	0.0	0.0	0.0	0.0	0.0	0.0	4.0	0.0	0.0	1.0
Trochammina ochracea	0.0	1.0	0.0	0.0	2.2	0.0	0.0	4.3	6.6	2.1	0.0	1.8	0.0	1.8	3.8	4.0	6.2	0.0	0.0
Bolivina spp.	1.1	0.0	0.0	0.0	0.0	0.0	0.0	0.7	0.0	0.0	0.0	0.0	0.0	0.0	0.0	0.0	0.0	0.0	0.0
Brizalina spp.	1.1	12.7	12.5	11.6	7.5	0.0	0.0	11.5	13.8	5.2	0.0	5.3	4.5	9.0	15.4	9.6	10.1	0.0	0.0
Bulimina spp.	0.0	0.0	0.5	0.0	0.0	0.0	0.0	0.7	3.0	0.0	0.0	0.0	0.0	2.4	0.8	0.0	0.0	0.0	0.0
Cyclogyra involvens	0.5	0.0	0.0	0.0	1.5	0.0	0.0	0.0	0.0	0.5	0.0	0.0	0.0	0.0	0.0	4.0	0.0	0.0	0.0
Eggerella spp.	0.0	0.0	0.0	0.0	0.0	0.0	0.0	0.0	0.0	0.0	0.0	0.0	0.0	0.0	0.0	0.8	0.0	0.0	0.0
Elphidium spp.	0.0	71.1	48.1	60.4	0.0	0.0	0.0	25.2	38.9	18.8	0.0	16.8	45.0	34.3	43.8	18.4	27.0	0.0	0.0
Fissurina spp.	0.0	0.0	0.0	1.2	0.0	0.0	0.0	0.0	0.0	0.0	0.0	0.0	0.0	0.0	0.0	0.0	0.0	0.0	0.0
Fursenkoina spp.	0.0	2.5	2.4	0.6	3.0	0.0	0.0	3.6	0.0	2.1	1.7	2.7	0.0	0.0	4.6	0.0	0.0	2.9	0.0
Gavelinopsis	0.0	0.0	0.0	0.0	0.0	0.0	0.0	0.7	0.0	0.0	0.0	0.0	0.0	0.0	0.0	4.8	0.0	0.0	0.0
Glabratella millettii	0.0	0.0	0.0	0.0	0.0	0.0	0.0	2.9	1.8	0.0	0.0	0.0	0.0	4.2	0.0	0.0	0.0	0.0	0.0
Globigerina spp.	0.0	3.4	0.0	1.2	0.0	0.0	0.0	0.0	0.0	0.0	0.0	0.0	0.0	0.0	0.0	0.8	0.0	0.0	0.0
Haynesina spp.	0.0	0.0	7.2	0.0	0.0	0.0	20.0	5.0	16.8	2.1	3.4	11.5	0.0	9.0	10.8	0.8	4.5	0.0	0.0
lagena spp.	0.0	0.0	0.0	0.0	0.0	0.0	0.0	0.0	0.6	0.0	0.0	0.0	0.0	0.0	0.0	0.0	0.6	0.0	0.0
Massilina secans	0.0	0.0	0.0	0.0	0.0	0.0	0.0	0.0	0.0	0.0	0.0	0.0	0.0	0.0	0.0	4.0	0.0	0.0	0.0
Quinqueloculina spp.	0.0	1.0	1.0	0.6	6.7	0.5	4.3	0.7	3.6	1.0	0.0	2.7	1.8	0.0	6.2	0.8	1.1	0.0	0.0
Total	188	204	208	164	134	218	70	139	167	192	58	113	111	166	130	125	178	70	103

Table A1.5 Live foraminifera percentages for transect OBSS1.

OBSS1 (live)	1	2	3	4	5	6	7	8	9	10	11	12	13	14	15	16	17	18	19	20	21	22
B. pseudomacresens	0.0	0.0	0.0	25.1	3.7	6.1	6.1	0.0	0.0	0.0	0.0	0.0	0.0	0.0	0.0	0.0	1.0	0.0	0.0	0.0	0.0	0.0
Cribrostomoides jeffreysii	0.0	0.0	0.0	0.0	0.0	0.0	0.0	0.0	0.0	0.0	0.0	0.0	0.0	0.0	0.0	0.0	0.0	0.0	0.0	0.0	1.8	0.0
Eggerella spp.	0.0	0.0	0.0	0.0	0.0	0.0	0.0	0.0	0.0	0.0	0.0	0.0	0.0	0.0	0.0	0.0	0.0	0.0	0.0	0.0	0.0	0.0
Haplophragmoides spp.	52.4	78.0	67.6	47.1	23.9	30.7	43.0	2.7	1.8	2.4	52.6	23.5	8.0	14.6	0.9	0.0	2.0	0.0	10.1	2.0	5.3	0.9
J.macrescens	27.0	7.0	1.4	5.4	40.4	20.1	10.9	0.0	0.0	11.9	10.5	0.0	6.0	6.3	10.7	0.0	0.0	3.5	5.1	38.8	21.1	39.3
M. fusca	9.5	2.0	18.3	12.6	22.9	21.2	16.4	11.6	31.2	26.2	15.8	47.1	34.0	24.0	31.3	1.0	0.0	21.2	32.9	2.0	12.3	8.0
Textularia spp.	0.0	0.0	0.0	0.0	0.0	0.0	0.0	0.0	0.0	0.0	0.0	0.0	0.0	0.0	0.0	0.0	0.0	0.0	0.0	0.0	0.0	0.9
Tiphotrocha comprimata	0.0	0.0	0.0	0.0	0.0	0.0	0.0	0.0	0.0	0.0	0.0	0.0	0.0	0.0	0.0	0.0	0.0	0.0	0.0	0.0	1.8	0.0
T. inflata	7.9	0.0	4.2	0.9	1.6	0.0	0.3	0.0	0.0	0.0	2.6	0.0	0.0	0.0	0.0	0.0	0.0	0.0	1.3	22.4	8.8	6.3
Ammonia spp.	0.0	0.0	4.2	4.9	2.1	21.2	22.5	85.7	65.3	59.5	18.4	23.5	46.0	54.2	56.3	99.0	95.0	75.2	45.6	30.6	49.1	43.8
Bolivina spp.	0.0	0.0	0.0	0.0	0.0	0.0	0.0	0.0	0.0	0.0	0.0	0.0	0.0	0.0	0.0	0.0	0.0	0.0	0.0	0.0	0.0	0.0
Brizalina spp.	0.0	0.0	0.0	0.0	0.0	0.0	0.0	0.0	0.0	0.0	0.0	0.0	0.0	0.0	0.0	0.0	0.0	0.0	3.8	0.0	0.0	0.0
Cyclogyra involvens	0.0	0.0	0.0	0.4	0.0	0.0	0.0	0.0	0.0	0.0	0.0	0.0	0.0	0.0	0.0	0.0	1.0	0.0	0.0	0.0	0.0	0.0
Elphidium spp.	0.0	0.0	0.0	0.0	0.0	0.0	0.0	0.0	0.0	0.0	0.0	5.9	4.0	0.0	0.0	0.0	0.0	0.0	0.0	0.0	0.0	0.0
Haynesina spp.	0.0	0.0	0.0	0.0	0.0	0.0	0.0	0.0	0.0	0.0	0.0	0.0	0.0	0.0	0.0	0.0	0.0	0.0	1.3	0.0	0.0	0.0
Quinqueloculina spp.	0.0	0.0	4.2	3.6	4.8	0.6	0.7	0.0	1.8	0.0	0.0	0.0	2.0	1.0	0.9	0.0	1.0	0.0	0.0	4.1	0.0	0.9
Turrispirillina spp.	5.0	0.0	0.0	0.0	0.3	0.0	0.0	0.0	0.0	0.0	0.0	0.0	0.0	0.0	0.0	0.0	0.0	0.0	0.0	0.0	0.0	0.0
Total	63	87	71	223	188	179	293	112	170	42	38	17	50	96	112	414	101	113	79	49	57	112

Table A1.6 Live foraminifera percentages for transect OBSS2.

OBSS2 (live)	1	2	3	4	5	6	7	8	9	10	11	12	13	14	15	16	17	18	19
B.pseudomacresens	0.0	0.0	6.7	16.7	33.3	22.2	0.0	0.0	21.4	0.0	0.0	0.0	0.0	0.0	0.0	0.0	0.0	0.0	0.0
Haplophragmoides spp.	25.0	44.4	53.3	33.3	0.0	77.8	54.5	100.0	42.9	5.3	97.2	84.2	66.7	60.0	14.8	33.3	9.1	5.6	0.0
J. macrescens	62.5	11.1	13.3	50.0	55.6	0.0	27.3	0.0	35.7	26.3	0.0	0.0	0.0	0.0	29.6	33.3	27.3	33.3	33.3
M. fusca	12.5	44.4	20.0	0.0	11.1	0.0	18.2	0.0	0.0	0.0	1.4	15.8	33.3	30.0	14.8	0.0	9.1	2.8	0.0
Trochammina inflata	0.0	0.0	0.0	0.0	0.0	0.0	0.0	0.0	0.0	57.9	1.4	0.0	0.0	10.0	18.5	33.3	9.1	47.2	16.7
Ammonia beccarii spp.	0.0	0.0	6.7	0.0	0.0	0.0	0.0	0.0	0.0	0.0	0.0	0.0	0.0	0.0	3.7	0.0	27.3	11.1	50.0
Quinqueloculina spp.	0.0	0.0	0.0	0.0	0.0	0.0	0.0	0.0	0.0	0.0	0.0	0.0	0.0	0.0	14.8	0.0	18.2	0.0	0.0
Rosalina spp.	0.0	0.0	0.0	0.0	0.0	0.0	0.0	0.0	0.0	0.0	0.0	0.0	0.0	0.0	3.7	0.0	0.0	0.0	0.0
Total	8	9	15	6	9	9	11	2	14	19	71	19	9	20	27	3	11	72	6

Table A1.7 Live foraminifera percentages for transect OBSS3.

OBSS3 (live)	1	2	3	4	5	6	7	8	9	10	11	12	13	14	15	16	17	18	19	20	21	22
B. pseudomacresens	0.0	8.9	15.2	8.0	0.0	0.0	0.0	0.0	0.0	0.0	0.0	0.0	0.0	0.0	0.0	0.0	0.0	0.0	0.0	0.0	0.0	0.0
Cribrostomoides jeffreysii	0.0	0.0	0.0	0.0	0.0	0.0	0.0	0.0	0.0	0.0	0.0	6.7	0.0	22.6	5.7	5.9	0.0	0.0	1.3	7.5	3.8	0.0
Haplophragmoides spp.	8.6	29.7	32.9	30.0	67.2	32.2	59.0	47.3	31.3	23.5	12.5	6.7	0.0	3.2	15.1	7.0	0.7	2.1	0.0	8.8	0.0	2.4
J. macrescens	89.8	50.0	45.6	50.0	30.7	39.0	33.3	17.6	47.5	39.2	16.7	36.7	8.1	32.3	49.1	24.8	15.5	6.3	33.8	28.8	40.4	33.9
M. fusca	1.6	4.9	5.1	5.0	1.3	23.3	2.8	25.7	8.8	7.8	12.5	13.3	86.5	9.7	3.8	1.9	2.7	5.6	2.5	1.3	2.9	0.8
Trochammina inflata	0.0	3.3	1.3	7.0	0.9	5.5	4.9	9.5	12.5	29.4	54.2	36.7	5.4	32.3	26.4	58.9	64.2	76.1	62.5	53.8	51.9	59.8
Ammonia beccarii spp.	0.0	0.4	0.0	0.0	0.0	0.0	0.0	0.0	0.0	0.0	0.0	0.0	0.0	0.0	0.0	0.0	0.7	2.1	0.0	0.0	0.0	0.0
Brizalina spp.	0.0	0.4	0.0	0.0	0.0	0.0	0.0	0.0	0.0	0.0	4.2	0.0	0.0	0.0	0.0	0.0	0.0	0.0	0.0	0.0	0.0	0.0
Cyclogyra involvens	0.0	0.0	0.0	0.0	0.0	0.0	0.0	0.0	0.0	0.0	0.0	0.0	0.0	0.0	0.0	0.0	13.5	7.0	0.0	0.0	0.0	0.8
Elphidium spp.	0.0	2.0	0.0	0.0	0.0	0.0	0.0	0.0	0.0	0.0	0.0	0.0	0.0	0.0	0.0	0.4	0.0	0.0	0.0	0.0	0.0	1.6
Gavelinopsis	0.0	0.4	0.0	0.0	0.0	0.0	0.0	0.0	0.0	0.0	0.0	0.0	0.0	0.0	0.0	0.0	0.0	0.0	0.0	0.0	0.0	0.0
Haynesina spp.	0.0	0.0	0.0	0.0	0.0	0.0	0.0	0.0	0.0	0.0	0.0	0.0	0.0	0.0	0.0	0.0	2.0	0.0	0.0	0.0	0.0	0.0
Nonion depressulus	0.0	0.0	0.0	0.0	0.0	0.0	0.0	0.0	0.0	0.0	0.0	0.0	0.0	0.0	0.0	0.0	0.0	0.0	0.0	0.0	0.0	0.0
Quinqueloculina spp.	0.0	0.0	0.0	0.0	0.0	0.0	0.0	0.0	0.0	0.0	0.0	0.0	0.0	0.0	0.0	1.1	0.7	0.7	0.0	0.0	1.0	0.8
Total	128	142	79	100	466	146	144	74	80	51	24	30	37	31	53	270	148	142	80	80	104	127

Table A1.8 Live foraminifera percentages for transects from Decoy Marsh.

Decoy Marsh (live)	1	2	3	4	5	6	7	8	9	10	11	12	13	14	15	16	17	18
B. pseudomacresens	34.1	80.0	7.9	1.1	0.0	0.0	0.0	5.2	5.5	5.3	7.2	12.6	3.3	0.0	0.0	0.0	0.0	0.0
Cribrostomoides jeffreysii	0.0	0.0	0.0	0.5	0.0	0.0	0.0	0.0	0.0	0.0	0.0	0.0	0.0	0.0	0.0	0.0	0.0	0.0
Haplophragmoides spp.	9.5	3.8	2.1	5.8	1.1	3.8	15.8	8.6	0.9	0.0	4.0	0.0	0.9	0.0	0.0	0.0	0.0	0.0
J. macrescens	33.3	12.5	85.7	92.6	95.8	96.3	56.2	81.0	86.4	84.0	87.1	85.4	95.8	100.0	98.4	100.0	95.0	100.0
M. fusca	23.0	3.8	4.3	0.0	3.2	0.0	6.2	0.0	1.8	6.4	0.7	0.3	0.0	0.0	0.0	0.0	0.0	0.0
Trochammina inflata	0.0	0.0	0.0	0.0	0.0	0.0	17.8	4.3	0.0	0.0	0.0	0.0	0.0	0.0	0.0	0.0	0.0	0.0
Ammonia beccarii spp.	0.0	0.0	0.0	0.0	0.0	0.0	0.0	0.0	1.8	0.0	0.0	0.0	0.0	0.0	0.0	0.0	0.0	0.0
Brizalina spp.	0.0	0.0	0.0	0.0	0.0	0.0	0.0	0.9	0.0	0.0	0.0	0.0	0.0	0.0	0.0	0.0	0.0	0.0
Fursenkoina spp.	0.0	0.0	0.0	0.0	0.0	0.0	0.0	0.0	0.0	0.0	0.0	0.0	0.0	0.0	0.0	0.0	0.0	0.0
Haynesina spp.	0.0	0.0	0.0	0.0	0.0	0.0	0.0	0.0	0.0	0.0	0.0	0.0	0.0	0.0	1.6	0.0	0.0	0.0
Quinqueloculina spp.	0.0	0.0	0.0	0.0	0.0	0.0	4.1	0.0	3.6	4.3	1.0	1.7	0.0	0.0	0.0	0.0	5.0	0.0
Total	126	80	140	365	189	80	146	116	110	94	402	302	212	48	122	48	101	90

Table A1.9 Fossil foraminifera percentages from OB5.

OB5	2	3	4	5	6	7	8	9	10	11	12	13	14	15	16	17	18	19	20	21	22	23	24
Cribrostomoides jeffreysii	0.7	1.3	2.8	0.3	0.0	2.6	1.3	2.4	8.3	0.0	3.7	6.5	2.4	4.5	6.5	1.3	0.5	0.0	0.4	6.0	1.3	0.0	0.0
Eggerella spp.	1.3	0.0	0.0	0.0	0.0	0.0	0.0	0.0	0.0	0.0	0.0	0.0	0.0	0.0	0.0	0.0	0.0	0.0	0.0	0.0	0.0	0.0	0.0
Haplophragmoides spp.	0.0	0.0	0.0	0.0	0.0	0.0	0.0	4.9	1.7	0.0	0.0	0.0	3.6	6.7	18.2	53.6	29.9	15.7	3.3	5.6	14.5	23.1	40.0
J. macrescens	0.7	3.2	2.8	2.0	2.0	4.1	2.6	0.0	8.3	18.5	7.4	29.0	46.4	14.0	27.3	7.9	22.5	67.8	84.4	24.7	54.7	49.3	45.9
M. fusca	0.0	0.0	0.0	0.0	0.0	0.0	0.0	0.0	0.0	0.0	3.7	0.0	1.2	24.7	0.0	18.5	17.6	10.3	4.7	12.1	6.5	4.1	6.1
Textularia spp.	12.0	7.0	0.0	0.0	0.0	0.0	0.0	0.0	1.7	0.0	0.0	0.0	0.0	0.0	0.0	0.0	0.0	0.0	0.0	0.0	0.0	0.0	0.0
T. inflata	0.0	0.6	0.0	0.0	0.0	0.5	0.0	9.8	0.0	0.0	7.4	0.0	0.0	1.1	1.3	0.0	0.5	0.0	0.9	0.0	1.6	2.7	1.6
Trochammina ochracea	1.3	7.0	5.7	8.6	2.0	5.1	6.6	26.8	16.7	48.1	66.7	46.8	33.3	44.9	24.7	13.9	17.6	0.8	0.4	9.3	1.2	1.8	0.4
Ammonia beccarii spp.	8.7	3.8	0.3	1.3	0.7	2.6	0.0	0.0	0.0	3.7	0.0	0.0	0.0	0.0	0.0	0.0	0.0	0.8	0.3	1.4	0.7	0.0	0.2
Astacolus crepidulus	0.0	0.0	0.0	0.0	0.0	0.0	0.0	0.0	0.0	0.0	0.0	0.0	0.0	0.0	0.0	0.0	0.0	0.0	0.0	0.0	0.0	0.0	0.0
Bolivina spp.	14.0	9.5	15.3	21.9	27.5	21.0	19.9	2.4	1.7	0.0	0.0	6.5	1.2	0.0	0.0	0.0	0.0	0.4	0.3	25.1	1.5	0.0	0.0
Brizalina spp.	11.3	8.9	5.4	7.9	6.5	2.6	4.0	4.9	8.3	1.9	0.0	0.0	1.2	0.0	0.0	0.0	0.0	0.0	0.0	0.0	0.7	0.0	0.0
Bulimina spp.	0.7	1.3	2.0	0.0	0.7	0.5	1.3	0.0	1.7	1.9	0.0	0.0	0.0	0.0	1.3	0.0	0.5	0.0	0.0	1.9	0.1	0.5	0.0
Bulimnella spp.	0.0	2.5	2.5	0.0	2.0	2.1	4.6	2.4	1.7	0.0	0.0	1.6	0.0	1.7	0.0	1.3	0.5	0.4	0.7	0.0	1.3	0.9	0.2
Cyclogyra involvens	0.0	0.0	0.3	0.0	0.0	0.0	1.3	0.0	0.0	0.0	0.0	0.0	0.0	0.0	0.0	2.0	0.0	0.0	0.0	0.0	0.6	0.9	1.6
Elphidium spp.	38.0	44.3	49.0	40.7	42.5	45.6	46.4	34.1	35.0	13.0	7.4	4.8	2.4	0.0	10.4	1.3	8.6	1.5	3.9	0.0	13.8	2.3	1.6
Fissurina spp.	0.0	0.0	0.6	2.3	0.0	0.0	0.0	0.0	0.0	0.0	0.0	0.0	0.0	0.0	0.0	0.0	0.0	0.0	0.1	0.0	0.0	0.0	0.0
Fursenkoina spp.	4.7	6.3	6.2	6.6	3.3	5.1	3.3	12.2	10.0	13.0	3.7	4.8	6.0	0.6	9.1	0.0	1.6	0.4	0.5	1.4	0.3	0.0	0.0
Gavelinopsis	0.0	1.9	2.5	0.0	0.0	0.0	0.0	0.0	0.0	0.0	0.0	0.0	0.0	0.0	0.0	0.0	0.0	0.0	0.0	0.9	0.4	0.0	0.0
Glabratella millettii	6.7	0.6	2.0	6.3	9.2	5.6	5.3	0.0	5.0	0.0	0.0	0.0	0.0	0.0	1.3	0.0	0.0	1.5	0.0	8.4	0.1	0.0	0.0
Globigerina spp.	0.0	0.6	0.0	0.0	2.0	0.0	0.0	0.0	0.0	0.0	0.0	0.0	0.0	0.0	0.0	0.0	0.0	0.0	0.0	1.4	0.1	0.0	0.0
Haynesina spp.	0.0	0.0	1.4	1.7	0.0	2.6	2.6	0.0	0.0	0.0	0.0	0.0	0.0	0.0	0.0	0.0	0.0	0.0	0.1	0.0	0.1	0.0	0.0
lagena spp.	0.0	1.3	0.0	0.0	0.0	0.0	0.0	0.0	0.0	0.0	0.0	0.0	0.0	0.6	0.0	0.0	0.0	0.0	0.0	0.0	0.0	0.0	0.0
Nonion depressulus	0.0	0.0	0.0	0.0	0.0	0.0	0.0	0.0	0.0	0.0	0.0	0.0	2.4	0.0	0.0	0.0	0.0	0.4	0.0	0.0	0.0	0.0	0.0
Nonionella spp.	0.0	0.0	1.1	0.0	1.3	0.0	0.0	0.0	0.0	0.0	0.0	0.0	0.0	0.0	0.0	0.0	0.0	0.0	0.0	0.0	0.0	0.0	0.0
Quinqueloculina spp.	0.0	0.0	0.0	0.3	0.7	0.0	0.7	0.0	0.0	0.0	0.0	0.0	0.0	1.1	0.0	0.0	0.0	0.0	0.1	1.9	0.1	14.5	2.2
Total	150	162	350	304	150	196	150	82	120	108	54	128	168	176	154	151	188	261	1068	212	706	200	596

Table A1.9 Fossil foraminifera percentages from OB5 continued

OB5	25	26	27	28	29	30	31	32	33	34	35	36	41	46	51
Cribrostomoides jeffreysii	0.4	0.9	0.8	0.3	0.0	0.3	0.0	0.6	0.0	0.0	0.4	0.0	0.7	0.0	0.6
Eggerella spp.	0.0	0.0	0.0	0.0	0.0	0.0	0.0	0.0	0.0	0.0	0.0	0.0	0.0	0.0	0.0
Haplophragmoides spp.	16.1	10.5	4.7	9.2	6.8	16.4	11.8	18.7	2.5	3.0	2.7	12.4	0.7	5.6	4.8
J. macrescens	22.8	56.1	49.2	51.4	8.2	47.8	6.5	14.5	21.6	31.0	11.9	16.3	15.2	19.7	9.5
M. fusca	1.3	17.0	10.9	22.1	3.1	5.7	1.4	5.6	4.5	5.4	3.4	5.9	0.9	4.4	6.9
Textularia spp.	0.0	0.0	0.0	0.0	0.0	0.0	0.2	0.0	0.0	0.0	0.0	0.0	0.0	0.0	1.3
T. inflata	0.0	0.9	0.0	1.6	0.0	2.8	1.4	15.7	43.4	58.0	68.3	48.7	57.9	33.5	44.3
Trochammina ochracea	3.6	0.9	6.3	2.7	0.5	2.0	0.8	2.8	0.2	0.5	0.3	2.2	0.2	0.6	1.5
Ammonia beccarii spp.	0.0	0.0	0.0	0.2	0.6	0.4	0.8	1.2	0.0	0.0	0.0	1.0	0.0	1.9	4.8
Astacolus crepidulus	0.0	0.0	0.0	0.0	0.0	0.0	0.0	0.0	0.0	0.0	0.0	0.0	0.2	0.0	0.0
Bolivina spp.	0.4	0.0	0.0	0.3	0.0	0.0	0.0	4.2	0.0	0.0	0.0	0.0	0.4	0.0	0.0
Brizalina spp.	0.0	0.0	0.0	0.5	0.0	0.0	0.6	1.8	0.0	0.0	0.0	0.4	0.2	3.8	3.0
Bulimina spp.	0.0	0.0	0.0	0.0	0.0	0.0	0.6	0.2	0.0	0.0	0.0	0.0	0.0	0.0	0.9
Bulimnella spp.	0.4	0.3	0.0	0.3	0.0	0.0	1.0	0.6	0.0	0.0	0.3	0.2	0.0	0.0	1.5
Cyclogyra involvens	0.4	0.6	6.3	3.6	3.1	16.4	3.5	7.2	4.1	0.1	2.6	3.5	1.1	3.4	0.4
Elphidium spp.	1.8	0.0	6.3	1.0	1.2	3.4	3.1	18.1	4.1	1.5	3.3	2.6	3.5	25.7	15.8
Fissurina spp.	0.0	0.0	0.0	0.0	0.0	0.0	0.0	0.0	0.0	0.0	0.0	0.0	0.0	0.0	0.0
Fursenkoina spp.	0.4	0.3	0.0	0.0	0.0	0.0	0.2	1.2	0.0	0.0	0.3	0.0	0.4	0.3	0.6
Gavelinopsis	0.0	0.0	0.0	0.0	0.0	0.0	0.0	0.0	0.0	0.0	0.0	0.0	0.0	0.0	0.6
Glabratella millettii	0.0	0.0	0.0	0.0	0.0	0.0	0.0	0.0	0.0	0.0	0.0	0.6	0.0	0.0	1.9
Globigerina spp.	0.0	0.0	0.0	0.0	0.0	0.0	0.0	0.0	0.0	0.0	0.0	0.0	0.0	0.0	0.0
Haynesina spp.	0.0	0.0	0.0	0.0	0.0	0.0	0.0	0.0	0.0	0.0	0.0	0.0	0.0	0.0	0.0
lagena spp.	0.0	0.0	0.0	0.0	0.0	0.0	0.0	0.2	0.0	0.0	0.0	0.0	0.2	0.0	0.2
Nonion depressulus	0.0	0.0	0.0	0.0	0.0	0.0	0.0	1.8	0.0	0.0	0.0	0.0	0.0	0.0	0.0
Nonionella spp.	0.0	0.0	0.0	0.0	0.0	0.0	0.0	0.0	0.0	0.0	0.0	0.0	0.0	0.0	0.0
Quinqueloculina spp.	52.2	12.6	15.6	6.8	76.4	4.8	68.0	5.6	19.5	0.5	6.4	6.3	18.4	0.9	1.3
Total	150	319	150	1070	207	1435	194	551	368	2793	714	562	379	322	465

Table A1.10 Fossil foraminifera percentages from DMC1.

DMC1	2	3	4	5	6	7	8	9	10	11	12
B. pseudomacresens	10.0	21.5	14.0	6.0	11.3	15.2	28.5	19.9	8.7	15.8	18.0
Cribrostomoides jeffreysii	0.7	0.0	0.0	0.0	0.0	0.0	0.0	0.0	0.0	0.0	0.0
Haplophragmoides spp.	13.3	8.9	19.1	22.7	11.3	41.7	27.2	32.5	36.0	9.9	17.0
J. macrescens	76.0	68.4	65.7	66.7	64.9	39.7	40.4	33.8	24.0	23.0	23.0
M. fusca	0.0	1.3	1.1	2.7	12.6	2.0	4.0	9.3	31.3	39.5	38.0
Trochammina inflata	0.0	0.0	0.0	1.3	0.0	1.3	0.0	4.6	0.0	11.8	4.0
Trochammina ochracea	0.0	0.0	0.0	0.7	0.0	0.0	0.0	0.0	0.0	0.0	0.0
Total	150	158	178	150	151	151	151	151	150	152	100

Table A2.1 Correlation matrix of environmental variables from OBSS1 with p values.

OBSS1	Cl	Br	Si	Al	Ti	Ca	Mg	K	Fe	Mn	Cr	Cu	Pb	Ni	Zn
Cl	0	0.000	0.000	0.000	0.001	0.000	0.000	0.000	0.901	0.018	0.481	0.000	0.000	0.001	0.000
Br	**0.891**	0	0.000	0.000	0.012	0.000	0.000	0.006	0.626	0.001	0.977	0.000	0.001	0.000	0.000
Si	**-0.835**	-0.751	0	0.000	0.000	0.000	0.000	0.000	0.424	0.063	0.017	0.000	0.000	0.028	0.000
Al	**-0.768**	-0.696	**0.943**	0	0.000	0.000	0.000	0.000	0.039	0.506	0.001	0.006	0.013	0.236	0.015
Ti	**-0.615**	-0.477	**0.901**	**0.941**	0	0.000	0.001	0.000	0.017	0.972	0.000	0.097	0.031	0.810	0.171
Ca	**-0.682**	**-0.658**	**0.875**	**0.894**	**0.844**	0	0.001	0.000	0.100	0.529	0.015	0.006	0.009	0.059	0.027
Mg	**-0.776**	**-0.645**	**0.709**	**0.744**	**0.603**	**0.584**	0	0.000	0.179	0.547	0.090	0.003	0.003	0.159	0.002
K	**-0.636**	-0.515	**0.875**	**0.954**	**0.967**	**0.805**	**0.699**	0	0.007	0.865	0.000	0.074	0.048	0.974	0.122
Fe	-0.025	0.098	0.160	0.400	0.456	0.323	0.267	0.508	0	0.000	0.008	0.094	0.128	0.013	0.046
Mn	0.453	**0.610**	-0.363	-0.134	-0.007	-0.127	-0.121	0.034	**0.703**	0	0.083	0.000	0.003	0.000	0.000
Cr	-0.142	0.006	0.456	**0.606**	**0.731**	0.465	0.333	**0.717**	0.501	0.339	0	0.305	0.687	0.020	0.250
Cu	**0.840**	**0.898**	**-0.681**	-0.519	-0.326	-0.518	**-0.550**	-0.350	0.329	**0.724**	0.205	0	0.000	0.000	0.000
Pb	**0.752**	**0.596**	**-0.678**	-0.472	-0.415	-0.493	**-0.556**	-0.385	0.300	**0.547**	0.081	**0.777**	0	0.000	0.000
Ni	**0.613**	**0.763**	-0.423	-0.236	-0.048	-0.368	-0.279	-0.007	0.471	**0.802**	0.446	**0.839**	**0.628**	0	0.000
Zn	**0.854**	**0.879**	**-0.628**	-0.463	-0.271	-0.424	**-0.563**	-0.305	0.388	**0.743**	0.229	**0.977**	**0.790**	**0.818**	0
Rb	**-0.717**	**-0.640**	**0.842**	**0.946**	**0.890**	**0.781**	**0.688**	0.929	0.449	-0.038	**0.660**	-0.445	-0.337	-0.102	-0.417
Sr	-0.440	-0.394	**0.600**	**0.779**	**0.745**	**0.828**	0.442	**0.740**	**0.689**	0.303	**0.612**	-0.132	-0.061	0.015	-0.044
Zr	-0.064	-0.175	0.050	0.161	0.120	0.025	-0.017	0.137	0.231	0.044	0.187	0.017	0.413	0.093	0.025
Sand	0.167	0.248	-0.531	**-0.673**	**-0.681**	**-0.714**	-0.208	-0.647	-0.445	-0.133	**-0.650**	0.012	-0.104	-0.090	-0.095
Clay	-0.137	-0.190	0.467	**0.587**	**0.610**	**0.607**	0.088	**0.550**	0.298	0.083	**0.644**	0.057	0.111	0.149	0.134
Silt	-0.170	-0.257	0.533	0.676	**0.679**	**0.722**	0.239	0.655	0.476	0.145	**0.628**	-0.034	0.097	0.067	0.079
-1-0	-0.043	-0.141	-0.343	-0.462	**-0.616**	-0.480	0.020	-0.492	-0.467	-0.338	**-0.700**	-0.321	-0.150	-0.339	-0.402
0-1	0.155	0.318	-0.476	**-0.560**	-0.542	**-0.623**	-0.242	**-0.559**	-0.304	0.020	-0.457	0.151	-0.034	0.027	0.053
1-2	0.112	0.210	-0.520	**-0.633**	**-0.675**	**-0.691**	-0.192	**-0.643**	-0.424	-0.109	**-0.636**	0.005	-0.084	-0.103	-0.105
2-3	0.080	0.133	-0.515	**-0.639**	**-0.712**	**-0.694**	-0.141	**-0.650**	-0.467	-0.175	**-0.698**	-0.079	-0.105	-0.164	-0.193
3-4	0.235	0.246	-0.332	-0.489	-0.400	-0.481	-0.171	-0.377	-0.319	-0.151	-0.403	0.028	-0.125	-0.012	-0.029
4-5	-0.332	-0.411	0.416	0.189	0.212	0.306	0.089	0.162	-0.347	-0.579	-0.160	-0.594	-0.505	-0.552	-0.543
5-6	-0.459	**-0.577**	**0.707**	**0.752**	**0.681**	**0.816**	0.360	**0.648**	0.266	-0.205	0.406	-0.434	-0.173	-0.332	-0.323
6-7	-0.002	-0.055	0.325	0.547	**0.551**	0.523	0.205	**0.569**	**0.615**	0.385	**0.651**	0.199	0.316	0.313	0.291
7-8	0.024	-0.031	0.321	0.531	**0.548**	0.538	0.152	0.542	**0.555**	0.357	**0.665**	0.239	0.297	0.311	0.328
8-9	-0.097	-0.137	0.446	**0.607**	**0.638**	**0.646**	0.159	**0.594**	0.471	0.237	**0.666**	0.126	0.139	0.201	0.216
9-10	-0.134	-0.184	0.457	**0.572**	**0.592**	**0.600**	0.089	0.531	0.275	0.075	**0.625**	0.054	0.099	0.143	0.132
LOI	**0.915**	**0.892**	**-0.918**	**-0.882**	**-0.743**	**-0.827**	**-0.711**	**-0.757**	-0.081	0.452	-0.269	**0.835**	**0.693**	**0.589**	**0.795**

Table A2.1 Correlation matrix of environmental variables from OBSS1 with p values continued.

OBSS1	Rb	Sr	Zr	Sand	Clay	Silt	-1-0	0-1	1-2	2-3	3-4	4-5	5-6	6-7	7-8	8-9	9-10	LOI
Cl	0.000	0.022	0.751	0.406	0.496	0.396	0.831	0.439	0.578	0.690	0.238	0.090	0.016	0.990	0.907	0.629	0.506	0.000
Br	0.000	0.042	0.382	0.213	0.342	0.196	0.484	0.106	0.294	0.509	0.216	0.033	0.002	0.783	0.878	0.497	0.357	0.000
Si	0.000	0.001	0.805	0.004	0.014	0.004	0.080	0.012	0.005	0.006	0.091	0.031	0.000	0.098	0.102	0.020	0.016	0.000
Al	0.000	0.000	0.424	0.000	0.001	0.000	0.015	0.002	0.000	0.000	0.010	0.346	0.000	0.003	0.004	0.001	0.002	0.000
Ti	0.000	0.000	0.553	0.000	0.001	0.000	0.001	0.004	0.000	0.000	0.039	0.288	0.000	0.003	0.003	0.000	0.001	0.000
Ca	0.000	0.000	0.902	0.000	0.001	0.000	0.011	0.001	0.000	0.000	0.011	0.120	0.000	0.005	0.004	0.000	0.001	0.000
Mg	0.000	0.021	0.931	0.297	0.663	0.229	0.921	0.225	0.338	0.482	0.393	0.659	0.065	0.306	0.450	0.427	0.660	0.000
K	0.000	0.000	0.496	0.000	0.003	0.000	0.009	0.002	0.000	0.000	0.052	0.420	0.000	0.002	0.004	0.001	0.004	0.000
Fe	0.019	0.000	0.247	0.020	0.131	0.012	0.014	0.123	0.028	0.014	0.105	0.076	0.180	0.001	0.003	0.013	0.165	0.689
Mn	0.850	0.125	0.827	0.508	0.681	0.472	0.084	0.922	0.588	0.384	0.452	0.002	0.306	0.047	0.068	0.234	0.711	0.018
Cr	0.000	0.001	0.351	0.000	0.000	0.000	0.000	0.017	0.000	0.000	0.037	0.426	0.036	0.000	0.000	0.000	0.000	0.176
Cu	0.020	0.511	0.935	0.951	0.777	0.865	0.102	0.453	0.980	0.697	0.889	0.001	0.024	0.319	0.230	0.531	0.788	0.000
Pb	0.085	0.764	0.032	0.607	0.581	0.629	0.454	0.866	0.678	0.601	0.534	0.007	0.387	0.108	0.132	0.490	0.624	0.000
Ni	0.614	0.942	0.646	0.657	0.459	0.739	0.084	0.893	0.609	0.413	0.953	0.003	0.091	0.112	0.114	0.315	0.477	0.001
Zn	0.031	0.826	0.901	0.637	0.504	0.695	0.038	0.794	0.601	0.335	0.888	0.003	0.100	0.140	0.095	0.280	0.513	0.000
Rb	0	0.000	0.145	0.000	0.002	0.000	0.023	0.003	0.001	0.001	0.008	0.663	0.000	0.001	0.003	0.001	0.002	0.000
Sr	**0.766**	0	0.183	0.000	0.000	0.000	0.000	0.005	0.000	0.000	0.001	0.657	0.000	0.000	0.000	0.000	0.000	0.002
Zr	0.288	0.264	0	0.221	0.416	0.189	0.461	0.378	0.316	0.312	0.215	0.881	0.056	0.160	0.315	0.424	0.515	0.620
sand	-0.660	**-0.747**	-0.244	0	0.000	0.000	0.000	0.000	0.000	0.000	0.000	0.855	0.000	0.000	0.000	0.000	0.000	0.019
clay	**0.578**	**0.657**	0.163	-0.913	0	0.000	0.000	0.000	0.000	0.000	0.000	0.416	0.000	0.000	0.000	0.000	0.000	0.064
silt	**0.662**	**0.749**	0.260	-0.991	0.851	0	0.000	0.000	0.000	0.000	0.000	0.980	0.000	0.000	0.000	0.000	0.000	0.015
-1-0	-0.435	**-0.658**	-0.148	0.682	-0.715	-0.647	0	0.128	0.001	0.000	0.004	0.231	0.022	0.000	0.000	0.000	0.000	0.469
0-1	**-0.548**	-0.528	-0.177	0.860	-0.707	-0.877	0.300	0	0.000	0.000	0.091	0.168	0.000	0.000	0.000	0.000	0.000	0.028
1-2	-0.613	**-0.679**	-0.200	0.961	-0.848	-0.962	0.618	0.936	0	0.000	0.013	0.495	0.000	0.000	0.000	0.000	0.000	0.037
2-3	-0.612	**-0.735**	-0.202	0.967	-0.884	-0.959	0.785	0.825	0.971	0	0.003	0.869	0.000	0.000	0.000	0.000	0.000	0.056
3-4	-0.498	**-0.611**	-0.247	0.696	-0.701	-0.668	0.535	0.332	0.472	0.556	0	0.012	0.002	0.000	0.000	0.000	0.000	0.052
4-5	0.088	-0.089	0.030	0.037	-0.163	0.005	0.238	-0.273	-0.137	-0.033	0.476	0	0.099	0.149	0.081	0.246	0.399	0.050
5-6	**0.715**	**0.701**	0.372	-0.846	0.663	0.874	-0.438	-0.799	-0.821	-0.791	-0.574	0.324	0	0.000	0.000	0.000	0.000	0.000
6-7	**0.585**	**0.699**	0.278	-0.924	0.782	0.936	-0.635	-0.765	-0.865	-0.878	-0.709	-0.285	0.706	0	0.000	0.000	0.000	0.178
7-8	0.543	**0.695**	0.201	-0.939	0.862	0.930	-0.700	-0.735	-0.865	-0.897	-0.754	-0.341	0.665	0.972	0	0.000	0.000	0.234
8-9	**0.594**	**0.728**	0.160	-0.959	0.940	0.930	-0.741	-0.747	-0.890	-0.927	-0.745	-0.231	0.700	0.899	0.960	0	0.000	0.078
9-10	**0.559**	**0.642**	0.131	-0.899	0.997	0.835	-0.706	-0.697	-0.836	-0.872	-0.689	-0.169	0.646	0.765	0.848	0.931	0	0.071
LOI	**-0.832**	**-0.578**	-0.100	0.450	-0.361	-0.462	0.146	0.423	0.403	0.373	0.378	-0.381	**-0.712**	-0.267	-0.237	-0.345	-0.353	0

Table A2.2 Correlation matrix of environmental variables from OBSS2 with p values.

OBSS2	Cl	Br	Al	Ti	Ca	Mg	K	Fe	Mn	Cr	Cu	Pb	Ni	Zn	Rb	Sr	Zr
Cl	0	0.122	0.178	0.369	0.697	0.484	0.178	0.312	0.009	0.734	0.522	0.074	0.600	0.390	0.364	0.166	0.634
Br	0.357	0	0.000	0.001	0.000	0.001	0.005	0.216	0.000	0.001	0.003	0.003	0.133	0.003	0.000	0.023	0.003
Al	-0.314	**-0.734**	0	0.000	0.000	0.000	0.000	0.132	0.042	0.000	0.753	0.017	0.175	0.654	0.000	0.039	0.208
Ti	-0.212	**-0.664**	**0.961**	0	0.000	0.000	0.000	0.066	0.132	0.000	0.842	0.013	0.156	0.701	0.000	0.027	0.090
Ca	-0.093	**-0.776**	**0.740**	**0.776**	0	0.000	0.001	0.860	0.131	0.000	0.065	0.001	0.747	0.037	0.000	0.000	0.008
Mg	-0.166	**-0.682**	**0.922**	**0.903**	**0.797**	0	0.000	0.201	0.149	0.000	0.498	0.004	0.330	0.337	0.000	0.007	0.142
K	-0.314	**-0.598**	**0.974**	**0.973**	**0.678**	**0.879**	0	0.028	0.119	0.000	0.682	0.074	0.037	0.804	0.000	0.080	0.420
Fe	0.238	0.289	0.349	0.419	0.042	0.299	0.492	0	0.022	0.089	0.005	0.881	0.000	0.014	0.178	0.399	0.115
Mn	**0.567**	0.709	-0.458	-0.348	-0.349	-0.335	-0.360	0.510	0	0.192	0.196	0.540	0.516	0.263	0.055	0.879	0.256
Cr	-0.081	**-0.662**	**0.862**	**0.856**	**0.755**	**0.819**	**0.851**	0.390	-0.305	0	0.591	0.019	0.359	0.389	0.000	0.003	0.243
Cu	-0.152	**0.623**	-0.075	-0.048	-0.421	-0.161	0.098	**0.598**	0.302	-0.128	0	0.003	0.000	0.000	0.473	0.048	0.000
Pb	-0.409	**0.623**	-0.527	-0.544	**-0.705**	-0.616	-0.409	-0.036	0.146	-0.518	**0.623**	0	0.237	0.002	0.004	0.000	0.002
Ni	-0.125	0.347	0.315	0.329	-0.077	0.230	0.469	**0.737**	0.154	0.216	**0.866**	0.277	0	0.000	0.357	0.539	0.004
Zn	-0.203	**0.629**	-0.107	-0.092	-0.469	-0.226	0.059	0.540	0.263	-0.204	**0.976**	**0.646**	**0.846**	0	0.351	0.018	0.000
Rb	-0.215	**-0.775**	**0.960**	**0.900**	**0.745**	**0.892**	**0.908**	0.314	-0.435	**0.863**	-0.170	**-0.617**	0.218	-0.220	0	0.008	0.234
Sr	0.322	**-0.507**	0.465	0.494	**0.825**	**0.587**	0.401	0.200	0.036	**0.632**	-0.448	**-0.756**	-0.146	-0.524	**0.575**	0	0.112
Zr	0.113	**-0.633**	0.294	0.389	**0.579**	0.340	0.191	-0.363	-0.267	0.274	-0.710	**-0.643**	-0.609	-0.717	0.279	0.367	0
Sand	-0.052	0.088	-0.528	**-0.581**	-0.415	-0.618	**-0.576**	-0.508	-0.097	-0.359	-0.227	0.308	-0.556	-0.207	-0.455	-0.305	0.007
Clay	-0.153	-0.345	**0.629**	**0.633**	0.351	**0.648**	**0.642**	0.413	-0.093	0.475	0.060	-0.385	0.322	0.005	**0.597**	0.205	0.110
Silt	0.200	0.260	-0.124	-0.077	0.046	-0.057	-0.090	0.072	0.183	-0.133	0.156	0.090	0.209	0.193	-0.162	0.085	-0.116
2-3	-0.233	-0.064	0.096	0.080	0.077	-0.037	0.119	0.224	0.004	0.105	0.243	0.129	0.096	0.259	0.111	0.098	-0.083
3-4	-0.037	0.110	**-0.562**	**-0.613**	-0.413	**-0.631**	**-0.609**	-0.528	-0.067	-0.351	-0.235	0.328	-0.560	-0.227	-0.497	-0.296	-0.001
4-5	0.294	-0.081	-0.409	-0.389	-0.091	-0.353	-0.519	**-0.553**	0.035	-0.275	-0.551	-0.222	-0.770	-0.549	-0.348	-0.011	**0.554**
5-6	0.144	-0.169	-0.070	-0.147	0.062	-0.037	-0.196	-0.424	-0.196	-0.084	-0.459	-0.305	-0.416	-0.416	-0.079	0.024	0.326
6-7	-0.051	0.362	0.033	0.029	-0.077	0.063	0.136	0.405	0.223	0.036	0.475	0.376	**0.561**	0.483	-0.017	-0.003	**-0.581**
7-8	-0.086	0.246	0.178	0.225	0.044	0.196	0.302	0.511	0.150	0.115	0.567	0.254	**0.687**	**0.561**	0.132	0.044	-0.496
8-9	-0.272	-0.221	**0.594**	**0.608**	0.259	0.535	**0.655**	0.420	-0.171	0.362	0.305	-0.119	**0.580**	0.298	0.528	0.031	-0.088
9-10	-0.110	-0.251	**0.549**	**0.558**	0.301	**0.588**	**0.573**	0.462	0.021	0.426	0.127	-0.334	0.350	0.058	0.533	0.217	0.026
LOI	-0.016	**0.840**	**-0.836**	**-0.831**	**-0.860**	**-0.850**	**-0.742**	-0.128	0.364	**-0.781**	0.465	**0.868**	0.099	0.512	-0.890	**-0.728**	**-0.619**

Table A2.2 Correlation matrix of environmental variables from OBSS1 with p values continued.

OBSS2	Sand	Clay	Silt	2-3	3-4	4-5	5-6	6-7	7-8	8-9	9-10	LOI
Cl	0.829	0.519	0.397	0.323	0.876	0.208	0.544	0.830	0.718	0.247	0.643	0.946
Br	0.711	0.136	0.269	0.787	0.644	0.733	0.476	0.116	0.296	0.348	0.286	0.000
Al	0.017	0.003	0.603	0.688	0.010	0.074	0.770	0.891	0.453	0.006	0.012	0.000
Ti	0.007	0.003	0.748	0.738	0.004	0.090	0.537	0.903	0.340	0.004	0.011	0.000
Ca	0.069	0.129	0.848	0.747	0.070	0.701	0.794	0.748	0.855	0.270	0.198	0.000
Mg	0.004	0.002	0.813	0.876	0.003	0.126	0.877	0.793	0.409	0.015	0.006	0.000
K	0.008	0.002	0.706	0.617	0.004	0.019	0.408	0.566	0.195	0.002	0.008	0.000
Fe	0.022	0.071	0.763	0.342	0.017	0.011	0.062	0.077	0.021	0.065	0.040	0.590
Mn	0.683	0.698	0.439	0.987	0.778	0.885	0.407	0.346	0.527	0.471	0.930	0.115
Cr	0.120	0.034	0.577	0.660	0.129	0.241	0.726	0.880	0.630	0.117	0.061	0.000
Cu	0.337	0.801	0.511	0.302	0.319	0.012	0.042	0.034	0.009	0.191	0.594	0.039
Pb	0.187	0.094	0.705	0.587	0.158	0.346	0.191	0.102	0.280	0.618	0.150	0.000
Ni	0.011	0.167	0.376	0.686	0.010	0.000	0.068	0.010	0.001	0.007	0.131	0.678
Zn	0.380	0.985	0.414	0.271	0.335	0.012	0.068	0.031	0.010	0.202	0.808	0.021
Rb	0.044	0.005	0.496	0.642	0.026	0.133	0.741	0.942	0.580	0.017	0.015	0.000
Sr	0.192	0.385	0.722	0.680	0.205	0.962	0.921	0.991	0.855	0.897	0.357	0.000
Zr	0.978	0.645	0.626	0.729	0.996	0.011	0.160	0.007	0.026	0.713	0.913	0.004
Sand	0	0.035	0.032	0.269	0.000	0.003	0.635	0.034	0.002	0.001	0.045	0.115
Clay	-0.473	0	0.013	0.403	0.042	0.106	0.320	0.251	0.669	0.000	0.000	0.013
Silt	-0.481	-0.545	0	0.832	0.033	0.318	0.596	0.000	0.019	0.674	0.012	0.402
2-3	0.260	-0.198	-0.051	0	0.472	0.862	0.245	0.852	0.749	0.745	0.493	0.781
3-4	0.981	-0.458	-0.478	0.171	0	0.002	0.519	0.031	0.001	0.001	0.057	0.082
4-5	0.636	-0.372	-0.235	-0.041	0.646	0	0.011	0.001	0.000	0.000	0.097	0.980
5-6	0.113	-0.235	0.126	-0.273	0.153	0.555	0	0.215	0.003	0.028	0.184	0.721
6-7	-0.476	-0.269	0.721	0.045	-0.483	-0.697	-0.290	0	0.000	0.478	0.309	0.204
7-8	-0.651	0.102	0.519	0.076	-0.661	-0.881	-0.636	0.789	0	0.005	0.553	0.618
8-9	-0.663	0.735	-0.100	-0.078	-0.662	-0.768	-0.490	0.168	0.599	0	0.000	0.134
9-10	-0.453	0.986	-0.549	-0.163	-0.431	-0.382	-0.310	-0.240	0.141	0.708	0	0.032
LOI	0.363	**-0.546**	0.198	-0.066	0.398	0.006	-0.085	0.296	0.119	-0.347	-0.481	0

Table A2.3 Correlation matrix of environmental variables from OBSS3 with p values.

OBSS3	Cl	Br	Al	Ti	Ca	Mg	K	Fe	Mn	Cr	Cu	Pb	Ni	Zn	Rb	Sr	Zr
Cl	0	0.005	0.000	0.000	0.019	0.307	0.000	0.000	0.000	0.000	0.007	0.001	0.005	0.000	0.000	0.000	0.001
Br	0.504	0	0.231	0.003	0.049	0.336	0.175	0.000	0.029	0.004	0.003	0.000	0.000	0.001	0.001	0.011	0.049
Al	**0.620**	0.226	0	0.000	0.004	0.000	0.000	0.000	0.000	0.000	0.005	0.005	0.006	0.000	0.000	0.000	0.030
Ti	**0.767**	0.523	**0.888**	0	0.000	0.017	0.000	0.000	0.000	0.000	0.000	0.000	0.000	0.000	0.000	0.000	0.000
Ca	0.424	0.362	0.510	**0.614**	0	0.374	0.005	0.000	0.003	0.000	0.000	0.000	0.001	0.000	0.001	0.000	0.011
Mg	0.193	-0.182	**0.712**	0.433	0.168	0	0.000	0.106	0.212	0.245	0.619	0.998	0.790	0.328	0.066	0.078	0.827
K	**0.642**	0.254	**0.984**	**0.911**	0.499	**0.667**	0	0.000	0.000	0.000	0.004	0.003	0.003	0.000	0.000	0.000	0.010
Fe	**0.754**	0.606	**0.800**	**0.924**	**0.694**	0.301	**0.821**	0	0.000	0.000	0.000	0.000	0.000	0.000	0.000	0.000	0.001
Mn	**0.830**	0.399	**0.630**	**0.754**	0.527	0.235	**0.674**	**0.814**	0	0.000	0.001	0.000	0.003	0.000	0.000	0.000	0.000
Cr	**0.620**	0.505	**0.755**	**0.841**	**0.642**	0.219	**0.766**	**0.883**	**0.664**	0	0.000	0.000	0.000	0.000	0.000	0.000	0.001
Cu	0.480	0.524	0.503	**0.638**	**0.651**	0.095	0.510	**0.839**	**0.582**	**0.722**	0	0.000	0.000	0.000	0.000	0.000	0.023
Pb	**0.597**	**0.622**	0.498	**0.685**	**0.657**	0.001	0.528	**0.882**	**0.681**	**0.782**	**0.957**	0	0.000	0.000	0.000	0.000	0.006
Ni	0.501	**0.693**	0.493	**0.673**	**0.585**	0.051	0.527	**0.834**	0.522	**0.662**	**0.903**	**0.908**	0	0.000	0.000	0.000	0.038
Zn	**0.756**	**0.596**	**0.727**	**0.880**	**0.690**	0.185	**0.750**	**0.978**	**0.788**	**0.897**	**0.873**	**0.930**	**0.836**	0	0.000	0.000	0.001
Rb	**0.748**	**0.574**	**0.861**	**0.937**	**0.597**	0.341	**0.879**	**0.927**	**0.721**	**0.905**	**0.624**	**0.702**	**0.682**	**0.889**	0	0.000	0.003
Sr	**0.752**	0.460	**0.841**	**0.908**	0.779	0.327	**0.848**	**0.943**	**0.789**	**0.910**	**0.726**	**0.787**	**0.680**	**0.932**	**0.934**	0	0.001
Zr	**0.575**	0.363	0.397	**0.677**	0.458	0.042	0.465	**0.580**	**0.613**	**0.578**	0.414	0.493	0.381	**0.595**	0.520	**0.557**	0
sand	**-0.619**	**-0.817**	-0.527	**-0.778**	**-0.662**	0.019	-0.562	**-0.871**	**-0.634**	**-0.775**	**-0.758**	**-0.844**	**-0.865**	**-0.862**	**-0.807**	**-0.783**	**-0.568**
clay	0.474	**0.662**	0.446	**0.619**	**0.636**	-0.082	0.481	**0.775**	0.534	**0.673**	**0.813**	**0.862**	**0.881**	**0.787**	**0.665**	**0.703**	0.360
silt	**0.626**	**0.820**	0.525	**0.783**	**0.647**	-0.007	**0.559**	**0.861**	**0.633**	**0.770**	**0.724**	**0.815**	**0.835**	**0.849**	0.808	**0.774**	**0.589**
-1-0	-0.392	**-0.558**	-0.226	-0.360	-0.433	0.062	-0.249	-0.491	-0.382	-0.494	-0.372	-0.444	-0.416	-0.479	-0.506	-0.455	-0.317
0-1	-0.475	**-0.652**	-0.282	**-0.554**	**-0.550**	0.226	-0.340	**-0.617**	-0.497	**-0.673**	-0.449	**-0.601**	-0.523	**-0.636**	**-0.650**	**-0.617**	**-0.593**
1-2	**-0.563**	**-0.777**	-0.420	**-0.711**	**-0.593**	0.136	-0.469	**-0.763**	**-0.572**	**-0.718**	**-0.641**	**-0.740**	**-0.730**	**-0.766**	**-0.728**	**-0.702**	**-0.652**
2-3	**-0.622**	**-0.785**	**-0.568**	-0.771	**-0.650**	-0.115	**-0.573**	**-0.871**	**-0.616**	**-0.697**	**-0.792**	**-0.827**	**-0.883**	**-0.850**	**-0.761**	**-0.751**	-0.472
3-4	-0.390	-0.421	-0.513	-0.517	-0.414	-0.275	-0.515	-0.658	-0.448	-0.484	**-0.663**	**-0.664**	**-0.766**	**-0.624**	**-0.546**	**-0.546**	-0.036
4-5	0.337	0.240	0.009	0.223	0.102	-0.233	0.011	0.153	0.245	0.149	0.019	0.062	-0.073	0.183	0.171	0.167	0.514
5-6	**0.658**	**0.753**	0.529	**0.777**	**0.595**	-0.002	0.542	**0.803**	**0.643**	**0.721**	**0.618**	**0.691**	**0.652**	**0.789**	**0.770**	**0.747**	**0.637**
6-7	0.552	**0.773**	**0.554**	**0.749**	**0.641**	0.095	**0.587**	**0.834**	**0.575**	**0.765**	**0.691**	**0.782**	**0.833**	**0.810**	**0.804**	**0.755**	0.440
7-8	0.437	**0.681**	0.476	**0.636**	**0.554**	0.101	0.515	**0.743**	0.473	**0.659**	**0.673**	**0.745**	**0.841**	**0.718**	**0.688**	**0.645**	0.338
8-9	0.391	**0.656**	0.389	**0.565**	0.525	-0.050	0.430	**0.706**	0.454	**0.599**	**0.734**	**0.791**	**0.885**	**0.701**	**0.603**	**0.596**	0.323
9-10	0.468	**0.660**	0.418	**0.598**	**0.621**	-0.119	0.454	**0.759**	0.523	**0.655**	**0.802**	**0.849**	**0.868**	**0.773**	**0.649**	**0.684**	0.355
LOI	-0.135	0.477	-0.525	-0.271	0.135	**-0.583**	-0.494	-0.021	-0.114	-0.202	0.313	0.316	0.426	0.019	-0.237	-0.196	-0.106

Table A2.3 Correlation matrix of environmental variables from OBSS3 with p values continued.

OBSS3	sand	clay	silt	-1-0	0-1	1-2	2-3	3-4	4-5	5-6	6-7	7-8	8-9	9-10	LOI
Cl	0.000	0.008	0.000	0.032	0.008	0.001	0.000	0.033	0.069	0.000	0.002	0.016	0.033	0.009	0.477
Br	0.000	0.000	0.000	0.001	0.000	0.000	0.000	0.020	0.202	0.000	0.000	0.000	0.000	0.000	0.008
Al	0.003	0.014	0.003	0.230	0.130	0.021	0.001	0.004	0.961	0.003	0.001	0.008	0.034	0.022	0.003
Ti	0.000	0.000	0.000	0.051	0.001	0.000	0.000	0.003	0.236	0.000	0.000	0.000	0.001	0.000	0.147
Ca	0.000	0.000	0.000	0.017	0.002	0.001	0.000	0.023	0.593	0.001	0.000	0.002	0.003	0.000	0.477
Mg	0.919	0.668	0.970	0.744	0.231	0.474	0.545	0.141	0.215	0.992	0.619	0.594	0.793	0.533	0.001
K	0.001	0.007	0.001	0.185	0.066	0.009	0.001	0.004	0.956	0.002	0.001	0.004	0.018	0.012	0.005
Fe	0.000	0.000	0.000	0.006	0.000	0.000	0.000	0.000	0.419	0.000	0.000	0.000	0.000	0.000	0.911
Mn	0.000	0.002	0.000	0.037	0.005	0.001	0.000	0.013	0.191	0.000	0.001	0.008	0.012	0.003	0.549
P	0.000	0.002	0.001	0.066	0.025	0.004	0.000	0.006	0.242	0.000	0.003	0.017	0.018	0.002	0.553
Cr	0.000	0.000	0.000	0.006	0.000	0.000	0.000	0.007	0.433	0.000	0.000	0.000	0.000	0.000	0.284
Cu	0.000	0.000	0.000	0.043	0.013	0.000	0.000	0.000	0.922	0.000	0.000	0.000	0.000	0.000	0.092
Pb	0.000	0.000	0.000	0.014	0.000	0.000	0.000	0.000	0.745	0.000	0.000	0.000	0.000	0.000	0.089
Ni	0.000	0.000	0.000	0.022	0.003	0.000	0.000	0.000	0.702	0.000	0.000	0.000	0.000	0.000	0.019
Zn	0.000	0.000	0.000	0.007	0.000	0.000	0.000	0.000	0.333	0.000	0.000	0.000	0.000	0.000	0.919
Rb	0.000	0.000	0.000	0.004	0.000	0.000	0.000	0.002	0.367	0.000	0.000	0.000	0.000	0.000	0.207
Sr	0.000	0.000	0.000	0.012	0.000	0.000	0.000	0.002	0.378	0.000	0.000	0.000	0.001	0.000	0.298
Zr	0.001	0.051	0.001	0.088	0.001	0.000	0.009	0.850	0.004	0.000	0.015	0.068	0.082	0.054	0.578
sand	0	0.000	0.000	0.002	0.000	0.000	0.000	0.000	0.311	0.000	0.000	0.000	0.000	0.000	0.118
clay	-0.856	0	0.000	0.032	0.000	0.000	0.000	0.000	0.632	0.000	0.000	0.000	0.000	0.000	0.041
silt	-0.995	0.803	0	0.002	0.000	0.000	0.000	0.001	0.205	0.000	0.000	0.000	0.000	0.000	0.154
-1-0	0.535	-0.393	-0.545	0	0.001	0.002	0.005	0.497	0.127	0.002	0.005	0.038	0.074	0.027	0.261
0-1	0.785	-0.601	-0.794	0.574	0	0.000	0.002	0.446	0.022	0.000	0.000	0.001	0.001	0.000	0.304
1-2	0.947	-0.745	-0.955	0.532	0.856	0	0.000	0.069	0.026	0.000	0.000	0.000	0.000	0.000	0.178
2-3	0.928	-0.805	-0.921	0.502	0.533	0.802	0	0.000	0.597	0.000	0.000	0.000	0.000	0.000	0.110
3-4	0.605	-0.721	-0.564	0.129	0.144	0.337	0.721	0	0.002	0.106	0.000	0.000	0.000	0.000	0.230
4-5	-0.192	-0.091	0.238	-0.285	-0.415	-0.405	-0.101	0.534	0	0.001	0.767	0.174	0.194	0.720	0.634
5-6	-0.877	0.642	0.893	-0.546	-0.772	-0.905	-0.798	-0.301	0.564	0	0.000	0.001	0.002	0.000	0.613
6-7	-0.948	0.810	0.944	-0.499	-0.692	-0.833	-0.906	-0.732	-0.057	0.743	0	0.000	0.000	0.000	0.195
7-8	-0.877	0.792	0.865	-0.380	-0.582	-0.743	-0.842	-0.789	-0.255	0.562	0.952	0	0.000	0.000	0.079
8-9	-0.863	0.894	0.830	-0.331	-0.564	-0.748	-0.811	-0.770	-0.244	0.544	0.871	0.942	0	0.000	0.015
9-10	-0.844	0.997	0.789	-0.404	-0.602	-0.738	-0.791	-0.698	-0.068	0.637	0.789	0.766	0.877	0	0.034
LOI	-0.291	0.375	0.267	-0.212	-0.194	-0.253	-0.298	-0.226	-0.090	0.096	0.243	0.326	0.438	0.389	0

Table A2.4 Correlation matrix of environmental variables from DMSS1 with p values.

DMSS1	Cl	Br	Al	Ti	Ca	Mg	K	Fe	Mn	Cr	Cu	Pb	Ni	Zn	Rb	Sr	Zr
Cl	0	0.799	0.585	0.451	0.206	0.651	0.482	0.985	0.382	0.572	0.138	0.041	0.448	0.728	0.493	0.870	0.021
Br	0.093	0	0.431	0.379	0.290	0.491	0.342	0.000	0.134	0.800	0.683	0.576	0.890	0.383	0.051	0.940	0.188
Al	-0.197	-0.282	0	0.000	0.017	0.000	0.000	0.760	0.969	0.000	0.301	0.010	0.000	0.012	0.117	0.002	0.084
Ti	-0.270	-0.313	**0.976**	0	0.025	0.001	0.000	0.664	0.989	0.000	0.494	0.008	0.001	0.033	0.116	0.003	0.023
Ca	0.438	-0.372	**0.730**	**0.697**	0	0.000	0.025	0.434	0.938	0.034	0.778	0.540	0.113	0.182	0.660	0.009	0.646
Mg	0.164	-0.248	**0.901**	**0.891**	**0.918**	0	0.001	0.687	0.648	0.002	0.956	0.169	0.010	0.048	0.187	0.001	0.287
K	-0.252	-0.336	**0.979**	**0.991**	**0.698**	**0.885**	0	0.638	0.944	0.000	0.424	0.007	0.002	0.026	0.148	0.005	0.032
Fe	-0.007	**0.913**	-0.111	-0.158	-0.279	-0.146	-0.170	0	0.358	0.784	0.356	0.991	0.484	0.181	0.037	0.586	0.305
Mn	0.311	0.507	0.014	-0.005	0.028	0.166	-0.026	0.326	0	0.979	0.420	0.877	0.721	0.843	0.221	0.480	0.371
Cr	-0.204	-0.092	**0.967**	**0.919**	**0.671**	**0.845**	**0.924**	0.100	0.010	0	0.122	0.009	0.000	0.001	0.044	0.001	0.160
Cu	-0.503	0.148	0.364	0.246	-0.102	0.020	0.286	0.328	-0.288	0.522	0	0.072	0.152	0.041	0.311	0.651	0.671
Pb	**-0.652**	-0.202	**0.766**	**0.779**	0.221	0.472	**0.782**	0.004	-0.057	**0.771**	**0.591**	0	0.013	0.076	0.158	0.069	0.013
Ni	-0.271	0.050	**0.910**	**0.865**	0.532	**0.765**	**0.848**	0.251	0.130	**0.948**	0.488	**0.749**	0	0.003	0.013	0.002	0.215
Zn	-0.126	0.310	**0.750**	**0.673**	0.459	**0.636**	**0.693**	0.460	0.072	**0.880**	**0.652**	**0.585**	**0.836**	0	0.006	0.018	0.569
Rb	-0.246	**0.629**	0.527	0.529	0.159	0.454	0.492	**0.662**	0.425	**0.645**	0.357	0.483	**0.746**	**0.791**	0	0.038	0.514
Sr	0.060	0.027	**0.848**	**0.837**	**0.769**	**0.890**	**0.807**	0.197	0.253	**0.870**	0.164	**0.595**	**0.858**	**0.725**	**0.659**	0	0.325
Zr	**-0.712**	-0.453	**0.572**	**0.705**	0.167	0.374	**0.675**	-0.362	-0.318	0.480	0.154	**0.747**	0.430	0.205	0.235	0.348	0
sand	-0.363	-0.458	-0.328	-0.220	-0.487	-0.472	-0.221	-0.504	-0.140	-0.476	-0.281	0.084	-0.449	**-0.693**	-0.531	-0.504	0.346
clay	0.418	0.198	0.484	0.494	**0.656**	**0.724**	0.463	0.097	0.370	0.458	-0.296	-0.080	0.458	0.466	0.538	**0.588**	0.014
silt	0.302	0.469	0.243	0.118	0.379	0.344	0.127	**0.549**	0.059	0.419	0.400	-0.075	0.389	**0.664**	0.460	0.417	-0.399
0-1	-0.431	-0.469	-0.311	-0.204	-0.510	-0.489	-0.203	-0.485	-0.245	-0.448	-0.210	0.116	-0.421	**-0.657**	-0.522	-0.514	0.389
1-2	-0.431	-0.469	-0.311	-0.204	-0.510	-0.489	-0.203	-0.485	-0.245	-0.448	-0.210	0.116	-0.421	**-0.657**	-0.522	-0.514	0.389
2-3	-0.431	-0.469	-0.311	-0.204	-0.510	-0.489	-0.203	-0.485	-0.245	-0.448	-0.210	0.116	-0.421	**-0.657**	-0.522	-0.514	0.389
3-4	-0.028	-0.298	-0.405	-0.325	-0.374	-0.428	-0.332	-0.434	0.185	-0.535	-0.421	-0.061	-0.530	**-0.710**	-0.506	-0.420	0.091
4-5	0.009	-0.217	**0.642**	**0.719**	**0.695**	**0.761**	**0.730**	-0.177	-0.033	**0.605**	-0.047	0.408	0.413	0.502	0.347	**0.639**	0.534
5-6	0.370	0.235	0.354	0.325	**0.610**	**0.568**	0.326	0.193	0.005	0.437	0.056	-0.110	0.301	**0.595**	0.419	0.465	-0.086
6-7	0.104	**0.638**	-0.269	-0.423	-0.277	-0.307	-0.414	**0.636**	0.133	-0.066	0.504	-0.250	0.007	0.270	0.222	-0.138	-0.653
7-8	0.079	0.487	-0.124	-0.288	-0.172	-0.225	-0.269	**0.664**	-0.047	0.080	**0.601**	-0.059	0.163	0.336	0.173	0.022	-0.568
8-9	0.439	-0.083	**0.595**	0.474	**0.740**	**0.704**	0.477	0.085	0.137	**0.594**	0.076	0.083	**0.630**	0.486	0.244	**0.647**	-0.212
9-10	0.352	0.133	0.483	0.506	**0.647**	**0.714**	0.471	0.039	0.262	0.448	-0.300	-0.084	0.445	0.437	0.502	**0.554**	0.082
LOI	0.258	0.612	**-0.821**	**-0.882**	**-0.685**	**-0.779**	**-0.897**	0.455	0.277	**-0.715**	-0.100	**-0.658**	**-0.564**	-0.417	-0.160	**-0.615**	**-0.769**

Table A2.4 Correlation matrix of environmental variables from DMSS1 with p values continued.

DMSS1	sand	clay	silt	0-1	1-2	2-3	3-4	4-5	5-6	6-7	7-8	8-9	9-10	LOI
Cl	0.302	0.230	0.397	0.214	0.214	0.214	0.939	0.980	0.293	0.774	0.829	0.204	0.319	0.471
Br	0.184	0.584	0.172	0.172	0.172	0.172	0.403	0.546	0.513	0.047	0.154	0.821	0.713	0.060
Al	0.356	0.157	0.498	0.382	0.382	0.382	0.245	0.045	0.316	0.452	0.733	0.070	0.157	0.004
Ti	0.541	0.147	0.745	0.572	0.572	0.572	0.359	0.019	0.360	0.223	0.420	0.166	0.135	0.001
Ca	0.153	0.039	0.280	0.132	0.132	0.132	0.287	0.026	0.061	0.438	0.635	0.014	0.043	0.029
Mg	0.168	0.018	0.331	0.151	0.151	0.151	0.217	0.011	0.087	0.388	0.531	0.023	0.020	0.008
K	0.540	0.178	0.726	0.573	0.573	0.573	0.349	0.017	0.358	0.234	0.452	0.163	0.170	0.000
Fe	0.138	0.790	0.100	0.155	0.155	0.155	0.210	0.625	0.594	0.048	0.036	0.816	0.914	0.186
Mn	0.700	0.292	0.870	0.496	0.496	0.496	0.608	0.928	0.989	0.715	0.898	0.706	0.465	0.438
Cr	0.165	0.183	0.228	0.194	0.194	0.194	0.111	0.064	0.207	0.857	0.825	0.070	0.195	0.020
Cu	0.432	0.406	0.252	0.561	0.561	0.561	0.225	0.898	0.877	0.137	0.066	0.834	0.399	0.783
Pb	0.817	0.827	0.838	0.749	0.749	0.749	0.866	0.242	0.763	0.487	0.871	0.820	0.817	0.039
Ni	0.193	0.183	0.266	0.226	0.226	0.226	0.115	0.235	0.398	0.985	0.653	0.051	0.197	0.090
Zn	0.026	0.175	0.036	0.039	0.039	0.039	0.022	0.140	0.069	0.450	0.343	0.154	0.207	0.231
Rb	0.115	0.109	0.181	0.122	0.122	0.122	0.135	0.326	0.228	0.537	0.633	0.496	0.140	0.660
Sr	0.137	0.074	0.231	0.128	0.128	0.128	0.226	0.047	0.175	0.704	0.952	0.043	0.097	0.059
Zr	0.327	0.969	0.253	0.267	0.267	0.267	0.804	0.112	0.814	0.041	0.086	0.557	0.822	0.009
sand	0	0.062	0.000	0.000	0.000	0.000	0.001	0.370	0.002	0.065	0.118	0.053	0.073	0.932
clay	-0.608	0	0.221	0.047	0.047	0.047	0.149	0.109	0.016	0.753	0.485	0.088	0.000	0.392
silt	-0.977	0.425	0	0.000	0.000	0.000	0.001	0.545	0.008	0.019	0.035	0.091	0.245	0.898
0-1	0.992	-0.639	-0.959	0	0.000	0.000	0.003	0.357	0.002	0.073	0.153	0.051	0.062	0.979
1-2	0.992	-0.639	-0.959	1.000	0	0.000	0.003	0.357	0.002	0.073	0.153	0.051	0.062	0.979
2-3	0.992	-0.639	-0.959	1.000	1.000	0	0.003	0.357	0.002	0.073	0.153	0.051	0.062	0.979
3-4	0.887	-0.492	-0.880	0.830	0.830	0.830	0	0.377	0.011	0.136	0.148	0.087	0.118	0.594
4-5	-0.318	0.538	0.218	-0.327	-0.327	-0.327	-0.314	0	0.042	0.206	0.192	0.646	0.098	0.003
5-6	-0.857	0.735	0.779	-0.854	-0.854	-0.854	-0.759	0.651	0	0.517	0.830	0.240	0.014	0.417
6-7	-0.603	-0.114	0.719	-0.590	-0.590	-0.590	-0.506	-0.438	0.233	0	0.001	0.659	0.684	0.058
7-8	-0.527	-0.251	0.668	-0.488	-0.488	-0.488	-0.492	-0.450	0.078	0.881	0	0.359	0.421	0.166
8-9	-0.627	0.567	0.562	-0.630	-0.630	-0.630	-0.568	0.167	0.409	0.160	0.325	0	0.105	0.443
9-10	-0.590	0.990	0.406	-0.608	-0.608	-0.608	-0.526	0.553	0.744	-0.147	-0.287	0.542	0	0.323
LOI	0.031	-0.304	0.047	0.010	0.010	0.010	0.193	**-0.823**	-0.290	**0.615**	0.475	-0.274	-0.349	0

Table A2.5 Correlation matrix of environmental variables from DMSS2 with p values.

DMSS2	Cl	Br	Al	Ti	Ca	Mg	K	Fe	Mn	Cr	Cu	Pb	Ni	Zn	Rb	Sr	Zr
Cl	0	0.012	0.005	0.936	0.896	0.001	0.001	0.000	0.000	0.001	0.001	0.011	0.001	0.001	0.007	0.013	0.012
Br	**0.564**	0	0.000	0.966	0.002	0.018	0.000	0.000	0.010	0.002	0.001	0.000	0.000	0.002	0.000	0.740	0.000
Al	**0.613**	**0.737**	0	0.201	0.469	0.000	0.000	0.000	0.024	0.000	0.000	0.000	0.000	0.000	0.000	0.033	0.000
Ti	0.020	0.010	0.307	0	0.187	0.137	0.179	0.479	0.993	0.213	0.347	0.110	0.583	0.327	0.669	0.022	0.757
Ca	-0.032	**-0.669**	-0.177	0.317	0	0.580	0.336	0.252	0.772	0.349	0.457	0.136	0.234	0.455	0.005	0.016	0.103
Mg	**0.697**	0.535	**0.882**	0.354	0.136	0	0.000	0.000	0.011	0.000	0.000	0.001	0.000	0.000	0.006	0.003	0.001
K	**0.688**	**0.763**	**0.977**	0.322	-0.234	**0.862**	0	0.000	0.013	0.000	0.000	0.000	0.000	0.000	0.000	0.027	0.000
Fe	**0.731**	**0.743**	**0.900**	0.173	-0.276	**0.809**	**0.929**	0	0.006	0.000	0.000	0.000	0.000	0.000	0.000	0.076	0.000
Mn	**0.794**	**0.572**	0.514	0.002	-0.071	**0.570**	**0.557**	**0.604**	0	0.046	0.027	0.048	0.008	0.026	0.011	0.024	0.031
Cr	**0.695**	**0.658**	**0.892**	0.299	-0.228	**0.754**	**0.927**	**0.878**	0.463	0	0.000	0.000	0.000	0.000	0.000	0.057	0.000
Cu	**0.718**	**0.679**	**0.923**	0.229	-0.182	**0.797**	**0.945**	**0.955**	0.505	**0.924**	0	0.000	0.000	0.000	0.000	0.027	0.000
Pb	**0.567**	**0.743**	**0.886**	0.378	-0.355	**0.679**	**0.924**	**0.874**	0.459	**0.884**	**0.906**	0	0.000	0.000	0.000	0.033	0.000
Ni	**0.712**	**0.759**	**0.917**	0.134	-0.287	**0.817**	**0.930**	**0.975**	**0.586**	**0.871**	**0.952**	**0.881**	0	0.000	0.000	0.075	0.000
Zn	**0.677**	**0.672**	**0.917**	0.238	-0.182	**0.829**	**0.935**	**0.974**	0.508	**0.887**	**0.973**	**0.875**	**0.960**	0	0.000	0.039	0.000
Rb	**0.594**	**0.981**	**0.819**	0.105	-0.615	**0.609**	**0.850**	**0.810**	**0.569**	**0.755**	**0.769**	**0.851**	**0.825**	**0.755**	0	0.394	0.000
Sr	**0.559**	0.082	0.492	0.521	0.544	**0.638**	0.507	0.417	0.515	0.443	0.505	0.491	0.418	0.476	0.207	0	0.474
Zr	**-0.562**	**-0.773**	**-0.889**	0.076	0.386	**-0.709**	**-0.856**	**-0.861**	-0.496	**-0.804**	**-0.841**	**-0.758**	**-0.900**	**-0.826**	**-0.809**	-0.175	0
sand	-0.501	**-0.757**	**-0.868**	0.059	0.367	**-0.659**	**-0.808**	**-0.777**	-0.438	**-0.769**	**-0.794**	**-0.750**	**-0.817**	**-0.751**	**-0.801**	-0.217	**0.931**
clay	0.535	**0.859**	**0.821**	0.040	-0.436	**0.618**	**0.794**	**0.732**	**0.597**	**0.726**	**0.723**	**0.753**	**0.800**	**0.696**	**0.876**	0.243	**-0.845**
silt	0.445	**0.682**	**0.795**	-0.131	-0.341	**0.598**	**0.722**	**0.730**	0.338	**0.698**	**0.740**	**0.668**	**0.759**	**0.688**	**0.719**	0.137	**-0.897**
2-3	-0.201	**-0.570**	**-0.614**	0.273	0.371	-0.470	-0.521	-0.529	-0.253	-0.406	-0.479	-0.447	**-0.564**	-0.484	**-0.582**	0.054	**0.771**
3-4	-0.497	**-0.751**	**-0.842**	0.072	0.368	**-0.629**	**-0.779**	**-0.768**	-0.414	**-0.756**	**-0.785**	**-0.731**	**-0.809**	**-0.731**	**-0.788**	-0.186	**0.922**
4-5	**-0.785**	**-0.808**	**-0.862**	-0.018	0.328	**-0.722**	**-0.867**	**-0.876**	**-0.612**	**-0.856**	**-0.881**	**-0.820**	**-0.906**	**-0.834**	**-0.855**	-0.377	**0.878**
5-6	0.105	0.452	0.532	-0.143	-0.312	0.359	0.440	0.461	0.036	0.460	0.467	0.440	0.509	0.422	0.473	-0.071	**-0.637**
6-7	**0.652**	**0.763**	**0.842**	-0.075	-0.336	**0.663**	**0.803**	**0.835**	0.510	**0.793**	**0.842**	**0.756**	**0.862**	**0.793**	**0.801**	0.270	**-0.912**
7-8	**0.735**	**0.764**	**0.878**	-0.024	-0.278	**0.738**	**0.858**	**0.856**	**0.582**	**0.821**	**0.871**	**0.770**	**0.875**	**0.821**	**0.808**	0.346	**-0.923**
8-9	**0.684**	**0.817**	**0.858**	-0.059	-0.398	**0.688**	**0.842**	**0.810**	**0.555**	**0.800**	**0.818**	**0.787**	**0.853**	**0.770**	**0.860**	0.298	**-0.899**
9-10	0.511	**0.836**	**0.799**	0.033	-0.453	**0.596**	**0.775**	**0.729**	**0.599**	**0.713**	**0.705**	**0.760**	**0.804**	**0.682**	**0.860**	0.241	**-0.835**
LOI	**0.581**	**0.947**	**0.738**	-0.053	**-0.578**	0.528	**0.753**	**0.730**	**0.562**	**0.702**	**0.700**	**0.721**	**0.758**	**0.659**	**0.935**	0.109	**-0.803**

Table A2.5 Correlation matrix of environmental variables from DMSS2 with p values continued.

DMSS2	sand	clay	silt	2-3	3-4	4-5	5-6	6-7	7-8	8-9	9-10	LOI
Cl	0.029	0.018	0.056	0.409	0.030	0.000	0.668	0.002	0.000	0.001	0.025	0.009
Br	0.000	0.000	0.001	0.011	0.000	0.000	0.052	0.000	0.000	0.000	0.000	0.000
Al	0.000	0.000	0.000	0.005	0.000	0.000	0.019	0.000	0.000	0.000	0.000	0.000
Ti	0.811	0.869	0.592	0.257	0.770	0.940	0.559	0.759	0.921	0.811	0.895	0.828
Ca	0.123	0.062	0.153	0.118	0.121	0.170	0.193	0.160	0.249	0.092	0.051	0.010
Mg	0.002	0.005	0.007	0.042	0.004	0.000	0.132	0.002	0.000	0.001	0.007	0.020
K	0.000	0.000	0.000	0.022	0.000	0.000	0.059	0.000	0.000	0.000	0.000	0.000
Fe	0.000	0.000	0.000	0.020	0.000	0.000	0.047	0.000	0.000	0.000	0.000	0.000
Mn	0.061	0.007	0.157	0.296	0.078	0.005	0.883	0.026	0.009	0.014	0.007	0.012
Cr	0.000	0.000	0.001	0.084	0.000	0.000	0.047	0.000	0.000	0.000	0.001	0.001
Cu	0.000	0.000	0.000	0.038	0.000	0.000	0.044	0.000	0.000	0.000	0.001	0.001
Pb	0.000	0.000	0.002	0.055	0.000	0.000	0.060	0.000	0.000	0.000	0.000	0.000
Ni	0.000	0.000	0.000	0.012	0.000	0.000	0.026	0.000	0.000	0.000	0.000	0.000
Zn	0.000	0.001	0.001	0.036	0.000	0.000	0.072	0.000	0.000	0.000	0.001	0.002
Rb	0.000	0.000	0.001	0.009	0.000	0.000	0.041	0.000	0.000	0.000	0.000	0.000
Sr	0.372	0.316	0.576	0.826	0.445	0.111	0.773	0.264	0.147	0.216	0.319	0.658
Zr	0.000	0.000	0.000	0.000	0.000	0.000	0.003	0.000	0.000	0.000	0.000	0.000
sand	0	0.000	0.000	0.000	0.000	0.000	0.000	0.000	0.000	0.000	0.000	0.000
clay	-0.885	0	0.000	0.003	0.000	0.000	0.007	0.000	0.000	0.000	0.000	0.000
silt	-0.969	0.778	0	0.000	0.000	0.000	0.000	0.000	0.000	0.000	0.000	0.000
2-3	0.820	-0.648	-0.838	0	0.000	0.005	0.002	0.000	0.000	0.000	0.003	0.009
3-4	0.989	-0.867	-0.985	0.793	0	0.000	0.000	0.000	0.000	0.000	0.000	0.000
4-5	0.886	-0.871	-0.832	0.612	0.882	0	0.017	0.000	0.000	0.000	0.000	0.000
5-6	-0.759	0.598	0.836	-0.665	-0.811	-0.539	0	0.001	0.020	0.008	0.005	0.007
6-7	-0.952	0.835	0.947	-0.729	-0.964	-0.949	0.683	0	0.000	0.000	0.000	0.000
7-8	-0.923	0.819	0.888	-0.724	-0.910	-0.956	0.528	0.964	0	0.000	0.000	0.000
8-9	-0.944	0.895	0.881	-0.727	-0.920	-0.965	0.587	0.946	0.960	0	0.000	0.000
9-10	-0.872	0.990	0.771	-0.649	-0.858	-0.857	0.617	0.824	0.793	0.877	0	0.000
LOI	**-0.819**	**0.913**	**0.755**	**-0.585**	**-0.827**	**-0.852**	**0.598**	**0.809**	**0.787**	**0.849**	**0.889**	0

Table A2.6 Correlation matrix of environmental variables from OB1 with p values

OB1	Al	Ti	Ca	Mg	K	Fe	Mn	Cl	Br	Cd	Cu	Ni	Pb	Rb	Sr	Zn	Zr
Al	0	0.000	0.509	0.000	0.000	0.000	0.855	0.906	0.000	0.088	0.225	0.000	0.983	0.000	0.882	0.831	0.000
Ti	**0.664**	0	0.001	0.000	0.000	0.000	0.212	0.079	0.295	0.107	0.359	0.000	0.431	0.469	0.376	0.093	0.351
Ca	-0.069	0.326	0	0.500	0.654	0.000	0.000	0.007	0.000	0.134	0.000	0.013	0.062	0.000	0.000	0.000	0.000
Mg	**0.882**	**0.667**	0.070	0	0.000	0.000	0.475	0.152	0.001	0.280	0.211	0.002	0.470	0.000	0.834	0.661	0.000
K	**0.933**	**0.804**	-0.047	**0.832**	0	0.000	0.610	0.603	0.000	0.099	0.584	0.000	0.809	0.000	0.308	0.438	0.000
Fe	**0.628**	0.427	-0.410	0.492	0.723	0	0.000	0.163	0.000	0.754	0.931	0.000	0.511	0.000	0.003	0.216	0.000
Mn	-0.019	-0.129	-0.469	-0.074	0.053	0.402	0	0.895	0.000	0.066	0.000	0.001	0.000	0.941	0.000	0.128	0.118
Cl	-0.012	-0.181	-0.275	-0.148	0.054	0.144	0.014	0	0.000	0.401	0.288	0.015	0.062	0.001	0.754	0.325	0.000
Br	0.440	0.109	**-0.597**	0.329	0.454	0.480	0.389	0.385	0	0.572	0.000	0.017	0.000	0.000	0.000	0.000	0.000
Cd	0.176	0.166	0.155	0.112	0.170	-0.033	-0.190	0.087	0.059	0	0.287	0.941	0.915	0.600	0.243	0.361	0.580
Cu	-0.126	0.095	0.416	-0.129	-0.057	-0.009	-0.358	0.110	-0.568	0.110	0	0.001	0.000	0.201	0.002	0.000	0.560
Ni	0.469	0.383	-0.255	0.312	**0.605**	**0.743**	0.346	0.249	0.245	-0.008	0.337	0	0.001	0.000	0.086	0.000	0.000
Pb	0.002	-0.082	0.192	-0.075	-0.025	0.068	-0.412	0.192	-0.443	0.011	**0.834**	0.331	0	0.016	0.000	0.000	0.030
Rb	**0.609**	0.075	-0.490	0.398	0.541	0.501	0.008	0.325	0.522	0.055	-0.132	0.478	0.247	0	0.794	0.691	0.000
Sr	-0.015	-0.092	**0.672**	0.022	-0.106	-0.297	-0.432	0.033	-0.356	0.121	0.314	-0.177	0.414	0.027	0	0.012	0.353
Zn	-0.022	0.173	0.353	-0.046	0.081	0.128	-0.157	0.102	-0.470	0.095	**0.933**	0.527	**0.754**	-0.041	0.257	0	0.607
Zr	**-0.656**	-0.097	0.520	-0.441	**-0.610**	**-0.698**	-0.161	-0.383	**-0.589**	-0.057	0.060	**-0.601**	-0.223	**-0.842**	0.096	-0.053	0
LOI	0.325	-0.019	-0.170	0.241	0.254	0.155	0.086	0.353	0.398	0.129	-0.148	0.124	-0.116	0.208	-0.019	-0.078	-0.417
sand	-0.374	-0.215	-0.131	-0.274	-0.331	-0.165	0.319	-0.026	0.283	0.017	-0.333	-0.334	-0.465	-0.405	-0.236	-0.362	0.336
silt	0.157	0.151	0.230	0.139	0.185	0.022	-0.209	-0.021	-0.210	-0.067	0.151	0.149	0.213	0.237	0.234	0.193	-0.142
clay	0.281	0.104	-0.068	0.183	0.205	0.169	-0.168	0.049	-0.125	0.045	0.240	0.242	0.332	0.239	0.049	0.233	-0.251

Table A2.7 Correlation matrix of environmental variables from OB1 with p values continued.

OB1	LOI	sand	silt	clay
Al	0.001	0.000	0.128	0.006
Ti	0.857	0.036	0.145	0.317
Ca	0.099	0.205	0.025	0.515
Mg	0.019	0.007	0.179	0.076
K	0.013	0.001	0.072	0.046
Fe	0.134	0.110	0.835	0.101
Mn	0.409	0.002	0.042	0.104
Cl	0.000	0.806	0.842	0.636
Br	0.000	0.005	0.041	0.227
Cd	0.214	0.873	0.520	0.667
Cu	0.151	0.001	0.145	0.019
Ni	0.231	0.001	0.148	0.018
Pb	0.261	0.000	0.038	0.001
Rb	0.043	0.000	0.021	0.019
Sr	0.853	0.021	0.023	0.639
Zn	0.454	0.000	0.061	0.023
Zr	0.000	0.001	0.169	0.014
LOI	0	0.840	0.351	0.261
sand	-0.021	0	0.000	0.000
silt	-0.097	-0.563	0	0.003
clay	0.116	-0.615	-0.306	0

Table A2.8 Correlation matrix of environmental variables from OB4 with p values.

OB4	Al	Ti	Ca	Mg	K	Fe	Mn	Cl	Br	Cr	Cu	Ni	Pb	Rb	Sr
Al	0	0.000	0.000	0.000	0.000	0.007	0.013	0.174	0.000	0.000	0.841	0.001	0.251	0.000	0.009
Ti	**0.715**	0	0.876	0.000	0.000	0.027	0.212	0.016	0.924	0.000	0.007	0.000	0.050	0.000	0.092
Ca	-0.474	-0.019	0	0.000	0.000	0.328	0.000	0.000	0.000	0.147	0.000	0.903	0.078	0.000	0.000
Mg	**0.795**	0.487	-0.431	0	0.000	0.011	0.194	0.012	0.000	0.107	0.086	0.012	0.659	0.000	0.059
K	**0.937**	**0.770**	-0.451	**0.717**	0	0.018	0.004	0.157	0.000	0.000	0.652	0.001	0.867	0.000	0.001
Fe	0.315	0.258	0.116	0.296	0.277	0	0.000	0.037	0.025	0.023	0.022	0.000	0.010	0.003	0.000
Mn	-0.289	-0.148	**0.583**	-0.154	-0.333	**0.658**	0	0.697	0.247	0.603	0.014	0.092	0.317	0.027	0.000
Cl	0.161	-0.281	**-0.562**	0.292	0.168	0.244	0.046	0	0.000	0.000	0.000	0.199	0.000	0.000	0.817
Br	0.428	-0.011	**-0.685**	0.462	0.429	0.262	-0.137	**0.904**	0	0.033	0.000	0.852	0.003	0.000	0.231
Cr	**0.538**	**0.687**	0.172	0.190	**0.534**	0.265	-0.062	-0.482	-0.250	0	0.000	0.000	0.000	0.004	0.971
Cu	-0.024	0.315	**0.583**	-0.202	-0.054	0.268	0.286	**-0.699**	**-0.633**	**0.630**	0	0.000	0.000	0.064	0.001
Ni	0.395	0.474	0.014	0.293	0.365	**0.624**	0.199	-0.152	-0.022	**0.521**	**0.590**	0	0.000	0.004	0.148
Pb	0.136	0.230	0.208	0.053	0.020	0.300	0.119	-0.433	-0.346	0.462	**0.731**	**0.600**	0	0.597	0.004
Rb	**0.813**	0.417	**-0.645**	**0.640**	**0.749**	0.340	-0.259	0.448	**0.657**	0.336	-0.218	0.335	0.063	0	0.120
Sr	-0.306	-0.199	**0.669**	-0.222	-0.379	**0.539**	**0.769**	0.028	-0.142	0.004	0.373	0.171	0.332	-0.184	0
Zn	-0.019	0.266	0.489	-0.111	-0.068	0.436	0.413	**-0.510**	-0.476	0.461	**0.884**	**0.725**	**0.659**	-0.134	0.407
Zr	-0.342	0.222	**0.587**	-0.342	-0.368	-0.250	0.130	**-0.679**	**-0.680**	0.154	0.448	-0.066	0.222	**-0.541**	0.146
Hg	0.160	0.278	0.445	0.066	0.038	0.361	0.337	-0.483	-0.439	**0.623**	**0.859**	**0.600**	**0.737**	0.023	0.448
LOI	0.381	-0.054	**-0.739**	0.427	0.342	0.181	-0.259	**0.740**	0.828	-0.213	-0.465	0.119	0.033	**0.612**	-0.173

Table A2.8 Correlation matrix of environmental variables from OB4 with p values continued.

OB4	Zn	Zr	Hg	LOI
Al	0.877	0.003	0.345	0.001
Ti	0.023	0.059	0.096	0.648
Ca	0.000	0.000	0.006	0.000
Mg	0.349	0.003	0.698	0.000
K	0.570	0.001	0.824	0.003
Fe	0.000	0.033	0.028	0.125
Mn	0.000	0.274	0.042	0.027
Cl	0	0.000	0.002	0.000
Br	0.000	0	0.007	0.000
Cr	0.000	0.194	0	0.070
Cu	0.000	0.000	0.000	0
Ni	0.000	**0.580**	0.000	0.317
Pb	0.000	0.059	0.000	**0.784**
Rb	0.259	0.000	**0.894**	0.000
Sr	0.000	0.219	0.005	0.143
Zn	0.000	0.008	0.000	0.001
Zr	0.307	0.000	0.057	0.000
Hg	**0.811**	0.315	0.000	0.059
LOI	-0.376	**-0.601**	-0.314	0.000

Table A2.9 Correlation matrix of environmental variables from OB5 with p values.

OB5	Al	Ti	Ca	Mg	K	Fe	Mn	P	Cl	Br	Cr	Cu	Ni	Pb	Rb	Sr	Zn	Zr	Hg
Al	0	0.000	0.000	0.000	0.000	0.000	0.342	0.000	0.000	0.127	0.000	0.000	0.000	0.000	0.000	0.000	0.000	0.000	0.596
Ti	**0.884**	0	0.000	0.000	0.000	0.000	0.047	0.000	0.001	0.021	0.000	0.000	0.000	0.000	0.000	0.000	0.000	0.000	0.620
Ca	0.410	0.459	0	0.000	0.000	0.000	0.000	0.007	0.983	0.000	0.000	0.000	0.006	0.000	0.012	0.000	0.000	0.000	0.469
Mg	**0.919**	**0.780**	0.431	0	0.000	0.000	0.725	0.006	0.000	0.805	0.000	0.000	0.000	0.000	0.000	0.000	0.000	0.000	0.680
K	**0.962**	**0.928**	0.420	**0.836**	0	0.000	0.035	0.000	0.001	0.026	0.000	0.000	0.000	0.000	0.000	0.000	0.000	0.001	0.682
Fe	**0.564**	**0.614**	0.500	0.384	**0.704**	0	0.000	0.000	0.052	0.203	0.000	0.000	0.000	0.000	0.000	0.000	0.000	0.771	0.410
Mn	0.105	0.217	0.429	0.039	0.230	**0.702**	0	0.000	0.001	0.614	0.185	0.019	0.005	0.003	0.035	0.000	0.000	0.948	0.578
P	0.426	0.492	0.291	0.300	0.487	0.646	**0.592**	0	0.383	0.009	0.039	0.308	0.012	0.037	0.000	0.000	0.075	0.037	0.637
Cl	0.515	0.356	0.002	**0.702**	0.350	-0.213	-0.350	-0.096	0	0.853	0.014	0.164	0.717	0.336	0.077	0.459	0.823	0.000	0.646
Br	0.168	0.252	**-0.604**	0.027	0.244	0.140	0.056	0.282	0.021	0	0.695	0.001	0.040	0.007	0.003	0.010	0.013	0.837	0.327
Cr	**0.726**	**0.658**	0.438	0.623	**0.762**	0.543	0.146	0.225	0.266	-0.043	0	0.000	0.000	0.000	0.000	0.000	0.000	0.096	0.588
Cu	0.522	0.436	**0.552**	0.472	**0.560**	**0.547**	0.256	0.112	0.153	-0.360	**0.744**	0	0.000	0.000	0.000	0.000	0.000	0.773	0.036
Ni	**0.692**	**0.705**	0.300	0.523	**0.794**	**0.732**	0.305	0.275	0.040	0.225	**0.740**	**0.686**	0	0.000	0.000	0.000	0.000	0.675	0.234
Pb	0.534	0.475	0.519	0.462	**0.594**	**0.617**	0.324	0.228	0.106	-0.295	**0.805**	**0.868**	**0.697**	0	0.000	0.000	0.000	0.736	0.086
Rb	**0.863**	**0.839**	0.274	**0.678**	**0.933**	**0.736**	0.230	0.470	0.194	0.324	**0.748**	**0.547**	**0.855**	**0.623**	0	0.000	0.000	0.166	0.398
Sr	**0.549**	**0.613**	**0.864**	0.470	**0.616**	**0.797**	0.650	0.583	-0.082	-0.281	**0.552**	**0.611**	**0.558**	**0.650**	**0.573**	0	0.000	0.013	0.211
Zn	0.500	0.460	**0.615**	0.405	**0.559**	**0.661**	0.402	0.195	-0.025	-0.269	**0.691**	**0.878**	**0.763**	**0.801**	**0.548**	**0.708**	0	0.956	0.116
Zr	0.374	**0.621**	0.393	0.459	0.357	0.032	-0.007	0.227	0.408	-0.023	0.183	-0.032	0.046	0.037	0.153	0.269	-0.006	0	0.785
Hg	0.059	0.055	0.080	0.046	0.045	0.091	0.062	0.052	0.051	-0.108	0.060	0.229	0.131	0.188	0.093	0.138	0.173	-0.030	0
sand	-0.129	-0.008	0.254	-0.047	-0.131	-0.166	0.002	0.007	0.000	-0.275	-0.116	-0.031	-0.194	-0.032	-0.256	0.057	0.004	0.347	-0.142
clay	0.267	0.068	-0.138	0.199	0.210	0.004	-0.165	0.021	0.145	0.138	0.213	0.076	0.170	0.072	0.267	-0.069	0.083	-0.224	-0.052
silt	-0.080	-0.046	-0.145	-0.109	-0.034	0.162	0.127	-0.024	-0.113	0.166	-0.051	-0.029	0.060	-0.024	0.045	-0.003	-0.069	-0.170	0.181
2-3	-0.037	0.062	0.095	0.009	0.005	-0.048	0.013	0.084	0.025	-0.027	-0.015	0.059	-0.030	-0.002	-0.075	0.013	0.059	0.196	-0.093
3-4	-0.143	-0.014	0.298	-0.057	-0.145	-0.155	0.034	0.009	-0.031	-0.314	-0.132	-0.045	-0.193	-0.035	-0.267	0.096	0.012	0.359	-0.109
4-5	-0.273	-0.133	0.089	-0.166	-0.328	-0.334	-0.057	-0.030	0.033	-0.210	-0.345	-0.329	-0.444	-0.310	-0.480	-0.145	-0.256	0.469	-0.200
5-6	-0.158	-0.129	0.082	-0.029	-0.226	-0.216	-0.001	-0.037	0.111	-0.222	-0.243	-0.161	-0.345	-0.206	-0.364	-0.113	-0.155	0.308	-0.157
6-7	0.092	0.045	-0.125	0.003	0.188	0.335	0.160	0.036	-0.151	0.232	0.254	0.259	0.348	0.261	0.348	0.117	0.170	-0.415	0.239
7-8	0.142	0.103	-0.100	0.038	0.220	0.313	0.105	0.022	-0.111	0.223	0.245	0.235	0.373	0.234	0.381	0.147	0.167	-0.389	0.269
8-9	0.229	0.113	-0.076	0.113	0.253	0.238	0.014	-0.002	-0.032	0.160	0.228	0.177	0.330	0.180	0.369	0.104	0.176	-0.365	0.156
9-10	0.262	0.076	-0.119	0.193	0.206	0.015	-0.151	0.040	0.130	0.141	0.217	0.082	0.185	0.078	0.263	-0.046	0.109	-0.212	-0.018
LOI	0.189	0.137	**-0.591**	0.072	0.235	0.064	-0.023	0.119	0.126	0.754	0.157	-0.078	0.322	0.006	0.369	-0.270	-0.078	-0.259	-0.014
DBD	-0.159	-0.160	0.403	0.023	-0.260	-0.330	-0.217	-0.250	0.060	-0.651	-0.226	-0.057	-0.382	-0.108	-0.409	0.026	-0.090	0.316	-0.071

Table A2.9 Correlation matrix of environmental variables from OB5 with p values continued.

OB5	sand	clay	silt	2-3	3-4	4-5	5-6	6-7	7-8	8-9	9-10	LOI	DBD
Al	0.241	0.014	0.469	0.740	0.194	0.012	0.152	0.404	0.196	0.036	0.016	0.085	0.148
Ti	0.945	0.537	0.680	0.573	0.896	0.228	0.241	0.682	0.349	0.305	0.494	0.215	0.146
Ca	0.020	0.212	0.189	0.392	0.006	0.421	0.460	0.257	0.365	0.490	0.281	0.000	0.000
Mg	0.673	0.070	0.323	0.933	0.608	0.131	0.792	0.976	0.734	0.305	0.078	0.513	0.838
K	0.234	0.055	0.758	0.967	0.187	0.002	0.038	0.088	0.044	0.020	0.060	0.031	0.017
Fe	0.131	0.973	0.141	0.666	0.159	0.002	0.048	0.002	0.004	0.029	0.892	0.560	0.002
Mn	0.987	0.135	0.250	0.908	0.757	0.605	0.993	0.147	0.340	0.899	0.170	0.839	0.047
P	0.947	0.849	0.830	0.449	0.933	0.789	0.741	0.742	0.842	0.986	0.719	0.281	0.022
Cl	0.997	0.190	0.304	0.821	0.780	0.767	0.317	0.170	0.315	0.773	0.237	0.254	0.588
Br	0.011	0.212	0.131	0.808	0.004	0.055	0.042	0.034	0.041	0.147	0.201	0.000	0.000
Cr	0.293	0.052	0.644	0.896	0.231	0.001	0.026	0.020	0.025	0.037	0.048	0.155	0.039
Cu	0.779	0.490	0.795	0.593	0.684	0.002	0.143	0.017	0.031	0.108	0.461	0.480	0.605
Ni	0.077	0.123	0.586	0.788	0.078	0.000	0.001	0.001	0.000	0.002	0.092	0.003	0.000
Pb	0.769	0.517	0.830	0.988	0.755	0.004	0.060	0.016	0.032	0.102	0.483	0.955	0.330
Rb	0.019	0.014	0.683	0.495	0.014	0.000	0.001	0.001	0.000	0.001	0.016	0.001	0.000
Sr	0.605	0.534	0.977	0.910	0.383	0.188	0.306	0.288	0.181	0.346	0.678	0.013	0.812
Zn	0.973	0.451	0.534	0.591	0.913	0.019	0.158	0.123	0.130	0.110	0.323	0.482	0.417
Zr	0.001	0.040	0.123	0.073	0.001	0.000	0.004	0.000	0.000	0.001	0.052	0.018	0.003
Hg	0.198	0.641	0.099	0.398	0.324	0.068	0.153	0.028	0.013	0.158	0.869	0.897	0.522
sand	0	0.000	0.000	0.000	0.000	0.000	0.066	0.000	0.000	0.000	0.001	0.002	0.000
clay	-0.385	0	0.000	0.118	0.000	0.000	0.029	0.342	0.784	0.000	0.000	0.003	0.048
silt	-0.693	-0.399	0	0.000	0.000	0.027	0.897	0.000	0.000	0.037	0.000	0.483	0.006
2-3	0.714	-0.172	-0.575	0	0.000	0.020	0.792	0.005	0.001	0.001	0.187	0.550	0.155
3-4	0.973	-0.406	-0.649	0.588	0	0.000	0.076	0.000	0.000	0.000	0.000	0.001	0.000
4-5	0.575	-0.422	-0.241	0.254	0.596	0	0.000	0.000	0.000	0.000	0.000	0.000	0.000
5-6	0.202	-0.238	-0.014	0.029	0.195	0.712	0	0.000	0.000	0.000	0.025	0.001	0.000
6-7	-0.538	-0.105	0.616	-0.306	-0.548	-0.749	-0.410	0	0.000	0.001	0.253	0.002	0.000
7-8	-0.611	0.030	0.583	-0.357	-0.589	-0.842	-0.759	0.800	0	0.000	0.797	0.002	0.000
8-9	-0.634	0.515	0.227	-0.370	-0.615	-0.791	-0.760	0.362	0.756	0	0.000	0.002	0.000
9-10	-0.371	0.988	-0.403	-0.145	-0.388	-0.406	-0.244	-0.126	0.028	0.513	0	0.004	0.040
LOI	-0.327	0.317	0.078	-0.066	-0.366	-0.417	-0.352	0.341	0.337	0.329	0.315	0	0.000
DBD	0.472	-0.216	-0.300	0.156	0.501	0.503	0.413	-0.525	-0.513	-0.405	-0.225	**-0.674**	0

Table A2.10 Correlation matrix of environmental variables from PB1 with p values.

PB1	Si	Al	Ti	Ca	Mg	K	Fe	Mn	Cl	Br	Cr	Cu	Ni	Pb	Rb	Sr	Zn	Zr	LOI
Si	0.000	0.000	0.000	0.239	0.003	0.002	0.000	0.000	0.000	0.000	0.000	0.001	0.000	0.000	0.000	0.000	0.000	0.001	0.000
Al	-0.517	0.000	0.000	0.952	0.000	0.000	0.000	0.017	0.000	0.000	0.000	0.000	0.000	0.000	0.000	0.000	0.000	0.054	0.000
Ti	-0.477	**0.958**	0.000	0.604	0.000	0.000	0.000	0.032	0.000	0.000	0.000	0.000	0.000	0.000	0.000	0.000	0.000	0.489	0.000
Ca	0.146	-0.008	0.065	0.000	0.480	0.995	0.974	0.142	0.008	0.227	0.805	0.020	0.816	0.473	0.222	0.275	0.337	0.001	0.060
Mg	-0.357	**0.896**	**0.874**	0.088	0.000	0.000	0.000	0.016	0.000	0.000	0.000	0.000	0.000	0.000	0.000	0.000	0.000	0.088	0.000
K	-0.370	**0.962**	**0.935**	0.001	**0.917**	0.000	0.000	0.034	0.000	0.000	0.000	0.000	0.000	0.000	0.000	0.000	0.000	0.015	0.000
Fe	**-0.797**	**0.733**	**0.685**	0.004	**0.650**	**0.670**	0.000	0.000	0.000	0.000	0.000	0.004	0.000	0.000	0.000	0.000	0.000	0.000	0.000
Mn	**-0.629**	0.290	0.263	0.181	0.293	0.259	**0.749**	0.000	0.000	0.000	0.299	0.931	0.000	0.628	0.022	0.000	0.018	0.000	0.000
Cl	**-0.725**	0.532	0.517	-0.324	0.501	0.542	**0.735**	**0.619**	0.000	0.000	0.002	0.354	0.000	0.139	0.000	0.000	0.000	0.000	0.000
Br	**-0.709**	0.441	0.444	-0.150	0.466	0.463	**0.752**	**0.735**	**0.948**	0.000	0.067	0.613	0.000	0.495	0.000	0.000	0.001	0.000	0.000
Cr	-0.505	**0.869**	**0.859**	0.031	**0.699**	**0.777**	**0.603**	0.129	0.365	0.225	0.000	0.000	0.000	0.000	0.000	0.000	0.000	0.715	0.001
Cu	-0.389	**0.617**	**0.692**	0.284	0.490	0.508	0.348	0.011	0.115	0.063	**0.757**	0.000	0.000	0.000	0.000	0.084	0.000	0.025	0.057
Ni	**-0.760**	**0.896**	**0.892**	0.029	**0.768**	**0.831**	**0.843**	0.480	**0.682**	**0.634**	**0.834**	**0.683**	0.000	0.000	0.000	0.000	0.000	0.016	0.000
Pb	-0.535	**0.766**	**0.763**	0.089	**0.569**	**0.623**	0.496	0.060	0.183	0.085	**0.879**	**0.859**	**0.770**	0.000	0.000	0.002	0.000	0.204	0.017
Rb	**-0.676**	**0.933**	**0.884**	-0.151	**0.763**	**0.848**	**0.731**	0.279	0.534	0.425	**0.851**	**0.626**	**0.898**	**0.832**	0.000	0.000	0.000	0.058	0.000
Sr	**-0.786**	0.537	0.458	0.135	0.458	0.447	**0.931**	**0.803**	**0.586**	**0.657**	0.415	0.213	**0.682**	0.372	0.575	0.000	0.000	0.001	0.000
Zn	**-0.630**	**0.705**	**0.714**	0.119	0.551	**0.609**	**0.638**	0.288	0.445	0.384	0.773	**0.799**	**0.862**	**0.790**	**0.714**	0.502	0.000	0.469	0.000
Zr	0.381	-0.237	-0.086	0.386	-0.210	-0.295	-0.421	-0.416	**-0.669**	**-0.628**	-0.045	0.273	-0.295	0.157	-0.233	-0.383	-0.090	0.000	0.000
LOI	**-0.797**	**0.578**	**0.568**	-0.231	0.543	0.564	**0.762**	**0.634**	**0.964**	**0.951**	0.410	0.234	**0.757**	0.290	**0.601**	**0.636**	0.534	**-0.616**	0.000

Table A2.11 Correlation matrix of environmental variables from PB3 with p values.

PB3	Si	Al	Ti	Ca	Mg	K	Fe	Mn	Cl	Br	Cr	Cu	Ni	Pb	Rb	Sr	Zn	Zr	LOI
Si	0.000	0.000	0.000	0.134	0.000	0.000	0.000	0.000	0.000	0.000	0.000	0.000	0.000	0.000	0.000	0.000	0.000	0.845	0.000
Al	**-0.655**	0.000	0.000	0.789	0.000	0.000	0.000	0.005	0.000	0.000	0.000	0.000	0.000	0.000	0.000	0.000	0.000	0.151	0.000
Ti	**-0.672**	**0.967**	0.000	0.106	0.000	0.000	0.000	0.000	0.000	0.000	0.000	0.000	0.000	0.000	0.000	0.000	0.000	0.002	0.000
Ca	**-0.163**	0.029	0.175	0.000	0.307	0.758	0.067	0.000	0.001	0.002	0.124	0.000	0.245	0.002	0.833	0.000	0.000	0.000	0.008
Mg	**-0.659**	**0.955**	**0.922**	0.112	0.000	0.000	0.000	0.001	0.000	0.000	0.000	0.000	0.000	0.000	0.000	0.000	0.000	0.172	0.000
K	-0.541	**0.964**	**0.930**	-0.034	**0.921**	0.000	0.000	0.041	0.000	0.000	0.000	0.000	0.000	0.000	0.000	0.000	0.000	0.221	0.000
Fe	**-0.832**	**0.919**	**0.936**	0.198	**0.896**	**0.862**	0.000	0.000	0.000	0.000	0.000	0.000	0.000	0.000	0.000	0.000	0.000	0.117	0.000
Mn	-0.426	0.303	0.424	**0.866**	0.343	0.221	0.506	0.000	0.123	0.399	0.000	0.000	0.000	0.000	0.009	0.000	0.000	0.000	0.782
Cl	-0.546	0.583	0.554	-0.349	0.542	0.547	0.554	-0.168	0.000	0.000	0.000	0.029	0.000	0.003	0.000	0.283	0.002	0.229	0.000
Br	-0.526	**0.716**	0.672	-0.337	**0.699**	**0.733**	**0.691**	-0.092	**0.755**	0.000	0.000	0.051	0.000	0.027	0.000	0.020	0.002	0.225	0.000
Cr	**-0.620**	**0.840**	**0.863**	0.167	**0.753**	**0.788**	**0.801**	0.388	0.434	0.381	0.000	0.000	0.000	0.000	0.000	0.000	0.000	0.001	0.000
Cu	**-0.756**	**0.691**	**0.755**	0.442	**0.654**	0.594	**0.814**	**0.700**	0.235	0.211	0.820	0.000	0.000	0.000	0.000	0.000	0.000	0.003	0.000
Ni	**-0.811**	**0.916**	**0.924**	0.127	**0.868**	**0.863**	**0.948**	0.408	0.577	**0.603**	**0.883**	**0.844**	0.000	0.000	0.000	0.000	0.000	0.196	0.000
Pb	**-0.816**	**0.632**	**0.681**	0.327	**0.606**	0.534	0.777	0.571	0.317	0.238	**0.758**	**0.936**	**0.827**	0.000	0.000	0.000	0.000	0.029	0.000
Rb	**-0.677**	**0.957**	**0.926**	-0.023	**0.902**	**0.936**	**0.899**	0.279	0.584	**0.716**	**0.822**	**0.681**	**0.900**	**0.629**	0.000	0.000	0.000	0.259	0.000
Sr	**-0.679**	**0.609**	**0.688**	**0.697**	**0.643**	0.533	0.758	**0.840**	0.117	0.250	0.596	**0.807**	**0.691**	**0.718**	**0.628**	0.000	0.000	0.001	0.001
Zn	**-0.743**	**0.780**	**0.826**	0.384	**0.747**	**0.692**	**0.860**	**0.661**	0.337	0.324	**0.849**	**0.951**	**0.896**	**0.874**	**0.775**	**0.799**	0.000	0.007	0.000
Zr	0.021	0.156	0.336	0.500	0.149	0.133	0.170	0.425	-0.131	-0.132	0.339	0.317	0.141	0.236	0.123	0.356	0.289	0.000	0.380
LOI	**-0.685**	**0.776**	**0.736**	-0.284	**0.761**	**0.765**	**0.776**	-0.030	**0.804**	**0.911**	0.537	0.403	**0.748**	0.464	**0.795**	0.366	0.510	-0.096	0.000

Table A2.12 Correlation matrix of environmental variables from DMC1 with p values.

DMC1	Cl	Br	Al	Ti	Ca	Mg	K	Fe	Mn	Cr	Cu	Pb	Ni	Zn	Rb	Sr	Zr	Hg
Cl	0	0.000	0.506	0.493	0.000	0.007	0.265	0.001	0.000	0.136	0.366	0.687	0.044	0.040	0.000	0.047	0.002	0.245
Br	**0.766**	0	0.066	0.149	0.000	0.000	0.045	0.000	0.000	0.006	0.195	0.256	0.000	0.005	0.000	0.001	0.001	0.217
Al	0.106	0.286	0	0.000	0.735	0.000	0.000	0.000	0.652	0.000	0.001	0.000	0.000	0.000	0.000	0.000	0.000	0.114
Ti	0.109	0.227	**0.982**	0	0.652	0.000	0.000	0.000	0.573	0.000	0.002	0.001	0.000	0.001	0.000	0.000	0.000	0.165
Ca	**0.825**	0.786	0.054	0.072	0	0.005	0.404	0.011	0.000	0.762	0.491	0.310	0.367	0.677	0.000	0.099	0.017	0.892
Mg	0.412	0.544	**0.905**	**0.895**	0.421	0	0.000	0.000	0.008	0.000	0.025	0.026	0.000	0.003	0.000	0.000	0.021	0.181
K	0.176	0.311	**0.989**	**0.990**	0.132	**0.935**	0	0.000	0.369	0.000	0.002	0.001	0.000	0.001	0.000	0.000	0.000	0.138
Fe	0.477	**0.696**	**0.729**	**0.671**	0.388	**0.780**	**0.718**	0	0.020	0.000	0.000	0.000	0.000	0.000	0.000	0.000	0.771	0.075
Mn	0.793	**0.685**	0.072	0.089	**0.952**	0.402	0.142	0.359	0	0.632	0.705	0.514	0.360	0.521	0.000	0.085	0.043	0.909
Cr	0.234	0.415	**0.820**	**0.754**	0.048	**0.708**	**0.785**	**0.825**	0.076	0	0.000	0.000	0.000	0.000	0.000	0.000	0.520	0.015
Cu	0.143	0.204	0.510	0.455	-0.109	0.345	0.459	**0.548**	-0.060	**0.812**	0	0.000	0.000	0.000	0.006	0.000	0.436	0.005
Pb	0.064	0.179	**0.550**	0.491	-0.160	0.343	0.491	**0.593**	-0.104	**0.858**	**0.940**	0	0.000	0.000	0.005	0.000	0.709	0.011
Ni	0.312	0.516	**0.836**	**0.780**	0.143	**0.763**	**0.804**	**0.896**	0.145	**0.926**	**0.766**	**0.768**	0	0.000	0.000	0.000	0.648	0.007
Zn	0.318	0.427	**0.558**	0.483	0.066	0.452	0.509	**0.762**	0.102	**0.886**	**0.920**	**0.919**	**0.876**	0	0.000	0.000	0.153	0.006
Rb	**0.608**	**0.906**	**0.639**	**0.580**	**0.597**	**0.779**	**0.646**	**0.889**	0.516	**0.699**	0.415	0.423	**0.797**	0.625	0	0.000	0.225	0.058
Sr	0.309	0.489	**0.844**	**0.831**	0.258	**0.804**	**0.841**	**0.886**	0.269	**0.826**	**0.630**	**0.653**	**0.923**	0.757	0.777	0	0.159	0.034
Zr	-0.466	-0.494	0.526	**0.618**	-0.368	0.354	**0.549**	-0.046	-0.313	0.102	-0.123	-0.059	0.073	-0.224	-0.191	0.221	0	0.487
Hg	0.183	0.195	0.247	0.218	0.022	0.211	0.233	0.278	0.018	0.373	0.428	0.390	0.410	0.415	0.295	0.328	-0.110	0
sand	-0.421	-0.558	-0.028	0.061	-0.308	-0.108	0.022	-0.494	-0.262	-0.300	-0.255	-0.280	-0.389	-0.435	-0.500	-0.226	**0.583**	-0.293
clay	0.408	0.535	0.073	-0.041	0.182	0.090	0.009	0.532	0.200	0.462	0.500	0.493	0.509	**0.663**	0.512	0.306	**-0.632**	0.361
silt	0.403	0.536	0.013	-0.064	0.329	0.107	-0.030	0.457	0.268	0.235	0.166	0.200	0.332	0.343	0.470	0.190	-0.537	0.257
0-1	-0.164	-0.256	-0.097	-0.039	-0.166	-0.135	-0.059	-0.353	-0.159	-0.155	-0.037	-0.087	-0.235	-0.160	-0.266	-0.161	0.220	-0.187
1-2	-0.222	-0.327	-0.049	-0.013	-0.221	-0.095	-0.018	-0.352	-0.203	-0.120	0.021	-0.039	-0.231	-0.151	-0.318	-0.158	0.232	-0.198
2-3	-0.360	-0.468	-0.047	0.022	-0.238	-0.111	0.003	-0.460	-0.192	-0.265	-0.206	-0.243	-0.366	-0.378	-0.437	-0.206	0.473	-0.275
3-4	-0.521	**-0.671**	0.026	0.142	-0.354	-0.071	0.072	-0.490	-0.297	-0.386	-0.444	-0.426	-0.421	**-0.593**	**-0.565**	-0.239	**0.787**	-0.323
4-5	-0.515	**-0.714**	0.011	0.128	-0.374	-0.101	0.037	-0.499	-0.294	-0.397	-0.461	-0.413	-0.428	**-0.610**	**-0.606**	-0.293	**0.777**	-0.349
5-6	-0.177	-0.245	-0.005	0.016	-0.135	-0.099	-0.043	-0.074	-0.057	-0.094	-0.181	-0.050	-0.098	-0.163	-0.193	-0.125	0.193	-0.081
6-7	0.511	**0.714**	-0.030	-0.133	0.429	0.094	-0.067	0.517	0.340	0.301	0.303	0.301	0.398	0.488	**0.602**	0.251	**-0.749**	0.327
7-8	0.534	**0.733**	0.006	-0.099	0.426	0.147	-0.028	**0.560**	0.318	0.337	0.323	0.305	0.432	0.512	**0.631**	0.289	**-0.741**	0.349
8-9	0.517	**0.686**	0.036	-0.078	0.349	0.140	-0.010	**0.561**	0.276	0.395	0.388	0.366	0.467	**0.570**	**0.606**	0.287	**-0.720**	0.333
9-10	0.390	0.515	0.088	-0.025	0.169	0.101	0.023	0.534	0.191	0.460	0.482	0.484	0.509	**0.650**	0.503	0.306	**-0.602**	0.365
LOI	**0.664**	**0.558**	**0.745**	**0.777**	**0.546**	**0.884**	**0.811**	**0.673**	0.539	**0.642**	0.390	0.363	**0.669**	0.468	**0.704**	**0.714**	0.219	0.222
DBD	-0.338	-0.229	0.340	0.312	-0.312	0.234	0.298	0.099	-0.338	0.182	0.005	0.094	0.126	0.005	-0.037	0.075	0.364	-0.067

Table A2.12 Correlation matrix of environmental variables from DMC1 with p values continued.

DMC1	sand	Clay	silt	0-1	1-2	2-3	3-4	4-5	5-6	6-7	7-8	8-9	9-10	LOI	DBD
Cl	0.005	0.007	0.008	0.299	0.158	0.019	0.000	0.000	0.262	0.001	0.000	0.000	0.011	0.000	0.029
Br	0.000	0.000	0.000	0.102	0.034	0.002	0.000	0.000	0.117	0.000	0.000	0.000	0.000	0.000	0.144
Al	0.861	0.646	0.937	0.541	0.758	0.766	0.869	0.945	0.975	0.850	0.971	0.822	0.579	0.000	0.028
Ti	0.702	0.795	0.689	0.807	0.933	0.892	0.371	0.420	0.922	0.401	0.532	0.622	0.873	0.000	0.045
Ca	0.047	0.248	0.033	0.292	0.159	0.129	0.022	0.015	0.392	0.005	0.005	0.024	0.285	0.000	0.044
Mg	0.498	0.571	0.499	0.395	0.549	0.485	0.657	0.525	0.532	0.553	0.354	0.377	0.524	0.000	0.136
K	0.891	0.953	0.850	0.713	0.912	0.982	0.653	0.815	0.786	0.672	0.860	0.950	0.886	0.000	0.055
Fe	0.001	0.000	0.002	0.022	0.022	0.002	0.001	0.001	0.640	0.000	0.000	0.000	0.000	0.000	0.531
Mn	0.093	0.204	0.087	0.314	0.198	0.222	0.056	0.059	0.718	0.028	0.040	0.077	0.225	0.000	0.029
Cr	0.053	0.002	0.134	0.328	0.448	0.090	0.012	0.009	0.555	0.053	0.029	0.010	0.002	0.000	0.248
Cu	0.104	0.001	0.293	0.816	0.894	0.191	0.003	0.002	0.251	0.051	0.037	0.011	0.001	0.011	0.976
Pb	0.072	0.001	0.204	0.583	0.807	0.120	0.005	0.007	0.753	0.053	0.050	0.017	0.001	0.018	0.554
Ni	0.011	0.001	0.032	0.134	0.141	0.017	0.006	0.005	0.535	0.009	0.004	0.002	0.001	0.000	0.426
Zn	0.004	0.000	0.026	0.310	0.339	0.014	0.000	0.000	0.302	0.001	0.001	0.000	0.000	0.002	0.977
Rb	0.001	0.001	0.002	0.088	0.040	0.004	0.000	0.000	0.220	0.000	0.000	0.000	0.001	0.000	0.816
Sr	0.150	0.048	0.229	0.309	0.318	0.190	0.127	0.059	0.429	0.108	0.064	0.065	0.048	0.000	0.639
Zr	0.000	0.000	0.000	0.162	0.139	0.002	0.000	0.000	0.222	0.000	0.000	0.000	0.000	0.163	0.018
Hg	0.060	0.019	0.101	0.236	0.210	0.078	0.037	0.023	0.610	0.034	0.024	0.031	0.017	0.158	0.672
sand	0	0.000	0.000	0.000	0.000	0.000	0.000	0.000	0.009	0.000	0.000	0.000	0.000	0.756	0.408
clay	-0.864	0	0.000	0.000	0.000	0.000	0.000	0.000	0.486	0.000	0.000	0.000	0.000	0.659	0.263
silt	-0.988	0.777	0	0.000	0.000	0.000	0.000	0.001	0.002	0.000	0.000	0.000	0.000	0.799	0.487
0-1	0.793	-0.535	-0.830	0	0.000	0.000	0.005	0.421	0.000	0.000	0.000	0.000	0.000	0.859	0.801
1-2	0.846	-0.595	-0.877	0.878	0	0.000	0.003	0.356	0.000	0.000	0.000	0.000	0.000	0.846	0.542
2-3	0.968	-0.811	-0.964	0.780	0.858	0	0.000	0.006	0.002	0.000	0.000	0.000	0.000	0.783	0.764
3-4	0.838	-0.874	-0.782	0.424	0.444	0.733	0	0.000	0.961	0.000	0.000	0.000	0.000	0.490	0.143
4-5	0.565	-0.721	-0.487	0.128	0.146	0.421	0.876	0	0.004	0.000	0.000	0.000	0.000	0.319	0.098
5-6	-0.399	0.111	0.465	-0.611	-0.626	-0.472	0.008	0.436	0	0.539	0.885	0.910	0.336	0.243	0.232
6-7	-0.920	0.837	0.897	-0.613	-0.657	-0.825	-0.933	-0.804	0.098	0	0.000	0.000	0.000	0.608	0.136
7-8	-0.884	0.811	0.859	-0.558	-0.591	-0.798	-0.929	-0.840	-0.023	0.974	0	0.000	0.000	0.419	0.234
8-9	-0.910	0.908	0.863	-0.566	-0.606	-0.834	-0.949	-0.827	0.018	0.952	0.969	0	0.000	0.440	0.257
9-10	-0.867	0.996	0.782	-0.549	-0.615	-0.822	-0.855	-0.682	0.152	0.821	0.791	0.890	0	0.680	0.335
LOI	-0.049	0.070	0.041	0.028	0.031	-0.044	-0.110	-0.158	-0.184	0.081	0.128	0.122	0.066	0	0.803
DBD	0.131	-0.177	-0.110	0.040	0.097	0.048	0.230	0.258	0.188	-0.234	-0.188	-0.179	-0.152	0.040	0

Appendix 3

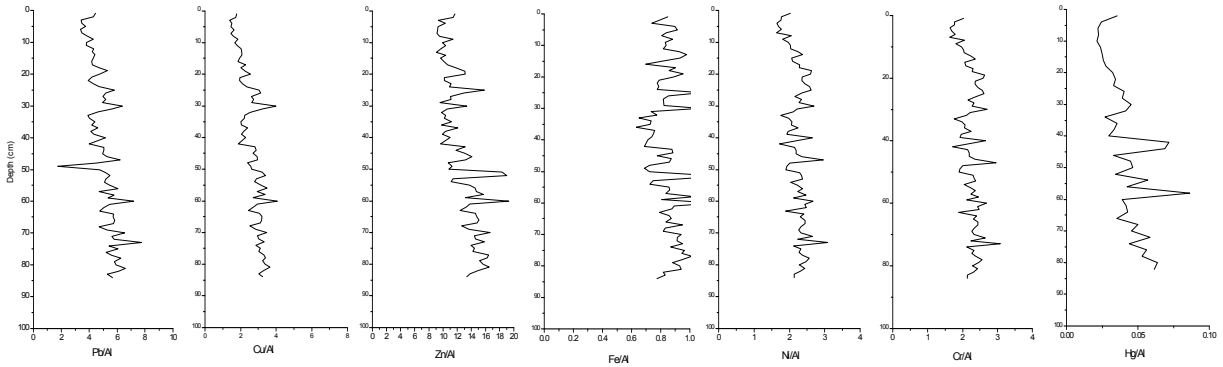

Figure A3.1 OB5 profiles of heavy metal ratios with Al.

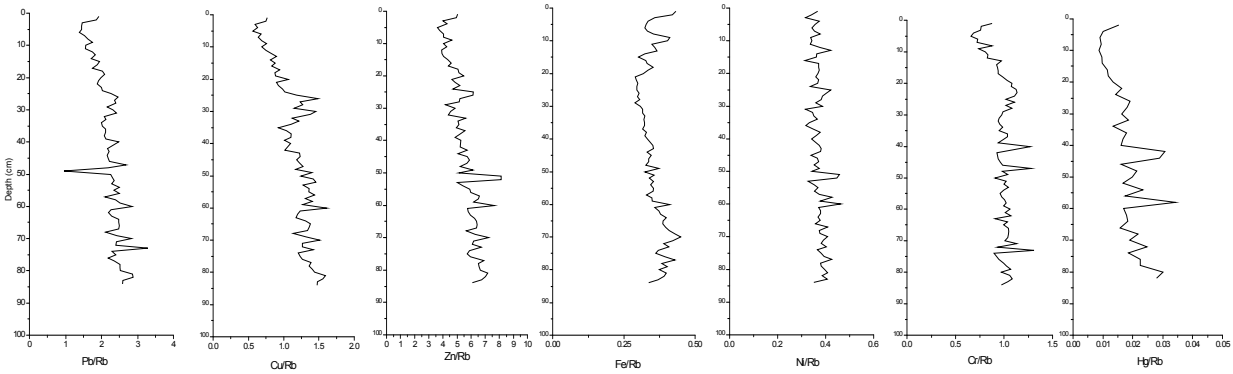

Figure A3.2 OB5 profiles of heavy metal ratios with Rb.

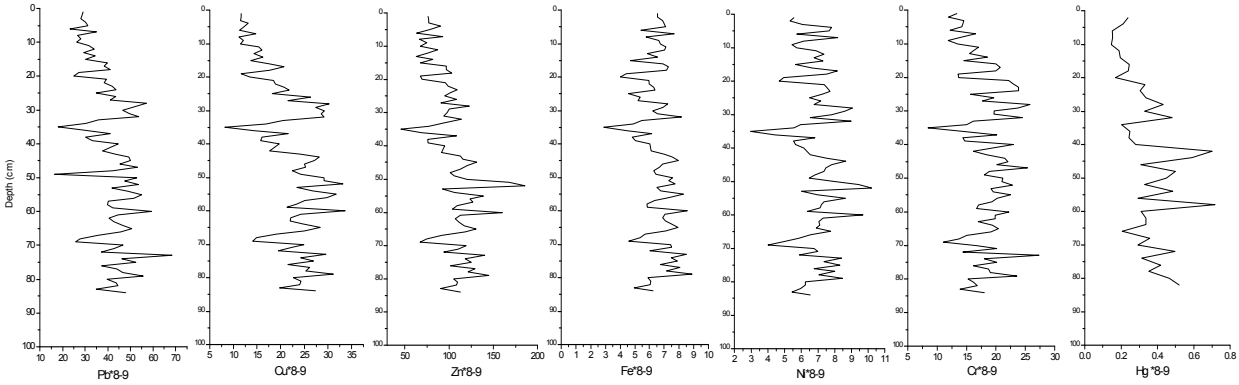

Figure A3.3 OB5 profiles of heavy metal ratios with grain size fraction 8-9 Φ.

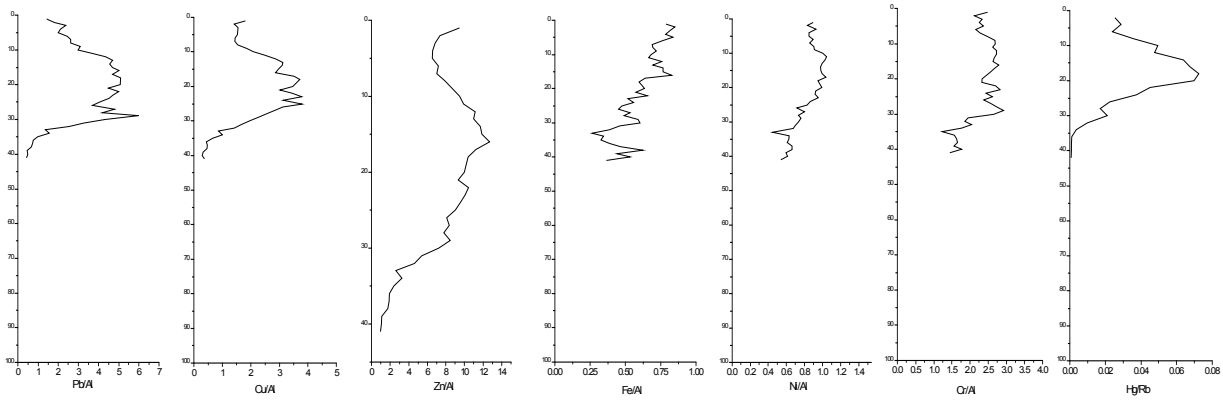

Figure A3.4 DMC1 profiles of heavy metal ratios with Al.

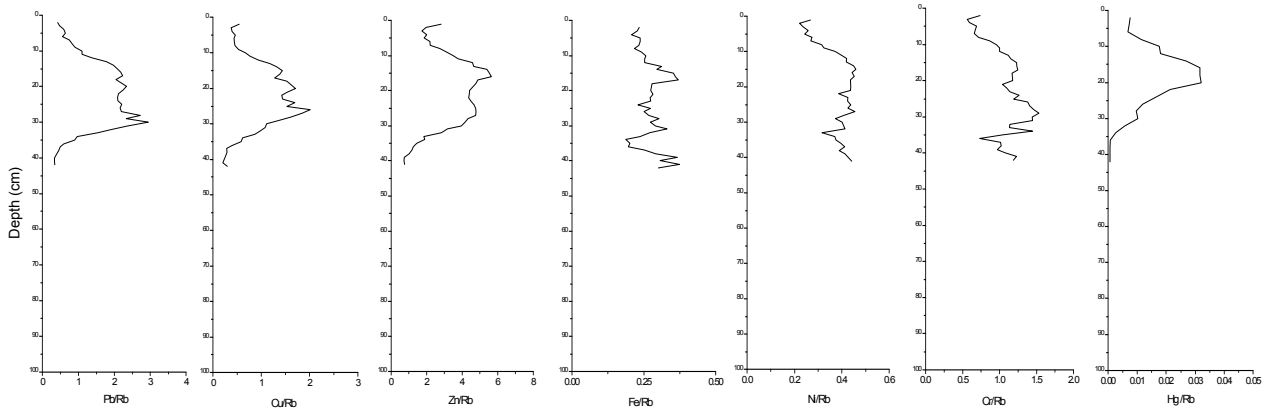

Figure A3.5 DMC1 profiles of heavy metal ratios with Rb.

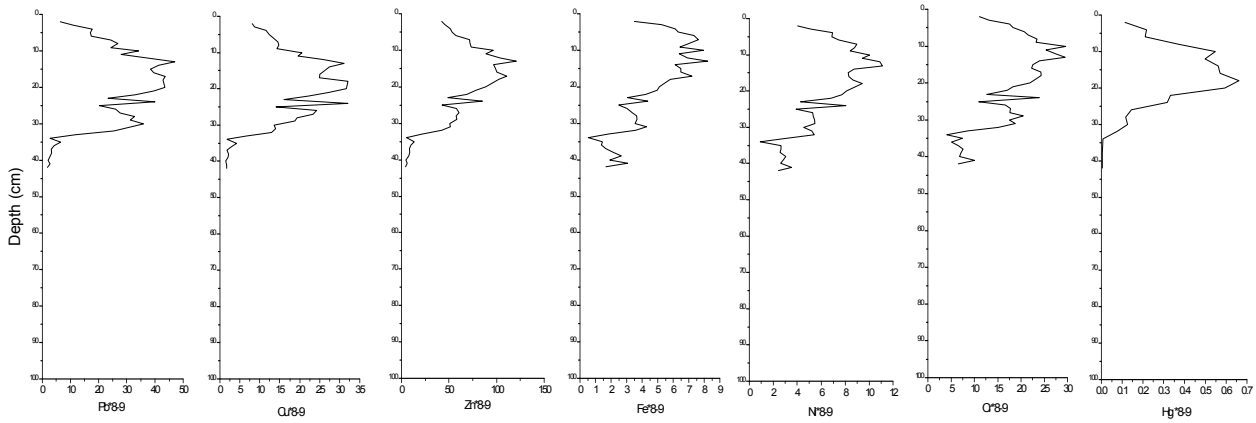

Figure A3.6 DMC1 profiles of heavy metal ratios with grain size fraction 8-9 Φ.

Appendix 4

Report on the radiometric analysis of a sediment core from Oglet Bay and Decoy Marsh saltmarshes in the Mersey Estuary

P.G.Appleby and G.T.Piliposyan Environmental Radioactivity Research Centre University of Liverpool

Methods

Dried sediment samples from the Oglet Bay cores OB5 and DMC1 in the Mersey Estuary were analysed for ^{210}Pb, ^{226}Ra, ^{137}Cs and ^{241}Am by direct gamma assay in the Liverpool University Environmental Radioactivity Laboratory using Ortec HPGe GWL (well-type) and GMX series coaxial low background intrinsic germanium detectors (Appleby et al., 1986). ^{210}Pb was determined via its gamma emissions at 46.5 keV, and ^{226}Ra by the 295 keV and 352 keV γ-rays emitted by its daughter radionuclide ^{214}Pb following 3 weeks storage in sealed containers to allow radioactive equilibration. ^{137}Cs and ^{241}Am were measured by their emissions at 662 keV and 59.5 keV respectively. The absolute efficiencies of the detectors were determined using calibrated sources and sediment samples of known activity. Corrections were made for the effect of self absorption of low energy γ-rays within the sample (Appleby et al., 1992).

Results OB5

Cs-137 and Am-241 records

The ^{137}Cs activity (figure 5.26 1a) had a maximum value quite near the base of the core, in the 72-73 cm sample. Above this peak, concentrations remain relatively high up to a depth of around 30 cm, but decline fairly steeply towards the top of the core. ^{241}Am concentrations (figure 5.26b) also have a maximum value in the 72-73 cm sample though towards the top of the core they decline less rapidly than those of ^{137}Cs. The ^{241}Am/^{137}Cs activity ratio varies from around 0.25 near the base of the core to around 0.5 in sediments in the top 10 cm. Both radionuclides have very high inventories. The calculated values are 813,880 Bq m^{-2} of ^{137}Cs and 209,200 Bq m^{-2} of ^{241}Am, though since there are evidently significant amounts below the base of the core, these figures underestimate the true inventories contained in the sediment record at this location. For comparison, the highest values previously obtained for saltmarsh cores from the Dee estuary were ~670,000 Bq m^{-2} of ^{137}Cs and ~60,000 Bq m^{-2} of ^{241}Am.

Lead-210 Activity

Total ^{210}Pb activity exceeded that of the supporting ^{226}Ra in all samples analysed (figure 5.26a). Unsupported ^{210}Pb activities, calculated by subtracting ^{226}Ra concentrations from the total ^{210}Pb concentrations, are very low and do not decline significantly with depth, supporting the inference from the ^{137}Cs /^{241}Am record that the core spans no more than a few decades.

Core Chronology OB5

Since discharges of ^{137}Cs from the Sellafield nuclear installation peaked during the years 1974-78, and discharges of ^{241}Am between during the years 1974-75, it is reasonable to suppose that sediments in the 72-73 cm sample containing the highest ^{137}Cs and ^{241}Am date from the period 1974-78. This implies a mean sedimentation rate since the mid-1970s of 1.7 g cm^{-2} y^{-1} (2.3 cm y^{-1}). Because of the incomplete nature of the ^{210}Pb record it is not possible to calculate an independent ^{210}Pb chronology. A chronology spanning the past 40 years can however be calculated by using the ^{137}Cs/^{241}Am date as a reference point (Appleby 2001). The results, shown in figure 2.28 and given in detail in table 5.6, suggest a significant acceleration in the sedimentation rate during past few decades, from around 0.9 g cm^{-2} y^{-1} (1.2 cm y^{-1}) before 1980 to around 3 g cm^{-2} y^{-1} (4 cm y^{-1}) during the past few years. Since the ^{210}Pb inventory suggests a mean supply rate that is well in excess of the atmospheric flux, it appears that the core is from a site subject to significant sediment focussing.

Results DMC1

Cs-137 and Am-241 records

The onset of significant concentrations of ^{137}Cs (figure 5.27a) occurred at a depth of around 20 cm. Above this level concentrations rose steeply, reaching a well defined peak in sediments between depths of 11-13 cm. ^{241}Am concentrations (figure 5.27b) followed a similar pattern, though the onset occurred very slightly later and the peak was a little sharper and contained in the 11-12 cm section. The inventories of these two radionuclides were 85710 Bq m^{-2} of ^{137}Cs and 24,938 Bq m^{-2} of ^{241}Am. Although high, they are just 10% of the values recorded in the nearby Oglet Bay core. Since the peaks in the Oglet Bay core occur at a much greater depth the difference is probably due to a much greater degree of sediment focussing at the Oglet Bay site.

Lead-210 Activity

Although unsupported ^{210}Pb activity (calculated by subtracting ^{226}Ra concentrations from the total ^{210}Pb concentrations) declined irregularly with depth (figure 5.27c), the overall trend was more-or-less exponential. This suggests that sedimentation rates have been relatively constant at least in recent decades.

Core Chronology DMC1

Since the discharge of ^{137}Cs from the Sellafield nuclear installation peaked during the years 1974-78, and the discharge of ^{241}Am in 1974, it is reasonable to suppose that sediments between 11-13 cm containing the highest ^{137}Cs and ^{241}Am concentrations date from the period 1974-78. This implies a mean sedimentation rate since the mid-1970s of 0.22 g cm^{-2} y^{-1} (0.35 cm y^{-1}). Since high ^{137}Cs and ^{241}Am concentrations in the 18-19 cm sample suggest that sediments at this depth post-date the onset of high Sellafield discharges in the late 1960s, it does however appear that accumulation rates in the preceding decade were significantly higher.

The $^{137}Cs/^{241}Am$ chronology is consistent with that determined from the ^{210}Pb record which indicates a mean sedimentation rate in recent decades of between 0.17 g cm^{-2} y^{-1} (CRS model) and 0.21 g cm^{-2} y^{-1} (CIC model). The lower value given by the CRS model may be due to uncertainties in the calculation of the ^{210}Pb inventory, possibly due to the suggested much higher sedimentation rate in the earlier part of the record. Revised CRS model calculations using the $^{137}Cs/^{241}Am$ date as a reference point (Appleby 2001) date the 18-19 cm sample to the early 1960s. The non-monotonic feature in the ^{210}Pb record between 12-16 cm is associated with a brief episode of more rapid accumulation. The results of these calculations are shown in figure 5.29 and given in detail in table 5.7. Because of the very low ^{210}Pb concentrations below 20 cm it is not possible to date sediments from the deeper sections of the core.

Appendix 5

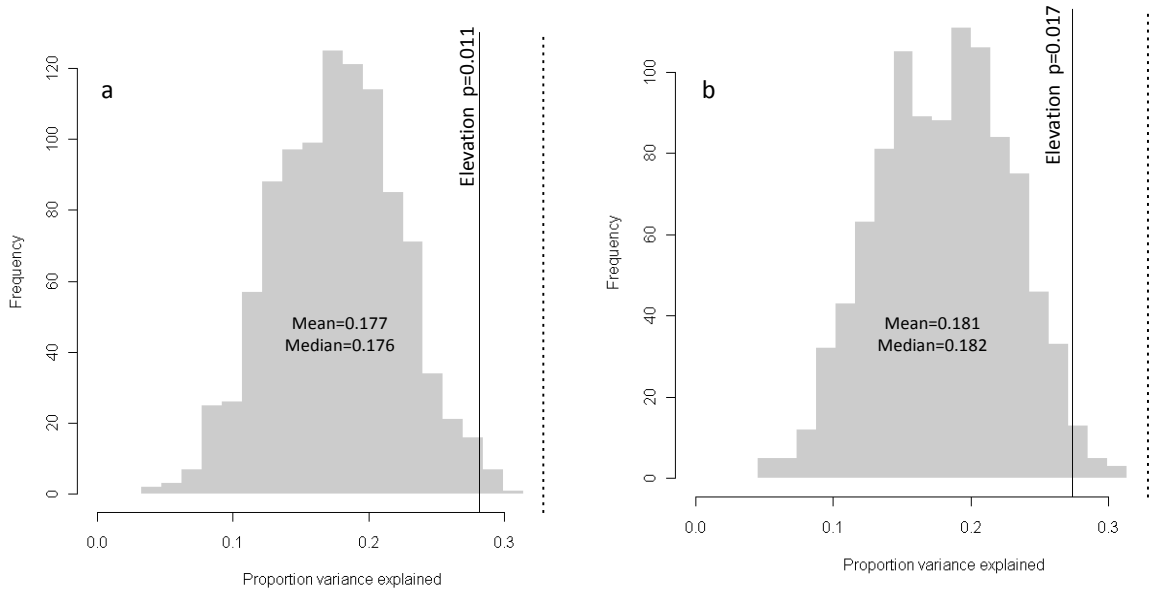

Figure A5.1 Histogram of the proportion of variance in the OB5 record explained by 999 WAPLS transfer functions trained by random data. Solid black line is the proportion of variance explained by transfer functions trained by a) OB b) OB b datasets. Dotted black line is the proportion of the variance explained by the 1st axis of a PCA of OB5.

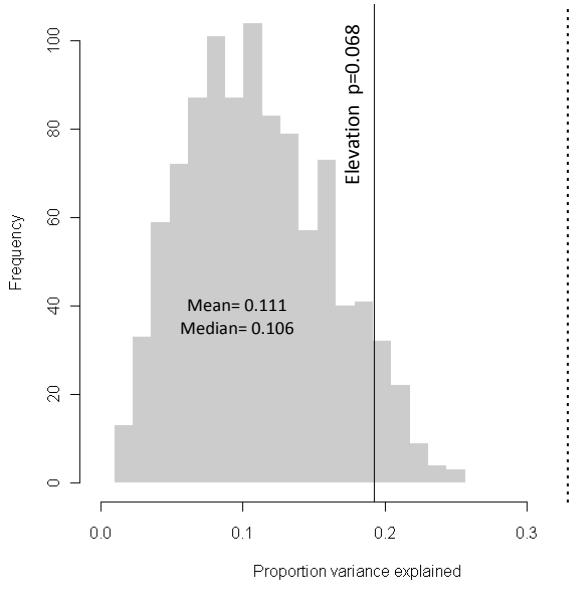

Figure A5.2Histogram of the proportion of variance in the OB5 record explained by 999 MAT transfer functions trained by random data. Solid black line is the proportion of variance explained by transfer functions trained by OB dataset. Dotted black line is the proportion of the variance explained by the 1st axis of a PCA of OB5.

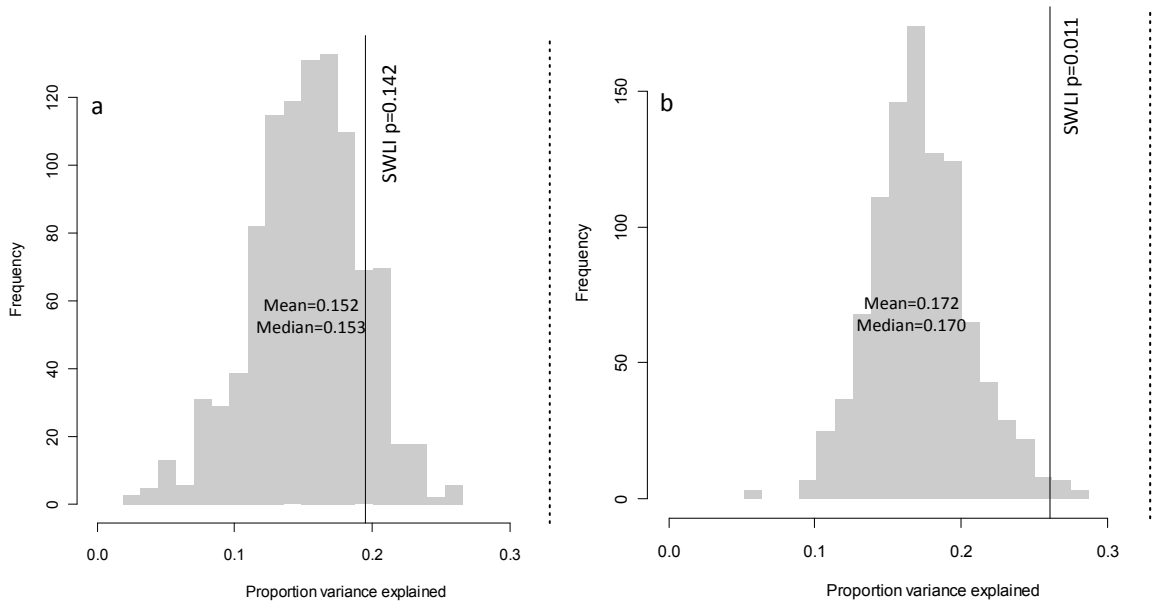

Figure A5.3 Histogram of the proportion of variance in the OB5 record explained by 999 WAPLS transfer functions trained by random data. Solid black line is the proportion of variance explained by transfer functions trained by a) H&E 7a b) H&E 7b datasets. Dotted black line is the proportion of the variance explained by the 1st axis of a PCA of OB5.